

University of Nottingham

UK | CHINA | MALAYSIA

A metabolic investigation into the effects of various perturbations on human macrophage

Alaa Mahmood Abuawad; MSc

Abstract

The “omics” sciences refer to a group of analytical platforms that aim to collectively characterise and quantify the pools of biological molecules such as genes (genomics), transcripts (transcriptomics), proteins (proteomics) and metabolites (metabolomics), which will be translated into the structure and the function of organisms, tissues or cells. Metabolomics concerns with identification and quantification of small molecules that represent the end products of the biological processes in a biological system. Liquid chromatography (LC)-mass spectrometry (MS)-based metabolomics approach is a powerful tool that has been widely used for disease diagnostics, biomarker discovery and drug toxicity. Moreover, LC-MS-based approaches have been employed to investigate the function of immune cells and immune responses by monitoring level changes of signalling molecules. Macrophages constitute a heterogeneous population of functionally distinct immune cells involved in several physiological and pathological processes. They play a crucial role in innate and adaptive immunity to protect the body from any invading danger. In addition, macrophages display remarkable plasticity by changing their phenotype and function in response to environmental cues displaying a wide spectrum of different functional phenotypes.

In this thesis, untargeted LC-MS-based metabolite profiling was applied to characterise THP-1 macrophages and differentiate between M1 and M2 phenotypes to identify key characteristic metabolites for each polarisation state. The so-called M1 and M2 macrophages are often considered as the extremes of polarisation states and representative of pro- and anti-inflammatory ends of the macrophage spectrum, respectively. The results showed that M1 and M2 macrophages have distinct metabolic profiles. Sphingolipid, pyrimidine and purine metabolism were significantly changed in M1 macrophages, whereas arginine, proline, alanine, aspartate and glutamate metabolism were significantly altered in M2 macrophages compared to naïve macrophages (M0). These data provided

functional readouts that show unique metabolic signatures for each phenotype, hence, could contribute to a better understanding of M1 and M2 functional properties, potenially paving the way for developing new therapeutics targeting different immune diseases.

In the second part of this thesis, the investigation of THP-1 macrophages polarisation and plasticity were extended to encompass the functional classification of macrophages; classically activated macrophages (M1), wound healing macrophages (M2) and regulatory macrophages (Mreg). LC-MS-based global metabolic profiling was carried out to differentiate between the metabolic profiles of these three subsets of macrophages revealing a distinct metabolic signature for M1 and M2 macrophages compared to M0 macrophages. However, Mreg showed a similar metabolic profile to M0 macrophages. Also, M0 and Mreg showed similar metabolic profiles after challenging them with lipopolysaccharide (LPS) where the significantly changed metabolites were similar to the characteristic key metabolites of M1. Moreover, the plasticity and stability of M1 and M2 macrophages were investigated using LC-MS-based global metabolic profiling after treating M1 macrophages with M2 inducer cytokines and vice versa. The results revealed that M1 macrophages are more stable than M2 macrophages. However, M2 showed the possibility of reversing to M1 phenotype showing a similar metabolic profile of M1 macrophages, whereas M1 macrophage did not reverse and their metabolic profiles remain more similar to their original M1 phenotype, indicationg that M1 macrophages are more stable than M2 macrophages.

In the third part of this thesis, LC-MS-based global metabolic profiling was used to distinguish between the impact of Gram-positive bacteria and Gram-negative bacteria on THP-1 macrophages challenged by the secretomes of *Staphylococcus aureus (S. aureus)* and *Pseudomonas aeruginosa (P. aeruginosa)*, and to find the key metabolites in each bacterial infection. Results revealed a distinct metabolic impact of each bacteria. This effect was clear in some metabolic pathways such as glycine and serine metabolism, sphingolipids metabolism, glycerophospholipids (GLs) metabolism, alanine, aspartate and glutamate metabolism and tryptophan metabolism *S. aureus* and *P. aeruginosa* showed differential impacts. However,

some similarities were shown in the impact on arginine and proline metabolism indicating a different response of macrophages to the secretome of different types of bacteria.

Finally, the ageing process in humans and its consequences on health and society have recently attracted more attention. Therefore, exploring the impact of ageing on macrophages using LC-MS-based global metabolic profiling was conducted on primary macrophages from young and old people in the steady state and in the LPS-stimulated state. However, young and old macrophages showed no difference in their metabolic profiles in both steady state and LPS stimulation, indicating no impact of ageing on macrophages metabolic profile. However, this result could be due to interindividual variabilities or the small sample size.

In conclusion, these results highlight LC-MS-based metabolomics as a promising approach to investigate immune responses under versatile conditions such as polarisation, bacterial infection and ageing. Furthermore, the efficiency of the technique aids the understanding of the mechanisms that underpin these responses, which could be utilised in developing novel therapeutics for manipulating immune diseases.

Dedication

To the one and only the one

To my soulmate, my friend and my

husband

Majdi Gogazeh

Acknowledgements

First and foremost, I take this opportunity to express my sincere gratitude to my principal supervisor Dr Dong-Hyun Kim for all precious support and constructive guidance throughout my thesis. I would like to express special appreciation and thanks for my co-supervisors, Prof. Amir Ghaemmaghami and Prof. David Barrett for their help and support.

I would like to convey my deep gratitude to Dr Salah Abdelrazig for his support as an advisor and friend throughout my PhD. Many thanks for Dr Catherine Ortori for her help and advice. I would also like to thank Dr Manuel Romero for his contribution and help in the bacterial chapter, Dr Chidimma Mbadugha for her contribution in macrophages characterisation. Also, many thanks to all members of the Centre for Analytical Biosciences and immunology group for their help and knowledge.

Very importantly, I would like to gratefully thank all my friends for their invaluable support and being always by my side, especially in hard times through PhD journey; Tamara Athamneh, Areen Al shweiat, Ola Al Fawares, Malak Jaber, Mohmmad Al Natour, Abdolelah Jaradat, Haneen Abu zaid, Razan Al Momani, Rasha Khader, Shahd Talhouni, Madiha Al awamie, Mussarat Wahid, Reem Al zaheri and every one share me every single time in this journey.

I would like to thank the Applied science private university in Jordan for awarding me the PhD Scholarship and sponsoring my study.

I would like to express my warm thanks from my deep heart to my Mom, Dad, sisters and brothers; Innas, Mohammad, Maysaa, Afnan, Ahmad, Omar, Aseel and Amer, my nephews and nieces for their continuous encouragement and warm feeling providing me with strength that I need to keep it up. I also would like to thank my Father in law Mohammad Ali Gogazeh for his support in my PhD.

Last but not least, very special gratitude to my amazing small family; my husband and my kids, Mohammad and Leen, that the completion of this PhD would have been not possible without their sacrifices, steadfast support and encouragement. Also, for sharing me all the delights and memories in Nottingham, thanks from my deep heart lovely family.

Publications

- Sherman HG, Jovanovic C, **Abuawad A**, Kim D-H, Collins H, Dixon JE, et al. Mechanistic insight into heterogeneity of trans-plasma membrane electron transport in cancer cell types. Biochimica et Biophysica Acta (BBA) - Bioenergetics. 2019;1860(8):628-39.

- **Abuawad, A.,** Mbadugha, C., Ghaemmaghami, A.M. et al. Metabolic characterisation of THP-1 macrophage polarisation using LC–MS-based metabolite profiling. Metabolomics 16, 33 (2020).

Contents

Abstract i

Dedication iv

Acknowledgements v

Publications vii

Contents viii

Table of figures xi

Table of Tables xvii

List of Abbreviations xix

1. General introduction 1

1.1. Metabolomics 2

1.1.1. Approaches of metabolomics 3

1.1.2. Cell-based metabolomics 4

1.1.2.1. Cell-based metabolomics workflow. 5

1.1.2.1.5. Advantages of cell-based metabolomics 15

1.1.2.1.6 Limitations and challenges of cell-based metabolomics 16

1.1.2.1.7. Application of cell metabolomics 16

1.2. Macrophages 17

1.2.1. Pattern recognition receptors. 19

1.2.2. Macrophage polarisation. 21

1.2.3. Macrophages polarisation and diseases. 26

1.2.4. Macrophages metabolism 29

1.3. Bacterial infection 34

1.3.1. Infectious diseases 35

1.3.2. Staphylococcus aureus. 37

1.3.3. Pseudomonas aeruginosa 38

1.3.4. Background of the problem 39

1.4. Ageing 41

1.4.1. Ageing and the immune system. 43

1.4.2. Ageing and macrophages. 44

1.4.3. Background of the problem 46

1.5. Aims and objectives. 48

2. Metabolic characterisation of THP-1 macrophage polarisation using LC-MS-based metabolite profiling 50

2.1. Introduction 51
2.2. Materials and methods 55
2.2.1. Materials 55
2.2.2. Methods 56
2.2.2.3. Sample preparation and metabolite extraction 57
2.3. Results and discussion 59
2.3.1. Macrophages characterisation using surface markers and cytokine profile 59
2.3.2. Untargeted metabolomics analysis of THP-1 polarised macrophages. . 63
2.3.3. Feature selection and identification of potential biomarker metabolites. 64
2.3.4. Pathway analysis 70
2.4. Conclusion 79
3. Investigation of the metabolic functional plasticity of macrophages using untargeted LC-MS metabolomics 86
3.1. Introduction 87
3.2. Materials and methods 95
3.2.1. Materials 95
3.2.2. Methods. 96
3.3. Results and discussion 100
3.3.1. Macrophages polarisation 100
3.3.2. Challenging M0 and Mreg with LPS 116
3.3.3. Macrophage plasticity 126
3.4. Conclusion 135
4. Treatment of macrophages with the secretomes of Gram-negative and -positive bacteria induces distinct metabolics signatures 178
4.1. Introduction 179
4.2. Materials and methods 184
4.2.1. Materials 184
4.2.2. Methods 184
4.2.2.3. Sample preparation and metabolite extraction 185
4.3. Results and discussion 188
4.3.1. Metabolic profiling of macrophages treated with the bacterial sectretome (bacterial cell culture medium). 188
4.3.2. Multivariate analysis 189
4.3.3. Pathway analysis 192
4.3.4. *P. aeruginosa* compared to mutant *P. aeruginosa* (PALT13) 207

4.4. Conclusion....210

5. Investigating the impact of ageing on human macrophages using LC-MS-based metabolite profiling....222

5.1. Introduction....223

5.2. Materials and methods....229

5.2.1. Materials....229

5.2.2. Methods....230

5.3. Results and discussion....233

5.3.2. Untargeted metabolomic analysis of macrophages....233

5.4. Conclusion....240

6. Conclusion and future work....241

6.1. Conclusion....242

6.2. Future work....247

References....249

Appendix....279

Table of figures

Figure 1.1: Schematic workflow of general cell metabolomics studies (24). 5
Figure 1.2: A common quenching and extraction approach used in the analysis of intracellular metabolites of adherent cells (24) 10
Figure 1.3: A schematic of ion formation in electrospray ionisation (71). 13
Figure 1.4: Origin of tissue-resident macrophages: bone marrow-derived monocytes yolk sac-derived macrophages and fetal liver-derived monocytes (112). 19
Figure 1.5: Pattern recognition receptors with their ligands (115). 21
Figure 1.6: Macrophage polarisation into classically activated macrophages, wound healing macrophages and regulatory macrophages in response to cytokines secreted in the micro-environment (108) 23
Figure 1.7: comparison of the cell wall in Gram-positive and Gram-negative bacteria (235) 35
Figure 1.8: Global Health Estimates 2016: Deaths by Cause, Age, Sex, by Country and by Region, 2000-2016. Geneva, World Health Organization; 2018. 36
Figure 1.9: The Hallmarks of Ageing (273) 42
Figure 1.10: Summary of the impact of ageing on macrophage function in mice as ageing affects many aspects of macrophage function (275). 45
Figure 2.1: Morphology of cytokine polarised THP-1 cells. Cells were stained with phalloidin (green) and DAPI (blue) for the visualization of cytoskeleton. Images were taken at 10x magnification; scale bar = 100µm. 61
Figure 2.2: Expression of surface markers by cytokine polarized THP-1 macrophages. A) Immunofluorescent images of showing mannose receptor (green) and calprotectin (red) expression; nuclei were stained with DAPI (blue). B) Mean fluorescent intensity (MFI) of M1, M2 and M0 cells. Data are presented as mean ± SD, (n=6). 62
Figure 2.3: Cytokine expression by macrophages. Following 6 h PMA activation, cells were treated with GM-CSF (50 ng/ml), LPS (100 ng/mL) and IFN-γ (20 ng/mL) or M-CSF (50 ng/mL) and IL-4 (20 ng/mL) for up to 72 h to generate M1 or M2 polarised cells, respectively. A) TNF-α B) IL-1β expression. Data are presented as mean ± SD (n=3). 63
Figure 2.4: Functional categories of the intracellular metabolites produced by THP-1 macrophages. In total, 575 metabolites were putatively identified in THP-1 macrophage extracts using LC-MS-based metabolite profiling. 64
Figure 2.5: OPLS-DA scores plots of macrophages extracts after polarisation toward M1 and M2 states and their corresponding unpolarised (M0) controls. (A) M1 and M2 macrophage samples and their respective unpolarised controls (R^2 = 0.647 and Q^2 = 0.847). (B) Two-way orthogonal comparison between M0 and M1 (R^2 = 0.664 and Q^2 = 0.899). (C) Two-way orthogonal comparison between M0 and M2 (R^2 = 0.711 and Q^2 = 0.838). M0 (yellow circles), M1 (blue squares), and M2 (purple triangles). n=6. 65
Figure 2.6: Summary of pathway analysis by MetaboAnalyst. The top-pathways are ranked by the gamma-adjusted p-values for permutation per pathway (y-axis) and the total number of hits per pathway (x-axis). The colour graduated from white to yellow, orange and red as the values of both x and y increase. (A) Metabolic pathways significantly changed in M1 macrophages. (B) Metabolic pathways significantly changed in M2 macrophages. 71

Figure 2.7: GLs and sphingolipids that significantly affected upon polarisation. (A) PC (14:2/16:0), (B) PS (18:0/20:4), and (C) PE (18:1/22:6) represent some GLs that increased significantly in M1 or M2 macrophages compared to M0 macrophages. (D) Ceramide (d18:1/24:0), (E) Ceramide (d18:1/22:0) and (F) Ceramide (d18:1/16:0) as potential key characteristic metabolites of M1 macrophages and their significant increase compared to M0 and M2 macrophages..... 73
Figure 2.8: Significant metabolic pathways upon polarisation of THP-1 macrophages toward M1 and M2 states with bar graphs of key metabolites that significantly changed. The other metabolites were either identified with no significant change (pyruvate, citrate, G6P, glutamate, ornithine and arginine) or not detected. Metabolic enzymes are as follows; 1: pyruvate dehydrogenase, 2: pyruvate carboxylase, 3: glutamate-aspartate aminotransferase, 4: L-aspartate N-acetyltransferase, 5: N-acetylglutamate synthetase, 6: formiminoglutamase, 7: imidazolonepropionase, 8: tryptophan 5-monooxygenase, 9: arylalkylamine N-acetyltransferase, 10: ornithine aminotransferase, 11: Arg-1, 12: ribosylpyrimidine nucleosidase, 13: pyrimidine-nucleoside phosphorylase. G6P: glucose 6-phosphate, PRPP: 5-phosphoribosyl 1-pyrophosphate, F6P: fructose 6-phosphate. The bar charts show the peak intensity (y-axis) of corresponding metabolites, from the top to the bottom and left to right (cytidine, N-acetyl-L-aspartate, N-acetyl-L-glutamate, 4-imidazolone-5-propanoate, 5-hydroxy-tryptophan and N-acetylserotonine). M0 in yellow, M1 in blue and M2 in purple. 79
Figure 3.1: Colour wheel of macrophage activation (109). A broad spectrum of macrophages is demonstrated where the primary three colours illustrate the main three activation states; classically activated macrophages(M1) (red), wound healing (M2 or alternatively activated) macrophages (yellow) and regulatory macrophages (Mreg) (blue). 88
Figure 3.2: Expression of surface markers by cytokine polarized THP-1 macrophages. A) Immunofluorescent images of showing mannose receptor (green) and calprotectin (red) expression; nuclei were stained with DAPI (blue). Scale bar = 100 µm..B) Mean fluorescent intensities of M1, M2 and M0 cells. *** $P \leq 0.001$, **** $P \leq 0.0001$. Data are presented as mean ± SD (n=6). 102
Figure 3.3: Cytokine expression by M0, M1 and M2 macrophages. A) TNF-α, B) IL-1β, C) CCL-18 expression. * $P \leq 0.05$, **** $P \leq 0.0001$. Data are presented as mean ± SD (n=3). 103
Figure 3.4: Cytokine expression by M0, M1, M2, and Mreg macrophages of TGF-β. As TGF-β and IL-10 are used to generate Mreg, 10 ng/ml TGF-β and 10 ng/ml Il-10 in complete media were analysed by ELISA and the obtained concentration was deduced from Mreg samples to get the concentration of TGF-β produced by Mreg upon polarisation. . ** $P \leq 0.01$, *** $P \leq 0.001$. Data are presented as mean ± SD (n=3)..... 103
Figure 3.5: OPLS-DA scores plots of macrophage extracts after polarisation toward M1, M2 and Mreg states and their corresponding unpolarised (M0) controls. (A) M1, M2 and Mreg macrophage samples and their respective unpolarised controls ($R^2 = 0.854$ and $Q^2 = 0.975$). (B) Two-way orthogonal comparison between M0 and M1 ($R^2 = 0.812$ and $Q^2 = 0.99$). (C) Two-way orthogonal comparison between M0 and M2 ($R^2 = 0.702$ and $Q^2 = 0.992$). (D) Two-way orthogonal comparison between M0 and Mreg ($R^2 = 0.504$ and $Q^2 = 0.960$). M0 (green pentagons), M1 (yellow diamonds), M2 (pink hexagons) and Mreg (dark blue circles). n=6..... 106
Figure 3.6: Box and whisker plots for significantly increased metabolites in M1 macrophages. Significant increase in these metabolites; 5-hydroxy-l-tryptophan

(Ceramide (d18:1/16:0); and cytidine, indicates enhanced activity of their corresponding pathways as characteristic for M1 macrophages, representing tryptophan metabolism, sphingolipids metabolism, and pyrimidine metabolism respectively. The whiskers illustrate minimum to maximum and the line in the box represent the median. n=6 .. 108
Figure 3.7: Box and whisker plots for significantly increased metabolites in M1 macrophages. Significant increase in these metabolites; 5-hydroxyindoleacetaldehyde; hypoxanthine, adenosine and deoxyadenosine, indicates enhanced activity of their corresponding pathways as characteristic for M1 macrophages, representing tryptophan metabolism, and purine metabolism, respectively. The whiskers illustrate minimum to maximum and the line in the box represent the median. n=6 110
Figure 3.8: Box and whisker plots for significantly decreased metabolites in M1 macrophages. Significant decrease in these metabolites; L-malate, 2-oxoglutarate and NAD+; L-aspartate and N-acetyl-L-aspartate; and N-acetyl-L-glutamate; indicates decreased activity of their corresponding pathways; representing TCA, metabolism; aspartate and glutamate metabolism, respectively. The whiskers illustrate minimum to maximum and the line in the box represent the median. n=6. 112
Figure 3.9: Schematic diagram of the significantly affected metabolic pathways upon polarisation of macrophages into M1 and M2 phenotypes. Red arrows represent M1 and green arrows represent M2 macrophages. Ascending arrows indicate an increase and descending arrows indicate a decrease in the levels of the metabolites. 113
Figure 3.10: Box and whisker plots with for significantly decreased metabolites in M2 macrophages. Significant increase in these metabolites; 4-imidazolone-5-propanoate and N-formimino-L-glutamate (intermediates in aspartate and glutamate metabolism) in addition to N-acetyl-L-glutamate and N-acetyl-L-aspartate (Figure 3.3) that represent aspartate and glutamate metabolism and; arginine and proline metabolism, respectively, indicating enhanced activity of these pathways. The whiskers illustrate minimum to maximum and the line in the box represent the median. n=6 115
Figure 3.11: Box and whisker plots for significantly decreased metabolites in M2 macrophages. Significant decrease in these metabolites; L-glutamine and L-formylkynurenine representing glutamate metabolism and tryptophan metabolism, respectively. The whiskers illustrate minimum to maximum and the line in the box represent the median. n=6 116
Figure 3.12: OPLS-DA scores plots of macrophage extracts after polarisation toward M1, M2 and Mreg states and their corresponding unpolarised (M0) controls in addition to M0 treated with LPS and Mreg treated with LPS for 24 hrs. (A) M1, M2, Mreg, M0-LPS and Mreg-LPS macrophage samples and their respective unpolarised controls (R^2 = 0.881 and $Q^{2=}$ 0.982). (B) Two-way orthogonal comparison between M0 and M1 (R^2 = 0.817 and Q^2 = 0.996). (C) Two-way orthogonal comparison between M0 and M2 (R^2 = 0.821 and Q^2 = 0.997). (D) Two-way orthogonal comparison between M0 and Mreg (R^2 = 0.615 and Q^2 = 0.989). (E) Two-way orthogonal comparison between M0 and M0-LPS (R^2 = 0.820 and Q^2 = 0.998). (F) Two-way orthogonal comparison between M0 and Mreg-LPS (R^2 = 0.875 and Q^2 = 0.860). M0 (green pentagons), M1 (yellow diamonds), M2 (pink hexagons), Mreg (dark blue circles), M0-LPS (red pentagon) and Mreg-LPS (light blue circles). n=6. 119
Figure 3.13: Box and whisker plots with for significantly increased metabolites in M1 macrophages in the experiment of challenging with LPS. Significant increase in the metabolites; 5-hydroxy-l-tryptophan and N-acetylserotonin; cytidine; hypoxanthine and adenosine; indicates enhanced activity of their corresponding pathways as characteristic

for M1 macrophages, representing tryptophan metabolism, pyrimidine metabolism and purine metabolism, respectively. The whiskers illustrate minimum to maximum and the line in the box represent the median. n=6. 121
Figure 3.14: Box and whisker plots for significantly decreased metabolites in M1 macrophages in the experiment of challenging with LPS. Significant decrease in these metabolites; L-malate, 2-oxoglutarate and NAD+; L-aspartate, N-acetyl-L-aspartate; L-glutamate and N-acetyl-L-glutamate; indicates decreased activity of their corresponding pathways; representing TCA, metabolism; aspartate and glutamate metabolism, respectively. The whiskers illustrate minimum to maximum and the line in the box represent the mediann=6. 123
Figure 3.15: Box and whisker plots for significantly increased metabolites in M0-LPS macrophages in the experiment of challenging with LPS. Significant increase in the metabolites; L-serine (glycine and serine metabolism) and 4-aminobutanoate (alanine, aspartate and glutamate metabolism) in addition to cytidine; hypoxanthine and adenosine in Figure 3.13. The whiskers illustrate minimum to maximum and the line in the box represent the median. n=6. 124
Figure 3.16: Box and whisker plots for significantly decreased metabolites in M0-LPS macrophages in the experiment of challenging with LPS Significant decrease in the metabolites; NADH (an intermediate in TCA cycle) and L-asparagine (an intermediate in alanine, aspartate and glutamate metabolism) in addition to N-acetyl-L-glutamate shown in Figure 3.14. The whiskers illustrate minimum to maximum and the line in the box represent the median. n=6 125
Figure 3.17: OPLS-DA scores plots of macrophage extracts after polarisation toward M1, M2 and reversing M1 and M2 for 24 (M1-M2-24 and M2-M1-24) and 48 hours (M1-M2-48 and M2-M1-48) and their corresponding unpolarised (M0) as a control. (A) M1, M2, M1-M2-24, M1-M2-48, M2-M1-24 and M2-M1-48 macrophage samples and their respective unpolarised controls (R2 = 0.905 and Q2 = 0.962). (B) A comparison between M1, M2-M1-24 and M2-M1-48 (R2 = 0.678 and Q2 = 0.979). (C) A comparison between M2, M1-M2-24 and M1-M2-48 (R2 = 0.889 and Q2 = 0.992).M0 (green pentagons), M1 (yellow diamonds), M2 (pink hexagons), M1-M2-24(dark blue squares), M1-M2-48 (dark green triangles), M2-M1-24 (light blue stars), M2-M1-48 (red circles). n=6..... 128
Figure 3.18: bar charts for the significantly changed metabolites in M2-M1-24 vs M1 macrophages, which showed a similar trend of M1 macrophages. N-acetyl-L-aspartate was significantly decreased, where 5-hydroxy-L-tryptophan and deoxyadenosine were significantly increased.n=6, data are presented as mean ± SEM. 130
Figure 3.19: bar charts for the significantly changed metabolites in M2-M1-48 vs M1 macrophages, which showed a similar trend of M1 macrophages. L-Tryptophan, L-arginine and L-1-pyrroline-3-hydroxy-5-carboxylate. In addition to N-acetyl-L-glutamate were significantly decreased, whereas deoxyadenosine was significantly increased in both (Figure 3.18). n=6, data are presented as mean ± SEM 130
Figure 3.20: bar charts for the significantly changed metabolites M1-M2-24 vs M2 macrophages, which showed a similar trend of M1 macrophages which are L-asparagine, NAD+, PC(20:4/P-18:1), 4-imidazolone-5-propanoate and L-ornithine, in addition to L-tryptophan (Figure 3.19), and N-acetyl-L-glutamate (Figure 3.18). n=6, data are presented as mean ± SEM. 132
Figure 3.21: 3D bar chart for the significantly changed metabolites in M2-M1-48 vs M2 macrophages, which showed similar trend of M1 macrophages which is L-valine, in addition to L-asparagine, PC(20:4/P-18:1), 4-imidazolone-5-propanoate and L-ornithine

(Figure 3.20), L-tryptophan and L-arginine (Figure 3.19), and N-acetyl-L-glutamate (Figure 3.18). n=6, data are presented as mean ± SEM. 133
Figure 4.1: Functional categories of the intracellular metabolites produced by macrophages, treated (S-S-M, P-S-M and Mut.P-S-M) and un-treated. 189
Figure 4.2: OPLS-DA scores plots and heatmap of macrophages extracts after treatment with the sectretomes of S. aureus, P. aeruginosa, Mut. P. aeruginosa and their corresponding untreated control (M0). (A) OPLS-DA scores plot of S-S-M, P-S-M and Mut.P-S-Mand M0 (R2 = 0.870 and Q2 = 0.988). (B) Heatmap of S-S-M, P-S-M and Mut.P-S-Mand M0 with clear clustering between the groups. (C) Two-way orthogonal comparison between P-S-M and untreated M0 (R2 = 0.838 and Q2 = 0.999). (D) Two-way orthogonal comparison between S-S-M and untreated M0 (R2 = 0.842 and Q2 = 0.998). M0 (dark blue squares), P-S-M (red triangles), S. aureus (light blue stars) and Mut.P-S-M (green circles). n=6..... 192
Figure 4.3: A summary of pathway analysis by MetaboAnalyst. The top pathways were ranked by the gamma-adjusted p-values for permutation per pathway (Y-axis) and the total number of hits per pathway (X-axis). The colour graduated from white to yellow, orange and red as the values of both x and y increase, red circles the most significantly changed metabolic pathway, and the pale yellowish are the least significantly changed metabolites. (A) Metabolic pathways significantly changed in P. aeruginosa sectretome treated macrophages. (B) Metabolic pathways significantly changed in S. aureus sectretome treated macrophages. 193
Figure 4.4: Significantly changed metabolites involved in amino acids metabolism in both P-S-M and S-S-M with the same trend (decrease or increase). L-1-Pyrroline-3-hydroxy-5-carboxylate, creatinine, L-glutamate 5-semialdehyde, L-citrulline and phosphocreatine represent arginine and proline metabolism. L-serine from glycine, serine and threonine metabolism. n=6, data are presented as mean ± SEM. 198
Figure 4.5: Amino acids relevant differentially and significantly changed metabolites in P-S-M and S-S-M. Sarcosine, guanidinoacetate and creatine represent Glycine, serine and threonine metabolism. O-acetylcarnitine, and L-asparagine represent alanine and aspartate metabolism, L-kynurenine and L-formylkynurenine represent tryptophan metabolism. n=6, data are presented as mean ± SEM. 201
Figure 4.6: Schematic pathway analysis shows the significant altered metabolites in their relevant pathways. 202
Figure 4.7: Differentially and significantly changed metabolites in S-S-M and P-S-M. FA(24:6) of fatty acyls. Ceramide (d18:1/16:0), Ceramide (d18:1/24:0) and Ceramide (d18:2/16:0) represent sphingolipid metabolism. LysoPE (0:0/22:5), LysoPE (0:0/20:5), PE (18:1) PE (18:1/20:4) represent GLs metabolism. n=6, data are presented as mean ± SEM. 206
Figure 4.8: Two-way OPLS-DA comparison between P-S-M and Mut.P-S-M. (R2 = 0.551 and Q2 = 0.983). P-S-M (red triangles), and Mut.P-S-M (green circles). n=6. 207
Figure 4.9: The metabolites significantly and differentially increased in Mut.P-S-M P-S-M. n=6, data are presented as mean ± SEM. 209
Figure 5.1: The proportion of individuals aged 60 years or older is expected to increase. The total world population and the number of people aged 60 years or older in 2000, and the projected values for 2025 and 2050, are shown. The figure also shows that individuals aged 60 years or older currently constitute 10% of the world population and this value is projected to increase to 22% in 2050. The figure is based on statistics from the World Health Organization website (280)..... 223

Figure 5.2: Functional categories of the intracellular metabolites produced by macrophages..... 234
Figure 5.3: PCA score plot of young and old macrophages samples. Young (red squares), old (green circles) and QCs (dark blue diamonds). n=9 and 6 for young and old, respectively..... 235
Figure 5.4: OPLS-DA score plot of young and old macrophages samples. Young (red squares), old (green circles), R2: 0.376 and Q2: -0.048. n=9 and 6 for young and old, respectively..... 236
Figure 5.5: PCA score plot of young and old macrophages samples treated with LPS (young-LPS and old-LPS) respectively. Young (yellow squares) and old (purple circles). n=6 and 7 for young and old, respectively. 237
Figure 5.6: OPLS-DA score plot of LPS treated young and old macrophages (young-LPS and old-LPS) respectively. Young (yellow squares) and old (purple circles). R2: 0.307 and Q2: -0.057. n=6 and 7 for young and old, respectively..... 237

Table of Tables

Table 2.1: The significant metabolites in THP-1 macrophages upon polarisation into M1 and M2. 67
Table 2.2: A list of 90 significantly changed metabolites in M1 macrophages with VIP >1 and FDR < 0.05 compared to M0 as a result of investigation M0, M1 and M2. 81
Table 2.3: A list of 49 significantly changed metabolites in M2 macrophages with VIP >1 and FDR < 0.05 compared to M0 as a result of investigation M0, M1 and M2. 84
Table 3.1: A list of 82 significantly changed metabolites in M1 with VIP > 1 and FDR < 0.05 compared to M0 as a result of investigation M0, M1, M2 and Mreg. 136
Table 3.2: a list of 74 significantly changed metabolites in M2 macrophages with VIP > 1 and FDR < 0.05 compared to M0 as a result of investigation M0, M1, M2 and Mreg. .. 140
Table 3.3: A list of 46 significantly changed metabolites in Mreg with VIP > 1 and FDR < 0.05 compared to M0 as a result of investigation M0, M1, M2 and Mreg. 143
Table 3.4: A list of 112 significantly changed metabolites in M1 macrophages with VIP > 1 and FDR < 0.05 compared to M0 as a result of investigation M0, M1, M2, Mreg, M0-LPS and Mreg-LPS. 145
Table 3.5: A list of 84 significantly changed ions in M2 macrophages with VIP > 1 and FDR < 0.05 compared to M0 as a result of investigation M0, M1, M2, Mreg, M0-LPS and Mreg-LPS. 150
Table 3.6: A list of 25 significantly changed metabolites in Mreg macrophages with VIP > 1 and FDR < 0.05 compared to M0 as a result of investigation M0, M1, M2, Mreg, M0-LPS and Mreg-LPS. 155
Table 3.7: A list of 54 significantly changed metabolites in M0-LPS with VIP > 1 and FDR < 0.05 compared to M0 as a result of investigation M0, M1, M2, Mreg, M0-LPS and Mreg-LPS. 157
Table 3.8: A list of 41 significantly changed metabolites in Mreg-LPS with VIP > 1 and FDR < 0.05 compared to M0 as a result of investigation M0, M1, M2, Mreg, M0-LPS and Mreg-LPS. 160
Table 3.9: A list of 54 significantly changed metabolites in M2-M1-24 with VIP > 1 and FDR < 0.05 compared to M1 as a result of investigation M1, M2-M1-24 and M2-M1-48. 163
Table 3.10: A list of 36 of significantly changed in M2-M1-48 with VIP > 1 and FDR < 0.05 compared to M1 as a result of investigation M1, M2-M1-24 and M2-M1-48. 166
Table 3.11: A list of 89 significantly changed metabolites in M1-M2-24 with VIP > 1 and FDR < 0.05 compared to M2 as a result of investigation M2, M1-M2-24 and M1-M2-48. 168
Table 3.12: A list of 104 significantly changed metabolites in M1-M2-48 with VIP > 1 and FDR < 0.05 compared to M2 as a result of investigation M2, M1-M2-24 and M1-M2-48. 173
Table 4.1: A list of the 83 significantly changed metabolites in S. aureus secretome treated macrophages with VIP > 1 and FDR < 0.05 compared to M0 211
Table 4.2: A list of 75 significantly changed metabolites in P. aeruginosa secretome treated macrophages with VIP > 1 and FDR < 0.05 compared to M0. 215

Table 4.3: A list of 28 significantly changed metabolites in mut. P.aeruginosa (PALT 13) secretome treated macrophages with VIP >1 and FDR < 0.05 Compared to P.aeruginosa (PA01) secretome treated macrophages. 220

List of Abbreviations

APCI	Atomic pressure chemical ionization
APPI	Atmospheric pressure photo ionization
Arg-1	Arginase-1
CLRs	C-lectin type receptors
Da	Dalton
DAMP	Damage associated molecular pattern
DCs	Dendritic cells
DNA	Deoxyribonucleic acid
ER	Endoplasmic reticulum
ESI	Electrospray ionisation
FAB	Fast atom bombardment
FBS	Foetal bovine serum
FDR	False discovery rate
FTICR	Fourier transform ion cyclotron
GC-MS	Gas chromatography-mass spectrometry
GLs	Glycerophospholipids
GM-SCF	Granulocyte macrophage colony-stimulating factor
HPLC	High-performance liquid chromatography
HILIC	Hydrophilic interaction liquid chromatography
HIV 1	Human immunodeficiency virus 1
HMDB	Human metabolic database.

HRMS	High resolution mass spectrometry
IDO	Indoleamine 2,3-dioxygenase
IDSA	Infectious diseases society of America
IFN-γ	Interferon gamma
IL	Interleukin
iNOS	inducible nitric oxide synthase
IT	Ion trap
LC	Liquid chromatography
LPS	lipopolysaccharide
M-CSF	Macrophage colony-stimulating factor
MS	Mass spectrometry
MHC	Major histocompatibility complex
Mreg	Regulatory macrophages
mRNA	Messenger ribonucleic acid
ml	Millilitre
NLRs	Nod-like receptors
NMR	Nuclear magnetic resonance spectroscopy
NO	Nitric oxide
P. aeruginosa	*Pseudomonas aeruginosa*
PAMP	Pathogen associated molecular pattern
PMA	Phorbol-12-myristate-13-acetate
PBS	Phosphate buffer solution
PC	phosphatidylcholines

PE	Phosphatidylethanolamines
PG	Phosphatidylglycerols
PI	Phosphatidylinositols
PPP	Pentose phosphate pathway
PRRs	Pathogen recognition receptors
PSMs	Phenol-soluble modulins
RLRs	Retinoic-acid-inducible gene I like receptors
ROS	Reactive oxygen species
RP-LC	Reverse phase liquid chromatography
S. aureus	*Staphylococcus aureus*
ssRNA	Single-stranded ribonucleic acid
TSB	Tryptic soy broth
TGF-β	Transforming growth factor beta
TLRs	Toll-like receptors
TNF-α	Tumour necrosis factor- α
TFA	Trifluoroacetic acid
TOF	Time of flight
TCA	Tricarboxylic acid

Chapter one

1. General introduction

1.1. Metabolomics

Omics science refer to a group of analytical methodologies that aim to achieve the collective characterisation and quantification of pools of biological molecules, such as genes, transcripts, proteins and metabolites, which are translated into the structure, function and dynamics of cells or organisms (1). The omics studies include genomics (DNA), transcriptomics (mRNA), proteomics (proteins), and metabolomics (metabolites) (2, 3). Genomics can be defined as a comprehensive approach to analyse the function and structure of DNA (1). It is a promising approach for understanding the diversity of biological systems at the genome level, which will provide a deep insight into the origin of individual features and disease susceptibility (2). Genomics also includes the analysis of gene expression through transcriptomic approaches (4) while proteomics is described as a systematic analysis of all proteins in the biological sample to provide a comprehensive insight of the structure, regulation and function of these systems. Proteomics has a complementary role to genomics as the measured proteins are transcribed genes. (2).

Metabolomics is defined as a comprehensive qualitative and quantitative analysis of small molecules (<1500 Da) in a given state. Metabolome can be defined as a complete set of all metabolites present in biological samples such as a cell, tissue, organ or organism at a given time (5). The metabolomics covers a diverse range of molecules with different chemical structures and different physico-chemical properties, including hormones, metabolic intermediates and signalling molecules (e.g. carbohydrates, lipids, organic acids, vitamins, aldehydes, ketones, amino acids, steroids, nucleic acids, etc.) (6-9).

Metabolomics provides a comprehensive investigation into the physiological processes that occur in biological systems and captures the complexity of the whole metabolic activities of the systems in response to any pathological or environmental perturbations (4). Metabolomics also provides the most relevant insight into cellular phenotypes (10). However, Genomics and proteomics do not account for differences in phenotype (11) This highlight the need for metabolomics as a complementary tool to genomics and proteomics and other omics to unravel the physiological state of biological samples.

1.1.1. Approaches of metabolomics

Metabolomics can be divided into two major approaches, untargeted and targeted. Untargeted metabolomics involves the global metabolite profiling of the biological samples without any previous information about the identity or the nature of the detected metabolites (12). This approach provides qualitative and relative quantitative information for a wide range of metabolites. Untargeted metabolomics is effective in comparing the changes in metabolites in response to biotic and/or abiotic perturbations (e.g. biological processes) and exposure to stimuli (e.g. drug, toxins)(13). Consequently, it has the potential to be used to uncover the role of metabolic pathways and the discovery of biomarker metabolites which represent diagnostic features of particular conditions, such as diseases (14). Therefore, the application of this approach generates new hypotheses (12). On the other hand, targeted metabolomics is mainly concerned with the quantitative analysis of a pre-defined single metabolite, pathway or group of metabolites based on prior knowledge of a biological system (14-16). In

the targeted approach, the specific signals of pre-defined metabolites are used to determine the accurate concentrations of the selected metabolites (14).

1.1.2. Cell-based metabolomics

Over the last decade, cell-based metabolomics has been used widely in many biomedical fields as a promising approach. However, focusing on the metabolic profile of the whole organism does not take into account the different cell types in the body.

Given that various cells in the same organism have different functions and responses under different conditions, it is crucial to focus on specific cells rather than the whole organism. Focusing on specific cells and identification of metabolic markers offer a comprehensive understanding of their functions and phenotypes under different conditions, leading to the development of potential therapeutics targeting these cells. This highlights the need and importance of cell-based metabolomics (17). The cell-based metabolomics approach involves the study of exo-metabolome (collection of all extracellular metabolites) and the endo-metabolome (collection of all intracellular metabolites). Extracellular metabolomics (called footprinting) has several applications in optimising the conditions of cell growth, analysing drug effects (e.g. toxicology), and identifying biomarkers for several diseases (18-20). Footprinting is a powerful technique because it often requires minimal sample preparation without metabolic quenching or extensive metabolite extraction from a cell or organism (17). In contrast, the measurement of intracellular metabolites is more challenging as it often requires additional sample preparation steps, such as metabolite extraction

from a cell or organism. However it provides valuable intracellular information about cell phenotyping, identification pivotal metabolic changes corresponding to physiological processes, and the interpretation of different signals in response to a variety of stimuli (21-23).

In general, both approaches, intracellular (fingerprint) and extracellular (footprint) metabolic profiles are complementing each other to give better insight into the metabolites and their corresponding metabolic pathways in a given state (17).

1.1.2.1. Cell-based metabolomics workflow.

The workflow of cell-based metabolomics starts with experimental design, followed by the culture of the cells of interest, sample preparation (metabolic quenching and metabolite extraction), data acquisition, and finally data processing and analysis (Figure 1.1) (17)

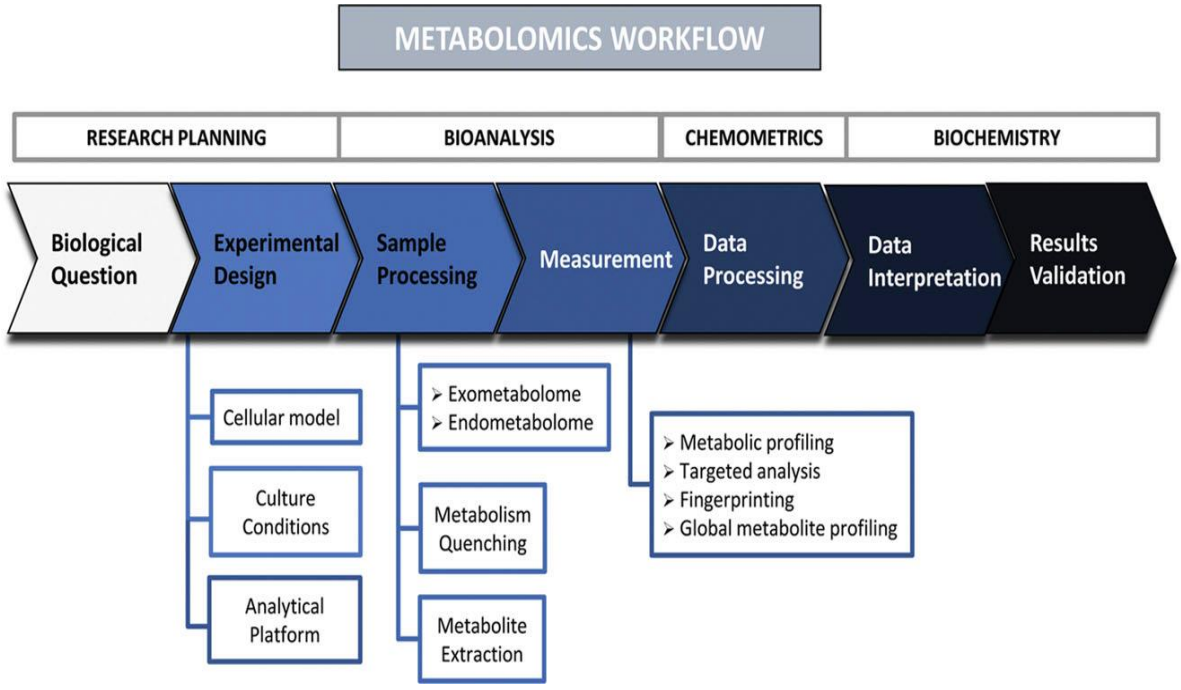


Figure 1.1: Schematic workflow of general cell metabolomics studies (24).

1.1.2.1.1. Experimental design

In vitro cell studies must obtain reliable and reproducible results that reflect the *in vivo* situation. Therefore, it is crucial to establish a proper experimental design which answers biological and/or clinical questions of interest. Several experimental protocols have been developed by researchers over the years. The choice of the best protocol is based on the objective of the study and the factors that influence the results. (24). In this sense, to reduce variations and biased results, an experimental design must achieve replication and randomisation**.** In cell-based metabolomics, randomisation can protect the experiment against external factors such as cells population, sample stability, instrumentation stability and variability resulted from different personnel (17), whereas replication is very important to ensure statistical power. Both biological and technical replicates are crucial to incorporate. (17, 25).

1.1.2.1.2. Sample collection and preparation

Any methods for sample preparation in cell-based metabolomics (Figure 1.1) should be reproducible, rapid and minimal. To avoid degradation and/or loss of metabolites during sample preparation, a well-designed metabolic quenching is required (26). Sample preparation depends on the cell type, culture system (adherent or non-adherent), the nature of the metabolites of interest and whether they are extracellular and/or intracellular (24). The sample collection mainly involves separation of cells from culture medium. Cell type determines the separation procedure (24). For an adherent culture, cells must be detached from the surface of the culture flask (27, 28) whereas filtration or centrifugation is used

to separate the cells from media in non-adherent cell cultures (29). Adherent cells are harvested mechanically with cell scrapers or by using trypsin/EDTA solutions (enzymatic reactions) (24). However, the use of trypsinisation has been reported to alter the metabolite profile (30). In this context, a previous study has compared a cell scraper with trypsinisation as harvesting methods, demonstrating that fewer metabolites were recovered after trypsinisation compared to a cell scraper (31).

1.1.3.2.1. Cell quenching

Metabolic profiles represent the physiological state of cells at the time of preparing the sample (32). As such, a quenching step is critical for the determination of both intracellular and extracellular metabolites at a given time. Metabolic quenching aims to terminate enzymatic activities to prevent the degradation of metabolites and the alteration of the composition of the sample because many of metabolites are extremely labile and have a rapid turnover rate of less than 1-2 s (33). Therefore, cellular metabolism should be stopped immediately before metabolite extraction to minimise metabolite turnover rates and loss of important metabolites (34). Quenching metabolic activities is usually achieved by rapidly changing pH or temperature (35). However, the choice of suitable quenching procedures depends on the nature of the sample and the type of cells. Cells in suspension cultures are usually quenched by snap freezing, cold isotonic saline solutions (e.g. aqueous isotonic NaCl solution), or cold aqueous methanol solution (36). On the other hand, the quenching of adherent cells might involve an extra step which is the washing of cells with a saline buffer (warm or cold), such as phosphate-buffered saline or aqueous isotonic NaCl solution, prior

to quenching. It is important to wash the cells and the culture vessels to remove the residual medium that may lead to contaminationof the metabolite profile or impairing the performance of the analysis process by ion suppression (37, 38).

1.1.3.2.2. Metabolite extraction

To date, several extraction protocols have been developed and optimised for intracellular metabolites (30, 34, 39-41). The study objective must be taken into consideration to select the suitable extraction procedure. In untargeted metabolomics, an extraction process should be non-selective, efficient and compatible with multiple analytical platforms. However, due to the complex chemical diversity of the endogenous metabolome, there is no universal protocol which is capable of extracting all intracellular metabolites equally and efffeciently (42). On the other hand, an extraction procedure which is selective toward a specific class of metabolites must be applied in a targeted metabolomics approach (43). Several organic solvents are usually used to extract intracellular metabolites. For example, pure or aqueous solutions, chlorinated or non-chlorinated, or a combination, and at different temperatures (44). Several studies have used different solvents for the extraction of intracellular metabolites from suspension or adherent cells. For example, aqueous acetonitrile (36), aqueous methanol (22), or pure methanol (45) in asuspension culture. Other studies using adherent cells have shown the applicability of some other solvents to extract the metabolites; aqueous mixtures with solvents (e.g., methanol (46), chloroform (47), methanol and trifluoroacetic acid(48), chloroform and methanol (49)), pure organic solvents (e.g. methanol (50), chloroform (51)), and mixtures of organic solvents (e.g.

chloroform and methanol (52) at different temperatures (e.g., boiling water, 90˚C, 50˚C, room temperature, ice-cold, 4˚C) (53). Repeating extraction cycles with the same solvents or different solvents may enhance the efficiency of the extraction process (53).

A recent study has considered eight extraction protocols to extract metabolites from cultured mammalian cells to study the effect of three parameters (washing step before extraction, temperature, and pH). The results showed that pH and temperature have minimal effects on the ion intensities, while washing cells before the extraction showed significant effects on intensities of the measured mass ions (54). To optimise an efficient protocol for the metabolomics study of Panc-1 cell line, four procedures were tested for of the number of detected metabolites and the efficiency of the extraction procedure. The results showed that direct scraping for harvesting and methanol/chloroform/H_2O as an extraction solvent represent the optimum procedure (27).

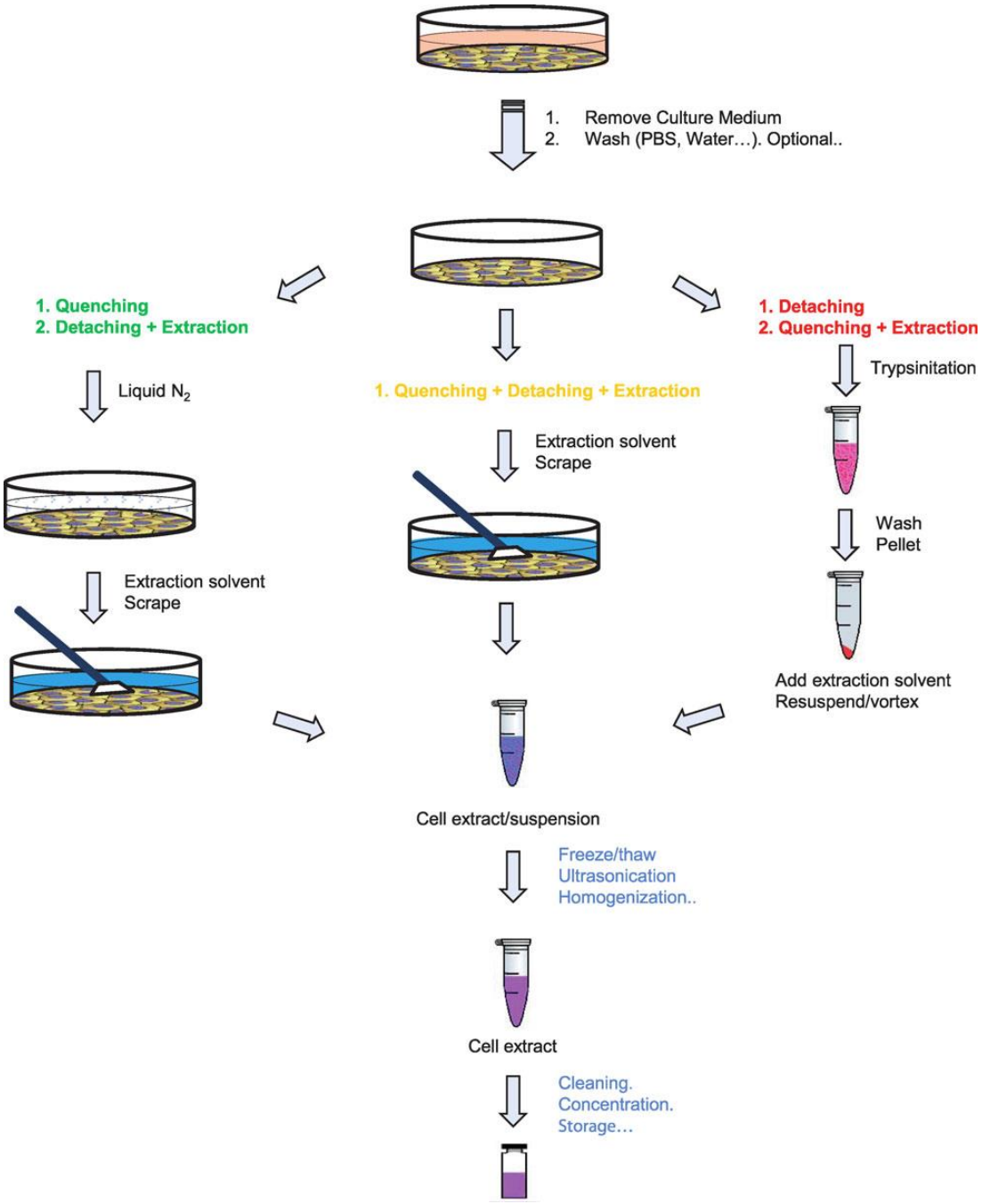


Figure 1.2: A common quenching and extraction approach used in the analysis of intracellular metabolites of adherent cells (24)

1.1.2.1.3. Measuring metabolites and analytical procedures.

The chemical complexity of the metabolome requires multiple analytical platforms to measure a broad range of metabolites (55). Over the last years, the most used platforms in metabolomics area are nuclear magnetic resonance (NMR) and mass

spectrometry (MS) (56). NMR outperforms MS in the sense that there is no need for sample preparation with biofluid samples and there is a direct correlation between the produced signal and the compound abundance, resulting from a linear response. However, NMR has limitations including low sensitivity and selectivity. This leads to the need for a more sensitive and powerful alternative. Mass spectroscopy has currently emerged as an approach that meets these demands due to its high sensitivity and selectivity (57). In order to improve metabolites coverage, MS is coupled to separation techniques such as gas chromatography (GC) or liquid chromatography (LC) for metabolite separation prior to the analysis and detection by MS. Each analytical technique has advantages and disadvantages. Therefore, there is no universal approach which promises all the desired advantages such as sensitivity, selectivity, ease of sample preparation and high resolving power (57). GC-MS has the highest resolving power and is a highly selective technique, but it is not suitable to analyse non-volatile and polar compounds (amino acids, sugars, nucleosides, etc) and requires an additional sample preparation such as metabolite derivatisation (58)**.** However, LC-MS has become the most widely used technique that avoids the above-mentioned drawbacks of other techniques (57).

1.1.2.1.3.1. LC-MS cell-based metabolomics.

Diverse types of columns (stationary phase) with different chromatography chemistry can be applied in cell-based LC-MS metabolomics studies including; reverse-phase (RP) columns (e.g. C18) and hydrophilic interaction chromatography (HILIC). Choosing the most suitable column depends on the

objectives of the study and the metabolites of interest. In this sense, non-polar metabolites (e.g., lipids) are separated well by RP columns. However, ionic or polar metabolites, due to their weak retention in such a stationary phase, are difficult to be separated. The use of HILIC separation in cell metabolomics has been steadily increased since it is carried out using elution solvent gradient on hydrated silica stationary phase, starting with the majority of an organic solvent which is decreased gradually in favour of water to end with a high proportion of water (27, 59).

Mass spectrometry detects the compounds and provides specific chemical information such as accurate masses of the parent ions which consequently help in identifying chemical compounds based on a mass-to-charge ratio (*m/z*) (60). Basically, three main parts compose the mass spectrometer; ion source, mass analyser, and detector. The molecules are ionised in an ion source to produce ions that are resolved by the mass analyser in either electromagnetic field or in a time-of-flight tube to be measured at the end by the detector. There are several types of the source of ionisation; atmospheric pressure chemical ionization (APCI), fast atom bombardment (FAB), atmospheric pressure photoionization (APPI) and electrospray ionization (ESI). ESI has been widely used since it provides "soft ionisation" that induces little or no fragmentation. It permits the analysis of thermolabile and non-volatile biomolecules without affecting their chemical structures (61)

The principle of ESI is illustrated in Figure 1.3. At atmosphere pressure, the sample enters the ion source of the MS via a capillary tube where a high voltage (2-5kV) is applied. The difference in voltage between inside the ion source and the

entrance of MS induces an electrical gradient along the path of charged droplets. As the droplets move forward, the solvent evaporates increasing the intensity of the charge and the Coulombic repulsion inside the droplet, leading to the dissociation of large droplets into smaller ones. This process continues until gaseous ions enter the MS for detection based on a mass to charge ratio (m/z) (62, 63). APPI and APCI also induce little or no fragmentation and they play a complementary role to ESI in analysing non-polar and thermally stable metabolites (e.g. lipids).

Several types of mass analyser could be used: e.g. time-of-flight (TOF), quadrupole, Fourier transform ion cyclotron (FTICR), Orbitrap and ion trap (IT). Furthermore, two types of analysers or more can be combined. To improve the identification of metabolites high resolution mass spectrometers (HRMS). TOF, Orbitrap and FTICR, which are used due to their high resolving power and mass accuracy (mass accuracy <3 ppm) (64-66)

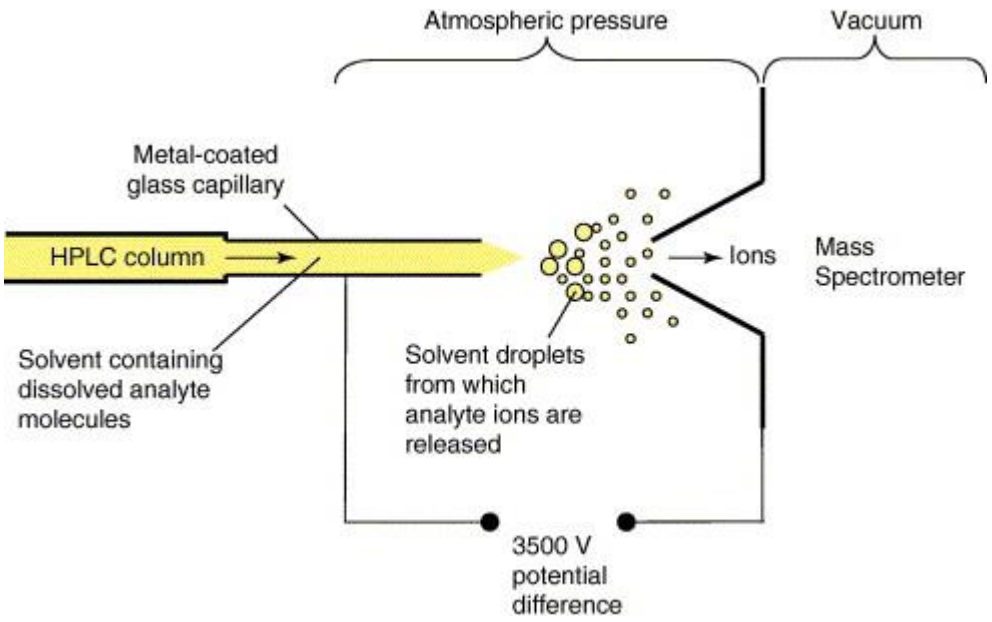


Figure 1.3: A schematic of ion formation in electrospray ionisation (71).

1.1.2.1.4. Data processing and analysis

Due to numerous acquired features from LC-MS (retention time, mass-to-charge ratio (*m/z*), and signal intensity) and the complexity of the acquired data from MS system, efficient data pre-processing is required to reduce its multi-dimensionality. Many software packages have been developed to help in data pre-processing, data analysis and metabolite identification such as Markerlynx, Markerview, Masshunter, XCMS, MZmine, and MzMatch (67, 68).

For processing raw LC-MS data, XCMS and mzMatch are the most widely used software for untargeted peak-picking and peak matching, respectively (69, 70). IDEOM is a user-friendly data processing tool which is a macro-based excel spreadsheet incorporated with XCMS and mzMatch, which allows automated filtering and annotation of metabolites (71). Human metabolic database (HMDB) (72), and METLIN (73) are examples of available online databases which provide potential identification (5, 24).

Metabolites are identified with two levels of confidence; level 1 (L1) identification was performed by matching retention times and accurate masses of authentic standards and level 2 (L2) identification was carried out when the predicted retention times were employed due to the lack of standards according to the metabolomics standards initiative (74, 75).

Such complex LC-MS data require efficient techniques to extract useful information about metabolites that allow classification and biomarker discovery. The statistical multivariate analysis (MVA) can be divided into two approaches:

unsupervised and supervised methods. Unsupervised analysis can be carried out by hierarchical clustering analysis (HCA) or principal component analysis (PCA). Supervised analysis can be carried out by different methods such as partial least squares–discriminant analysis (PLS-DA) or orthogonal partial least squares discriminant analysis (OPLS-DA) (76, 77). These approaches are used for classification of the metabolites and find the similarities and differences between sample groups in response to different stimulators. Such classifications can lead to information about physiological processes and exploration of metabolic activities (17).

MetaboAnalyst is a web-based tool for processing metabolomics data. It accepts different data inputs such as NMR and MS spectra, and MS peak lists. It can also provide data pre-processing, multivariate analysis and pathway analysis (78).

1.1.2.1.5. Advantages of cell-based metabolomics

Cell-based metabolomics offers many advantages. One main advantages is that it is subjected to fewer biological variables than human subjects or animal models, such as environmental exposures, confounding factors such as sex, age, health state, and interindividual variations. Various types of cells and perturbations can be used *in vitro.* Also, cells can be subjected to more extreme conditions than humans (79). Furthermore, cell-based studies require no ethical considerations, unlike studies applied to humans or animals (17). Metabolomics has an important advantage for cell-based studies is that it can be used to analyse intracellular and

extracellular metabolites. Therefore, this approach can enhance our understanding of metabolic activities (44).

1.1.2.1.6 Limitations and challenges of cell-based metabolomics

In spite of the aforementioned advantages, as any other approach, cell-based metabolomics has limitations and challenges. Several issues are related to sample preparation (27, 80), such as metabolic quenching and metabolite extraction which are time-consuming that may result in degrading labile metabolites (17). Also, the growth media variability in term of nutrients, additives and formulation affect the metabolic profile of the cells. Moreover, differences in the proliferation rate between cells, and cell ages (passage number) influence metabolic state (17). All these factors, collectively, could affect the accuracy, repeatability and reproducibility of metabolomics results (81). Also, the output of cell-based metabolomics, as other metabolomics, is represented in a huge amount of complex data which often require multivariate analysis techniques. However, this problem is becoming easier to be tackled due to the growing and high quality of data pre-processing software (82).

1.1.2.1.7. Application of cell metabolomics

Metabolomics research related to health, disease and biology has been performed using various types of samples including body fluids (83), tissue extract (84), as well as mammalian cells (17).

Many applications have been reported and shown that cell-based metabolomics is a promising approach in various research fields including toxicology (85), cell

phenotyping (86), biotechnology (22), biomarker discovery (50), diagnosis, and treatment of diseases (44). In the last few years, many studies have shown the feasibility of cell metabolomics in studying immune cells and metabolic alteration of these cells in response to external stimuli (87, 88).

1.2. Macrophages

Macrophages are effector phagocytic immune cells. They are widely distributed throughout the body (89, 90). Ilya Metchnikoff, who has won the Nobel prize for his work on immunity and phagocytosis, first discovered macrophages in 1892. He first referred to large phagocytic cells as macrophages (the big eaters in Greek) and demonstrated their presence in all vertebrates and invertebrates (91-93). In 1924, Aschoff et al have introduced the concept of a reticuloendothelial system and described macrophages as the main member of this system, side to side with phagocytic endothelia and reticulum cells (94). Later, van Furth team has introduced the mononuclear phagocyte system and proposed that all macrophages, including resident macrophages or those which activated in inflammation, are derived from monocytes originated from a bone marrow precursor and circulated in the blood (Figure 1.4) (95-97). Nevertheless, in the last years, many studies have extensively revised the whole picture of macrophages origin, considering the functional differences between circulating macrophages and tissue resident macrophages. Interestingly, some tissue-resident macrophages are developed prenatally and persist until adulthood. More specifically, these tissue-resident macrophages are now believed to be derived

from the yolk sac and fetal liver of embryos and can renew themselves (Figure 1.4) (98-104).

Macrophages play a pivotal role in innate and adaptive immune system (105). They, together with natural killers such as eosinophils, dendritic cells and neutrophils, represent the first line of immune defence to recognise and eliminate invading microbes including viruses bacteria and fungi (106, 107). Another crucial role of macrophages is in maintenance of tissue homeostasis (107, 108). Generally, macrophages demonstrate a range of functions such as the clearance of senescent cells, elimination of tumour cells and pathogens, maintenance of tissue integrity and homeostasis, modulation of extracellular matrix and control of tissue cell growth (107).

Macrophages are avid phagocytic cells that clear a massive amount of erythrocytes every day (approximately 2 x 10^{11} cells which is equal to 3 kg of haemoglobin and iron per annum that is reused by the host) (109, 110). This clearance is a metabolic contribution that is crucial for host survival (108). Also, macrophages efficiently and rapidly clear the debris of the apoptotic cells (111).

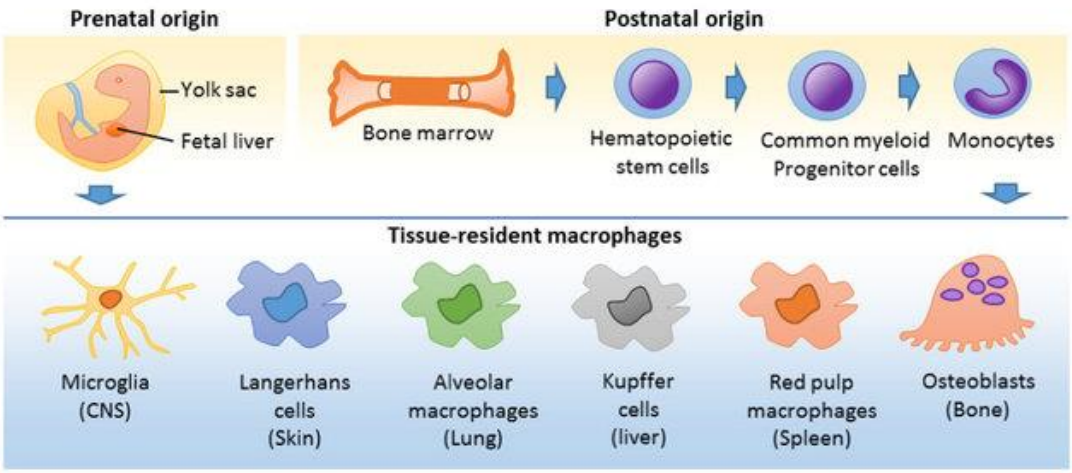


Figure 1.4: Origin of tissue-resident macrophages: bone marrow-derived monocytes yolk sac-derived macrophages and fetal liver-derived monocytes (112).

1.2.1. Pattern recognition receptors.

In the last years, the recognition of pathogen associated molecules has attracted more interest and taken place in immunity studies (113). Pattern recognition receptors (PRRs) are the main players in recognising pathogens and driving signalling cascade by the expression of inflammatory molecules to eliminate the pathogen (114, 115). They recognise patterns of microbial species called pathogen associated molecular patterns (PAMPs). It is also confirmed that they also recognise endogenous molecules resulted from damaged cells which are called damage associated molecular patterns (DAMPs) (114).

Toll-like receptors (TLRs), which are transmembrane proteins, are the first family of PRRs identified in 1997 (116). Nowadays three other families have been identified; (i) cytoplasmic proteins such as nucleotide binding and oligomerization domain (NOD)-like receptors (NLRs), (ii) retinoic-acid-inducible gene I (RIG-I) like

receptors (RLRs), (iii) C-type lectin receptors (CLRs) (117). The ligation of these receptors plays a cooperative role in mediating an adaptive and innate response (114). In the recent years, identification of PRR families is not the sole aim of the research, however, researchers have been also interested in the area of the ligand identification (117) (Figure 1.5). The TLR family ligands include nucleic acids, peptides, carbohydrate, and lipids which are widely distributed in microorganisms (e.g., bacteria and viruses). Until now, studies have identified 13 TLRs (118). However, the NLR family includes 34 members at least (119), that recognise the structures of peptidoglycans and peptides in bacteria (120). The TLRs are considered to be the more efficient family in terms of recognising invaders (121). As both TLRs and NLRs recognise the bacterial components, they synergistically induce the production of proinflammatory cytokines (120). Regarding other families, RLRs recognise virus components and cover a broad spectrum of ssRNA as ligands. In this context, several studies have shown the involvement of RIG-like receptors in antiviral responses (122). Lastly, the C-type lectin receptors (CLRs) represent a large family that is characterised with a carbohydrate-recognition domain. There are a further 17 subclasses in this family based on the number and arrangement of carbohydrate recognition domains (123, 124). Mannose receptors are examples of CLRs which play an important role in the uptake and recognition of allergens (125).

PRRs	Localization	Ligand	Origin of the Ligand
TLR			
TLR1	Plasma membrane	Triacyl lipoprotein	Bacteria
TLR2	Plasma membrane	Lipoprotein	Bacteria, viruses, parasites, self
TLR3	Endolysosome	dsRNA	Virus
TLR4	Plasma membrane	LPS	Bacteria, viruses, self
TLR5	Plasma membrane	Flagellin	Bacteria
TLR6	Plasma membrane	Diacyl lipoprotein	Bacteria, viruses
TLR7 (human TLR8)	Endolysosome	ssRNA	Virus, bacteria, self
TLR9	Endolysosome	CpG-DNA	Virus, bacteria, protozoa, self
TLR10	Endolysosome	Unknown	Unknown
TLR11	Plasma membrane	Profilin-like molecule	Protozoa
RLR			
RIG-I	Cytoplasm	Short dsRNA, 5′triphosphate dsRNA	RNA viruses, DNA virus
MDA5	Cytoplasm	Long dsRNA	RNA viruses (Picornaviridae)
LGP2	Cytoplasm	Unknown	RNA viruses
NLR			
NOD1	Cytoplasm	iE-DAP	Bacteria
NOD2	Cytoplasm	MDP	Bacteria
CLR			
Dectin-1	Plasma membrane	β-Glucan	Fungi
Dectin-2	Plasma membrane	β-Glucan	Fungi
MINCLE	Plasma membrane	SAP130	Self, fungi

Figure 1.5: Pattern recognition receptors with their ligands (115).

1.2.2. Macrophage polarisation.

Macrophages represent a heterogeneous population of immune cells. They display remarkable plasticity in which they change their phenotype and function in response to microenvironment cues (126-128). Macrophage polarisation is a discipline where macrophage cells are directed toward distinct phenotype and function as a response to microenvironmental signals such as microbial, parasitic, and viral antigens, cytokines or apoptotic cells (129-132). Therefore, the macrophage polarisation has arisen as a key concept in immunology, diseases pathogenesis, inflammation and tissue homeostasis (105, 133-138).

In the last several years, researchers have made considerable efforts to describe and classify macrophages based on their biology, functions, production of cytokines and surface markers (105, 139). In this regard, macrophages have been

classified into two major phenotypes with distinct and opposing activities that constitute the extremes of the broad spectrum of macrophage polar models: (i) pro-inflammatory M1 macrophages (classically activated macrophages) and (ii) anti-inflammatory M2 macrophages (alternatively activated macrophages) (105, 108, 131, 140). However, the observed macrophage activities in chronic inflammation or cancer have implied that the M1/M2 model does not describe the different macrophage subpopulations and hence does not reflect the whole picture of the polarisation model (135, 141-143). Based on the activating signal, M2 macrophages can be further classified into three subsets including M2a, M2b and M2c (105).

Given the expansion of the macrophage subsets, more promising classification should be dependant on the fundamental macrophage functions. The main proposed functions of macrophages can be summarised in host defence, tissue repair and immune regulation. In addition to M1 and M2 macrophages, regulatory macrophages, which are the same as M2c, have emerged as a third main subset based on the functional classification (108) (Figure 1.6).

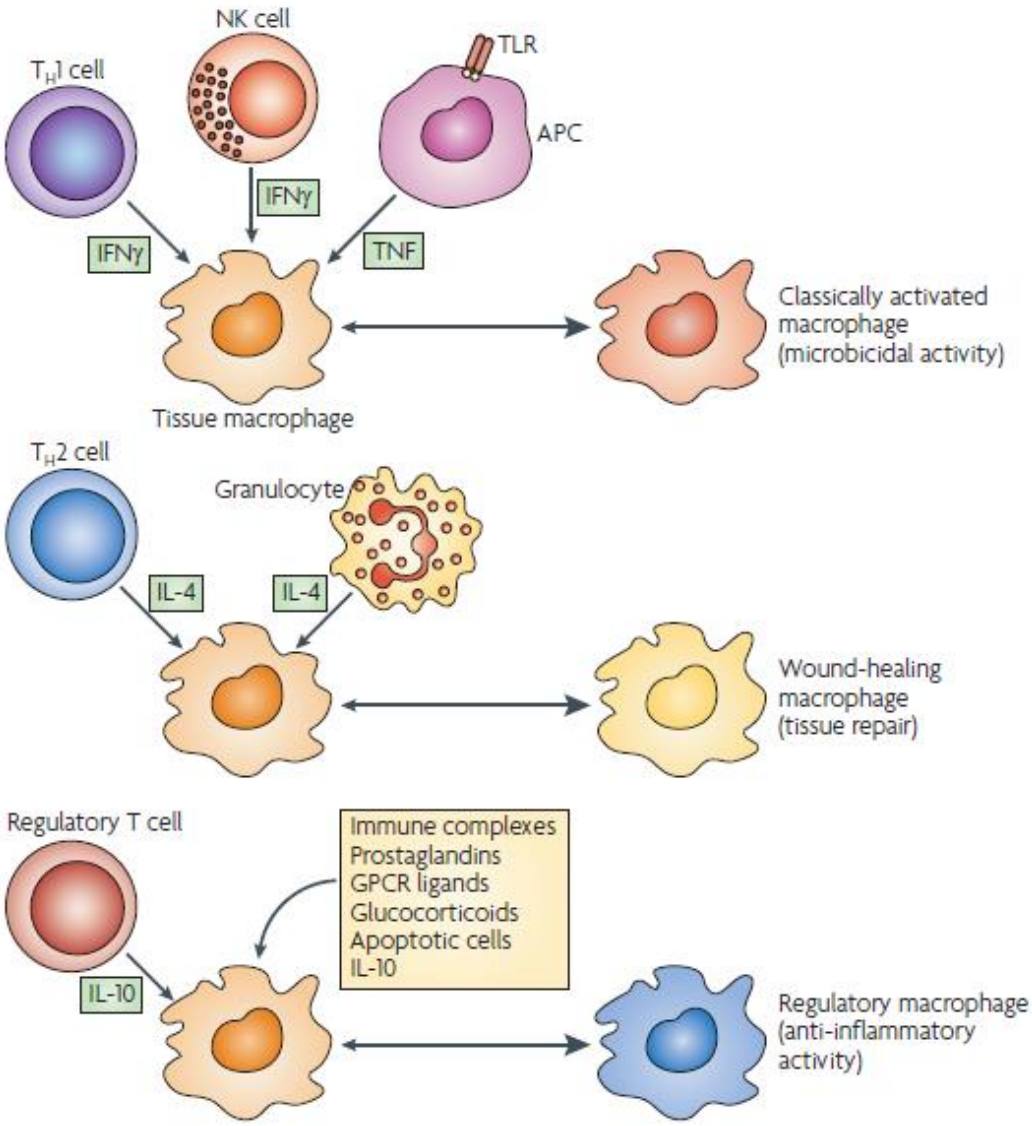


Figure 1.6: Macrophage polarisation into classically activated macrophages (M1), wound healing macrophages (M2) and regulatory macrophages (Mreg) in response to cytokines secreted in the micro-environment (108)

1.2.2.1. M1 pro-inflammatory macrophages (classically activated macrophages).

M1 macrophages can be obtained during an immune response as a result of the exposure of naïve macrophages (M0) to granulocyte macrophage colony-stimulating factor (GM-SCF), Th1 cytokines such as interferon gamma (IFN-γ) and tumour necrosis factor-α (TNF-α) or other toll-like receptor (TLR) ligands such as

Gram-negative bacterial lipopolysaccharide (LPS) (105, 129, 144, 145). M1 macrophages have been characterised with a high production of the pro-inflammatory cytokines including interleukin-1β (IL-1β), TNF-α, IL-12, IL-23, IL-6 and cyclooxygenase-2 (COX-2) (131). The production of these pro-inflammatory molecules induces the production of reactive oxygen species (ROS) and nitrogen radicals which are responsible for killing pathogens during infections (146, 147). Functionally, M1 macrophages play a crucial role in pathogen clearance in infection through enhancing the endocytic activity, acidification of phagosome and production of ROS (148, 149). Therefore, macrophages can be characterised by their microbicidal and tumoricidal activity and mediate tissue damage by ROS generation, consequently, impairment of wound healing and tissue generation (150, 151). Although it has been clear that M1 macrophages are the main component of host defence, the excessive production of pro-inflammatory macrophages can contribute to chronic inflammatory autoimmune diseases (152). To protect against such progression and to inhibit chronic inflammation, a regulatory mechanism is developed and driven by M2 macrophages which are anti-inflammatory players (153).

1.2.2.2. Anti-inflammatory macrophage M2 (alternatively activated macrophages).

Similar to M1 macrophages, M2 macrophages can appear as a response to adaptive or innate immunity (154). Generally, they can be generated by the exposure to Th2 cytokines including IL-4 and IL-13 (155, 156). IL-4 is believed to be

the first signal released in response to tissue injury. Additionally, chitin (a biopolymer found in some parasites and fungi) triggers IL-4 release and hence, converts resting macrophages into wound healing macrophages (M2 macrophages) (157). The released IL-4 induces the production of ornithine from arginine by arginase-1. Ornithine is the precursor of collagen and polyamines that contributes to extracellular matrix production in case of wound healing (158). M2 macrophages are involved in tissue repair and wound healing (132, 159, 160), dampening of inflammation (161), parasite clearance (162, 163), tissue remodelling (164) and tumour progression (165-167).

1.1.2.3. Regulatory macrophages.

Regulatory macrophages have been recognised as a third main population of macrophages as a result of the functional expansion of M2 macrophages. They are developed in response to adaptive and innate immunity as well as M1 and M2 macrophages (108). Also, stress responses could trigger regulatory macrophages due to glucocorticoids released by adrenal cells. Glucocorticoids can inhibit the inflammatory activity of macrophages by downregulating the production of pro-inflammatory cytokines (168). Regulatory macrophages can develop at the late stage of an adaptive immune activity, where their principal function is to knock down immune responses and terminate the inflammation (169). Immune complexes in the presence of TLR agonist can induce the generation of regulatory macrophages (M2b) (170). IL-10, transforming growth factor beta (TGF-β) or glucocorticoids also induce regulatory macrophages (M2c) (105, 146). However,

other stimulators can give arise to regulatory macrophages such as apoptotic cells (154), prostaglandin (171) and adenosine (143, 172). Despite the diversity in the stimulators that can generate regulatory macrophages, they are characterised by a high production of IL-10, TGF-β and low production of IL-12 (108, 170). IL-10 and TGF-β are immunosuppressive cytokines that inhibit the activity and production of pro-inflammatory cytokines such as IL-12, IL-6 and TNF-α. TGF-β acts as immunosuppressive cytokines (108, 173).

1.2.3. Macrophages polarisation and diseases.

As previously mentioned, macrophage subsets plays a crucial role in the clearance of pathogens, tissue repair and wound healing, resolution of inflammation and tissue homeostasis (105, 133-138). However, inappropriate regulation of macrophage immune responses and the disturbed balance in M1/M2 phenotypes are associated with chronic inflammation, leading to several autoimmune diseases (174) such as rheumatoid arthritis (175), multiple sclerosis (176) and Crohn's disease (177), alcoholic and non-alcoholic liver diseases (178), atherosclerosis (179), obesity and diabetes (180). In these autoimmune diseases, M1 macrophages represent the main source of inflammatory cytokines (IL-1β, TNF-α, IL-23, IL-12 and IL-18) that mediate and drive the chronic inflammatory state (181-183).

Rheumatoid arthritis is a chronic autoimmune disease where the synovial lining of the joint is inflamed (184). A rheumatoid arthritis lesion is characterised by macrophage infiltration and the high number of the sub-lining macrophages in the early active disease. Nevertheless, as the degree of synovial macrophage

infiltration increases, the degree of joint erosion increases (183). Alcoholic liver disease is a complex disorder characterised by progressive tissue damage and dysfunction of the liver. Liver chronic alcoholic inflammation is associated with the increased sensitivity of resident macrophages to phagocytosis or polarisation by TLR4 ligands, leading to dysregulation in the pro-inflammatory mediator expression (185, 186).

Crohn's disease as a chronic inflammatory disorder mainly affects the gastrointestinal tract. It develops as a result of an irregular interaction between the immune system and the bowel contents (187).

Multiple sclerosis is a chronic inflammatory disorder. It is characterised by demyelination of the central nervous system. Generally, It affects people between 20 and 50 years old leading to neurological disability among young adults (188, 189). Multiple demyelinated lesions are the main characteristic of this disease (190). It has been evident that macrophages are involved in the pathogenesis of multiple sclerosis in a complex role where they contribute to axonal damage and lesion formation. However, macrophages provide repair mechanisms (191, 192). Macrophages are abundant in the lesions and the inflammatory reaction that occurs during active demyelination is regulated by activated macrophages which secrete plenty of pro-inflammatory cytokines, nitric oxide, glutamate and reactive oxygen species which promote tissue damage (193-195).

Atherosclerosis, an inflammatory chronic disease, is a progressive cardiovascular disease hallmarked by the accumulation of macrophages within the vascular wall and formation of atherosclerotic plaques in medium and large size arteries (196,

197). These plaques are composed of necrotic cores, lipids, endothelial cells inflamed smooth muscle cells and foam cells (196-198). Foam cells are a type of macrophages accumulated in plaques promoting atherosclerosis progression. They have an impaired ability to migrate, leading to hampering the resolution of inflammation. Macrophages contribute to secreting the pro-inflammatory mediators in the plaques (198, 199).

Moreover, macrophages have a principal role in cancer. Generally, M1 macrophages attack and kill tumour cells with their cytotoxic activity whereas M2 macrophages stimulate angiogenesis and hence induce tumour growth (200, 201). Tumour-associated macrophages are the main player linking cancer to inflammation that represents the majority of infiltrating leukocytes of a tumour environment (165). They mainly display an M2 phenotype, having an immune-suppressive function and producing growth factors for tumour growth (165). In the early stages of cancer and tumour associated macrophages, they display M1 macrophages with appreciated cytotoxic activity, however, these macrophages change their phenotype into M2 macrophages due to the anti-inflammatory mediators and growth factors released by the tumour micro-environment at the late stages (165, 167, 202, 203).

In the context of macrophage polarisation, M1/M2 ratio is a key player in human health and diseases. The reduction in this ratio is favoured in chronic inflammation diseases. However, the increase in the ratio is favoured in cancer (204). This implies the importance of macrophage plasticity and reversibility which could lead to promising therapeutic strategies (105, 108). Therewith, the extent of such

plasticity and the mechanisms that regulate the phenotypic changes are still not fully understood (205). Identifying the biomarkers for macrophage phenotypes can lead to the development of novel approaches that can potentially manipulate macrophages and interrogate the desired macrophages phenotype (108). Biomarkers and their relative metabolic pathways can be manipulated by targeting specific pathways or enzymes in a specific reaction to suppress or enhance a certain pathway at a given pathological condition.

1.2.4. Macrophages metabolism

Recently, immunometabolism of macrophages has emerged in the field of immunology, highlighting the crucial role of metabolism in the shaping of the functional phenotypes of macrophages in response to micro-environment cues (206, 207). Under stress conditions, macrophages adjust their metabolic activities to meet the demand for energy which is necessary for the functionality and growth of cells (208). Generally, oxygen level, cytokines, nutrient availability and growth factors represent environmental signals that induce metabolic alterations (209). For instance, macrophages respond to hypoxia by switching their metabolic pathways from oxidative phosphorylation to glycolysis (206, 210). Furthermore, macrophage polarisation is associated with a metabolic trait of the cells where M1 and M2 macrophages adopt distinct metabolic regulation of glucose, iron, amino acids and folate (206, 211). They show a metabolic switch to the glycolysis pathway in response to Th1 cytokines, LPS and IL-12 (M1 macrophages polarising stimuli). However, a minimal effect on glucose metabolism is shown in response

to IL-4 and IL-13 (M2 polarising stimuli) (212). Since LPS and IFN-γ, which induce M1 phenotype, are associated with acute infection, they need a robust and quick anti-microbial activity in such hypoxic conditions. Therefore, a shift to an anaerobic pathway such as glycolysis is considered to be the best choice to meet the energy demand, in addition to the suppression of fatty acid oxidation and mitochondrial activity (212-214). On the other hand, the role of M2 macrophages in tissue repair and wound healing requires a sustained energy supply. Such a requirement is met by oxidative phosphorylation and fatty acid oxidation. Therefore, M2 macrophages are characterised by a high mitochondrial activity and oxidative phosphorylation, in addition to β-oxidation of fatty acid-based respiratory activity (212, 215).

Amino acid metabolism is also linked to the macrophage functional phenotype. M1 macrophages are distinctive with the expression of Nitric oxide synthase (iNOS), the enzyme that facilitates the production of NO which has anti-microbial activity and cytotoxicity. However, there is no production of NO in M2 macrophages but instead, they express Arg-1 that is required in the production of polyamines which are necessary for cell proliferation, collagen synthesis and tissue remodelling. Nevertheless, the production of polyamines has been shown to drive M2 phenotype (211, 215).

Another subtle difference in metabolic signature between M1 and M2 macrophages is displayed in iron metabolism (206, 216). M1 macrophages were reported to express high levels of proteins such as ferritin that contribute to iron storage and low levels of ferroportin that exports iron. In contrast, M2

macrophages have shown to express high levels of ferroportin and low levels of ferritin. This contrasting metabolic behaviour is clearly linked to the different M1 and M2 functions. Iron is necessary for bacterial growth and its low level in M1 serves as bacteriostatic supporting host defence in infection. However, the high level of iron released in M2 macrophages is required for tissue repair but promotes tumour progression (133, 216). Based on these aspects, a metabolic signature may give key information that links the macrophage polarisation to their functional activity.

1.2.5. Background of the problem

As discussed previously, M1 and M2 macrophages are discriminated differentially by their sets of cytokines, chemokines and their receptors (217) as well as a distinct metabolic signature (section 1.2.4). Also, it has been discussed that the macrophage phenotypes play a pivotal role in many diseases when there is an imbalance in the M1/M2 ratio or excessive activity of M1 or M2 macrophages. In addition to the importance of activating regulatory macrophages in some places such as for the resolution of excessive inflammation. Therefore, the characterisation of macrophage phenotypes by finding characteristic molecular markers for each phenotype has been of high importance. Moreover, as macrophages have been well described with its heterogeneity and plasticity, this can be advantageous in modulating the immune system by being directed or switched to the suitable phenotype based on physiological condition. Many studies have been carried out to characterise macrophage phenotypes. For

instance, THP-1 macrophages have recently been investigated in order to characterise M1 and M2 subsets based on their chemokine and surface receptors. The authors have demonstrated that this approach could be not suitable for the discrimination between macrophages subsets, in particular, M2 subset which was shown to be less well defined (159). Moreover, Lopez-Castejon et al have discriminated M1 and M2 macrophages based on their gene expression profile (218). Nevertheless, the profiling of gene expression does not account for functional phenotypes and cannot address the complexity in the biological samples (219). However, an overlap in the expression of surface markers between macrophage subsets have been reported (220). Therefore, there is an urgent need for a more informative approach that allows a deeper insight into molecular mechanisms responsible for distinctive functional subsets. Metabolomics can represent such an approach characterising macrophage subsets to complement other approaches. Metabolomics approach allows an understanding of the harmony between the functions of immune cells and their metabolism, thereby providing valuable information which can be recruited in manipulating the cellular activity. (221). For instance, metabolic profiling for the patient pre and post smallpox vaccination has allowed the identification of potential biomarkers relevant to adverse reactions of vaccine (222, 223).

Recently, metabolomics has been used to show some key metabolites that characterise different macrophage phenotypes and their ability to modulate the function of macrophages. For instance, Rattigan et al. have performed LC-MS metabolomics approach to investigate whether LPS and IFN-γ have a synergetic effect or antagonistic effect on the metabolic profile of mice macrophages. They

revealed a number of metabolites increased similarly in both LPS and IFN-γ treated macrophages such as L-glutamate, succinate and itaconate. However, inosine monophosphate was increased in LPS treated samples but not in the samples challenged with LPS and IFN-γ together. However, metabolites involved in glycolysis (3-phospho D glycerate and 1,6-bisphosphate) and pentose phosphate pathway (erythrose 4-phosphate and ribose 5-phosphate) have been shown to be triggered primarily by LPS. These pathways are hallmarks of M1 macrophages (224). Using LC-MS metabolomics, Mills et al. have shown that itaconate is an anti-inflammatory metabolite which has an important role in regulating macrophages functions (225). Another study using LC-MS metabolite profiling of macrophages in response to LPS has identified succinate as a participant in innate immune signalling where its increase leads to boosting the production of IL-1β during inflammation (226). Additionally, a recent study has used transcriptomics and LC-MS metabolomics to investigate the polarisation and the distinct metabolic profiles of M1 and M2 macrophages in mice. They have demonstrated that M2 macrophages activate glutamine catabolism and UDP-GlcNAc-related modules. On the other hand, they have identified interruption in the tricarboxylic acid (TCA) cycle between isocitrate and 2-oxoglutarate as a hallmark for M1 macrophages (227). Although tremendous efforts have been made to investigate macrophages and their polarisation states, there is still a gap of knowledge in distinguishing the metabolic profiles of macrophage subsets and key metabolites to understand the mechanisms of human macrophages polarisation in human. Therefore, our study used a human cell line (THP-1) and LC-MS metabolic profiling to identify key metabolites for each macrophage subset. The translation of key metabolites and

pathways to human health represent a promising prospect in the light of the link between macrophage phenotypes and disease.

1.3. Bacterial infection

Bacteria are single-celled microorganisms that exist together in communities of millions. Many types of bacteria live in different places within or on our body in addition to surrounding environments where we are in daily contact. They constitute a complex system without harming or causing diseases. In this case, the bacteria are referred as commensal bacteria and are non-pathogenic (228, 229). On the other hand, pathogenic bacteria can cause serious harms and infectious disease (229). Based on staining properties with Gram's stain, pathogenic bacteria can be categorised into two main types: Gram-positive and Gram-negative bacteria. A cell wall can be found in both Gram-negative and Gram-positive bacteria with subtle differences in the structure and composition as can be seen in Figure 1.7. The cell wall is primarily made of peptidoglycan which is a highly cross-linked polymer of amino acids and amino sugars (muramic acid and N-acetyl glucosamine). Gram-positive bacteria have a distinctly thicker peptidoglycan layer compared to Gram-negative bacteria and covalently linked to teichuronic acids or teichoic acids in Gram-positive bacteria (230). The peptidoglycan layer is responsible for the protection of bacteria from bursting and from the antibacterial immune system components such as lysozyme. Also, the peptidoglycan layer defines the shape of bacteria (231, 232). An outer membrane is another feature that distinguishingly exists in Gram-negative bacteria only. The outer membrane is a lipid bilayer composed of glycolipids (233). Lipopolysaccharide (LPS) is the

principal glycolipid in the outer membrane. It is a strong stimulus that triggers a human innate response and is considered an indicator of infection (234).

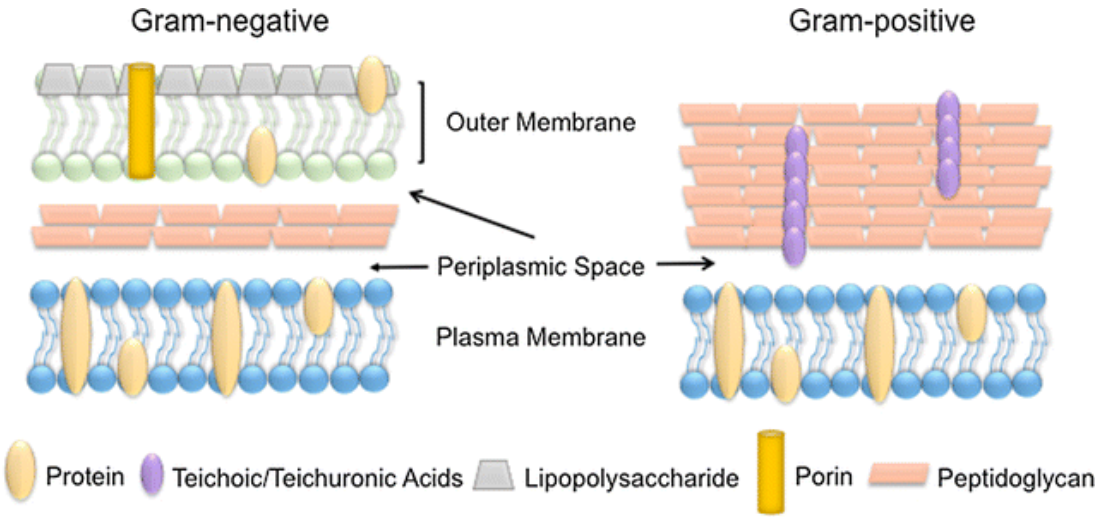


Figure 1.7: comparison of the cell wall in Gram-positive and Gram-negative bacteria (235)

1.3.1. Infectious diseases

Life-threatening infectious diseases affect millions of people every year (236). The development of bacterial strains which are resistant to antimicrobial agents has become a worldwide burden. It was estimated, by the US Center for Disease Control and Prevention, that more than 23,000 deaths have resulted from antibiotic-resistant infections each year. The infections caused by such resistant bacteria cause a longer hospital stay, high rate of hospitalisation and a higher rate of death which have been consequently reflected in increasing the cost associated with these infections (237). Based on World Health Organisation (WHO) report (Global Health Estimates 2016: Deaths by Cause, Age, Sex, by Country and by Region, 2000-2016.WHO; 2018.), infectious diseases have been reported as one of

the top 10 causes of death globally, particularly, the lower respiratory tract infections (Figure 1.8). *Pseudomonas aeruginosa* and Enterobacteriaceae family are among the most common Gram-negative bacteria encountered. However, in Gram-positive bacteria, *Staphylococcus aureus, Enterococcus spp*., viridans streptococci and coagulase-negative staphylococci are more common (238). Many pathogenic bacteria have evolved multidrug resistance, which is a leading cause of infectious diseases in such as bacteraemia, skin and soft tissue infections, urinary tract infections and respiratory tract infections (239, 240). The ESKAPE pathogen family encompasses Gram-negative and Gram-positive bacteria. This acronym stands for *Enterococcus faecium, Staphylococcus aureus, Klebsiella pneumoniae, Acinetobacter baumannii, Pseudomonas aeruginosa, and Enterobacter* species (241). These bacteria are leading causes of many of the serious infectious diseases mentioned above (239, 240).

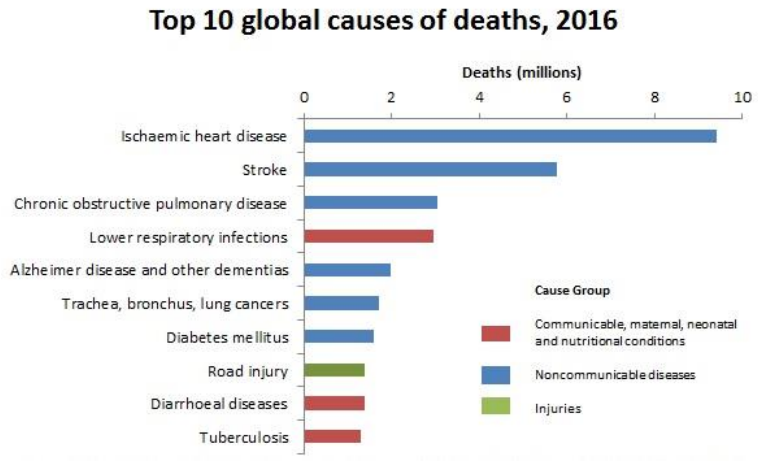


Figure 1.8: Global Health Estimates 2016: Deaths by Cause, Age, Sex, by Country and by Region, 2000-2016. Geneva, World Health Organization; 2018.

1.3.2. Staphylococcus aureus.

Staphylococcus aureus (S. aureus), a Gram-positive bacterium, is an opportunistic human pathogen which colonises the skin and the respiratory tract (242, 243). *S. aureus* causes a wide range of infectious diseases such as infective endocarditis (IE), bacteremia, osteoarticular, device-related, skin and soft tissue and pleuropulmonary infections (239). These infections are commonly treated with Vancomycin, an effective antibiotic against *S. aureus* strains (244). However, bacteria have evolved resistant mechanisms, leading to the emergence of antibiotic resistant strains. Bacterial communities can alter their phenotype in term of gene expressions, growth and protein productions. Also, they can show remarkable tolerance to environmental stresses (245). Therefore, understanding the mechanisms of pathogenicity is of high priority (241). It has been reported that the professional pathogenicity system of *S. aureus* is multifactorial including various virulence factors where toxins are the main players (246). *S. aureus* toxins can be mainly divided into three groups: exfoliative toxins, the pore-forming toxins and superantigens. Pore-forming toxins can be subdivided into four groups; hemolysin-α (α-toxin), hemolysin-β, phenol-soluble, and phenol-soluble modulins (PSMs) leukotoxins (247). Since this professional system of *S. aureus* toxins can respond to and resist a wide range of environmental conditions, a mechanistic understanding of this system aids in the better control of staphylococcal infectious diseases. *S. aureus* toxin system is associated with some diseases such as staphylococcal scalded skin syndrome, toxic shock syndrome, deep-seated skin infections or necrotizing pneumonia (248, 249). However, these toxins can lead to

a weak immune response due to their capability of damaging host cells, modulating immune responses, or degrading the intracellular connections (247).

1.3.3. Pseudomonas aeruginosa

Pseudomonas aeruginosa (P.aeruginosa), a Gram-negative bacterium, is a major opportunistic pathogen of humans. It is a versatile bacterium that is widespread in coastal marine and soil marsh habitats, as well as on animal and plant tissues (250). *P. aeruginosa* causes 10% to 20% of infections in hospitals. It is often associated with nosocomial infections in immunocompromised individuals. In this regard, *P. aeruginosa* is responsible for approximately 40% of deaths in the intensive care unit in pneumatic patients using ventilators (251, 252). Moreover, *P. aeruginosa* induces various infections in human including respiratory infections, wound infections, bacteraemia and urinary tract infections. Also, they cause a life-threatening chronic infection in patients with cystic fibrosis (252). Since *P. aeruginosa* is a member of "ESKAPE" family which are infamous with their antibiotic resistance, these pathogens are on the priority of Infectious Diseases Society of America (IDSA) to develop novel therapeutic options (253). Many antimicrobials are deemed to be effective against *P. aeruginosa* including ceftazidime, cefepime, imipenem, piperacillin, meropenem, piperacillin, tazobactam, levofloxacin, ciprofloxacin, aztreonam, tobramycin, amikacin and gentamicin (254). However, *P. aeruginosa* has developed an antimicrobial drug resistance over the years by the virulence factors and metabolic adaptability which make the eradication of these bacteria extremely challenging (255). Pathogenicity

of *P. aeruginosa* depends on a wide range of virulence factors including adhesion, enterotoxin, exotoxin (e.g. exotoxin A, and four type three (T3) secreted effectors exoenzyme T, exoenzyme S, exoenzyme Y and exoenzyme U), products of secondary metabolites and enzymes (e.g. proteolytic enzymes, phospholipase) (256, 257).

1.3.4. Background of the problem

Considering emerging antibiotic-resistant strains of Gram-negative and Gram-positive bacteria, there is a strong requirement to find promising approaches for early diagnosis and novel therapeutics for bacterial infections (253). Currently, the non-molecular tests for diagnosis of bacterial infections are the routine practice in the laboratories including clinical symptoms assessment and culture of the microorganism from blood or tissue samples. However, diagnostic tests have been described as inaccurate, time-consuming and, most importantly, not sensitive (258). Other options are available but very expensive, such as a real-time polymerase chain reaction (PCR) (258). In this context, the development of new approaches for the diagnosis of various infections become urgent. Therefore, more interest has been directed toward identifying disease-specific biomarkers and signatures (259).

In bacterial infections, innate immunity is among the first line of host defence and macrophages are one of the main players in immune responses against bacteria (260). Researchers have made significant efforts to understand the immune response in bacterial infections. Thus, many studies have investigated the importance of metabolism in order to understand the mechanism of infections

(261-265). Based on the differences of the cell wall components in Gram-negative and Gram-positive bacteria, each of them is recognised by different receptors. Immune cells, particularly macrophages, recognise LPS of Gram-negative bacteria by TLR-4, but they recognise peptidoglycan of Gram-positive by TLR-2 (266, 267). Therefore, different mechanisms of action and impact can be investigated by the metabolic profiles of macrophage.

As mentioned earlier, LC-MS-based metabolomics is an effective approach for biomarker discovery and disease diagnosis, as well as the investigation of metabolic pathway alterations in response to external signals (268). LC-MS metabolomics provides a distinctive insight into the bacterial infections due to its remarkable ability to identify a wide range of metabolites involved in immune responses and the pathways disturbed upon infection (269). The application of metabolomics to address the pathogenesis of bacterial and viral infections have dramatically increased recently. Researchers have used this approach to successfully investigate the metabolic origin of several microorganisms identifying the key metabolites in the pathogen-host interaction.

In chapter four, we have chosen *P. aeruginosa* as a Gram-negative bacteria and *S. aureus* as a Gram-positive bacteria in order to investigate whether they have differential impacts on the metabolic profile of macrophages, leading to identifying the key metabolites and metabolic pathways that are differentially changed by each bacterium. The potential biomarkers can help the development of an early diagnostic tool and novel and targeted therapeutic strategies.

1.4. Ageing

Ageing is defined as a time-dependent decline in the physiological functions of most cells and tissues and is associated with increased morbidity and can lead to death. The era of ageing research started 30 years ago by the successful isolation of long-lived strains in *Caenorhabditis elegans* (270). The world population is currently seeing a dramatic increase in the number of aged individuals (more than 60 years old), which could be due to the development of public health policies and socioeconomics as well as the fast progression in medicine (271). Based on WHO statistics, 10% is the proportion of aged individuals in 2000. However, it is predicted to be 22% by 2050 (Facts about ageing; WHO, 2018). In the last 150 years, the global average life span has been increased from 40 years to approximately unprecedented 80 years (272). Despite the apparent advantages of a long lifespan, undesirable consequences on society and individuals are associated. In fact, aged individuals progressively lose the physiological integrity which consequently leads to the impairment of functions and high vulnerability to death (273). In old individuals, there is a homeostasis loss resulting in increased susceptibility to infectious diseases and decline in the immune response against pathogens leading to high morbidity due to infectious diseases compared to young individuals (273, 274). Lo´pez-Otı´n et al have identified the potential molecular and cellular hallmarks of ageing (Figure 1.9). These hallmarks include: epigenetic alterations, deregulated nutrient sensing, telomere attrition, loss of proteostasis, genomic instability, cellular senescence, altered cellular communication, mitochondrial dysfunction, and stem cell exhaustion (273). As a consequence, many challenges have arisen in society and individuals. Aging associated with

chronic diseases and increased susceptibility to infectious diseases negatively affects the quality of life for elderly people. Moreover, the number of elderly individuals requiring special care (which affects the health care system economically) has increased, as well as the cost of caring for those elderly people (271, 275). Therefore, new approaches that can delay the unfavourable effects of ageing can have benefits for society and individuals.



Figure 1.9: The Hallmarks of Ageing (273)

1.4.1. Ageing and the immune system.

A functional immune system is crucial as a protection line of the host and plays a pivotal role in survival against foreign pathogens. In human and several other species, the immune system declining with ageing has been evident and referred as immunosenescence (276). The main characteristics of immunosenescence include a higher incidence of autoimmune diseases, low-grade inflammation persistence (referred as inflammaging), impaired ability to fight foreign antigens, wound healing impairment, and higher incidence of bacterial infections (such as respiratory tract infections, skin and soft tissues infections and urinary tract infections). Also, these infections are described with more severity in old individuals (276-278). Nevertheless, the immunosenescence consequences are not limited to infections and the decline in immune system functions is related to increased cancer incidence due to a decrease in antitumour function (279). Immunosenescence is partially described by cellular senescence. Therefore, it is necessary to take into account the cellular-intrinsic changes and defects, in addition to the microenvironment of antigen exposure upon immunosenescence (280).

The innate immune system constitutes the first line of defence against pathogens. It is represented by the skin and epithelial linings which constitute a barrier for the prevention of pathogen entry or by antimicrobial secretions that retard the infections in these sites. Once these barriers are breached by the pathogen, tissue macrophages secrete chemokines and cytokines to initiate inflammation (281). Upon ageing, the high incidence of infectious disease implies a possible impairment of macrophages and epithelial cell function as efficient barriers and

defects in their ability to detect pathogens and initiate an appropriate antimicrobial response (282).

The adaptive immune system displays antigen-specific responses which take longer than innate immune responses and it is found only in vertebrates (92). T cells and B cells are activated by interacting with dendritic cells and macrophages (antigen-presenting cells). Thus, they proliferate and migrate to the inflammation site (275). However, the adaptive immune system deteriorates with ageing, and so the functions of T cells, B cells, macrophages and dendritic cells, and the cytokine secretion all decline with ageing (282).

1.4.2. Ageing and macrophages.

Many functions of macrophages have been demonstrated to be impaired upon ageing. In detail, TLR activation is affected by ageing, leading to decreased secretion of inflammatory cytokines from macrophages. Such an effect has been reported by Renshaw et al. and Boehmer et al. showing a decreased amount of TNF-α and IL-6 in response to TLR ligands by splenic and thioglycollate-elicited peritoneal macrophages in old mice when compared to young mice (283, 284). Also, a decreased secretion of IL-6, IL-1β, IL-12 and TNF-α, and increased IL-10 in splenic macrophages have been demonstrated by Chelvarajan et al. in response to LPS in old mice (285). In the aspect of polarisation, a decreased expression of M1 and M2 markers from old mice was reported by Mahbub et al. (286). Nevertheless, Kelly et al. have demonstrated that ageing leads to polarising macrophages into M2-like phenotype in mice, where ocular macrophages of old mice showed a decrease in TNF-α and IL-12 levels, and increase in IL-10 level (287). Interestingly,

an increase in M2 macrophages have been demonstrated in lymph nodes, bone marrow and spleen of old mice. Thus, it is clear that results regarding the effect of ageing on macrophages are conflicting and opposing. Also, this conflict has been reported in terms of phagocytosis. Reduced phagocytosis has been reported in salmonella infection with ageing (288). However, Lynch et al. have noticed an increase in phagocytic activity in old rat microglia (289). Moreover, it was reported that there is an impairment of wound healing ability in both rodents and human with ageing. More specifically, a substantial delay in collagen synthesis, reepithelialisation and angiogenesis have been demonstrated in aged mice compared to young mice (290). Figure 1.10 summarises the impact of ageing upon macrophage function.

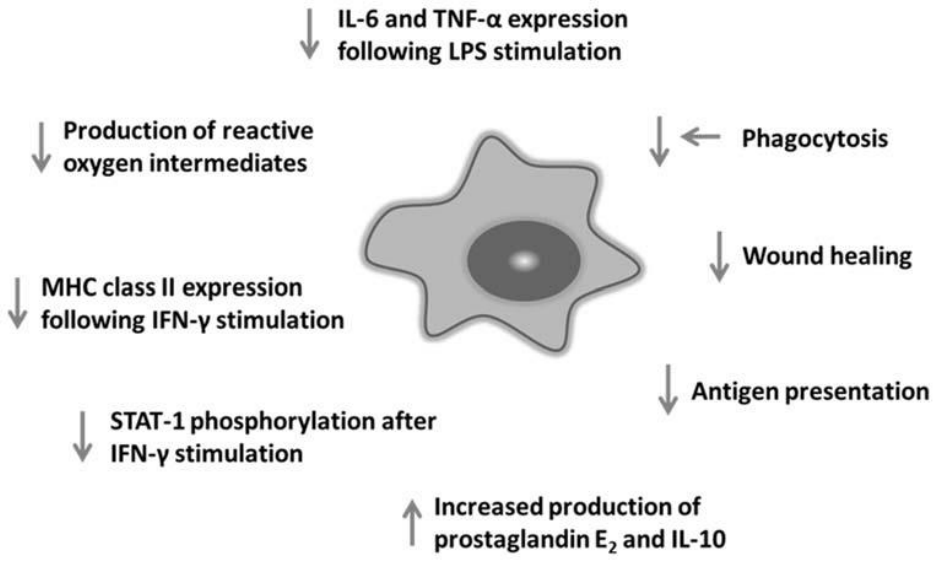


Figure 1.10: Summary of the impact of ageing on macrophage function in mice as ageing affects many aspects of macrophage function (275).

1.4.3. Background of the problem

As mentioned earlier, ageing has increasingly become important as a topical area that attracts more attention because of its negative consequences on both the individual's health and society as a whole. To date, the ageing process has not been fully understood. Environmental and genetic factors seem to be involved, but more informative descriptions are required to give a full understanding of the ageing process, with an aim to minimise ageing negative consequences of ageing (291, 292). To date, most information on ageing has been acquired from non-human studies. Although ageing is associated with a decline in metabolism (293), only a few metabolomics studies have been performed to study ageing using animal models (mice, dogs, and rats) (294-296), and very few metabolomics studies have been published to investigate ageing impacts on human (297). Lawton et al. have performed metabolic profiling using GC- and LC-MS in plasma from a cohort of 269 individuals to investigate the impact of ageing. They revealed significant metabolites associated with ageing, which are relevant to lipid metabolism, energy metabolism and oxidative stress (298). Also, Zhonghao et al. have used a metabolomics approach on human serum demonstrating that metabolic profiles are age-related and can give important information about ageing consequences, such as impairment of mitochondrial functions and fatty acid oxidation (297). These studies highlight the efficiency of metabolomics in the understanding of ageing complexity, which in turn can be applied successfully in the area of discoveries that enhance healthy ageing.

A fully functioning immune system is fundamental for maintaining human health and macrophages are considered as central effector cells in adaptive and innate

immunity. Therefore, age-associated deterioration of macrophage functions is likely to have substantial consequences on the health of aged individuals (275).

The strong association of metabolism and immune system contributes to the emergance of the immunometabolism field, which has dramatically grown in the past years (206, 299). The role of metabolism in the immune system and the crucial roles of immune cells in diseases have led to questions and critical opportunities of utilising immunometabolism in therapeutics to enhance healthy ageing.

Macrophages constitute central effector cells in adaptive and innate immunity. Therefore, age-associated deterioration of macrophages functions are more likely to have substantial consequences on the health of aged individuals (275). Recently, the effect of ageing on macrophages has attracted attention. However, conflicting results have been demonstrated in the literature. For instance, a decrease in TLR-4 expression was suggested as the cause of age-associated changes in TLR signalling (283), whereas others demonstrated no change in the surface expression of TLR-4 in response to LPS in mice upon ageing (284). Also, in contrast to murine studies, no change in the production of pro-inflammatory cytokines, IL-1β, TNF-α, or IL-6 in response to TLR-4 stimulation in monocyte-derived macrophages from both old and young individuals has been discovered (300). Another recent metabolomics study has demonstrated non-responsiveness of aged macrophages to LPS in the first hours of stimulation, and a delayed response has been reported in old mice compared to young mice (301).

Despite the decline of immune system with ageing and the tight coupling between the metabolism and the immune system, macrophages particularly, very few metabolomics studies have been performed to study the impact of ageing on humans. Also, the impact of ageing on macrophages have demonstrated conflicting results specially between mice and humans, which means that the aging impact on mice does not always reflect on human ageing. This urges more studies to focus on human ageing. In our study, for the first time, we used LC-MS metabolic profiling to investigate the impact of ageing on human monocyte-derived macrophages in a steady state and LPS activation state.

1.5. Aims and objectives.

The aim of this PhD project is to investigate macrophages as effector cells in the immune system using a comprehensive and robust cell-based LC-MS metabolic profiling approach. Different aspects and functions of macrophages are investigated, including macrophage polarisation and subsets, macrophage responses against bacterial infections and finally macrophages with ageing.

The main objectives of this project are using LC-MS metabolic profiling to:

- Characterise M1 and M2 phenotypes in THP-1 macrophages in order to identify the biomarkers and characteristic metabolites of each polarisation state (Chapter two)
- Investigate the metabolic plasticity of functional macrophages subsets (M1, M2 and regulatory macrophages (Mreg)), investigate the effect of LPS on the metabolic responses of Mreg and explore the plasticity and stability of macrophages subsets (Chapter three)

- Discover the impact of the secretomes of Gram-negative and Gram-positive represented by *P. aeruginosa and S. aureus*, respectively, on the metabolic profile of macrophages in order to investigate affected pathways which could be targeted in developing novel therapeutics (Chapter four).
- Reveal the effect of ageing on metabolic profiles of macrophages to investigate the metabolic pathways that underpin the expected ageing consequences in immune system originated from macrophages (Chapter five).

Chapter Two

2. Metabolic characterisation of THP-1 macrophage polarisation using LC-MS-based metabolite profiling.

2.1. Introduction

Macrophages as effector cells in the immune system, play a critical role in innate and adaptive immunity (105). They are a heterogeneous population of cells with a high degree of plasticity and ability to acquire distinct functional phenotypes in response to different environmental changes and stimuli such as microbial, parasitic, and viral antigens, or apoptotic cells (129). Many macrophage populations have now been identified that display a broad spectrum of functional phenotypes (136). However, two major populations of macrophages with distinct functions represent the extreme polarisation states of macrophages: pro-inflammatory M1 macrophages and anti-inflammatory M2 macrophages (140). M1 macrophages play a crucial role against infectious microbes (e.g. bacteria and viruses) and tumour progression whereas M2 macrophages are involved in tissue repair, wound healing, and in response against parasitic infections (159).

Resting or naïve macrophages (M0) can be polarised to a pro-inflammatory M1 phenotype by exposure to granulocyte macrophage colony-stimulating factor (GM-CSF), Th1 cytokines like interferon gamma (IFN-γ) and tumour necrosis factor alpha (TNF-α), and other toll-like receptor (TLR) ligands, such as bacterial lipopolysaccharide (LPS). Polarisation towards anti-inflammatory M2 phenotype, on the other hand, is primarily induced via exposure to macrophage colony-stimulating factor (M-CSF) and Th2 cytokines like IL-4 or IL-13 (105, 129). The balance between pro- and anti-inflammatory macrophage phenotypes plays a central role in the maintenance of tissue homeostasis under steady-state conditions and after exposure to pathogens and tissue damage (175, 302). This is

exemplified by various autoimmune (e.g. rheumatoid arthritis (175), multiple sclerosis (176) and Crohn's disease (177)) and chronic inflammatory diseases (e.g. alcoholic and non-alcoholic liver diseases (178), atherosclerosis (179), and diabetes (180)) where dysregulation in macrophage function is thought to play a central role (177, 302, 303). However, the molecular events that control M1 and M2 polarisation and underpin different functions of pro- and anti-inflammatory macrophages are still poorly understood (218).

Characterisation of macrophage polarisation has been studied widely. Chanput et al recently reported characterisation of THP-1 macrophages for both M1 and M2 phenotypes using the expression of chemokines and surface marker receptors. This study demonstrated that chemokines and surface receptors could be inappropriate markers for characterising different macrophage polarising states, particularly for the M2 subset which was less sharply defined because chemokines are affected by secondary cell-cell signals that are crucial to driving M2 polarization (159). In another study, Lopez-Castejon et al have shown specific gene expression profile which controls M1 and M2 macrophages phenotypes (218). Also, Sierra-Filardi et al demonstrated a characteristic high expression of CCR2 and CCL2 genes in M1 and M2 macrophages respectively (304). However, gene expression profiling does not account for differences in functional phenotype and cannot reveal the complexity of biological samples (219). Furthermore, a great overlap in the expression of surface markers has been reported between different macrophage subsets and more importantly deciphering function based on surface phenotype is not always possible (220).

Therefore, there is a need for more functional biological readouts that not only allow better classification of different macrophage subsets but also provide better insight into the molecular mechanisms that underpin distinct functional and phenotypical subsets. Given the mounting evidence highlighting a strong correlation between the metabolic state and the functional phenotype of macrophages, metabolite profiling could prove a powerful tool for better classification and understanding of different macrophage phenotypes (212, 305). For example, M1 macrophages have been characterized by high levels of glycolysis and flux through the pentose phosphate pathway (PPP), and an increase in tricarboxylic acid (TCA) cycle metabolites particularly, such as: citrate, succinate and itaconate. Moreover, M1 macrophages have increased fatty acids synthesis (212, 227). On the other hand, M2 macrophages adopt oxidative phosphorylation and fatty acid oxidation (215). These key metabolic differences between M1 and M2 macrophages are widely accepted. However, the metabolic mechanisms that underpin the orchestrating of their profiles remain not well understood. Also, M1 macrophages are distinctive with the expression of inducible nitric oxide synthase (iNOS) that facilitates the production of NO, which has anti-microbial activity and cytotoxicity whereas M2 macrophages express Arg-1 instead that is required in the production of polyamines which are necessary for cell proliferation, collagen synthesis and tissue remodelling (211, 215).

Liquid chromatography (LC)-mass spectrometry (MS)-based metabolomics is a powerful tool for quantifying metabolites as well as for identifying known and unknown compounds in biological samples (306). Therefore, this technique has

been used widely for disease diagnostic biomarker discovery (307) as well as evaluation of drug toxicity (308). In addition, LC-MS-based approaches have been employed to investigate the function of immune cells and immune responses by monitoring level changes of signalling molecules. Tannahill et al have revealed succinate as an inflammatory signal in lipopolysaccharide (LPS)-activated bone marrow-derived macrophages (BMDMs) using LC-MS metabolomics approach (88). Also, Hollenbaugh et al have demonstrated that LC-MS/MS metabolomics was an effective approach to monitor various metabolic alterations in Human immunodeficiency virus 1 (HIV-1)-infected primary human CD4+ T cells and a macrophage model system (309). Moreover, LC-MS metabolomics has been effectively used to monitor LPS-induced changes in amino acid metabolism of macrophage-like cell line (RAW 264.7) and to identify relevant pathways (310). In the context of macrophages polarisation, a recent study has used integrated transcriptomics and LC-MS-based metabolomics to investigate the polarisation and the distinct metabolic profiles of M1 and M2 macrophages in mice. They demonstrated that M2 macrophages activate glutamine catabolism and UDP-N-acetylglucosamine (UDP-GlcNAc)-related modules. On the other hand, they identified interruption in the TCA cycle between isocitrate and 2-oxoglutarate in M1 macrophages, leading to an interruption in oxidative phosphorylation (OXPHOS) (227). Using LC-MS metabolomics, Mills et al. have shown that itaconate is an anti-inflammatory metabolite which has an important role in the regulation of macrophages functions (225). However, Rattigan et al. demonstrated a complex role of itaconate as both an inflammatory and anti-inflammatory key metabolite (224). Moreover, another metabolomics study of

macrophages has identified succinate as a participant in innate immune signalling in response to LPS (M1 macrophages) where its increase results from impaired TCA cycle and leads to a boost in the production of the inflammatory cytokine, IL-1β during inflammation (226). Also, Freemerman et al demonstrated that driving glucose uptake and metabolism through glucose transporters in macrophages induces a proinflammatory response and metabolomics analysis revealed an increase in glycolysis, PPP, purine and pyrimidine metabolism (311). However, full metabolic signature of human macrophage polarisation states has not yet been investigated.

In this study, untargeted LC-MS-based metabolite profiling was employed to characterise M1 and M2 phenotypes in THP-1 macrophages in order to identify the key characteristic metabolites of each polarisation state in these cells. Our data clearly showed a distinct metabolic signature and associated changes of relevant metabolites in M1 and M2 macrophages which could not only provide a better understanding of the functional properties of different macrophage subsets but also pave the way for identifying new key characteristic metabolites and potential therapeutic targets in different inflammatory diseases.

2.2. Materials and methods

2.2.1. Materials

THP-1 cell line was purchased from ATCC, USA. RPMI 1640 medium, phosphate buffered saline (PBS) and *E. coli* lipopolysaccharide were purchased from Sigma-Aldrich, UK. GM-CSF, M-CSF and IL-4 were purchased from Miltenyi Biotec,

Germany. IFN-γ was purchased from R&D Systems, USA. Methanol and acetonitrile were purchased from Fisher Scientific, UK. All solvents were LC-MS grade.

2.2.2. Methods

2.2.2.1. Cell culture

Human THP-1 cells were cultured and differentiated as previously described in (159). Briefly, THP-1 cells were grown in T75 tissue culture flasks using RPMI 1640 supplemented with 10% heat-inactivated fetal bovine serum (FBS), 1% L-glutamine, and 1% penicillin-streptomycin. Cells were then incubated at 37 °C and 5% CO_2.

2.2.2.2. Differentiation and polarisation of THP-1 cells

THP-1 cells were differentiated into naïve macrophage-like state (M0) by treating with phorbol-12-myristate-13-acetate (PMA). Six million cells were seeded per flask (T25 tissue culture flask), and then the cells were treated with PMA containing media with a final concentration of 50 ng/ml of PMA and incubated for 6 h. After the incubation period, the cells were further treated with either 50 ng/ml GM-CSF, 100 ng/mL LPS and 20 ng/mL IFN-γ or 50 ng/mL M-CSF and 20 ng/mL IL-4 for up to 72 h to generate M1 or M2 polarised cells, respectively (312). This polarisation protocol is adapted from previous studies (312, 313) and the cell phenotypes were confirmed by conventional assays (Figures 2.1 and 2.2). Cells treated with PMA only were used as controls (M0). Six biological replicates for each condition were prepared.

2.2.2.3. Sample preparation and metabolite extraction

After incubation for 72 h, the media containing PMA and polarising agents were removed. The cells were then washed once with pre-warmed PBS (37 °C) and 500 µl pre-cooled methanol at -48 °C was used for metabolic quenching and metabolite extraction. The cells were harvested using a plastic scraper whilst being kept on ice and the extracts were transferred into pre-cooled fresh tubes (4 °C). The cell extract was vortexed for 1 h and centrifuged at 16,100 ×g for 10 min at 4 °C. After the centrifugation, the supernatants were transferred into pre-cooled fresh tubes (4 °C) and they were then dried under vacuum and reconstituted in 70 µl of methanol. The samples were stored at -80 °C prior to LC-MS analysis. To assess the instrument performance, an intrastudy quality control (QC) sample was prepared by mixing equal volume of each sample.

2.2.2.4. Analytical methodologies

LC-MS-based metabolite profiling was performed on an Accela system coupled to an Exactive MS (Thermo Fisher Scientific, Hemel Hempstead, UK) operating with electrospray ionisation (ESI) running in the negative (ESI-) and positive (ESI+) modes as previously described in (314). Briefly, the spray voltage was 4500 V (ESI+) and 3500 V (ESI-), the capillary voltage was 40 V (ESI+) and 30 V (ESI-), tube lens voltage was 70 V for both modes and skimmer voltage was 20 V (ESI+) and 18 V (ESI-). The temperature for capillary and probe was maintained at 275 °C and 150 °C, respectively. Chromatographic separation was carried out using ZIC-pHILIC (4.6 × 150 mm and 5 µm particle size, Merck Sequant). The mobile phase

composed of 20 mM ammonium carbonate in water (solvent A) and 100% acetonitrile (solvent B). Metabolites were separated according to a linear gradient as following: 0-15 min (20% A), 15-17 min (95% A), and 17-24 min (20% A) at 300 µl/min flow rate. The injection volume of 10 µl and the column was kept at 45 ^{o}C.

2.2.2.5. Data processing and metabolites identification

To process raw data obtained from LC-MS, XCMS and mzMatch were used for untargeted peak-picking and peak matching, respectively (69, 70). IDEOM was employed for putative metabolite identification and noise filtering with default parameters (315). Briefly, retention time (RT) for identification of authentic standards was 5%, RT for identification for calculated RT was 50 %, mass accuracy for mass identification was 3ppm. Metabolites were identified with two levels of confidence; level 1 (L1) identification was performed by matching retention times and accurate masses of authentic standards and level 2 (L2) identification was carried out when the predicted retention times were employed due to the lack of standards according to the metabolomics standards initiative (74, 75).

Pre-processed data were analysed by performing multivariate and univariate analysis. Orthogonal partial least squares-discriminant analysis (OPLS-DA) was carried out by SIMCA-P v13.0.2 (Umetrics, Umea, Sweden) as a supervised multivariate model. This multivariate analysis was used as the first step for visualising data with sample classes and evaluating the metabolome changes in M0, M1, and M2 groups. The key mass ions representing potential characteristic metabolites were determined based on variable importance in projection (VIP) values obtained from two-way orthogonal comparisons. Mass ions with VIP

values greater than one were considered as discriminant key characteristic metabolites. Univariate analysis was also performed in parallel to multivariate analysis to identify significant mass ions. T-test with false discovery rate (FDR) correction was performed using MetaboAnalyst (24) to determine the significantly changed mass ions between unpolarised THP-1 macrophages (M0) and polarised groups (M1 and M2). MetaboAnalayst and the Kyoto Encyclopedia of Genes and Genomes (KEGG) database were used to analyse and visualise the affected pathway.

2.3. Results and discussion

2.3.1. Macrophages characterisation using surface markers and cytokine profile

As previously mentioned, macrophages adopt a range of phenotypes in response to different micro-environmental stimuli. To generate M1 cells, naïve THP-1 macrophages were treated with GM-CSF, LPS (a potent endotoxin) and a Th1 cytokine, IFN-γ, while M2 cells were generated using M-CSF and a Th2 cytokine, IL4. These biomolecules have been shown to drive macrophage polarisation down the pro-inflammatory or anti-inflammatory path, respectively (217, 316). To confirm the efficiency of the polarisation approach used in this study, the morphology, surface phenotypic markers and cytokine profile of cells in response to different cytokine treatments were analysed. For the visualisation of the cell cytoskeleton, different macrophage subsets were stained with fluorescently labelled phalloidin. M1 cells showed a less rounded and elongated morphology while M2 cells appeared rounded and stretched, displaying a ‘fried egg-like’

morphology; M0 cells had rounded but less stretched cells (Figure 2.1). Results obtained were in line with existing morphological data for different macrophage subsets (317, 318). To find out the surface phenotype of each cell population, immunofluorescence staining for calprotectin and mannose receptor (MR) (319), which have been associated with M1 and M2 cells, respectively (317), was carried out. As shown in Figure 2.2, M1 cells expressed higher levels of calprotectin and lower levels of MR compared to M2 and M0 cells. On the other hand, M2 cells expressed the highest level of MR with no calprotectin expression. Additionally, the levels of cytokines in the supernatants collected from the macrophage subsets were analysed by enzyme-linked immunosorbent assay (318). M1 cells expressed significantly higher levels of pro-inflammatory cytokines, TNF-α and IL-1β compared to M2 and M0 macrophages (Figure 2.3). As anticipated, our polarisation approach induced distinct M1 and M2 macrophages, characterised by increased expression of pro-inflammatory (calprotectin, TNF-α, IL-1β) or anti-inflammatory markers (319), respectively.

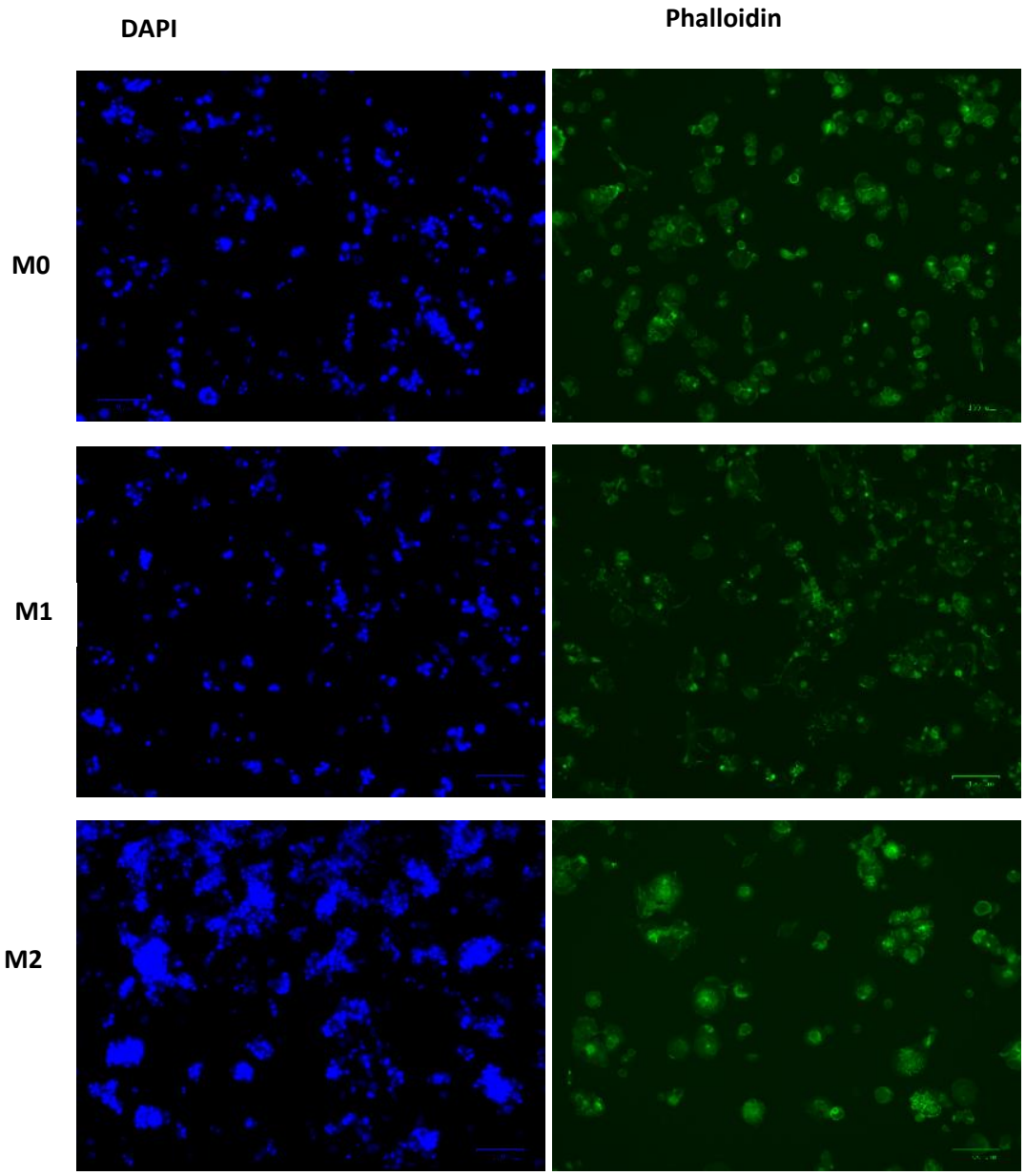


Figure 2.1: Morphology of cytokine polarised THP-1 cells. Cells were stained with phalloidin (green) and DAPI (blue) for the visualization of cytoskeleton. Images were taken at 10x magnification; scale bar = 100µm.

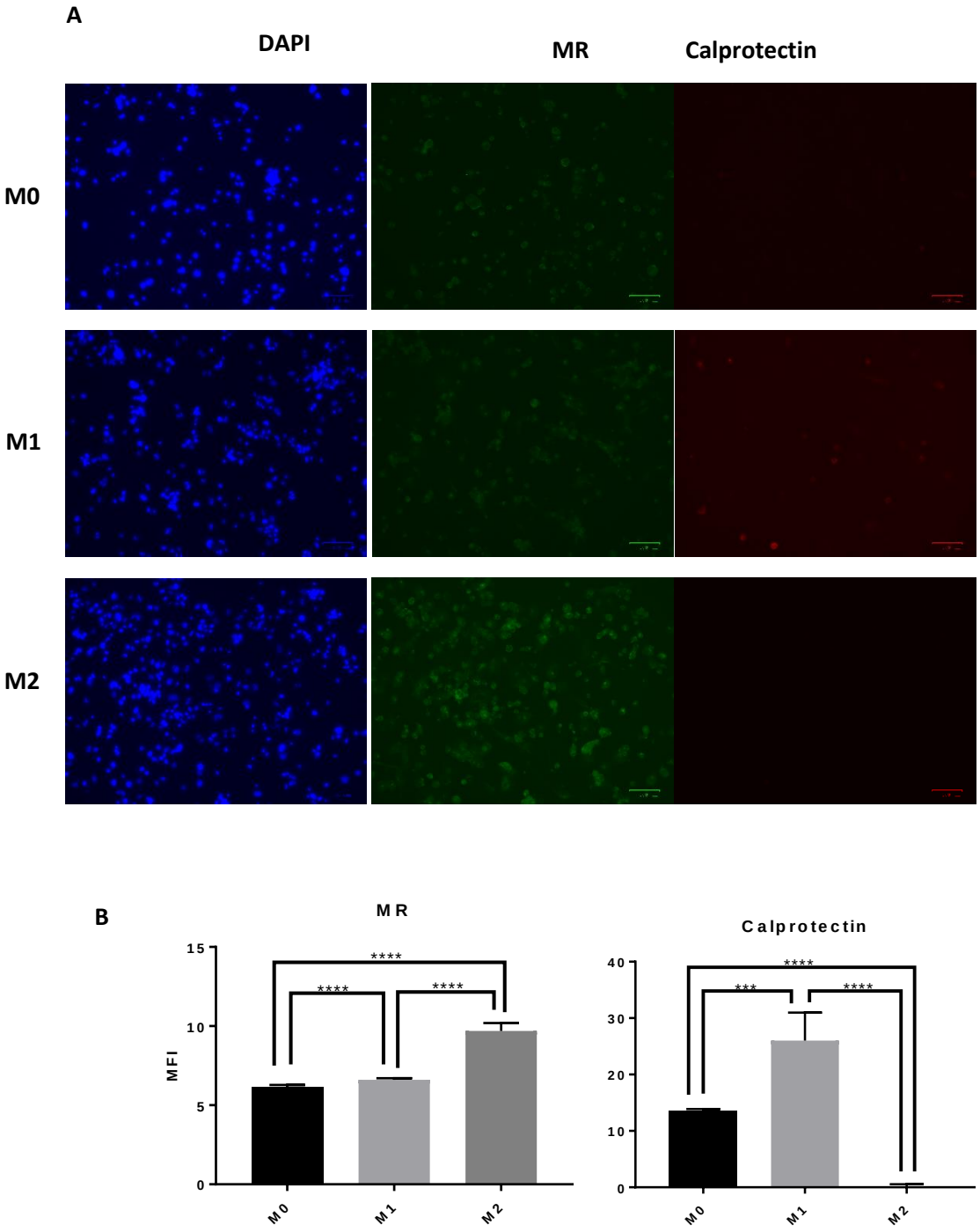


Figure 2.2: Expression of surface markers by cytokine polarized THP-1 macrophages. A) Immunofluorescent images of showing mannose receptor (green) and calprotectin (red) expression; nuclei were stained with DAPI (blue). B) Mean fluorescent intensity (MFI) of M1, M2 and M0 cells. Data are presented as mean ± SD, (n=6).

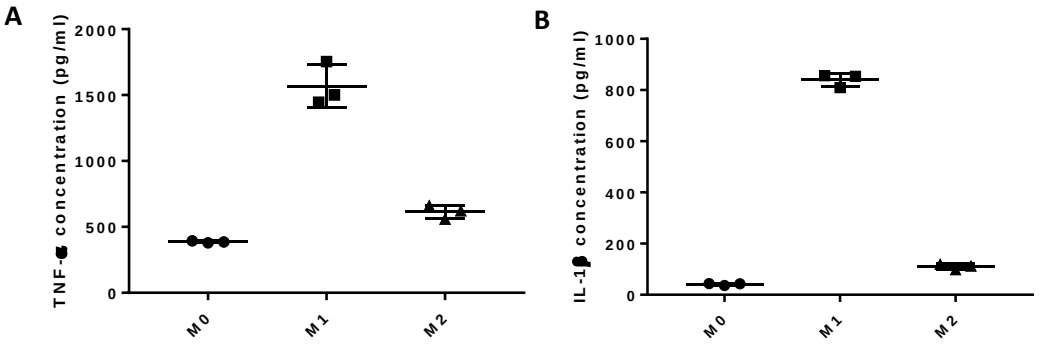


Figure 2.3: Cytokine expression by macrophages. Following 6 h PMA activation, cells were treated with GM-CSF (50 ng/ml), LPS (100 ng/mL) and IFN-γ (20 ng/mL) or M-CSF (50 ng/mL) and IL-4 (20 ng/mL) for up to 72 h to generate M1 or M2 polarised cells, respectively. A) TNF-α B) IL-1β expression. Data are presented as mean ± SD (n=3).

2.3.2. Untargeted metabolomics analysis of THP-1 polarised macrophages.

In order to explore the changes in the metabolic profile of THP-1 macrophages upon polarisation to M1 and M2 subsets and identify potential key characteristic metabolites for each macrophage polarisation state, the extracted intracellular metabolites from M0 group (unpolarised) and polarised groups were analysed using LC-MS. 5474 features were detected in positive and negative mode with a total of 575 metabolites identified putatively (Appendix, Table A1). Figure 2.4 shows the chemical composition of THP-1 macrophages with the biological classifications of the identified metabolites. The metabolome was mainly constituted of glycerophospholipids (20%) and amino acids (17%), respectively followed by fatty acyls (7%), other lipids (6%), carbohydrate (5%), nucleotide (3%), sphingolipids (3%), co-factors and vitamins (2%), and energy metabolites (1%).

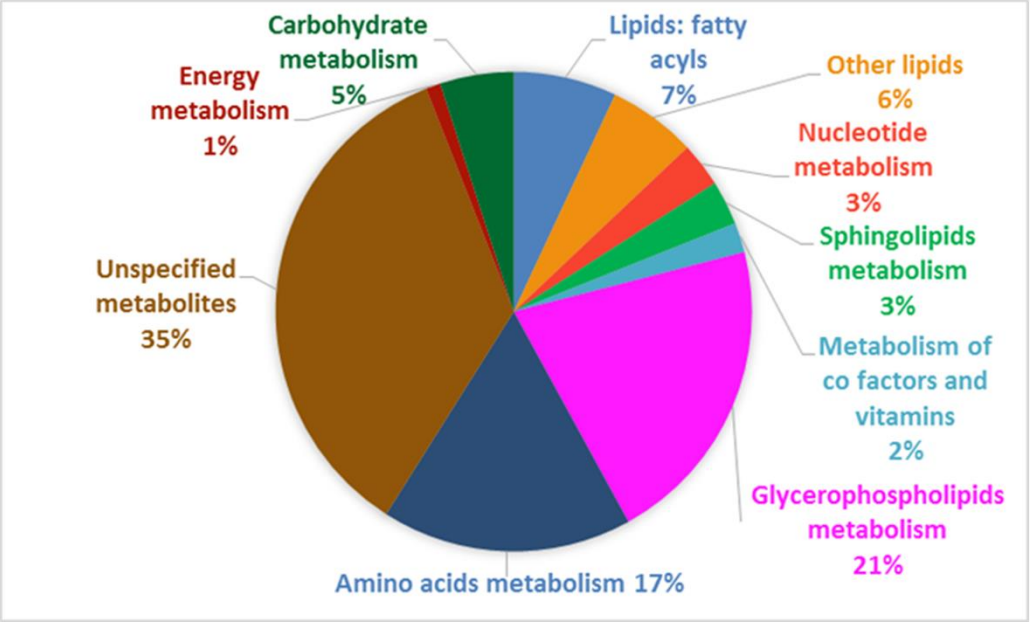


Figure 2.4: Functional categories of the intracellular metabolites produced by THP-1 macrophages. In total, 575 metabolites were putatively identified in THP-1 macrophage extracts using LC-MS-based metabolite profiling.

2.3.3. Feature selection and identification of potential biomarker metabolites.

In order to reveal the key metabolites representing potential key characteristic metabolites for the two polarisation states of macrophages, the pre-processed data were imported to SIMCA-P to perform multivariate analysis. OPLS-DA was performed on the detected featues to distinguish M0, M1 and M2 groups. OPLS-DA scores plot showed tight clustering of the six replicates within each group and clear separation between the three different groups (M0, M1, and M2 macrophages) with R^2 and Q^2 values of 0.647 and 0.847, respectively (Figure 2.5). R^2 measures the fitting of the model to the original data and Q^2 represents the cross validation that provides the measure of the prediction ability of this model (320). R^2 and Q^2 values should be greater than 0.5 to imply that the model is valid, and the prediction ability is accepted (321, 322). Six replicates were deemed to

be valid for this type of cell line-based studies (306, 323). This separation indicated a distinctive metabolic signature of M1, M2 and M0 macrophages.

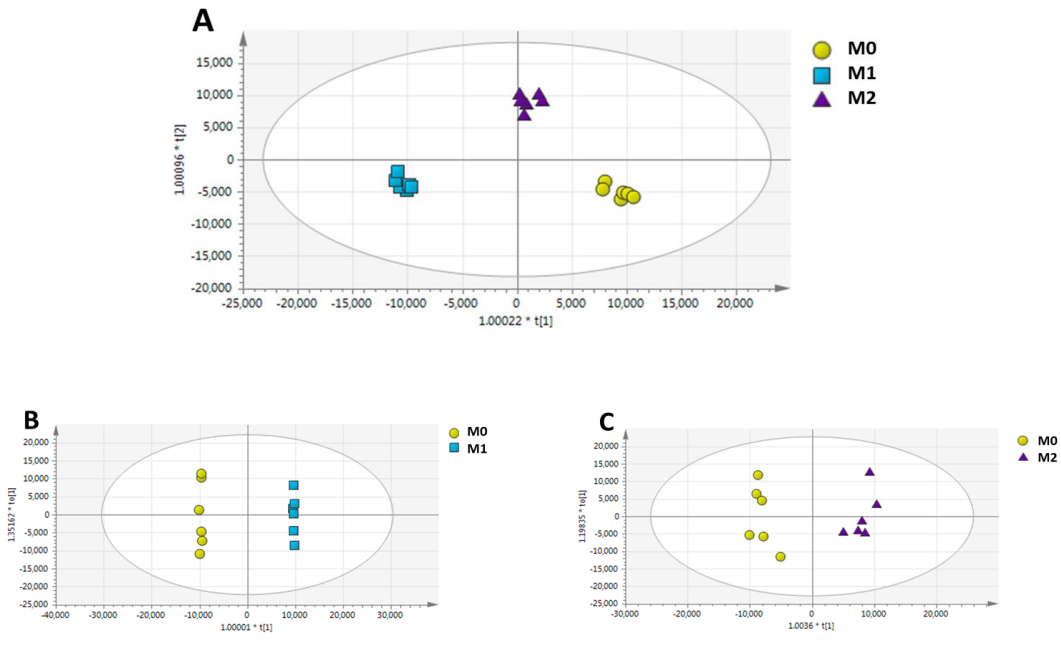


Figure 2.5: OPLS-DA scores plots of macrophages extracts after polarisation toward M1 and M2 states and their corresponding unpolarised (M0) controls. (A) M1 and M2 macrophage samples and their respective unpolarised controls (R^2 = 0.647 and Q^2 = 0.847). (B) Two-way orthogonal comparison between M0 and M1 (R^2 = 0.664 and Q^2 = 0.899). (C) Two-way orthogonal comparison between M0 and M2 (R^2 = 0.711 and Q^2 = 0.838). M0 (yellow circles), M1 (blue squares), and M2 (purple triangles). n=6.

Two-way comparison illustrated in Figure 2.5B and C was performed to determine the mass ions which contributed to the separation between M0 and M1 or M2 macrophages based on their VIP values. The mass ions with VIP values greater than one were considered as potential key mass ions (324). OPLS-DA scores plot showed a clear separation between M0 and M1 groups (Figure 2.5B) with R^2 and Q^2 values of 0.664 and 0.899, respectively, demonstrating acceptable OPLS-DA models (324). In parallel, univariate t-test with FDR correction was performed to

identify significantly changed mass ions (FDR < 0.05) in M1 compared to the corresponding control (M0). Combination of the multivariate and univariate analysis revealed 90 significantly changed metabolites in M1 macrophages. Similarly, in Figure 2.5C, OPLS-DA scores plot showed a clear separation between M0 and M2 macrophages with Q^2 and R^2 values of 0.838 and 0.711, respectively. Again, univariate t-test with FDR correction was performed in parallel to identify significant mass ions changed in M2 group compared to the corresponding control (M0), revealing 49 significantly changed metabolites in M2 macrophages. Table 2.1 shows the top twenty significant metabolites with higher fold changes (1.97 to 15.44) in M1 and M2. Tables 2.2 and 2.3 show the significantly changed metabolites in M1 and M2 compared to M0, respectively.

Table 2.1: The significant metabolites in THP-1 macrophages upon polarisation into M1 and M2.

Putative metabolite	Exact mass	RT (min)	Formula	PubChem ID	ID confidence	Polarization state	Fold change	FDR
5-Hydroxy-L-tryptophan	220.0847	9.21	$C_{11}H_{12}N_2O_3$	439280	L2	M1	15.44	4.12E-06
Ceramide (d18:1/22:1)	619.5899	5.03	$C_{40}H_{77}NO_3$	53481052	L2	M1	4.77	0.0002
Cytidine	243.0854	11.26	$C_9H_{13}N_3O_5$	6175	L1	M1	3.74	0.0029
C14 Ceramide	509.4806	5.12	$C_{32}H_{63}NO_3$	5282310	L2	M1	3.45	6.36E-05
Ceramide (d18:1/16:0)	537.5120	5.10	$C_{34}H_{67}NO_3$	5283564	L2	M1	3.96	0.0012
Ceramide (d18:1/18:0)	565.5435	5.10	$C_{36}H_{71}NO_3$	53481047	L2	M1	4.73	0.0156
Ceramide (d18:1/22:0)	621.6068	5.10	$C_{40}H_{79}NO_3$	53481048	L2	M1	6.84	0.0122

Ceramide (d18:1/24:0)	649.6385	5.10	$C_{42}H_{83}NO_3$	5283576	L2	M1	5.76	0.0128
3-(4-hydroxyphenyl) pyruvate	180.0423	8.52	$C_9H_8O_4$	5318321	L2	M2	2.19	0.0024
3-Dehydroxycarnitine	145.1102	6.15	$C_7H_{15}NO_2$	725	L2	M2	3.47	0.0078
4-Imidazolone-5-propanoate	156.0534	9.76	$C_6H_8N_2O_3$	128	L2	M2	2.08	6.3E-05
Alpha-CEHC	278.1517	4.65	$C_{16}H_{22}O_4$	9943542	L2	M2	2.67	6.3E-05
Ala-Ala	160.0847	8.59	$C_6H_{12}N_2O_3$	5460362	L2	M2	1.94	0.0023
N-Ac-L-Asp	175.0480	11.16	$C_6H_9NO_5$	65065	L2	M2	1.07	0.0065
N-Ac-L-Glu	189.0636	10.85	$C_7H_{11}NO_5$	185	L1	M2	3.57	0.0046
PC(O-14:0/16:0)	691.5514	5.27	$C_{38}H_{78}NO_7P$	24779275	L2	M2	2.12	0.0076

PC(P-20:0/0:0)	535.3997	5.66	$C_{28}H_{58}NO_6P$	52924063	L2	M2	3.99	0.0139
N-Acetylserotonin	218.1055	6.34	$C_{12}H_{14}N_2O_2$	903	L2	M1 / M2	6.78/3.04	0.001/0.017

(+) indicates the metabolite increase upon polarisation. M1 and M2 indicate the polarisation states. ID confidence represents the level of metabolite identification based on MSI standard (74, 75). Ala-Ala: D-Alanyl-l-Alanine, N-Ac-L-Asp: N-acetyl-L-aspartate, N-Ac-L-Glu: N-acetyl-L-glutamate

2.3.4. Pathway analysis

For a further investigation to identify the metabolic pathways significantly altered by M1 and M2 polarisation states, a summary of pathway analysis is illustrated in Figure 2.6A and B. Figure 2.6A and B show that glycerophospholipids (GLs) metabolism was significantly changed in M1 as well as M2 compared to M0. Glycerophospholipids constitute the main components of the cell membrane (325). They mainly include phosphatidylcholines (PC), phosphatidylethanolamines (PE), phosphatidylserines (PS), phosphatidylinositols (PI), and phosphatidylglycerols (PG) (325). The level of GLs in polarised macrophages (M1 and M2) was significantly increased and this results clearly from the increased levels of PC, PS and PE (Tables 2.2 and 2.3). Figure 2.7A, B and C show different GLs such as PC (14:2/16:0), PS (18:0/20:4), and PE (18:1/22:6) that significantly increased in M1 or M2. This agrees with recent research where Zhang et al detected an increase in the composition of medium- and long-chain polyunsaturated GLs, such as PS, PC, PE, and PI upon macrophages polarisation into M1 and M2 phenotypes, compared to M0 (326). Generally, lipid metabolism contributes to the pro- or anti-inflammatory functions of macrophages by meeting energetic requirements and modulating membrane fluidity (327). However, GLs are also involved in multiple biological processes, such as inflammation and cell differentiation (328).

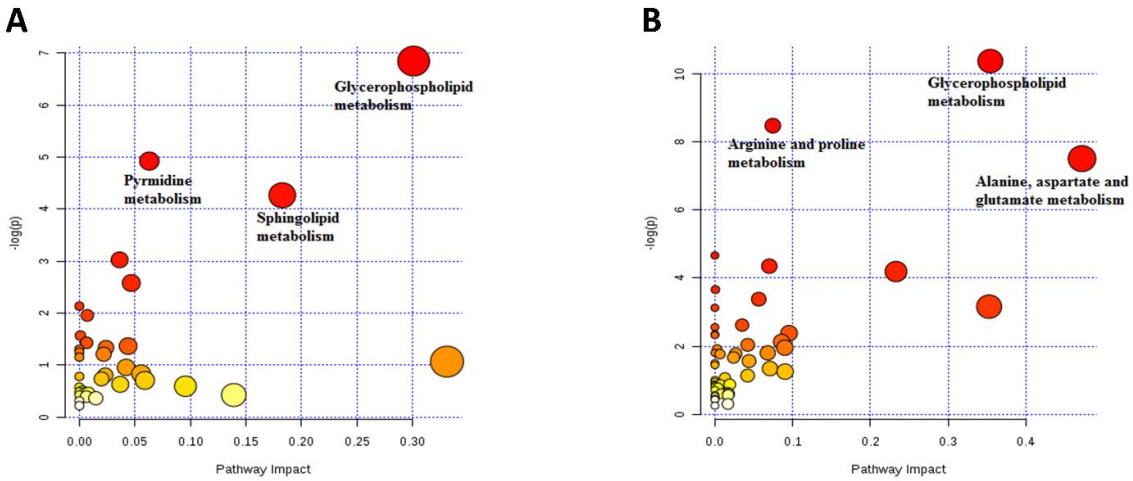


Figure 2.6: Summary of pathway analysis by MetaboAnalyst. The top-pathways are ranked by the gamma-adjusted p-values for permutation per pathway (y-axis) and the total number of hits per pathway (x-axis). The colour graduated from white to yellow, orange and red as the values of both x and y increase. (A) Metabolic pathways significantly changed in M1 macrophages. (B) Metabolic pathways significantly changed in M2 macrophages.

Sphingolipids and pyrimidine metabolisms were significantly altered in M1 macrophages as shown in Figure 2.6A. Sphingolipids constitute a large class of bioactive and structural lipids representing the main lipid component of the eukaryotic plasma membrane. Sphingolipids are metabolised by a family of enzymes that regulate their metabolic interconnected network (329). In recent years, different aspects of sphingolipid function has been investigated, including its role in inflammation (330), signalling pathways and metabolism (331). The key metabolite in sphingolipids metabolism is ceramide which is generated either through sphingolipid metabolism or in a *de novo* pathway at the endoplasmic reticulum (ER) (332). This obvious alteration in sphingolipid pathway is attributed to a significant increase in the levels of some sphingolipids and ceramides which could be considered as potential key characteristic metabolites for M1 macrophages. The levels of sphingolipids such as Ceramide (d18:1/24:0),

Ceramide (d18:1/22:0) and Ceramide (d18:1/16:0) were significantly increased in M1 macrophages as shown in Figure 2.7D, E, and F, respectively. It was demonstrated that stimulation of macrophages (RAW264.7) with LPS or another TLR-4 agonist elevate ceramide levels by multiple mechanisms, including the *de novo* synthesis pathway (333). Similarly, Cuschieri et al. reported that the formation of ceramide could be involved in the gathering of Toll-like receptor (TLR) as a response to bacterial antigens such as lipopolysaccharide (LPS) (334). Gathering and activation of TLR-4 in response to LPS drives a switch from oxidative phosphorylation to glycolysis which increases reactive oxygen species (ROS) production (210), although our data showed no significant changes in the glycolysis intermediates. ROS is important for killing bacterial cells, which is a significant function of M1 macrophages (159). Others showed an increase in ceramide levels and inducing TLR4-mediated response in both leukaemia and epithelial cells in response to microbial ligands such as LPS (335). Furthermore, a recent lipidomic study demonstrated an increase in the total cellular sphingolipids after TLR4 activation of murine macrophages (RAW 264.7 cells). Therefore, our results are in line with previous studies showing an increase in ceramide production in pro-inflammatory macrophages. However, the mechanism responsible for the increase in the synthesis of sphingolipids in TLR4 stimulated cells is still unknown (336).

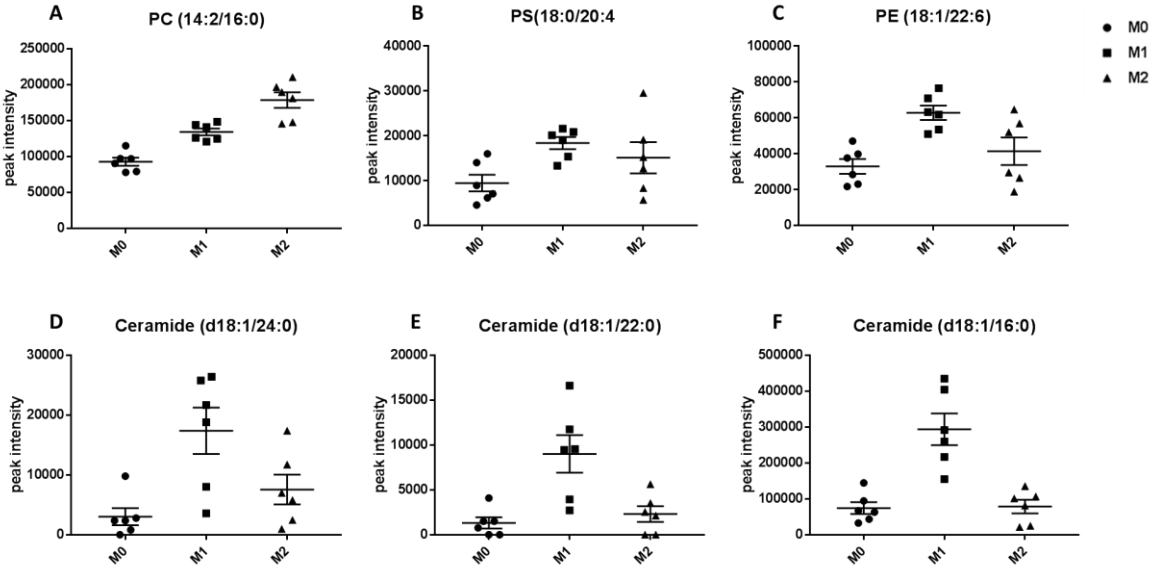


Figure 2.7: GLs and sphingolipids that significantly affected upon polarisation. (A) PC (14:2/16:0), (B) PS (18:0/20:4), and (C) PE (18:1/22:6) represent some GLs that increased significantly in M1 or M2 macrophages compared to M0 macrophages. (D) Ceramide (d18:1/24:0), (E) Ceramide (d18:1/22:0) and (F) Ceramide (d18:1/16:0) as potential key characteristic metabolites of M1 macrophages and their significant increase compared to M0 and M2 macrophages.

Pyrimidine metabolism was another significantly perturbed pathway in M1 macrophages as can be seen in Figure 2.6A. Pyrimidine is found in the form of nucleic acid and vitamins in living systems. It represents the basic nucleus in RNA and DNA. Therefore, it has been found to be involved in several biological activities (337). Biologically, pyrimidines are considered as a very important class of molecules and represent the most abundant member of the diazines family with uracil and thymine (338). Numerous studies in the literature showed a broad range of therapeutic activity of pyrimidine nucleus-containing compounds such as antibacterial (339) and antitubercular (340) compounds. Our results showed a significant increase in cytidine that can be used as potential new key characteristic metabolites for M1 macrophages (Figure 2.8). This metabolite is an intermediate in pyrimidine metabolism (KEGG map 00240). Increase in the levels of pyrimidines

could result from the pentose phosphate pathway (PPP) (KEGG map 00030) which is well known to be induced in M1 macrophages, and it enhances the production of pyrimidines as previously reported (212). Unexpectedly then, metabolites involved in the PPP showed no significant change in our results unexpectedly. Intensive research has been carried out to investigate the activity of pyrimidines in inflammation. Bonnert et al. reported a remarkable activity of pyrimidine derivatives against inflammation and immune disorders such as rheumatoid arthritis, atherosclerosis, and Crohn's disease (341). Furthermore, Nargund et al. showed potent antibacterial activity of pyrimidine derivatives against various gram-negative and gram-positive bacteria (339). Collectively, these studies have revealed the activity of pyrimidines in inflammation and bacterial attack which is a pivotal role for M1 macrophages (159). Also, along with pyrimidines, purines are key components in the production of RNA and DNA. They have a crucial role in the energy system (e.g. ATP generation) (342) and enhanced PPP flux increases the production of purines as well as pyrimidines (343). Our data demonstrated a significant increase in the purines; hypoxanthine and inosine (Table 2.2). In agreement with our results, hypoxanthine was reported to be increased in the presence of LPS (344). Pyrimidines and purines can be used for activated cell biosynthesis and provide NADPH, which is the substrate for NADPH oxidase in order to produce reactive oxygen species (343) that act as a bacterial killing mechanism (345) representing the main function of M1 macrophages. Furthermore, a previous study showed that the purine analogue 6-N-hydroxylaminopurine has antibacterial and antiviral activity (346).

Figure 2.8 shows two metabolites with a significant increase that could also be considered as potential key characteristic metabolites for M1 macrophages: 5-hydroxy-L-tryptophan and N-acetylserotonin intermediates in tryptophan metabolism (KEGG map 00380). 5-hydroxy-L-tryptophan are generated as a result of tryptophan breakdown by tryptophan hydroxylase (KEGG R01814) and is followed by the reaction KEGG R02701 producing serotonin. N-acetylserotonin is produced from serotonin by the reaction KEGG R02911. The precursor tryptophan is an amino acid required for metabolic functions and protein synthesis. It cannot be synthesised in the body, therefore, it must be supplied in the form of proteins. Although many studies have focused on the role of tryptophan metabolism in the last decades, its role and that of its intermediates in the immune system are not yet fully understood. However, tryptophan metabolism and inflammatory responses are thought to be associated with several diseases and pathological conditions (347). For instance, Tarique et al revealed a role of 5-hydroxy-L-tryptophan in innate immunity as it attracts mast cells to the inflammation site (348). Moreover, Nakumura et al. showed that 5-hydroxy-L-tryptophan enhanced phagocytosis in murine macrophages (349), a key property by which M1 macrophages eliminate foreign particles (350).

On the other hand, arginine, proline metabolism, and alanine, aspartate and glutamate metabolism were all significantly altered in M2 macrophages (Figure 2.6B). L-Arginine is considered as a non-essential amino acid at the whole organism level, but it is important to be supplemented in certain diseases (351). It is believed that mammalian arginine metabolism and its cellular regulation is a complex process (352). L-Arginine is produced from *de novo* arginine production

or cellular protein break-down. Many amino acids are involved in the biosynthesis of arginine such as L-citrulline, L-ornithine and L-glutamine. Furthermore, L-arginine represents a precursor for the synthesis of urea, nitric oxide, L-glutamate, polyamines, L-proline, and creatine (353). Corraliza et al previously demonstrated a key aspect of arginine metabolism which showed that different enzymes involved in arginine metabolism are promoted in macrophages based on their polarisation state (M1 or M2). Arginine in macrophages is catabolised by either iNOS in M1 macrophages (producing NO and citrulline) or Arg-1 in M2 macrophages (producing L-ornithine, polyamines (putrescine, spermidine and spermine), and urea, which are involved critically in wound healing and tissue repair function of M2 macrophages) (354). In agreement with this statement, our results showed a significant increase in L-citrulline (Table 2.2). This has been proved by Sugimoto et al demonstrating excessive increase in L-citrulline in LPS-activated macrophages (355). Figure 2.8 shows three of the potential key characteristic metabolites for M2 macrophages; N-acetyl-L-glutamate, N-acetyl-L-aspartate, and 4-imidazolone-5-propanoate that significantly increased in these cells. N- acetyl-L-glutamate is produced by a reaction of acetyl-CoA with L-glutamate (KEGG R00259). Acetyl-CoA is generated from β-oxidation of fatty acids which was proved to be utilised in M2 macrophages (319). However, L-glutamate is interconverted from L-ornithine by the enzyme ornithine aminotransferase (KEGG R00667). As aforementioned, L-ornithine is known to be produced in M2 macrophages from L-arginine via Arg-1, and is represented as a substrate for the enzyme ornithine decarboxylase in the synthesis of polyamines induced in M2 macrophages (305). The other significantly altered pathway in M2 macrophages

was alanine, aspartate, and glutamate metabolism, which is connected to the TCA cycle. No significant change was observed in TCA cycle intermediates, which could indicate an intact and functioning TCA cycle tightly linked to fully functioning OXPHOS of mitochondria. OXPHOS was reported as a hallmark of M2 macrophages (212). Therefore, L-aspartate could be driven from the TCA cycle by oxaloacetate (KEGG R00355) and consequently to be consumed in a reaction with acetyl-CoA to produce N-acetyl L-aspartate by L-aspartate N-acetyltransferase (KEGG R487), which could explain the decrease in the level of L-aspartate and increase in the level of N-acetyl-L-aspartate. 4-Imidazolone-5-propanoate could represent another source for glutamate (KEGG R02288 and R02285) which, in addition to producing N-acetyl L-glutamate, could feed into the TCA cycle by being converted to 2-oxoglutarate by glutamate dehydrogenase.

Since many lipid classes have been detected and significantly changed in M1 or M2 macrophages, a more detailed lipidomic study will be another prospective approach, potentially revealing the lipid signature of M1 and M2 macrophages and will be a complementary dataset to existing metabolomics data, therby providing a more clear picture of macrophages response.

Surprisingly, glycolysis, PPP and OXPHOS showed no significant difference in their intermediates. These metabolic pathways represent hallmarks for M1 (glycolysis and PPP) and M2 macrophages (OXPHOS which connectes to the TCA cycle) as discussed earlier. These results can be due to different reasons.

Firstly, macrophages heterogenicity and diversity enable the generation of an infinite number of phenotypes with different profiles under the impact of varying stimuli (356, 357). Our protocol of polarisation used multiple stimuli for M1 and

M2 macrophages namely LPS, GM-CSF and IFN-γ for M1 macrophages and IL-4 and M-CSF for M2 macrophages. However, most of the studies used LPS or/and IFN-γ for M1 and IL-4 for M2 macrophages. GM-CSF and M-CSF can give rise to pro-inflammatory and anti-inflammatory macrophages, respectively, and so it is expected that they impact the metabolic signature of macrophage phenotypes (224, 358). It was already reported that using LPS alone, IFN-γ alone or both of them together give rise to different metabolic responses of macrophages (224). Therefore, metabolic responses to different stimuli can be sufficiently different, contradictory and seriously complex. This, in turn, suggests that the studies with single or limited number of stimuli do not reflect the complexity of the picture *in vivo* (224).

Secondly, and most importantly, most of the previous studies discussed the metabolic signature of M1 and M2 in mice macrophages (either primary or cell line stimulated with *in vitro* stimuli) whereas our experiment was conducted using a human cell line (THP-1 cells). In fact, macrophages from different species, residing in different tissues or arising from different progenitors, may show different biological and metabolic signatures, even to defined stimuli (357, 359). This could highlight the need to focus on primary human macrophages in future studies to acquire a more accurate reflection of the biology and signature of macrophages. However the large number of cells required for conventional metabolomics studies and access to human tissue limit the feasibility of such studies.

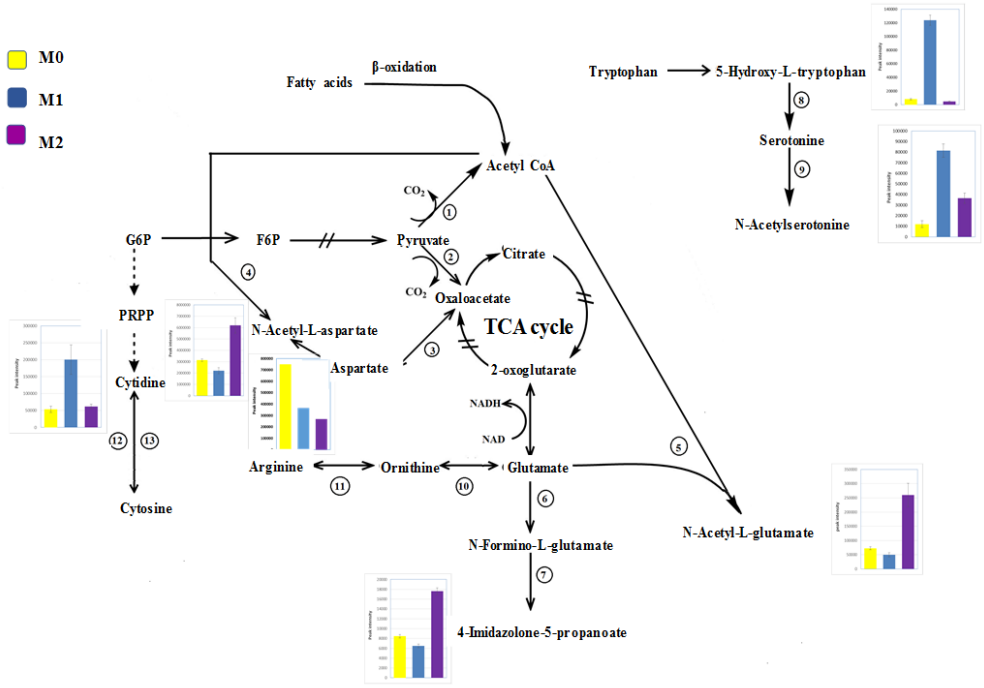


Figure 2.8: Significant metabolic pathways upon polarisation of THP-1 macrophages toward M1 and M2 states with bar graphs of key metabolites that significantly changed. The other metabolites were either identified with no significant change (pyruvate, citrate, G6P, glutamate, ornithine and arginine) or not detected. Metabolic enzymes are as follows; 1: pyruvate dehydrogenase, 2: pyruvate carboxylase, 3: glutamate-aspartate aminotransferase, 4: L-aspartate N-acetyltransferase, 5: N-acetylglutamate synthetase, 6: formiminoglutamase, 7: imidazolonepropionase, 8: tryptophan 5-monooxygenase, 9: arylalkylamine N-acetyltransferase, 10: ornithine aminotransferase, 11: Arg-1, 12: ribosylpyrimidine nucleosidase, 13: pyrimidine-nucleoside phosphorylase. G6P: glucose 6-phosphate, PRPP: 5-phosphoribosyl 1-pyrophosphate, F6P: fructose 6-phosphate. The bar charts show the peak intensity (y-axis) of corresponding metabolites, from the top to the bottom and left to right (cytidine, N-acetyl-L-aspartate, N-acetyl-L-glutamate, 4-imidazolone-5-propanoate, 5-hydroxy-tryptophan and N-acetylserotonine). M0 in yellow, M1 in blue and M2 in purple.

2.4. Conclusion

In this study, LC-MS metabolite profiling was used successfully to characterise M0, M1 and M2 macrophages. Furthermore, uni- and multivariate analyses demonstrated that this technique is sensitive enough to detect subtle changes in a wide range of metabolites upon polarisation of macrophages, and to identify the distinct metabolic signature of M1 and M2 phenotypes. Various metabolic

pathways were significantly affected in these macrophage phenotypes. Given the significant number of diseases associated with each phenotype (such as chronic inflammatory diseases or cancer progression), the identified key metabolites will improve the understanding of underlying mechanisms in macrophages polarisation. Moreover, this data provides new insight for the rational design of novel immune modulatory strategies, such as targeting specific pathways associated with different macrophage subsets in inflammatory diseases. Future studies should take into consideration different type of stimuli for macrophage polarisation to resemble the multiple stimuli present *in vivo* to account for the diverse range of signalling pathways resulting in different immune-metabolic responses (360). Furthermore, the origin of macrophages for investigation of metabolic signatures of different macrophage subsets should be considered since it could represent essential biochemical information revealing key pathways in specific disease.

Table 2.2: A list of 90 significantly changed metabolites in M1 macrophages with VIP >1 and FDR < 0.05 compared to M0 as a result of investigation M0, M1 and M2.

Putative metabolite	Mass	RT	FORMULA	Polarity	confidence	Pathway	Fold change	VIP	FDR
(R)-2-Hydroxyglutarate	148.0372	11.39	C5H8O5	-	L2	glutamate degradation V (via hydroxyglutarate)	0.4588657	1.61396	0.039922
(R)-3-Hydroxyisobutyrate	104.0474	6.36	C4H8O3	-	L2	Synthesis and degradation of ketone bodies, Butanoate metabolism	1.9896751	1.426	0.0001958
[FA (24:0)]	366.3498	4.61	C24H46O2	-	L2	Fatty Acids and Conjugates	2.9080981	1.53879	6.364E-05
[PC (18:1/18:0)]	771.6142	5.23	C44H86NO7P	+	L2	Glycerophosphocholines	1.3434902	1.16075	0.0047806
[PC (18:1/20:4)]	793.5983	5.19	C46H84NO7P	+	L2	Glycerophosphocholines	1.2266434	1.18263	0.011226
[PE (18:1/18:1)]	729.5679	5.23	C41H80NO7P	+	L2	Glycerophosphoethanolamines	1.3716125	1.44945	0.0013425
[PE (18:1/20:4)]	751.5519	4.98	C43H78NO7P	+	L2	Glycerophosphoethanolamines	1.8162713	1.56562	0.0008069
[PE (18:1/16:0)]	745.5622	5.25	C41H80NO8P	+	L2	Glycerophosphoethanolamines	1.2464637	1.14849	0.0018658
Cer(d18:1/24:0)]	647.6217	5.08	C42H81NO3	-	L2	Ceramides	3.4769324	1.19891	0.024851
2-Dehydro-3-deoxy-L-rhamnonate	162.0528	10.83	C6H10O5	-	L2	Fructose and mannose metabolism	2.7364767	1.56051	7.236E-05
2-Isopropylmaleate	158.0579	9.62	C7H10O4	+	L2	Valine, leucine and isoleucine biosynthesis	0.4073122	1.69547	0.0008301
3-(4-Hydroxyphenyl)lactate	182.0580	8.59	C9H10O4	-	L2	Tyrosine metabolism	1.3139861	1.13373	3.863E-05
3-Dehydroxycarnitine	145.1102	6.15	C7H15NO2	+	L2	Lysine degradation	0.4012641	1.64648	0.0019279
5-Guanidino-2-oxopentanoate	173.0801	12.57	C6H11N3O3	+	L2	D-Arginine and D-ornithine metabolism	2.6067972	1.47798	6.278E-05
5-Hydroxy-L-tryptophan	220.0847	9.21	C11H12N2O3	+	L2	Tryptophan metabolism	15.440052	1.81415	4.12E-06
5-Methylcytosine	125.0589	10.30	C5H7N3O	+	L2	Pyrimidine metabolism	1.3362091	1.03866	0.0003178
9-Hexadecenoylcarnitine	397.3191	5.94	C23H43NO4	+	L2	Unkown	1.4004592	1.09065	0.0002782
Acetylcarnitine	203.1159	10.22	C9H17NO4	+	L1	Alanine and aspartate metabolism	0.3964063	1.69794	0.0025236
Acetyl-L-homoserine	161.0688	10.32	C6H11NO4	+	L2	Methionine metabolism, Sulfur metabolism	0.1205693	1.67246	0.0003508
Butanal	72.0575	5.63	C4H8O	+	L2	Butanoate metabolism	2.5094028	1.0095	0.023452
Butanoylcarnitine	231.1470	9.12	C11H21NO4	+	L2	Fatty acyl carnitines	0.4423101	1.6989	0.0011102
C14 Ceramide	509.4806	5.12	C32H63NO3	-	L2	Ceramides	3.4485921	1.72342	6.364E-05
Ceramide (d18:1/16:0)	537.5120	5.10	C34H67NO3	-	L2	Ceramides	3.9594337	1.53252	0.001163
Cer(d18:1/22:1)	619.5899	5.03	C40H77NO3	+	L2	Unkown	4.7441121	1.79543	0.0002108
Cer(d18:2/16:0)	535.4962	5.06	C34H65NO3	+	L2	Ceramides	3.2946682	1.81496	0.0005041
Ceramide (d18:1/18:0)	565.5435	5.10	C36H71NO3	-	L2	Ceramides	4.7293243	1.29817	0.015575
Ceramide (d18:1/22:0)	621.6068	5.10	C40H79NO3	-	L2	Ceramides	6.8365827	1.37832	0.01216
Ceramide (d18:1/24:0)	649.6385	5.10	C42H83NO3	-	L2	Sphingolipid metabolism	5.7565016	1.37038	0.012765
Cytidine	243.0854	11.26	C9H13N3O5	+	L2	Pyrimidine metabolism	3.7401287	1.33796	0.0029739

D-Alanyl-D-alanine	160.0847	8.59	C6H12N2O3	+	L2	Glycine, serine and threonine metabolism	0.1212499	1.30515	0.043204
D-Glucosamine	179.0793	11.92	C6H13NO5	+	L2	Aminosugars metabolism	3.0428155	1.01226	0.035371
D-Serine	105.0425	9.20	C3H7NO3	+	L2	Glycine, serine and threonine metabolism	0.3752761	1.8317	0.0008298
Glucosyl Ceramide (d18:1/16:0)	699.5656	5.22	C40H77NO8	+	L2	Sphingolipid metabolism	1.9820743	1.67088	0.0002726
Hypoxanthine	136.0384	10.48	C5H4N4O	+	L1	Purine metabolism	3.2251723	1.18439	0.011034
Inosine	268.0808	10.64	C10H12N4O5	+	L1	Purine metabolism	2.392361	1.44625	8.62E-05
L-4-Hydroxyglutamate semialdehyde	147.0531	9.09	C5H9NO4	-	L2	Arginine and proline metabolism	0.3720393	1.79681	0.0025224
L-Carnitine	161.1051	11.42	C7H15NO3	+	L1	Lysine degradation	0.2476222	1.73776	5.912E-05
L-Citrulline	175.0957	12.87	C6H13N3O3	+	L1	Arginine and proline metabolism	1.8081303	1.31619	8.928E-05
L-Formylkynurenine	236.0797	9.81	C11H12N2O4	+	L2	Tryptophan metabolism	0.2445689	1.70852	0.0016923
LPA(0:0/16:0)	410.2432	5.96	C19H39O7P	-	L2	Glycerophosphates	0.3112683	1.68082	0.0004082
LysoPC(20:4)	543.3319	5.84	C28H50NO7P	+	L2	Glycerophosphocholines	1.4114174	1.05496	0.012229
LysoPC(O-18:0)	509.3845	5.85	C26H56NO6P	+	L2	Glycerophosphocholines	0.3056905	1.67314	0.039922
LysoPE(20:4/0:0)	501.2855	5.65	C25H44NO7P	-	L2	Glycerophosphoethanolamines	1.4041255	1.37538	0.0002448
N6-Methyl-L-lysine	160.1211	18.13	C7H16N2O2	+	L2	Unkown	0.2418615	1.65213	0.004186
N-Acetyl-aspartyl-glutamate	304.0904	12.17	C11H16N2O8	+	L2	Unkown	0.3612467	1.49729	0.049634
N-Acetylserotonin	218.1055	6.34	C12H14N2O2	+	L2	Tryptophan metabolism	6.7770448	1.48859	0.0010383
PC (14:2/16:0)	689.5357	5.28	C38H76NO7P	+	L2	Glycerophosphocholines	1.4463718	1.61404	0.0006606
PC(18:3/20:2)	807.5778	5.20	C46H82NO8P	+	L2	Glycerophosphocholines	1.37197	1.32265	0.0033732
PC(18:4/16:0)	737.5365	5.01	C42H76NO7P	+	L2	Glycerophosphocholines	2.0685673	1.48334	0.0009997
PC(20:4/18:1)	791.5823	5.19	C46H82NO7P	+	L2	Glycerophosphocholines	1.211511	1.07465	0.0042565
PC(36:1)	787.6086	5.22	C44H86NO8P	+	L2	Glycerophosphocholines	1.3020443	1.19977	0.0008097
PC(36:5)	779.5462	5.22	C44H78NO8P	+	L2	Glycerophosphocholines	1.4370487	1.48023	0.0008097
PC(38:3)	811.6087	5.19	C46H86NO8P	+	L2	Glycerophosphocholines	1.648231	1.64426	0.0010716
PC(38:4)	809.5935	5.19	C46H84NO8P	+	L2	Glycerophosphocholines	1.6222362	1.59211	0.0013506
PC(40:6)	833.5931	5.17	C48H84NO8P	+	L2	Glycerophosphocholines	1.5343041	1.4549	0.0033732
PC(O-14:0/16:0)	691.5514	5.27	C38H78NO7P	+	L2	Glycerophosphocholines	1.2517243	1.30383	0.0006748
PE (18:1/22:6)	775.5513	4.96	C45H78NO7P	+	L2	Glycerophosphoethanolamines	1.9076807	1.55335	0.00084
PE(16:0/P-18:1)	701.5358	5.03	C39H76NO7P	+	L2	Glycerophosphoethanolamines	1.3339304	1.13595	0.0027997
PE(18:3/P-18:1)	723.5201	4.99	C41H74NO7P	+	L2	Glycerophosphoethanolamines	1.7448897	1.62812	0.0021401
PE(18:4/18:1)	721.5059	5.00	C41H72NO7P	+	L2	Glycerophosphoethanolamines	1.5626594	1.48152	0.0040577
PE(20:2/P-18:1)	753.5684	5.03	C43H80NO7P	+	L2	Glycerophosphoethanolamines	1.8470652	1.42235	0.0009797
PE(20:4/P-18:1)	749.5362	4.98	C43H76NO7P	+	L2	Glycerophosphoethanolamines	1.4448463	1.33537	0.0034652

PE(22:4/18:1)	777.5681	4.97	C45H80NO7P	+	L2	Glycerophosphoethanolamines	1.762977	1.41166	0.0020269
PE(38:1)	773.5937	5.22	C43H84NO8P	+	L2	Glycerophosphoethanolamines	1.4781266	1.34164	0.0004448
PE(38:4)	767.5469	4.98	C43H78NO8P	+	L2	Glycerophosphoethanolamines	1.4136741	1.25727	0.0027997
PE-NMe2(16:0/16:0)	719.5479	5.27	C39H78NO8P	+	L2	Glycerophosphoethanolamines	1.6099193	1.64099	0.0004816
Phenylacetylglycine	193.0741	5.94	C10H11NO3	+	L2	Phenylalanine metabolism	1.4676181	1.4675	0.0065423
PI(18:1/16:0)	836.5413	4.58	C43H81O13P	-	L2	Glycerophosphoinositols	1.7416124	1.24926	0.0004649
PI(22:3/18:3)	910.5575	4.57	C49H83O13P	-	L2	Glycerophosphoinositols	1.7390753	1.17829	0.0004835
Propanoylcarnitine	217.1314	9.60	C10H19NO4	+	L2	OxidationofBranchedFattyAcids	0.3544564	1.72163	0.0004816
PS(14:1/20:0)	761.5203	4.53	C40H76NO10P	+	L2	Glycerophosphoserines	1.5953295	1.0984	0.0020638
PS(18:0/20:3)	813.5521	4.57	C44H80NO10P	-	L2	Glycerophosphoserines	2.0028467	1.32271	0.0002223
PS(18:0/20:4)	811.5364	4.56	C44H78NO10P	+	L2	Glycerophosphoserines	1.9436778	1.33938	0.000124
PS(18:0/22:5)	837.5518	4.46	C46H80NO10P	+	L2	Glycerophosphoserines	1.7844548	1.39458	0.0001545
PS(20:0/16:1)	789.5518	4.54	C42H80NO10P	+	L2	Glycerophosphoserines	2.9874572	1.56878	0.0004082
PS(20:2/20:2)	839.5667	4.46	C46H82NO10P	+	L2	Glycerophosphoserines	1.7955461	1.39244	0.000223
PS(22:4/18:2)	835.5363	4.50	C46H78NO10P	+	L2	Glycerophosphoserines	2.0352945	1.39935	0.0003069
PS(22:4/22:6)	883.5361	4.43	C50H78NO10P	+	L2	Glycerophosphoserines	2.3844392	1.55085	6.216E-05
PS(34:0)	763.5362	4.46	C40H78NO10P	+	L2	Glycerophosphoserines	1.4068633	1.11855	0.0003265
SM(d16:1/18:0)	702.5672	5.48	C39H79N2O6P	+	L2	Ceramide phosphocholines (sphingomyelins)	1.2070616	1.43981	0.001459
SM(d18:0/18:1)	730.5986	5.43	C41H83N2O6P	+	L2	Ceramide phosphocholines (sphingomyelins)	1.5399486	1.33938	0.0007682
SM(d18:1/14:0)	674.5359	5.53	C37H75N2O6P	+	L2	Ceramide phosphocholines (sphingomyelins)	1.3565472	1.33905	0.0010327
SM(d18:1/24:1)	812.6769	5.37	C47H93N2O6P	+	L2	Ceramide phosphocholines (sphingomyelins)	1.3764327	1.04412	0.0010621
sn-Glycerol 3-phosphate	172.0136	10.62	C3H9O6P	-	L2	Glycerolipid metabolism, Glycerophospholipid metabolism	0.2566792	1.75052	0.0002695
Sphinganine	301.2980	8.57	C18H39NO2	+	L2	Sphingolipid metabolism	2.9761328	1.56024	0.0001958
Taurine	125.0146	12.57	C2H7NO3S	-	L1	Bile acid biosynthesis, Taurine and hypotaurine metabolism	0.3620067	1.57292	0.0076734
UDP	404.0022	12.08	C9H14N2O12P2	+	L2	Pyrimidine metabolism, Peptidoglycan biosynthesis, Zeatin biosynthesis	0.3100687	1.5728	0.017991
UDP-glucose	566.0546	12.05	C15H24N2O17P2	-	L2	Pentose and glucuronate interconversions_Galactose metabolism_ Glycerolipid metabolism	0.3000922	1.55475	0.01545
Unknown	251.1004	11.28	C9H17NO7	+	L2	Unkown	1.3673617	1.01578	0.0006361
Urate	168.0282	10.82	C5H4N4O3	-	L1	Purine metabolism	3.3611123	1.32579	0.0023349

Table 2.3: A list of 49 significantly changed metabolites in M2 macrophages with VIP >1 and FDR < 0.05 compared to M0 as a result of investigation M0, M1 and M2.

Putative metabolite	Mass	RT	FORMULA	Polarity	confidence	Pathway	Fold change	VIP	FDR
(R)-3-Hydroxyisobutyrate	104.0474	6.36	C4H8O3	-	L2	Synthesis and degradation of ketone bodies, Butanoate metabolism	1.4014654	1.34709	0.0064985
(R)-S-Lactoylglutathione	379.1049	9.83	C13H21N3O8S	-	L2	Pyruvate metabolism	1.4966868	1.42873	0.022049
[PC (14:0/14:0)]	677.4992	5.31	C36H72NO8P	+	L2	Glycerophosphocholines	1.8658495	1.96493	0.0048737
[PC (14:0/16:1)]	703.5147	5.28	C38H74NO8P	+	L2	Glycerophosphocholines	1.9080661	2.00081	0.004828
[PE (16:0)]	453.2852	5.78	C21H44NO7P	-	L2	Glycerophosphoethanolamines	1.2927405	1.24381	0.029212
[PE (18:1/18:1)]	729.5679	5.23	C41H80NO7P	+	L2	Glycerophosphoethanolamines	1.5093621	1.54137	0.020218
[PE (18:1/16:0)]	745.5622	5.25	C41H80NO8P	+	L2	Glycerophosphoethanolamines	1.3304285	1.51883	0.028836
[PI (18:1)]	598.3117	4.88	C27H51O12P	-	L2	Glycerophosphoinositols	1.5437296	1.59909	0.0014524
2-Dehydro-3-deoxy-L-rhamnonate	162.0528	10.83	C6H10O5	-	L2	Fructose and mannose metabolism	1.3335512	1.24689	0.049719
3-(4-Hydroxyphenyl)lactate	182.058	8.59	C9H10O4	-	L2	Tyrosine metabolism	1.5144459	1.48091	0.0023996
3-(4-Hydroxyphenyl)pyruvate	180.0423	8.52	C9H8O4	-	L2	Tyrosine metabolism	2.1960245	1.91781	0.00023885
3-Dehydroxycarnitine	145.1103	6.15	C7H15NO2	+	L2	LysineDegradation	3.4716562	1.84808	0.0077514
3-Hydroxypropanoate	90.0316	8.58	C3H6O3	-	L2	beta-Alanine metabolism	1.4665792	1.27702	0.013893
3-Oxopropanoate	88.016	8.58	C3H4O3	-	L2	inositol metabolism	1.3867007	1.25087	0.01065
4-Guanidinobutanoate	145.085	12.81	C5H11N3O2	+	L2	Arginine and proline metabolism	1.2743668	1.30255	0.0018806
4-Imidazolone-5-propanoate	156.0534	9.76	C6H8N2O3	+	L2	Histidine metabolism	2.0771499	2.09699	0.000063409
5-Guanidino-2-oxopentanoate	173.0801	12.57	C6H11N3O3	+	L2	D-Arginine and D-ornithine metabolism	1.7905876	1.59038	0.025214
5-Oxoproline	129.0426	12.30	C5H7NO3	+	L2	Arginine and proline metabolism	0.4249075	2.00896	0.0070659
Acetylcarnitine	203.1159	10.22	C9H17NO4	+	L1	Alanine and aspartate metabolism	1.5501257	1.7943	0.000063409
Alpha-CEHC	278.1517	4.65	C16H22O4	-	L2	Unkown	2.6792906	2.09007	0.000063409
cis-4-Hydroxy-L-proline	131.0581	6.39	C5H9NO3	-	L2	beta-Alanine metabolism	1.3354658	1.43019	0.0024831
D-Alanyl-D-alanine	160.0847	8.59	C6H12N2O3	+	L2	D-Alanine metabolism, Peptidoglycan biosynthesis	1.9421829	1.86698	0.0022883
D-Glucose	180.0634	13.68	C6H12O6	-	L2	Glycolysis / Gluconeogenesis, Pentose phosphate pathway, Galactose metabolism	1.4534073	1.60783	0.0065046
Ethanolamine phosphate	141.019	12.22	C2H8NO4P	+	L1	Glycine, serine and threonine metabolism, Glycerophospholipid metabolism, Sphingolipid metabolism	0.2154285	1.91923	0.0065046
L-Arabinonate	166.0478	10.45	C5H10O6	-	L2	Ascorbate and aldarate metabolism	0.4092484	1.943	0.0014846

L-Aspartate	133.0375	11.70	C4H7NO4	+	L1	Alanine and aspartate metabolism, Arginine and proline metabolism, Glycine, serine and threonine metabolism	0.357658	1.85773	0.033331
L-Citrulline	175.0957	12.87	C6H13N3O3	+	L1	Arginine and proline metabolism	1.4454629	1.39716	0.026857
L-Glutamine	146.069	12.40	C5H10N2O3	+	L2	Glutamate metabolism, Purine metabolism, Pyrimidine metabolism	0.4415041	1.98876	0.0068791
L-isoleucyl-L-proline	228.1475	8.45	C11H20N2O3	+	L2	Unkown	1.3438305	1.32193	0.037075
L-Threonine	119.0582	8.63	C4H9NO3	+	L2	Glycine, serine and threonine metabolism	1.7829006	1.71354	0.027182
LysoPC(20:1)	549.3791	5.75	C28H56NO7P	+	L2	Glycerophosphocholines	1.7051858	1.56413	0.042342
LysoPC(O-18:0)	509.3845	5.85	C26H56NO6P	+	L2	Glycerophosphocholines	1.8955321	1.79146	0.014839
LysoPE(0:0/18:1)	479.3009	5.68	C23H46NO7P	+	L2	Glycerophosphoethanolamines	1.4069216	1.43028	0.03756
N6,N6,N6-Trimethyl-L-lysine	188.1525	17.07	C9H20N2O2	+	L2	Lysine degradation	1.2700148	1.2452	0.0045426
N-Acetyl-L-aspartate	175.048	11.16	C6H9NO5	-	L2	Alanine and aspartate metabolism	1.9732171	1.76301	0.0065046
N-Acetyl-L-glutamate	189.0636	10.85	C7H11NO5	-	L1	Arginine and proline metabolism	3.5762347	1.7778	0.0046059
N-Acetylserotonin	218.1055	6.34	C12H14N2O2	+	L2	Tryptophan metabolism	3.0364009	1.73641	0.01704
Orthophosphate	97.9769	12.27	H3O4P	-	L2	Oxidative phosphorylation, Photosynthesis	0.5285257	1.79644	0.011852
PC (14:2/16:0)	689.5357	5.28	C38H76NO7P	+	L2	Glycerophosphocholines	1.925988	1.82917	0.0046059
PC(O-14:0/16:0)	691.5514	5.27	C38H78NO7P	+	L2	Glycerophosphocholines	2.1274348	1.82917	0.0076202
PC(P-20:0/0:0)	535.3997	5.66	C28H58NO6P	+	L2	Glycerophosphocholines	3.9908331	1.76311	0.013893
PE-NMe2(16:0/16:0)	719.5479	5.27	C39H78NO8P	+	L2	Glycerophosphoethanolamines	1.552891	1.65126	0.021553
PG(20:4/18:0)	798.5411	4.41	C44H79O10P	-	L2	Glycerophosphoglycerols	1.4318493	1.12465	0.047803
SM(d16:1/18:0)	702.5672	5.48	C39H79N2O6P	+	L2	Ceramide phosphocholines (sphingomyelins)	1.3565023	1.57145	0.01704
SM(d18:1/14:0)	674.5359	5.53	C37H75N2O6P	+	L2	Ceramide phosphocholines (sphingomyelins)	1.6109135	1.80329	0.0062761
sn-Glycerol 3-phosphate	172.0136	10.62	C3H9O6P	+	L2	Glycerolipid metabolism, Glycerophospholipid metabolism	0.469526	1.79171	0.03959
Succinyl-L-homoserine	219.0742	10.84	C8H13NO6	-	L2	Methionine metabolism, Sulfur metabolism	1.3171557	1.28564	0.016311
Taurine	125.0146	12.57	C2H7NO3S	-	L1	Bile acid biosynthesis, Taurine and hypotaurine metabolism	0.2848399	1.97174	0.00093585
Vinylacetylglycine	143.0582	8.60	C6H9NO3	+	L2	Unkown	1.3758858	1.69191	0.0074154

Chapter Three

3. Investigation of the metabolic functional plasticity of macrophages using untargeted LC-MS metabolomics

3.1. Introduction

Orchestrating innate and adaptive immunity is a complex process, whereas the host defence must be promoted and the maladaptive collateral cell damage must be limited. Nowadays, it is increasingly evident that specialised immune cells such as macrophages and dendritic cells must undergo phenotypic alteration to maintain homeostasis by serving appropriate functions in discrete context (361). Macrophages are highly plastic and heterogeneous cells that play a fundamental role with unique functions in homeostasis and immunity, both innate and adaptive (130, 131). In the last two decades, much work has been performed on the description of macrophages subsets. Phenotypes of activated macrophages are defined and described based on their biology and functions. Accordingly, two major populations of macrophages with distinct functions represent the extreme of a wide spectrum of macrophage activation states: pro-inflammatory M1 macrophages (classically activated macrophages) and anti-inflammatory M2 macrophages (alternatively activated macrophages) (105, 108, 131, 140). However, observations acquired from the implication of macrophages in cancer or chronic inflammation demonstrated a much wider spectrum of macrophages depending on the signals received from the microenvironment (135, 141, 142). In this context, M2 macrophages have been rapidly expanded to encompass further subsets such as M2a, M2b and M2c (105). Three functions have been proposed for macrophages: host defence, tissue repair and immune regulation. Given this functional classification, regulatory macrophages (Mreg) have emerged as a third population. This functional plasticity of macrophages can be shown in the colour

wheel (Figure 3.1), where the three primary colours designating the main functional populations of macrophages. Red represents classically activated macrophages, yellow represents wound healing macrophages, and blue represents regulatory macrophages. For secondary colours, such as green, orange or purple in the colour wheel, further macrophage populations can be evolved that can share characteristics of more than one of the main macrophage populations, resulting in a wider spectrum of functional macrophage populations (108).

In fact, many different macrophage subsets have not yet been identified, and may constitute a broad spectrum of the population according to function (105, 108). Nevertheless, the extent of such functional plasticity and the underlying mechanisms that govern the phenotypic alteration remain not fully understood (205).

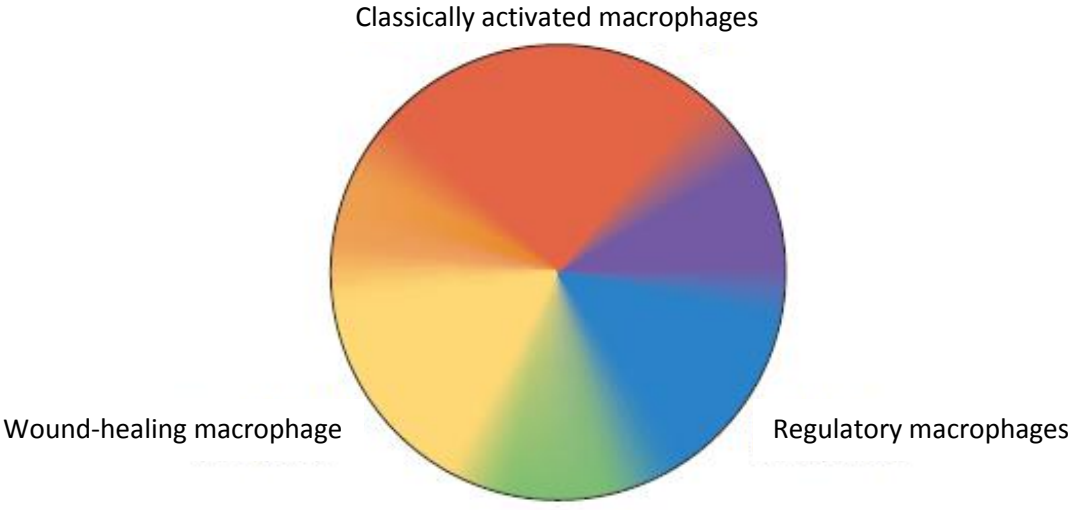


Figure 3.1: Colour wheel of macrophage activation (109). A broad spectrum of macrophages is demonstrated where the primary three colours illustrate the main three activation states; classically activated macrophages(M1) (red), wound healing (M2 or alternatively activated) macrophages (yellow) and regulatory macrophages (Mreg) (blue).

As mentioned above, macrophages are highly plastic cells that can change their phenotype in response to different environmental cues, such as pathogens or biological processes (362). Therefore, the polarisation of macrophages has evolved as a key area in understanding disease pathogenesis, inflammation and tissue homeostasis (131, 133, 135, 363). However, macrophages can be polarised or change their phenotype in different ways, depending on exposure to endogenous or exogenous factors (361). Resting macrophages (naïve macrophages, M0) can be polarised to the M1 macrophage phenotype by exposure to granulocyte macrophage colony-stimulating factor (GM-SCF), Th1 cytokines such as interferon gamma (IFN-γ) and tumour necrosis factor alpha (TNF-α), and other toll-like receptor (TLR) ligands such as Gram-negative bacterial lipopolysaccharide (LPS) (105, 129, 140, 159, 312, 364, 365). The M2 macrophage phenotype can be induced by encountering resting macrophages with macrophage colony-stimulating factor (M-CSF), or Th2 cytokines like IL-4 or IL-13 (105, 129, 140, 159, 312, 364, 365). In addition, regulatory macrophages can be generated by IL-10, transforming growth factor beta (TGF-β), or corticosteroids (105, 146). Based on functional classification, M1 macrophages are key players against infectious microbes such as bacteria and viruses, and against tumour progression. M2 macrophages play a crucial role in wound healing, tissue repair and in response to parasite infections. However, regulatory macrophages (deactivated macrophages, Mreg) are considered as suppressor macrophages that terminate inflammatory immune responses to avoid the immunopathological consequences of excessive and prolonged M1 macrophage responses (159, 366), such as chronic inflammation, leading to several autoimmune diseases (174).

Moreover, regulatory macrophages play a crucial role in inducing tolerance of organ transplants (367).

As mentioned in section 1.2.2, M1 macrophages are characterised by their ability to secrete high levels proinflammatory cytokines, such as TNF-α, IL-12, IL-1β, and IL-6 (368). They play a crucial role in enhancing phagocytic activity and the ability to clear invading pathogens (149). The microbicidal activity of M1 is mediated by various mechanisms, such as acidification of the phagosome, ceasing of iron and nutrients for the invading microorganisms, and synthesis of nitric oxide (NO) and reactive oxygen species (ROS) (369-371).

Similarly, M2 polarised macrophages can be developed as a response to innate or adaptive immunity cues such as IL-4 and other granulocytes which are released during tissue injury (156). Additionally, M2 macrophages can be developed against fungi and parasite, in response to their structural biopolymer, chitin (157). *In vitro*, IL-4 and/or IL-13-induced M2 macrophages were unsuccessful presenting antigen to T cells, with a minimal amount of pro-inflammatory cytokines being produced. Therefore, there is no production of toxic NO or ROS which are responsible for bacterial killing and pathogen clearance (345, 372). Nevertheless, the primary function of M2 macrophages is related to tissue repair and wound healing by stimulating arginase activity leading to producing ornithine from arginine, which is the precursor of secretion of the component of collagen and polyamines, resulting in production of the component of extracellular matrix (158, 373).

Regulatory macrophages, as well as M1 and M2 macrophages, are developed in response to innate and adaptive immunity. They form in the later stages of adaptive immunity and attenuate the immune response and terminate inflammation (168, 169). Various ways to generate regulatory macrophages have been reported. For example, *in vitro* stimulation with a TLR agonist in the presence of immunoglobulin G immune complexes gives rise to regulatory macrophages producing high levels of immunosuppressive cytokines (170). Apoptotic cells (154) and other molecules can induce the generation of regulatory macrophages such as prostaglandin (171) and IL-10, TGF-β, or corticosteroid (105). They are all characterised by high production of IL-10 and TGF-β, and low production of IL-12 (108, 170). Although regulatory macrophages have previously been classified as M2, subtle differences between the two type have been described. For instance, regulatory macrophages can present the antigen to T cells and do not contribute to extracellular matrix production (372). Moreover, there are functional differences between subsets of regulatory macrophages based on the stimulator which induces their polarisation (108). Additionally, as discussed earlier in section 1.2.3, the different phenotypes of macrophages are associated with several diseases resulting, mainly, from disturbance of the balance of macrophages subsets (174). Therefore, the identification of biomarkers for each subset targeted by specific therapeutics has become of high importance (108).

This plasticity of macrophage phenotypes plays a critical function in maintaining homeostasis (361). Switching from M1 to M2 is important in termination of excessive inflammation reactions. However, switching from M2 to M1 dampens the bactericidal properties and triggers the resolution of inflammation.

Macrophages can shift their functional phenotypes reversibly in response to changes in cytokines in their micro-environment (such as IFN-γ, IL-4, IL-10) or in response to other stimulants (such as lipopolysaccharide(LPS)) (374). Also, longevity and stability of polarised macrophages have been investigated extensively and they suggest that macrophage phenotypes change over time. However, the mechanism has not been well defined, as no clear evidence shows whether this change is because the polarised macrophages are switched to the resting state, or a new population of macrophages migrates to the tissue site and replaces the original polarised cells (108).

Although numerous genomic studies have investigated macrophage polarisation in response to a variety of stimuli (TLR ligands, bacteria, M1 or M2 promotors), no studies have shown the successful construction of new and comprehensive models of a macrophage polarisation spectrum (375-378). Transcriptomics gives useful insight into the function and regulation of immune cells. For instance, Miller et al and Gautier et al have produced datasets defining the main transcriptional profile in dendritic cells and murine macrophages, respectively, under steady state (379, 380). Other studies on molecular interactions between different proteins of the immune system provided mechanistic insights into immune cell function. However, differences in the genetic background of mice and the stimulation condition were the challenges in these transcriptomic studies (381, 382). Additionally, the subtle difference between gene profiles from mice and human's immune cells is another challenge (383, 384). Unfortunately, it remains not fully understood how polarisation of immune cells, macrophages particularly, is transcriptionally regulated (137).

Recently, cell metabolism regulation and its pivotal role in the immune system have been recognised and attracted more attention (385, 386). Immune responses including immune cell differentiation (387), antigen presenting (388) and the immune system role in tissue repair (389) have been shown to be directly linked to cell metabolism. Therefore, the role of the immune system in regulating whole body metabolism has become increasingly of interest (390). In regard to macrophages, it has been shown that phenotypic changes are driven by alterations in the metabolic environment (391). Both macrophages and dendritic cells undergo extensive metabolic reprogramming as a response to microenvironmental signals, such as pathogens, cytokines or hypoxia (392). As aforementioned, macrophages display high heterogeneity with diverse subsets (M1, M2 and Mreg). The unique metabolic programming of each subset is believed to produce distinct metabolic profile which are effectively regulated by its function, surface marker expression and cytokine release (392, 393). To date, the immune metabolic base of diverse macrophage subsets has not been fully explored (359). Therefore, it remains to be fully investigated how activation of human macrophages is metabolically controlled.

Metabolomics can provide a quantitative and qualitative description of the metabolites which represent the end products of cellular processes or metabolic activities of a cell (5, 6). It describes the changes in the metabolic pathways occurring in response to various pathophysiological conditions or exposure to different stimuli (e.g. drugs, toxins, or pathogens). Therefore, metabolomics provides valuable metabolic information and the insight into cellular phenotype

and biochemistry of living systems, and is complementary to genomics, transcriptomics and proteomics (6, 11).

Untargeted metabolomics using liquid chromatography (LC)-mass spectrometry (MS) is a promising approach for identifying and quantifying metabolites in biological samples because of its high sensitivity and specificity (394). Several studies have implied the importance of analysing metabolic networks in macrophages (378, 395). These studies demonstrate how the analytical and technological advances can contribute to exploring the structurally complex network in immune cells (139). Untargeted LC-MS metabolomics has been widely used for disease diagnostic biomarker discovery (396) and evaluation of drug toxicity (21). Moreover, it has been used in immunometabolism field for linking changes in metabolites during important immune cell processes to their functions (397). LC-MS metabolomics has been applied to study stem cell differentiation (398), immune cells activation (399), and autoimmune diseases (400) Several studies have used metabolomics to characterise mice macrophage subsets revealing some characteristic metabolic pathways such as glycolysis, the pentose phosphate pathway (PPP) and glutamine metabolism (224-227). Unfortunately, all these studies focused only on classically activated and/or alternatively activated macrophages without investigating the metabolic profile of regulatory macrophages. Moreover, the plasticity and stability of macrophage phenotypes over time has not been fully understood. The plasticity and stability play a critical role in monitoring several pathological conditions such as in tumour where M1 is changed to M2 over time, promoting tumour progress (401). Also, switching from M2 to M1 phenotype protects from allergic and asthmatic reactions, whereas

switching from M1 to M2 phenotype protects from excessive inflammation (402, 403). Some bacteria induce switching from M1 to M2 phenotype to avoid the bactericidal function of M1 macrophages. For example, *Yersinia enterocolitica* induces the production of TGFβ1 and IL-4 and activation of Arg-1 (hallmarks of M2 phenotype) in mice macrophages (404).

In this study LC-MS metabolic profiling of the human THP-1 cell line was conducted to characterise three main functional macrophage subsets (i.e. M1, M2 and Mreg). In addition to shedding light on the stability of these phenotypes by investigating the stability of polarised macrophages to M1 and M2, we investigated their plasticity by the ability to change their phenotypes in response to environmental changes by being exposed to opposite polarising cytokines. Our data showed distinct metabolic profiles of M1 or M2 compared to M0, whereas Mreg and M0 showed similar metabolic profiles. Furthermore, M1 phenotype showed higher stability than M2 against environmental changes. These results showed that LC-MS metabolomics identified metabolites implicated in macrophage phenotype according to individual pathological conditions, and that their phenotypes could be manipulated by targeting metabolic pathway with novel strategies.

3.2. Materials and methods

3.2.1. Materials

THP-1 cell line was purchased from ATCC, USA. RPMI 1640 medium, phosphate buffered saline (PBS) and *E. coli* lipopolysaccharide were purchased from Sigma-Aldrich, UK. GM-CSF, M-CSF and IL-4 were purchased from Miltenyi Biotec,

Germany. IFN-γ, TGF-β and IL-10 were purchased from R&D Systems, USA. Methanol and acetonitrile were purchased from Fisher Scientific, UK. All solvents were LC-MS grade.

3.2.2. Methods.

3.2.2.1. Culture of THP-1 cells.

Human THP-1 cells were cultured and differentiated as previously described in (159). Briefly, THP-1 cells were grown in RPMI 1640 supplemented with 10% heat-inactivated fetal bovine serum (FBS), 1% L-glutamine, and 1% penicillin-streptomycin. Cells were then incubated at 37 °C and 5% CO_2.

3.2.2.2. Differentiation of THP-1 cells.

THP-1 cells were differentiated into naïve macrophage-like state (M0) by treating with phorbol-12-myristate-13-acetate (PMA). Six million cells were seeded per flask (T25 tissue culture flask), and then the cells were grown in media containing 50 ng/ml of PMA and incubated for 24 h. The PMA-containing media then was removed and replaced with fresh complete media for further 24 h incubation.

3.2.2.3. Polarisation of THP-1 macrophages.

After 24 h resting period, the cells were treated with either 50ng/ml GM-CSF, 100 ng/mL LPS and 20 ng/mL IFN-γ to generate M1 cells, 50 ng/mL M-CSF and 20 ng/mL IL-4 to generate M2 cells or 10 ng/ml IL-10 and 10 ng/ml TGF-β to generate Mreg cells and incubated for 72 h . This protocol was adapted from the previous study described in (312). Unpolarised naïve macrophages (M0) were used as controls. Six replicates for each condition were prepared.

3.2.2.4. Challenging M0 and Mreg with LPS.

After 72 h of incubation, both M0 and Mreg cells were treated with 100 ng/ml LPS for 24 h to generate M0-LPS and Mreg-LPS. Six replicates of each condition were prepared.

3.2.2.5. Macrophage plasticity and stability investigation

To investigate the plasticity and stability of macrophages after polarisation into M1 and M2 (section 3.2.2), M1 macrophages were exposed to M2 polarising agents (50ng/ml M-CSF and 20 ng/ml IL-4) and incubated for 24 h or 48 h to generate M1-M2-24 or M1-M2-48, respectively. Also, M2 macrophages were exposed to M1 polarising agents (50 ng/ml GM-CSF, 100 ng/ml LPS and 20 ng/ml IFN-γ) and incubated for 24 or 48 h to generate M2-M1-24 or M2-M1-48, respectively. Six replicates of each condition were prepared.

3.2.2.6. Sample preparation and metabolite extraction.

After the incubation time, the media containing PMA and polarising agents were removed. The cells were then washed once with 500 µl pre-warmed PBS (37 °C) and pre-cooled methanol at -48 °C was used for metabolism quenching and metabolite extraction. The cells were harvested using a plastic scraper whilst being kept on ice and the extracts were transferred into pre-cooled fresh tubes (4 °C). The cell extracts were vortexed for 1 h and centrifuged at 16,100 ×g for 10 min at 4 °C. After the centrifugation, the supernatants were transferred into pre-cooled fresh tubes (4 °C) and they were then dried under vacuum and reconstituted with 70 µl of methanol. The samples were stored at -80 °C prior to LC-MS analysis. To

assess the instrument performance, an intrastudy quality control (QC) sample was prepared by mixing an equal volume of all the samples.

3.2.2.7. Analytical technologies.

LC-MS-based metabolite profiling was performed on an Accela system coupled to an Exactive MS (Thermo Fisher Scientific, Hemel Hempstead, UK) operating with electrospray ionisation (ESI) running in the negative (ESI-) and positive (ESI+) modes as previously described in (314). Briefly, the spray voltage was 4500 V (ESI+) and 3500 V (ESI-), the capillary voltage was 40 V (ESI+) and 30 V (ESI-), tube lens voltage was 70 V for both modes and skimmer voltage was 20 V (ESI+) and 18 V (ESI-). The temperature for capillary and probe was maintained at 275 °C and 150 °C, respectively. Chromatographic separation was carried out using ZIC-pHILIC (4.6 x 150 mm and 5 µm particle size, Merck Sequant). The mobile phase composed of 20 mM ammonium carbonate in water (solvent A) and 100% acetonitrile (solvent B). Metabolites were separated according to a linear gradient as following: 0-15 min (20% A), 15-17 min (95% A), and 17-24 min (20% A) at 300 µl/min flow rate. The injection volume of 10 µl and the column was kept at 45 ^{o}C.

3.2.2.8. Data processing and metabolites identification.

To process raw data obtained from LC-MS, XCMS and mzMatch were used for untargeted peak-picking and peak matching, respectively (69, 70). IDEOM was employed for putative metabolite identification and noise filtering with default parameters (315). Briefly, RT for identification of authentic standards was 5%, RT for identification for calculated RT was 50%, mass accuracy for mass identification was 3 ppm. Metabolites were identified with two levels of confidence; level 1 (L1)

identification by matching retention times and accurate masses of authentic standards and level 2 (L2) identification when the predicted retention times were employed due to the lack of standards according to the metabolomics standards initiative (75, 405). Pre-processed data were analysed by performing multivariate and univariate analysis. Orthogonal partial least squares-discriminant analysis (OPLS-DA) was carried out by SIMCA-P v13.0.2 (Umetrics, Umea, Sweden) as a supervised multivariate model. This multivariate analysis was used as the first step for visualising data with sample classes and evaluating the metabolome changes in macrophages subtypes groups. The key mass ions representing potential biomarkers were determined based on VIP values obtained from two-way orthogonal comparisons. Mass ions with VIP values greater than one were considered as discriminant biomarkers (324). Univariate analysis was also performed in parallel to multivariate analysis to identify significant mass ions. T-test with FDR correction was performed using MetaboAnalyst (24) to determine the significantly changed mass ions between M0 and M1, M2 or Mreg in the first part, between M0 and M0-LPS or Mreg-LPS in the second part, between M1 and M2-M1-24 or M2-M1-48, and between M2 and M1-M2-24 or M1-M2-48 in the third part. MetaboAnalayst and the Kyoto Encyclopaedia of Genes and Genomes (KEGG) database were used to analyse and visualise the affected pathway. Results and discussion.

3.3. Results and discussion

3.3.1. Macrophages polarisation

3.3.1.1. Macrophages characterisation

As mentioned earlier, macrophages display a wide range of functional phenotypes in response to environmental cues. Naïve THP-1 (M0) macrophages were treated with GM-CSF, LPS and a Th1 cytokine, IFN-γ. To generate M2 macrophages, M0 cells were treated with M-CSF and a Th2 cytokine, IL4 whereas IL-10 and TGF-β have been used to generate Mreg macrophages. These biomolecules have been reported to polarise macrophages into M1, M2, Mreg cells (105, 217, 316). To find out the surface phenotypes of M1 and M2 macrophages, immunofluorescence staining for calprotectin and mannose receptor (MR), which are evident to be markers for M1 and M2 cells, respectively (317), was carried out. As shown in Figure 3.2, consistent with chapter two section 2.3.1 and the literature (317), M1 cells significantly expressed higher levels of calprotectin and lower levels of MR compared to M2 and M0 cells. On the other hand, M2 cells significantly expressed the highest level of MR with very low calprotectin expression. Additionally, an enzyme-linked immunosorbent assay (ELISA) was used to analyse the cytokine and chemokine profiles of polarised macrophages. The levels of cytokines and chemokines in the supernatants collected from the macrophage subsets were analysed. M1 macrophages showed a significantly higher level of pro-inflammatory cytokines, IL1β and TNF-α compared to M0 and M2 macrophages. On the other hand, CC chemokine ligand 18 (CCL18) was expressed significantly higher in M2 compared to M0 and M1 macrophages (Figure 3.3). These results confirm the efficiency of our polarisation approach in inducing distinct M1 and M2

phenotypes. M1 macrophages were characterised by a significant amount of pro-inflammatory markers secreted such as IL1β and TNF-α (368), whereas CCL18 has been deemed a marker for M2 macrophages (406). Regarding Mreg macrophages, Figure 3.4 demonstrated significantly increased expression of TGF-β in Mreg macrophages compared to M0, M1 and M2 macrophages, as expected since Mreg macrophages are defined by secreted TGF-β (108, 407).

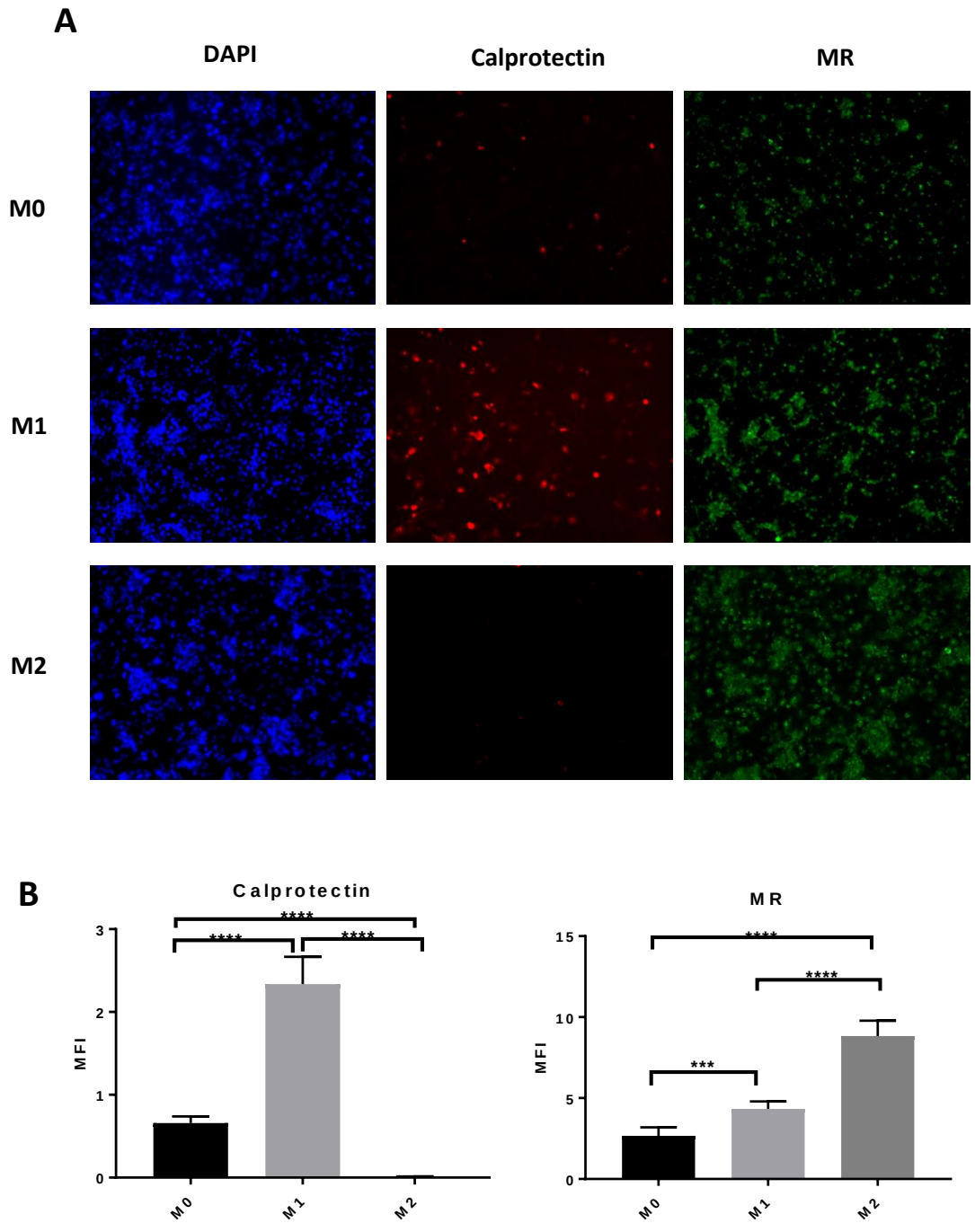


Figure 3.2: Expression of surface markers by cytokine polarized THP-1 macrophages. A) Immunofluorescent images of showing mannose receptor (green) and calprotectin (red) expression; nuclei were stained with DAPI (blue). Scale bar = 100 µm..B) Mean fluorescent intensities of M1, M2 and M0 cells. *** P ≤ 0.001, **** P ≤ 0.0001. Data are presented as mean ± SD (n=6).

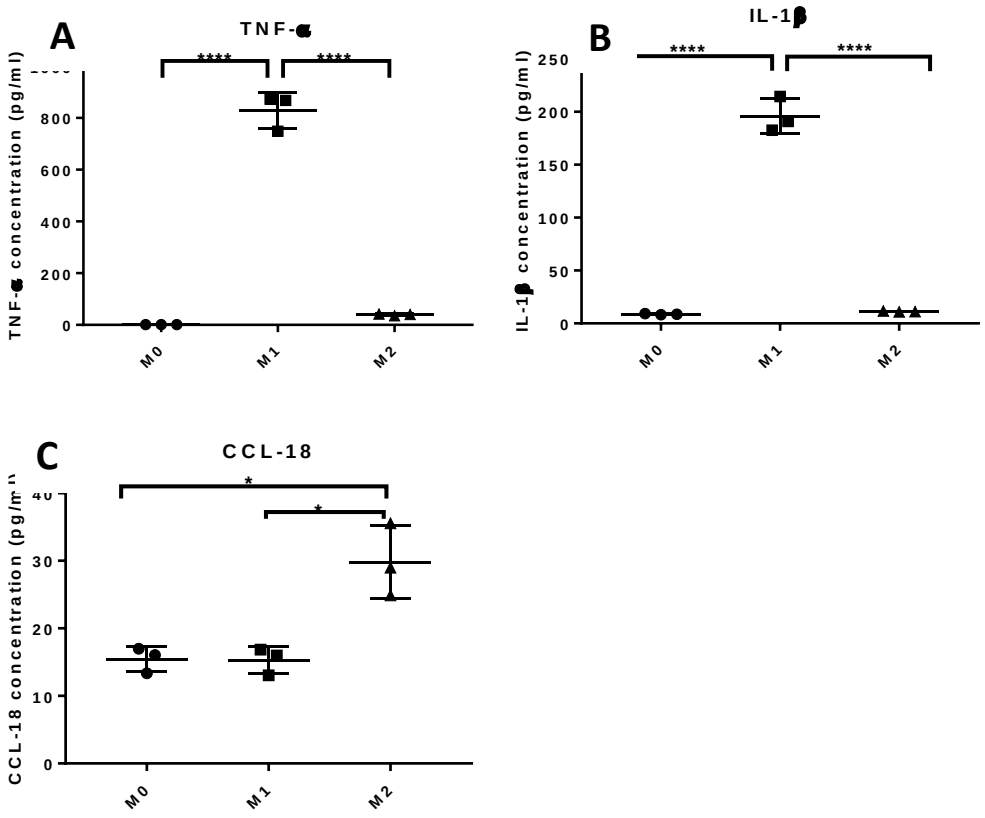


Figure 3.3: Cytokine expression by M0, M1 and M2 macrophages. A) TNF-α, B) IL-1β, C) CCL-18 expression. * P ≤ 0.05, **** P ≤ 0.0001. Data are presented as mean ± SD (n=3).

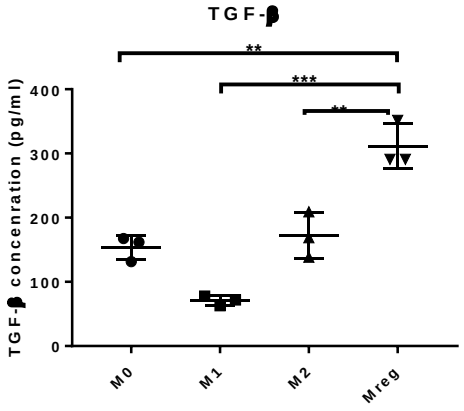


Figure 3.4: Cytokine expression by M0, M1, M2, and Mreg macrophages of TGF-β. As TGF-β and IL-10 are used to generate Mreg, 10 ng/ml TGF-β and 10 ng/ml Il-10 in complete media were analysed by ELISA and the obtained concentration was deduced from Mreg samples to get the concentration of TGF-β produced by Mreg upon polarisation. . ** P ≤ 0.01, *** P ≤ 0.001. Data are presented as mean ± SD (n=3).

3.3.1.2. Features selection.

As a result of processing data and using IDEOM for identification, a total of 405 metabolites were putatively identified (Appendix, Table A2). In order to investigate and visualise the inherent metabolic differences of M0, M1, M2 and Mreg macrophages, the pre-processed data were imported to SIMCA-P (version 13.2) to carry out multivariate analysis. OPLS-DA (supervised multivariate analysis) was performed to discover the discriminative mass ions. Figure 3.5A shows a OPLS-DA scores plot which illustrates the tight clustering of six replicates within each group with R^2 and Q^2 values of 0.854 and 0.975, respectively. Moreover, Figure 3.5A shows a clear separation between M0 and M1 or M2 indicating different metabolic profiles for each of M0, M1 or M2 macrophages. However, no clear separation is shown between M0 and Mreg macrophages, which could imply similar metabolic profiles of these phenotypes. To find out which ions were responsible for the separation between groups of interest, a two-way comparison of OPLS-DA model was carried out and shown in Figure 3.5 (B, C and D). The mass ions were ranked according to their VIP values to identify the most discriminative ions. As mentioned earlier in section 2.3.3, the mass ions with VIP > 1 were considered as potential biomarkers (324). Independent univariate analysis, t-test with FDR correction was performed, accompanied by the multivariate analysis. Most significantly changed mass ions were selected based on VIP > 1 and FDR < 0.05.

Figure 3.5B illustrates a OPLS-DA scores plot that shows a clear separation between M0 and M1 macrophages with R^2 and Q^2 values of 0.812 and 0.990, respectively, demonstrating an acceptable and valid model (324). After

performing univariate analysis in parallel, 82 metabolites with VIP > 1 and FDR < 0.05 were identified as significant key metabolites (Table 3.1). Similarly, the OPLS-DA scores plot in Figure 3.5C shows a clear separation between M0 and M2 macrophages with R^2 and Q^2 values of 0.702 and 0.992, respectively, indicating the validity of the model. 74 metabolites were revealed as significant key metabolites for M2 (VIP > 1 and FDR < 0.05) (Table 3.2). However, a two-way comparison by OPLS-DA scores plot shows the separation between M0 and Mreg with R^2 and Q^2 values of 0.504 and 0.960, respectively. Fewer metabolites were significantly changed between M0 and Mreg (46 metabolites) (Table 3.3) compared to the previous two comparisons. However, only one metabolite showed a fold change greater than 1.5 (increasing or decreasing) indicating the similarity in the metabolic profile between M0 and Mreg macrophages (Figure 3.5D)

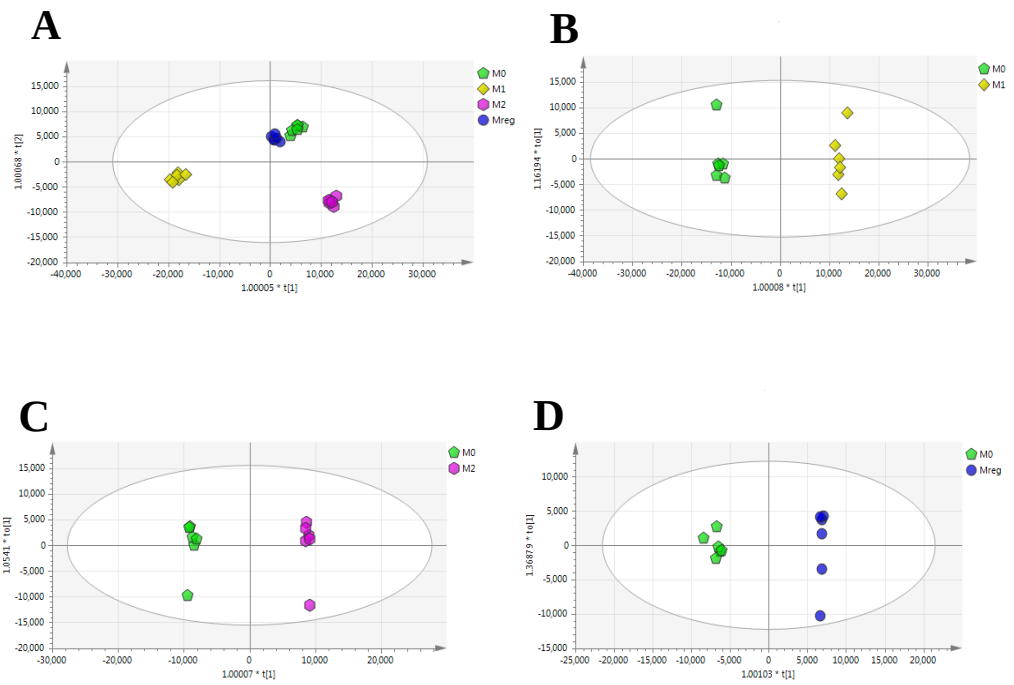


Figure 3.5: OPLS-DA scores plots of macrophage extracts after polarisation toward M1, M2 and Mreg states and their corresponding unpolarised (M0) controls. (A) M1, M2 and Mreg macrophage samples and their respective unpolarised controls (R^2 = 0.854 and Q^2 = 0.975). (B) Two-way orthogonal comparison between M0 and M1 (R^2 = 0.812 and Q^2 = 0.99). (C) Two-way orthogonal comparison between M0 and M2 (R^2 = 0.702 and Q^2 = 0.992). (D) Two-way orthogonal comparison between M0 and Mreg (R^2 = 0.504 and Q^2 = 0.960). M0 (green pentagons), M1 (yellow diamonds), M2 (pink hexagons) and Mreg (dark blue circles). n=6.

3.3.1.3. Pathway analysis

To further investigation to identify the metabolic pathways significantly altered by macrophages polarisation states, the characteristic key metabolites for each phenotype have been explored. In line with what was revealed in Chapter two, M1 and M2 macrophages showed a distinct metabolic profile that was distinguished by several significant characteristic key metabolites

In agreement with the first chapter section 2.3.4, 5-hydroxy-L-tryptophan (an intermediate in tryptophan metabolism pathway), Ceramide (d18:1/16:0) (an intermediate in sphingolipid metabolism), cytidine (an intermediate in pyrimidine metabolism pathway) (Figure 3.6) and other intermediates in glycerophospholipid

(GLs) metabolism (Table 3.1) show significant increase upon polarisation into M1 phenotype. Also, a significant increase in 5-hydroxyindoleacetaldehyde, an intermediate in the tryptophan metabolic pathway, were demonstrated (Figure 3.7). Tryptophan metabolism plays an appreciated role in inflammatory responses associated with several pathological conditions (347). Furthermore, its role in innate immunity in attracting mast cells to inflammation site has been reported by Tarique et al (348). However, it was reported with boosting phagocytosis in murine macrophages (349). Regarding the increase in GLs, it was discussed earlier in section 2.3.4 that GLs are involved in several biological processes including inflammation and cell differentiation (328). Moreover, lipid metabolism in general has an important role in maintaining M1 and M2 functions by meeting energetic requirements and modulating membrane fluidity (327).

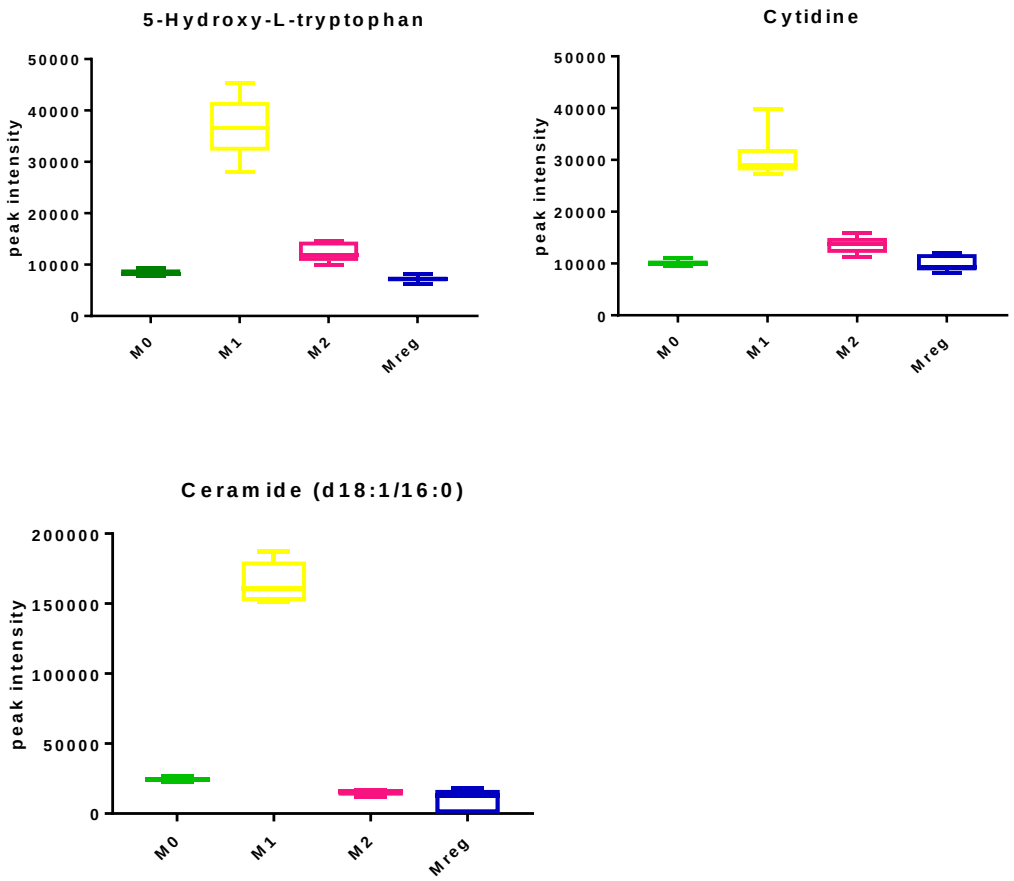


Figure 3.6: Box and whisker plots for significantly increased metabolites in M1 macrophages. Significant increase in these metabolites; 5-hydroxy-l-tryptophan (Ceramide (d18:1/16:0); and cytidine, indicates enhanced activity of their corresponding pathways as characteristic for M1 macrophages, representing tryptophan metabolism, sphingolipids metabolism, and pyrimidine metabolism respectively. The whiskers illustrate minimum to maximum and the line in the box represent the median. n=6

Deoxyadenosine, adenosine, and hypoxanthine were, also, characteristically increased in M1 macrophages (Figure 3.7). These purines showed a significant increase with high fold changes (6.41, 4.54 and 4.39 respectively). Purines along with pyrimidines are key components in the production of RNA and DNA (408). They have a crucial role in energy generation (e.g., ATP). Moreover, they act as a signal metabolite that contributes to sugar transport and cell growth control (342, 409). The activation of macrophages toward the M1 phenotype, as mentioned

earlier in section 3.3.1.1, induces a metabolic switch from oxidative phosphorylation to glycolysis, enhanced PPP and decreased tricarboxylic acid (TCA) cycle activity (31, 226, 410). The enhancement of PPP activity increases the production of pyrimidines and purines, which consequently can be used for the activated cell biosynthesis and provide NADPH, which is the substrate for NADPH oxidase, to produce ROS (343) that act as a bacterial killing mechanism (345). Although no significant change was shown in PPP, our results showed a significant increase in purines (deoxyadenosine, adenosine, and hypoxanthine), which agrees with section 2.3.4 that showed a significant increase in purines such as hypoxanthine and inosine. Furthermore, adenosine has been reported to have synergistic effects with LPS to enhance lactate production implying the role of adenosine in promoting LPS-induced glycolysis increase (411). Also, hypoxanthine was reported to be increased in the presence of LPS (344). In purine metabolism pathway, hypoxanthine is converted to xanthine, by the enzyme xanthine oxidase, producing the ROS, H_2O_2 as a by-product (412). Also, a previous study showed that the purine analogue (6-N-hydroxylaminopurine) has antibacterial and antiviral activity (346). AL-Janabi et al, in another study, demonstrated the antibacterial activity of the purine and caffeine against *Staphylococcus aureus* and *Bacillus subtilis* (413) where the clearance of pathogens such as bacteria is the responsibility of M1 macrophages (159). Our results show increase in the levels of purines in Figure 3.7.

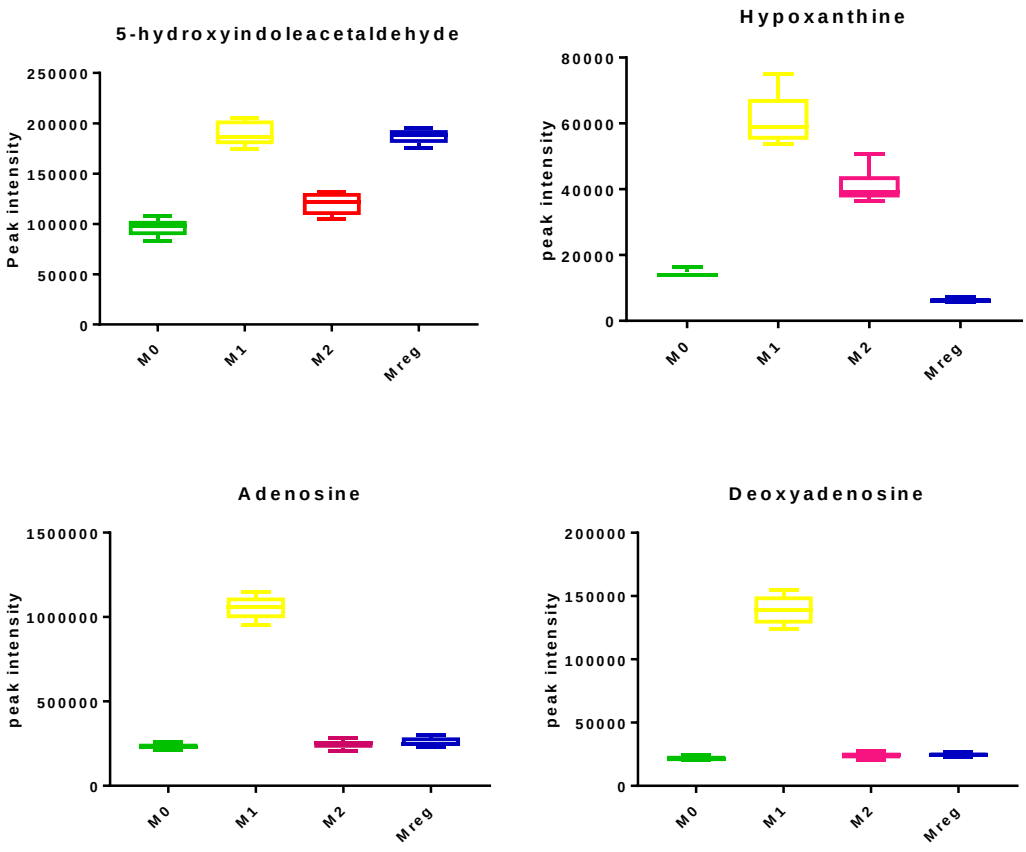


Figure 3.7: Box and whisker plots for significantly increased metabolites in M1 macrophages. Significant increase in these metabolites; 5-hydroxyindoleacetaldehyde; hypoxanthine, adenosine and deoxyadenosine, indicates enhanced activity of their corresponding pathways as characteristic for M1 macrophages, representing tryptophan metabolism, and purine metabolism, respectively. The whiskers illustrate minimum to maximum and the line in the box represent the median. n=6

On the other hand, 21 metabolites were significantly decreased in M1 macrophages compared to M0 macrophages. The significant metabolites include L-malate, 2-oxoglutarate, NAD+, L-glutamate, N-acetylcarnitine, L-aspartate, N-acetyl-L-aspartate, N-acetyl-L-glutamate, L-tryptophan and *myo*-inositol (Table 3.2). L-malate, 2-oxoglutarate and NAD+ are intermediates in the TCA cycle and oxidative phosphorylation (Figures 3.8 and 3.9). The TCA cycle and glycolysis represent important pathways in cellular processes (414). Mitochondria are the main regulators of metabolism, which produce ATP by oxidative phosphorylation as a source of energy via the TCA cycle (415). M1 macrophages metabolism is characterised by increased glycolysis and reduced oxidative phosphorylation activities associated with impairment of TCA cycle (416). This agrees with our

results in Figure 3.8 showing a decrease in the levels of L-malate, 2-oxoglutarate and NAD+. The TCA cycle involves a series of metabolites including citrate, aconitate, isocitrate, 2-oxoglutarate, succinate, fumarate, malate and oxaloacetate (Figure 3.9). Also, a decrease in L-aspartate level was shown (Figure 3.8). The TCA cycle was reported two have two break points in M1 macrophages (417). The first break occurs with the enzyme succinate dehydrogenase which produces fumarate from succinate (227). A break at this point could reduce the production of fumarate as well as malate, which could explain the decrease in the level of malate. The second break occurs after citrate which is evident to be accumulated in LPS-activated and M1 macrophages (226, 227) as a result of inhibition of isocitrate dehydrogenase which converts isocitrate to 2-oxoglutarate (227). This is likely the reason for the decrease in the level of 2-oxoglutarate. Citrate is required bioenergetic demands of M1 macrophages including fatty acid biosynthesis (418). Once it is in the cytosol, it is cleaved by citrate lyase producing acetyl-CoA and oxaloacetate. Increased acetyl-CoA will enhance the biosynthesis of fatty acids, which plays a critical role in M1 macrophages inflammatory response and signalling (419). The utilisation of acetyl-CoA in fatty acid biosynthesis decreases the amount of acetyl-CoA that is available for other reactions with, such as the TCA and conversion of L-glutamate and L-aspartate to N-acetyl-L- glutamate and N-acetyl-L-aspartate, respectively. In this regard, our results showed a decrease in N-acetyl-L-glutamate and N-acetyl-L-aspartate in M1 macrophages (Figure 3.8) indicating a disturbance in their relevant pathways as discussed earlier in section 2.3.4. Figure 3.9 summarises the pathway analysis and shows how the significantly changed metabolites are connected in their corresponding pathways.

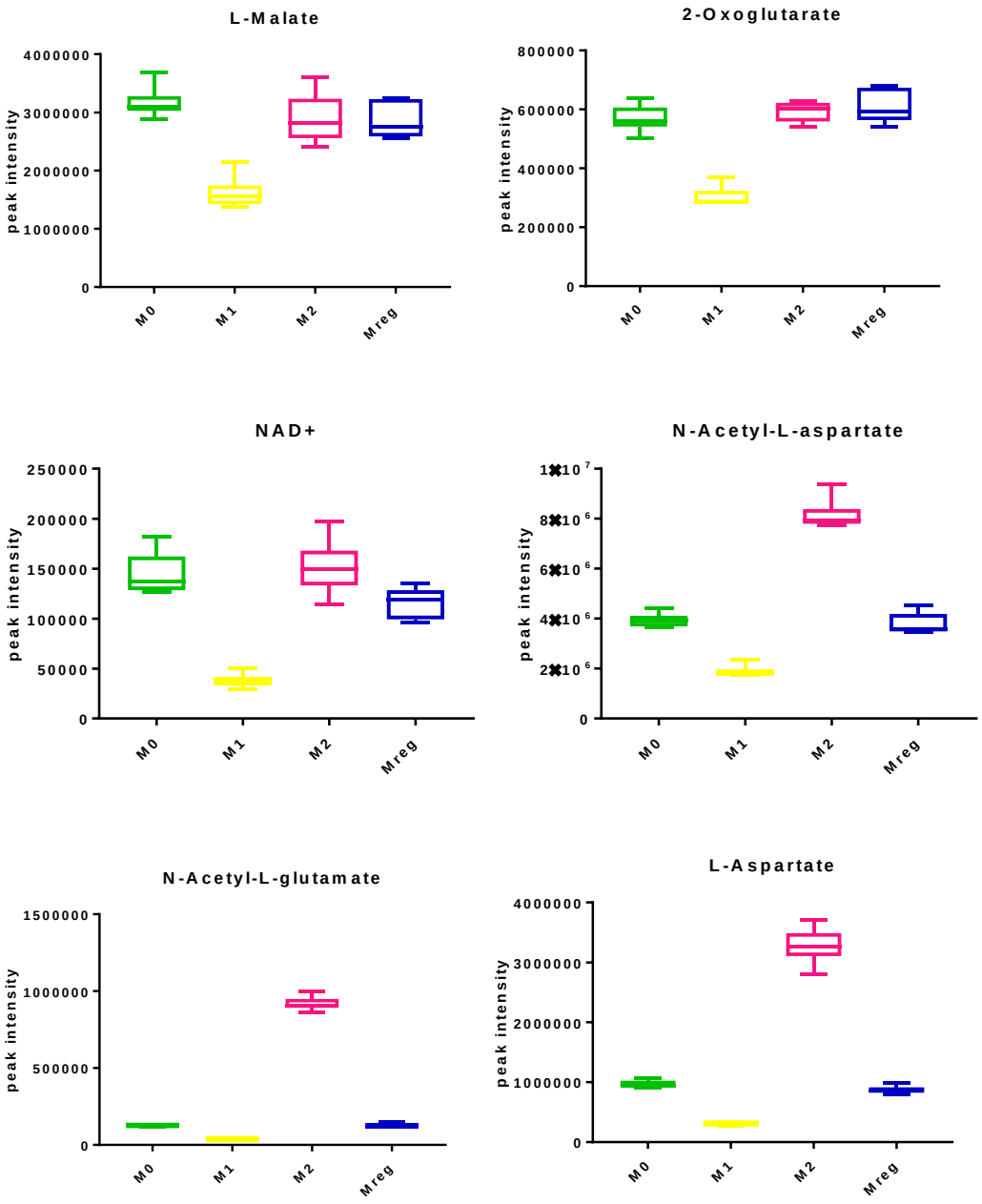


Figure 3.8: Box and whisker plots for significantly decreased metabolites in M1 macrophages. Significant decrease in these metabolites; L-malate, 2-oxoglutarate and NAD+; L-aspartate and N-acetyl-L-aspartate; and N-acetyl-L-glutamate; indicates decreased activity of their corresponding pathways; representing TCA, metabolism; aspartate and glutamate metabolism, respectively. The whiskers illustrate minimum to maximum and the line in the box represent the median. n=6.

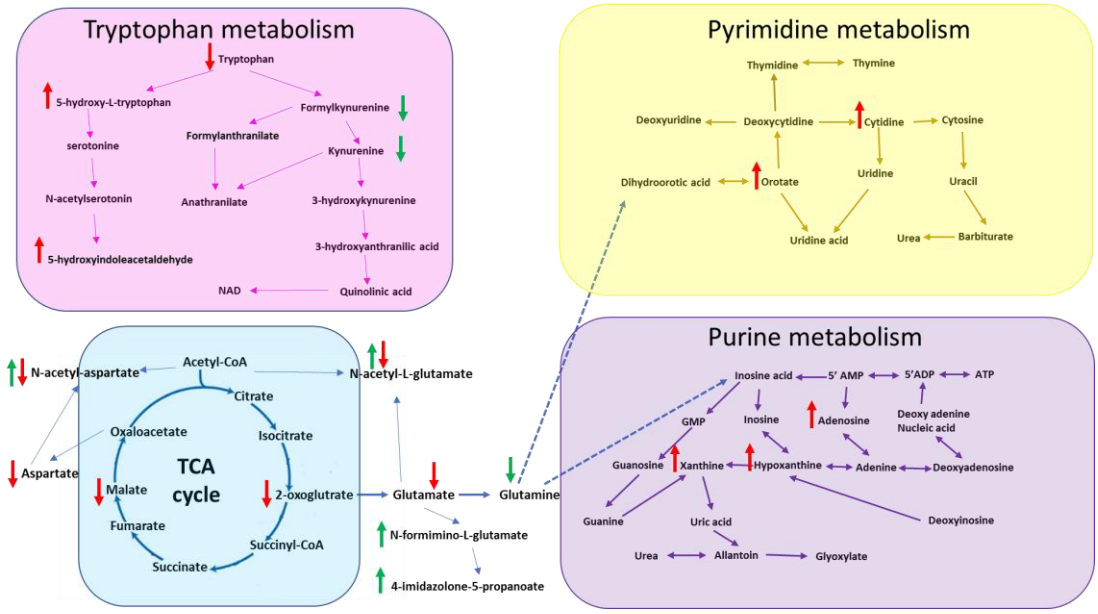


Figure 3.9: Schematic diagram of the significantly affected metabolic pathways upon polarisation of macrophages into M1 and M2 phenotypes. Red arrows represent M1 and green arrows represent M2 macrophages. Ascending arrows indicate an increase and descending arrows indicate a decrease in the levels of the metabolites.

In contrast to M1 macrophages, N-acetyl-L-glutamate, N-acetyl-L-aspartate were distinctively increased in M2 macrophage (Figure 3.8), which agreed with results shown in chapter two, section 2.3.4. Also, M2 cells showed a significant increase in N-Formimino-L-glutamate and 4-imidazolone-5-propanoate (Figure 3.10) with the former converted to the later by the enzyme imidazolonepropionase. The increase in 4-imidazolone-5-propanoate matched that observed in chapter two, section 2.3.4. N-Formimino-L-glutamate is produced from L-glutamate by formiminoglutamase. L-glutamate is interconverted from L-ornithine by the enzyme ornithine aminotransferase. Production of L-ornithine from L-arginine increases via the arginase-1 path, which is a hallmark in M2 macrophages (305). Increased production of L-glutamate from this pathway could therefore explain the increase in N-Formimino-L-glutamate and 4-imidazolone-5-propanoate.

Furthermore L-glutamate could feed TCA cycle by being converted to 2-oxoglutarate by the enzyme glutamate dehydrogenase (Figure 3.9).

On the other hand, L-glutamine and L-formylkynurenine showed a significant decrease in M2 macrophages (Figure 3.11). L-Glutamine is the most abundant free amino acid in the body which plays a crucial role in several cellular processes including oxidative fuel, redox potential, signalling pathways and extracellular matrix synthesis (420, 421). Glutaminase and glutamine synthetase are the most important enzymes in L-glutamine metabolism. Glutaminase catalyses the conversion of L-glutamine to L-glutamate (422). Several fates for L-glutamine have been identified. Mainly, it undergoes extensive metabolism to produce L-glutamate. L-glutamate, as aforementioned is converted to 2-oxoglutarate by glutamate dehydrogenase, converted to L-ornithine which represent a substrate for ornithine decarboxylase in the synthesis of polyamines induced in M2 macrophages (305) or reacted with acetyl-CoA by N-acetylglutamate synthetase to produce N-acetyl-L-glutamate which showed a significant increase in M2 macrophages. These three fates could explain the significant decrease in L-glutamine.

Based on these results discussed above, identifying characteristic key metabolites in M1 or M2 showed distinct metabolic signature for each phenotype demonstrating the implication of metabolism in regulation of macrophages phenotypes. This is illustrated in the significant disturbance of several metabolic pathways such as TCA cycle, purine metabolism, pyrimidine metabolism and tryptophan metabolism in M1, or arginine and proline metabolism and aspartate

and glutamate metabolism in M2 macrophages showing distinct metabolic profile for M1 or M2 macrophages. As discussed earlier in the introduction section1.2.2, macrophages polarisation associated with several diseases, as a result of disturbed M1/M2 balance, such as chronic inflammatory and autoimmune diseases (174-180). Strategies to use the key identified metabolites in the manipulation of macrophages polarisation, targeting and interfering with the identified metabolic pathways, could be promising in the prevention of inflammation consequences and help to resolve associated diseases.

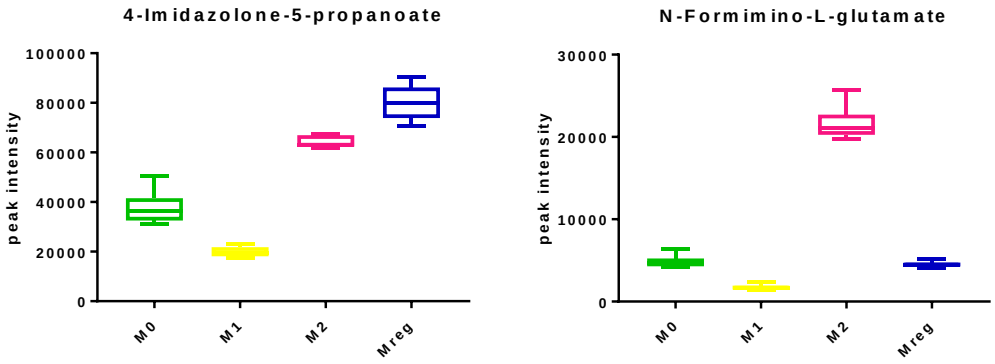


Figure 3.10: Box and whisker plots with for significantly decreased metabolites in M2 macrophages. Significant increase in these metabolites; 4-imidazolone-5-propanoate and N-formimino-L-glutamate (intermediates in aspartate and glutamate metabolism) in addition to N-acetyl-L-glutamate and N-acetyl-L-aspartate (Figure 3.3) that represent aspartate and glutamate metabolism and; arginine and proline metabolism, respectively, indicating enhanced activity of these pathways. The whiskers illustrate minimum to maximum and the line in the box represent the median. n=6

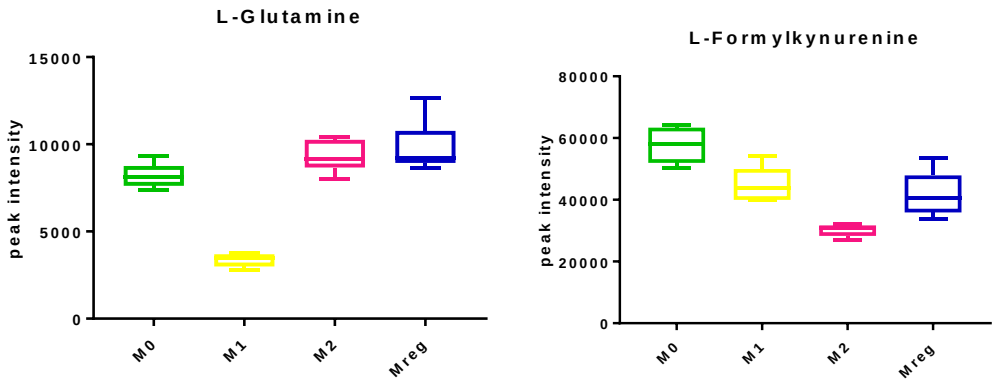


Figure 3.11: Box and whisker plots for significantly decreased metabolites in M2 macrophages. Significant decrease in these metabolites; L-glutamine and L-formylkynurenine representing glutamate metabolism and tryptophan metabolism, respectively. The whiskers illustrate minimum to maximum and the line in the box represent the median. n=6

Mreg macrophages, as mentioned earlier, showed a similar metabolic profile to M0 macrophages. Although 46 metabolites demonstrated significant difference, only hypoxanthine showed a fold change greater than 1.5 implying the similarity in their metabolic profiles. Mreg macrophages are suppressor cells that dampen the immune response and limit inflammation (169) and interestingly, they showed a significant decrease in the level of hypoxanthine compared to M0 macrophages (Figure 3.7). Hypoxanthine is an oxidative stress and inflammation marker (355). Therefore, decreasing the levels in the oxidative stress and inflammation markers could be linked to the function of Mreg in dampening the inflammation.

3.3.2. Challenging M0 and Mreg with LPS.

3.3.2.1. Feature selection

Since M0 and Mreg macrophages showed similar metabolic profiles at the steady state, a further challenge was conducted in an attempt to differentiate Mreg cells by investigating their response and behaviour to LPS (a potent inducer of the

inflammatory response *in vivo* and *in vitro*) (423). Based on the macrophage polarisation aspect discussed earlier in the introduction, M0 will trigger an inflammatory phenotype and Mreg will behave as a suppressor in response to LPS. Therefore, M0 and Mreg were treated with LPS for 24 hrs, followed by LC-MS-based metabolic profiling in an attempt to metabolically distinguish between these groups.

513 metabolites were putatively identified using IDEOM (Appendix, Table A3). OPLS-DA scores plot (Figure 3.12A) shows a tight clustering of six replicates within each group with R^2 and Q^2 values of 0.881 and 0.982, respectively, indicating a good OPLS-DA model (324). Consistently with the first experiment, a clear separation was shown between M0 and each of M1, M2, LPS-treated M0 (M0-LPS) or LPS-treated Mreg (Mreg-LPS). Nevertheless, a slight separation was shown between Mreg and M0 macrophages. Two-way comparisons of OPLS-DA models were acquired as shown in Figure 3.12 (B,C,D,E and F), and similarly showed clear separations between M1 and M0 macrophages (R^2 and Q^2 values of 0.817 and 0.996), M2 and M0 macrophages (R^2 and Q^2 values of 0.821 and 0.997), M0 and Mreg (R^2 and Q^2 values of 0.615 and 0.989), M0 and M0-LPS macrophages (R^2 and Q^2 values of 0.820 and 0.998) and M0 and Mreg-LPS macrophages (R^2 and Q^2 values of 0.875 and 0.860). The combination of multivariate analysis and univariate analyses, with the same workflow as mentioned earlier in section 3.3.1.1, revealed characteristic key metabolites. 112 metabolites were significantly changed in M1 compared to M0 macrophages where purine, pyrimidine, and tryptophan relevant metabolites showed a significant increase, and TCA cycle intermediate showed a significant decrease (Table 3.4). 84

metabolites have been revealed as significant metabolites upon polarisation of M0 into M2 macrophages (Table 3.5). However, only 25 metabolites were significantly changed in Mreg macrophages which showed and of there only cytidine was significantly increased with fold change greater than 1.5 (Table 3.6). 54 and 41 metabolites were significantly changed in M0-LPS and Mreg-LPS, respecively (Tables 3.7 and 3.8). To some extent, the challenged groups (M0-LPS and Mreg-LPS), showed a similar trend to M1 macrophages where metabolites from purine and pyrimidine metabolism showed significant increase (Tables 3.7 and 3.8) and (Figure 3.13).

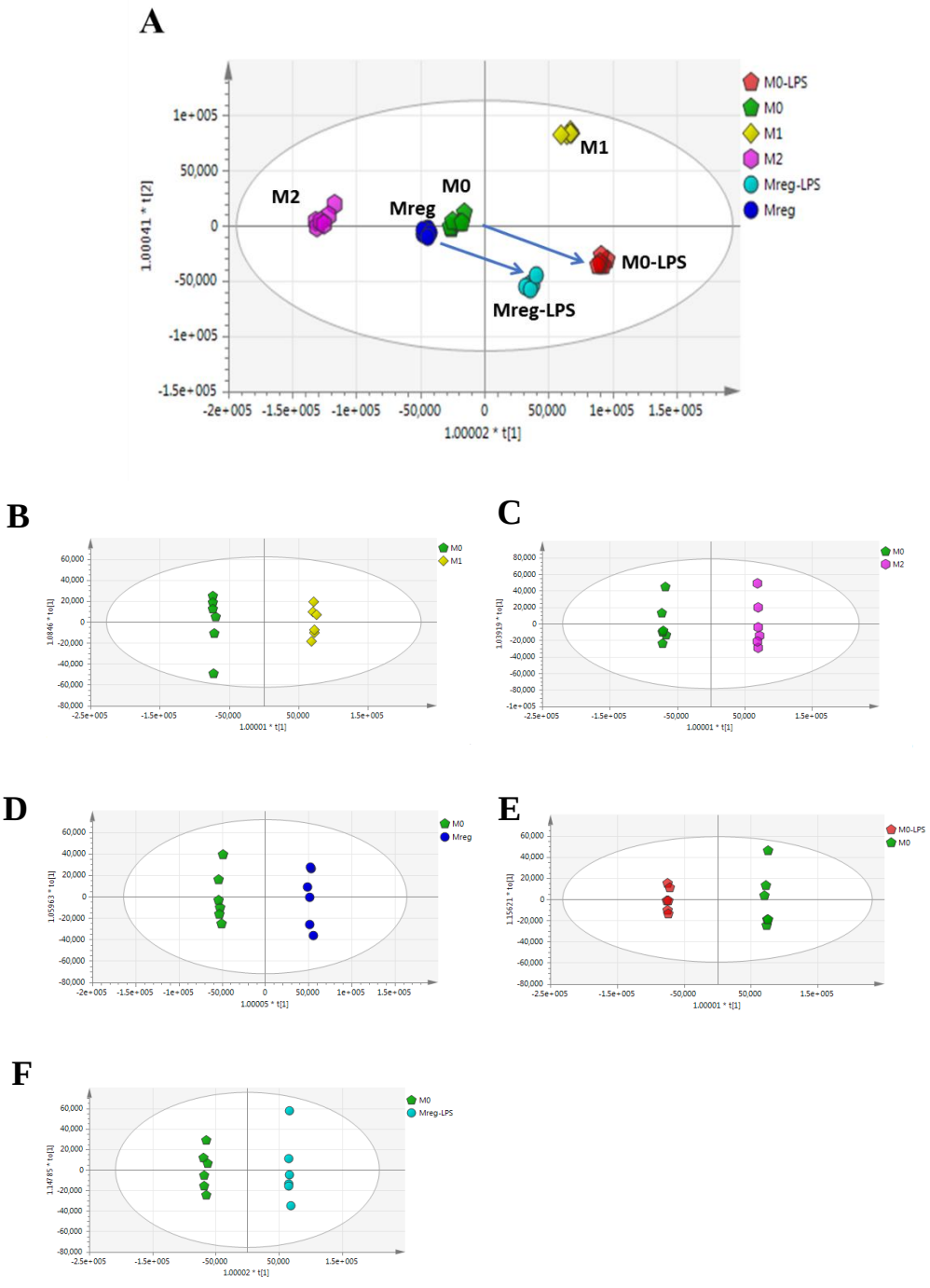


Figure 3.12: OPLS-DA scores plots of macrophage extracts after polarisation toward M1, M2 and Mreg states and their corresponding unpolarised (M0) controls in addition to M0 treated with LPS and Mreg treated with LPS for 24 hrs. (A) M1, M2, Mreg, M0-LPS and Mreg-LPS macrophage samples and their respective unpolarised controls (R^2 = 0.881 and Q^2 = 0.982). (B) Two-way orthogonal comparison between M0 and M1 (R^2 = 0.817 and Q^2 = 0.996). (C) Two-way orthogonal comparison between M0 and M2 (R^2 = 0.821 and Q^2 = 0.997). (D) Two-way orthogonal comparison between M0 and Mreg (R^2 = 0.615 and Q^2 = 0.989). (E) Two-way orthogonal comparison between M0 and M0-LPS (R^2 = 0.820 and Q^2 = 0.998). (F) Two-way orthogonal comparison between M0 and Mreg-LPS (R^2 = 0.875 and Q^2 = 0.860). M0 (green pentagons), M1 (yellow diamonds), M2 (pink hexagons), Mreg (dark blue circles), M0-LPS (red pentagon) and Mreg-LPS (light blue circles). n=6.

3.3.2.2. Pathway analysis

For further analysis of the results, the characteristic metabolites for each group (M1, M2, M0-LPS and Mreg-LPS macrophages) compared to M0 were explored. In agreement with the first experiment in the section 3.3.1.2., purines (hypoxanthine and adenosine), pyrimidine (cytidine), 5-hydroxy-L-tryptophan, N-acetylserotonin and other GLs were significantly increased in M1 macrophages compared to M0 (Figure 3.13) whereas O-acetyl carnitine, L-glutamate, L-aspartate, N-acetyl-L-glutamate, N-acetyl-L-aspartate, L-malate, 2-oxoglutarate, and NAD+ were significantly decreased (Figure 3.14). On the other hand, in agreement with section 3.3.1.2, N-acetyl-L-glutamate and N-acetyl L-aspartate were significantly increased in M2 macrophages compared to M0 (Figure 3.114). In addition to significantly increased levels of 2-oxoglutarate, which is intermediate in the TCA cycle

. Hypoxanthine and cytidine, which were revealed as increased characteristic metabolites of M1 macrophages, showed a significant decrease in M2 macrophages (Figure 3.13). The opposite behaviour of key characteristic metabolites in M1 or M2 agree with that M1 and M2 subsets are the opposite extreme phenotype where their response and function opposes each other (364).

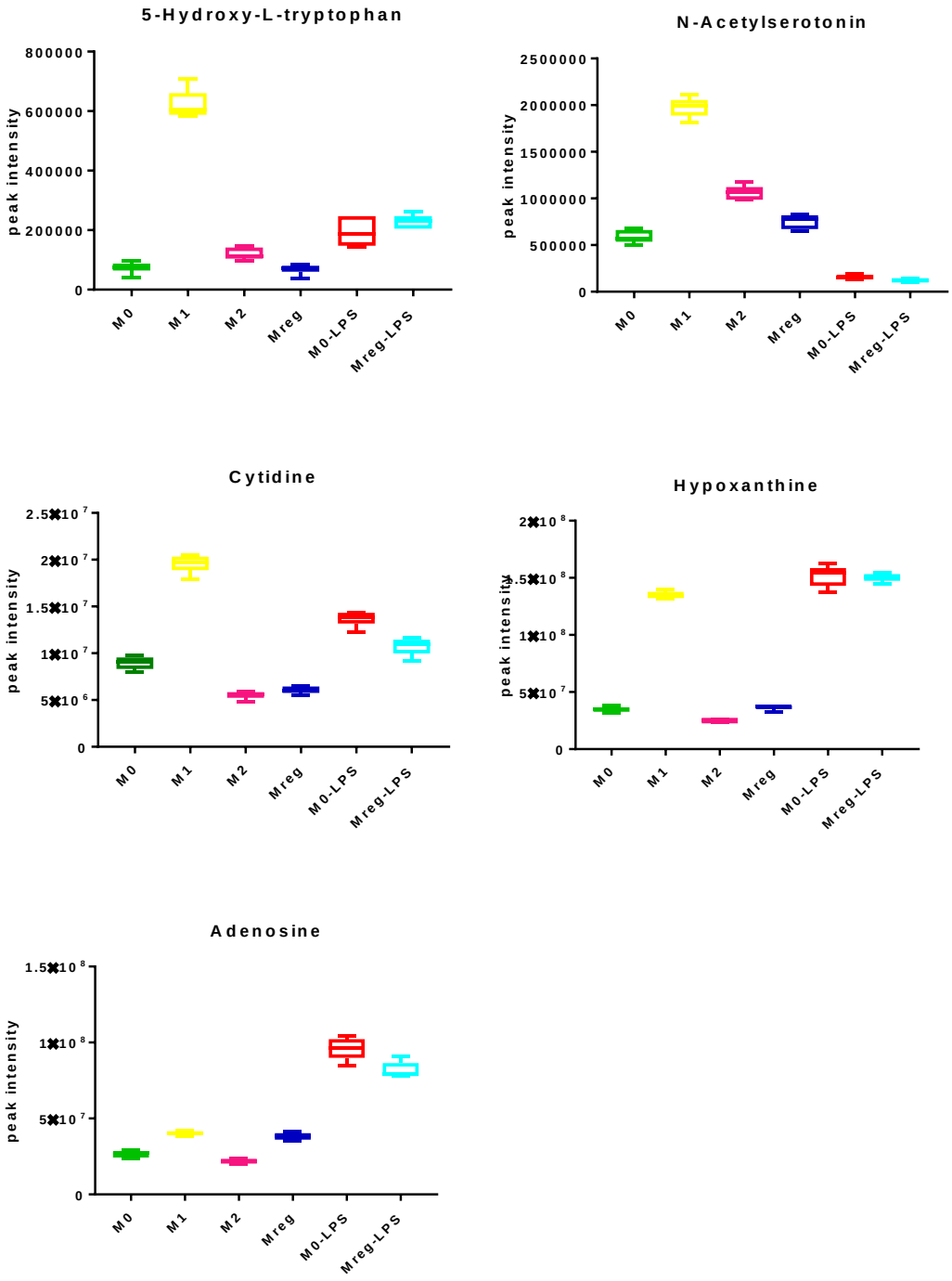
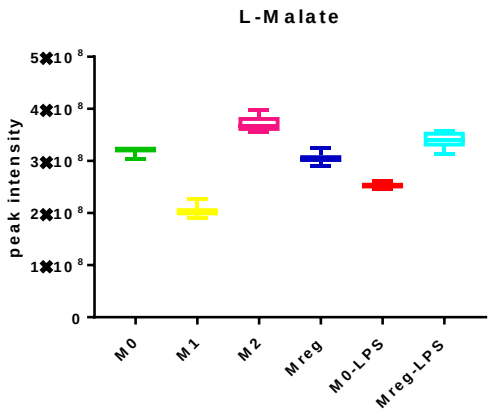
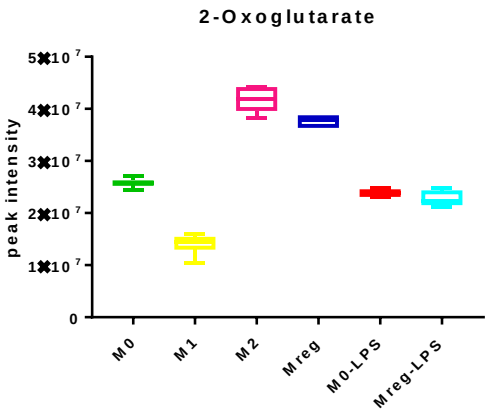
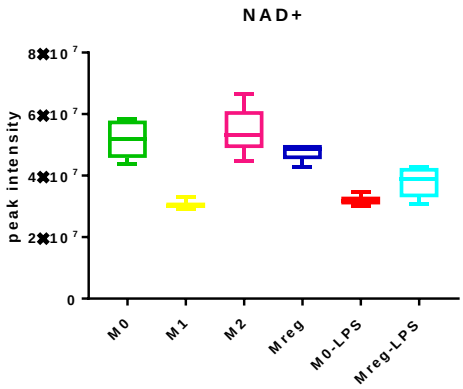
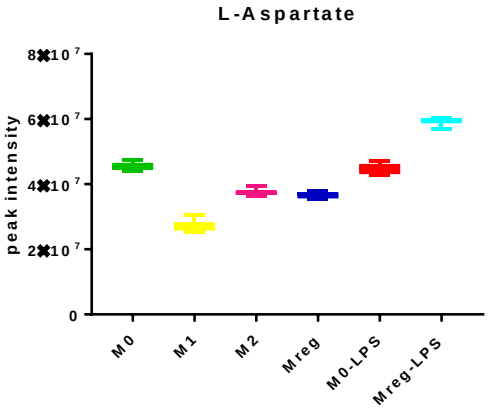


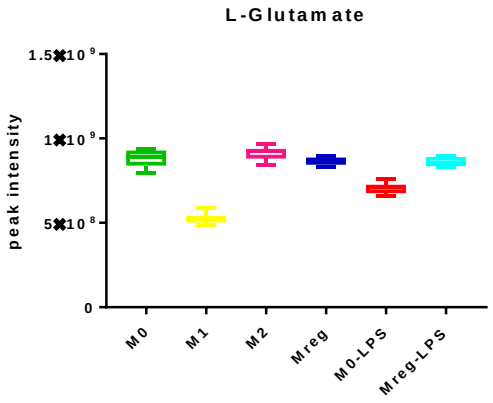
Figure 3.13: Box and whisker plots with for significantly increased metabolites in M1 macrophages in the experiment of challenging with LPS. Significant increase in the metabolites; 5-hydroxy-l-tryptophan and N-acetylserotonin; cytidine; hypoxanthine and adenosine; indicates enhanced activity of their corresponding pathways as characteristic for M1 macrophages, representing tryptophan metabolism, pyrimidine metabolism and purine metabolism, respectively. The whiskers illustrate minimum to maximum and the line in the box represent the median. n=6.

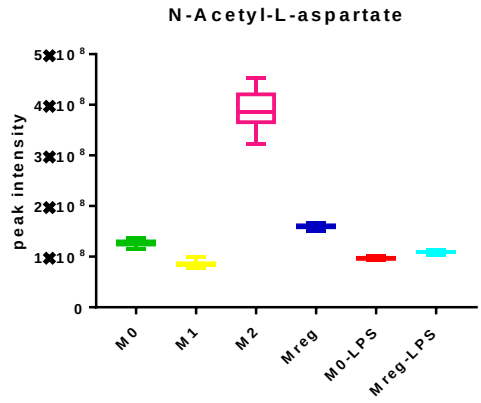

L-Malate
peak intensity
5✖10 8
4✖10 8
3✖10 8
2✖10 8
1✖10 8
0
M0
M1
M2
Mreg
M0-LPS
Mreg-LPS


2-Oxoglutarate
peak intensity
5✖10 7
4✖10 7
3✖10 7
2✖10 7
1✖10 7
0
M0
M1
M2
Mreg
M0-LPS
Mreg-LPS


NAD+
peak intensity
8✖10 7
6✖10 7
4✖10 7
2✖10 7
0
M0
M1
M2
Mreg
M0-LPS
Mreg-LPS


L-Aspartate
peak intensity
8✖10 7
6✖10 7
4✖10 7
2✖10 7
0
M0
M1
M2
Mreg
M0-LPS
Mreg-LPS


L-Glutamate
peak intensity
1.5✖10 9
1✖10 9
5✖10 8
0
M0
M1
M2
Mreg
M0-LPS
Mreg-LPS


N-Acetyl-L-aspartate
peak intensity
5✖10 8
4✖10 8
3✖10 8
2✖10 8
1✖10 8
0
M0
M1
M2
Mreg
M0-LPS
Mreg-LPS

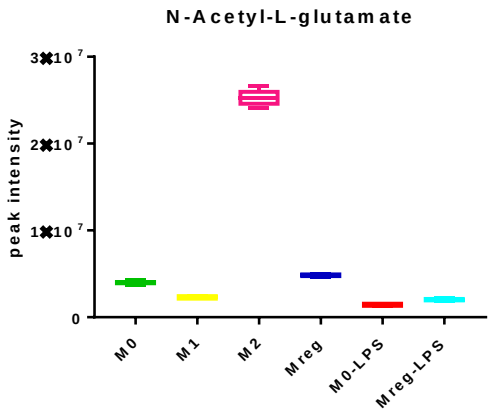


Figure 3.14: Box and whisker plots for significantly decreased metabolites in M1 macrophages in the experiment of challenging with LPS. Significant decrease in these metabolites; L-malate, 2-oxoglutarate and NAD+; L-aspartate, N-acetyl-L-aspartate; L-glutamate and N-acetyl-L-glutamate; indicates decreased activity of their corresponding pathways; representing TCA, metabolism; aspartate and glutamate metabolism, respectively. The whiskers illustrate minimum to maximum and the line in the box represent the mediann=6.

Mreg macrophages showed a similar metabolic profile to M0 in this experiment Although 25 metabolites were significantly changed, only cytidine showed a significant decrease as compared to M0 with a fold change greater than 1.5 (Figure 3.13). Our results in the previous section and chapter two identified cytidine as a key characteristic metabolite of M1 macrophages. M1 macrophages are inflammatory cells that are activated in inflammation. A decrease in cytidine in Mreg may indicate their suppressor activity in inflammation. As we aimed to investigate the behaviour of M0 and Mreg macrophages in response to LPS, their metabolic profiles upon LPS treatment were studied. The metabolic profile of M0-LPS revealed a significant increase in hypoxanthine, adenosine, cytidine, glycerophospholipids (GLs), L-serine and 4-aminobutanoate (Figures 3.13 and 3.15). The conversion of serine to glycine plays a critical role in the one-carbon pathway, which is a key metabolic pathway in maintaining redox balance under

oxidative stress or hypoxia, both which are induced by bacterial invasion (424-426). The increased L-serine level (Figure3.15) may indicate a contribution of this metabolite in maintaining the redox balance in LPS-M0 which undergo oxidative stress as a result of LPS treatment. Ma et al have demonstrated that serine availability can be used as a checkpoint metabolite indicating the efficient immune response of primary T cells (427). 4-aminobutanoate is an intermediate in the 4-aminobutanoate shunt pathway. This pathway was reported to promote polarisation of mouse macrophages into M1 phenotype (428). However, a significant decrease was shown in the level of N-acetyl-L-glutamate NADH and L-asparagine (Figures 3.13 and 3.16). N-acetyl-L glutamate was discussed in section 2.3.4 as a key characteristic significantly decreased metabolite in M1. Taken together, M0-LPS, to some extent, showed a similar metabolic profile to M1 macrophages which is perhaps not surprising, as LPS is a potent inflammatory stimulator that induces the generation of M1 macrophages (105).

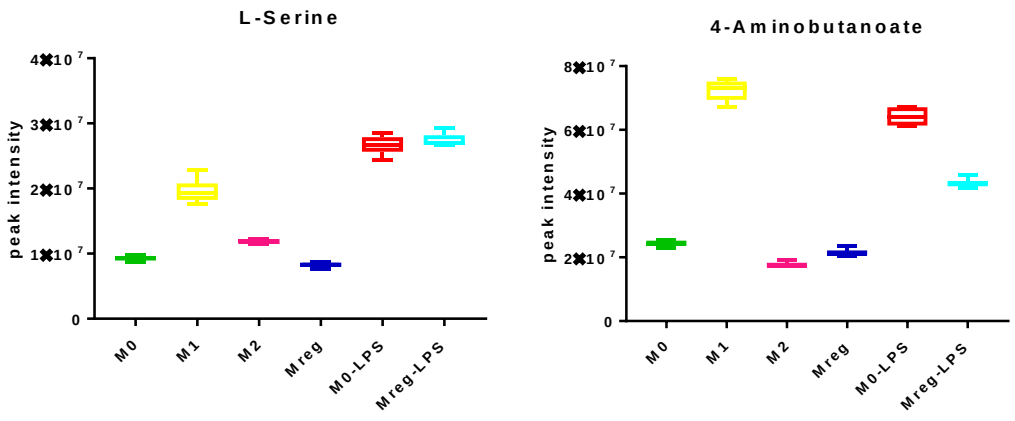


Figure 3.15: Box and whisker plots for significantly increased metabolites in M0-LPS macrophages in the experiment of challenging with LPS. Significant increase in the metabolites; L-serine (glycine and serine metabolism) and 4-aminobutanoate (alanine, aspartate and glutamate metabolism) in addition to cytidine; hypoxanthine and adenosine in Figure 3.13. The whiskers illustrate minimum to maximum and the line in the box represent the median. n=6.

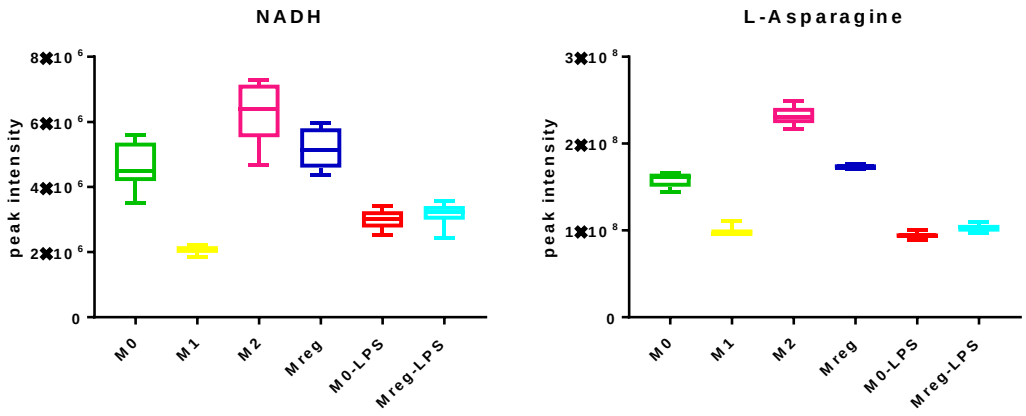


Figure 3.16: Box and whisker plots for significantly decreased metabolites in M0-LPS macrophages in the experiment of challenging with LPS Significant decrease in the metabolites; NADH (an intermediate in TCA cycle) and L-asparagine (an intermediate in alanine, aspartate and glutamate metabolism) in addition to N-acetyl-L-glutamate shown in Figure 3.14. The whiskers illustrate minimum to maximum and the line in the box represent the median. n=6

Similarly, for Mreg-LPS macrophages compared to M0 (Table 3.8), its metabolic profile demonstrated a significant increase in hypoxanthine, adenosine, L-serine and 4-aminobutanoate (Figures 3.13 and 3.15), and a significant decrease in L-asparagine and N-acetyl-L-glutamate (Figures 3.14 and 3.16). Based upon these significantly changed metabolites in both M0-LPS and Mreg-LPS, it can be clearly seen that they display a similar response to LPS. Interestingly, their metabolic profile and significantly changed metabolites are highly similar to those of M1 macrophages. For instance, all M1, M0-LPS and Mreg-LPS showed a significant increase in adenosine and hypoxanthine, where hypoxanthine is considered as an inflammation biomarker (355). Also, these three groups showed a significant decrease in N-acetyl-L-glutamate, indicating that M0 and Mreg could be polarised into M1-like macrophages in response to LPS. As can be seen in Figure 3.8, the OPLS-DA model showed the movement of both M0 and Mreg in response to LPS, in the same trend toward the side of M1. M1, M0-LPS and Mreg-LPS showed a

clear separation which means that they did not show identical metabolic profiles, but the similarity in their significantly changed metabolites was obvious. This separation could be due to the heterogeneity of macrophages which can display an infinite number of phenotypes that can share some characteristics of the main subsets, as discussed earlier (section 3.1).

3.3.3. Macrophage plasticity.

3.3.3.1. Feature selection.

Macrophages are highly plastic cells which alter their phenotypes in response to different environmental cues such as microbial, parasitic, and viral antigens, cytokines or apoptotic cells (129-131). In order to investigate the plasticity and reversibility of macrophages, naïve macrophages (M0) were polarised into M1 and M2. Then, in an attempt to reverse the functional phenotypes, M1 macrophages were exposed to M2 polarising agents (M-CSF and IL-4) and M2 macrophages were exposed to M1 polarising agents (GM-CSF, LPS and IFN-γ) for 24 and 48 h. After the treatment, their metabolic profiles were studied. 440 metabolites were identified using IDEOM (Appendix, Table A4). In Figure 3.17A, OPLS-DA score plot with R^2 and Q^2 values of 0.905 and 0.962, respectively, demonstrated a valid model (324). And the clustering of six replicates within each group indicating good repeatability. This OPLS-DA scores plot in Figure 3.17A also shows a clear separation between M0, M1 and M2 macrophages which agrees with our previous results in this chapter (Figures 3.5 and 3.12) and chapter two (Figure 2.5). M2 macrophages clearly tended toward original M1 macrophages

when they treated with M1 polarising agent for 24 and 48 h (M2-M1-24 and M2-M1-48, respectively), which could indicate that the metabolic profiles of M2-M1-24 and M2-M1-48 became similar to that of M1 macrophages (Figure 3.17A). However, when M2-M1-24 and M2-M1-48 compared directly to the original M1 macrophages (Figure 3.17B), the OPLS-DA scores plot and it shows a clear separation between M1 polarising agent treated M2 and M1 macrophages with R^2 and Q^2 values of 0.678 and 0.979. To determine the key mass ions which are characteristic to each condition uni- and multivariate analyses were performed. 54 metabolites in M2-M1-24 have shown significant difference while 36 were revealed as significantly changed mass ions in M2-M1-48 compared to M1 (Tables 3.9 and 3.10, respectively).

In the same context, Figure 3.17A showed that M1 macrophages challenged with M2 polarising cytokines for 24 and 48 hrs (M1-M2-24 and M1-M2-48, respectively) tended away from M1 macrophages. M1-M2-24 and M1-M2-48 were compared to M2 separately in the OPLS-DA scores plot (Figure 3.13C). A clear separation is shown with R^2 and Q^2 values of 0.889 and 0.992 indicating acceptable model. 89 metabolites in M1-M2-24 showed a significant difference, while 104 were revealed as significantly changed mass ions in M1-M2-48 compared to M2 (Tables 3.11 and 3.12, respectively).

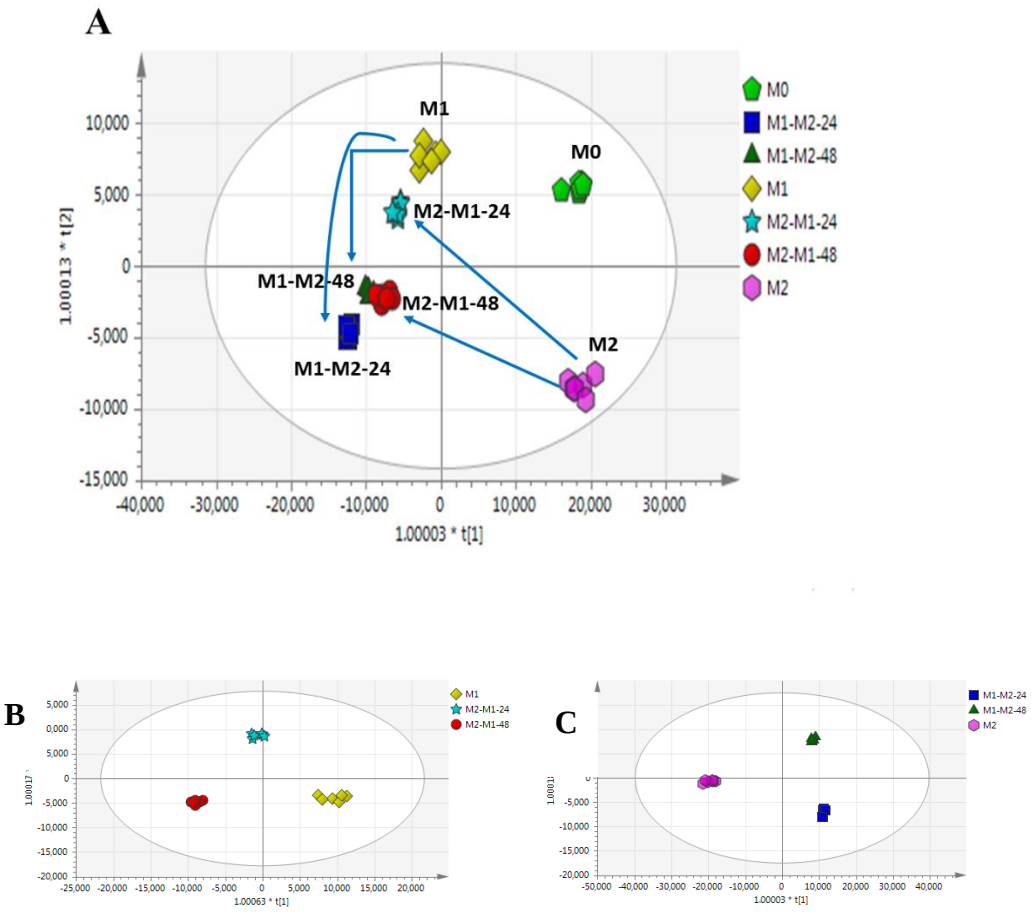


Figure 3.17: OPLS-DA scores plots of macrophage extracts after polarisation toward M1, M2 and reversing M1 and M2 for 24 (M1-M2-24 and M2-M1-24) and 48 hours (M1-M2-48 and M2-M1-48) and their corresponding unpolarised (M0) as a control. (A) M1, M2, M1-M2-24, M1-M2-48, M2-M1-24 and M2-M1-48 macrophage samples and their respective unpolarised controls (R2 = 0.905 and Q2 = 0.962). (B) A comparison between M1, M2-M1-24 and M2-M1-48 (R2 = 0.678 and Q2 = 0.979). (C) A comparison between M2, M1-M2-24 and M1-M2-48 (R2 = 0.889 and Q2 = 0.992).M0 (green pentagons), M1 (yellow diamonds), M2 (pink hexagons), M1-M2-24(dark blue squares), M1-M2-48 (dark green triangles), M2-M1-24 (light blue stars), M2-M1-48 (red circles). n=6.

3.3.3.2. Pathway analysis.

In order to investigate the metabolic pathways that significantly changed by exposing M1 and M2 macrophages to the opposing polarising agents, the significantly changed metabolites were linked to their corresponding pathways.

The metabolic profile of M1 macrophages was compared to the metabolic profile of M2-M1-24. Out of the 54 significantly changed metabolites, 32 metabolites

showed fold changes greater than 1.5 (Table 3.9) between these two groups. Despite these fold changes, most of these metabolites have the same trend of M1 (decrease or increase) when compared to control (M0 macrophages) which could indicate the similarity in their metabolic profile. For instance, N-acetyl-L-glutamate was decreased in both (the fold changes are 0.60 and 0.82 in M1 and M2-M1-24, respectively) compared to M0, whereas deoxyadenosine and 5-hydroxy-L-tryptophan were increased in both (the fold changes are 3.09 and 3.15 in M1, 15.6 and 6.27 in M2-M1-24, respectively) compared to M0 (Figure 3.18). These metabolites revealed as key characteristically changed metabolites in M1 macrophages with the same trend (section 3.3.1.2). Similarly, M2-M1-48 showed significant changes in 36 metabolites compared to M1 macrophages (Table 3.10). Again, most of these metabolites showed the same trends (increase or decrease) of M1 macrophages when compared to control (M0 macrophages). For example L-tryptophan, L-arginine and L-1-Pyrroline-3-hydroxy-5-carboxylate were decreased in both, M1 and M2-M1-48 whereas deoxyadenosine was increased in both (the fold changes were 0.47, 0.43, 0.56, 0.68, and 3.09, respectively in M1, 0.73, 0.78, 0.64, 0.76 and 9.5 respectively in M2-1-48) compared to M0 (Figures 3.18 and 3.19). These results also indicate similar metabolic profiles of M1 macrophages and M2-M1-48 macrophages.

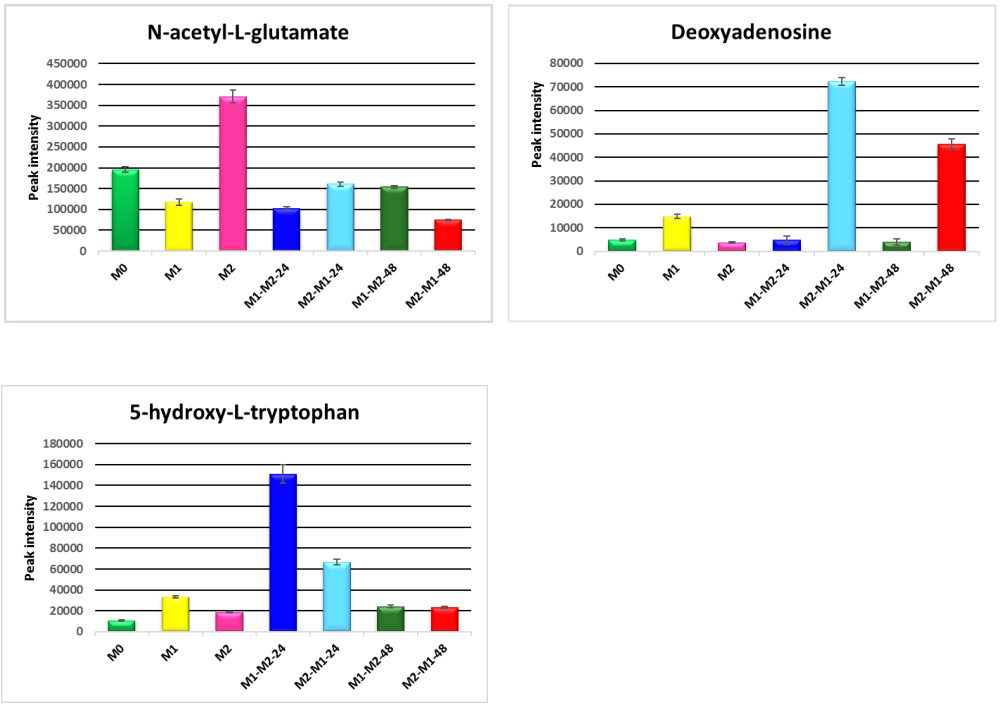


Figure 3.18: bar charts for the significantly changed metabolites in M2-M1-24 vs M1 macrophages, which showed a similar trend of M1 macrophages. N-acetyl-L-aspartate was significantly decreased, where 5-hydroxy-L-tryptophan and deoxyadenosine were significantly increased.n=6, data are presented as mean ± SEM.

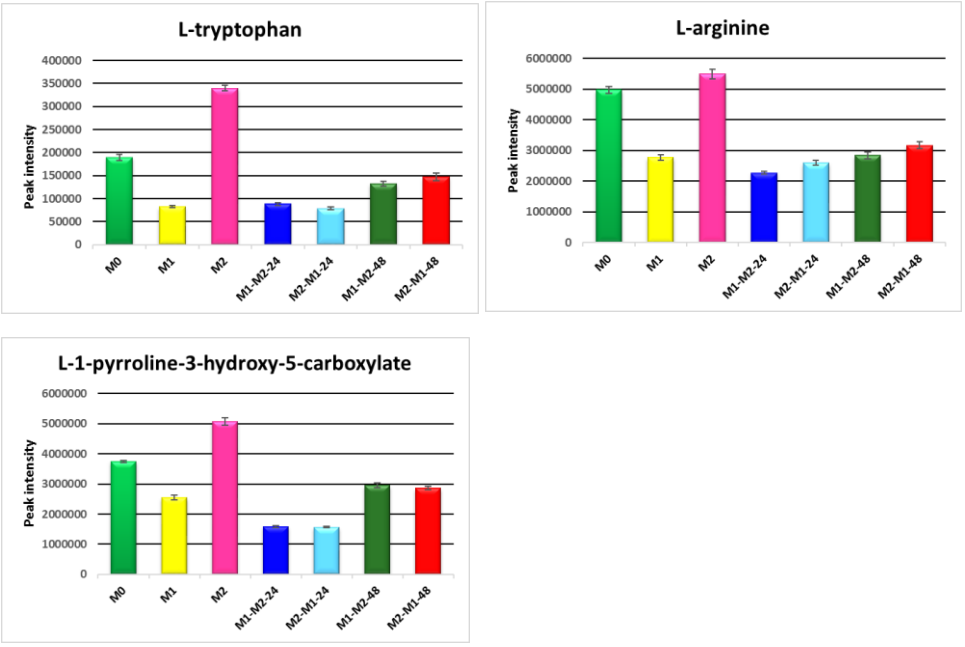


Figure 3.19: bar charts for the significantly changed metabolites in M2-M1-48 vs M1 macrophages, which showed a similar trend of M1 macrophages. L-Tryptophan, L-arginine and L-1-pyrroline-3-hydroxy-5-carboxylate. In addition to N-acetyl-L-glutamate were significantly decreased, whereas deoxyadenosine was significantly increased in both (Figure 3.18). n=6, data are presented as mean ± SEM

As mentioned earlier, a significant number of metabolites showed a significant change between M2 and either M1-M2-24 or M1-M2-48 indicating different metabolic profiles (89 or 104 metabolites respectively, Tables 3.11 and 3.12). Most of these metabolites such as L-asparagine, L-tryptophan, N-acetyl-L-glutamate, 4-imidazolone-5-propanoate, NAD+, L-ornithine, and PC (20:4/P-18:1) were significantly changed in M1-M2-24 compared to M2. However, they still showed the same trend (decrease or increase) to M1 when compared to M0 macrophages (Figures 3.18, 3.19, and 3.20). A higher number of metabolites (104 metabolites) showed a significant change upon extending reversing time into 48 h compared to M2 (Table 3.12). These metabolites are shown in Figures 3.18-3.21, including L-valine, L-arginine, L-ornithine, L-asparagine, L-tryptophan, N-acetyl-L-glutamate, 4-imidazolone-5-propanoate, PC (20:4/P-18:1) and some PCs (Table 3.12). Interestingly, all these metabolites showed the same trend of M1 when compared M0 macrophages, implying that the metabolic profile of M1-M2-48 was more similar to that of M1 than that of M2 phenotype.

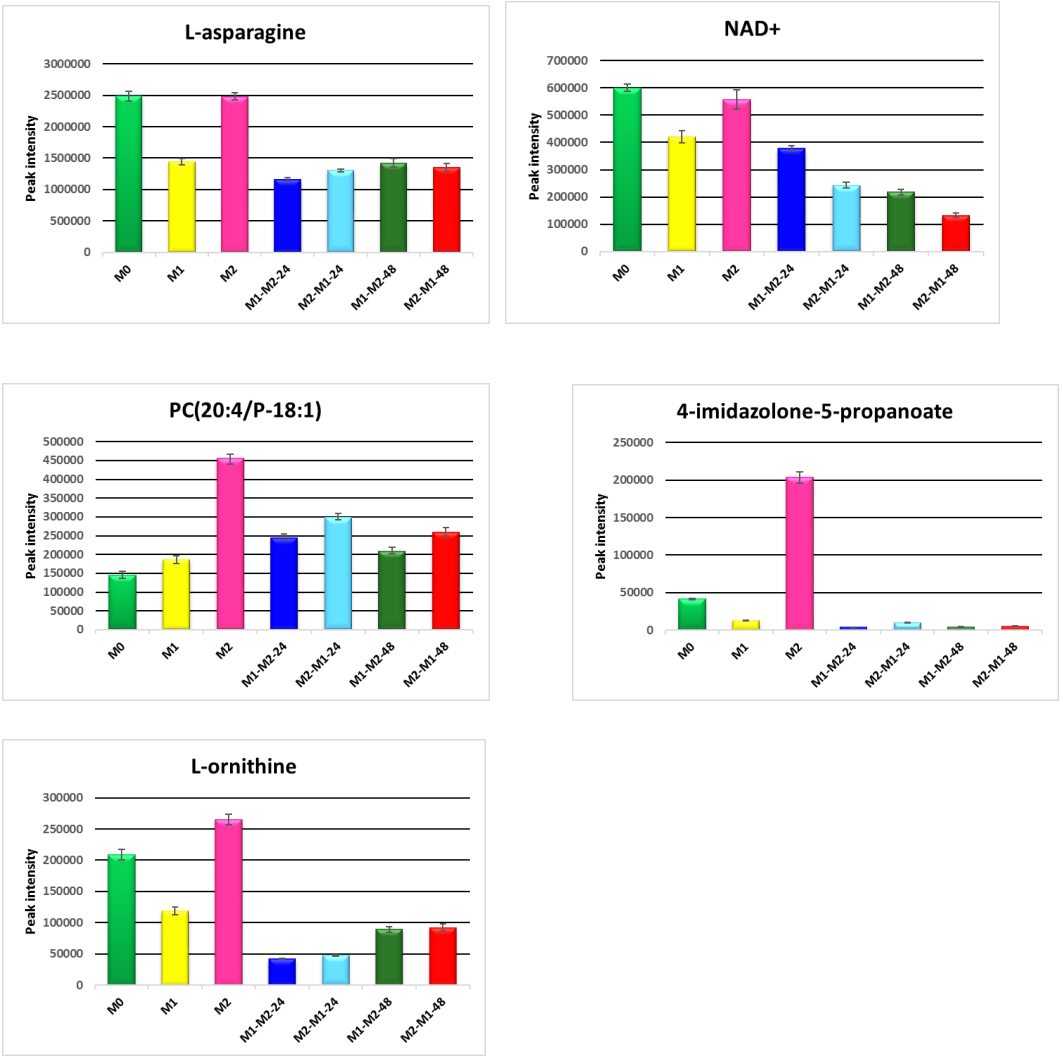


Figure 3.20: bar charts for the significantly changed metabolites M1-M2-24 vs M2 macrophages, which showed a similar trend of M1 macrophages which are L-asparagine, NAD+, PC(20:4/P-18:1), 4-imidazolone-5-propanoate and L-ornithine, in addition to L-tryptophan (Figure 3.19), and N-acetyl-L-glutamate (Figure 3.18). n=6, data are presented as mean ± SEM.

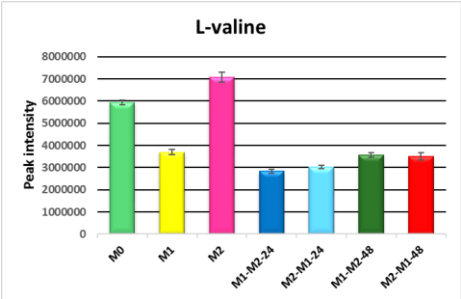


Figure 3.21: 3D bar chart for the significantly changed metabolites in M2-M1-48 vs M2 macrophages, which showed similar trend of M1 macrophages which is L-valine, in addition to L-asparagine, PC(20:4/P-18:1), 4-imidazolone-5-propanoate and L-ornithine (Figure 3.20), L-tryptophan and L-arginine (Figure 3.19), and N-acetyl-L-glutamate (Figure 3.18). n=6, data are presented as mean ± SEM.

Based on the previous observations, the results showed that M1 macrophages are more stable and resistant to change their phenotype than M2 macrophages. Upon trying to reverse them, M1 macrophages treated with M2 polarising agents for 24 and 48 hrs showed metabolic profile closer to their original M1 state than that of M2 macrophages (Figure 3.17). However, M2 macrophages challenged with M1 polarising agents for 24 and 48 hrs showed a metabolic profile different to their original M2 state, but instead more similar metabolic profile to M1 macrophages. M1 and M2 macrophages are a mirror image of Th1 and Th2 polarisation of T cells, respectively (155). These results agree with a previous study which demonstrated that human Th1 cells, which were generated using IL-12 were stable and not affected significantly when re-stimulated with IL-4 (Th2 polarising agent). In contrast, Th2 cells generated by IL-4, were not stable and could be easily converted to into Th0 or Th1 cells when re-stimulated with IL-12 (429). Similarly, Coffman et al have reported that Th2 phenotype could give rise to Th1 phenotype after re-stimulation with IL-12 (430).

As discussed in section 3.1, switching macrophage phenotypes plays a significant role in inflammatory and autoimmune diseases, as well as bacterial infections (431). Protection from allergic and asthmatic reactions can be obtained from Switching M2 to M1, whereas switching M1 to M2 phenotype can protect from excessive inflammation (402, 403). Also, some bacteria can reprogram M1 to M2 to avoid the bactericidal effect of M1, hence promoting their progression. Also, M1 macrophages have cytotoxic effects on early stage tumour cells (432). However, as the tumour progresses and grows, the tumour microenvironment influences macrophages markedly leading to switch in macrophage phenotype to more closely resemble regulatory macrophages (401, 432). Therefore, our results provide significant information in terms of determining the plasticity of macrophages phenotype to be taken into consideration in the discipline of monitoring and reprogramming macrophage phenotype and function. The M2 phenotype was shown to be easier to switche and less stable than M1. This should be taken into consideration in which switching between macrophage phenotypes could be a therapeutic route to developing novel medicines and technologies for treating relevant diseases. For example, in tumour, it is preferred for M1 to be active with their cytotoxic activity for a longer time in order to stop tumour progression. In other cases, such as excessive inflammation which can develop autoimmune diseases, there is a need to reprogram proinflammatory macrophages to the anti-inflammatory state to terminate the inflammation.

3.4. Conclusion

The study of immunometabolism based on *in vitro* macrophage systems could offer key information on the interplay between cell function and metabolism. Herein, LC-MS-based metabolite profiling was used to investigate and characterise different macrophage populations (M0, M1, M2 and Mreg). The sensitivity and specificity of this approach enabled a statistical assessment performing uni- and multi-variate analyses to reveal the characteristic metabolites extracted from different polarisation states. Various metabolites were significantly changed in each polarisation state implying a distinct metabolic profile for M1 and M2 macrophages. However, Mreg showed a similar metabolic profile to that of M0, even after challenge with LPS. Autoimmune diseases such as rheumatoid arthritis, Crohn's disease, and multiple sclerosis are associated with the excessive activity of M1 macrophages, and tumour killing mechanisms are mediated by M1 macrophages (177, 303, 433). On the other hand, M2 macrophages are believed to boost tumour growth (433). Therefore, the potential that characteristic metabolites could be targeted to manipulate M1 or M2 macrophages and could lead to a novel therapeutic approach for treating tumours and immune diseases. Moreover, this approach successfully investigated the stability of M1 and M2 macrophages implying that the M1 phenotype is stable and not easily switched to the M2 phenotype, whereas M2 showed a less stable and more plastic phenotype. This study provides informative data which could be taken into consideration in the development of macrophages reprogramming and immune modulatory strategies.

Table 3.1: A list of 82 significantly changed metabolites in M1 with VIP > 1 and FDR < 0.05 compared to M0 as a result of investigation M0, M1, M2 and Mreg.

Putative metabolite	Mass	RT	FORMULA	Polarity	confidence	Pathway	Fold change	FDR	VIP
L-Alanine	89.0477	10.78	C3H7NO2	+	L2	Alanine and aspartate metabolism, Taurine and hypotaurine metabolism,	0.5910674	3.4803E-06	4.27078
L-Lactate	90.0317	7.72	C3H6O3	-	L1	Pyruvate metabolism	0.74433312	0.00067402	4.01618
4-Aminobutanoate	103.0633	11.03	C4H9NO2	+	L1	Arginine and proline metabolism, Glutamate metabolism, beta-Alanine metabolism, Butanoate metabolism	3.27345779	9.2929E-09	4.9334
Choline	103.0997	10.04	C5H13NO	+	L2	Glycine, serine and threonine metabolism, Glycerophospholipid metabolism	0.77634392	0.000015304	5.06087
Hypotaurine	109.0197	11.08	C2H7NO2S	+	L2	Taurine and hypotaurine metabolism	0.71818796	0.000076231	1.1076
L-Proline	115.0633	9.75	C5H9NO2	+	L1	Arginine and proline metabolism, Novobiocin biosynthesis	0.76210595	0.000019175	11.882
Guanidinoacetate	117.0538	11.63	C3H7N3O2	+	L1	Glycine, serine and threonine metabolism, Arginine and proline metabolism	0.50158592	6.2839E-08	1.97431
Taurine	125.0147	11.30	C2H7NO3S	+	L1	Bile acid biosynthesis, Taurine and hypotaurine metabolism	0.72422127	9.1814E-06	2.41315
(4E)-2-Oxohexenoic acid	128.0473	4.91	C6H8O3	+	L2	4-nitrotoluene degradation II	1.49580224	0.000025815	3.91235
5,6-Dihydrothymine	128.0586	10.76	C5H8N2O2	+	L2	Pyrimidine metabolism	0.81578366	0.0043388	1.31758
L-1-Pyrroline-3-hydroxy-5-carboxylate	129.0426	7.90	C5H7NO3	+	L2	Arginine and proline metabolism	0.86310599	0.033484	4.70826
(S)-3-Methyl-2-oxopentanoic acid	130.0631	4.78	C6H10O3	-	L2	Valine, leucine and isoleucine degradation, Valine, leucine and isoleucine biosynthesis	0.73807418	0.00013967	1.3122
L-Leucine	131.0946	8.86	C6H13NO2	+	L1	Valine, leucine and isoleucine degradation, Valine, leucine and isoleucine biosynthesis	0.84654372	0.0012935	4.96011
L-Asparagine	132.0535	11.06	C4H8N2O3	+	L2	Alanine and aspartate metabolism, Tetracycline biosynthesis, Cyanoamino acid metabolism, Nitrogen metabolism	0.8554587	0.0026876	2.30689
L-Aspartate	133.0374	10.44	C4H7NO4	+	L2	Alanine and aspartate metabolism, Arginine and proline metabolism, Glycine, serine and threonine metabolism, Lysine biosynthesis, Arginine and proline metabolism, Histidine metabolism, beta-Alanine metabolism, Cyanoamino acid metabolism, Carbon fixation	0.32413821	1.8317E-08	3.83937
L-Malate	134.0216	11.36	C4H6O5	-	L2	Citrate cycle (TCA cycle), Glutamate metabolism, Alanine and aspartate metabolism, Pyruvate metabolism, Glyoxylate and dicarboxylate	0.51023569	0.000010993	5.80121

						metabolism, Carbon fixation, Reductive carboxylate cycle (CO2 fixation)			
[FA trihydroxy(4:0)]	136.0372	9.23	C4H8O5	-	L2	Ascorbate and aldarate metabolism	0.71767949	0.00092306	1.2544
Hypoxanthine	136.0385	8.76	C5H4N4O	+	L1	Purine metabolism	4.38764858	1.1238E-09	5.9356
4-Trimethylammoniobutanoate	145.1102	9.59	C7H15NO2	+	L2	Lysine degradation	0.4516021	1.0842E-07	3.59513
2-Oxoglutarate	146.0215	11.27	C5H6O5	-	L2	Citrate cycle (TCA cycle), Ascorbate and aldarate metabolism, Glutamate metabolism, Alanine and aspartate metabolism, Lysine biosynthesis, Histidine metabolism, D-Glutamine and D-glutamate metabolism, Glyoxylate and dicarboxylate metabolism	0.53201048	0.000003357	2.41995
(R)-3-Hydroxy-3-methyl-2-oxopentanoate	146.0579	4.78	C6H10O4	+	L2	Valine, leucine and isoleucine biosynthesis	1.53095492	2.4774E-07	3.49383
L-Glutamate	147.0531	10.36	C5H9NO4	+	L1	Arginine and proline metabolism, Glutamate metabolism, Histidine metabolism, D-Glutamine and D-glutamate metabolism, Glutathione metabolism_Butanoate metabolism_C5-Branched dibasic acid metabolism_Porphyrin and chlorophyll metabolism_Nitrogen metabolism	0.61338229	5.0499E-07	10.7239
(R)-2-Hydroxyglutarate	148.0372	10.84	C5H8O5	-	L2	glutamate degradation V (via hydroxyglutarate)	0.54599951	0.000012083	2.17822
L-Methionine	149.0510	9.06	C5H11NO2S	+	L1	Methionine metabolism	0.90474192	0.0075267	2.46189
Xanthine	152.0334	9.21	C5H4N4O2	-	L1	Purine metabolism, Caffeine metabolism	2.59505995	5.9135E-06	1.74975
L-Histidine	155.0695	11.10	C6H9N3O2	+	L2	Histidine metabolism, beta-Alanine metabolism	0.7145422	0.000063413	3.29887
Orotate	156.0171	8.41	C5H4N2O4	-	L1	Pyrimidine metabolism	4.53636558	0.000002445	1.10051
L-Rhamnose	164.0685	8.78	C6H12O5	+	L2	Fructose and mannose metabolism	1.29275927	0.000090681	1.00553
Formylanthranilate	165.0427	4.92	C8H7NO3	-	L2	Tryptophan metabolism	2.77217369	1.8173E-06	1.04036
L-Phenylalanine	165.0790	8.21	C9H11NO2	+	L2	Phenylalanine metabolism, Phenylalanine, tyrosine and tryptophan biosynthesis, Phenylpropanoid biosynthesis, Alkaloid biosynthesis II	0.8435426	0.00031862	3.59198
N(pi)-Methyl-L-histidine	169.0851	9.89	C7H11N3O2	+	L2	Histidine metabolism	0.81640794	0.00034739	1.00105
sn-Glycerol 3-phosphate	172.0137	10.04	C3H9O6P	-	L2	Glycerolipid metabolism, Glycerophospholipid metabolism	0.42606612	1.0368E-06	3.78068
N-Acetyl-L-aspartate	175.0481	10.40	C6H9NO5	-	L2	Alanine and aspartate metabolism	0.4763034	7.5563E-07	6.776
5-Hydroxyindoleacetaldehyde	175.0633	4.14	C10H9NO2	+	L2	Tryptophan metabolism	2.71076977	4.4579E-06	1.71909
L-Citrulline	175.0957	11.20	C6H13N3O3	+	L2	Arginine and proline metabolism	0.73903731	0.00019519	1.60279
D-Glucosamine	179.0794	11.03	C6H13NO5	+	L2	Aminosugars metabolism	1.74118279	4.9617E-06	2.97878

myo-Inositol	180.0634	12.13	C6H12O6	-	L1	Inositol metabolism, Galactose metabolism, Ascorbate and aldarate metabolism, Streptomycin biosynthesis, Inositol phosphate metabolism	0.31358669	0.000010379	2.02227
L-Tyrosine	181.0740	10.17	C9H11NO3	+	L2	Tyrosine metabolism, Phenylalanine, tyrosine and tryptophan biosynthesis, Novobiocin biosynthesis, Thiamine metabolism, Phenylpropanoid biosynthesis, Alkaloid biosynthesis I	1.34962718	4.1433E-06	2.252
3-(4-Hydroxyphenyl)lactate	182.0579	7.65	C9H10O4	-	L2	Tyrosine metabolism	3.60083365	2.0651E-06	1.84868
D-Sorbitol	182.0791	10.47	C6H14O6	+	L2	Fructose and mannose metabolism, Galactose metabolism	1.59172259	0.00010052	2.10388
N-Acetyl-L-glutamate	189.0637	10.08	C7H11NO5	-	L1	Arginine and proline metabolism	0.2937601	3.4322E-09	1.42945
Phenylacetylglycine	193.0740	4.91	C10H11NO3	+	L2	Phenylalanine metabolism	1.23996118	0.0086703	1.42737
D-Gluconic acid	196.0583	10.02	C6H12O7	-	L2	Pentose phosphate pathway	0.44892405	0.000027101	1.08998
O-Acetylcarnitine	203.1158	8.36	C9H17NO4	+	L1	Alanine and aspartate metabolism	0.37379056	1.3395E-06	13.3209
L-Tryptophan	204.0900	9.48	C11H12N2O2	+	L2	Tryptophan metabolism, Phenylalanine, tyrosine and tryptophan biosynthesis, Indole and ipecac alkaloid biosynthesis	0.4070365	3.8788E-09	1.79877
sn-glycero-3-Phosphoethanolamine	215.0559	10.87	C5H14NO6P	-	L2	Glycerophospholipid metabolism, Ether lipid metabolism	0.38506994	4.1009E-07	4.47559
2-C-Methyl-D-erythritol 4-phosphate	216.0400	11.06	C5H13O7P	-	L2	Biosynthesis of steroids	1.35217145	0.0014436	4.56082
5-Hydroxy-L-tryptophan	220.0848	7.98	C11H12N2O3	+	L2	Tryptophan metabolism	4.38217667	3.3657E-06	2.28474
Cytidine	243.0855	9.55	C9H13N3O5	+	L2	Pyrimidine metabolism	2.56934463	1.2694E-06	2.20472
Deoxyadenosine	251.1019	7.13	C10H13N5O3	+	L1	Purine metabolism	6.40954834	1.3368E-08	1.63077
Hexadecanoic acid	256.2404	3.89	C16H32O2	-	L2	Fatty acid biosynthesis, Fatty acid elongation in mitochondria, Fatty acid metabolism, Biosynthesis of unsaturated fatty acids	1.18521273	0.029711	2.38098
sn-glycero-3-Phosphocholine	257.1029	10.03	C8H20NO6P	+	L1	Glycerophospholipid metabolism, Ether lipid metabolism	0.75337995	0.000014305	22.855
[FA (18:2)]	266.2610	3.94	C18H34O	+	L2	Fatty alcohols	2.73637324	0.00004707	2.69959
Adenosine	267.0968	7.78	C10H13N5O4	+	L1	Purine metabolism	4.543874	5.8236E-09	4.32093
Octadecanoic acid	284.2717	4.03	C18H36O2	-	L2	Fatty acid biosynthesis, Biosynthesis of unsaturated fatty acids	1.34866001	0.00088522	7.14501
Glutathione disulfide	306.0760	11.19	C20H32N6O12S2	+	L1	Glutamate metabolism, Glutathione metabolism	0.45649669	1.4164E-06	1.9828
Phenolsulfonphthalein	354.0563	4.90	C19H14O5S	-	L2	0	1.49473138	0.001111	2.45752
[FA methoxy,trihydrox] prostadiene	354.2771	3.98	C21H38O4	+	L2	Eicosanoids	1.66760495	0.0017277	1.28001
[GL (18:0)]	358.3084	3.94	C21H42O4	+	L2	Monoradylglycerols	2.50415536	0.000025977	11.8695

S-Adenosyl-L-homocysteine	384.1217	9.69	C14H20N6O5S	+	L2	Methionine metabolism	0.31876851	3.2273E-06	1.15227
[PC (18:0)]	523.3642	4.41	C26H54NO7P	+	L2	Glycerophosphocholines	1.83398898	0.000010977	1.79775
Ceramide (d18:1/16:0)]	537.5122	3.72	C34H67NO3	+	L2	Ceramides	6.72527452	2.1365E-08	1.78188
UDP-N-acetyl-D-glucosamine	607.0815	10.38	C17H27N3O17P2	-	L2	Aminosugars metabolism, Lipopolysaccharide biosynthesis, Peptidoglycan biosynthesis	0.26562296	2.0774E-07	2.94949
NAD+	663.1091	9.59	C21H27N7O14P2	+	L2	Oxidative phosphorylation, Glutamate metabolism, Nicotinate and nicotinamide metabolism	0.26990803	1.8623E-06	2.53374
SM(d18:1/14:0)	674.5361	4.06	C37H75N2O6P	+	L2	Ceramide phosphocholines (sphingomyelins)	1.85961145	0.00067363	1.05572
SM(d16:1/18:1)	700.5514	3.98	C39H77N2O6P	+	L2	Phosphosphingolipids	1.93220396	0.000012684	1.60072
Ceramide (d18:1/16:0)]	702.5673	3.94	C39H79N2O6P	+	L2	Ceramide phosphocholines (sphingomyelins)	1.17414961	0.0033839	1.68216
PE(18:3/P-18:1)	723.5202	3.71	C41H74NO7P	+	L2	Glycerophosphoethanolamines	1.51085702	0.000015392	1.34431
1-Hexadecanoyl-2-octadecenoyl)-sn-glycero-3-phosphonocholine	743.5827	3.81	C42H82NO7P	+	L2	Glycerophosphonocholines	1.27858239	0.00057827	1.30227
PE(36:1)	745.5622	3.81	C41H80NO8P	+	L2	Glycerophosphoethanolamines	1.1614813	0.013923	1.10053
PC(16:0/P-18:0)	745.5984	3.80	C42H84NO7P	+	L2	Glycerophosphocholines	1.1380074	0.014768	1.30564
PC(34:2)	757.5620	3.81	C42H80NO8P	+	L2	Glycerophosphocholines	1.22311943	0.0018247	2.56631
PC(36:4)	781.5620	3.79	C44H80NO8P	+	L2	Glycerophosphocholines	1.60436134	0.00001516	3.39696
PC(36:1)	787.6081	3.78	C44H86NO8P	+	L2	Glycerophosphocholines	1.34788786	0.00054396	1.79172
[PC (18:1/20:4)]	793.5983	3.78	C46H84NO7P	+	L2	Glycerophosphocholines	1.34002592	0.00033994	1.42806
PC(20:2/P-18:1)	795.6134	3.76	C46H86NO7P	+	L2	Glycerophosphocholines	1.54613209	0.000021062	1.02568
PC(38:5)	807.5779	3.79	C46H82NO8P	+	L2	Glycerophosphocholines	1.44551513	0.000054339	2.37145
PC(38:4)	809.5937	3.77	C46H84NO8P	+	L2	Glycerophosphocholines	1.81031284	5.9366E-07	2.50104
PC(38:3)	811.6090	3.77	C46H86NO8P	+	L2	Glycerophosphocholines	1.6267107	0.000027101	1.27086
PC(40:6)	833.5924	3.75	C48H84NO8P	+	L2	Glycerophosphocholines	1.63370412	0.000016747	1.48949
PC(40:5)	835.6093	3.75	C48H86NO8P	+	L2	Glycerophosphocholines	1.61957309	0.000025959	1.15688
PI(38:4)	886.5569	3.57	C47H83O13P	-	L2	Glycerophosphoinositols	0.62718074	0.00015924	1.12711

Table 3.2: a list of 74 significantly changed metabolites in M2 macrophages with VIP > 1 and FDR < 0.05 compared to M0 as a result of investigation M0, M1, M2 and Mreg.

Putative metabolite	Mass	RT	FORMULA	Polarity	confidence	Pathway	Fold change	VIP	FDR
L-Alanine	89.0477	10.78	C3H7NO2	+	L2	Alanine and aspartate	1.30368522	4.9687	0.00028081
Orthophosphate	97.9770	11.28	H3O4P	-	L2	Oxidative phosphorylation, Photosynthesis	0.79535804	3.60477	0.0013151
L-Serine	105.0426	11.37	C3H7NO3	+	L1	Glycine, serine and threonine metabolism, Methionine metabolism, Cysteine metabolism	0.74795882	1.61634	0.0012516
(L)-1-Pyrroline-5-carboxylate	113.0478	10.97	C5H7NO2	-	L2	Glutamate metabolism, Arginine and proline metabolism	2.00635141	1.7643	0.0014892
5,6-Dihydrouracil	114.0429	9.17	C4H6N2O2	+	L2	Pyrimidine metabolism, beta-Alanine metabolism, Pantothenate and CoA biosynthesis	1.42166023	1.81905	0.0002303
L-Proline	115.0633	9.75	C5H9NO2	+	L1	Arginine and proline metabolism, Novobiocin biosynthesis	1.17400582	13.5084	0.0015133
Guanidinoacetate	117.0538	11.63	C3H7N3O2	+	L1	Glycine, serine and threonine metabolism, Arginine and proline metabolism	5.461508	8.24144	1.5758E-10
L-Valine	117.0790	8.82	C5H11NO2	+	L2	Valine, leucine and isoleucine degradation, Valine, leucine and isoleucine biosynthesis	1.14980008	6.11209	0.0073837
Succinate	118.0267	10.83	C4H6O4	-	L2	Citrate cycle (TCA cycle), Oxidative phosphorylation, Glutamate metabolism	1.37125077	1.03471	0.00036492
L-Threonine	119.0583	10.59	C4H9NO3	+	L2	Glycine, serine and threonine metabolism, Valine, leucine and isoleucine biosynthesis	1.18924083	2.77246	0.0093809
Taurine	125.0147	11.30	C2H7NO3S	+	L1	Bile acid biosynthesis, Taurine and hypotaurine metabolism	0.67474278	3.66933	3.7304E-06
2-Oxohexenoic acid	128.0473	4.91	C6H8O3	+	L2	4-nitrotoluene degradation II	0.7832302	3.30659	0.0072255
5,6-Dihydrothymine	128.0586	10.76	C5H8N2O2	+	L2	Pyrimidine metabolism	1.22680378	2.15329	0.00065886
(S)-3-Methyl-2-oxopentanoic acid	130.0631	4.78	C6H10O3	-	L2	Valine, leucine and isoleucine degradation, Valine, leucine and isoleucine biosynthesis	1.33097224	2.08791	0.000044197
Creatine	131.0694	10.77	C4H9N3O2	+	L1	Glycine, serine and threonine metabolism, Arginine and proline metabolism	1.29659199	19.4221	0.00038328
L-Leucine	131.0946	8.86	C6H13NO2	+	L1	Valine, leucine and isoleucine degradation, Valine, leucine and isoleucine biosynthesis	1.09131924	4.9661	0.018955
L-Asparagine	132.0535	11.06	C4H8N2O3	+	L2	Alanine and aspartate metabolism, Tetracycline biosynthesis	1.10317588	2.51753	0.029563
L-Aspartate	133.0374	10.44	C4H7NO4	+	L2	Alanine and aspartate metabolism, Arginine and proline metabolism, Glycine, serine and threonine metabolism	3.39704055	10.0092	2.274E-07
[FA trihydroxy (4:0)]	136.0372	9.23	C4H8O5	-	L2	Ascorbate and aldarate metabolism	1.18281113	1.33946	0.0094931

4-Guanidinobutanoate	145.0851	11.03	C5H11N3O2	+	L2	Arginine and proline metabolism	1.47161928	1.18482	0.000022507
3-Hydroxy-3-methyl-2-oxopentanoate	146.0579	4.78	C6H10O4	+	L2	Valine, leucine and isoleucine biosynthesis	0.78664819	2.88286	0.0015003
L-Glutamine	146.0690	10.88	C5H10N2O3	+	L1	Glutamate metabolism, Purine metabolism _D-Glutamine and D-glutamate metabolism.	0.64343147	17.3687	1.6963E-06
(L)-2-Hydroxyglutarate	148.0372	10.84	C5H8O5	-	L2	glutamate degradation	1.59994264	3.47019	0.000036695
L-Methionine	149.0510	9.06	C5H11NO2S	+	L1	Methionine metabolism	1.15683814	4.61835	0.0025767
Phenylpropanoate	150.0680	4.73	C9H10O2	-	L2	Phenylalanine metabolism	2.09397644	1.69697	9.8838E-07
L-Histidine	155.0695	11.10	C6H9N3O2	+	L2	Histidine metabolism, beta-Alanine metabolism	1.43339232	5.74041	0.000016454
4-Imidazolone-5-propanoate	156.0535	7.09	C6H8N2O3	-	L2	Histidine metabolism	1.70019774	1.04465	0.000059035
Allantoin	158.0439	11.36	C4H6N4O3	+	L2	Unknown	0.53640158	1.10531	0.0031771
O-Acetyl-L-homoserine	161.0688	8.63	C6H11NO4	+	L2	Methionine metabolism	1.44776315	4.49929	0.000010846
L-Rhamnose	164.0685	8.78	C6H12O5	+	L2	Fructose and mannose metabolism	0.69706979	1.37124	0.0018592
L-Phenylalanine	165.0790	8.21	C9H11NO2	+	L2	Phenylalanine metabolism	1.14921616	4.77877	0.001874
3-(3-Hydroxy-phenyl)-propanoic acid	166.0630	4.90	C9H10O3	-	L2	Phenylalanine metabolism	5.1454175	1.26972	2.4711E-07
N-Formimino-L-glutamate	174.0641	8.55	C6H10N2O4	+	L2	Histidine metabolism	4.81078239	1.00835	6.8466E-07
N-Acetyl-L-aspartate	175.0481	10.40	C6H9NO5	-	L2	Alanine and aspartate metabolism	2.06867333	13.4581	9.9425E-07
L-Citrulline	175.0957	11.20	C6H13N3O3	+	L2	Arginine and proline metabolism	1.14331055	1.52174	0.012241
D-Glucosamine	179.0794	11.03	C6H13NO5	+	L2	Aminosugars metabolism	0.8045273	2.00783	0.0017426
myo-Inositol	180.0634	12.13	C6H12O6	-	L1	Inositol metabolism, Galactose metabolism_ metabolism_Inositol phosphate metabolism	1.42521181	2.07024	0.0030956
L-Tyrosine	181.0740	10.17	C9H11NO3	+	L2	Tyrosine metabolism	1.12893042	1.67891	0.015364
3-(4-Hydroxyphenyl) lactate	182.0579	7.65	C9H10O4	-	L2	Tyrosine metabolism	3.4647346	2.52501	8.1605E-08
N6,N6,N6-Trimethyl-L-lysine	188.1525	15.31	C9H20N2O2	+	L2	Lysine degradation	1.29824884	1.61166	0.000044437
N-Acetyl-L-glutamate	189.0637	10.08	C7H11NO5	-	L1	Arginine and proline metabolism	7.20954174	5.89031	6.5786E-10
Phenylacetylglycine	193.0740	4.91	C10H11NO3	+	L2	Phenylalanine metabolism	1.27167038	2.17183	0.0070028
[FA (10:1/2:0)]	200.1049	4.76	C10H16O4	+	L2	Fatty Acids and Conjugates	0.74346803	1.90323	0.00025935
L-Kynurenine	208.0849	8.82	C10H12N2O3	+	L2	Tryptophan metabolism	0.68090021	2.52752	0.00015415
Phosphocreatine	211.0359	10.46	C4H10N3O5P	+	L2	Arginine and proline metabolism	1.34949533	4.78401	0.00035986
sn-glycero-3-Phosphoethanolamine	215.0559	10.87	C5H14NO6P	-	L2	Glycerophospholipid metabolism, Ether lipid metabolism	1.20804105	3.34671	0.0027972
2-C-Methyl-D-erythritol 4-phosphate	216.0400	11.06	C5H13O7P	-	L2	Biosynthesis of steroids	0.82491566	4.4721	0.0026389
Propanoylcarnitine	217.1314	7.75	C10H19NO4	+	L2	Oxidation of Branched Fatty Acids	1.27635937	3.34242	0.0024232
L-Formylkynurenine	236.0797	8.02	C11H12N2O4	+	L2	Tryptophan metabolism	0.5220933	1.08131	8.0239E-06

sn-glycero-3-Phosphocholine	257.1029	10.03	C8H20NO6P	+	L1	Glycerophospholipid metabolism, Ether lipid metabolism	0.91417714	16.9486	0.010191
Octadecanoic acid	284.2717	4.03	C18H36O2	-	L2	Fatty acid biosynthesis, Biosynthesis of unsaturated fatty acids	0.86503274	5.88141	0.010033
2-Oxooctadecanoic acid	298.2508	3.81	C18H34O3	+	L2	Fatty Acids and Conjugates	1.4728387	1.02395	0.0041073
Glutathione disulfide	306.0760	11.19	C20H32N6O12S2	+	L1	Glutamate metabolism, Glutathione metabolism	0.85530564	1.20635	0.030872
AMP	347.0632	9.59	C10H14N5O7P	+	L2	Purine metabolism, Zeatin biosynthesis	0.70677272	1.19524	0.0019574
[PC (16:2)]	481.3533	4.49	C24H52NO6P	+	L2	Glycerophosphocholines	1.26601288	1.43978	0.0001743
UDP-N-acetyl-D-glucosamine	607.0815	10.38	C17H27N3O17P2	-	L2	Aminosugars metabolism, Lipopolysaccharide biosynthesis, Peptidoglycan biosynthesis	0.68476779	2.59322	0.00020036
PC(30:0)	705.5307	3.85	C38H76NO8P	+	L2	Glycerophosphocholines	1.45674587	3.224	0.00066337
[PC (14:2/18:0)]	719.5836	3.84	C40H82NO7P	+	L2	Glycerophosphocholines	1.24956606	1.14552	0.00764
PE(18:3)	723.5202	3.71	C41H74NO7P	+	L2	Glycerophosphoethanolamines	0.71410548	1.36096	0.00045202
PC(32:1)	731.5463	3.83	C40H78NO8P	+	L2	Glycerophosphocholines	1.65707116	8.3114	0.000034906
PC(32:0)	733.5626	3.82	C40H80NO8P	+	L2	Glycerophosphocholines	0.83808094	2.01645	0.026505
PE(36:2)	743.5467	3.79	C41H78NO8P	+	L2	Glycerophosphoethanolamines	1.3996198	1.16782	0.0021958
1-Hexadecanoyl-2-(octadecenoyl)-sn-glycero-3-phosphonocholine	743.5827	3.81	C42H82NO7P	+	L2	Glycerophosphonocholines	1.31926741	1.88892	0.003579
PC(16:0/P-18:0)	745.5984	3.80	C42H84NO7P	+	L2	Glycerophosphocholines	1.37738391	3.37461	0.00030728
[PE (16:1/22:6)]	747.5199	3.68	C43H74NO7P	+	L2	Glycerophosphoethanolamines	0.70601069	1.19321	0.00043237
PC(36:4)	781.5620	3.79	C44H80NO8P	+	L2	Glycerophosphocholines	0.86983969	1.93879	0.017497
PC(36:1)	787.6081	3.78	C44H86NO8P	+	L2	Glycerophosphocholines	0.82199988	1.76365	0.0017633
PS(36:1)	789.5523	3.57	C42H80NO10P	-	L2	Glycerophosphoserines	0.27774596	2.46207	9.1219E-06
PG(22:6)	866.5101	3.53	C50H75O10P	-	L2	Glycerophosphoglycerols	0.56618512	1.01277	0.000049238
PS(44:10)	883.5360	3.53	C50H78NO10P	+	L2	Glycerophosphoserines	0.54262297	1.28648	0.00035269
PI(38:4)	886.5569	3.57	C47H83O13P	-	L2	Glycerophosphoinositols	0.42028258	2.0086	0.000012837

Table 3.3: A list of 46 significantly changed metabolites in Mreg with VIP > 1 and FDR < 0.05 compared to M0 as a result of investigation M0, M1, M2 and Mreg.

Putative metabolite	Mass	RT	FORMULA	Polarity	confidence	Pathway	Fold change	VIP	FDR
(1-Ribosylimidazole)-4-acetate	258.0852	8.01	C10H14N2O6	+	L2	Histidine metabolism	0.71874071	3.32871	0.00086979
(R)-2-Hydroxyglutarate	148.0372	10.84	C5H8O5	-	L2	glutamate degradation	1.16398315	2.04506	0.036458
[GL (18:0)]	358.3084	3.94	C21H42O4	+	L2	Monoradylglycerols	1.40527267	10.1536	0.012813
[PC (14:2/16:0)]	691.5514	3.85	C38H78NO7P	+	L2	Glycerophosphocholines	1.18144086	1.15525	0.034028
[PC (14:2/18:0)]	719.5836	3.84	C40H82NO7P	+	L2	Glycerophosphocholines	1.30691845	1.72517	0.0017887
[PC (16:2)]	481.3533	4.49	C24H52NO6P	+	L2	Glycerophosphocholines	0.84802795	1.34064	0.0052852
[PC (18:0)]	523.3642	4.41	C26H54NO7P	+	L2	Glycerophosphocholines	1.2470667	1.61727	0.0097919
[ST hydrox] 3alpha,12alpha-Dihydroxy-5beta-chol-6-en-24-oic Acid	390.2771	3.85	C24H38O4	+	L2	Bile acids and derivatives	0.8137069	3.29368	0.00049801
4-Aminobutanoate	103.0633	11.03	C4H9NO2	+	L1	Arginine and proline metabolism, Glutamate metabolism, beta-Alanine metabolism, Butanoate metabolism	0.93528522	1.26933	0.037815
4-Trimethylammoniobutanoate	145.1102	9.59	C7H15NO2	+	L2	Lysine degradation	0.88917714	2.49942	0.031497
Acetoacetate	102.0317	9.63	C4H6O3	+	L2	Valine, leucine and isoleucine degradation, Tyrosine metabolism, Propanoate metabolism	0.68636409	1.02295	0.000091688
gamma-Amino-gamma-cyanobutanoate	128.0586	8.38	C5H8N2O2	+	L2	Cyanoamino acid metabolism	1.18796924	1.47067	0.00093318
Guanidinoacetate	117.0538	11.63	C3H7N3O2	+	L1	Glycine, serine and threonine metabolism, Arginine and proline metabolism	1.2048983	2.22311	0.000057093
Hypoxanthine	136.0385	8.76	C5H4N4O	+	L1	Purine metabolism	0.41588091	4.40337	2.1787E-07
Itaconate	130.0267	7.78	C5H6O4	-	L2	C5-Branched dibasic acid metabolism	1.16319782	1.17447	0.049463
L-1-Pyrroline-3-hydroxy-5-carboxylate	129.0426	7.90	C5H7NO3	+	L2	Arginine and proline metabolism	0.8685846	8.57764	0.042942
L-Citrulline	175.0957	11.20	C6H13N3O3	+	L2	Arginine and proline metabolism	0.79457235	2.48637	0.0032958
L-Glutamate	147.0531	10.36	C5H9NO4	+	L1	Arginine and proline metabolism, Glutamate metabolism, Glutathione metabolism	0.91207359	8.54113	0.0054277
L-Leucine	131.0946	8.86	C6H13NO2	+	L1	Valine, leucine and isoleucine degradation, Valine, leucine and isoleucine biosynthesis	0.91580096	6.49204	0.0078472
L-Methionine	149.0510	9.06	C5H11NO2S	+	L1	Methionine metabolism	0.87135864	5.58269	0.00078179
L-Phenylalanine	165.0790	8.21	C9H11NO2	+	L2	Phenylalanine metabolism, Phenylalanine, tyrosine and tryptophan biosynthesis	0.85001798	6.37891	0.00054046
L-Serine	105.0426	11.37	C3H7NO3	+	L1	Glycine, serine and threonine metabolism, Methionine metabolism, Cysteine metabolism,	0.71241261	2.31254	0.00013158
L-Tryptophan	204.0900	9.48	C11H12N2O2	+	L2	Tryptophan metabolism, Phenylalanine, tyrosine and tryptophan biosynthesis	0.73656445	2.13036	2.5289E-06

L-Tyrosine	181.0740	10.17	C9H11NO3	+	L2	Tyrosine metabolism	0.88909809	1.98119	0.032974
N(pi)-Methyl-L-histidine	169.0851	9.89	C7H11N3O2	+	L2	Histidine metabolism	0.90634798	1.1436	0.044205
NAD+	663.1091	9.59	C21H27N7O14P2	+	L2	Oxidative phosphorylation, Glutamate metabolism, Nicotinate and nicotinamide metabolism	0.73851916	2.4753	0.010817
N-Formyl-L-methionine	177.0460	4.92	C6H11NO3S	-	L2	Methionine metabolism	0.78926271	1.88161	0.002013
N-Methylethanolamine phosphate	155.0346	10.23	C3H10NO4P	+	L2	Glycerophospholipid metabolism	0.77919782	1.03443	0.00061092
O-Acetyl-L-homoserine	161.0688	8.63	C6H11NO4	+	L2	Methionine metabolism.	1.46925228	5.95037	0.000016273
Octadecanoic acid	284.2717	4.03	C18H36O2	-	L2	Fatty acid biosynthesis, Biosynthesis of unsaturated fatty acids	1.13850507	7.26959	0.0493
Propanoylcarnitine	217.1314	7.75	C10H19NO4	+	L2	Oxidation of Branched Fatty Acids	0.73565083	4.29802	0.0018359
Orthophosphate	97.9770	11.28	H3O4P	-	L2	Oxidative phosphorylation, Photosynthesis, Peptidoglycan biosynthesis	1.22251162	4.48377	0.028549
PC(16:0/P-18:0)	745.5984	3.80	C42H84NO7P	+	L2	Glycerophosphocholines	1.13820736	2.39879	0.024517
PC(32:0)	733.5626	3.82	C40H80NO8P	+	L2	Glycerophosphocholines	1.26147569	3.51248	0.010893
PC(32:2)	729.5307	3.85	C40H76NO8P	+	L2	Glycerophosphocholines	1.17953796	1.18708	0.044627
PC(36:1)	787.6081	3.78	C44H86NO8P	+	L2	Glycerophosphocholines	1.16925623	2.01485	0.043903
PC(36:2)	785.5932	3.79	C44H84NO8P	+	L2	Glycerophosphocholines	1.1836604	4.55349	0.0070263
PC(38:4)	809.5937	3.77	C46H84NO8P	+	L2	Glycerophosphocholines	1.15181155	1.73588	0.015701
PE(18:3)	723.5202	3.71	C41H74NO7P	+	L2	Glycerophosphoethanolamines	1.17100671	1.28321	0.01104
PE(20:4)	749.5360	3.71	C43H76NO7P	+	L2	Glycerophosphoethanolamines	1.38979386	1.42945	0.025906
PE(34:1)	717.5308	3.82	C39H76NO8P	+	L2	Glycerophosphoethanolamines	1.25298531	1.19473	0.020692
PE(36:2)	743.5467	3.79	C41H78NO8P	+	L2	Glycerophosphoethanolamines	1.28290305	1.14782	0.049096
Phenylacetylglycine	193.0740	4.91	C10H11NO3	+	L2	Phenylalanine metabolism	1.21520923	2.55785	0.0053363
Pyridoxine	169.0739	7.21	C8H11NO3	+	L2	Vitamin B6 metabolism	0.86149324	2.75732	0.030997
Tetradecanoic acid	228.2090	3.86	C14H28O2	-	L2	Fatty acid biosynthesis	0.79345777	2.05771	0.037293

Table 3.4: A list of 112 significantly changed metabolites in M1 macrophages with VIP > 1 and FDR < 0.05 compared to M0 as a result of investigation M0, M1, M2, Mreg, M0-LPS and Mreg-LPS.

Putative metabolite	Mass	RT	FORMULA	POLARITY	confidence	Pathway	Fold change	VIP	FDR
Hexadecenoic acid	254.2246	3.51	C16H30O2	-	L2	Fatty acid biosynthesis	1.43848618	2.74311	2.72767E-06
(R)-2-Hydroxyglutarate	148.0372	10.69	C5H8O5	-	L1	glutamate degradation V (via hydroxyglutarate)	0.61655946	1.68546	1.73558E-08
(S)-3-Methyl-2-oxopentanoic acid	130.0631	4.45	C6H10O3	-	L2	Valine, leucine and isoleucinemetabolism	0.71040728	1.31471	3.42152E-06
(L)-Malate	134.0216	11.20	C4H6O5	-	L1	Citrate cycle (TCA cycle), Glutamate metabolism, Alanine and aspartate metabolism, Pyruvate metabolism	0.63242015	3.75835	4.27248E-08
[FA (20:4)]	304.2402	3.50	C20H32O2	-	L2	Fatty Acids and Conjugates	2.275636	2.24008	3.84439E-09
[FA (6:0)]	259.1784	4.51	C13H25NO4	+	L2	Fatty acyl carnitines	0.48601794	2.06272	6.41175E-07
[FA (8:0)]	144.1151	3.89	C8H16O2	-	L2	Fatty acid biosynthesis	1.45422493	1.30035	1.77473E-06
[FA methyl(14:0)]	242.2246	3.53	C15H30O2	-	L2	Fatty Acids and Conjugates	1.43658271	3.95363	6.0376E-06
[FA trihydroxy(4:0)]	136.0373	9.35	C4H8O5	-	L2	Ascorbate and aldarate metabolism	1.07666863	1.53254	0.018538129
[GL (18:0)]	358.3085	3.77	C21H42O4	-	L2	Monoradylglycerols	1.48255489	3.81887	3.23123E-07
[PC (16:0/18:1)]	759.5777	6.41	C42H82NO8P	+	L2	Glycerophosphocholines	0.61969789	1.31766	6.06731E-06
[PC (18:0)]	523.3645	7.25	C26H54NO7P	+	L2	Glycerophosphocholines	1.65781385	1.09916	1.27933E-05
[PC (18:1/18:1)]	785.5934	6.44	C44H84NO8P	+	L2	Glycerophosphocholines	0.63909897	1.40053	1.77638E-06
Ceramide (d18:1/14:0)]	229.2406	4.34	C14H31NO	+	L2	Sphingoid bases	2.77136595	2.1982	2.16695E-06
Ceramide (d18:1/16:0)]	537.5121	4.29	C34H67NO3	+	L2	Ceramides	5.15995143	2.91484	2.59566E-09
[ST hydrox] 3alpha,12alpha-Dihydroxy-5beta-chol-6-en-24-oic Acid	390.2769	4.41	C24H38O4	+	L2	Bile acids and derivatives	2.31418639	4.10291	1.66142E-09
2,3-Dimethylmaleate	144.0424	10.25	C6H8O4	+	L2	Nicotinate and nicotinamide metabolism	1.64434734	2.64852	0.000902918
2,5-Dioxopentanoate	130.0268	6.97	C5H6O4	-	L2	Ascorbate and aldarate metabolism, Arginine and proline metabolism	0.87162665	5.15668	0.000361002
2-Amino-4-hydroxy-6-(D-erythro-1,2,3-trihydroxypropyl)-7,8- dihydropteridine	255.0967	10.93	C9H13N5O4	+	L2	Folate biosynthesis	24.7453969	1.33644	7.98005E-10
2-C-Methyl-D-erythritol 4-phosphate	216.0401	10.92	C5H13O7P	-	L2	Biosynthesis of steroids	1.2899577	1.00279	2.62655E-05
2-Dehydro-3-deoxy-L-rhamnonate	162.0529	10.08	C6H10O5	-	L2	Fructose and mannose metabolism	1.42772751	1.53793	4.221E-06
2-Oxoglutarate	146.0216	11.10	C5H6O5	-	L2	Citrate cycle (TCA cycle), Ascorbate and aldarate metabolism, Glutamate metabolism, Alanine and aspartate metabolism	0.54730026	9.65222	7.13002E-07
3-(4-Hydroxyphenyl)lactate	182.0580	7.37	C9H10O4	-	L2	Tyrosine metabolism	3.34518875	1.43985	1.4892E-10

3-(4-Hydroxyphenyl)pyruvate	180.0423	7.31	C9H8O4	-	L2	Tyrosine metabolism	4.04388475	1.64722	2.63032E-08
3-Hydroxyanthranilate	153.0426	9.34	C7H7NO3	+	L2	Tryptophan metabolism, Carbazole degradation	2.66673547	1.49159	1.74849E-09
4-Aminobutanoate	103.0633	10.90	C4H9NO2	+	L2	Arginine and proline metabolism, Glutamate metabolism_Butanoate metabolism	2.99110131	20.9512	6.74324E-10
4-Guanidinobutanoate	145.0852	10.88	C5H11N3O2	+	L2	Arginine and proline metabolism	1.28155153	5.3179	3.13542E-06
4-Pyridoxolactone	165.0427	4.52	C8H7NO3	-	L2	Vitamin B6 metabolism	1.75088585	5.3792	8.70771E-06
4-Trimethylammoniobutanoate	145.1103	9.53	C7H15NO2	+	L2	Lysine degradation	0.49718519	1.01084	6.60207E-09
5-Acetamidopentanoate	159.0895	9.31	C7H13NO3	+	L2	Lysine degradation	0.44467487	1.66038	5.78824E-10
5-Hydroxy-L-tryptophan	220.0847	7.79	C11H12N2O3	+	L2	Tryptophan metabolism	8.25334527	24.6399	6.74518E-10
8-Amino-7-oxononanoate	187.1208	4.50	C9H17NO3	+	L2	Biotin metabolism	0.65661907	2.9153	2.6811E-05
Adenosine	267.0967	7.76	C10H13N5O4	+	L1	Purine metabolism	1.50946704	4.50335	5.5995E-07
ADP	427.0294	10.38	C10H15N5O10P2	+	L2	Oxidative phosphorylation_Purine metabolism	0.48576661	3.25273	0.000104034
CDP-choline	244.0538	10.15	C14H26N4O11P2	+	L2	Glycerophospholipid metabolism	0.41270282	4.28923	2.44684E-05
Citrate	192.0270	12.14	C6H8O7	-	L2	Citrate cycle (TCA cycle), Glutamate metabolism, Alanine and aspartate metabolism	0.70860988	1.3983	0.006336691
Creatine	131.0694	10.63	C4H9N3O2	+	L1	Glycine, serine and threonine metabolism, Arginine and proline metabolism	0.9542483	6.26518	0.014605109
Creatinine	113.0590	8.21	C4H7N3O	+	L1	Arginine and proline metabolism	0.86510576	3.21495	0.002644392
Cytidine	243.0857	9.44	C9H13N3O5	+	L1	Pyrimidine metabolism	2.18072654	3.01153	1.13774E-08
D-Gluconic acid	196.0583	10.03	C6H12O7	-	L1	Pentose phosphate pathway	1.48823512	1.93396	3.21784E-06
D-Glucose	180.0634	11.93	C6H12O6	-	L2	Glycolysis / Gluconeogenesis, Pentose phosphate pathway, Galactose metabolism,	0.33348594	1.41759	6.35309E-10
Dodecanoic acid	200.1776	3.61	C12H24O2	-	L2	Fatty acid biosynthesis	1.6175167	1.49744	2.44036E-07
D-Sorbitol	182.0791	10.35	C6H14O6	+	L2	Fructose and mannose metabolism, Galactose metabolism	2.42693905	2.35084	1.50314E-07
Glutathione disulfide	306.0760	11.02	C20H32N6O12S2	+	L1	Glutamate metabolism, Glutathione metabolism	0.7360926	2.23423	0.009997179
Glyceraldehyde	90.0318	7.33	C3H6O3	-	L2	GlycerolipidMetabolism	0.66854248	7.00791	5.9622E-07
Glycine	75.0321	11.26	C2H5NO2	+	L1	Purine metabolism, Glycine, serine and threonine metabolism, Lysine degradation_Glutathione metabolism	0.69266407	8.97258	3.75759E-05

Guanidinoacetate	117.0538	11.49	C3H7N3O2	+	L1	Glycine, serine and threonine metabolism_Arginine and proline metabolism	0.0976572	5.71626	1.87961E-09
Hexadecanoic acid	256.2402	3.51	C16H32O2	-	L2	Fatty acid biosynthesis	0.86421743	1.16217	0.001359232
Hypotaurine	109.0198	10.91	C2H7NO2S	+	L2	Taurine and hypotaurine metabolism	0.33375477	18.044	8.27922E-10
Hypoxanthine	136.0385	8.64	C5H4N4O	+	L1	Purine metabolism	3.86173709	7.38045	2.3989E-11
Inosine	268.0808	8.87	C10H12N4O5	+	L1	Purine metabolism	4.34932184	2.12758	7.0839E-09
L-Alanine	89.0477	10.76	C3H7NO2	+	L1	Alanine and aspartate metabolism	0.51192607	2.25692	3.87991E-09
L-Arginine	174.1117	17.73	C6H14N4O2	+	L1	Arginine and proline metabolism_D-Arginine and D-ornithine metabolism	0.92957231	2.61861	0.037052933
L-Asparagine	132.0535	10.93	C4H8N2O3	+	L1	Alanine and aspartate metabolism	0.62075843	3.47458	5.47692E-07
L-Aspartate	133.0376	10.57	C4H7NO4	-	L1	Alanine and aspartate metabolism, Arginine and proline metabolism, Glycine, serine and threonine metabolism	0.59768504	7.38343	2.95573E-08
L-Citrulline	175.0957	11.06	C6H13N3O3	+	L1	Arginine and proline metabolism	2.7051333	1.26822	1.80835E-10
L-Glutamate	147.0531	10.32	C5H9NO4	+	L1	Arginine and proline metabolism, Glutamate metabolism, Histidine metabolism, D-Glutamine and D-glutamate metabolism	0.59427494	1.70176	3.90876E-07
L-Glutamate 5-semialdehyde	131.0583	10.55	C5H9NO3	-	L2	Arginine and proline metabolism	0.50435819	6.3827	9.20644E-09
L-Kynurenine	208.0848	8.75	C10H12N2O3	+	L2	Tryptophan metabolism	0.82630856	2.15674	0.00018635
L-Leucine	131.0946	8.54	C6H13NO2	+	L1	Valine, leucine and isoleucine degradation, Valine, leucine and isoleucine biosynthesis	0.91921764	3.37401	0.00660688
L-Methionine	149.0511	9.01	C5H11NO2S	+	L2	Methionine metabolism	0.90653499	6.90296	0.011687944
L-Methionine S-oxide	165.0459	9.69	C5H11NO3S	+	L2	Methionine metabolism	1.41333327	4.25381	0.000186409
L-Phenylalanine	165.0790	8.12	C9H11NO2	+	L2	Phenylalanine metabolism, Phenylalanine, tyrosine and tryptophan biosynthesis	0.81783613	1.05462	6.87075E-05
L-Proline	115.0633	9.65	C5H9NO2	+	L1	Arginine and proline metabolism, Novobiocin biosynthesis	0.89790713	1.40511	8.89499E-05
L-Serine	105.0427	11.25	C3H7NO3	+	L1	Glycine, serine and threonine metabolism	2.10553159	6.20145	4.15145E-07
L-Threonine	119.0583	10.54	C4H9NO3	+	L2	Glycine, serine and threonine metabolism, Valine, leucine and isoleucine biosynthesis	0.50308397	13.2403	3.29384E-08
L-Tyrosine	181.0739	10.05	C9H11NO3	+	L2	Tyrosine metabolism	0.91558596	2.60605	0.047882461
L-Valine	117.0790	8.74	C5H11NO2	+	L2	Valine, leucine and isoleucine metabolism	0.93201912	2.62739	0.009713149
LysoPC(18:0)	523.3640	4.07	C26H54NO7P	+	L2	Glycerophosphocholines	1.55462837	2.85833	1.0012E-05
N(pi)-Methyl-L-histidine	169.0851	9.25	C7H11N3O2	+	L2	Histidine metabolism	0.81729772	2.1004	1.74122E-05

N4-Acetylaminobutanal	129.0790	7.25	C6H11NO2	+	L2	Arginine and proline metabolism	0.40487632	6.05825	1.85398E-07
N6,N6,N6-Trimethyl-L-lysine	188.1524	14.79	C9H20N2O2	+	L2	Lysine degradation	0.79335875	2.29485	0.000284772
N6-Methyl-L-lysine	160.1212	15.81	C7H16N2O2	+	L1	0	0.50774123	1.79506	7.90777E-06
N-Acetyl-L-aspartate	175.0480	10.23	C6H9NO5	-	L2	Alanine and aspartate metabolism	0.61005686	1.13634	2.25748E-09
N-Acetyl-L-glutamate	189.0637	9.84	C7H11NO5	-	L2	Arginine and proline metabolism	0.5718298	2.04714	6.63268E-08
N-Acetylserotonin	218.1055	5.34	C12H14N2O2	+	L2	Tryptophan metabolism	3.37638706	1.31323	2.78342E-09
NAD+	331.5545	9.52	C21H27N7O14P2	+	L2	Oxidative phosphorylation, Nicotinate and nicotinamide metabolism	0.58879177	2.06708	1.92096E-05
NADH	332.5625	9.35	C21H29N7O14P2	+	L2	Oxidative phosphorylation	0.44544743	4.30476	2.20275E-05
N-Formyl-L-methionine	177.0459	4.51	C6H11NO3S	-	L2	Methionine metabolism	0.77213071	3.38678	3.37142E-06
N-Methylethanolamine phosphate	155.0347	10.13	C3H10NO4P	+	L2	Glycerophospholipid metabolism	0.70457409	1.08717	0.000215104
O-Acetylcarnitine	203.1158	8.34	C9H17NO4	+	L1	Alanine and aspartate metabolism	0.34184451	1.03631	6.47338E-10
O-Acetyl-L-homoserine	161.0689	7.32	C6H11NO4	-	L2	Methionine metabolism, Sulfur metabolism	0.53191082	1.03476	1.90728E-06
Butanoylcarnitine	231.1471	7.32	C11H21NO4	+	L2	Fatty acyl carnitines	0.50020228	7.82695	9.00887E-10
Propanoylcarnitine	217.1314	5.39	C10H19NO4	+	L2	Oxidation of Branched Fatty Acids	0.45611174	1.26404	2.64833E-09
Orotate	156.0172	8.16	C5H4N2O4	-	L2	Pyrimidine metabolism	3.20896733	6.69604	3.2984E-11
O-Succinyl-L-homoserine	219.0742	9.86	C8H13NO6	-	L2	Methionine metabolism, Sulfur metabolism	0.40823736	1.0862	1.93E-08
PC(30:0)	705.5308	3.59	C38H76NO8P	+	L2	Glycerophosphocholines	0.57675014	2.00695	7.53116E-09
PC(32:0)	733.5609	3.64	C40H80NO8P	+	L2	Glycerophosphocholines	0.75479592	1.33229	6.73002E-07
PC(32:1)	731.5464	3.56	C40H78NO8P	+	L2	Glycerophosphocholines	0.76409883	3.35278	2.84747E-08
PC(34:1)	759.5774	3.65	C42H82NO8P	+	L2	Glycerophosphocholines	0.89598693	1.3421	0.000155386
PC(34:2)	757.5620	3.54	C42H80NO8P	+	L2	Glycerophosphocholines	0.88857554	1.66782	8.20915E-05
PC(36:2)	785.5932	3.54	C44H84NO8P	+	L2	Glycerophosphocholines	0.86787476	1.26837	1.43691E-05
PC(36:3)	783.5773	3.52	C44H82NO8P	+	L2	Glycerophosphocholines	1.10334976	1.11708	0.002476507
PC(36:4)	781.5620	3.52	C44H80NO8P	+	L2	Glycerophosphocholines	1.28440707	1.46441	4.06885E-06
PC(38:4)	809.5926	3.51	C46H84NO8P	+	L2	Glycerophosphocholines	1.36087301	1.07736	9.63243E-07
Phenylpropanoate	150.0681	4.45	C9H10O2	-	L2	Phenylalanine metabolism	1.79433946	3.01045	1.79532E-07
Phenylpyruvate	164.0474	4.48	C9H8O3	-	L2	Phenylalanine metabolism	9.79014438	1.44753	3.6647E-09
Phosphocreatine	211.0358	10.31	C4H10N3O5P	+	L2	Arginine and proline metabolism	0.82471903	1.08825	0.002610008
Pyridoxine	169.0738	7.34	C8H11NO3	+	L2	Vitamin B6 metabolism	1.16348181	5.09707	0.000306001
Pyruvate	88.0161	7.29	C3H4O3	-	L2	Glycolysis / Gluconeogenesis, Citrate cycle (TCA cycle), Pentose phosphate pathway_ Alanine and aspartate metabolism_	0.5949559	13.7683	2.04199E-08

sn-glycero-3-Phosphocholine	257.1029	9.93	C8H20NO6P	+	L1	Glycerophospholipid metabolism, Ether lipid metabolism	0.86334112	5.53025	9.29255E-06
sn-glycero-3-Phosphoethanolamine	215.0559	10.77	C5H14NO6P	+	L2	Glycerophospholipid metabolism, Ether lipid metabolism	0.3567385	1.42873	1.37599E-10
sn-Glycerol 3-phosphate	172.0137	9.96	C3H9O6P	-	L2	Glycerolipid metabolism, Glycerophospholipid metabolism	0.5118049	4.44549	2.07594E-09
Taurine	125.0147	11.25	C2H7NO3S	-	L2	Bile acid biosynthesis, Taurine and hypotaurine metabolism	0.48848754	1.47129	5.73941E-10
Tetradecanoic acid	228.2090	3.55	C14H28O2	-	L2	Fatty acid biosynthesis	1.50760128	1.49765	2.6292E-08
Triethanolamine	149.1052	8.65	C6H15NO3	+	L2	Glycerophospholipid metabolism	0.74828584	2.82427	5.21195E-06
UDP-glucose	566.0547	11.02	C15H24N2O17P2	-	L2	Pentose and glucuronate interconversions, Galactose metabolism, Pyrimidine metabolism	0.45086927	1.25475	1.38434E-06
UDP-N-acetyl-D-glucosamine	607.0812	10.23	C17H27N3O17P2	-	L2	Aminosugars metabolism _Peptidoglycan biosynthesis	0.32523428	1.90651	9.93862E-09
Xanthine	152.0334	9.00	C5H4N4O2	-	L1	Purine metabolism, Caffeine metabolism	1.51529183	2.09654	1.08567E-06

Table 3.5: A list of 84 significantly changed ions in M2 macrophages with VIP > 1 and FDR < 0.05 compared to M0 as a result of investigation M0, M1, M2, Mreg, M0-LPS and Mreg-LPS.

Putative metabolite	Mass	RT	FORMULA	POLARITY	confidence	Pathway	M2	VIP	FDR
Adenosine	267.0967	7.76	C10H13N5O4	+	L1	Purine metabolism	0.8160371	4.91739	0.001759945
ADP	427.0294	10.38	C10H15N5O10P2	+	L2	Oxidative phosphorylation, Photosynthesis, Purine metabolism, Zeatin biosynthesis	0.53440044	3.51417	4.38157E-05
Propanoylcarnitine	217.1314	7.69	C10H19NO4	+	L2	Oxidation of Branched Fatty Acids	1.66850053	1.14369	1.51807E-07
Butanoylcarnitine	231.1471	7.32	C11H21NO4	+	L2	Fatty acyl carnitines	1.16715611	1.61471	8.68007E-05
Dodecanoic acid	200.1776	3.61	C12H24O2	-	L2	Fatty acid biosynthesis	1.22046182	21.748	7.60623E-05
Tetradecanoic acid	228.2090	3.55	C14H28O2	-	L2	Fatty acid biosynthesis	1.25205954	2.25766	1.07029E-05
Hexadecanoic acid	256.2402	3.51	C16H32O2	-	L2	Fatty acid biosynthesis, Fatty acid elongation in mitochondria, Fatty acid metabolism, Biosynthesis of unsaturated fatty acids	0.70883992	1.93237	3.64596E-06
[FA (18:1)]	281.2719	4.92	C18H35NO	+	L2	Fatty amides	0.73032499	3.94926	0.028281391
Glutathione disulfide	306.0760	11.02	C20H32N6O12S2	+	L1	Glutamate metabolism, Glutathione metabolism	0.82135605	2.07545	0.00118311
NADH	332.5625	9.35	C21H29N7O14P2	+	L2	Oxidative phosphorylation	1.35498767	3.03625	0.011094442
[GL (18:0)]	358.3085	3.77	C21H42O4	-	L2	Monoradylglycerols	1.39493456	4.59543	3.29706E-07
[ST hydrox] 3alpha,12alpha-Dihydroxy-5beta-chol-6-en-24-oic Acid	390.2769	4.41	C24H38O4	+	L2	Bile acids and derivatives	1.8839245	1.62684	4.88778E-08
Glycine	75.0321	11.26	C2H5NO2	+	L1	Bile acid biosynthesis, Purine metabolism, Glycine, serine and threonine metabolism, Lysine degradation, Thiamine metabolism, Porphyrin and chlorophyll metabolism, Nitrogen metabolism	1.24299219	17.458	2.9064E-05
Hypotaurine	109.0198	10.91	C2H7NO2S	+	L2	Taurine and hypotaurine metabolism	1.06999258	1.04189	0.013078332
Taurine	125.0147	11.25	C2H7NO3S	-	L2	Bile acid biosynthesis, Taurine and hypotaurine metabolism	0.84512405	5.08562	1.56224E-05
PC(30:0)	705.5308	3.59	C38H76NO8P	+	L2	Glycerophosphocholines	1.35792179	1.23491	5.21432E-07
Glyceraldehyde	90.0318	7.33	C3H6O3	-	L2	GlycerolipidMetabolism	1.24492614	20.5103	3.82626E-06
Guanidinoacetate	117.0538	11.49	C3H7N3O2	+	L1	Glycine, serine and threonine metabolism, Arginine and proline metabolism	2.27073183	6.46166	5.84407E-08
L-Alanine	89.0477	10.76	C3H7NO2	+	L1	Alanine and aspartate metabolism, Cysteine metabolism, Taurine and hypotaurine metabolism, Selenoamino acid metabolism, D-Alanine metabolism, Carbon fixation, Reductive carboxylate cycle (CO2 fixation)	1.90413168	18.879	9.58186E-08

L-Serine	105.0427	11.25	C3H7NO3	+	L1	Glycine, serine and threonine metabolism, Methionine metabolism, Cysteine metabolism, Cyanoamino acid metabolism, Sphingolipid metabolism, Methane metabolism, Sulfur metabolism	1.27636018	16.7902	2.57273E-06
D-Glyceraldehyde 3-phosphate	169.9980	11.01	C3H7O6P	-	L2	Glycolysis / Gluconeogenesis, Pentose phosphate pathway, Inositol metabolism, Pentose and glucuronate interconversions, Fructose and mannose metabolism, Galactose metabolism, Biosynthesis of steroids, Clavulanic acid biosynthesis, Methane metabolism	2.27849494	2.36549	4.62273E-08
sn-Glycerol 3-phosphate	172.0137	9.96	C3H9O6P	-	L2	Glycerolipid metabolism, Glycerophospholipid metabolism	1.0905703	3.57368	0.010108296
PC(32:1)	731.5464	3.56	C40H78NO8P	+	L2	Glycerophosphocholines	1.4176004	2.23047	1.35861E-08
PC(34:2)	757.5620	3.54	C42H80NO8P	+	L2	Glycerophosphocholines	1.31540943	2.1116	4.96234E-06
PC(34:1)	759.5774	3.65	C42H82NO8P	+	L2	Glycerophosphocholines	0.94786598	1.19036	0.0126611
PC(36:4)	781.5620	3.52	C44H80NO8P	+	L2	Glycerophosphocholines	0.84620738	1.31584	0.000867933
PC(36:2)	785.5932	3.54	C44H84NO8P	+	L2	Glycerophosphocholines	1.0612167	1.14941	0.010598004
Phosphocreatine	211.0358	10.31	C4H10N3O5P	+	L2	Arginine and proline metabolism	1.55139824	15.9802	4.86784E-06
L-Malate	134.0216	11.20	C4H6O5	-	L1	Citrate cycle (TCA cycle), Glutamate metabolism, Alanine and aspartate metabolism, Pyruvate metabolism, Glyoxylate and dicarboxylate metabolism, Carbon fixation, Reductive carboxylate cycle (CO2 fixation)	1.15473649	10.3332	0.000167308
Creatinine	113.0590	8.21	C4H7N3O	+	L1	Arginine and proline metabolism	1.11930999	8.55896	0.010381781
L-Aspartate	133.0376	10.57	C4H7NO4	-	L1	Alanine and aspartate metabolism, Arginine and proline metabolism, Glycine, serine and threonine metabolism, Lysine biosynthesis, Arginine and proline metabolism, Histidine metabolism, beta-Alanine metabolism	0.82719614	2.85278	1.93662E-06
L-Asparagine	132.0535	10.93	C4H8N2O3	+	L1	Alanine and aspartate metabolism, Tetracycline biosynthesis, Cyanoamino acid metabolism, Nitrogen metabolism	1.46558754	1.05788	1.36569E-06
[FA trihydroxy(4:0)]	136.0373	9.35	C4H8O5	-	L2	Ascorbate and aldarate metabolism	1.08219065	1.68801	0.030273624
Creatine	131.0694	10.63	C4H9N3O2	+	L1	Glycine, serine and threonine metabolism, Arginine and proline metabolism	1.12052232	1.99119	7.23305E-05

4-Aminobutanoate	103.0633	10.90	C4H9NO2	+	L2	Arginine and proline metabolism, Glutamate metabolism, beta-Alanine metabolism, Butanoate metabolism	0.72666389	1.853	9.69417E-07
L-Threonine	119.0583	10.54	C4H9NO3	+	L2	Glycine, serine and threonine metabolism, Valine, leucine and isoleucine biosynthesis, Porphyrin and chlorophyll metabolism	1.12787969	8.57068	0.009416671
L-Glutamine	146.0691	10.77	C5H10N2O3	+	L1	Glutamate metabolism, Purine metabolism, Pyrimidine metabolism, D-Glutamine and D-glutamate metabolism, Nitrogen metabolism	0.52953603	5.82404	8.66762E-08
L-Arabinonate	166.0478	9.99	C5H10O6	-	L2	Ascorbate and aldarate metabolism	2.12113698	5.19458	6.32333E-09
4-Guanidinobutanoate	145.0852	10.88	C5H11N3O2	+	L2	Arginine and proline metabolism	1.88800683	3.07333	3.60272E-08
L-Valine	117.0790	8.74	C5H11NO2	+	L2	Valine, leucine and isoleucine degradation, Valine, leucine and isoleucine biosynthesis, Penicillin and cephalosporin biosynthesis, Propanoate metabolism, Pantothenate and CoA biosynthesis	1.11587573	1.39841	0.000335233
L-Methionine	149.0511	9.01	C5H11NO2S	+	L2	Methionine metabolism	1.4086555	4.14164	2.2543E-06
L-Methionine S-oxide	165.0459	9.69	C5H11NO3S	+	L2	Methionine metabolism	1.38073861	2.53034	0.00016736
2-C-Methyl-D-erythritol 4-phosphate	216.0401	10.92	C5H13O7P	-	L2	Biosynthesis of steroids	0.89379196	2.189	0.000463148
sn-glycero-3-Phosphoethanolamine	215.0559	10.77	C5H14NO6P	+	L2	Glycerophospholipid metabolism, Ether lipid metabolism	1.33495908	6.68521	0.000118332
Hypoxanthine	136.0385	8.64	C5H4N4O	+	L1	Purine metabolism	0.71477428	6.09821	9.28427E-06
Adenine	135.0545	8.04	C5H5N5	+	L2	Purine metabolism, Zeatin biosynthesis	1.40189193	6.95569	5.50822E-06
2,5-Dioxopentanoate	130.0268	6.97	C5H6O4	-	L2	Ascorbate and aldarate metabolism, Arginine and proline metabolism	0.86745685	10.3821	0.000237279
2-Oxoglutarate	146.0216	11.10	C5H6O5	-	L2	Citrate cycle (TCA cycle), Ascorbate and aldarate metabolism, Glutamate metabolism, Alanine and aspartate metabolism, Lysine biosynthesis, Histidine metabolism, D-Glutamine and D-glutamate metabolism, Glyoxylate and dicarboxylate metabolism	1.62171952	2.0134	3.2588E-07
L-1-Pyrroline-3-hydroxy-5-carboxylate	129.0427	7.75	C5H7NO3	-	L2	Arginine and proline metabolism	1.1908595	2.74271	0.000156364
N-Carbamoyl-L-aspartate	176.0433	11.45	C5H8N2O5	-	L2	Pyrimidine metabolism, Alanine and aspartate metabolism	1.21768745	1.03269	0.053673017
2-Hydroxyglutarate	148.0372	10.69	C5H8O5	-	L1	glutamate degradation V (via hydroxyglutarate)	1.59481451	1.73223	9.60731E-09
L-Proline	115.0633	9.65	C5H9NO2	+	L1	Arginine and proline metabolism, Novobiocin biosynthesis	1.17232923	3.67684	8.83964E-06
L-Glutamate 5-semialdehyde	131.0583	10.55	C5H9NO3	-	L2	Arginine and proline metabolism	1.51371127	4.38057	8.98213E-07

L-4-Hydroxyglutamate semialdehyde	147.0532	7.98	C5H9NO4	-	L2	Arginine and proline metabolism	1.32424207	4.71982	1.12344E-05
(S)-3-Methyl-2-oxopentanoic acid	130.0631	4.45	C6H10O3	-	L2	Valine, leucine and isoleucine degradation, Valine, leucine and isoleucine biosynthesis	2.00382557	2.94763	6.57754E-09
2-Dehydro-3-deoxy-L-rhamnonate	162.0529	10.08	C6H10O5	-	L2	Fructose and mannose metabolism	1.3278251	3.91953	7.13424E-05
5-Guanidino-2-oxopentanoate	173.0800	10.70	C6H11N3O3	+	L2	D-Arginine and D-ornithine metabolism	4.67692876	1.57286	1.2029E-08
N-Formyl-L-methionine	177.0459	7.29	C6H11NO3S	-	L2	Methionine metabolism	1.16818983	2.63605	0.003361394
O-Acetyl-L-homoserine	161.0689	7.32	C6H11NO4	-	L2	Methionine metabolism, Sulfur metabolism	1.23551754	1.42204	0.00304429
D-Glucose	180.0634	11.93	C6H12O6	-	L2	Glycolysis / Gluconeogenesis, Pentose phosphate pathway, Galactose metabolism, Starch and sucrose metabolism, Streptomycin biosynthesis, Indole and ipecac alkaloid biosynthesis	2.25740924	1.29173	1.32575E-09
D-Gluconic acid	196.0583	10.03	C6H12O7	-	L1	Pentose phosphate pathway	2.21766154	1.30172	2.46888E-10
L-Citrulline	175.0957	11.06	C6H13N3O3	+	L1	Arginine and proline metabolism	2.67172719	3.55829	1.36525E-08
L-Leucine	131.0946	8.54	C6H13NO2	+	L1	Valine, leucine and isoleucine degradation, Valine, leucine and isoleucine biosynthesis	1.33341303	8.43063	9.69417E-07
L-Arginine	174.1117	17.73	C6H14N4O2	+	L1	Arginine and proline metabolism, Clavulanic acid biosynthesis, D-Arginine and D-ornithine metabolism	1.22974097	2.38064	5.44686E-05
D-Glucuronolactone	176.0321	10.92	C6H8O6	-	L2	Ascorbate and aldarate metabolism	0.55247709	2.85825	4.91493E-07
N-Acetyl-L-aspartate	175.0480	10.23	C6H9NO5	-	L2	Alanine and aspartate metabolism	2.52975438	3.6936	1.69768E-08
N(pi)-Methyl-L-histidine	169.0851	9.25	C7H11N3O2	+	L2	Histidine metabolism	1.45842786	3.59902	2.55146E-07
N-Acetyl-L-glutamate	189.0637	9.84	C7H11NO5	-	L2	Arginine and proline metabolism	6.31944963	1.27628	2.06781E-10
4-Trimethylammoniobutanoate	145.1103	9.53	C7H15NO2	+	L2	Lysine degradation	1.1841506	3.43829	0.000245107
N6-Methyl-L-lysine	160.1212	15.81	C7H16N2O2	+	L1	0	1.26811115	1.11131	0.028108914
O-Succinyl-L-homoserine	219.0742	9.86	C8H13NO6	-	L2	Methionine metabolism, Sulfur metabolism	1.64751603	1.95803	3.48002E-06
[FA (8:0)] octanoic acid	144.1151	3.89	C8H16O2	-	L2	Fatty acid biosynthesis	1.27750597	1.13873	3.65178E-05
3-(2-Hydroxyphenyl)propanoate	166.0630	6.72	C9H10O3	-	L2	Phenylalanine metabolism, Fluorene degradation	6.33524036	1.67438	4.77664E-08
3-(4-Hydroxyphenyl)lactate	182.0580	7.37	C9H10O4	-	L2	Tyrosine metabolism	3.07682965	1.39372	1.31904E-08
L-Phenylalanine	165.0790	8.12	C9H11NO2	+	L2	Phenylalanine metabolism, Phenylalanine, tyrosine and tryptophan biosynthesis, Phenylpropanoid biosynthesis, Alkaloid biosynthesis II	1.43060633	2.87382	3.82626E-06
L-Tyrosine	181.0739	10.05	C9H11NO3	+	L2	Tyrosine metabolism, Phenylalanine, tyrosine and tryptophan biosynthesis, Novobiocin biosynthesis, Thiamine metabolism, Phenylpropanoid biosynthesis, Alkaloid biosynthesis I	1.35272735	1.97086	2.59787E-05

Deoxycytidine	227.0905	8.58	C9H13N3O4	+	L2	Pyrimidine metabolism	0.72712823	8.80696	2.66063E-06
Cytidine	243.0857	9.44	C9H13N3O5	+	L1	Pyrimidine metabolism	0.61747353	1.9804	6.5788E-06
8-Amino-7-oxononanoate	187.1208	4.50	C9H17NO3	+	L2	Biotin metabolism	2.52913649	1.50587	3.0783E-08
O-Acetylcarnitine	203.1158	8.34	C9H17NO4	+	L1	Alanine and aspartate metabolism	1.42055583	1.00084	1.29402E-05
N6,N6,N6-Trimethyl-L-lysine	188.1524	14.79	C9H20N2O2	+	L2	Lysine degradation	1.72958132	1.63679	1.19578E-05
Phenylpyruvate	164.0474	4.48	C9H8O3	-	L2	Phenylalanine metabolism, Phenylalanine, tyrosine and tryptophan biosynthesis	5.99228884	5.1919	1.34334E-07
3-(4-Hydroxyphenyl)pyruvate	180.0423	7.31	C9H8O4	-	L2	Tyrosine metabolism, Phenylalanine, tyrosine and tryptophan biosynthesis, Novobiocin biosynthesis, Alkaloid biosynthesis I, Biosynthesis of vancomycin group antibiotics	3.0925572	2.72538	2.08513E-07

Table 3.6: A list of 25 significantly changed metabolites in Mreg macrophages with VIP > 1 and FDR < 0.05 compared to M0 as a result of investigation M0, M1, M2, Mreg, M0-LPS and Mreg-LPS.

Putative metabolite	Mass	RT	FORMULA	POLARITY	confidence	Pathway	Fold change	VIP	FDR
(R)-2-Hydroxyglutarate	148.0372	10.69	C5H8O5	-	L1	glutamate degradation V (via hydroxyglutarate)	1.20747133	4.41495	1.58472E-06
L-Malate	134.0216	11.20	C4H6O5	-	L1	Citrate cycle (TCA cycle), Glutamate metabolism, Alanine and aspartate metabolism, Pyruvate metabolism	0.94982608	1.43349	0.034411904
2-Dehydro-3-deoxy-L-rhamnonate	162.0529	10.08	C6H10O5	-	L2	Fructose and mannose metabolism	1.1192582	2.37526	0.020301572
2-Oxoglutarate	146.0216	11.10	C5H6O5	-	L2	Citrate cycle (TCA cycle) _Glutamate metabolism, Alanine and aspartate metabolism	1.4631015	6.95177	7.46557E-08
3-(4-Hydroxyphenyl) lactate	182.0580	7.37	C9H10O4	-	L2	Tyrosine metabolism	1.14776125	1.25542	0.01719459
4-Aminobutanoate	103.0633	10.90	C4H9NO2	+	L2	Arginine and proline metabolism, Glutamate metabolism, beta-Alanine metabolism, Butanoate metabolism	0.88393505	3.17736	0.002819363
Adenosine	267.0967	7.76	C10H13N5O4	+	L1	Purine metabolism	1.4298947	4.59523	2.4593E-05
Cytidine	243.0857	9.44	C9H13N3O5	+	L1	Pyrimidine metabolism	0.67537665	3.93261	3.08425E-05
D-Glucose	180.0634	11.93	C6H12O6	-	L2	Glycolysis / Gluconeogenesis, Pentose phosphate pathway, Galactose metabolism,	0.70644144	3.72516	2.8246E-07
L-1-Pyrroline-3-hydroxy-5-carboxylate	129.0427	7.75	C5H7NO3	-	L2	Arginine and proline metabolism	0.90162963	4.05053	0.005314746
L-4-Hydroxyglutamate semialdehyde	147.0532	7.98	C5H9NO4	-	L2	Arginine and proline metabolism	1.11616504	1.25188	0.010645061
L-Alanine	89.0477	10.76	C3H7NO2	+	L1	Alanine and aspartate metabolism, Cysteine metabolism, Taurine and hypotaurine metabolism,	1.0989203	8.25587	0.008426512
L-Asparagine	132.0535	10.93	C4H8N2O3	+	L1	Alanine and aspartate metabolism	1.09391404	7.23486	0.006529199
L-Serine	105.0427	11.25	C3H7NO3	+	L1	Glycine, serine and threonine metabolism, Methionine metabolism, Cysteine metabolism,	0.88776392	13.6655	0.00196185
L-Threonine	119.0583	10.54	C4H9NO3	+	L2	Glycine, serine and threonine metabolism, Valine, leucine and isoleucine biosynthesis	0.77262006	6.26612	7.59393E-05
N-Acetyl-L-aspartate	175.0480	10.23	C6H9NO5	-	L2	Alanine and aspartate metabolism	1.10123038	2.25617	0.004160038
N-Acetyl-L-glutamate	189.0637	9.84	C7H11NO5	-	L2	Arginine and proline metabolism	1.21133999	2.21875	7.22028E-05
O-Acetyl-L-homoserine	161.0689	7.32	C6H11NO4	-	L2	Methionine metabolism, Sulfur metabolism	1.16578649	1.28341	0.008139759
Butanoylcarnitine	231.1471	7.32	C11H21NO4	+	L2	Fatty acyl carnitines	1.09171464	5.20596	0.012337457
Propanoylcarnitine	217.1314	7.69	C10H19NO4	+	L2	OxidationofBranchedFattyAcids	1.28840811	4.38108	1.06067E-05
PC(36:4)	781.5620	3.52	C44H80NO8P	+	L2	Glycerophosphocholines	0.89916443	1.1876	0.004319353
Phosphocreatine	211.0358	10.31	C4H10N3O5P	+	L2	Arginine and proline metabolism	1.0976769	2.91711	0.016275336

sn-glycero-3-Phosphoethanolamine	215.0559	10.77	C5H14NO6P	+	L2	Glycerophospholipid metabolism, Ether lipid metabolism	1.19462807	1.10614	2.82985E-05
Taurine	125.0147	11.25	C2H7NO3S	-	L2	Bile acid biosynthesis, Taurine and hypotaurine metabolism	1.12147035	1.78759	0.000113705
Tetradecanoic acid	228.2090	3.55	C14H28O2	-	L2	Fatty acid biosynthesis	1.39245116	3.07065	1.33654E-07

Table 3.7: A list of 54 significantly changed metabolites in M0-LPS with VIP > 1 and FDR < 0.05 compared to M0 as a result of investigation M0, M1, M2, Mreg, M0-LPS and Mreg-LPS..

Putative metabolite	Mass	RT	FORMULA	POLARITY	confidence	Pathway	Fold change	VIP	FDR
2-Hydroxyglutarate	148.0372	10.69	C5H8O5	-	L1	glutamate degradation V (via hydroxyglutarate)	0.65840896	5.87517	4.14376E-09
(S)-3-Methyl-2-oxopentanoic acid	130.0631	4.45	C6H10O3	-	L2	Valine, leucine and isoleucine degradation, Valine, leucine and isoleucine biosynthesis	0.51363196	3.50365	9.85264E-08
L-Malate	134.0216	11.20	C4H6O5	-	L1	Citrate cycle (TCA cycle), Glutamate metabolism, Alanine and aspartate metabolism, Pyruvate metabolism, Glyoxylate and dicarboxylate metabolism, Carbon fixation, Reductive carboxylate cycle (CO2 fixation)	0.78955121	8.84904	2.4292E-07
[GL (18:0)]	358.3085	3.77	C21H42O4	-	L2	Monoradylglycerols	2.05547887	2.7181	2.1215E-10
[ST hydrox] 3alpha,12alpha-Dihydroxy-5beta-chol-6-en-24-oic Acid	390.2769	4.41	C24H38O4	+	L2	Bile acids and derivatives	1.99232658	1.51013	5.11143E-09
2-C-Methyl-D-erythritol 4-phosphate	216.0401	10.92	C5H13O7P	-	L2	Biosynthesis of steroids	1.31122635	2.05927	6.91364E-07
2-Dehydro-3-deoxy-L-rhamnonate	162.0529	10.08	C6H10O5	-	L2	Fructose and mannose metabolism	0.87648084	3.72419	0.007672046
2-Oxoglutarate	146.0216	11.10	C5H6O5	-	L2	Citrate cycle (TCA cycle), Ascorbate and aldarate metabolism, Glutamate metabolism, Alanine and aspartate metabolism, Lysine biosynthesis, Histidine metabolism, D-Glutamine and D-glutamate metabolism, Glyoxylate and dicarboxylate metabolism	0.92647189	6.28988	0.003045714
3-(4-Hydroxyphenyl) lactate	182.0580	7.37	C9H10O4	-	L2	Tyrosine metabolism	1.64446405	2.84882	6.39127E-08
4-Aminobutanoate	103.0633	10.90	C4H9NO2	+	L2	Arginine and proline metabolism, Glutamate metabolism, beta-Alanine metabolism, Butanoate metabolism	2.64927507	23.1051	1.07555E-09
4-Trimethylammoniobutanoate	145.1103	9.53	C7H15NO2	+	L2	Lysine degradation	0.55872542	1.46594	2.62754E-08
5-Guanidino-2-oxopentanoate	173.0800	10.70	C6H11N3O3	+	L2	D-Arginine and D-ornithine metabolism	3.57810024	1.57841	1.08559E-08
8-Amino-7-oxononanoate	187.1208	4.50	C9H17NO3	+	L2	Biotin metabolism	1.35889617	24.3981	0.00076385
Adenosine	267.0967	7.76	C10H13N5O4	+	L1	Purine metabolism	3.58834552	2.38514	1.68796E-08
Creatine	131.0694	10.63	C4H9N3O2	+	L1	Glycine, serine and threonine metabolism, Arginine and proline metabolism	0.73167388	1.52316	5.2165E-07
Cytidine	243.0857	9.44	C9H13N3O5	+	L1	Pyrimidine metabolism	1.52420246	3.5403	3.04293E-06
Deoxycytidine	227.0905	8.58	C9H13N3O4	+	L2	Pyrimidine metabolism	0.38443142	1.0337	7.11684E-09
D-Glucose	180.0634	11.93	C6H12O6	-	L2	Glycolysis / Gluconeogenesis, Pentose phosphate pathway, Galactose metabolism, Starch and	0.49989297	2.01296	6.48087E-10

						sucrose metabolism, Streptomycin biosynthesis, Indole and ipecac alkaloid biosynthesis			
Dodecanoic acid	200.1776	3.61	C12H24O2	-	L2	Fatty acid biosynthesis	1.20910181	6.27254	0.000313936
Glyceraldehyde	90.0318	7.33	C3H6O3	-	L2	GlycerolipidMetabolism	0.66520253	9.41636	1.27283E-07
Guanidinoacetate	117.0538	11.49	C3H7N3O2	+	L1	Glycine, serine and threonine metabolism, Arginine and proline metabolism	0.27657488	5.73497	2.35935E-08
Hypotaurine	109.0198	10.91	C2H7NO2S	+	L2	Taurine and hypotaurine metabolism	0.72595056	5.68636	1.75527E-06
Hypoxanthine	136.0385	8.64	C5H4N4O	+	L1	Purine metabolism	4.34351693	7.56025	2.46008E-09
L-1-Pyrroline-3-hydroxy-5-carboxylate	129.0427	7.75	C5H7NO3	-	L2	Arginine and proline metabolism	0.70258539	7.43626	7.83649E-07
L-Alanine	89.0477	10.76	C3H7NO2	+	L1	Alanine and aspartate metabolism, Cysteine metabolism, Taurine and hypotaurine metabolism, Selenoamino acid metabolism, D-Alanine metabolism, Carbon fixation, Reductive carboxylate cycle (CO2 fixation)	0.27320702	25.4176	9.498E-11
L-Asparagine	132.0535	10.93	C4H8N2O3	+	L1	Alanine and aspartate metabolism, Tetracycline biosynthesis, Cyanoamino acid metabolism, Nitrogen metabolism	0.59465911	2.3278	1.62826E-07
L-Glutamate	147.0531	10.32	C5H9NO4	+	L1	Arginine and proline metabolism, Glutamate metabolism, Histidine metabolism, D-Glutamine and D-glutamate metabolism, Glutathione metabolism_Butanoate metabolism_C5-Branched dibasic acid metabolism_Porphyrin and chlorophyll metabolism_Nitrogen metabolism	0.80144529	10.2027	9.80277E-05
L-Glutamate 5-semialdehyde	131.0583	10.55	C5H9NO3	-	L2	Arginine and proline metabolism	0.5500766	5.39611	3.7351E-08
L-Glutamine	146.0691	10.77	C5H10N2O3	+	L1	Glutamate metabolism, Purine metabolism, Pyrimidine metabolism, D-Glutamine and D-glutamate metabolism, Nitrogen metabolism	1.27692226	3.79905	3.07843E-05
L-Leucine	131.0946	8.54	C6H13NO2	+	L1	Valine, leucine and isoleucine degradation, Valine, leucine and isoleucine biosynthesis	0.87132149	7.51541	0.000610157
L-Methionine	149.0511	9.01	C5H11NO2S	+	L2	Methionine metabolism	0.84403353	3.18131	8.2736E-05
L-Phenylalanine	165.0790	8.12	C9H11NO2	+	L2	Phenylalanine metabolism, Phenylalanine, tyrosine and tryptophan biosynthesis, Phenylpropanoid biosynthesis, Alkaloid biosynthesis II	0.78499004	1.33455	2.70703E-05
L-Proline	115.0633	9.65	C5H9NO2	+	L1	Arginine and proline metabolism, Novobiocin biosynthesis	0.72348429	11.9488	6.79982E-08
L-Serine	105.0427	11.25	C3H7NO3	+	L1	Glycine, serine and threonine metabolism, Methionine metabolism, Cysteine metabolism, Cyanoamino acid metabolism, Sphingolipid	2.86184579	9.3074	4.98176E-09

						metabolism, Methane metabolism, Sulfur metabolism			
L-Threonine	119.0583	10.54	C4H9NO3	+	L2	Glycine, serine and threonine metabolism, Valine, leucine and isoleucine biosynthesis, Porphyrin and chlorophyll metabolism	0.71559583	14.247	8.51119E-06
L-Tyrosine	181.0739	10.05	C9H11NO3	+	L2	Tyrosine metabolism, Phenylalanine, tyrosine and tryptophan biosynthesis, Novobiocin biosynthesis, Thiamine metabolism, Phenylpropanoid biosynthesis, Alkaloid biosynthesis I	0.81207335	2.61975	0.00046618
N(pi)-Methyl-L-histidine	169.0851	9.25	C7H11N3O2	+	L2	Histidine metabolism	0.7621793	3.92936	7.56679E-06
N6,N6,N6-Trimethyl-L-lysine	188.1524	14.79	C9H20N2O2	+	L2	Lysine degradation	0.72081493	1.25587	2.53633E-05
N-Acetyl-L-aspartate	175.0480	10.23	C6H9NO5	-	L2	Alanine and aspartate metabolism	0.73745899	2.82928	4.75934E-08
N-Acetyl-L-glutamate	189.0637	9.84	C7H11NO5	-	L2	Arginine and proline metabolism	0.35908037	1.18791	9.89778E-09
NADH	332.5625	9.35	C21H29N7O14P2	+	L2	Oxidative phosphorylation	0.64758556	2.49708	0.000915461
N-Carbamoyl-L-aspartate	176.0433	11.45	C5H8N2O5	-	L2	Pyrimidine metabolism, Alanine and aspartate metabolism	0.33295334	1.66544	2.39259E-05
O-Acetylcarnitine	203.1158	8.34	C9H17NO4	+	L1	Alanine and aspartate metabolism	0.6927402	7.70802	9.8896E-07
O-Acetyl-L-homoserine	161.0689	7.32	C6H11NO4	-	L2	Methionine metabolism, Sulfur metabolism	0.64671881	2.60978	2.59657E-05
Butanoylcarnitine	231.1471	7.32	C11H21NO4	+	L2	Fatty acyl carnitines	0.89192587	3.6547	5.23252E-05
Propanoylcarnitine	217.1314	7.69	C10H19NO4	+	L2	OxidationofBranchedFattyAcids	0.81611411	5.73355	0.000167475
O-Succinyl-L-homoserine	219.0742	9.86	C8H13NO6	-	L2	Methionine metabolism, Sulfur metabolism	0.27137113	5.79545	7.59927E-09
PC(36:4)	781.5620	3.52	C44H80NO8P	+	L2	Glycerophosphocholines	1.1930939	1.21707	3.24948E-05
Phosphocreatine	211.0358	10.31	C4H10N3O5P	+	L2	Arginine and proline metabolism	0.52841418	1.86478	2.08355E-07
Pyridoxine	169.0738	7.34	C8H11NO3	+	L2	Vitamin B6 metabolism	1.39834544	2.4956	3.30296E-06
sn-glycero-3-Phosphocholine	257.1029	9.93	C8H20NO6P	+	L1	Glycerophospholipid metabolism, Ether lipid metabolism	0.94822782	1.16235	0.007295548
sn-glycero-3-Phosphoethanolamine	215.0559	10.77	C5H14NO6P	+	L2	Glycerophospholipid metabolism, Ether lipid metabolism	0.59350974	7.2802	8.94591E-08
Taurine	125.0147	11.25	C2H7NO3S	-	L2	Bile acid biosynthesis, Taurine and hypotaurine metabolism	0.86872498	4.40876	0.000155747
Tetradecanoic acid	228.2090	3.55	C14H28O2	-	L2	Fatty acid biosynthesis	1.30494226	2.63087	2.56737E-06

Table 3.8: A list of 41 significantly changed metabolites in Mreg-LPS with VIP > 1 and FDR < 0.05 compared to M0 as a result of investigation M0, M1, M2, Mreg, M0-LPS and Mreg-LPS.

Putative metabolite	Mass	RT	FORMULA	POLARITY	confidence	Pathway	Fold change	VIP	FDR
2-Hydroxyglutarate	148.0372	10.69	C5H8O5	-	L2	glutamate degradation V (via hydroxyglutarate)	0.847765492	1.04179	9.34169E-06
(S)-3-Methyl-2-oxopentanoic acid	130.0631	4.45	C6H10O3	-	L2	Valine, leucine and isoleucine degradation, Valine, leucine and isoleucine biosynthesis	0.750994215	8.85181	7.03759E-05
L-Malate	134.0216	11.20	C4H6O5	-	L2	Citrate cycle (TCA cycle), Glutamate metabolism, Alanine and aspartate metabolism, Pyruvate metabolism, Glyoxylate and dicarboxylate metabolism, Carbon fixation, Reductive carboxylate cycle (CO2 fixation)	1.05748133	7.63673	0.04364152
[GL (18:0)] 1-octadecanoyl-rac-glycerol	358.3085	3.77	C21H42O4	-	L2	Monoradylglycerols	2.053368195	1.63729	6.42155E-08
[ST hydrox] 3alpha,12alpha-Dihydroxy-5beta-chol-6-en-24-oic Acid	390.2769	4.41	C24H38O4	+	L2	Bile acids and derivatives	2.266027031	2.46526	7.16042E-10
2-C-Methyl-D-erythritol 4-phosphate	216.0401	10.92	C5H13O7P	-	L2	Biosynthesis of steroids	1.211690484	3.06814	5.27481E-06
2-Dehydro-3-deoxy-L-rhamnonate	162.0529	10.08	C6H10O5	-	L2	Fructose and mannose metabolism	0.839734159	4.46391	0.004623387
2-Oxoglutarate	146.0216	11.10	C5H6O5	-	L2	Citrate cycle (TCA cycle), Ascorbate and aldarate metabolism, Glutamate metabolism, Alanine and aspartate metabolism, Lysine biosynthesis, Histidine metabolism, D-Glutamine and D-glutamate metabolism, Glyoxylate and dicarboxylate metabolism	0.883835366	7.76319	0.0029219
3-(4-Hydroxyphenyl) lactate	182.0580	7.37	C9H10O4	-	L2	Tyrosine metabolism	1.561837544	2.54968	3.51518E-07
4-Aminobutanoate	103.0633	10.90	C4H9NO2	+	L2	Arginine and proline metabolism, Glutamate metabolism, beta-Alanine metabolism, Butanoate metabolism	1.789573214	15.1258	6.70108E-09
4-Trimethylammoniobutanoate	145.1103	9.53	C7H15NO2	+	L2	Lysine degradation	0.720830367	11.2732	1.85869E-06
Adenosine	267.0967	7.76	C10H13N5O4	+	L2	Purine metabolism	3.058702107	2.57285	1.94506E-08
Creatine	131.0694	10.63	C4H9N3O2	+	L2	Glycine, serine and threonine metabolism, Arginine and proline metabolism	0.889433012	6.35851	0.000783384
Cytidine	243.0857	9.44	C9H13N3O5	+	L2	Pyrimidine metabolism	1.195225982	3.12133	0.006382697
Deoxycytidine	227.0905	8.58	C9H13N3O4	+	L2	Pyrimidine metabolism	0.597652672	1.61929	8.39636E-08

D-Glucose	180.0634	11.93	C6H12O6	-	L2	Glycolysis / Gluconeogenesis, Pentose phosphate pathway, Galactose metabolism, Starch and sucrose metabolism, Streptomycin biosynthesis, Indole and ipecac alkaloid biosynthesis	0.699776131	3.53008	2.83746E-07
Dodecanoic acid	200.1776	3.61	C12H24O2	-	L2	Fatty acid biosynthesis	1.62002089	3.40245	4.12408E-07
Glyceraldehyde	90.0318	7.33	C3H6O3	-	L2	GlycerolipidMetabolism	0.771749115	23.2107	2.15285E-06
Guanidinoacetate	117.0538	11.49	C3H7N3O2	+	L2	Glycine, serine and threonine metabolism, Arginine and proline metabolism	0.580198377	3.99382	1.55987E-06
Hypoxanthine	136.0385	8.64	C5H4N4O	+	L2	Purine metabolism	4.297732751	2.18413	9.86E-12
L-1-Pyrroline-3-hydroxy-5-carboxylate	129.0427	7.75	C5H7NO3	-	L2	Arginine and proline metabolism	0.793833799	1.81766	3.27011E-05
L-4-Hydroxyglutamate semialdehyde	147.0532	7.98	C5H9NO4	-	L2	Arginine and proline metabolism	0.603814256	4.58286	1.69253E-06
L-Alanine	89.0477	10.76	C3H7NO2	+	L1	Alanine and aspartate metabolism, Cysteine metabolism, Taurine and hypotaurine metabolism, Selenoamino acid metabolism, D-Alanine metabolism, Carbon fixation, Reductive carboxylate cycle (CO2 fixation)	0.409243492	17.0709	6.96536E-10
L-Asparagine	132.0535	10.93	C4H8N2O3	+	L2	Alanine and aspartate metabolism, Tetracycline biosynthesis, Cyanoamino acid metabolism, Nitrogen metabolism	0.65138903	1.4221	1.05226E-06
L-Glutamine	146.0691	10.77	C5H10N2O3	+	L2	Glutamate metabolism, Purine metabolism, Pyrimidine metabolism, D-Glutamine and D-glutamate metabolism, Nitrogen metabolism	1.256653782	7.37936	0.00043417
L-Proline	115.0633	9.65	C5H9NO2	+	L2	Arginine and proline metabolism, Novobiocin biosynthesis	0.769812241	16.6637	1.92827E-06
L-Serine	105.0427	11.25	C3H7NO3	+	L2	Glycine, serine and threonine metabolism, Methionine metabolism, Cysteine metabolism, Cyanoamino acid metabolism, Sphingolipid metabolism, Methane metabolism, Sulfur metabolism	2.943274084	4.97257	6.96536E-10
L-Threonine	119.0583	10.54	C4H9NO3	+	L2	Glycine, serine and threonine metabolism, Valine, leucine and isoleucine biosynthesis, Porphyrin and chlorophyll metabolism	0.802671937	7.97373	0.000128538
N-Acetyl-L-aspartate	175.0480	10.23	C6H9NO5	-	L2	Alanine and aspartate metabolism	0.925006109	1.21832	0.002131203
N-Acetyl-L-glutamate	189.0637	9.84	C7H11NO5	-	L2	Arginine and proline metabolism	0.506028437	2.3964	1.19523E-07
O-Acetylcarnitine	203.1158	8.34	C9H17NO4	+	L2	Alanine and aspartate metabolism	0.733867642	3.52509	1.23935E-05

O-Acetyl-L-homoserine	161.0689	7.32	C6H11NO4	-	L2	Methionine metabolism, Sulfur metabolism	0.768467338	1.37	0.001096379
Butanoylcarnitine	231.1471	7.32	C11H21NO4	+	L2	Fatty acyl carnitines	1.135827323	3.34137	0.001303718
Propanoylcarnitine	217.1314	7.69	C10H19NO4	+	L2	OxidationofBranchedFattyAcids	1.062907464	5.21905	0.017954859
PC(36:4)	781.5620	3.52	C44H80NO8P	+	L2	Glycerophosphocholines	1.087764493	1.46701	0.012369816
Phosphocreatine	211.0358	10.31	C4H10N3O5P	+	L2	Arginine and proline metabolism	0.738930235	1.4195	2.77084E-05
Pyridoxine	169.0738	7.34	C8H11NO3	+	L2	Vitamin B6 metabolism	1.547097691	1.17894	8.66226E-08
sn-glycero-3-Phosphoethanolamine	215.0559	10.77	C5H14NO6P	+	L2	Glycerophospholipid metabolism, Ether lipid metabolism	0.757704841	6.6049	1.58403E-05
Taurine	125.0147	11.25	C2H7NO3S	-	L2	Bile acid biosynthesis, Taurine and hypotaurine metabolism	0.925698763	7.11251	0.010382938
Tetradecanoic acid	228.2090	3.55	C14H28O2	-	L2	Fatty acid biosynthesis	1.545869334	1.34732	1.85682E-06

Table 3.9: A list of 54 significantly changed metabolites in M2-M1-24 with VIP > 1 and FDR < 0.05 compared to M1 as a result of investigation M1, M2-M1-24 and M2-M1-48.

Putative metabolite	Mass	RT	FORMULA	POLARITY	confidence	Pathway	Fold change	VIP	FDR
[GL (18:0)]	358.3083	4.14	C21H42O4	-	L2	Monoradylglycerols	1.23462333	1.08902	0.002915
[PC (14:0)]	467.3012	4.67	C22H46NO7P	+	L2	Glycerophosphocholines	2.26570479	1.45423	2.3719E-08
[PC (14:2/16:0)]	691.5517	3.94	C38H78NO7P	+	L2	Glycerophosphocholines	3.16582456	2.7963	1.6072E-07
[PC (14:2/18:0)]	719.5835	3.92	C40H82NO7P	+	L2	Glycerophosphocholines	2.69312036	1.82914	6.0581E-07
[PC (16:0)]	495.3325	4.59	C24H50NO7P	+	L2	Glycerophosphocholines	1.29252884	2.62532	0.00077256
[PC (16:1)]	493.3169	4.61	C24H48NO7P	+	L2	Glycerophosphocholines	2.43877156	2.34979	3.2369E-08
[PC (16:2)]	481.3533	4.60	C24H52NO6P	+	L2	Glycerophosphocholines	1.73628042	1.94909	1.2252E-06
[PC (18:1/18:0)]	771.6144	3.89	C44H86NO7P	+	L2	Glycerophosphocholines	1.82688019	1.965	1.3081E-06
[PC (18:1/20:4)]	793.5987	3.87	C46H84NO7P	+	L2	Glycerophosphocholines	1.61874718	2.28663	0.000010498
Ceramide (d18:1/16:0)]	702.5675	4.01	C39H79N2O6P	+	L2	Ceramide phosphocholines (sphingomyelins)	1.18393857	1.79816	0.0065574
1-Hexadecanoyl-2-octadecenoyl-sn-glycero-3-phosphonocholine	743.5828	3.91	C42H82NO7P	+	L2	Glycerophosphonocholines	1.83060721	3.19249	2.3729E-08
L-1-Pyrroline-5-carboxylate	113.0477	11.08	C5H7NO2	-	L2	Glutamate metabolism, Arginine and proline metabolism	1.51663448	1.8874	8.8169E-09
2-Amino-4-hydroxy-6-(D-erythro-1,2,3-trihydroxypropyl)-7,8- dihydropteridine	255.0967	11.30	C9H13N5O4	+	L2	Folate biosynthesis	1.42894812	1.57977	1.6783E-07
2-Dehydro-3-deoxy-L-rhamnonate	162.0528	10.28	C6H10O5	-	L2	Fructose and mannose metabolism	1.57982496	2.11698	5.4577E-09
3-Methyl-2-oxopentanoic acid	130.0631	4.87	C6H10O3	-	L2	Valine, leucine and isoleucine degradation, Valine, leucine and isoleucine biosynthesis	1.32512955	2.03605	0.00045931
5-Guanidino-2-oxopentanoate	173.0801	11.09	C6H11N3O3	+	L2	D-Arginine and D-ornithine metabolism	1.13659618	1.08041	0.000146
5-Hydroxyindoleacetaldehyde	175.0633	4.25	C10H9NO2	+	L2	Tryptophan metabolism	1.36888382	1.18004	0.00002012
5-Hydroxy-L-tryptophan	220.0847	8.05	C11H12N2O3	+	L2	Tryptophan metabolism	1.99181529	1.33098	6.8491E-10
5'-Methylthioadenosine	297.0896	7.18	C11H15N5O3S	+	L1	Arginine and proline metabolism, Methionine metabolism, Zeatin biosynthesis	1.80122688	3.30435	4.577E-09
Creatine	131.0695	11.00	C4H9N3O2	+	L1	Glycine, serine and threonine metabolism, Arginine and proline metabolism	1.3446254	16.446	0.000038125
Deoxyadenosine	251.1018	7.26	C10H13N5O3	+	L2	Purine metabolism	4.87568622	1.77984	4.5872E-11
D-Galactosamine	179.0794	10.64	C6H13NO5	+	L2	Galactose metabolism	1.46063511	1.64084	1.03E-09
Glutathione	307.0838	10.08	C10H17N3O6S	+	L1	Glutamate metabolism, Cysteine metabolism, Glutathione metabolism	1.24977215	4.83179	3.9325E-10

Guanidinoacetate	117.0538	11.88	C3H7N3O2	+	L1	Glycine, serine and threonine metabolism, Arginine and proline metabolism	2.01559949	3.54613	2.4709E-09
L-Aspartate	133.0375	10.80	C4H7NO4	-	L1	Alanine and aspartate metabolism, Arginine and proline metabolism, Glycine, serine and threonine metabolism, Lysine biosynthesis, Arginine and proline metabolism	2.06467359	3.99763	1.8947E-07
L-Carnitine	161.1052	9.83	C7H15NO3	+	L1	Lysine degradation	2.07725027	8.72321	1.7998E-10
L-Formylkynurenine	236.0797	8.11	C11H12N2O4	+	L2	Tryptophan metabolism	1.83431751	1.77327	1.8139E-07
L-Glutamate	147.0531	10.51	C5H9NO4	+	L1	Arginine and proline metabolism, Glutamate metabolism, Histidine metabolism, Glutathione metabolism_	1.28072647	9.2633	0.000055939
L-Glutamine	146.0691	11.03	C5H10N2O3	+	L1	Glutamate metabolism, Purine metabolism, Pyrimidine metabolism	1.25661497	12.8812	1.4274E-06
L-Malate	134.0215	11.50	C4H6O5	-	L2	Butanoate metabolism	1.69198601	9.81245	2.4709E-09
L-Serine	105.0426	11.55	C3H7NO3	+	L1	Glycine, serine and threonine metabolism, Methionine metabolism, Cysteine metabolism	1.82054254	3.28679	1.5803E-06
myo-Inositol	180.0634	12.25	C6H12O6	-	L1	Inositol metabolism, Galactose metabolism	3.60987724	4.41262	2.0375E-14
N-Acetyl-L-aspartate	175.0481	10.52	C6H9NO5	-	L2	Alanine and aspartate metabolism	2.07294769	9.45293	1.0653E-10
N-Acetyl-L-glutamate	189.0637	10.18	C7H11NO5	-	L2	Arginine and proline metabolism	1.37387744	1.42304	2.6219E-07
Nicotinamide	122.0480	7.19	C6H6N2O	+	L1	Nicotinate and nicotinamide metabolism	1.32799238	7.32121	4.681E-07
O-Acetyl-L-homoserine	161.0688	8.73	C6H11NO4	+	L2	Methionine metabolism, Sulfur metabolism	1.21530885	2.14221	1.3996E-07
Butanoylcarnitine	231.1470	7.40	C11H21NO4	+	L2	Fatty acyl carnitines	1.46090983	1.27976	0.00003205
Propanoylcarnitine	217.1314	7.94	C10H19NO4	+	L2	OxidationofBranchedFattyAcids	2.78540659	5.56353	2.1688E-11
PC(14:0/P-16:0)	689.5360	3.96	C38H76NO7P	+	L2	Glycerophosphocholines	2.50831224	1.83302	5.5886E-08
PC(16:0/P-18:0)	745.5985	3.90	C42H84NO7P	+	L2	Glycerophosphocholines	2.2081026	5.44174	1.6268E-08
PC(18:0/P-18:0)	773.6299	3.89	C44H88NO7P	+	L2	Glycerophosphocholines	1.94486803	1.42065	4.3391E-07
PC(20:4/P-18:1)	791.5827	3.87	C46H82NO7P	+	L2	Glycerophosphocholines	1.60647061	2.44151	2.8227E-06
PC(22:4/P-18:1)	819.6146	3.85	C48H86NO7P	+	L2	Glycerophosphocholines	1.47273464	1.01894	0.00007107
PC(30:0)	705.5309	3.94	C38H76NO8P	+	L2	Glycerophosphocholines	1.7625355	2.95427	2.3743E-07
PC(32:0)	733.5625	3.92	C40H80NO8P	+	L2	Glycerophosphocholines	1.86346719	2.71373	9.1299E-07
PC(32:1)	731.5463	3.93	C40H78NO8P	+	L2	Glycerophosphocholines	1.17957331	3.26493	0.00002921
PC(34:1)	759.5776	3.90	C42H82NO8P	+	L2	Glycerophosphocholines	1.18128026	5.10737	0.0012133
PC(34:2)	757.5619	3.91	C42H80NO8P	+	L2	Glycerophosphocholines	1.19783094	2.87678	0.00012698
PC(36:2)	785.5932	3.88	C44H84NO8P	+	L2	Glycerophosphocholines	1.32796403	4.39001	0.00018685
PC(O-16:0/12:0)	663.5202	3.99	C36H74NO7P	+	L2	Glycerophosphocholines	2.54768653	1.13809	1.8471E-06

Phosphocreatine	211.0359	10.57	C4H10N3O5P	+	L2	Arginine and proline metabolism	1.55232235	4.64227	2.7217E-07
Phosphodimethylethanolamine	169.0504	9.74	C4H12NO4P	+	L2	Glycerophospholipid metabolism	1.34734019	1.44265	5.2975E-08
Pyridoxine	169.0739	7.37	C8H11NO3	+	L1	Vitamin B6 metabolism	1.24219736	2.40116	0.000000163
S-Adenosyl-L-homocysteine	384.1217	9.82	C14H20N6O5S	+	L1	Methionine metabolism	3.30773691	2.36407	2.4398E-11

Table 3.10: A list of 36 of significantly changed in M2-M1-48 with VIP > 1 and FDR < 0.05 compared to M1 as a result of investigation M1, M2-M1-24 and M2-M1-48.

Putative metabolite	Mass	RT	FORMULA	POLARITY	confidence	Pathway	Fold chnge	VIP	FDR
[FA oxo,amino(6:0)]	145.0739	7.24	C6H11NO3	+	L2	Lysine degradation	1.55956469	1.08475	8.0912E-07
[PC (14:2/16:0)]	691.5517	3.94	C38H78NO7P	+	L2	Glycerophosphocholines	2.31738241	2.0212	1.6072E-07
[PC (14:2/18:0)]	719.5835	3.92	C40H82NO7P	+	L2	Glycerophosphocholines	2.30948269	1.4713	6.0581E-07
[PC (16:1)]	493.3169	4.61	C24H48NO7P	+	L2	Glycerophosphocholines	1.43246229	1.09339	3.2369E-08
[PC (18:1/18:0)]	771.6144	3.89	C44H86NO7P	+	L2	Glycerophosphocholines	1.60504236	1.48295	1.3081E-06
[PC (18:1/20:4)]	793.5987	3.87	C46H84NO7P	+	L2	Glycerophosphocholines	1.41589478	1.60393	0.000010498
Ceramide (d18:1/16:0)]	537.5123	3.82	C34H67NO3	+	L2	Ceramides	2.8945629	1.3925	3.5124E-11
1-Hexadecanoyl-2-sn-glycero-3-phosphonocholine	743.5828	3.91	C42H82NO7P	+	L2	Glycerophosphonocholines	1.544856	2.35431	2.3729E-08
L-1-Pyrroline-5-carboxylate	113.0477	11.08	C5H7NO2	-	L2	Glutamate metabolism, Arginine and proline metabolism	2.05190965	2.54099	8.8169E-09
2-Dehydro-3-deoxy-L-rhamnonate	162.0528	10.28	C6H10O5	-	L2	Fructose and mannose metabolism	1.28452648	1.34194	5.4577E-09
2-Oxoglutaramate	145.0375	8.43	C5H7NO4	-	L2	Glutamate metabolism	1.97793234	1.29116	5.2558E-11
2-Oxohexenoic acid	128.0473	5.10	C6H8O3	+	L2	4-nitrotoluene degradation II	2.30577274	2.62641	0.000012807
4-Hydroxyphenylacetaldehyde-oxime	151.0633	5.49	C8H9NO2	+	L2	Tyrosine metabolism	10.406263	5.13367	1.0921E-12
5-Hydroxyindoleacetaldehyde	175.0633	4.25	C10H9NO2	+	L2	Tryptophan metabolism	1.57642377	1.42051	0.00002012
Biotin	244.0882	7.22	C10H16N2O3S	+	L2	Biotin metabolism	1.68413919	1.00627	0.000014588
Creatinine	113.0589	8.50	C4H7N3O	+	L2	Arginine and proline metabolism	1.20978209	5.97362	0.00038244
Deoxyadenosine	251.1018	7.26	C10H13N5O3	+	L2	Purine metabolism	3.07537543	1.19882	4.5872E-11
D-Galactosamine	179.0794	10.64	C6H13NO5	+	L2	Galactose metabolism	2.20805232	2.58037	1.03E-09
Guanidinoacetate	117.0538	11.88	C3H7N3O2	+	L1	Glycine, serine and threonine metabolism, Arginine and proline metabolism	1.34515711	1.84582	2.4709E-09
L-1-Pyrroline-3-hydroxy-5-carboxylate	129.0427	8.04	C5H7NO3	-	L2	Arginine and proline metabolism	1.12360289	3.28322	3.1665E-09
L-Arginine	174.1117	18.31	C6H14N4O2	+	L1	Arginine and proline metabolism, Clavulanic acid biosynthesis, D-Arginine and D-ornithine metabolism	1.14411176	3.55787	0.0039498
L-Aspartate	133.0375	10.80	C4H7NO4	-	L1	Alanine and aspartate metabolism, Arginine and proline metabolism, Glycine, serine and threonine metabolism, Lysine biosynthesis,	1.78392802	3.06395	1.8947E-07
L-Tryptophan	204.0900	9.63	C11H12N2O2	+	L1	Tryptophan metabolism, Phenylalanine, tyrosine and tryptophan biosynthesis, Indole and ipecac alkaloid biosynthesis	1.79097414	1.69504	7.6573E-07
L-Tyrosine	181.0740	10.34	C9H11NO3	+	L1	Tyrosine metabolism, Phenylalanine, tyrosine and tryptophan biosynthesis	1.26438542	2.50858	3.6869E-07

N-Acetyl-L-aspartate	175.0481	10.52	C6H9NO5	-	L2	Alanine and aspartate metabolism	1.54872512	6.26633	1.0653E-10
Nicotinamide	122.0480	7.19	C6H6N2O	+	L1	Nicotinate and nicotinamide metabolism	1.24431996	5.70248	4.681E-07
Propanoylcarnitine	217.1314	7.94	C10H19NO4	+	L2	Oxidation of Branched Fatty Acids	1.23842939	1.70286	2.1688E-11
PC(14:0/P-16:0)	689.5360	3.96	C38H76NO7P	+	L2	Glycerophosphocholines	1.62811866	1.07137	5.5886E-08
PC(16:0/P-18:0)	745.5985	3.90	C42H84NO7P	+	L2	Glycerophosphocholines	1.82769579	4.1262	1.6268E-08
PC(18:0/P-18:0)	773.6299	3.89	C44H88NO7P	+	L2	Glycerophosphocholines	1.80876968	1.19436	4.3391E-07
PC(20:4/P-18:1)	791.5827	3.87	C46H82NO7P	+	L2	Glycerophosphocholines	1.40069307	1.7454	2.8227E-06
PC(32:0)	733.5625	3.92	C40H80NO8P	+	L2	Glycerophosphocholines	1.67061415	2.17664	9.1299E-07
Phenylacetylglycine	193.0739	5.14	C10H11NO3	-	L2	Phenylalanine metabolism	1.44426914	1.46049	1.9026E-06
PS(36:1)	789.5520	3.66	C42H80NO10P	-	L2	Glycerophosphoserines	1.57343085	1.1537	0.000011439
Pyridoxine	169.0739	7.37	C8H11NO3	+	L1	Vitamin B6 metabolism	1.69936462	4.23055	0.000000163
SM(d18:1/24:1)	812.6769	3.93	C47H93N2O6P	+	L2	Ceramide phosphocholines (sphingomyelins)	1.51783317	1.02528	0.00098791

Table 3.11: A list of 89 significantly changed metabolites in M1-M2-24 with VIP > 1 and FDR < 0.05 compared to M2 as a result of investigation M2, M1-M2-24 and M1-M2-48.

Putative metabolite	Mass	RT	FORMULA	POLARITY	confidence	Pathway	Fold change	VIP	FDR
(S)-3-Methyl-2-oxopentanoic acid	130.0631	4.87	C6H10O3	-	L2	Valine, leucine and isoleucine degradation, Valine, leucine and isoleucine biosynthesis	0.29029564	2.92049	4.9107E-12
[FA (12:4/2:0)]	222.0893	4.24	C12H14O4	-	L2	Fatty Acids and Conjugates	0.46482142	1.0519	7.3886E-10
[FA trihydroxy(4:0)]	136.0372	9.37	C4H8O5	-	L2	Ascorbate and aldarate metabolism	0.43719191	1.43739	1.3686E-08
[PC (14:0)]	467.3012	4.67	C22H46NO7P	+	L2	Glycerophosphocholines	0.2684851	1.37184	4.3608E-09
[PC (14:2/16:0)]	691.5517	3.94	C38H78NO7P	+	L2	Glycerophosphocholines	0.24470255	2.12211	8.3876E-15
[PC (14:2/18:0)]	719.5835	3.92	C40H82NO7P	+	L2	Glycerophosphocholines	0.18093875	2.12688	2.5371E-15
[PC (16:0)]	495.3325	4.59	C24H50NO7P	+	L2	Glycerophosphocholines	0.48551047	3.34691	2.0901E-11
[PC (16:1)]	493.3169	4.61	C24H48NO7P	+	L2	Glycerophosphocholines	0.25475622	2.26238	2.7765E-10
[PC (16:1)]	479.3376	4.55	C24H50NO6P	+	L2	Glycerophosphocholines	0.48901277	1.04693	4.6267E-10
[PC (16:2)]	481.3533	4.60	C24H52NO6P	+	L2	Glycerophosphocholines	0.19439765	2.45321	3.7396E-13
[PC (18:1/18:0)]	771.6144	3.89	C44H86NO7P	+	L2	Glycerophosphocholines	0.37507279	1.62754	5.7996E-09
[PC (18:1/20:4)]	793.5987	3.87	C46H84NO7P	+	L2	Glycerophosphocholines	0.6265459	1.47506	3.2408E-07
[PE (16:1)]	437.2907	4.45	C21H44NO6P	+	L2	Glycerophosphoethanolamines	0.38671809	1.19866	9.0283E-11
1-Hexadecanoyl-2-(octadecenoyl)-sn-glycero-3-phosphonocholine	743.5828	3.91	C42H82NO7P	+	L2	Glycerophosphonocholines	0.47509316	2.36425	3.8985E-12
2-Dehydro-3-deoxy-L-rhamnonate	162.0528	10.28	C6H10O5	-	L2	Fructose and mannose metabolism	0.25599645	1.99929	1.0551E-19
3-(4-Hydroxyphenyl)lactate	182.0579	7.78	C9H10O4	-	L2	Tyrosine metabolism	0.14484027	2.38366	3.7456E-17
4-Guanidinobutanoate	145.0851	11.26	C5H11N3O2	+	L2	Arginine and proline metabolism	0.20930972	1.74913	1.6423E-14
4-Imidazolone-5-propanoate	156.0535	8.73	C6H8N2O3	+	L2	Histidine metabolism	0.0194351	1.80012	3.2742E-14
4-Trimethylammoniobutanoate	145.1103	9.79	C7H15NO2	+	L2	Lysine degradation	0.25174072	2.87996	4.6568E-17
5-Guanidino-2-oxopentanoate	173.0801	11.09	C6H11N3O3	+	L2	D-Arginine and D-ornithine metabolism	0.35923903	1.78367	8.9727E-12
5'-Methylthioadenosine	297.0896	7.18	C11H15N5O3S	+	L1	Arginine and proline metabolism, Methionine metabolism, Zeatin biosynthesis	0.58111198	1.84381	8.9084E-09
Biotin	244.0882	7.22	C10H16N2O3S	+	L2	Biotin metabolism	0.39330774	1.00721	1.0127E-10
Creatine	131.0695	11.00	C4H9N3O2	+	L1	Glycine, serine and threonine metabolism, Arginine and proline metabolism	0.26818249	25.1879	1.4634E-14
Creatinine	113.0589	8.50	C4H7N3O	+	L2	Arginine and proline metabolism	0.41248613	9.18261	1.0006E-10
D-Galactosamine	179.0794	10.64	C6H13NO5	+	L2	Galactose metabolism	0.59560409	1.41011	1.0447E-09
D-Gluconic acid	196.0583	10.17	C6H12O7	-	L2	Pentose phosphate pathway	0.26841255	1.39833	1.3971E-13

D-Glyceraldehyde 3-phosphate	169.9980	11.37	C3H7O6P	-	L2	Glycolysis / Gluconeogenesis, Pentose phosphate pathway, Inositol metabolism, Pentose and glucuronate interconversions, Fructose and mannose metabolism, Galactose metabolism, Biosynthesis of steroids, Clavulanic acid biosynthesis, Methane metabolism	0.32932403	1.73602	1.0379E-14
D-Phenylalanine	165.0790	8.19	C9H11NO2	+	L2	Phenylalanine metabolism	0.31151427	8.79832	2.0011E-14
Glycine	75.0320	11.62	C2H5NO2	+	L2	Bile acid biosynthesis, Purine metabolism, Glycine, serine and threonine metabolism, Lysine degradation, Cyanoamino acid metabolism, Glutathione metabolism, Methane metabolism, Thiamine metabolism, Porphyrin and chlorophyll metabolism, Nitrogen metabolism	0.4895174	1.18759	0.001444
Guanidinoacetate	117.0538	11.88	C3H7N3O2	+	L1	Glycine, serine and threonine metabolism, Arginine and proline metabolism	0.17899831	3.07872	3.0733E-16
Hypotaurine	109.0198	11.27	C2H7NO2S	+	L2	Taurine and hypotaurine metabolism	0.42223089	1.48744	8.6852E-13
L-1-Pyrroline-3-hydroxy-5-carboxylate	129.0427	8.04	C5H7NO3	-	L2	Arginine and proline metabolism	0.31327276	7.52249	8.5875E-13
L-Alanine	89.0477	11.08	C3H7NO2	+	L2	Alanine and aspartate metabolism, Cysteine metabolism, Taurine and hypotaurine metabolism, Selenoamino acid metabolism, D-Alanine metabolism, Carbon fixation, Reductive carboxylate cycle (CO2 fixation)	0.2913485	4.90257	5.3167E-14
L-Arginine	174.1117	18.31	C6H14N4O2	+	L1	Arginine and proline metabolism, Clavulanic acid biosynthesis, D-Arginine and D-ornithine metabolism	0.41240348	7.2229	2.9034E-11
L-Asparagine	132.0535	11.21	C4H8N2O3	+	L2	Alanine and aspartate metabolism, Tetracycline biosynthesis, Cyanoamino acid metabolism, Nitrogen metabolism	0.46622961	4.62768	1.3884E-10
L-Aspartate	133.0375	10.80	C4H7NO4	-	L1	Alanine and aspartate metabolism, Arginine and proline metabolism, Glycine, serine and threonine metabolism, Lysine biosynthesis, Arginine and proline metabolism, Histidine metabolism, beta-Alanine metabolism, Cyanoamino acid metabolism, Carbon fixation	0.67306984	1.84773	1.6163E-07
L-Carnitine	161.1052	9.83	C7H15NO3	+	L1	Lysine degradation	0.49631245	4.79352	3.6181E-11
L-Glutamate 5-semialdehyde	131.0585	10.86	C5H9NO3	+	L2	Arginine and proline metabolism	0.3932074	10.6319	6.3145E-11

L-Histidine	155.0695	11.22	C6H9N3O2	+	L1	Histidine metabolism, beta-Alanine metabolism	0.3314781	5.87497	4.4458E-15
L-Leucine	131.0947	9.02	C6H13NO2	+	L1	Valine, leucine and isoleucine degradation, Valine, leucine and isoleucine biosynthesis	0.37624702	13.3215	2.4825E-12
L-Lysine	146.1055	16.99	C6H14N2O2	+	L2	Lysine biosynthesis, Lysine degradation, Biotin metabolism, Alkaloid biosynthesis II	0.25185431	1.9534	5.8437E-13
L-Methionine	149.0511	9.18	C5H11NO2S	+	L1	Methionine metabolism	0.32533971	8.68157	2.0179E-13
L-Methionine S-oxide	165.0460	9.84	C5H11NO3S	+	L2	Methionine metabolism	0.40902863	1.36713	1.8849E-09
L-Ornithine	132.0899	15.96	C5H12N2O2	+	L1	Arginine and proline metabolism, D-Arginine and D-ornithine metabolism, Glutathione metabolism	0.158907	1.90179	6.356E-13
L-Proline	115.0634	9.96	C5H9NO2	+	L1	Arginine and proline metabolism, Novobiocin biosynthesis	0.2603111	26.6273	4.9917E-11
L-Threonine	119.0583	10.77	C4H9NO3	+	L1	Glycine, serine and threonine metabolism, Valine, leucine and isoleucine biosynthesis, Porphyrin and chlorophyll metabolism	0.31190478	5.6	1.9249E-14
L-Tryptophan	204.0900	9.63	C11H12N2O2	+	L1	Tryptophan metabolism, Phenylalanine, tyrosine and tryptophan biosynthesis, Indole and ipecac alkaloid biosynthesis	0.25978411	2.02443	2.6647E-14
L-Tyrosine	181.0740	10.34	C9H11NO3	+	L1	Tyrosine metabolism, Phenylalanine, tyrosine and tryptophan biosynthesis, Novobiocin biosynthesis, Thiamine metabolism, Phenylpropanoid biosynthesis, Alkaloid biosynthesis I	0.44548389	3.19252	6.2424E-10
L-Valine	117.0790	9.67	C5H11NO2	+	L1	Valine, leucine and isoleucine degradation, Valine, leucine and isoleucine biosynthesis, Penicillin and cephalosporin biosynthesis, Propanoate metabolism, Pantothenate and CoA biosynthesis	0.40156537	8.26018	2.6068E-11
myo-Inositol	180.0634	12.25	C6H12O6	-	L1	Inositol metabolism, Galactose metabolism, Ascorbate and aldarate metabolism, Streptomycin biosynthesis, Inositol phosphate metabolism	0.56847347	1.76651	1.4873E-12
N(pi)-Methyl-L-histidine	169.0851	9.65	C7H11N3O2	+	L2	Histidine metabolism	0.25593202	2.70625	6.2975E-14
N2-(D-1-Carboxyethyl)-L-arginine	246.1329	10.48	C9H18N4O4	+	L2	Arginine and proline metabolism	0.06148687	2.56646	2.7203E-14
N6,N6,N6-Trimethyl-L-lysine	188.1525	15.36	C9H20N2O2	+	L2	Lysine degradation	0.23174232	2.31495	3.7763E-12
N6-Methyl-L-lysine	160.1211	16.41	C7H16N2O2	+	L1	0	0.33087363	1.21871	1.1495E-12
N-Acetyl-L-aspartate	175.0481	10.52	C6H9NO5	-	L2	Alanine and aspartate metabolism	0.43852952	6.53936	2.6429E-14

N-Acetyl-L-glutamate	189.0637	10.18	C7H11NO5	-	L2	Arginine and proline metabolism	0.27746994	2.07762	1.7911E-11
NAD+	663.1090	9.74	C21H27N7O14P2	+	L2	Oxidative phosphorylation, Glutamate metabolism, Nicotinate and nicotinamide metabolism	0.68001292	1.56068	1.833E-07
NADH	665.1253	9.55	C21H29N7O14P2	+	L1	Oxidative phosphorylation	0.31004947	1.309	1.1838E-10
N-Formyl-L-methionine	177.0460	5.17	C6H11NO3S	-	L2	Methionine metabolism	0.33277395	1.79351	2.2577E-10
Nicotinamide	122.0480	7.19	C6H6N2O	+	L1	Nicotinate and nicotinamide metabolism	0.68203086	4.45513	3.4499E-06
O-Acetylcarnitine	203.1158	8.54	C9H17NO4	+	L1	Alanine and aspartate metabolism	0.14119687	11.3123	1.42E-14
Butanoylcarnitine	231.1470	7.40	C11H21NO4	+	L2	Fatty acyl carnitines	0.54145881	1.02653	3.9604E-11
Propanoylcarnitine	217.1314	7.94	C10H19NO4	+	L2	OxidationofBranchedFattyAcids	0.26983899	3.05227	5.1678E-11
PC(14:0/P-16:0)	689.5360	3.96	C38H76NO7P	+	L2	Glycerophosphocholines	0.34924826	1.20626	5.0047E-12
PC(16:0/P-18:0)	745.5985	3.90	C42H84NO7P	+	L2	Glycerophosphocholines	0.33017649	4.51469	7.4727E-16
PC(18:0/P-18:0)	773.6299	3.89	C44H88NO7P	+	L2	Glycerophosphocholines	0.27318554	1.76503	4.2375E-13
PC(20:4/P-18:1)	791.5827	3.87	C46H82NO7P	+	L2	Glycerophosphocholines	0.5355122	1.8342	1.3884E-10
PC(22:4/P-18:1)	819.6146	3.85	C48H86NO7P	+	L2	Glycerophosphocholines	0.5126938	1.00847	4.8888E-10
PC(30:0)	705.5309	3.94	C38H76NO8P	+	L2	Glycerophosphocholines	0.44513078	2.27583	2.4915E-11
PC(30:1)	703.5150	3.95	C38H74NO8P	+	L2	Glycerophosphocholines	0.42805425	1.01999	5.0908E-11
PC(32:0)	733.5625	3.92	C40H80NO8P	+	L2	Glycerophosphocholines	0.52457059	2.15957	3.5489E-11
PC(32:1)	731.5463	3.93	C40H78NO8P	+	L2	Glycerophosphocholines	0.63428472	3.44559	3.7131E-11
PC(34:1)	759.5776	3.90	C42H82NO8P	+	L2	Glycerophosphocholines	0.77226097	4.35148	1.2302E-09
PC(34:2)	757.5619	3.91	C42H80NO8P	+	L2	Glycerophosphocholines	0.79972612	1.84673	3.0605E-08
PC(36:1)	787.6089	3.88	C44H86NO8P	+	L2	Glycerophosphocholines	0.5408956	2.86576	1.3902E-11
PC(36:2)	785.5932	3.88	C44H84NO8P	+	L2	Glycerophosphocholines	0.68381966	3.21748	1.8634E-10
PC(38:2)	813.6250	3.86	C46H88NO8P	+	L2	Glycerophosphocholines	0.4981075	1.16635	1.1449E-10
PE(16:0/P-18:1)	701.5361	3.83	C39H76NO7P	+	L2	Glycerophosphoethanolamines	0.25026366	1.29948	5.3127E-10
Phenylacetylglycine	193.0739	5.14	C10H11NO3	-	L2	Phenylalanine metabolism	0.26073438	2.03811	3.9975E-12
Phenyllactate	166.0630	5.11	C9H10O3	-	L2	Phenylalanine metabolism	0.03412898	2.49136	1.1846E-15
Phosphocreatine	211.0359	10.57	C4H10N3O5P	+	L2	Arginine and proline metabolism	0.40221508	3.57887	1.6795E-10
PS(36:1)	789.5520	3.66	C42H80NO10P	-	L2	Glycerophosphoserines	0.50591748	1.33922	7.5218E-08
Pyridine-2,3-dicarboxylate	167.0219	11.14	C7H5NO4	-	L2	Tryptophan metabolism, beta-Alanine metabolism, Nicotinate and nicotinamide metabolism	0.47635978	1.39467	3.3993E-14
Pyridoxine	169.0739	7.37	C8H11NO3	+	L1	Vitamin B6 metabolism	0.49211221	3.32502	4.4452E-09
SM(d18:1/24:1)	812.6769	3.93	C47H93N2O6P	+	L2	Ceramide phosphocholines (sphingomyelins)	0.58551136	1.02028	3.1836E-07

sn-glycero-3-Phosphocholine	257.1030	10.23	C8H20NO6P	+	L1	Glycerophospholipid metabolism, Ether lipid metabolism	0.56215124	25.2351	4.7421E-11
sn-glycero-3-Phosphoethanolamine	215.0559	11.04	C5H14NO6P	+	L2	Glycerophospholipid metabolism, Ether lipid metabolism	0.25730387	3.70687	1.3459E-14
sn-Glycerol 3-phosphate	172.0137	10.23	C3H9O6P	-	L2	Glycerolipid metabolism, Glycerophospholipid metabolism	0.32081553	3.30174	6.0652E-18
Taurine	125.0147	11.45	C2H7NO3S	+	L1	Bile acid biosynthesis, Taurine and hypotaurine metabolism	0.37671085	1.92017	1.8488E-12

Table 3.12: A list of 104 significantly changed metabolites in M1-M2-48 with VIP > 1 and FDR < 0.05 compared to M2 as a result of investigation M2, M1-M2-24 and M1-M2-48.

Putative metabolite	Mass	RT	FORMULA	POLARITY	confidence	Pathway	Fold change	VIP	FDR
[FA (12:4/2:0)]	222.0893	4.24	C12H14O4	-	L2	Fatty Acids and Conjugates	0.38791942	1.20498	7.3886E-10
[FA trihydroxy(4:0)]	136.0372	9.37	C4H8O5	-	L2	Ascorbate and aldarate metabolism	0.54844212	1.35433	1.3686E-08
[FA] Palmitoyl-carnitine	399.3350	4.54	C23H45NO4	+	L2	Fatty acyl carnitines	0.39919016	1.09305	3.3924E-08
[PC (14:0)]	467.3012	4.67	C22H46NO7P	+	L2	Glycerophosphocholines	0.1971749	1.54002	4.3608E-09
[PC (14:2/16:0)]	691.5517	3.94	C38H78NO7P	+	L2	Glycerophosphocholines	0.18251681	2.35784	8.3876E-15
[PC (14:2/18:0)]	719.5835	3.92	C40H82NO7P	+	L2	Glycerophosphocholines	0.15605221	2.30463	2.5371E-15
[PC (16:0)]	495.3325	4.59	C24H50NO7P	+	L2	Glycerophosphocholines	0.3724311	3.95633	2.0901E-11
[PC (16:1)]	493.3169	4.61	C24H48NO7P	+	L2	Glycerophosphocholines	0.17681931	2.54418	2.7765E-10
[PC (16:1)]	479.3376	4.55	C24H50NO6P	+	L2	Glycerophosphocholines	0.49574672	1.10816	4.6267E-10
[PC (16:2)]	481.3533	4.60	C24H52NO6P	+	L2	Glycerophosphocholines	0.15878661	2.67582	3.7396E-13
[PC (18:0)]	523.3642	4.49	C26H54NO7P	+	L2	Glycerophosphocholines	0.64050073	1.2859	3.5414E-07
[PC (18:1/18:0)]	771.6144	3.89	C44H86NO7P	+	L2	Glycerophosphocholines	0.29088909	1.88926	5.7996E-09
[PC (18:1/20:4)]	793.5987	3.87	C46H84NO7P	+	L2	Glycerophosphocholines	0.5560227	1.74031	3.2408E-07
[PE (16:1)]	437.2907	4.45	C21H44NO6P	+	L2	Glycerophosphoethanolamines	0.34985504	1.31904	9.0283E-11
[PE (18:1)]	479.3013	4.42	C23H46NO7P	+	L2	Glycerophosphoethanolamines	0.27524642	1.12345	7.0286E-10
1-Hexadecanoyl-2-(octadecenoyl)-sn-glycero-3-phosphonocholine	743.5828	3.91	C42H82NO7P	+	L2	Glycerophosphonocholines	0.38119728	2.74727	3.8985E-12
2-Dehydro-3-deoxy-L-rhamnonate	162.0528	10.28	C6H10O5	-	L2	Fructose and mannose metabolism	0.22231454	2.18012	1.0551E-19
2-Oxoglutarate	146.0215	11.38	C5H6O5	-	L2	Citrate cycle (TCA cycle), Ascorbate and aldarate metabolism, Glutamate metabolism, Alanine and aspartate metabolism, Lysine biosynthesis, Histidine metabolism, D-Glutamine and D-glutamate metabolism, Glyoxylate and dicarboxylate metabolism	0.60740601	1.71966	3.603E-07
3-(4-Hydroxyphenyl)lactate	182.0579	7.78	C9H10O4	-	L2	Tyrosine metabolism	0.12421146	2.5731	3.7456E-17
3-Methyl-2-oxopentanoic acid	130.0631	4.87	C6H10O3	-	L2	Valine, leucine and isoleucine degradation, Valine, leucine and isoleucine biosynthesis	0.35503062	2.96272	4.9107E-12
4-Guanidinobutanoate	145.0851	11.26	C5H11N3O2	+	L2	Arginine and proline metabolism	0.1927513	1.88518	1.6423E-14

4-Imidazolone-5-propanoate	156.0535	8.73	C6H8N2O3	+	L2	Histidine metabolism	0.02184181	1.91777	3.2742E-14
4-Trimethylammoniobutanoate	145.1103	9.79	C7H15NO2	+	L2	Lysine degradation	0.19624996	3.18524	4.6568E-17
5-Guanidino-2-oxopentanoate	173.0801	11.09	C6H11N3O3	+	L2	D-Arginine and D-ornithine metabolism	0.26242226	2.04799	8.9727E-12
5'-Methylthioadenosine	297.0896	7.18	C11H15N5O3S	+	L1	Arginine and proline metabolism, Methionine metabolism, Zeatin biosynthesis	0.36619898	2.48066	8.9084E-09
Creatine	131.0695	11.00	C4H9N3O2	+	L1	Glycine, serine and threonine metabolism, Arginine and proline metabolism	0.21560091	27.8227	1.4634E-14
Creatinine	113.0589	8.50	C4H7N3O	+	L2	Arginine and proline metabolism	0.52237075	8.76436	1.0006E-10
D-Galactosamine	179.0794	10.64	C6H13NO5	+	L2	Galactose metabolism	0.59783802	1.49943	1.0447E-09
D-Gluconic acid	196.0583	10.17	C6H12O7	-	L2	Pentose phosphate pathway	0.62776556	1.05275	1.3971E-13
D-Glyceraldehyde 3-phosphate	169.9980	11.37	C3H7O6P	-	L2	Glycolysis / Gluconeogenesis, Pentose phosphate pathway, Inositol metabolism, Pentose and glucuronate interconversions, Fructose and mannose metabolism, Galactose metabolism, Biosynthesis of steroids, Clavulanic acid biosynthesis, Methane metabolism	0.28174655	1.91662	1.0379E-14
D-Phenylalanine	165.0790	8.19	C9H11NO2	+	L2	Phenylalanine metabolism	0.41850146	8.61124	2.0011E-14
D-Sorbitol	182.0791	10.65	C6H14O6	-	L2	Fructose and mannose metabolism, Galactose metabolism	0.56928442	1.24958	1.7839E-08
Glutathione disulfide	612.1520	11.28	C20H32N6O12S2	+	L1	Glutamate metabolism, Glutathione metabolism	0.53048271	1.38726	0.00012909
Guanidinoacetate	117.0538	11.88	C3H7N3O2	+	L1	Glycine, serine and threonine metabolism, Arginine and proline metabolism	0.20245367	3.23643	3.0733E-16
Hexadecanoic acid	256.2404	3.92	C16H32O2	-	L2	Fatty acid biosynthesis, Fatty acid elongation in mitochondria, Fatty acid metabolism, Biosynthesis of unsaturated fatty acids	0.64264463	3.11457	0.000016138
Hypotaurine	109.0198	11.27	C2H7NO2S	+	L2	Taurine and hypotaurine metabolism	0.34676197	1.68963	8.6852E-13
L-1-Pyrroline-3-hydroxy-5-carboxylate	129.0427	8.04	C5H7NO3	-	L2	Arginine and proline metabolism	0.58177282	6.21057	8.5875E-13
L-Alanine	89.0477	11.08	C3H7NO2	+	L2	Alanine and aspartate metabolismTaurine and hypotaurine metabolismD-Alanine metabolism, Carbon fixation, Reductive carboxylate cycle (CO2 fixation)	0.33765308	5.05126	5.3167E-14
L-Arginine	174.1117	18.31	C6H14N4O2	+	L1	Arginine and proline metabolism, Clavulanic acid biosynthesis, D-Arginine and D-ornithine metabolism	0.51629424	6.94595	2.9034E-11
L-Asparagine	132.0535	11.21	C4H8N2O3	+	L2	Alanine and aspartate metabolism, Tetracycline biosynthesis, Cyanoamino acid metabolism, Nitrogen metabolism	0.57341911	4.36751	1.3884E-10

L-Aspartate	133.0375	10.80	C4H7NO4	-	L1	Alanine and aspartate metabolism, Arginine and proline metabolism, Glycine, serine and threonine metabolism, Lysine biosynthesis, Arginine and proline metabolism, Histidine metabolism, beta-Alanine metabolism, Cyanoamino acid metabolism, Carbon fixation	0.65879123	1.98636	1.6163E-07
L-Carnitine	161.1052	9.83	C7H15NO3	+	L1	Lysine degradation	0.42432701	5.48145	3.6181E-11
L-Glutamate 5-semialdehyde	131.0585	10.86	C5H9NO3	+	L2	Arginine and proline metabolism	0.45887524	10.6806	6.3145E-11
L-Histidine	155.0695	11.22	C6H9N3O2	+	L1	Histidine metabolism, beta-Alanine metabolism	0.43488779	5.75559	4.4458E-15
L-Leucine	131.0947	9.02	C6H13NO2	+	L1	Valine, leucine and isoleucine degradation, Valine, leucine and isoleucine biosynthesis	0.43415517	13.5255	2.4825E-12
L-Lysine	146.1055	16.99	C6H14N2O2	+	L2	Lysine biosynthesis, Lysine degradation, Biotin metabolism, Alkaloid biosynthesis II	0.32762422	1.97282	5.8437E-13
L-Malate	134.0215	11.50	C4H6O5	-	L2	Butanoate metabolism	0.89400421	2.02779	4.3808E-06
L-Methionine	149.0511	9.18	C5H11NO2S	+	L1	Methionine metabolism	0.39534752	8.75035	2.0179E-13
L-Methionine S-oxide	165.0460	9.84	C5H11NO3S	+	L2	Methionine metabolism	0.53480601	1.27771	1.8849E-09
L-Ornithine	132.0899	15.96	C5H12N2O2	+	L1	Arginine and proline metabolism, D-Arginine and D-ornithine metabolism, Glutathione metabolism	0.33726057	1.79377	6.356E-13
L-Proline	115.0634	9.96	C5H9NO2	+	L1	Arginine and proline metabolism, Novobiocin biosynthesis	0.30331987	27.4971	4.9917E-11
L-Threonine	119.0583	10.77	C4H9NO3	+	L1	Glycine, serine and threonine metabolism, Valine, leucine and isoleucine biosynthesis, Porphyrin and chlorophyll metabolism	0.39413163	5.60118	1.9249E-14
L-Tryptophan	204.0900	9.63	C11H12N2O2	+	L1	Tryptophan metabolism, Phenylalanine, tyrosine and tryptophan biosynthesis, Indole and ipecac alkaloid biosynthesis	0.38959049	1.9569	2.6647E-14
L-Tyrosine	181.0740	10.34	C9H11NO3	+	L1	Tyrosine metabolism, Phenylalanine, tyrosine and tryptophan biosynthesis, Novobiocin biosynthesis, Thiamine metabolism, Phenylpropanoid biosynthesis, Alkaloid biosynthesis I	0.66089827	2.60414	6.2424E-10
L-Valine	117.0790	9.67	C5H11NO2	+	L1	Valine, leucine and isoleucine degradation, Valine, leucine and isoleucine biosynthesis, Penicillin and cephalosporin biosynthesis, Propanoate metabolism, Pantothenate and CoA biosynthesis	0.50425988	7.98548	2.6068E-11

myo-Inositol	180.0634	12.25	C6H12O6	-	L1	Inositol metabolism, Galactose metabolism, Ascorbate and aldarate metabolism, Streptomycin biosynthesis, Inositol phosphate metabolism	0.23564414	2.52941	1.4873E-12
N(pi)-Methyl-L-histidine	169.0851	9.65	C7H11N3O2	+	L2	Histidine metabolism	0.3166153	2.76415	6.2975E-14
N2-(D-1-Carboxyethyl)-L-arginine	246.1329	10.48	C9H18N4O4	+	L2	Arginine and proline metabolism	0.1425822	2.61475	2.7203E-14
N6,N6,N6-Trimethyl-L-lysine	188.1525	15.36	C9H20N2O2	+	L2	Lysine degradation	0.28139745	2.38368	3.7763E-12
N6-Methyl-L-lysine	160.1211	16.41	C7H16N2O2	+	L1	0	0.29331986	1.33538	1.1495E-12
N-Acetyl-L-aspartate	175.0481	10.52	C6H9NO5	-	L2	Alanine and aspartate metabolism	0.46459633	6.80931	2.6429E-14
N-Acetyl-L-glutamate	189.0637	10.18	C7H11NO5	-	L2	Arginine and proline metabolism	0.41469824	1.98669	1.7911E-11
NAD+	663.1090	9.74	C21H27N7O14P2	+	L2	Oxidative phosphorylation, Glutamate metabolism, Nicotinate and nicotinamide metabolism	0.39142076	2.43901	1.833E-07
NADH	665.1253	9.55	C21H29N7O14P2	+	L1	Oxidative phosphorylation	0.34444862	1.35411	1.1838E-10
N-Formyl-L-methionine	177.0460	5.17	C6H11NO3S	-	L2	Methionine metabolism	0.41356684	1.78643	2.2577E-10
Nicotinamide	122.0480	7.19	C6H6N2O	+	L1	Nicotinate and nicotinamide metabolism	0.85947096	2.81024	3.4499E-06
O-Acetylcarnitine	203.1158	8.54	C9H17NO4	+	L1	Alanine and aspartate metabolism	0.12387205	12.1888	1.42E-14
Butanoylcarnitine	231.1470	7.40	C11H21NO4	+	L2	Fatty acyl carnitines	0.36468351	1.30319	3.9604E-11
Propanoylcarnitine	217.1314	7.94	C10H19NO4	+	L2	OxidationofBranchedFattyAcids	0.17396067	3.47178	5.1678E-11
Pantothenate	219.1106	7.20	C9H17NO5	+	L2	beta-Alanine metabolism, Pantothenate and CoA biosynthesis	0.35832102	5.80697	8.2692E-12
PC(14:0/P-16:0)	689.5360	3.96	C38H76NO7P	+	L2	Glycerophosphocholines	0.27502744	1.35909	5.0047E-12
PC(16:0/P-18:0)	745.5985	3.90	C42H84NO7P	+	L2	Glycerophosphocholines	0.21824623	5.20657	7.4727E-16
PC(18:0/P-18:0)	773.6299	3.89	C44H88NO7P	+	L2	Glycerophosphocholines	0.1668428	2.01886	4.2375E-13
PC(20:4/P-18:1)	791.5827	3.87	C46H82NO7P	+	L2	Glycerophosphocholines	0.45742725	2.12336	1.3884E-10
PC(22:4/P-18:1)	819.6146	3.85	C48H86NO7P	+	L2	Glycerophosphocholines	0.43597485	1.15812	4.8888E-10
PC(30:0)	705.5309	3.94	C38H76NO8P	+	L2	Glycerophosphocholines	0.3512296	2.63408	2.4915E-11
PC(30:1)	703.5150	3.95	C38H74NO8P	+	L2	Glycerophosphocholines	0.28899542	1.21906	5.0908E-11
PC(32:0)	733.5625	3.92	C40H80NO8P	+	L2	Glycerophosphocholines	0.54045728	2.26362	3.5489E-11
PC(32:1)	731.5463	3.93	C40H78NO8P	+	L2	Glycerophosphocholines	0.44320724	4.58403	3.7131E-11
PC(32:2)	729.5309	3.94	C40H76NO8P	+	L2	Glycerophosphocholines	0.46871677	1.1191	4.1165E-10
PC(34:1)	759.5776	3.90	C42H82NO8P	+	L2	Glycerophosphocholines	0.60349471	6.23858	1.2302E-09
PC(34:2)	757.5619	3.91	C42H80NO8P	+	L2	Glycerophosphocholines	0.60426847	2.90901	3.0605E-08
PC(36:1)	787.6089	3.88	C44H86NO8P	+	L2	Glycerophosphocholines	0.4217154	3.4453	1.3902E-11
PC(36:2)	785.5932	3.88	C44H84NO8P	+	L2	Glycerophosphocholines	0.47930373	4.45796	1.8634E-10

PC(38:2)	813.6250	3.86	C46H88NO8P	+	L2	Glycerophosphocholines	0.32680023	1.45403	1.1449E-10
PE(16:0/P-18:1)	701.5361	3.83	C39H76NO7P	+	L2	Glycerophosphoethanolamines	0.17444221	1.45979	5.3127E-10
PE(18:3)	723.5203	3.80	C41H74NO7P	+	L2	Glycerophosphoethanolamines	0.63270385	1.07487	9.3628E-06
PE(20:4/P-18:1)	749.5360	3.79	C43H76NO7P	+	L2	Glycerophosphoethanolamines	0.48607988	1.11136	2.3149E-07
PE(36:1)	745.5625	3.91	C41H80NO8P	+	L2	Glycerophosphoethanolamines	0.69231424	1.31727	0.000011218
PE(38:1)	773.5939	3.89	C43H84NO8P	+	L2	Glycerophosphoethanolamines	0.63330661	1.07571	1.9111E-07
PG(34:1)	748.5251	3.63	C40H77O10P	-	L2	Glycerophosphoglycerols	0.41623836	1.29401	2.9728E-08
Phenylacetylglycine	193.0739	5.14	C10H11NO3	-	L2	Phenylalanine metabolism	0.37273956	1.99725	3.9975E-12
Phosphocreatine	211.0359	10.57	C4H10N3O5P	+	L2	Arginine and proline metabolism	0.32620395	4.07188	1.6795E-10
Phosphodimethylethanolamine	169.0504	9.74	C4H12NO4P	+	L2	Glycerophospholipid metabolism	0.46126726	1.18009	2.077E-07
PI(38:4)	886.5575	3.66	C47H83O13P	-	L2	Glycerophosphoinositols	0.56664614	1.08116	0.00002354
PS(36:1)	789.5520	3.66	C42H80NO10P	-	L2	Glycerophosphoserines	0.46408184	1.50578	7.5218E-08
Pyridine-2,3-dicarboxylate	167.0219	11.14	C7H5NO4	-	L2	Tryptophan metabolism, beta-Alanine metabolism, Nicotinate and nicotinamide metabolism	0.33138844	1.68063	3.3993E-14
Pyridoxine	169.0739	7.37	C8H11NO3	+	L1	Vitamin B6 metabolism	0.69920935	2.66022	4.4452E-09
SM(d18:1/24:1)	812.6769	3.93	C47H93N2O6P	+	L2	Ceramide phosphocholines (sphingomyelins)	0.53860791	1.15799	3.1836E-07
sn-glycero-3-Phosphocholine	257.1030	10.23	C8H20NO6P	+	L1	Glycerophospholipid metabolism, Ether lipid metabolism	0.43772236	30.6916	4.7421E-11
sn-glycero-3-Phosphoethanolamine	215.0559	11.04	C5H14NO6P	+	L2	Glycerophospholipid metabolism, Ether lipid metabolism	0.1911428	4.12868	1.3459E-14
sn-Glycerol 3-phosphate	172.0137	10.23	C3H9O6P	-	L2	Glycerolipid metabolism, Glycerophospholipid metabolism	0.23365578	3.74238	6.0652E-18
Taurine	125.0147	11.45	C2H7NO3S	+	L1	Bile acid biosynthesis, Taurine and hypotaurine metabolism	0.2758871	2.21015	1.8488E-12
UDP-N-acetyl-D-glucosamine	607.0811	10.49	C17H27N3O17P2	-	L2	Aminosugars metabolism, Lipopolysaccharide biosynthesis, Peptidoglycan biosynthesis	0.38838258	1.76054	1.2639E-08

Chapter Four

4. Treatment of macrophages with the secretomes of Gram-negative and -positive bacteria induces distinct metabolics signatures

4.1. Introduction

Infectious diseases represent major health and economic challenges worldwide and have constantly feature amongst the top 10 causes of death globally (236, 434). Emergence of multiple drug-resistant bacteria in the community and hospital has become a worldwide concern, as resistant bacterial infections are associated with longer hospitalisation and an increase in death rate (435). Therefore, there is an urgent need for innovative and more efficient diagnostic and treatment approaches (436).

Staphylococcus aureus, an archetypal Gram-positive bacterium, represents a major human pathogen. It is an opportunistic bacteria normally colonising the skin and the respiratory tract causing a wide range of infectious diseases (242, 243). On the other hand, *Pseudomonas aeruginosa* is an opportunistic Gram-negative bacterium that can cause a serious infection in individuals with compromised immune defence system, for example in case of cystic fibrosis, severe burns or neutropenia (240, 256). Both *S. aureus* and *P. aeruginosa* are members of the ESKAPE pathogen group (*Enterococcus faecium, S. aureus, Klebsiella pneumoniae, Acinetobacter baumannii, P. aeruginosa, and Enterobacter* species) (241). They are leading causes of many serious diseases such as bacteraemia, skin and soft tissue infections, urinary tract infections and respiratory tract infections (239, 240). Unfortunately, uncontrolled use of antibiotics has led to the appearance of many strains of bacteria resistant to existing antibiotics (256). Given the severity of the infections caused by these two types bacteria and the antibiotic resistance they display, there is a substantial interest in understanding their pathobiology. Different studies have shown that the pathogenicity of bacteria is multifactorial

and caused by various virulence factors such as toxins, enzymes, adhesins, as well as the production of secondary metabolites (241, 246, 256).

A wide range of virulence factors enables the bacteria to avoid the immune system. Nevertheless, the immune system is able to recognise different features of pathogens by specific surface receptors called pathogen recognition receptors (PRRs). Notably, Toll-like receptors (TLRs), a transmembrane protein family, plays a crucial role in triggering immune responses against bacteria (437). Once the pathogen associated molecular patterns (PAMPs) are detected by TLRs, the latter induces the expression of co-stimulatory cell surface proteins and pro-inflammatory cytokines which initiate a cascade of anti-bacterial immune responses (438). Macrophages are effector immune cells that play a critical role in innate and adaptive immunity (105) and are characterised by expression of a wide range of PRRs, most popularly, TLRs (116, 439).

In vitro studies have identified distinct ligands for different TLRs. For instance, lipopolysaccharide (LPS), a component of the outer membrane of Gram-negative bacteria, is recognized by TLR4, whereas lipoteichoic acid (LTA) and peptidoglycan (PG) from the Gram-positive bacterial cell wall are recognized by TLR2 (266, 267). Hoshino et al have demonstrated the LPS hypo-response of macrophages and B cells from TLR4-deficient mice (267). In contrast, there has been doubt in the function of TLR2 as PG receptor since TLR2 was intensively studied using commercial Staphylococcus aureus PG preparations which could be contaminated by other cell wall components (440). In this context, Travassos et al have shown that the TLR2-PG mediated activity can in fact attributed to the presence of LTA in the cell wall of Gram-positive bacteria (438). *In vivo*, TLR2 and TLR4 represent

receptors for different bacterial cell wall components, where TLR2 recognises Gram-positive bacteria and TLR4 recognises Gram-negative bacteria (266). Given that Gram-negative and Gram-positive bacteria engage with a different set of TLRs that are linked to different signalling pathways, it is not surprising that different bacterial infections have distinct immunological profiles, but less is known about metabolic responses of immune cells to different types of a bacterial infection.

The emergence of antibiotic-resistant bacteria in the hospital and community urges the development of innovate approaches for diagnosis and treatment (435, 436, 441). Currently, culturing microorganisms from blood or other body fluids is the most commonly used for bacterial infection diagnosis. Molecular tests have been increasingly used in clinical laboratories, but not as a part of routine practice due to the high cost. However, non-molecular diagnostic tests, while cheaper, are time-consuming and have low accuracy which could provide erroneous information, especially in patients with immunodeficiency (258). Most crucially, these routine clinical tests are not sensitive enough, so at least 50% of cases of bacterial infections are undetected. These drawbacks of routine tests have led to an increased effort to identify disease-specific biomarkers or physiological signature that can be used in the prediction of the nature and the severity of bacterial infections. Such biomarkers can potentially lead to early diagnosis and selection of the optimal treatment at an early stage, hence improving health outcome (442). For instance, Wunderink et al demonstrated that procalcitonin, pro-inflammatory cytokine and peptide hormones are mainly produced in response to bacterial infections and considered to be a diagnostic biomarker to differentiate between viral and bacterial infections (443). However, relying on a

single biomarker does not always provide enough information because the metabolite can be an intermediate in more than one metabolic pathway. Moreover, the most challenging mission is to differentiate between infectious diseases caused by different strains of bacteria (444). Therefore, novel approaches are needed to improve the microbiological readout. In this context, in the last few years the research has moved from focusing on a single biomarker to a biosignature encompassing a set of reliable biomarkers (259) using different approaches, such as transcriptomics (445), proteomics (446) and metabolomics (447). Metabolomics permits tracking of signalling molecules and their relevant metabolic pathways in response to different perturbations including a bacterial attack or encountering other dangers (306). Hence metabolomics has already been applied in several infectious disease studies (87, 448-453). LC-MS based metabolomics has been used widely for disease diagnostic biomarker discovery due to its sensitivity and powerful quantification ability of low molecular metabolites in the biological samples (306, 454). Furthermore, it is an integral part in quantitative analysis in the clinical laboratory (455). Given the recent massive progression in data analysis capabilities accompanied by multivariate analysis techniques such as principle component analysis (PCA), orthogonal partial least squares-discriminant analysis (OPLS-DA) and univariate analysis, LC-MS metabolomics can routinely produce high quality, reliable results (456), leading to a better understanding and assessment of the biological condition (457).

To fill the gap of knowledge in diagnosis and treatment of bacterial infections, LC-MS-based metabolic profiling could represent a promising approach with its relative efficiency in the discovery of biomarkers (454). Together with, the crucial

pro-inflammatory role of macrophages infighting bacterial infections (88, 310). Metabolomics may have a dual benefit in the study of bacterial infections: (i) in a diagnostic role by revealing potential biomarkers and (ii) by increasing the chance for novel therapeutics by targeting relevant pathways.

LC-MS metabolomics has been successfully employed in bacterial infection studies by discovering the biomarkers and the changes in the metabolic pathways upon infection (87, 448-450). For example, Müller et al have applied non-targeted metabolomics to determine the metabolic alterations in HEP-2 cell in response to *Chlamydia pneumoniae* infection. This study showed significant alterations in amino acid, carbohydrate and lipid metabolism upon infection which could be potential biomarkers for diagnosis and drug targeting (448). In another metabolomics study, Antunes et al investigated the impact of *Salmonella* on the murine immunological response, revealing many metabolites significantly changed in response to *Salmonella* infection. In Particular, hormone pathways were shown to be most disrupted (458).

In this study, we performed LC-MS metabolic profiling to differentiate between the impact of the secretome (bacterial cell culture medium) from the Gram-positive *S. aureus* SH1000 and Gram-negative *P. aeruginosa* PAO1 bacterial pathogens on THP-1 macrophages. Moreover, in order to assess whether differences in the potential virulence of the bacterial strains used could alter THP-1 responses, metabolic profiles of macrophages exposed to the secretome of *P. aeruginosa* PAO1 Wild-Type (WT) and the *rsmAN* mutant PALT13 (459) were studied. RsmA and RsmN repress the translation of *P. aeruginosa* genes required for the establishment of chronic infections, including those encoding for type VI

secretion systems and exopolysaccharide biosynthesis (460-462). In addition, RsmA/N positively impact on acute infection-related phenotypes including motility, type II and III secretion systems, type IV pili, and secreted exoproteases and exotoxins (463-465). Therefore, the PALT13 strain, contrary to the WT, is impaired in acute infection-related phenotype and would cause chronic (usually biofilm-centered) infections.

This metabolomics approach was used to compare the impact of *P. aeruginosa* PAO1 and mutant *P. aeruginosa* (PALT13), revealing whether they display distinct impacts on the metabolic profiles of macrophages. This could offer a novel diagnostic approach and pave the way for new treatment of bacterial infections.

4.2. Materials and methods

4.2.1.Materials

THP-1 cell line was purchased from ATCC, USA. RPMI-1640 medium foetal bovine serum (FBS), phosphate buffered saline (PBS), 2 mM L-glutamine, 100 U/ml penicillin, 100 µg/ml streptomycin and tryptic soy broth (TSB) were purchased from Sigma-Aldrich, UK. 0.2 µm sterilised filters were purchased from Sartorius, UK. Methanol and acetonitrile were purchased from Fisher Scientific, UK. All solvents were LC-MS grade.

4.2.2. Methods

4.2.2.1. Cell culture and differentiation

Human THP-1 cells were cultured and differentiated as previously described in (159). Briefly, THP-1 cells were grown in T75 tissue culture flasks using RPMI 1640

supplemented with 10% heat-inactivated fetal bovine serum (FBS), 1% L-glutamine, and 1% penicillin-streptomycin. Cells were then incubated at 37 °C and 5% CO_2. THP-1 cells were differentiated into naïve macrophages state (M0) by treating with phorbol-12-myristate-13-acetate (PMA). Six million cells were seeded per flask (T25 tissue culture flask), and then the cells were treated with six ml of PMA-containing media with a final concentration of 50 ng/ml of PMA and incubated for 24 h.

4.2.2.2. Bacterial culture and cell treatment with bacterial secretome.

P. aeruginosa PAO1, *P. aeruginosa* PALT13 and *S. aureus* SH1000 in tryptic soy broth (TSB) were grown in 50 mL of culture media in 250 mL conical flasks with shaking (200 rpm) at 37°C. After 18 h of incubation, spent culture media were centrifuged, and supernatants were recovered and filter sterilised. 10% (600 µl) of spent culture media for each bacteria (*S. aureus* SH1000, WT *P. aeruginosa* PAO1 and *rsmAN* mutant *P. aeruginosa* PALT13),) were used to treat macrophages with incubation for 24 h. (henceforth referred to as S-S-M, P-S-M and Mut.P-S-M, respectively). This protocol was discussed and recommended by Shen-An Hwang (Department of Immunology, Myriad RBM institution, USA). Untreated M0 was set as a control. Six biological replicates of each condition were prepared.

4.2.2.3. Sample preparation and metabolite extraction

After incubated for 24 h, the media were removed. The cells were then washed once with pre-warmed PBS (37 °C) and 500 µl pre-cooled methanol at -48 °C was used for metabolism quenching and metabolite extraction. The cells were harvested using a plastic scraper whilst being kept on ice and the extracts were

transferred into pre-cooled fresh tubes (4 °C). The cell extracts were vortexed for 1 h at 4 °C and centrifuged at 16,100 ×g for 10 min at 4 °C. After the centrifugation, the supernatants were dried under vacuum and reconstituted with 70 µl methanol, and then stored at -80 °C prior to LC-MS analysis. To assess the instrument performance, a quality control (QC) sample was prepared by mixing an equal volume of all the samples.

4.2.2.4. Analytical methodologies

LC-MS-based metabolite profiling was performed on an Accela system coupled to an Exactive MS (Thermo Fisher Scientific, Hemel Hempstead, UK) operating with electrospray ionisation (ESI) running in the negative (ESI-) and positive (ESI+) modes as previously described in (314). Briefly, the spray voltage was 4500 V (ESI+) and 3500 V (ESI-), the capillary voltage was 40 V (ESI+) and 30 V (ESI-), and tube lens voltage was 70 V for both modes and skimmer voltage was 20 V (ESI+) and 18 V (ESI-). The temperature for capillary and probe was maintained at 275 °C and 150 °C, respectively. Chromatographic separation was carried out using ZIC-pHILIC (4.6 x 150 mm and 5 µm particle size, Merck Sequant). The mobile phase composed of 20 mM ammonium carbonate in water (solvent A) and 100% acetonitrile (solvent B). Metabolites were separated according to a linear gradient as following: 0-15 min (20% A), 15-17 min (95% A), and 17-24 min (20% A) at 300 µl/min flow rate. The injection volume was 10 µl and the column was kept at 45 ^{o}C.

4.2.2.4. Data processing and metabolites identification

To process raw data obtained from LC-MS, XCMS and mzMatch were used for untargeted peak-picking and peak matching, respectively (69, 70). IDEOM was performed for putative metabolite identification and noise filtering with default parameters (315). Briefly, RT for identification of authentic standards was 5%, RT for identification for calculated RT was 50%, ppm for mass identification was 3 ppm. Metabolites were identified with two levels of confidence; level 1 (L1) identification by matching retention times and accurate masses of authentic standards and level 2 (L2) identification when the predicted retention times were employed due to the lack of standards according to the metabolomics standards initiative (75, 405).

Pre-processed data were analysed by performing multivariate and univariate analysis. OPLS-DA was carried out by SIMCA-P v13.0.2 (Umetrics, Umea, Sweden) as a supervised multivariate model. This multivariate analysis was used as the first step for visualising data with sample classes and evaluating the metabolome differences between M0 and *P. aeruginosa or S. aureus,* and between *P. aeruginosa* and mutant *P. aeruginosa*. The key mass ions representing potential biomarkers were determined based on VIP values obtained from two-way orthogonal comparisons. Mass ions with VIP values greater than one were considered as discriminant biomarkers. Univariate analysis was also performed in parallel to multivariate analysis to identify significant mass ions. T-test with FDR correction was performed using Metaboanalyst (24) to determine the significantly changed mass ions between M0 and S-S-M or P-S-M and between P-S-M and

Mut.P-S-M. MetaboAnalayst and KEGG database were used to analyse and visualise the affected pathway.

4.3. Results and discussion

4.3.1. Metabolic profiling of macrophages treated with the bacterial sectretome (bacterial cell culture medium).

In order to explore the impact of the secretomes of *S. aureus, P. aeruginosa* and mutant *P .aeruginosa* on the metabolic profiles of macrophages, the extracted intracellular metabolites from M0 cells (control) and M0 treated cells (S-S-M, P-S-M and Mut.P-S-M) were analysed using LC-MS-based technique. A total of 503 metabolites were identified putatively by IDEOM (Appendix, Table A5). Figure 4.1 shows the chemical composition of macrophages upon the exposure of the bacterial secretomes (S-S-M, P-S-M and Mut.P-S-M) with the biological classifications of the identified metabolites. The metabolome was mainly composed of amino acids (18%) and glycerophoshpolipids (15%) followed by fatty acyls (9%), carbohydrates (6%), other lipids (4%), nucleotides (4%), co-factors and vitamins (3%), sphingolipids (2%), and energy metabolites (1%).

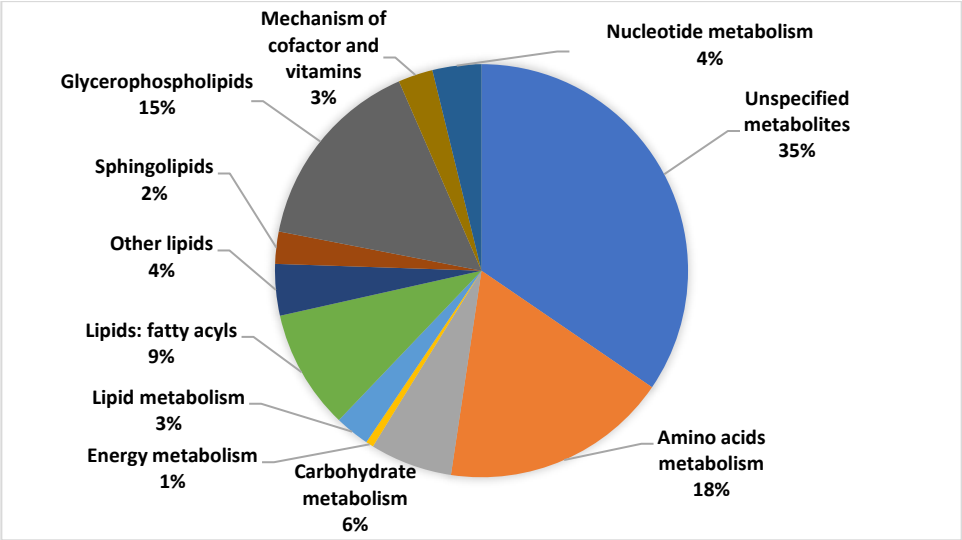


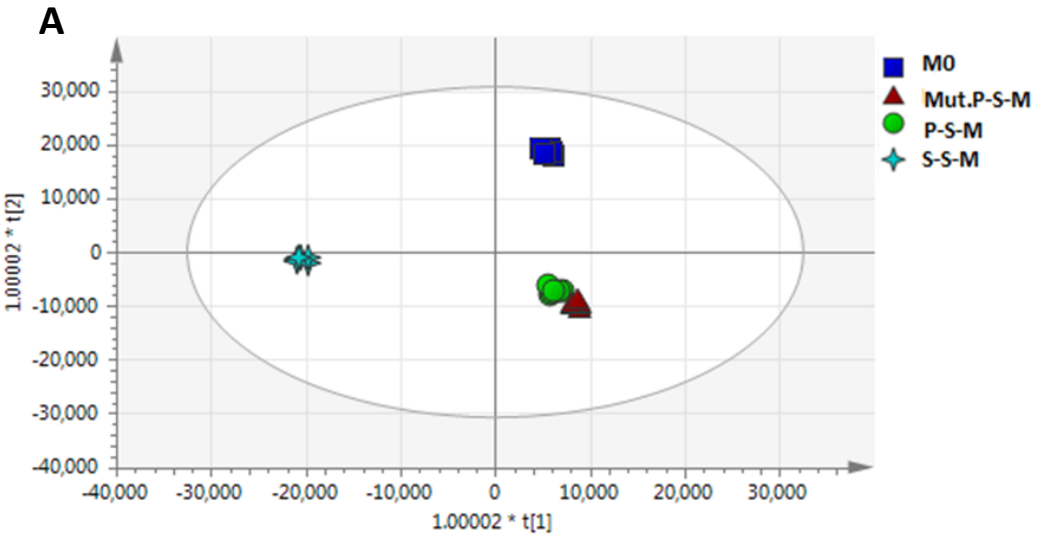
Figure 4.1: Functional categories of the intracellular metabolites produced by macrophages, treated (S-S-M, P-S-M and Mut.P-S-M) and un-treated.

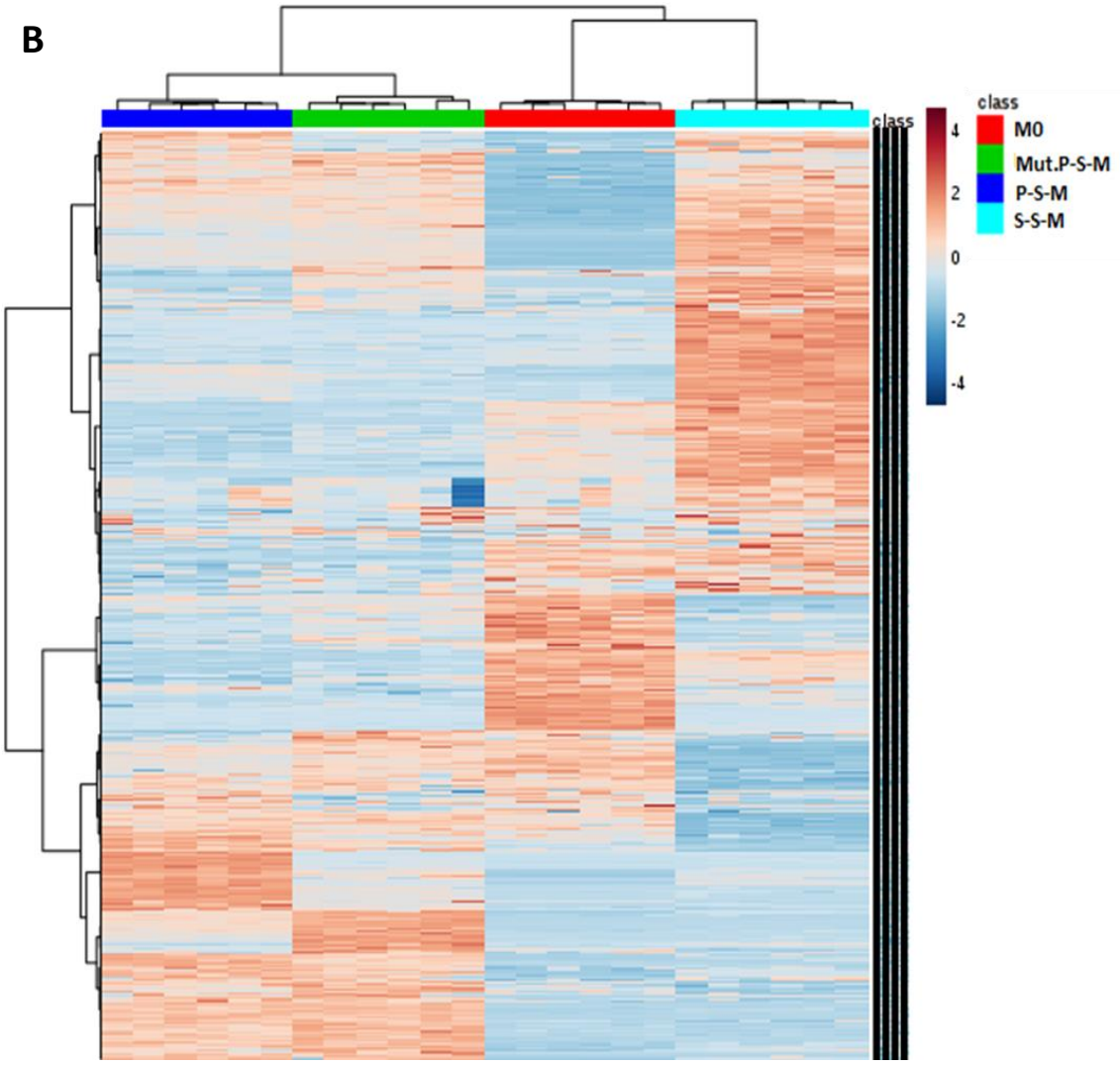
4.3.2. Multivariate analysis

In order to investigate and visualise the inherent metabolic difference between the macrophages challenged with the secretomes (S-S-M, P-S-M and Mut.P-S-M) a supervised OPLS-DA was performed for the comparison with the untreated macrophages as a control (M0). In Figure 4.2A, the OPLS-DA scores plot shows a tight clustering of six replicates within each group indicating the LC-MS analysis was reproducible. Also, a clear separation is shown between M0 and S-S-M, P-S-M or Mut.P-S-M with R^2 and Q^2 values of 0.87 and 0.988, respectively. This result shows two important points: firstly, that there is a change in the metabolic profiles of macrophages upon the exposure of the bacterial secretome, secondly, that there is a clear separation between S-S-M and P-S-M or Mut.P-S-M indicating that macrophages behave differently in response to sectretome exposure with a different type of bacteria, i.e. with the Gram-positive bacteria secretome (*S. aureus* secretome) or Gram-negative bacteria (*P. aeruginosa* PAO1 and *P.*

aeruginosa PALT13 secretomes). Interestingly, macrophages exposed to the spent culture media of *P. aeruginosa* and mutant *P. aeruginosa* are clustered closely (Figure 4.2A). This trend can be seen clearly in the heat map. Also, clustering and similar change patterns of many metabolites can be seen (Figure 4.2B). To investigate which features contributed to the separation between groups, two-way comparisons of OPLS-DA were performed as shown in Figure 4.2C and D. The faetures were ranked according to their VIP values to determine the most discriminative where the features with VIP > 1 were considered as potential biomarkers. Multivariate analysis was accompanied by t-test with FDR correction. Most significantly changed features with VIP > 1 and FDR < 0.05 were selected as potential characteristic metabolites.

As can be seen in Figure 4.2C, the OPLS-DA scores plot shows a clear separation between M0 and S-S-M with R^2 and Q^2 values of 0.664 and 0.899, respectively, demonstrating an acceptable and valid model (324). Based on the combination of multivariate and univariate analyses, 83 metabolites (VIP > 1 and FDR < 0.05) were identified as key metabolites (Table 4.1). Similarly, Figure 4.3D shows a OPLS-DA scores plot with a clear separation of M0 and P-S-M with R^2 and Q^2 values of 0.842 and 0.998, respectively (i.e. a strong model). 75 metabolites have met the two criteria (VIP > 1 and FDR < 0.05) for selection as significantly changing metabolites upon the exposure of the sectretome from *P. aeruginosa* (Table 4.2).


A
M0
Mut.P-S-M
P-S-M
S-S-M
30,000
20,000
10,000
0
-10,000
-20,000
-30,000
-40,000
1.00002 * t[2]
-40,000
-30,000
-20,000
-10,000
0
10,000
20,000
30,000
1.00002 * t[1]


B
class
class
M0
Mut.P-S-M
P-S-M
S-S-M
4
2
0
-2
-4

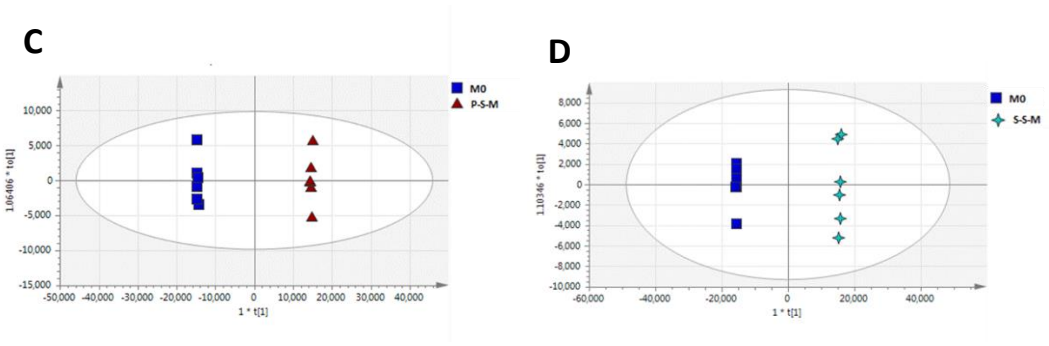


Figure 4.2: OPLS-DA scores plots and heatmap of macrophages extracts after treatment with the sectretomes of *S. aureus*, *P. aeruginosa*, Mut. *P. aeruginosa* and their corresponding untreated control (M0). (A) OPLS-DA scores plot of S-S-M, P-S-M and Mut.P-S-Mand M0 (R2 = 0.870 and Q2 = 0.988). (B) Heatmap of S-S-M, P-S-M and Mut.P-S-Mand M0 with clear clustering between the groups. (C) Two-way orthogonal comparison between P-S-M and untreated M0 (R2 = 0.838 and Q2 = 0.999). (D) Two-way orthogonal comparison between S-S-M and untreated M0 (R2 = 0.842 and Q2 = 0.998). M0 (dark blue squares), P-S-M (red triangles), S. aureus (light blue stars) and Mut.P-S-M (green circles). n=6.

4.3.3. Pathway analysis

To further identify the metabolic pathways that were significantly altered upon the exposure of the bacterial secretomes, a comprehensive pathway analysis was generated using MetaboAnalyst, as illustrated in Figure 4.3A and B. These data show that the significant number of altered metabolites caused by exposure to the bacterial sectretome exposure are relevant to amino acid metabolism as can be clearly seen in Figure 4.3. Amino acid metabolism is very important for the host cells to enhance the immune defense against pathogens. L-tryptophan, L-arginine and L-asparagine are the main amino acids which the pathogen competes with the host cells for (466). Disturbance of amino acid pathways has been noticed as a cell adaptation in bacterial infections. Therefore, targeting these pathways in the host has recently been highlighted as a novel approach to manipulate bacterial infections (467).

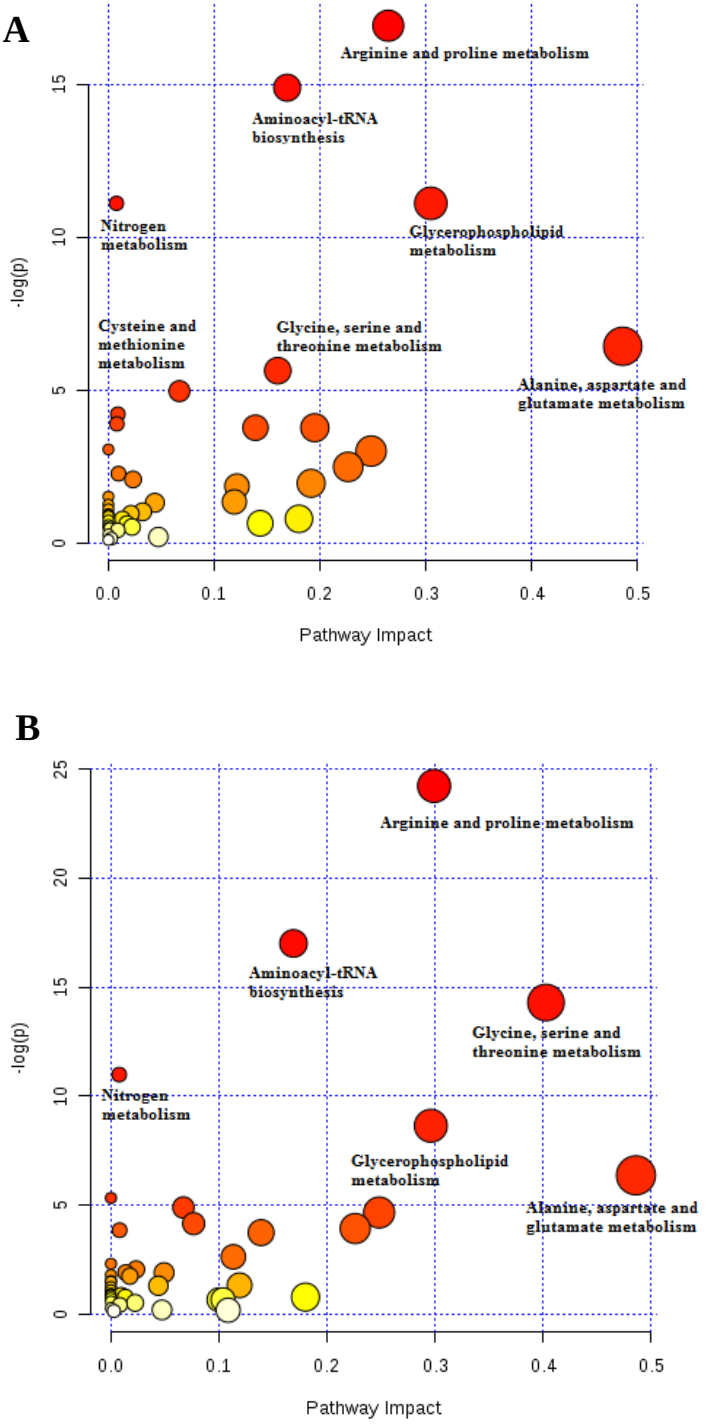


Figure 4.3: A summary of pathway analysis by MetaboAnalyst. The top pathways were ranked by the gamma-adjusted p-values for permutation per pathway (Y-axis) and the total number of hits per pathway (X-axis). The colour graduated from white to yellow, orange and red as the values of both x and y increase, red circles the most significantly changed metabolic pathway, and the pale yellowish are the least significantly changed metabolites. (A) Metabolic pathways significantly changed in *P. aeruginosa* sectretome treated macrophages. (B) Metabolic pathways significantly changed in *S. aureus* sectretome treated macrophages.

The arginine and proline metabolism pathway in Figure 4.3A and B showed the most significant alteration in response to the exposure of the secretomes from *S. aureus* and *P. aeruginosa* infection. This could be due to the significant decrease in the level of L-1-pyrroline-3-hydroxy-5-carboxylate, creatinine, L-glutamate 5-semialdehyde, L-citrulline and phosphocreatine- which are intermediates in the arginine and proline metabolism- in both *S. aureus* and *P. aeruginosa* secretomes treated macrophages (Figure 4.4). L-Arginine is considered as a non-essential amino acid at the whole organism level, but it is important to be supplemented in certain diseases such as gastritis, ulcer, hypertension and cardiovascular diseases (468). It is produced from *de novo* arginine biosynthesis or cellular protein break-down (469). Metabolic flexibility and interconvertibility are well recognised for L-arginine since it can be interconverted with a range of other amino acids such as L-glutamate and L-proline. In addition, it is involved in the synthesis of metabolites such as creatine, phosphocreatine, polyamines, nitric oxide and urea cycle metabolites (470-472). Normally, L-arginine is a substrate of two main enzymes, arginase and inducible type 2 nitric oxide synthase. It can be metabolised by arginase to produce ornithine and urea or oxidised by iNOS to produce L-citrulline and nitric oxide (NO) (353). Therefore, the competition of arginase with the iNOS is well studied for its activity in decreasing the production of NO. In addition to this competition, arginase was reported to inhibit the expression of iNOS, again limiting the production of NO (472). NO is a pivotal element of the immune response and is one of the most important antimicrobial agent of the host's first line of defence (473). Pathogenic bacteria adapt several mechanisms targeting arginine to protect itself against the immune system of a

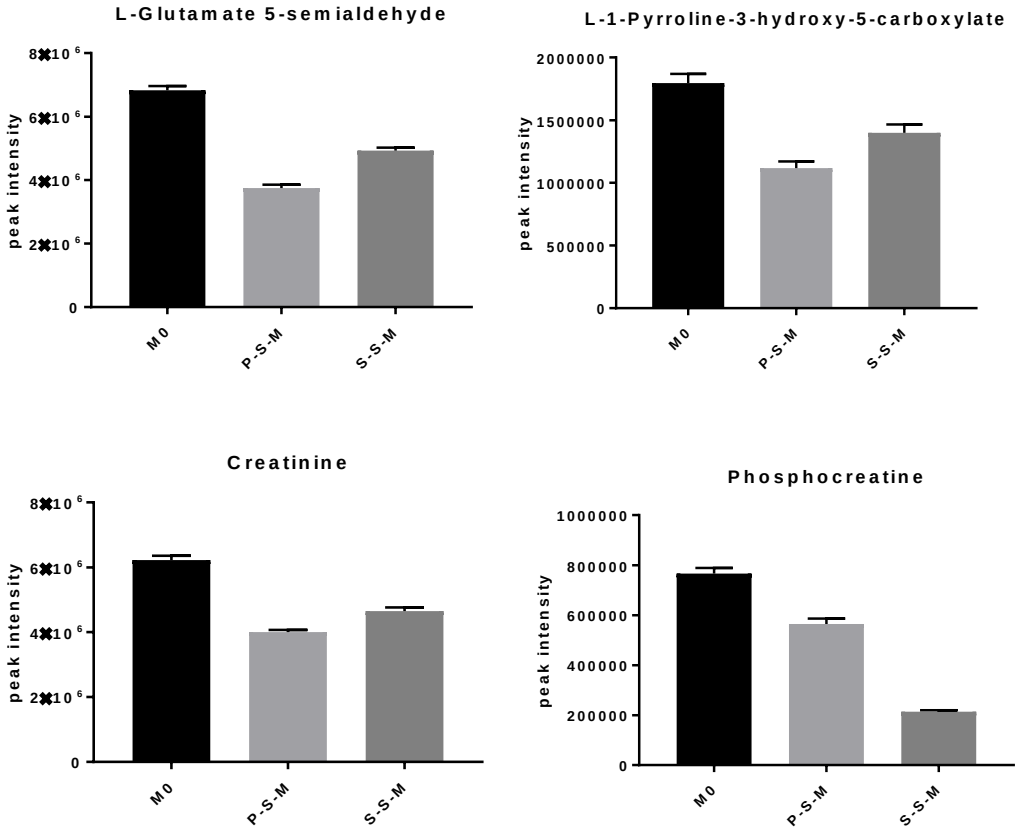
host cell. For instance, arginase diverts arginine away from iNOS to subvert an antimicrobial effect of macrophages (466). Moreover, pathogens upregulate the activity of arginase to decrease the availability of arginine as a substrate for iNOS (474, 475). The arginase produced by bacteria can also compete with iNOS in a similar manner to mammalian arginase to prevent NO production as a strategy of the bacteria to survive (476). The bacterial arginase was reported to be recruited to deplete L-arginine in macrophages (477). The depletion of L-arginine will consequently decrease the production of L-ornithine which is hydrolysed by ornithine aminotransferase followed by 1-pyrroline-5-carboxylate dehydrogenase to produce L-glutamate. Also, L-ornithine produces L-citrulline by ornithine carbamoyl transferase (471). Targeting the precursors such as L-arginine and L-ornithine by bacteria can explain the decrease in the level of intermediates such as L-citrulline, L-glutamate and other relevant metabolites (L-1-pyrroline-3-hydroxy-5-carboxylate, creatinine, L-glutamate 5-semialdehyde and phosphocreatine).

Glutathione is the most abundant low molecular weight thiol and it plays a crucial role in confronting the oxidative stress of the cells resulting from bacterial infection-induced ROS production (478, 479). The ratio of glutathione and glutathione disulphide (the oxidized form) represents the main redox balance in human cells (478). Our results showed that glutathione was significantly decreased whereas glutathione disulphide significantly increased in response to the exposure of the secretomes from *S. aureus* and *P. aeruginosa* (figure 4.4). This perturbation in the redox state indicates the oxidative stress condition of infected macrophages (480). Additionally, increase in the level of glutathione disulphide

was reported to increase the sensitivity to the oxidative stress (481). As aforementioned, one-carbon metabolism is appreciated for its role in maintaining redox balance. It contributes to the production of NADPH and glutathione as it provides a source of the methyl group required for the synthesis of glutathione and purines, and DNA methylation (482, 483). The production of glutathione from glycine occurs in all cell types (484). The significant decrease in glycine (Table 4.1 and 4.2) could explain the significant reduction of glutathione, indicating the redox imbalance and oxidative stress condition. A reduction in the availability of glycine was reported as a result of inflammation stimuli (485). Also, Fang et al suggested that glycine may become a limiting factor for the synthesis of glutathione (478). Another *in vivo* study showed that glycine availability was the limiting factor for glutathione production by erythrocyte in burned patients (486).

Glycine, serine, and threonine metabolism were amongst the most significantly altered amino acids upon the treatment with the secretomes from *S. aureus* and *P. aeruginosa* (Figure 4.3A and B). Glycine and serine are non-essential amino acids that are involved in the synthesis of nucleic acids, proteins and lipids as precursors for these processes (487). Serine is converted to glycine using the enzyme, serine hydroxymethyltransferase (424). This reaction plays a crucial role in the one-carbon pathway by supplying a methyl group required for the synthesis of proteins, glutathione and nucleotides. The one-carbon pathway has emerged as a key metabolic pathway in cell proliferation and immune functions. However, maintaining the redox balance and sustaining immune cell proliferation are crucial to confront oxidative stress or hypoxia that can be induced in the case of

bacterial infections (425, 426). In a recent study, Ma et al demonstrated that serine availability can serve as a checkpoint metabolite, indicating efficient immune response of primary T cells (427) which emphasises the pivotal role of this pathway in the immune response against challenging pathogens such as bacteria. Our data showed significant elevation of serine in S-S-M and P-S-M (Figure 4.4). Glycine can potentially enter the folate cycle by donating one carbon through the glycine cleavage process (488).



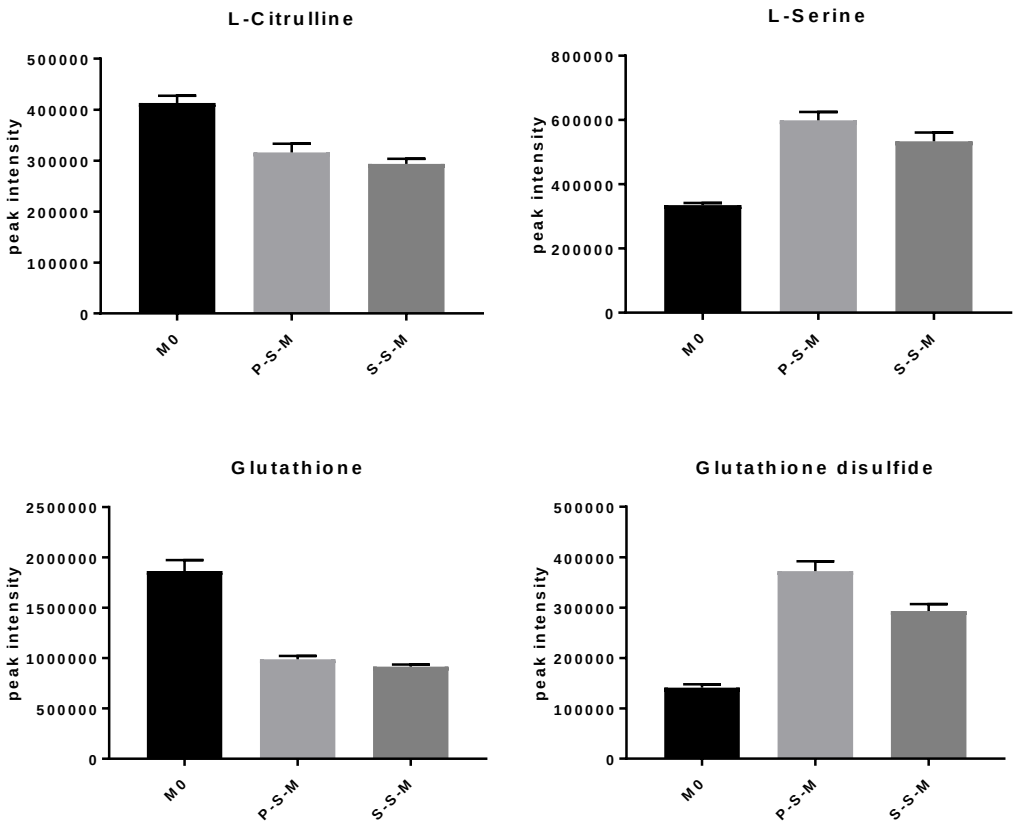


Figure 4.4: Significantly changed metabolites involved in amino acids metabolism in both P-S-M and S-S-M with the same trend (decrease or increase). L-1-Pyrroline-3-hydroxy-5-carboxylate, creatinine, L-glutamate 5-semialdehyde, L-citrulline and phosphocreatine represent arginine and proline metabolism. L-serine from glycine, serine and threonine metabolism. n=6, data are presented as mean ± SEM.

Interestingly, sarcosine, guanidinoacetate and creatine (Figure 4.5) were significantly and distinctly decreased in S-S-M, but not in P-S-M. Sarcosine is produced from glycine by the enzyme glycine N-methyltransferase [KEGG 2.1.1.20] or from creatine by the enzyme creatinase [KEGG 3.5.3.3]. Guanidinoacetate is also produced from glycine by the enzyme glycine amidinotransferase [KEGG 2.1.4.1], and then converted to creatine by the enzyme guanidinoacetate N-methyltransferase [KEGG 2.1.1.2]. A significant decrease in these three metabolites could be attributed to the implication of glycine in one-carbon metabolism by donating one carbon to the folate cycle producing more

purines and coordinating with glutathione and NADPH biosynthesis, thus maintaining redox balance (427). The crucial role of glycine and serine in maintaining redox balance was reported in cancer metabolism as well where the uptake of glycine and serine increased (483, 489, 490). However, insignificant changes in sarcosine and guanidinoacetate levels and a significant increase in creatine level were shown in P-S-M implying a differential impact of the secretomes of *S. aureus* or *P. aeruginosa* on macrophages. The difference in the metabolic responses of macrophages to the secretomes of *S. aureus* or *P. aeruginosa* can be applied in identifying more selective therapeutic targets in a certain pathway for each bacterial infection.

Another pathway that was altered significantly and differentially upon the bacterial secretome is alanine, aspartate, and glutamate metabolism (Figure 4.3A and B). O-Acetyl carnitine was significantly decreased in S-S-M but was increased in P-S-M (Figure 4.5). Conversely, asparagine was significantly increased in S-S-M but decreased in P-S-M (Figure 4.5). Asparagine is a major nitrogen source for the pathogens that infect the skin and human throat. It induces pathogen proliferation and expression of genes including those which are related to metabolism, virulence and growth (491). The different asparagine levels observed in response to the two secretomes may indicate distinct macrophage responses to each species and the different strategies that these bacteria use to survive.

Tryptophan metabolism showed a significant perturbation through a significant increase in tryptophan in both S-S-M and P-S-M. Interestingly, L-formylkynurenine showed a significant increase in S-S-M but not in P-S-M, while L-kynurenine showed a significant decrease in P-S-M but not in S-S-M (Figure 4.5*)*. Tryptophan

is an essential amino acid required for metabolic functions and protein synthesis. It cannot be produced in the body; therefore, it must be supplied in the form of proteins. In the last decades, more focus was directed on the role of tryptophan as an intermediate in the immune system, but its role still not fully understood. However, tryptophan metabolism and inflammatory responses are thought to be associated with several diseases and pathological conditions (347). Tryptophan is metabolised through L-kynurenine pathway by the enzyme indoleamine 2,3-dioxygenase (IDO) that is present in macrophages and dendritic cells. IDO is induced under the immune activation condition. IDO breaks L-tryptophan to produce L-formylkynurenine which is consequently metabolised by the enzyme kynurenine formamidase to produce L-kynurenine which is considered as an inflammatory marker (492). The increase in the level of L-formylkynurenine in S-S-M could be attributed to the stimulation and activation of macrophages. Unexpectedly, though, L-kynurenine showed no increase in response to the *S. aureus* secretome and a significant decrease in response to the *P. aeruginosa* secretome, suggesting that such effect is due to tolerance and local immunosuppression associated with an enhanced IDO activity which may indicate a stronger impact of on this pathway (493). Figure 4.6 represents a schematic pathway analysis of most amino acids related metabolites which were significantly changed in response to the treatment of the secretomes from *P. aeruginosa* and *S. aureus* in macrophages.

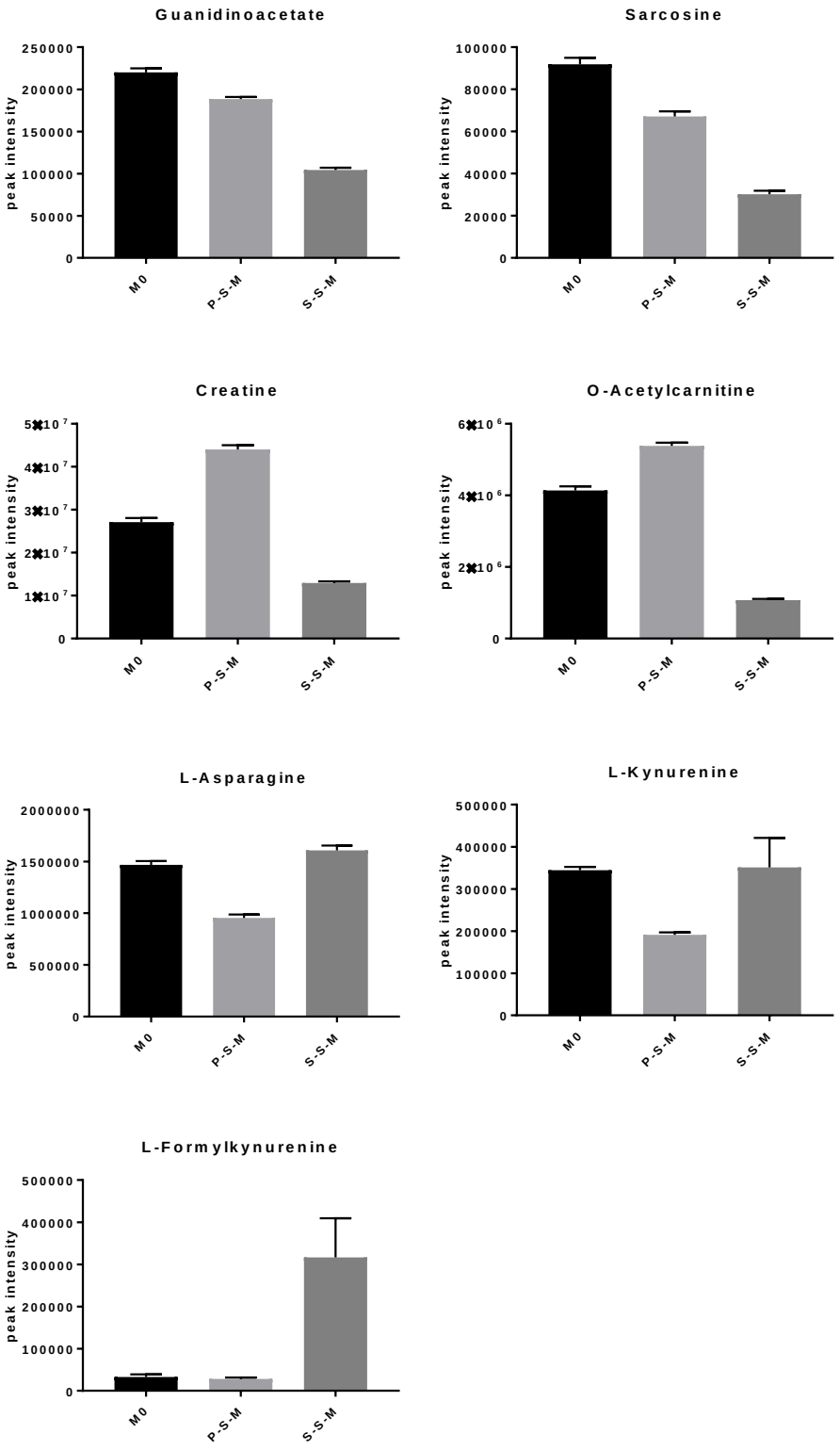


Figure 4.5: Amino acids relevant differentially and significantly changed metabolites in P-S-M and S-S-M. Sarcosine, guanidinoacetate and creatine represent Glycine, serine and threonine metabolism. O-acetylcarnitine, and L-asparagine represent alanine and aspartate metabolism, L-kynurenine and L-formylkynurenine represent tryptophan metabolism. n=6, data are presented as mean ± SEM.

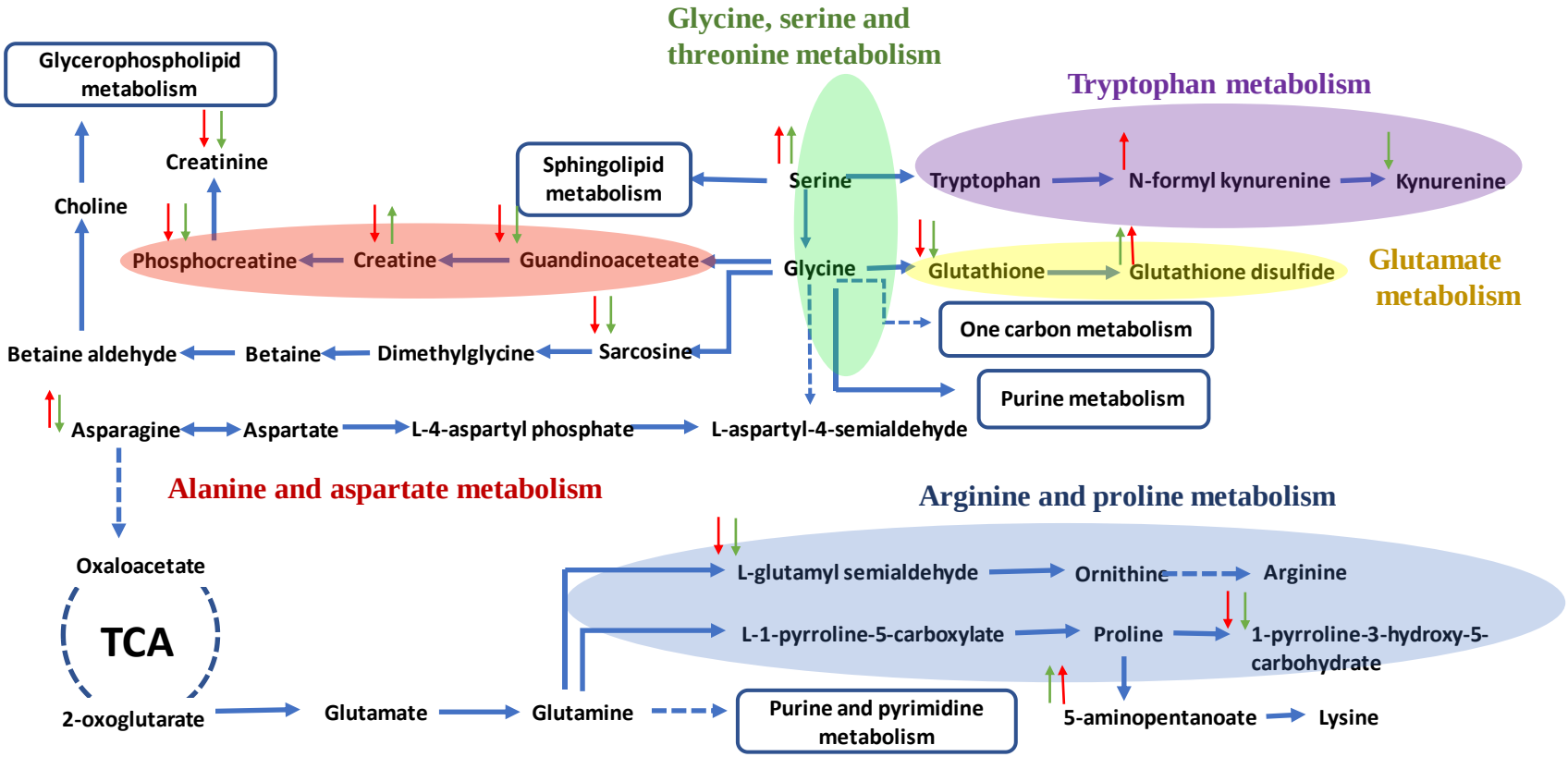


Figure 4.6: Schematic pathway analysis shows the significant altered metabolites in their relevant pathways.

Lipid metabolism appeared to be significantly altered in our results (Table 3.1 and 3.2). Generally, lipids constitute the main component of the cellular membranes. Furthermore, they are used as an energy source, in addition to its role in inflammation and infection as signalling molecules (494, 495). Excessive lipid remodelling during bacterial infections in macrophages has been increasingly reported. Moreover, each pathogen has its own strategy in manipulating the host metabolism, and infection outcome and disease susceptibility are extensively affected by the modulation of lipid metabolism in the host (496). The present results showed that some fatty acyls were significantly increased in S-S-M (Table 4.1), whereas no changes in these lipids were shown in P-S-M. Fatty acids can be produced in macrophages by *de novo* synthesis or taken up by the macrophages through the lipolysis of triglyceride-rich lipoproteins (497). Saka et al have demonstrated that several pathogens trigger the formation of lipid droplets in immune cells (498). These lipid droplets, in turn, produce other mediator lipids such as eicosanoids. This elaborates the significant increase in the levels of the eicosanoids such as [FA (24:6)] in S-S-M but not P-S-M (Figure 4.7). Many eicosanoids have been found to be increased by various bacterial infections, playing a key role as mediators in orchestration of immune responses (499).

Sphingolipids were also showed significantly altered in macrophages upon the exposure of the secretomes from *S. aureus* and *P. aeruginosa* (329). Recently, the functions of sphingolipids have been investigated in term of different aspects including their role in inflammation (330), signalling pathways and metabolism (331). The key metabolite in sphingolipids metabolism is ceramide, which is generated either through by hydrolysis of sphingomyelin or in a *de novo* pathway

at the endoplasmic reticulum (ER) (332). Ceramide (d18:1/24:0), Ceramide (d18:1/16:0) and Ceramide (d18:2/16:0), showed an increase in response to the treatment with both S-S-M and P-S-M with a substantially greater increase in S-S-M (Figure 4.7). These ceramides showed a high increase with fold changes of 44.82, 33.11 and 26.44, respectively. However, these ceramides showed an insignificant increase in the case of P-S-M. The ceramide-rich cellular membrane is important for bacterial infections response with important roles in apoptosis, phagosome trafficking, cell-cell interaction, phagocytosis, and macrophage maturation (500-503). Esen et al have demonstrated the crucial role of ceramides in *S. aureus*-induced apoptosis. *S. aureus* induces activation of the acid sphingomyelinase, which releases ceramides triggering the reorganisation of a sphingolipid-rich raft, leading to apoptosis. This study has indicated the possibility of preventing *S. aureus*-induced apoptosis by targeting acid sphingomyelinase (501). Also, Grassmé et al have reported similar results showing the role of *P. aeruginosa* in the activation of acid sphingomyelinase and release of ceramides in a sphingolipid-rich raft, leading to apoptosis (502). However, the behaviour of different ceramides in response to different pathogens is still not well understood (504). In agreement with our results, Lau et al have shown that Ceramide (d18:1/16:0) increased significantly in plasma samples of tuberculosis and community-acquired pneumonia patients, with a higher fold change in tuberculosis patients, suggesting a robust immune response in this case (504).

Glycerophospholipid metabolism as shown in Figure 4.3A and B was significantly perturbed in both S-S-M and P-S-M. Glycerophospholipids constitute the main components of the cell membrane bilayer (325). Several glycerophospholipid

subclasses have been identified as phosphatidylcholines (PC), phosphatidylethanolamines (PE), phosphatidylserines (PS), phosphatidylinositols (PI) and phosphatidylglycerols (PG) (326). Generally, lipid metabolism contributes to the pro- or anti-inflammatory functions of macrophages by meeting energetic requirements and modulating membrane fluidity (327). However, GLs are also involved in multiple biological processes, such as inflammation and cell differentiation (328). For instance, PEs increases upon bacterial infections. LysoPE (0:0/22:5), LysoPE (0:0/20:5) and PE (18:1) (Figure 4.7) showed a significant increase in P-S-M but to less extents and insignificantly increased in S-S-M. However, PE (18:1/20:4) was significantly increased in S-S-M but not in P-S-M (Figure 4.7). It has been reported that PE and PC were increased during the macrophage differentiation (505). In general, a versatile alteration has been observed of GLs upon treating macrophages with the secretome of *S. aureus* or *P. aeruginosa*. The exact lipid mediators to control bacterial infections still need to be identified. Alteration in glycerophospholipid metabolism upon infection has been evident in both pathogen and host, which make the understanding of metabolic interaction between host and pathogen more complicated (496).

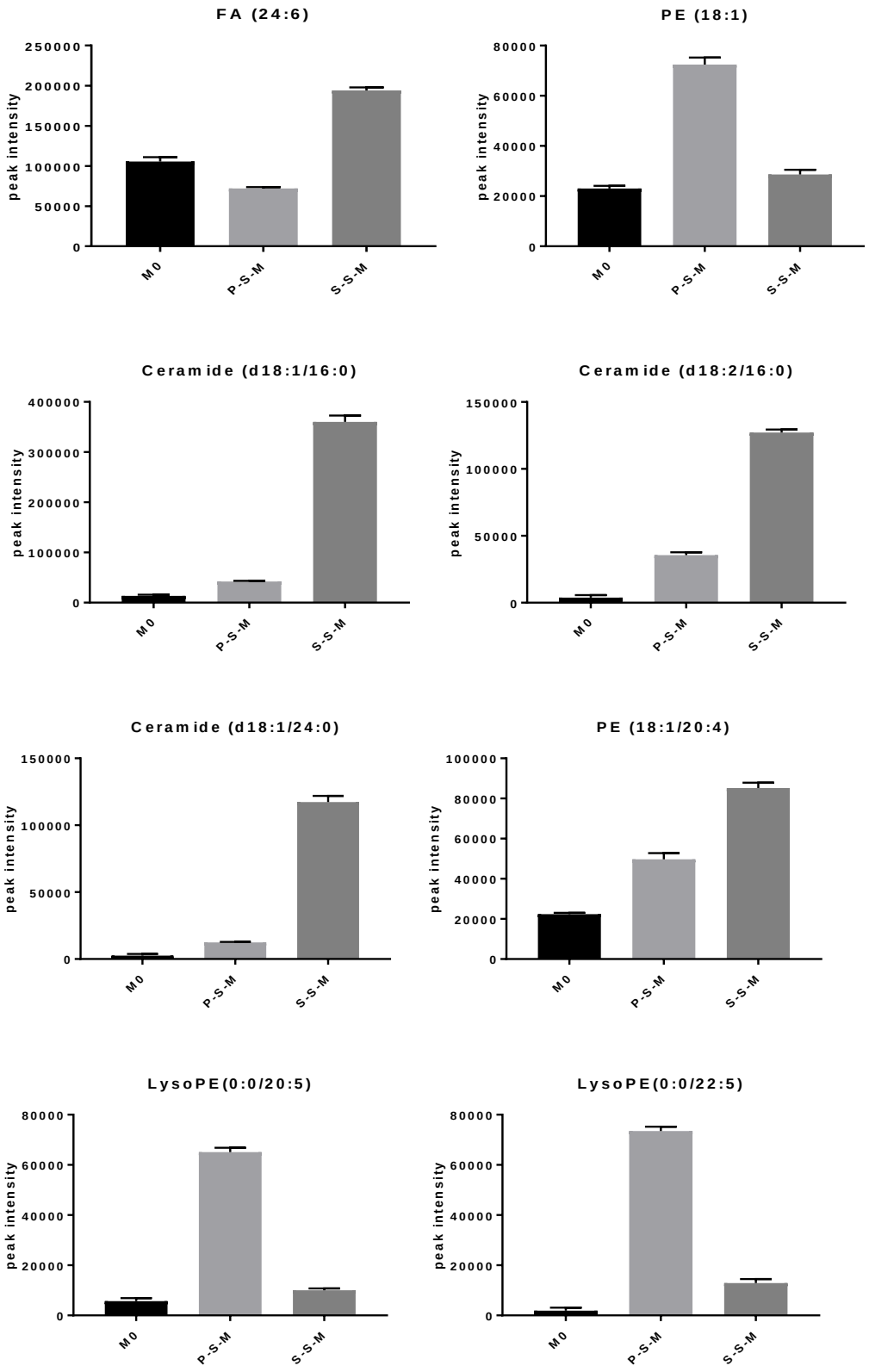


Figure 4.7: Differentially and significantly changed metabolites in S-S-M and P-S-M. FA(24:6) of fatty acyls. Ceramide (d18:1/16:0), Ceramide (d18:1/24:0) and Ceramide (d18:2/16:0) represent sphingolipid metabolism. LysoPE (0:0/22:5), LysoPE (0:0/20:5), PE (18:1) PE (18:1/20:4) represent GLs metabolism. n=6, data are presented as mean ± SEM.

4.3.4. *P. aeruginosa* compared to mutant *P. aeruginosa* (PALT13)

Regarding the macrophage responses to P-S-M or Mut.P-S-M, and given the small separation between these two groups in the OPLS-DA scores plot (Figure 4.2A), similar metabolic profiles for P-S-M and Mut.P-S-M was suggested. The two-way OPLS-DA scores plot in Figure 4.8 shows a separation between the two groups with R^2 and Q^2 values of 0.55 and 0.997, respectively. 28 metabolites were revealed as significantly changed metabolites (Table 4.3). However, only four of them showed a fold change >1.5 between P-S-M and Mut.P-S-M (Figure 4.9).

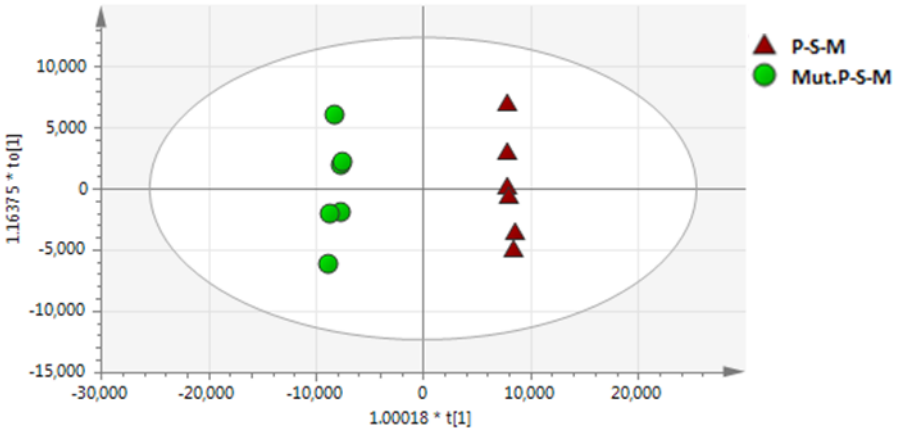


Figure 4.8: Two-way OPLS-DA comparison between P-S-M and Mut.P-S-M. (R2 = 0.551 and Q2 = 0.983). P-S-M (red triangles), and Mut.P-S-M (green circles). n=6.

Picolinic acid, N-acetyl-L-glutamate 5-semialdehyde, 5-guanidino-2-oxopentanoate, and 5-aminopentanoate were increased significantly in the Mut.P-S-M (Figure 4.9). Picolinic acid is a tryptophan catabolite and mounting evidence have demonstrated the association between L-tryptophan metabolism and anti-microbial activity of macrophages (506). It is produced as a result of consecutive reactions of L-tryptophan breakdown ending with 2-amino-3-carboxymuconic semialdehyde that produces picolinic acid by the enzyme, 2-amino-3-carboxymuconic semialdehyde decarboxylase (507). Picolinic acid has been extensively studied as a biologically active agent in macrophages due to its crucial immunological functions such as the activation of murine macrophages effector properties (507). Blasi et al have demonstrated the microbicidal activity of picolinic acid by showing that intracerebral administration protected mice against a lethal challenge with *Candida albicans*, an opportunistic pathogen (508). Also, picolinic acid has been reported as a co-stimulator with IFN-γ in triggering the expression of an inducible nitric oxide synthase, which is responsible for producing NO against bacterial invasion (509). N-Acetyl-L-glutamate 5-semialdehyde and 5-guanidino-2-oxopentanoate (intermediates in arginine and proline metabolism) also increased in Mut.P-S-M. Again, as L-arginine is being targeted by pathogenic bacteria to inhibit the production of NO (353), the levels of N-acetyl-L-glutamate 5-semialdehyde and 5-guanidino-2-oxopentanoate could be increased to compensate for the depleted L-arginine. The final metabolite that differentially increased in mutant *P. aeruginosa* is 5-aminopentanoate, which involved in lysine metabolism. The increase in 5-aminopentanoate could be attributed to an increase in L-lysine. L-lysine produces 5-aminopentanamide by

the enzyme lysine 2-monooxygenase (KEGG 3.5.1.30), which in turn produces 5-aminopentanoate by the enzyme, 5-aminopentanamidase (KEGG 3.5.1.30). Lysine was reported to have antimicrobial activity against herpes simplex virus (510). Based on this result, these four metabolites have been increased in both Mut.P-S-M and P-S-M*,* however, they showed a higher increase in Mut.P-S-M which could indicate higher impact of the mutant *P. aeruginosa* on macrophages. This could be attributed to the more chronic characteristic of mutant *P.aeruginosa* (PALT 13*)* compared to WT *P. aeruginosa.*

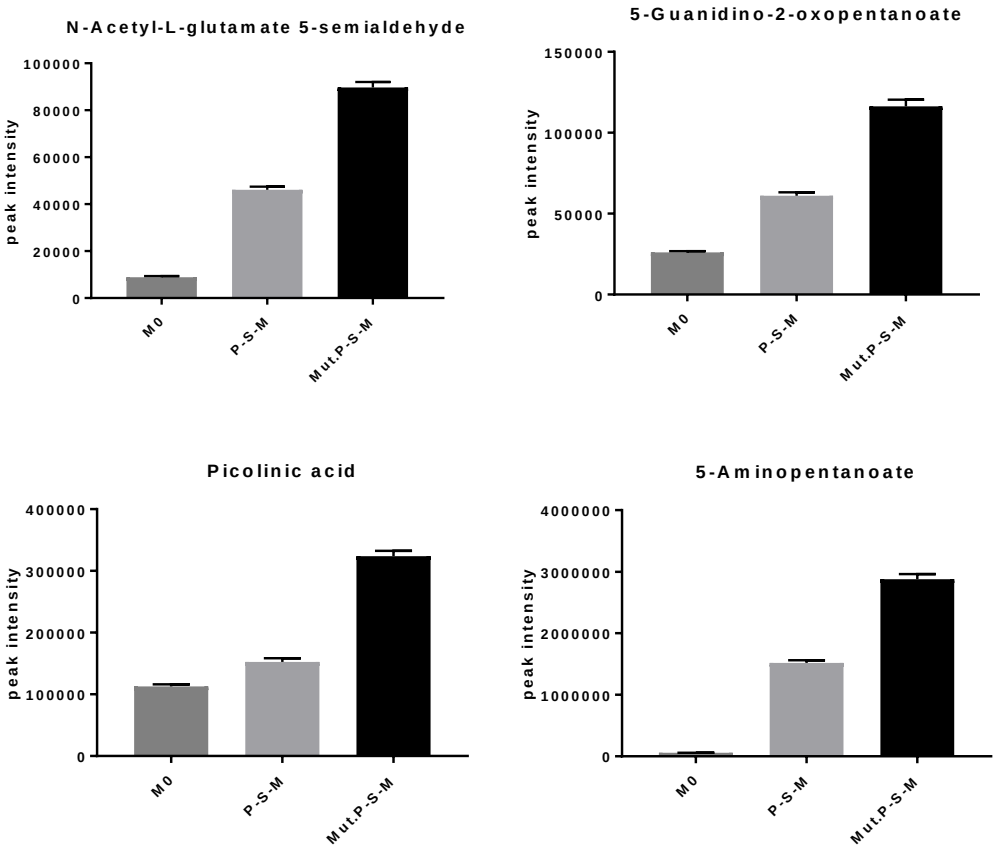


Figure 4.9: The metabolites significantly and differentially increased in Mut.P-S-M P-S-M. n=6, data are presented as mean ± SEM.

4.4. Conclusion

In this study, LC-MS metabolite profiling was shown to be a promising and effective approach to investigate the effect of Gram-positive and Gram-negative bacteria on macrophages metabolic profile. Treatment with the secretomes of *S. aureus* and *P. aeruginosa* led to distinct metabolic impacts on macrophages, despite some similarities. Glycine and serine metabolism, sphingolipid metabolism, GL metabolism, alanine, aspartate and glutamate metabolism and tryptophan metabolism showed different trends in macrophages treated with each secretome. However, the alteration of arginine and proline metabolism showed a similar trend in both bacteria secretome-challenged macrophages. This could imply that these Gram-positive and Gram-negative used different mechanisms in disturbing the host immune system, particularly the metabolism of macrophages. On the other hand, the secretome of *P. aeruginosa* and mutant *P. aeruginosa* showed a similar impact on macrophages, with only changes in few metabolites (i.e. picolinic acid, N-acetyl-L-glutamate 5-semialdehyde, 5-guanidino-2-oxopentanoate and 5-aminopentanoate). The identification of the key metabolites that can represent potential biomarkers could be translated to design a novel approach of early diagnosis of bacterial infectious diseases. Moreover, these key metabolites can be used for better understanding of the mechanisms underpinning the pathogenesis and resistance of these bacteria. Hence, this could lead to a new perspective in therapeutics by discovering innovative targeting strategies with selectivity toward Gram-positive or Gram-negative bacteria.

Table 4.1: A list of the 83 significantly changed metabolites in *S. aureus* secretome treated macrophages with VIP > 1 and FDR < 0.05 compared to M0

Putative metabolite	Mass	RT	FORMULA	Polarity	Confidence	Pathway	Fold change	VIP	FDR
(4E)-2-Oxohexenoic acid	128.0473	4.88	C6H8O3	+	L2	4-nitrotoluene degradation II	0.0339892	3.1584	4.359E-10
[FA (24:6)]	344.1777	4.21	C24H24O2	+	L2	Fatty Acids and Conjugates	1.8384652	2.44806	1.193E-07
[FA methoxy,trihydroxy]-prostadiene	354.2770	4.02	C21H38O4	+	L2	Eicosanoids	1.4892391	2.66052	3.138E-07
[GL (18:0)]	358.3084	4.02	C21H42O4	+	L2	Monoradylglycerols	1.1597151	2.52698	0.0116877
[PC (16:0)]	495.3325	4.39	C24H50NO7P	+	L2	Glycerophosphocholines	2.1797923	1.35857	2.733E-07
[PC (16:1)]	479.3376	4.37	C24H50NO6P	+	L2	Glycerophosphocholines	1.8995277	2.97738	2.185E-06
[PC (16:2)]	481.3533	4.43	C24H52NO6P	+	L2	Glycerophosphocholines	1.6336883	1.916	2.316E-06
[PC (18:1/18:0)]	771.6141	3.78	C44H86NO7P	+	L2	Glycerophosphocholines	1.6111977	2.23744	2.532E-06
[PC (18:1/20:4)]	793.5983	3.76	C46H84NO7P	+	L2	Glycerophosphocholines	2.1002155	15.9844	2.666E-07
[PE (18:1/20:4)]	751.5514	3.71	C43H78NO7P	+	L2	Glycerophosphoethanolamines	3.802419	1.1457	2.006E-09
Ceramide (d18:1/16:0)]	537.5122	3.81	C34H67NO3	-	L2	Ceramides	26.44311	1.55788	7.031E-10
Ceramide (d18:1/16:0)]	702.5673	3.91	C39H79N2O6P	+	L2	Ceramide phosphocholines (sphingomyelins)	0.142839	1.15147	2.798E-09
Ceramide (d18:1/24:0)]	647.6224	3.70	C42H81NO3	+	L2	Ceramides	44.815786	1.33461	1.299E-09
1-Hexadecanoyl-2-(octadecenoyl)-sn-glycero-3-phosphonocholine	743.5826	3.80	C42H82NO7P	+	L2	Glycerophosphonocholines	1.7811123	1.26228	2.78E-07
3-methyl-1-heptene	112.1252	3.90	C8H16	-	L2	Hydrocarbons	3.3657902	1.01797	1.283E-06
4-Guanidinobutanoate	145.0851	10.99	C5H11N3O2	+	L2	Arginine and proline metabolism	3.849495	2.1975	1.995E-10
5-Aminopentanoate	117.0790	10.94	C5H11NO2	-	L2	Lysine degradation, Arginine and proline metabolism	2.7102728	2.52089	1.625E-09
5'-Deoxyadenosine	251.1017	9.00	C10H13N5O3	+	L2	0	12.073153	18.8909	1.498E-08
5-Guanidino-2-oxopentanoate	173.0800	10.78	C6H11N3O3	+	L2	D-Arginine and D-ornithine metabolism	6.1603924	3.56544	1.914E-10
5'-Methylthioadenosine	297.0896	6.96	C11H15N5O3S	+	L2	Arginine and proline metabolism, Methionine metabolism, Zeatin biosynthesis	0.1913745	3.83405	3.096E-09
Acetylcholine	145.1102	9.55	C7H15NO2	+	L2	Glycerophospholipid metabolism	0.1644762	1.63653	7.514E-09

Adenine	135.0545	8.19	C5H5N5	-	L2	Purine metabolism, Zeatin biosynthesis	0.291833	2.40156	9.751E-10
Cer(d18:2/16:0)	535.4962	3.85	C34H65NO3	+	L2	Ceramides	33.112075	2.07448	3.133E-11
Creatine	131.0695	10.70	C4H9N3O2	-	L2	Glycine, serine and threonine metabolism, Arginine and proline metabolism	0.4772938	6.8233	9.65E-08
Creatinine	113.0589	8.23	C4H7N3O	-	L2	Arginine and proline metabolism	0.7475717	4.52161	3.926E-06
Cytidine	243.0855	9.53	C9H13N3O5	+	L1	Pyrimidine metabolism	5.249654	1.54426	5.815E-11
Cytosine	111.0433	9.44	C4H5N3O	+	L2	Pyrimidine metabolism	4.6167105	5.60597	2.274E-09
D-Glucosamine	179.0794	10.37	C6H13NO5	+	L1	Aminosugars metabolism	1.4756581	1.82869	0.0001232
D-Methionine	149.0510	8.93	C5H11NO2S	-	L2	Unknown	1.8184533	1.50714	2.819E-08
Glutathione	307.0839	9.81	C10H17N3O6S	+	L1	Glutamate metabolism, Cysteine metabolism, Glutathione metabolism	0.4905779	2.28637	5.544E-06
Glutathione disulfide	306.0760	11.05	C20H32N6O12S2	+	L1	Glutamate metabolism, Glutathione metabolism	2.0806558	2.3952	1.847E-06
Glycine	75.0320	11.38	C2H5NO2	+	L2	Glycine, serine and threonine metabolism, Lysine degradation, Glutathione metabolism, Methane metabolism, Thiamine metabolism	0.4570198	2.00104	5.584E-09
Guanidinoacetate	117.0538	11.60	C3H7N3O2	+	L1	Glycine, serine and threonine metabolism, Arginine and proline metabolism	0.4742266	1.29957	4.537E-09
Hypotaurine	109.0197	10.99	C2H7NO2S	+	L2	Taurine and hypotaurine metabolism	0.3399049	1.98454	7.959E-09
Hypoxanthine	136.0384	8.71	C5H4N4O	+	L1	Purine metabolism	32.149825	4.0612	2.237E-09
L-1-Pyrroline-3-hydroxy-5-carboxylate	129.0426	7.87	C5H7NO3	+	L2	Arginine and proline metabolism	0.7790454	1.2455	0.0013678
L-Asparagine	132.0535	10.90	C4H8N2O3	-	L2	Alanine and aspartate metabolism, Tetracycline biosynthesis, Nitrogen metabolism	1.0957808	1.05844	0.018366
L-Carnitine	161.1052	9.56	C7H15NO3	+	L1	Lysine degradation	0.1666537	2.01841	2.426E-08
L-Citrulline	175.0958	11.13	C6H13N3O3	+	L2	Arginine and proline metabolism	0.71067	4.92975	3.175E-05
L-Formylkynurenine	236.0797	7.90	C11H12N2O4	+	L2	Tryptophan metabolism	5.8482112	1.15769	2.526E-09
L-Glutamate	147.0531	10.21	C5H9NO4	+	L1	Arginine and proline metabolism, Glutamate metabolism, Glutathione metabolism_Butanoate metabolism	0.4483477	3.9985	4.736E-09
L-Glutamate 5-semialdehyde	131.0584	10.57	C5H9NO3	-	L2	Arginine and proline metabolism	0.7217336	4.27033	4.599E-07
L-Glutamine	146.0691	10.77	C5H10N2O3	-	L1	Glutamate metabolism, Purine metabolism, Pyrimidine metabolism	1.1281618	5.23266	0.0055292

L-Leucine	131.0947	8.55	C6H13NO2	+	L2	Valine, leucine and isoleucine degradation, Valine, leucine and isoleucine biosynthesis	1.7270754	4.26515	3.94E-06
L-Lysine	146.1055	16.74	C6H14N2O2	-	L2	Lysine biosynthesis, Lysine degradation, Biotin metabolism, Alkaloid biosynthesis II	5.793573	3.54547	2.673E-10
L-Methionine S-oxide	165.0459	9.57	C5H11NO3S	-	L2	Methionine metabolism	4.1835183	2.10768	3.562E-10
L-Phenylalanine	165.0790	8.07	C9H11NO2	+	L2	Phenylalanine metabolism, Phenylalanine, tyrosine and tryptophan biosynthesis, Phenylpropanoid biosynthesis, Alkaloid biosynthesis II	2.9884482	1.2876	3.996E-10
L-Proline	115.0633	9.68	C5H9NO2	+	L1	Arginine and proline metabolism, Novobiocin biosynthesis	1.2432343	1.93064	1.661E-05
L-Serine	105.0426	11.28	C3H7NO3	+	L1	Glycine, serine and threonine metabolism, Methionine metabolism, Cysteine metabolism	1.5930321	3.30448	2.891E-05
L-Tryptophan	204.0900	9.38	C11H12N2O2	+	L1	Tryptophan metabolism, Phenylalanine, tyrosine and tryptophan biosynthesis	6.1161048	7.49918	8.927E-11
L-Tyrosine	181.0740	10.04	C9H11NO3	+	L1	Tyrosine metabolism	2.3623719	1.07205	1.23E-07
N(pi)-Methyl-L-histidine	169.0851	9.46	C7H11N3O2	+	L1	Histidine metabolism	0.6123934	1.41722	3.565E-07
N6-Methyl-L-lysine	160.1212	16.19	C7H16N2O2	+	L1	Unknown	0.2276234	1.90608	9.582E-09
O-Acetylcarnitine	203.1158	8.31	C9H17NO4	+	L1	Alanine and aspartate metabolism	0.2586587	1.2915	9.484E-10
O-Propanoylcarnitine	217.1314	7.61	C10H19NO4	+	L2	OxidationofBranchedFattyAcids	0.149092	5.82142	5.028E-09
Pantothenate	219.1107	6.98	C9H17NO5	-	L2	beta-Alanine metabolism, Pantothenate and CoA biosynthesis	0.3369867	1.44963	2.908E-08
PC(16:0/P-18:0)	745.5984	3.80	C42H84NO7P	+	L2	Glycerophosphocholines	1.6662637	4.10374	2.501E-07
PC(20:2)	795.6138	3.76	C46H86NO7P	+	L2	Glycerophosphocholines	2.0621236	10.2294	1.579E-07
PC(30:0)	705.5308	3.84	C38H76NO8P	+	L2	Glycerophosphocholines	0.7890354	1.3485	0.0001836
PC(32:0)	733.5615	3.82	C40H80NO8P	+	L2	Glycerophosphocholines	1.6087076	1.1786	1.31E-06
PC(32:1)	731.5462	3.81	C40H78NO8P	+	L2	Glycerophosphocholines	0.8775841	1.10442	0.0039552
PC(32:2)	729.5307	3.83	C40H76NO8P	+	L2	Glycerophosphocholines	0.5587094	1.55328	1.921E-07
PC(34:1)	759.5775	3.79	C42H82NO8P	+	L2	Glycerophosphocholines	1.1848302	1.11383	0.0014767
PC(36:1)	787.6086	3.76	C44H86NO8P	+	L2	Glycerophosphocholines	1.9271518	1.45322	2.114E-06
PC(38:3)	811.6091	3.76	C46H86NO8P	+	L2	Glycerophosphocholines	1.3686502	4.86641	4.385E-05

PC(38:4)	809.5935	3.75	C46H84NO8P	+	L2	Glycerophosphocholines	2.3630143	3.07039	1.537E-08
PC(38:5)	807.5778	3.77	C46H82NO8P	+	L2	Glycerophosphocholines	1.6396553	1.57395	3.587E-07
PC(40:5)	835.6090	3.75	C48H86NO8P	+	L2	Glycerophosphocholines	2.1351713	9.46117	5.206E-09
PC(40:6)	833.5933	3.75	C48H84NO8P	+	L2	Glycerophosphocholines	1.7643985	3.17895	1.285E-06
PE(20:4)	749.5357	3.68	C43H76NO7P	+	L2	Glycerophosphoethanolamines	2.9638441	3.74339	3.681E-09
PE(34:0)	719.5469	3.83	C39H78NO8P	+	L2	Glycerophosphoethanolamines	1.7711682	1.44412	2.409E-05
PE(38:1)	773.5937	3.78	C43H84NO8P	+	L2	Glycerophosphoethanolamines	1.7809977	1.46758	9.474E-07
PE(38:4)	767.5470	3.72	C43H78NO8P	+	L2	Glycerophosphoethanolamines	2.7520707	1.07961	4.202E-09
Phosphocreatine	211.0360	10.31	C4H10N3O5P	-	L2	Arginine and proline metabolism	0.2792269	1.6292	1.674E-09
Phosphodimethylethanolamine	169.0504	9.46	C4H12NO4P	-	L2	Glycerophospholipid metabolism	0.1718706	10.2151	1.056E-08
PS(36:1)	789.5515	3.58	C42H80NO10P	+	L2	Glycerophosphoserines	2.7661578	4.07674	6.711E-08
Pyridoxine	169.0739	7.11	C8H11NO3	-	L2	Vitamin B6 metabolism	1.8635098	1.50163	8.779E-10
Sarcosine	89.0477	7.00	C3H7NO2	+	L2	Glycine, serine and threonine metabolism, Arginine and proline metabolism	0.3285352	1.08147	1.871E-08
SM(d16:1/18:1)	700.5510	3.97	C39H77N2O6P	+	L2	Phosphosphingolipids	0.0896636	1.2206	2.582E-10
SM(d18:1/14:0)	674.5362	3.99	C37H75N2O6P	+	L2	Ceramide phosphocholines (sphingomyelins)	0.0866166	1.15276	1.529E-09
sn-glycero-3-Phosphocholine	257.1030	9.96	C8H20NO6P	+	L2	Glycerophospholipid metabolism, Ether lipid metabolism	0.7212508	2.10253	8.823E-06
sn-glycero-3-Phosphoethanolamine	215.0558	10.79	C5H14NO6P	-	L2	Glycerophospholipid metabolism, Ether lipid metabolism	0.2321072	1.84288	2.434E-09

Table 4.2: A list of 75 significantly changed metabolites in *P. aeruginosa* secretome treated macrophages with VIP > 1 and FDR < 0.05 compared to M0.

Putative metabolite	Mass	RT	FORMULA	POLARITY	confidence	Pathway	Fold change	VIP	FDR
[FA (10:1/2:0)]	200.1049	4.70	C10H16O4	+	L2	Fatty Acids and Conjugates	0.59836	10.7415	8.263E-08
[FA (18:1)]	281.2719	4.17	C18H35NO	-	L2	Fatty amides	0.54922	7.96763	1.518E-08
[FA] O-Palmitoyl-R-carnitine	399.3349	4.38	C23H45NO4	+	L2	Fatty acyl carnitines	1.57508	2.48311	1.319E-06
[GL (16:0)]	330.2771	4.06	C19H38O4	+	L2	Monoradylglycerols	0.59490	4.58149	3.506E-06
[GL (18:0)]	358.3084	4.02	C21H42O4	+	L2	Monoradylglycerols	1.08931	2.36889	0.039856
[PC (14:0)]	467.3013	4.50	C22H46NO7P	+	L2	Glycerophosphocholines	0.90846	1.74498	0.0091875
[PC (16:0)]	495.3325	4.39	C24H50NO7P	+	L2	Glycerophosphocholines	1.33827	1.88486	2.586E-05
[PC (16:2)]	481.3533	4.43	C24H52NO6P	+	L2	Glycerophosphocholines	1.19573	1.01244	0.004821
[PC (22:6)]	567.3322	4.31	C30H50NO7P	+	L2	Glycerophosphocholines	1.43751	1.00054	1.391E-05
[PC methyl(12:2)]	439.3064	4.40	C21H46NO6P	+	L2	Glycerophosphocholines	0.86240	2.73204	0.0042027
[PE (18:1)]	479.3011	4.28	C23H46NO7P	+	L2	Glycerophosphoethanolamines	1.20388	1.09009	0.0021449
Ceramide (d18:1/16:0)]	702.5673	3.91	C39H79N2O6P	+	L2	Ceramide phosphocholines (sphingomyelins)	0.77628	2.58862	5.554E-05
3-Dehydroxycarnitine	145.1102	14.79	C7H15NO2	+	L2	LysineDegradation	0.80287	2.70761	0.0006009
4-Guanidinobutanoate	145.0851	10.99	C5H11N3O2	+	L2	Arginine and proline metabolism	0.58267	1.26398	0.0001031
5-Aminopentanoate	117.0790	10.94	C5H11NO2	+	L2	Lysine degradation, Arginine and proline metabolism	0.41067	1.91195	2.089E-06
5'-Methylthioadenosine	297.0896	6.96	C11H15N5O3S	+	L2	Arginine and proline metabolism, Methionine metabolism, Zeatin biosynthesis	2.85557	10.5009	5.685E-10
AMP	347.0631	9.41	C10H14N5O7P	+	L2	Purine metabolism, Zeatin biosynthesis	26.69349	1.09934	1.539E-05
CDP-choline	488.1074	10.13	C14H26N4O11P2	+	L2	Glycerophospholipid metabolism	4.53147	2.40587	1.813E-09
Choline	103.0997	17.85	C5H13NO	+	L2	Glycine, serine and threonine metabolism, Glycerophospholipid metabolism	2.84142	1.52172	3.026E-08
Creatine	131.0695	10.70	C4H9N3O2	-	L2	Glycine, serine and threonine metabolism, Arginine and proline metabolism	0.49708	1.71576	1.436E-06

Creatinine	113.0589	8.23	C4H7N3O	-	L2	Arginine and proline metabolism	3.50860	1.75537	2.036E-07
Cytosine	111.0433	9.44	C4H5N3O	+	L2	Pyrimidine metabolism	2.64261	2.15896	7.56E-07
D-Glucosamine	179.0794	10.37	C6H13NO5	+	L1	Aminosugars metabolism	3.12601	2.64939	3.598E-09
D-Methionine	149.0510	8.93	C5H11NO2S	+	L2	unknown	1.81332	1.25084	8.144E-07
D-Sorbitol	182.0791	10.39	C6H14O6	+	L2	Fructose and mannose metabolism, Galactose metabolism	0.64326	6.74141	6.915E-08
Glutathione	307.0839	9.81	C10H17N3O6S	-	L1	Glutamate metabolism, Cysteine metabolism, Glutathione metabolism	0.64226	8.87017	4.736E-07
Glutathione disulfide	306.0760	11.05	C20H32N6O12S2	+	L1	Glutamate metabolism, Glutathione metabolism	0.62348	3.19555	7.865E-06
Hypoxanthine	136.0384	8.71	C5H4N4O	+	L1	Purine metabolism	11.38694	1.111	5.696E-10
IMP	348.0471	10.51	C10H13N4O8P	+	L1	Purine metabolism	1.58905	3.75388	1.241E-06
L-1-Pyrroline-3-hydroxy-5-carboxylate	129.0426	7.87	C5H7NO3	+	L2	Arginine and proline metabolism	2.58559	1.16875	1.263E-07
L-Asparagine	132.0535	10.90	C4H8N2O3	+	L2	Alanine and aspartate metabolism, Tetracycline biosynthesis, Cyanoamino acid metabolism, Nitrogen metabolism	1.45750	1.47766	3.695E-06
L-Carnitine	161.1052	9.56	C7H15NO3	+	L1	Lysine degradation	0.52975	4.1242	1.603E-05
L-Citrulline	175.0958	11.13	C6H13N3O3	+	L2	Arginine and proline metabolism	1.62264	18.4905	3.887E-07
L-Glutamate	147.0531	10.21	C5H9NO4	+	L1	Arginine and proline metabolism, Glutamate metabolism, Histidine metabolism, D-Glutamine and D-glutamate metabolism, Glutathione metabolism_Butanoate metabolism_C5-Branched dibasic acid metabolism_Porphyrin and chlorophyll metabolism_Nitrogen metabolism	38.41263	1.22401	1.071E-10

L-Glutamate 5-semialdehyde	131.0584	10.57	C5H9NO3	-	L2	Arginine and proline metabolism	1.13202	1.20813	4.236E-12
L-Glutamine	146.0691	10.77	C5H10N2O3	+	L1	Glutamate metabolism, Purine metabolism, Pyrimidine metabolism, D-Glutamine and D-glutamate metabolism, Nitrogen metabolism	0.35932	1.91205	7.666E-08
L-Kynurenine	208.0849	8.73	C10H12N2O3	-	L1	Tryptophan metabolism	0.90775	9.84513	0.0106045
L-Leucine	131.0947	8.55	C6H13NO2	+	L2	Valine, leucine and isoleucine degradation, Valine, leucine and isoleucine biosynthesis	0.58264	3.38437	9.032E-06
L-Lysine	146.1055	16.74	C6H14N2O2	-	L2	Lysine biosynthesis, Lysine degradation, Biotin metabolism, Alkaloid biosynthesis II	1.64343	6.42516	8.301E-08
L-Methionine S-oxide	165.0459	9.57	C5H11NO3S	-	L2	Methionine metabolism	2.71175	1.45168	1.71E-07
L-Phenylalanine	165.0790	8.07	C9H11NO2	+	L2	Phenylalanine metabolism, Phenylalanine, tyrosine and tryptophan biosynthesis, Phenylpropanoid biosynthesis, Alkaloid biosynthesis II	5.72492	2.60994	5.018E-09
L-Proline	115.0633	9.68	C5H9NO2	+	L1	Arginine and proline metabolism, Novobiocin biosynthesis	0.23912	1.05967	2.148E-07
L-Serine	105.0426	11.28	C3H7NO3	+	L1	Glycine, serine and threonine metabolism, Methionine metabolism, Cysteine metabolism, Cyanoamino acid metabolism, Sphingolipid metabolism, Methane metabolism, Sulfur metabolism	2.00291	3.21639	2.589E-06
L-Tryptophan	204.0900	9.38	C11H12N2O2	+	L1	Tryptophan metabolism, Phenylalanine, tyrosine and tryptophan biosynthesis, Indole and ipecac alkaloid biosynthesis	1.23221	5.91392	4.608E-07
L-Tyrosine	181.0740	10.04	C9H11NO3	+	L1	Tyrosine metabolism, Phenylalanine, tyrosine and	0.55521	1.77232	4.811E-08

						tryptophan biosynthesis, Novobiocin biosynthesis, Thiamine metabolism, Phenylpropanoid biosynthesis, Alkaloid biosynthesis I			
LysoPC(20:4)	543.3323	4.34	C28H50NO7P	+	L2	Glycerophosphocholines	1.57829	1.20171	4.323E-05
LysoPE(0:0/20:5)	499.2699	4.28	C25H42NO7P	+	L2	Glycerophosphoethanolamines	0.69116	1.72538	1.604E-05
LysoPE(0:0/22:5)	527.3019	4.15	C27H46NO7P	-	L2	Glycerophosphoethanolamines	1.29657	1.07294	0.0002996
N(pi)-Methyl-L-histidine	169.0851	9.46	C7H11N3O2	+	L1	Histidine metabolism	0.62262	4.31285	1.049E-06
N2-Acetyl-L-lysine	188.1163	9.26	C8H16N2O3	+	L2	Lysine biosynthesis	39.07539	1.19111	1.394E-07
NAD+	663.1089	9.45	C21H27N7O14P2	+	L2	Oxidative phosphorylation, Glutamate metabolism, Nicotinate and nicotinamide metabolism	1.30032	4.9337	8.447E-06
N-Butyryl-L-homoserine lactone	171.0895	4.93	C8H13NO3	+	L2	Fatty amides	0.65008	3.20547	1.484E-06
O-Acetylcarnitine	203.1158	8.31	C9H17NO4	+	L1	Alanine and aspartate metabolism	0.50980	1.58639	3.516E-06
Propanoylcarnitine	217.1314	7.61	C10H19NO4	+	L2	Oxidation of Branched Fatty Acids	0.73708	1.94291	7.53E-05
PC(16:0/P-18:0)	745.5984	3.80	C42H84NO7P	+	L2	Glycerophosphocholines	4.54906	3.77695	4.432E-10
PC(28:0)	677.4993	3.89	C36H72NO8P	+	L2	Glycerophosphocholines	1.92622	1.05417	2.181E-08
PC(30:0)	705.5308	3.84	C38H76NO8P	+	L2	Glycerophosphocholines	0.17384	9.95638	5.226E-10
PC(32:0)	733.5615	3.82	C40H80NO8P	+	L2	Glycerophosphocholines	1.71440	1.35567	9.361E-08
PC(32:1)	731.5462	3.81	C40H78NO8P	+	L2	Glycerophosphocholines	0.23832	4.12602	1.59E-08
PC(32:2)	729.5307	3.83	C40H76NO8P	+	L2	Glycerophosphocholines	2.38368	1.3734	5.89E-06
PC(34:1)	759.5775	3.79	C42H82NO8P	+	L2	Glycerophosphocholines	12.26762	3.16616	6.166E-11
PC(36:1)	787.6086	3.76	C44H86NO8P	+	L2	Glycerophosphocholines	4.39863	1.1804	4.261E-09
PC(36:2)	785.5931	3.76	C44H84NO8P	+	L2	Glycerophosphocholines	1.78902	2.29307	2.459E-06
PC(38:2)	813.6249	3.76	C46H88NO8P	+	L2	Glycerophosphocholines	1.95928	1.01147	1.264E-07
PC(38:3)	811.6091	3.76	C46H86NO8P	+	L2	Glycerophosphocholines	2.09486	1.34126	2.491E-06
PC(38:4)	809.5935	3.75	C46H84NO8P	+	L2	Glycerophosphocholines	2.22793	1.53634	1.091E-09
PE(38:1)	773.5937	3.78	C43H84NO8P	+	L2	Glycerophosphoethanolamines	0.89594	1.07833	0.0254251
Phosphocreatine	211.0360	10.31	C4H10N3O5P	+	L2	Arginine and proline metabolism	2.49715	1.08633	2.57E-08
Phosphodimethylethanolamine	169.0504	9.46	C4H12NO4P	+	L2	Glycerophospholipid metabolism	0.76550	1.28333	0.0010371

PI(14:1(9Z)/0:0)	271.1242	4.01	C23H43O12P	+	L2	Glycerophosphoinositols	2.27992	3.38207	2.876E-08
SM(d16:1/18:1)	700.5510	3.97	C39H77N2O6P	+	L2	Phosphosphingolipids	0.44094	1.28658	4.08E-08
SM(d18:1/24:1)	812.6767	3.83	C47H93N2O6P	+	L2	Ceramide phosphocholines (sphingomyelins)	25.01565	1.06597	1.604E-10
sn-glycero-3-Phosphocholine	257.1030	9.96	C8H20NO6P	+	L2	Glycerophospholipid metabolism, Ether lipid metabolism	3.06994	2.47065	7.792E-09
sn-glycero-3-Phosphoethanolamine	215.0558	10.79	C5H14NO6P	-	L2	Glycerophospholipid metabolism, Ether lipid metabolism	2.18841	1.50271	1.451E-07

Table 4.3: A list of 28 significantly changed metabolites in mut. *P.aeruginosa* (PALT 13) secretome treated macrophages with VIP >1 and FDR < 0.05 Compared to *P.aeruginosa* (PA01) secretome treated macrophages.

Putative metabolite	Mass	RT	FORMULA	Polarity	Confidence	Pathway	Fold change P.aeruginosa	Fold change Mut.P	VIP	FDR
Glutathione	307.0839	9.81	C10H17N3O6S	+	L1	Glutamate metabolism, Cysteine metabolism, Glutathione metabolism	0.53	0.67	8.83945	4.35E-11
CDP-choline	488.1074	10.13	C14H26N4O11P2	+	L2	Glycerophospholipid metabolism	2.38	3.29	6.75123	3.27E-15
Linoleamide	279.2563	4.17	C18H33NO	+	L2	Fatty amides	0.89	1.06	2.08954	1.57E-08
[FA (18:1)]	281.2719	4.17	C18H35NO	+	L2	Fatty amides	0.80	1.04	1.22059	3.68E-08
[GL (16:0)]	330.2771	4.06	C19H38O4	+	L2	Monoradylglycerols	0.58	0.86	5.45836	1.94E-19
[GL (18:0)]	358.3084	4.02	C21H42O4	+	L2	Monoradylglycerols	0.58	0.77	9.50525	2.99E-19
[FA (24:6)]	344.1777	4.21	C24H24O2	+	L2	Fatty Acids and Conjugates	0.68	0.95	2.17161	0.0019314
[PC (16:1)]	493.3168	4.44	C24H48NO7P	+	L2	Glycerophosphocholines	1.13	1.25	1.54755	1.58E-18
[PC (20:5)]	541.3167	4.37	C28H48NO7P	+	L2	Glycerophosphocholines	2.55	3.48	1.283	2.24E-07
LysoPC(20:4)	543.3323	4.34	C28H50NO7P	+	L2	Glycerophosphocholines	2.84	3.76	1.00444	8.93E-16
[PC (22:6)]	567.3322	4.31	C30H50NO7P	+	L2	Glycerophosphocholines	2.50	2.98	1.00803	1.29E-15
PC(28:0)	677.4993	3.89	C36H72NO8P	+	L2	Glycerophosphocholines	2.23	2.90	1.53559	1.29E-05
PC(30:1)	703.5149	3.85	C38H74NO8P	+	L2	Glycerophosphocholines	1.08	1.24	1.29758	1.17E-09
PC(30:0)	705.5308	3.84	C38H76NO8P	+	L2	Glycerophosphocholines	1.34	1.49	1.38158	1.63E-13
Guanidinoacetate	117.0538	11.60	C3H7N3O2	+	L1	Glycine, serine and threonine metabolism, Arginine and proline metabolism	0.86	0.98	1.8765	1.40E-11
PS(O-16:0/20:1)	775.5738	3.87	C42H82NO9P	+	L2	Glycerophosphoserines	4.72	6.66	1.21519	5.00E-17
5-Aminopentanoate	117.0790	10.94	C5H11NO2	+	L2	Lysine degradation, Arginine and proline metabolism	26.69	50.58	1.1638	4.64E-13
D-Methionine	149.0510	8.93	C5H11NO2S	+	L2	0	1.64	1.84	1.90573	7.86E-17
sn-glycero-3-Phosphoethanolamine	215.0558	10.79	C5H14NO6P	-	L2	Glycerophospholipid metabolism, Ether lipid metabolism	1.13	1.34	2.76134	8.70E-09
L-Glutamate 5-semialdehyde	131.0584	10.57	C5H9NO3	-	L2	Arginine and proline metabolism	0.55	0.74	7.0829	2.47E-11
5-Guanidino-2-oxopentanoate	173.0800	10.78	C6H11N3O3	+	L2	D-Arginine and D-ornithine metabolism	2.34	4.45	3.54697	1.52E-11
L-Leucine	131.0947	8.55	C6H13NO2	+	L2	Valine, leucine and isoleucine degradation, Valine, leucine and isoleucine biosynthesis	1.23	1.38	5.70758	4.75E-12
N(pi)-Methyl-L-histidine	169.0851	9.46	C7H11N3O2	+	L1	Histidine metabolism	0.41	0.54	4.95591	0.0019466
N-Acetyl-L-glutamate 5-semialdehyde	173.0689	7.10	C7H11NO4	-	L2	Arginine and proline metabolism	5.20	10.10	5.49804	1.24E-11

3-Dehydroxycarnitine	145.1102	14.79	C7H15NO2	+	L2	LysineDegradation	2.71	3.40	1.33929	1.61E-09
L-Carnitine	161.1052	9.56	C7H15NO3	+	L1	Lysine degradation	0.17	0.26	3.77688	2.16E-16
O-Acetylcarnitine	203.1158	8.31	C9H17NO4	+	L1	Alanine and aspartate metabolism	1.30	1.52	1.77927	1.07E-14
Pantothenate	219.1107	6.98	C9H17NO5	-	L2	beta-Alanine metabolism, Pantothenate and CoA biosynthesis	0.59	0.80	1.7055	3.79E-12

Chapter Five

5. Investigating the impact of ageing on human macrophages using LC-MS-based metabolite profiling.

5.1. Introduction

Advances in medicine, socioeconomic development and public health policies have led to increasing the human life span (271). Globally, massive demographic changes in the population have been reported by the World Health Organization (WHO). Figure 5.1 shows the proportions of individuals over 60 years of age compared to the total global populations. Individuals over 60 years of age accounted for 10% of the total global population in 2000. However, WHO has reported that this will increase to 22% by 2050. Moreover, more than 18% of the current population in the UK are 65 years or older, which is expected to increase to 25% by 2031 (272). Similarly, the US Census Bureau has predicted that individuals over 60 years of age will represent 25% of the global population in 2050.

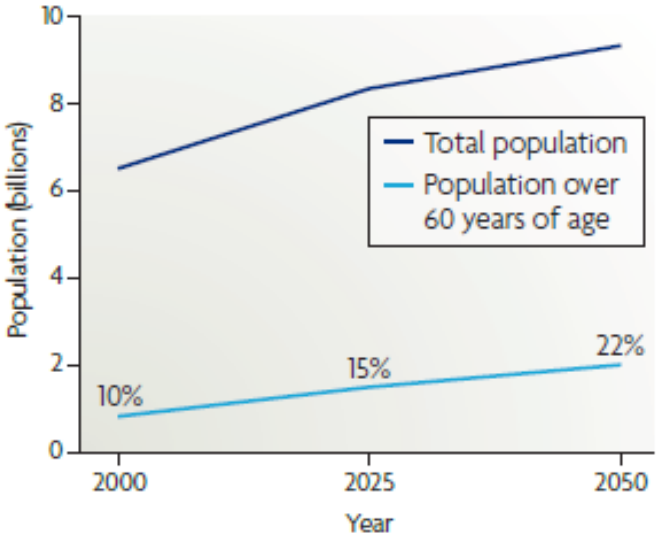


Figure 5.1: The proportion of individuals aged 60 years or older is expected to increase. The total world population and the number of people aged 60 years or older in 2000, and the projected values for 2025 and 2050, are shown. The figure also shows that individuals aged 60 years or older currently constitute 10% of the world population and this value is projected to increase to 22% in 2050. The figure is based on statistics from the World Health Organization website (280).

Although the longer life span is an advantage, new challenges caused by ageing have become significant issues to society. Ageing is associated with health deterioration and loss of physiological and mental integrity including chronic diseases and increased vulnerability to infections (273, 275). For instance, the high prevalence of respiratory system and urinary tract infections have been evident (511).

The immune system is an essential defensive tool against foreign pathogens including viruses and bacteria. Also, it plays a pivotal role in maintaining homeostasis. The immune system is divided into two main compartments: the innate and adaptive immune systems (512). The innate immune system represents the first line of defence in human body that serves an essential role against foreign invaders (275, 513). Innate immune cells encompass macrophages, neutrophils and dendritic cells, that all recognise and remove invasive pathogens. Adaptive immune cells include antigen-specific T and B cells that function to remove pathogens by producing antigen-specific antibodies or by cytotoxic reactions. When the innate immune system is unable to clear the pathogens, the adaptive immune system is immediately activated. Adaptive immune cells become activated once they interact with antigen presenting cells (APC) (514, 515). Age-associated decline of the innate and adaptive immune system has been extensively studied (514-517). For instance, the adaptive immune system in elderly individuals becomes unable to produce protective immunity, which can be reflected in unresponsiveness to vaccines (276). Moreover, the capacity to

activate T cells through antigen presentation is impaired in aged innate immune cells due to the downregulation of the expression of costimulatory molecules and Major histocompatibility complex (MHC) class II (518). This will, subsequently, introduce a new challenge in protecting elderly individuals from infectious diseases (276). For example, only 30–40% of elderly population are effectively responsive to the influenza vaccine (519), and so WHO has considered the development of vaccines which particularly target those elderly populations as a priority in the future research plans (520). Furthermore, ageing affects the immunoregulatory mechanisms of the immune system leading to increased risk of autoimmune diseases (521). Additionally, the morbidity and severity of these infections are believed to increase with ageing. For instance, a high prevalence of respiratory system and urinary tract infections have been evident. This can be seen in death rate increase owing to influenza, of which more than 90% occur in over-65 individuals every year (282, 511). Moreover, life-threatening diseases could develop as a result of occult infection with varicella zoster virus and tuberculosis in elderly people (522). These problems are primarily attributed to the age-related deterioration of the immune system and dysregulation of immune defensive functions (513), known as immunosenescence (523). Furthermore, the impairment of the immune system with ageing is accompanied by a decline in antitumor function leading to an increase in cancer incidence in elderly population, (279). Therefore, all these aspects of age-related immune system decline contribute to many socio-economic negative consequences such as an increased cost in caring of elderly people, which in turn affects the health care system significantly and introduces major economic consequences (271, 275). The

ageing-associated decline in the immune system activity, is likely a major cause of the high mortality and morbidity rate in elderly people.

To date, the age-related changes in the immune system are not fully understood. In addition to the significant conflicting and controversial conclusions in the literature (275), it has been suggested that the basis of immune system impairment is the same basis accounts for cellular senescence (275, 523, 524). Therefore, the importance of understanding the ageing effect on immune cells has been recognised as an important factor in the development of novel strategies to preserve the health of elderly people.

Macrophages, as effector cells, play a pivotal role in the innate and adaptive immune system (105). These potent immune cells, have many diverse immune functions, such as clearance of viruses, bacteria, parasites and tumour cells (525) by phagocytosis and producing nitrogen species and ROS. Macrophages also centrally initiate and propagate the inflammatory response by releasing a wide range of pro-inflammatory cytokines such as TNF-α, IL-6 and IL-1β (526, 527). Macrophages play a crucial role in the antigen presenting process to activate B and T cells (161). Another important role of macrophages is to maintain tissue homeostasis via apoptosis (scavenging dead cells) and growth factor production (138). Additionally, macrophages aid in efficient tissue repair and wound healing by debris clearance and secretion of fibrogenic and angiogenic factors (528). Macrophages can be characterized by the expression of a wide range of pathogen recognition receptors (PRRs) (116, 439). Through these receptors, macrophages can recognise the distinct pathogen products, called pathogen associated

molecular patterns (PAMPs). PRRs are classified into several classes including RIG-I like receptors (RLRs), Nod-like receptors (NLRs) and the most over-looked toll-like receptors (TLRs) (114). Binding of the pathogen ligand to the PRRs leads to production of pro-inflammatory cytokines, thus starting an inflammatory response. For instance, TLRs detect the bacterial lipopolysaccharide (LPS) from Gram-negative bacteria and lipoteichoic acid from Gram-positive bacteria) and viral nucleic acid (529). TLR activation induces the production of TNF-α, IL-6 and IL-1β, the pro-inflammatory cytokines (150).

The impact of ageing on macrophages has been studied and has attracted attention because of the impairment of the functional aspects of macrophages such as polarisation, phagocytosis, wound healing and TLR activation (282, 286, 527, 530). However, studies have yielded opposing results and conflicting conclusions which could be due to several factors, such as macrophage origin (spleen, bone-marrow, alveolus, or tissue), strain, sex, and different experimental conditions (used stimulant, culture condition, etc.). In addition, the difficulty of identifying the term 'healthy elderly subject' requires careful health screening (527, 531). Vida et al have evaluated the functions of mice macrophages with ageing (532). The levels of ROS and superoxide ions, oxidized and reduced glutathione, digestion capacity and phagocytosis were investigated. Their results showed increased oxidative stress, lower antioxidant defence and impaired macrophages functions in old mice (532). Related decline of macrophages functions at the genomic level has been reported (533). Chelvarajan et al revealed age-related reduction in the immune response (proinflammatory cytokines,

chemokines and their receptors) and signal transduction genes in aged mice (533). Genetic and environmental factors are believed to be involved, but further study required (291, 534-536). Based on genetic studies in animals, the various pathways implicated in ageing immune decline were related to metabolism (537-540). Metabolic system dysregulation, particularly in mitochondria, have been observed in humans and mice upon ageing (541-543), as well as significant changes occurring in many different types of molecules (268, 544). In fact, many processes have been reported to be affected by ageing in macrophages. However, whether metabolic dysregulation can contribute to (rather than be a result of) macrophage dysfunction with ageing is not fully known (301). Therefore, metabolomics could help investigate the molecular influence of ageing on macrophages.

Metabolomics is a promising approach for capturing the complexity of ageing through detecting the influenced metabolic pathways and link these effects to the function and phenotypes of interest. It was proposed that the basis of immune system deterioration by ageing is the same basis of the cells body impairment and the pathways that involved are related to metabolism (275, 537-540). LC-MS has been applied successfully to investigate immune cells functions and the signalling molecules in ageing. Menni et al have successfully employed LC-MS metabolite profiling in an age-related study on 1052 fasting individuals' serum in the UK, revealing that 22 metabolites were strongly correlated with age (545). Another metabolomics study on mice demonstrated that glucose, fatty acids and redox homeostasis were among the impacted pathways in muscle and liver of aged

animals (546). However, the impact of aging on immune system remains incompletely understood.

Despite the above only a few age-related metabolomics studies have been conducted on animals (mice, dogs and rats) (294-296), and very few metabolomics studies have been conducted in humans. For instance, Lawton et al have used GC- and LC-MS metabolomics to investigate the ageing effect using human plasma of 269 individuals (298). Their results showed changes in oxidative stress, lipid metabolism, energy metabolism, and protein metabolism associated with ageing (298). Due to the lack of metabolomics studies that investigate the ageing effect on human immune cells, global LC-MS cell-based metabolite profiling of aged macrophages could represent an informative approach that can be utilized to combat the health implications of ageing and increase healthspan.

In this study, LC-MS-based metabolite profiling was carried out to investigate the impact of ageing on human macrophages in steady state or LPS-stimulated state. Our data demonstrated that there is no significant difference between young and old macrophages in steady state and in LPS-stimulated cells. Further investigations on human macrophages are to be conducted.

5.2. Materials and methods

5.2.1. Materials.

Buffy coats from healthy donors were obtained from the National Blood Service Sheffield, UK. M-CSF, CD14 MicroBeads and LS columns were purchased from

Miltenyi Biotec, Histopaque-1077, RPMI-1640 medium foetal bovine serum (FBS), Phosphate Buffered Saline (PBS), 2 mM L-glutamine, 100 U/ml penicillin, and 100 µg/ml streptomycin all from Sigma-Aldrich, St. Louis, MO, USA. Methanol and acetonitrile were purchased from Fisher Scientific, UK, all solvents are LC-MS grade.

5.2.2. Methods.

5.2.2.1. Monocytes isolation

Macrophages were generated using the protocol described previously in (547, 548). Briefly, peripheral blood mononuclear cells (PBMCs) were isolated from the blood of healthy old donors for aged macrophages samples and from the buffy coat of healthy donors for young macrophages, by density gradient centrifugation using Histopaque-1077. Isolated PBMCs were counted and monocytes were isolated from PBMCs using magnetic cell separation system, MACS based on positive selection with CD14 Microbeads and LS columns. The generated monocytes were greater than 95% pure as determined by flow cytometry analysis of CD14 expression.

5.2.2. Macrophages culture and activation

Six million purified monocytes were suspended in 6 ml of RPMI-1640 medium supplemented with 10% FBS, 1% L-glutamine, 1% penicillin-streptomycin (referred as complete RPMI medium) for each sample and seeded in T25 tissue culture flasks. To obtain naïve macrophages, 50 ng/ml M-CSF was added to monocytes and incubated for 6 days at 37 °C and 5% CO_2 in a humidified incubator. On day three, 3 ml of complete RPMI-1640 medium were added containing 50 ng/ml M-

CSF. Six samples of macrophages purified from buffy coats of young individuals and 7 samples of macrophages purified from fresh blood samples of old macrophages.

5.2.2.1. Macrophage stimulation with LPS.

Stimulation was performed on another set of young macrophages (6 samples were purified from buffy coats) and old macrophages (7 samples were purified from old volunteers). On day six the medium containing M-CSF was removed and replaced with fresh complete RPMI-1640 medium. To stimulate macrophages, 100 ng/ml LPS was added and incubate for 24 hours at 37 °C and 5% CO_2 in a humidified incubator.

5.2.2.2. Sample preparation and metabolite extraction

After 6 days differentiation period or further 24 hrs treatment with LPS, the media was removed. Then, the cells were washed once with pre-warmed PBS at 37 °C. For metabolism quenching and metabolite extraction and the cells, 500 µL of pre-cooled methanol at -48 °C was used. The cells were harvested using a plastic scraper whilst being kept on ice and the extracts were transferred into pre-cooled fresh tubes at 4 °C. Followed by vortex the cell extract for 1 h and centrifugation at 16,100 xg for 10 min at 4 °C. After the centrifugation, the supernatants were dried under vacuum and reconstituted in 70 µL methanol. The extracts were then stored at -80 °C prior to LC-MS analysis. A quality control (QC) sample was prepared by mixing equal volume of each sample.

5.2.2.3. Analytical methodologies

Global LC-MS-based metabolite profiling was performed on an Accela system coupled to an Exactive MS (Thermo Fisher Scientific, Hemel Hempstead, UK) the ion source; electrospray ionisation (ESI) run in the negative (ESI-) and positive (ESI+) modes as previously described in (314). Briefly, the spray voltage was 4500 V (ESI+) and 3500 V (ESI-), capillary voltage was 30 V (ESI-) and 40 V (ESI+), and tube lens voltage was 70 V for the both negative and positive modes. skimmer voltage was 20 V (ESI+) and 18 V (ESI-). The temperature for capillary and probe was maintained at 275 °C and 150 °C, respectively. Chromatographic separation was carried out using ZIC-pHILIC (4.6 x 150 mm and 5 µm particle size, Merck Sequant). The mobile phase composed of 20 mM ammonium carbonate in water (solvent A) and 100% acetonitrile (solvent B). Metabolites were separated according to a linear gradient as follows: 0-15 min (20% A), 15-17 min (95% A), and 17-24 min (20% A) at 300 µl/min flow rate. The injection volume of 10 µl and the column was kept at 45 ^{o}C.

5.2.2.4. Data processing and metabolites identification

Raw LC-MS data were processed using XCMS and mzMatch for untargeted peak-picking and peak matching, respectively (69, 70). IDEOM was performed for putative metabolite identification and noise filtering with default parameters (315). Briefly, mass accuracy for mass identification was 3 ppm, RT for identification of authentic standards was 5%, RT for identification for calculated RT was 50 %. Metabolites were identified with confidence levels as follows; level 1 (L1) identification by matching retention times and accurate masses of authentic standards and level 2 (L2) identification when the predicted retention times were

employed due to the lack of standards according to the metabolomics standards initiative (75, 405).

Pre-processed data were analysed by performing multivariate and univariate analysis. PCA as an unsupervised model and OPLS-DA as a supervised model were carried out by SIMCA-P v13.0.2 (Umetrics, Umea, Sweden). This multivariate analysis was used as the first step for visualising data with sample classes and evaluating the metabolic difference between young and old macrophages. Also, to evaluate the metabolic difference between young-LPS and old-LPS. The key mass ions representing potential biomarkers were determined based on variable importance in projection (VIP) values obtained from two-way orthogonal comparisons. Mass ions with VIP values greater than one were considered as discriminant biomarkers. In parallel to multivariate analysis, univariate analysis was performed to identify significant mass ions. T-test with false discovery rate (FDR) correction was performed using MetaboAnalyst (24) to determine the significantly changed mass ions metabolic difference between young and old macrophages or between young-LPS and old-LPS

5.3. Results and discussion.

5.3.2. Untargeted metabolomic analysis of macrophages.

In order to explore the metabolome of macrophages, the extracted intracellular metabolites from young and old macrophages were analysed by LC-MS-based metabolite profiling. 4716 ions were detected with a total of 353 metabolites identified putatively using IDEOM (Appendix, Table A.6). Figure 5.2 shows the

molecular class composition of the macrophages metabolome with. Glycerophospholipids represent 18% of the identified metabolites, followed by 17% amino acids, 14% fatty acyls, 7% carbohydrates, 4% nucleotides, 3% sphingolipids, 3% other lipids, 2% biosynthesis of secondary metabolites, 2% of metabolites of cofactors and vitamins and 1% energy metabolism.

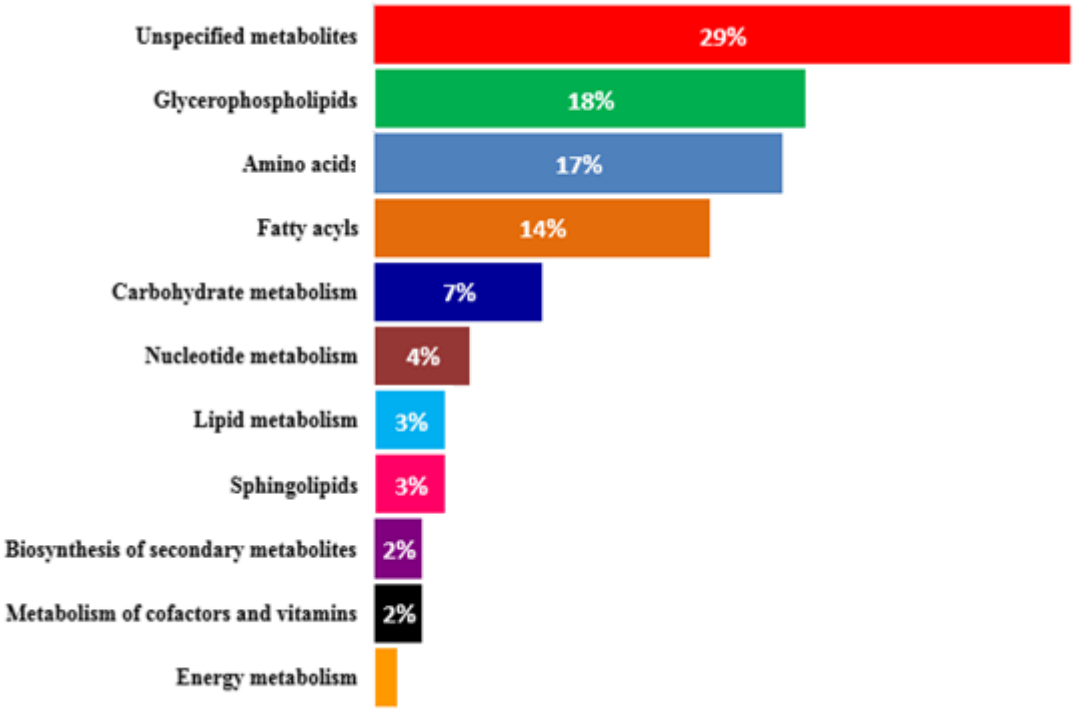


Figure 5.2: Functional categories of the intracellular metabolites produced by macrophages.

In order to investigate and compare the metabolic profiles of young and old macrophages, multivariate analysis using SIMCA-P version 13.2 has been performed. Figure 5.3 illustrated the unsupervised PCA modelling for young and old macrophages and showed no separation between these two groups. However, QC samples are clustered tightly in the PCA scores plot, indicating the stability of the method (549). For further investigation, supervised OPLS-DA modelling was conducted (Figure 5.4). The OPLS-DA showed a slight separation between young and old macrophages (R^2 and Q^2 were 0.376 and -0.048, respectively), indicating

there were no significant changes between the sample groups. R^2 measures the fitting of the model to the original data and Q^2 represents the cross validation that provides the measure of the prediction ability of this model (320). R^2 and Q^2 values should be greater than 0.5 to imply that the model is valid, and the prediction ability is accepted. R^2 and Q^2 ,below these values, indicate the invalidity of the model, and the prediction of the model is not accepted (321, 322). Also, univariate analysis showed that none of the ions have FDR values greater than 0.05. Multivariate and univariate analyses demonstrated that there is no significant difference between metabolomes of young and old macrophages under these conditions. This could be attributed to the individual variation or small sample size.

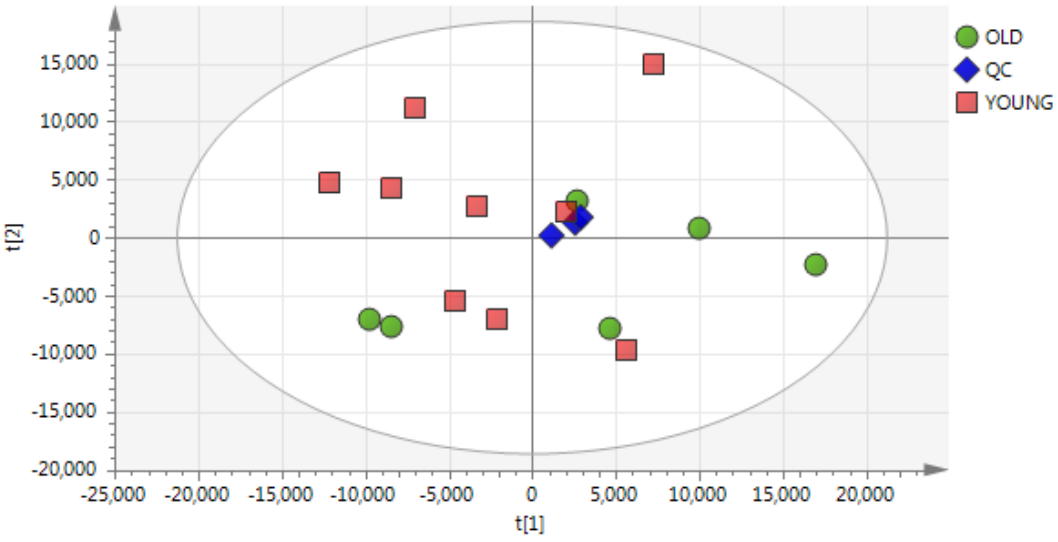


Figure 5.3: PCA score plot of young and old macrophages samples. Young (red squares), old (green circles) and QCs (dark blue diamonds). n=9 and 6 for young and old, respectively.

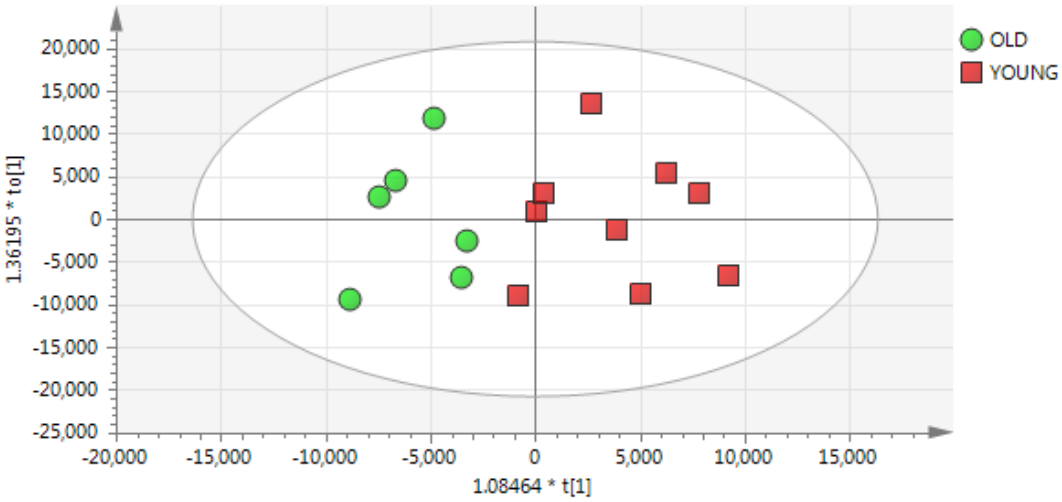


Figure 5.4: OPLS-DA score plot of young and old macrophages samples. Young (red squares), old (green circles), R^2: 0.376 and Q^2: -0.048. n=9 and 6 for young and old, respectively.

In order to investigate whether young and old macrophages show a different response to inflammatory stimuli, they were treated with LPS to produce young-LPS and old-LPS macrophages. 5711 ions were detected with a total of 385 metabolites identified using IDEOM (Appendix, Table A7). Figure 5.5 illustrates the PCA scores plot showing that there is no separation between young-LPS and old-LPS macrophages. The OPLS-DA scores plot in Figure 5.6 shows a slight separation, with R^2 and Q^2 values of 0.307 and -0.057, respectively. Based on these values, this model is invalid (321, 322). In addition, univariate analysis revealed that none of the ions has FDR values greater than 0.05. Based on these observations, no significant difference has been found between young-LPS and old-LPS macrophages under these conditions, implying the same response to LPS. Again,

this could be attributed to individual variation or small sample size. Larger sample size could reduce the effect of individual variations on the results.

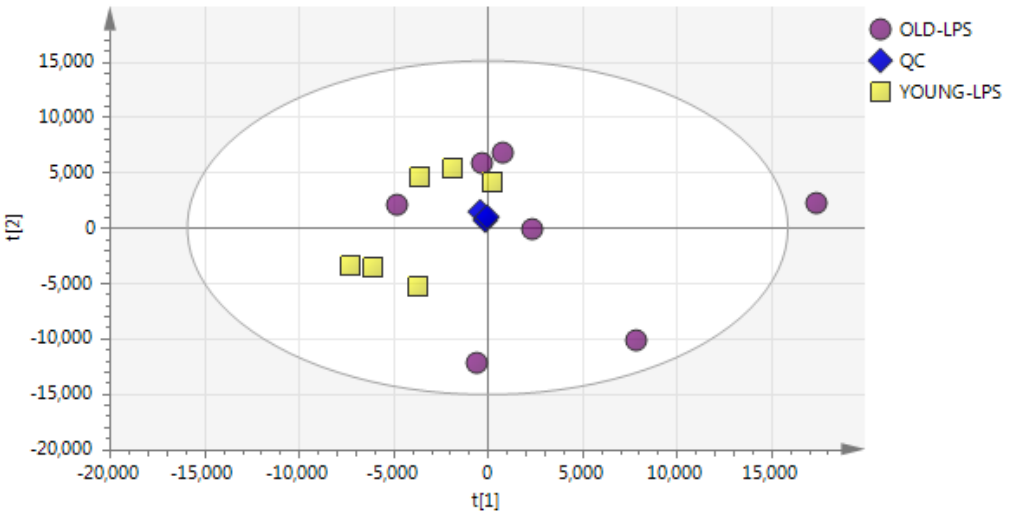


Figure 5.5: PCA score plot of young and old macrophages samples treated with LPS (young-LPS and old-LPS) respectively. Young (yellow squares) and old (purple circles). n=6 and 7 for young and old, respectively.

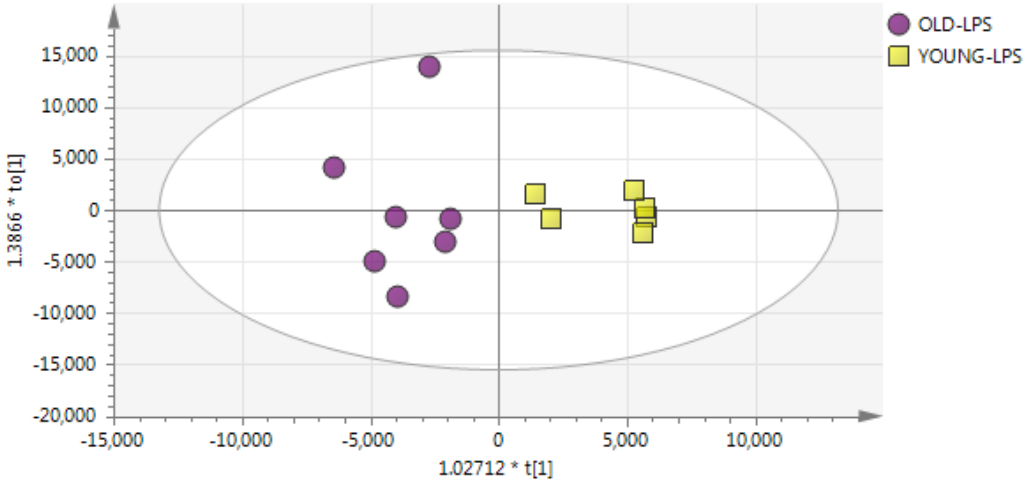


Figure 5.6: OPLS-DA score plot of LPS treated young and old macrophages (young-LPS and old-LPS) respectively. Young (yellow squares) and old (purple circles). R^2: 0.307 and Q^2: -0.057. n=6 and 7 for young and old, respectively.

Our results showed that there is no significant difference between young and old human macrophages in steady state and LPS-stimulated state. A recent metabolomics study that investigated the influence of ageing on mice macrophages demonstrated similar results for the metabolic profiles of young and old macrophages in the steady state (301). In LPS-stimulated macrophages, they demonstrated a significant difference between young and old mice metabolic profiles after four hours. However, after 16 hours stimulation, old macrophage profile were much similar to the young macrophages. This may expalian why our 24 hours-stimulated cells looked similar, implying that old macrophages showed a delay in the response to LPS stimulation (301). However, several other studies have investigated the effect of ageing on macrophages and demonstrated conflicting conclusions (527, 531). For instance, it was reported that thioglycollate-elicited peritoneal macrophages and splenic macrophages secreted lower amounts of the proinflammatory cytokines IL-6 and TNF-α in old compared to young mouse macrophages upon stimulation with TLR ligands (283). In addition, Boehmer et al. demonstrated that lower levels of IL-6 and TNF-α have been secreted in old mice in their thioglycollate-elicited peritoneal macrophages compared to young mice (284). Also, a reduction in the secretion of proinflammatory cytokines such as IL-1β, IL-6, IL-12 and TNF-α have been reported (285). In agreement with these studies, Chelvarajan et al. have demonstrated a reduction in the immune response generally and signal transduction gene particularly in old mice's macrophages as a response to LPS stimulation, in addition to the decrease in the levels of IL-6 and IL-1β with an increase of anti-inflammatory

cytokine IL-10 level (533). These changes in TLR signalling with age were suggested to be due to the decrease in TLR4 expression (283). However, TLR4 expression in macrophages have been unchanged with ageing, but the impairment of intracellular signalling could be the underlying mechanism (284). Others have proposed a reduction of CD14 expression which is a coreceptor for TLR4, could be implicated (285). In humans, several studies have been conducted to investigate the effects of ageing on cytokine production by monocytes. However, conflicting results were again demonstrated, since decreased, unchanged and increased cytokine production in response to LPS has been shown in human monocytes (282). Seidler et al. demonstrated no difference in the production of IL-6, IL-1β or TNF-α as a response to TLR4 stimulation in monocyte-derived macrophages from old and young individuals (300).

The phagocytosis function of macrophages has been investigated in the regard of ageing. In a previous study, a decrease in phagocytosis has been reported in macrophages from old mice (550). Linehan et al. investigated the phagocytosis of fluorescent particles in mice and showed significant impairment of phagocytosis in peritoneal macrophages in old mice compared to young mice *in vitro* and *in vivo.* However, they demonstrated that the changes in the microenvironment in the peritoneum upon ageing could be the reason underlying this impairment, rather than a defect in macrophages (275). In another study on rats, phagocytosis was shown to decline in neutrophils with age, while alveolar macrophages of the same model showed no change in phagocytosis (551). Also, an age-related decline in phagocytosis in mice has been demonstrated *in vivo* but not *in vitro* (552). Recently, Hearps et al. demonstrated impairment in phagocytosis by CD14+

monocytes from elderly individuals (553). However, an earlier study demonstrated no impact on phagocytosis in humans upon ageing (554).

As mentioned earlier, conflicting results could be attributed to several factors including the origin of macrophages, sex of individuals, strain and different experimental designs. Moreover, identifying healthy elderly subjects is challenging and requires careful health screening (527, 531).

5.4. Conclusion.

In this study, LC-MS metabolite profiling was used to investigate the effect of ageing on the metabolic profile of macrophages. Our results demonstrated that there is no significant difference between young and old macrophages in both steady state and upon LPS stimulation. This result could imply that there is no effect of ageing on human macrophages or could be attributed to the small sample size and the interindividual variation within the same group. The ageing process is a complex and highly challenging field, and confused by conflicting findings. This controversial data could be owed to the complexity of phenotypes that develop with age and the difficulty in studying such complex issue (275). In human models, particularly, *in vivo* and *ex vivo* experiments are challenging. Therefore, results are translated from rodents and mice to human, which is, as discussed earlier, not always an accurate reflection pf human system. In spite of the obstacles in this field, it is important to reveal the mechanisms underlying the age-related changes in the immune response. This urges more advanced strategies with more cohort research to study the effect of ageing on the immune system using a high number of samples to obtain reliable results.

Chapter Six

6. Conclusion and future work

6.1. Conclusion

The exploration of immunometabolism based on *in vitro* macrophages system could offer key information on the interplay between cell functions and metabolism. Given the mounting evidence highlighting a strong correlation between the metabolic state of macrophages and their functional activity or phenotype, metabolite profiling could be a powerful tool for a better understanding of different macrophage responses to different environmental cues (212, 305). Since LC-MS-based metabolomics approaches have expanded rapidly - especially with rapid progression in the sensitivity and selectivity of the instrument, data processing and analysis tools - LC-MS metabolomics can produce a high quality and reliable results (456).

In this work, a global LC-MS-based metabolite profiling approach was used to characterise macrophage polarisation and detect the subtle differences in the metabolic profiles of the macrophage functional subtypes. M1 and M2 subsets, as main polarisation states that represent the extremes of the wide range of macrophage polarisation, showed different metabolic responses upon polarisation indicating distinct metabolic signatures for M1 and M2 subsets. Different metabolic pathways were significantly and differentially affected as a result of polarisation, such as pyrimidine and sphingolipid metabolism in M1 macrophages. On the other hand, arginine and proline, alanine, aspartate and glutamate metabolism were disturbed significantly in M2 macrophages. Interestingly, neither glycolysis nor the tricarboxylic acid (TCA) cycle, which are reported in the literature as the hallmark metabolic pathways of M1 and M2,

respectively, showed any significant change. This could be attributed to the various polarisation protocols employed to generate a wide range of macrophages subsets and to the different species, since most of the reported conclusions were based on mice macrophages. The relevant characteristic metabolites for M1 and M2 that were identified in this work could be used as potential candidates in targeted therapy to treat several diseases, since the relationship of macrophage polarisation with cancer and certain autoimmune diseases (such chronic inflammatory diseases) have been evident. For instance, excessive activity of M1 is associated with rheumatoid arthritis, multiple sclerosis, and Crohn's disease (177, 303). Furthermore, M1 macrophages play a protective role against tumour development. On the other hand, M2 macrophages were reported to promote tumour progression and suppress anti-tumour adaptive immune responses (433). The identification of potential characteristic metabolites of M1 and M2 could also lead to a better understanding of the underlying mechanisms of macrophage polarisation which, in turn, could be utilised in the area of immune modulation and development of novel therapeutics (Chapter two).

LC-MS-based metabolite profiling was also successfully used to investigate the metabolic functional plasticity of macrophages. The work was expanded by including Mreg macrophages as a third main functional phenotype in addition to M1 and M2 macrophages. In agreement with chapter two, several metabolites were significantly distinguished in M1 or M2 macrophage demonstrating distinct metabolic signatures for each polarisation state. However, Mreg macrophages

showed a similar metabolic profile to control cells (M0), in both the steady state and the LPS-activated state, indicating that they respond to the polarisation and LPS exposure similarly at the molecular levels. The tryptophan pathway, sphingolipids, pyrimidine and purine metabolic pathways showed significant changes in their intermediates upon polarisation into M1. L-glutamate, N-acetyl-l-glutamate, N-acetyl-L-aspartate showed significant changes in M2 macrophages. Macrophages, as a heterogeneous and plastic cell type change their function and phenotype in response to environmental cues. Therefore, the plasticity of M1 and M2 macrophages was successfully investigated at the metabolic levels. M1 macrophages showed high stability and more resistance to changing their phenotype to that of M2. However, M2 macrophages demonstrated greater plasticity in changing their phenotype back to that of M1 macrophages. These results provide valuable information that can be translated into the interrogation of macrophages and reprogramming of phenotypes in certain immune-mediated diseases (Chapter three).

The emergence of antibiotic-resistant bacteria in the hospital and community urges the development of innovative approaches for diagnosis and treatment. LC-MS-based metabolite profiling was shown as a promising approach to investigate the impact of Gram-positive and Gram-negative bacteria (represented by the secretome of *S. aureus* and *P. aeruginosa*) upon the macrophage metabolic profile. The results demonstrated a differential effect of Gram-positive and Gram-negative bacteria secretomes upon macrophages. Alanine, aspartate and glutamate metabolism, sphingolipid metabolism, glycine and serine metabolism, and GL metabolism were differentially disturbed in macrophages in response to

the secretome of *S. aureus* and *P. aeruginosa*. However, a similar disturbance in arginine and proline metabolism were shown in macrophages in response to both *S. aureus* and *P. aeruginosa* secretomes. Despite some similarities, the results indicated that *S. aureus* and *P. aeruginosa* adopt different mechanisms to disturb macrophages, leading to different metabolic responses of macrophages. Moreover, *P. aeruginosa* (WT) and their mutant *P. aeruginosa* (PALT13) demonstrated a similar impact on the metabolic profile of macrophages. Significant increase in the levels of picolinic acid, N-acetyl-L-glutamate 5-semialdehyde, 5-guanidino-2-oxopentanoate and 5-aminopentanoate were shown in both *P. aeruginosa* (WT) and their mutant *P. aeruginosa* (PALT 13), with higher levels in *P. aeruginosa* (PALT 13), indicating the more chronic nature of this mutant. Therefore, different approaches would be required to discriminate strains of the same pathogen with different pathogenic potential (i.e. non-acute chronic infection vs rapidly progressing infection). Identification of potential biomarkers from these studies can be developed to provide an innovative approach for early bacterial diagnosis, potentially leading to earlier and more suitable treatments. Also, the significantly altered metabolic pathways could be selectively targeted by novel therapeutics specifically against Gram-positive or Gram-negative bacteria (Chapter four).

Ageing has attracted more attention recently due to the increase in the proportion of elderly people compared to the total populations of the globe. Ageing introduces new challenges to both individuals and society, particularly in health and diseases as it is associated with loss of physiological integrity, and increased vulnerability to infections (273, 275). LC-MS-based metabolite profiling was used

to explore the impact of ageing on the metabolic profile of macrophages. Based on our results, no significant differences were detected between young and old macrophages in either steady state or LPS activation. Conflicting results regarding ageing have been reported, likely due to the complexity of the aging process. Complex phenotypes can develope with ageing, which in addition to the challenges o performing *in vivo* and *ex vivo* experiments, makes study of this process challenging. Therefore, to date most studies have been based on rodents or mice. However, differences between species in terms of metabolism make the animal-based conclusions not entirely transferable to humans. Age-related changes in immune response and the mechanisms underpinning these changes are not fully understood. To investigate age-related changes in immune response, more sophisticated strategies encompassing a higher number of samples that could reflect the impact of ageing on immune cells and in particular macrophages are required. (Chapter five).

To conclude, LC-MS-based metabolite profiling, in this thesis, showed its value in investigating immune cell, response using THP-1 macrophages . Furthermore, identification of the key characteristic metabolites in different types of macrophage perturbation gives better insight into the mechanisms underpinning them. This has the potential to promote development of novel targeted therapeutics with selectivity towards each pathological condition. This thesis offered advantages over previous studies, since human cells were used where previous studies were largely based on animal cells. This issue may be the cause of disagreement of some of the results in this thesis with the literature, particularily regarding macropahges polarisation. This highlights the danger of

extrapolating results of animal macrophages studies to human macrophages, and suggests taking the variabiles between species into consideration. This thesis used a THP-1 cell line as a model for human macrophages in chapters two, three and four which is considered a limitation of this study. In fact, primary cells are favourable over a cell line in studying the biochemical and metabolic pathways of specific biological systems because they retain most of the phenotypic characteristics of the original tissue, i.e. they are more physiologically relevant (555). Another limitation of this study was the small sample size in chapter five studying the impact of ageing on macrophage, A better experimental design can be performed with higher number of volanteers to minimize the effect of interindividual variabilities on the results.

6.2. Future work

Based on this thesis, additional work which was beyond our scope would be beneficial. In this thesis, several classes of lipids showed significant changes upon polarisation with potential key characteristic lipids. Therefore, a comprehensive lipidomics study is our next step to investigate the exact chemical structures of those lipids which might be related to the different macrophage polarisation states. The lipidomics study requires the optimisation of extraction protocols to cover a wider range of lipids and optimised LC-MS methods. Combining lipidomics with metabolomics would provide a more comprehensive view of polarisation and macrophage responses.

Following the investigation of the impact of the secretomes from Gram-positive and Gram-negative bacteria on macrophages, *in vivo* study can be conducted by inducing actual bacterial infections to reflect actual host-pathogen interaction.

In the ageing study, a controlled larger group of subjects would be advantageous to reflect accurately the impact of ageing on the cellular processes and immune responses upon ageing, providing additional information. This could offer a further understanding of ageing consequences, leading to a better monitoring tool.

Stable isotope labeling provides vast improvements in both metabolite identification and pathway characterization. Improved confidence in molecular formula assignment can be achieved in cell-culture studies where cells can be grown on a uniformly 12C- (unlabeled) or uniformly 13C-labeled carbon source (556). In this case, the mass difference between labeled and unlabeled metabolites clearly defines the number of carbon atoms in each molecule, which significantly reduces the search space for identification of possible molecular formulas with an accurate mass that agrees with the detected mass (557). Using labelling approach in our study could improve the confidence level of metabolites identification, giving more accuarate insight into the altered pathways.

References

1. Klug WS, Ward SM. Concepts of Genetics: Pearson Benjamin Cummings; 2009.
2. Kordalewska M, Markuszewski MJ. Metabolomics in cardiovascular diseases. J Pharm Biomed Anal. 2015;113:121-36.
3. Aboud OA, Weiss RH. New opportunities from the cancer metabolome. Clin Chem. 2013;59(1):138-46.
4. Deidda M, Piras C, Bassareo PP, Cadeddu Dessalvi C, Mercuro G. Metabolomics, a promising approach to translational research in cardiology. IJC Metabolic & Endocrine. 2015;9:31-8.
5. Wikoff WR, Anfora AT, Liu J, Schultz PG, Lesley SA, Peters EC, et al. Metabolomics analysis reveals large effects of gut microflora on mammalian blood metabolites. Proceedings of the National Academy of Sciences. 2009;106(10):3698-703.
6. Nicholson JK, Lindon JC, Holmes E. 'Metabonomics': understanding the metabolic responses of living systems to pathophysiological stimuli via multivariate statistical analysis of biological NMR spectroscopic data. Xenobiotica. 1999;29(11):1181-9.
7. Zhao Y-Y, Lin R-C. UPLC–MSE application in disease biomarker discovery: The discoveries in proteomics to metabolomics. Chemico-Biological Interactions. 2014;215:7-16.
8. Junot C, Fenaille F, Colsch B, Becher F. High resolution mass spectrometry based techniques at the crossroads of metabolic pathways. Mass Spectrom Rev. 2014;33(6):471-500.
9. Collino S, Martin FP, Rezzi S. Clinical metabolomics paves the way towards future healthcare strategies. Br J Clin Pharmacol. 2013;75(3):619-29.
10. Nicholson JK, Wilson ID. Opinion: understanding 'global' systems biology: metabonomics and the continuum of metabolism. Nat Rev Drug Discov. 2003;2(8):668-76.
11. Holmes E, Wilson ID, Nicholson JK. Metabolic phenotyping in health and disease. Cell. 2008;134(5):714-7.
12. Raterink R-J, Lindenburg PW, Vreeken RJ, Ramautar R, Hankemeier T. Recent developments in sample-pretreatment techniques for mass spectrometry-based metabolomics. TrAC Trends in Analytical Chemistry. 2014;61:157-67.
13. Want EJ, Wilson ID, Gika H, Theodoridis G, Plumb RS, Shockcor J, et al. Global metabolic profiling procedures for urine using UPLC-MS. Nat Protoc. 2010;5(6):1005-18.
14. Agin A, Heintz D, Ruhland E, Chao de la Barca JM, Zumsteg J, Moal V, et al. Metabolomics – an overview. From basic principles to potential biomarkers (part 1). Médecine Nucléaire. 2016;40(1):4-10.
15. Álvarez-Sánchez B, Priego-Capote F, Luque de Castro MD. Metabolomics analysis I. Selection of biological samples and practical aspects preceding sample preparation. TrAC Trends in Analytical Chemistry. 2010;29(2):111-9.
16. Dudley E, Yousef M, Wang Y, Griffiths WJ. Targeted metabolomics and mass spectrometry. Adv Protein Chem Struct Biol. 2010;80:45-83.
17. Cuperlovic-Culf M, Barnett DA, Culf AS, Chute I. Cell culture metabolomics: applications and future directions. Drug Discov Today. 2010;15(15-16):610-21.

18. Forcisi S, Moritz F, Kanawati B, Tziotis D, Lehmann R, Schmitt-Kopplin P. Liquid chromatography-mass spectrometry in metabolomics research: mass analyzers in ultra high pressure liquid chromatography coupling. J Chromatogr A. 2013;1292:51-65.
19. Theodoridis G, Gika HG, Wilson ID. LC-MS-based methodology for global metabolite profiling in metabonomics/metabolomics. TrAC Trends in Analytical Chemistry. 2008;27(3):251-60.
20. Xu Y-J, Wang C, Ho WE, Ong CN. Recent developments and applications of metabolomics in microbiological investigations. TrAC Trends in Analytical Chemistry. 2014;56:37-48.
21. Jiao G, Li X, Zhang N, Qiu J, Xu H, Liu S. Metabolomics study on the cytotoxicity of graphene. RSC Advances. 2014;4(84):44712-7.
22. Chrysanthopoulos PK, Goudar CT, Klapa MI. Metabolomics for high-resolution monitoring of the cellular physiological state in cell culture engineering. Metab Eng. 2010;12(3):212-22.
23. Ruiz-Aracama A, Peijnenburg A, Kleinjans J, Jennen D, van Delft J, Hellfrisch C, et al. An untargeted multi-technique metabolomics approach to studying intracellular metabolites of HepG2 cells exposed to 2,3,7,8-tetrachlorodibenzo-p-dioxin. BMC Genomics. 2011;12:251.
24. Leon Z, Garcia-Canaveras JC, Donato MT, Lahoz A. Mammalian cell metabolomics: experimental design and sample preparation. Electrophoresis. 2013;34(19):2762-75.
25. Zhou B, Xiao JF, Tuli L, Ressom HW. LC-MS-based metabolomics. Mol Biosyst. 2012;8(2):470-81.
26. Vuckovic D. Current trends and challenges in sample preparation for global metabolomics using liquid chromatography-mass spectrometry. Anal Bioanal Chem. 2012;403(6):1523-48.
27. Bi H, Krausz KW, Manna SK, Li F, Johnson CH, Gonzalez FJ. Optimization of harvesting, extraction, and analytical protocols for UPLC-ESI-MS-based metabolomic analysis of adherent mammalian cancer cells. Anal Bioanal Chem. 2013;405(15):5279-89.
28. Dettmer K, Nurnberger N, Kaspar H, Gruber MA, Almstetter MF, Oefner PJ. Metabolite extraction from adherently growing mammalian cells for metabolomics studies: optimization of harvesting and extraction protocols. Anal Bioanal Chem. 2011;399(3):1127-39.
29. Bennett BD, Yuan J, Kimball EH, Rabinowitz JD. Absolute quantitation of intracellular metabolite concentrations by an isotope ratio-based approach. Nat Protoc. 2008;3(8):1299-311.
30. Teng Q, Huang W, Collette TW, Ekman DR, Tan C. A direct cell quenching method for cell-culture based metabolomics. Metabolomics. 2008;5(2):199-208.
31. Krawczyk CM, Holowka T, Sun J, Blagih J, Amiel E, DeBerardinis RJ, et al. Toll-like receptor-induced changes in glycolytic metabolism regulate dendritic cell activation. Blood. 2010;115(23):4742-9.
32. Paglia G, Hrafnsdottir S, Magnusdottir M, Fleming RM, Thorlacius S, Palsson BO, et al. Monitoring metabolites consumption and secretion in cultured cells using ultra-performance liquid chromatography quadrupole-time of flight mass spectrometry (UPLC-Q-ToF-MS). Anal Bioanal Chem. 2012;402(3):1183-98.
33. Weibel KE, Mor JR, Fiechter A. Rapid sampling of yeast cells and automated assays of adenylate, citrate, pyruvate and glucose-6-phosphate pools. Anal Biochem. 1974;58(1):208-16.
34. Sellick CA, Hansen R, Maqsood AR, Dunn WB, Stephens GM, Goodacre R, et al. Effective quenching processes for physiologically valid metabolite profiling of suspension cultured Mammalian cells. Anal Chem. 2009;81(1):174-83.

35. Winder CL, Dunn WB, Schuler S, Broadhurst D, Jarvis R, Stephens GM, et al. Global metabolic profiling of Escherichia coli cultures: an evaluation of methods for quenching and extraction of intracellular metabolites. Anal Chem. 2008;80(8):2939-48.
36. Dietmair S, Timmins NE, Gray PP, Nielsen LK, Kromer JO. Towards quantitative metabolomics of mammalian cells: development of a metabolite extraction protocol. Anal Biochem. 2010;404(2):155-64.
37. Wu Y, Li L. Development of Isotope Labeling Liquid Chromatography–Mass Spectrometry for Metabolic Profiling of Bacterial Cells and Its Application for Bacterial Differentiation. Analytical Chemistry. 2013;85(12):5755-63.
38. Fei F, Bowdish DM, McCarry BE. Comprehensive and simultaneous coverage of lipid and polar metabolites for endogenous cellular metabolomics using HILIC-TOF-MS. Anal Bioanal Chem. 2014;406(15):3723-33.
39. Duarte IF, Marques J, Ladeirinha AF, Rocha C, Lamego I, Calheiros R, et al. Analytical Approaches toward Successful Human Cell Metabolome Studies by NMR Spectroscopy. Analytical Chemistry. 2009;81(12):5023-32.
40. Yuan J, Bennett BD, Rabinowitz JD. Kinetic flux profiling for quantitation of cellular metabolic fluxes. Nat Protoc. 2008;3(8):1328-40.
41. Ritter JB, Genzel Y, Reichl U. Simultaneous extraction of several metabolites of energy metabolism and related substances in mammalian cells: optimization using experimental design. Anal Biochem. 2008;373(2):349-69.
42. Duportet X, Aggio RBM, Carneiro S, Villas-Bôas SG. The biological interpretation of metabolomic data can be misled by the extraction method used. Metabolomics. 2012;8(3):410-21.
43. Lorenz MA, Burant CF, Kennedy RT. Reducing time and increasing sensitivity in sample preparation for adherent mammalian cell metabolomics. Anal Chem. 2011;83(9):3406-14.
44. Madji Hounoum B, Blasco H, Emond P, Mavel S. Liquid chromatography–high-resolution mass spectrometry-based cell metabolomics: Experimental design, recommendations, and applications. TrAC Trends in Analytical Chemistry. 2016;75:118-28.
45. Sellick CA, Knight D, Croxford AS, Maqsood AR, Stephens GM, Goodacre R, et al. Evaluation of extraction processes for intracellular metabolite profiling of mammalian cells: matching extraction approaches to cell type and metabolite targets. Metabolomics. 2010;6(3):427-38.
46. Danielsson AP, Moritz T, Mulder H, Spegel P. Development and optimization of a metabolomic method for analysis of adherent cell cultures. Anal Biochem. 2010;404(1):30-9.
47. Fernandez C, Fransson U, Hallgard E, Spegel P, Holm C, Krogh M, et al. Metabolomic and proteomic analysis of a clonal insulin-producing beta-cell line (INS-1 832/13). J Proteome Res. 2008;7(1):400-11.
48. Korinek M, Sistek V, Mladkova J, Mikes P, Jiracek J, Selicharova I. Quantification of homocysteine-related metabolites and the role of betaine-homocysteine S-methyltransferase in HepG2 cells. Biomed Chromatogr. 2013;27(1):111-21.
49. Bai J, Wang MX, Chowbay B, Ching CB, Chen WN. Metabolic profiling of HepG2 cells incubated with S(−) and R(+) enantiomers of anti-coagulating drug warfarin. Metabolomics. 2011;7(3):353-62.
50. Cao B, Aa J, Wang G, Wu X, Liu L, Li M, et al. GC-TOFMS analysis of metabolites in adherent MDCK cells and a novel strategy for identifying intracellular metabolic markers for use as cell amount indicators in data normalization. Anal Bioanal Chem. 2011;400(9):2983-93.

51. Haynes CA, Allegood JC, Sims K, Wang EW, Sullards MC, Merrill AH, Jr. Quantitation of fatty acyl-coenzyme As in mammalian cells by liquid chromatography-electrospray ionization tandem mass spectrometry. J Lipid Res. 2008;49(5):1113-25.
52. Chong WP, Thng SH, Hiu AP, Lee DY, Chan EC, Ho YS. LC-MS-based metabolic characterization of high monoclonal antibody-producing Chinese hamster ovary cells. Biotechnol Bioeng. 2012;109(12):3103-11.
53. Selvarasu S, Ho YS, Chong WP, Wong NS, Yusufi FN, Lee YY, et al. Combined in silico modeling and metabolomics analysis to characterize fed-batch CHO cell culture. Biotechnol Bioeng. 2012;109(6):1415-29.
54. Ser Z, Liu X, Tang NN, Locasale JW. Extraction parameters for metabolomics from cultured cells. Anal Biochem. 2015;475:22-8.
55. Wojakowska A, Chekan M, Widlak P, Pietrowska M. Application of Metabolomics in Thyroid Cancer Research. International Journal of Endocrinology. 2015;2015:13.
56. Dunn WB, Bailey NJ, Johnson HE. Measuring the metabolome: current analytical technologies. Analyst. 2005;130(5):606-25.
57. Dettmer K, Aronov PA, Hammock BD. Mass spectrometry-based metabolomics. Mass Spectrom Rev. 2007;26(1):51-78.
58. Lenz EM, Wilson ID. Analytical strategies in metabonomics. J Proteome Res. 2007;6(2):443-58.
59. Narainsamy K, Cassier-Chauvat C, Junot C, Chauvat F. High performance analysis of the cyanobacterial metabolism via liquid chromatography coupled to a LTQ-Orbitrap mass spectrometer: evidence that glucose reprograms the whole carbon metabolism and triggers oxidative stress. Metabolomics. 2013;9(1):21-32.
60. Glauser G, Veyrat N, Rochat B, Wolfender JL, Turlings TC. Ultra-high pressure liquid chromatography-mass spectrometry for plant metabolomics: a systematic comparison of high-resolution quadrupole-time-of-flight and single stage Orbitrap mass spectrometers. J Chromatogr A. 2013;1292:151-9.
61. Fenn JB, Mann M, Meng CK, Wong SF, Whitehouse CM. Electrospray ionization for mass spectrometry of large biomolecules. Science. 1989;246(4926):64-71.
62. Watson AD. Thematic review series: systems biology approaches to metabolic and cardiovascular disorders. Lipidomics: a global approach to lipid analysis in biological systems. J Lipid Res. 2006;47(10):2101-11.
63. Han X, Gross RW. Shotgun lipidomics: Electrospray ionization mass spectrometric analysis and quantitation of cellular lipidomes directly from crude extracts of biological samples. Mass Spectrom Rev. 2005;24(3):367-412.
64. Denisov E, Damoc E, Lange O, Makarov A. Orbitrap mass spectrometry with resolving powers above 1,000,000. International Journal of Mass Spectrometry. 2012;325-327:80-5.
65. Krauss M, Singer H, Hollender J. LC-high resolution MS in environmental analysis: from target screening to the identification of unknowns. Anal Bioanal Chem. 2010;397(3):943-51.
66. Roy-Lachapelle A, Solliec M, Sinotte M, Deblois C, Sauve S. High resolution/accurate mass (HRMS) detection of anatoxin-a in lake water using LDTD-APCI coupled to a Q-Exactive mass spectrometer. Talanta. 2015;132:836-44.
67. Patterson AD, Li H, Eichler GS, Krausz KW, Weinstein JN, Fornace AJ, Jr., et al. UPLC-ESI-TOFMS-based metabolomics and gene expression dynamics inspector self-organizing metabolomic maps as tools for understanding the cellular response to ionizing radiation. Anal Chem. 2008;80(3):665-74.
68. Chokkathukalam A, Jankevics A, Creek DJ, Achcar F, Barrett MP, Breitling R. mzMatch-ISO: an R tool for the annotation and relative quantification of isotope-labelled mass spectrometry data. Bioinformatics (Oxford, England). 2013;29(2):281-3.

69. Tautenhahn R, Bottcher C, Neumann S. Highly sensitive feature detection for high resolution LC/MS. BMC bioinformatics. 2008;9:504.
70. Scheltema RA, Jankevics A, Jansen RC, Swertz MA, Breitling R. PeakML/mzMatch: a file format, Java library, R library, and tool-chain for mass spectrometry data analysis. Analytical chemistry. 2011;83(7):2786-93.
71. Creek DJ, Jankevics A, Burgess KEV, Breitling R, Barrett MP. IDEOM: an Excel interface for analysis of LC–MS-based metabolomics data. Bioinformatics (Oxford, England). 2012;28(7):1048-9.
72. Wishart DS, Jewison T, Guo AC, Wilson M, Knox C, Liu Y, et al. HMDB 3.0—The Human Metabolome Database in 2013. Nucleic acids research. 2012;41(D1):D801-D7.
73. Smith CA, O'Maille G, Want EJ, Qin C, Trauger SA, Brandon TR, et al. METLIN: a metabolite mass spectral database. Therapeutic drug monitoring. 2005;27(6):747-51.
74. Sumner L, Lei Z, Nikolau B, Saito K, Roessner U, Trengove R. Proposed quantitative and alphanumeric metabolite identification metrics2014. 1047-9 p.
75. Sumner LW, Amberg A, Barrett D, Beale MH, Beger R, Daykin CA, et al. Proposed minimum reporting standards for chemical analysis Chemical Analysis Working Group (CAWG) Metabolomics Standards Initiative (MSI). Metabolomics : Official journal of the Metabolomic Society. 2007;3(3):211-21.
76. Andersen AH, Rayens WS, Liu Y, Smith CD. Partial Least Squares for Discrimination in fMRI Data. Magnetic Resonance Imaging. 2012;30(3):446-52.
77. Brereton RG. Chemometrics for Pattern Recognition: Wiley; 2009.
78. Xia J, Psychogios N, Young N, Wishart DS. MetaboAnalyst: a web server for metabolomic data analysis and interpretation. Nucleic acids research. 2009;37(Web Server issue):W652-60.
79. Dunn WB, Broadhurst DI, Atherton HJ, Goodacre R, Griffin JL. Systems level studies of mammalian metabolomes: the roles of mass spectrometry and nuclear magnetic resonance spectroscopy. Chem Soc Rev. 2011;40(1):387-426.
80. Martineau E, Tea I, Loaec G, Giraudeau P, Akoka S. Strategy for choosing extraction procedures for NMR-based metabolomic analysis of mammalian cells. Anal Bioanal Chem. 2011;401(7):2133-42.
81. Antignac J-P, de Wasch K, Monteau F, De Brabander H, Andre F, Le Bizec B. The ion suppression phenomenon in liquid chromatography–mass spectrometry and its consequences in the field of residue analysis. Analytica Chimica Acta. 2005;529(1–2):129-36.
82. Kosmides AK, Kamisoglu K, Calvano SE, Corbett SA, Androulakis IP. Metabolomic fingerprinting: challenges and opportunities. Crit Rev Biomed Eng. 2013;41(3):205-21.
83. Cortes M, Pareja E, Castell JV, Moya A, Mir J, Lahoz A. Exploring mass spectrometry suitability to examine human liver graft metabonomic profiles. Transplant Proc. 2010;42(8):2953-8.
84. Wu H, Southam AD, Hines A, Viant MR. High-throughput tissue extraction protocol for NMR- and MS-based metabolomics. Anal Biochem. 2008;372(2):204-12.
85. Palmer JA, Smith AM, Egnash LA, Conard KR, West PR, Burrier RE, et al. Establishment and assessment of a new human embryonic stem cell-based biomarker assay for developmental toxicity screening. Birth Defects Res B Dev Reprod Toxicol. 2013;98(4):343-63.
86. Allen J, Davey HM, Broadhurst D, Heald JK, Rowland JJ, Oliver SG, et al. High-throughput classification of yeast mutants for functional genomics using metabolic footprinting. Nat Biotechnol. 2003;21(6):692-6.
87. Hollenbaugh JA, Munger J, Kim B. Metabolite profiles of human immunodeficiency virus infected CD4+ T cells and macrophages using LC-MS/MS analysis. Virology. 2011;415(2):153-9.

88. Tannahill GM, Curtis AM, Adamik J, Palsson-McDermott EM, McGettrick AF, Goel G, et al. Succinate is a danger signal that induces IL-1β via HIF-1α. Nature. 2013;496(7444):238-42.
89. Epelman S, Lavine KJ, Randolph GJ. Origin and functions of tissue macrophages. Immunity. 2014;41(1):21-35.
90. Nathan C. Metchnikoff's Legacy in 2008. Nat Immunol. 2008;9(7):695-8.
91. Takahashi K. Development and Differentiation of Macrophages and Related Cells

Historical Review and Current Concepts. Journal of Clinical and Experimental Hematopathology. 2001;41(1):1-31.
92. Cooper MD, Alder MN. The evolution of adaptive immune systems. Cell. 2006;124(4):815-22.
93. Tauber AI. Metchnikoff and the phagocytosis theory. Nature reviews Molecular cell biology. 2003;4(11):897-901.
94. Aschoff L. Das reticulo-endotheliale System. In: Kraus F, Meyer E, Minkowski O, Müller F, Sahli H, Schittenhelm A, et al., editors. Ergebnisse der Inneren Medizin und Kinderheilkunde: Sechsundzwanzigster Band. Berlin, Heidelberg: Springer Berlin Heidelberg; 1924. p. 1-118.
95. van Furth R, Cohn ZA, Hirsch JG, Humphrey JH, Spector WG, Langevoort HL. The mononuclear phagocyte system: a new classification of macrophages, monocytes, and their precursor cells. Bulletin of the World Health Organization. 1972;46(6):845-52.
96. Van Furth R. Current View on the Mononuclear Phagocyte System. Immunobiology. 1982;161(3):178-85.
97. Volkman A, Chang NC, Strausbauch PH, Morahan PS. Differential effects of chronic monocyte depletion on macrophage populations. Laboratory investigation; a journal of technical methods and pathology. 1983;49(3):291-8.
98. Ginhoux F, Greter M, Leboeuf M, Nandi S, See P, Gokhan S, et al. Fate mapping analysis reveals that adult microglia derive from primitive macrophages. Science (New York, NY). 2010;330(6005):841-5.
99. Schulz C, Perdiguero EG, Chorro L, Szabo-Rogers H, Cagnard N, Kierdorf K, et al. A Lineage of Myeloid Cells Independent of Myb and Hematopoietic Stem Cells. Science (New York, NY). 2012;336(6077):86.
100. Yona S, Kim KW, Wolf Y, Mildner A, Varol D, Breker M, et al. Fate mapping reveals origins and dynamics of monocytes and tissue macrophages under homeostasis. Immunity. 2013;38(1):79-91.
101. Hashimoto D, Chow A, Noizat C, Teo P, Beasley MB, Leboeuf M, et al. Tissue-resident macrophages self-maintain locally throughout adult life with minimal contribution from circulating monocytes. Immunity. 2013;38(4):792-804.
102. Epelman S, Lavine KJ, Beaudin AE, Sojka DK, Carrero JA, Calderon B, et al. Embryonic and adult-derived resident cardiac macrophages are maintained through distinct mechanisms at steady state and during inflammation. Immunity. 2014;40(1):91-104.
103. Guilliams M, De Kleer I, Henri S, Post S, Vanhoutte L, De Prijck S, et al. Alveolar macrophages develop from fetal monocytes that differentiate into long-lived cells in the first week of life via GM-CSF. The Journal of experimental medicine. 2013;210(10):1977-92.
104. Jakubzick C, Gautier EL, Gibbings SL, Sojka DK, Schlitzer A, Johnson TE, et al. Minimal differentiation of classical monocytes as they survey steady-state tissues and transport antigen to lymph nodes. Immunity. 2013;39(3):599-610.
105. Martinez FO, Sica A, Mantovani A, Locati M. Macrophage activation and polarization. Frontiers in bioscience : a journal and virtual library. 2008;13:453-61.

106. Mercer J, Greber UF. Virus interactions with endocytic pathways in macrophages and dendritic cells. Trends in microbiology. 2013;21(8):380-8.
107. Vega MA, Corbi A. Human macrophage activation: Too many functions and phenotypes for a single cell type. Inmunologia. 2006;25:248-72.
108. Mosser DM, Edwards JP. Exploring the full spectrum of macrophage activation. Nature reviews Immunology. 2008;8(12):958-69.
109. Andrews NC. Forging a field: the golden age of iron biology. Blood. 2008;112(2):219-30.
110. De Domenico I, McVey Ward D, Kaplan J. Regulation of iron acquisition and storage: consequences for iron-linked disorders. Nature reviews Molecular cell biology. 2008;9(1):72-81.
111. Kono H, Rock KL. How dying cells alert the immune system to danger. Nature reviews Immunology. 2008;8(4):279-89.
112. Pei Y, Yeo Y. Drug delivery to macrophages: Challenges and opportunities. Journal of Controlled Release. 2016;240:202-11.
113. Gordon S. Pattern Recognition Receptors: Doubling Up for the Innate Immune Response. Cell. 2002;111(7):927-30.
114. Takeuchi O, Akira S. Pattern recognition receptors and inflammation. Cell. 2010;140(6):805-20.
115. Akira S, Uematsu S, Takeuchi O. Pathogen recognition and innate immunity. Cell. 2006;124(4):783-801.
116. Medzhitov R, Preston-Hurlburt P, Janeway CA, Jr. A human homologue of the Drosophila Toll protein signals activation of adaptive immunity. Nature. 1997;388(6640):394-7.
117. Kumagai Y, Akira S. Identification and functions of pattern-recognition receptors. J Allergy Clin Immunol. 2010;125(5):985-92.
118. Takeda K, Kaisho T, Akira S. Toll-like receptors. Annu Rev Immunol. 2003;21:335-76.
119. Chen G, Shaw MH, Kim YG, Nunez G. NOD-like receptors: role in innate immunity and inflammatory disease. Annu Rev Pathol. 2009;4:365-98.
120. Sabbah A, Chang TH, Harnack R, Frohlich V, Tominaga K, Dube PH, et al. Activation of innate immune antiviral responses by Nod2. Nat Immunol. 2009;10(10):1073-80.
121. Yerkovich ST, Upham JW. 12 - Interactions between allergens and dendritic cells: pattern recognition receptors and their function in the pathogenesis of allergic respiratory diseases A2 - Williams, Marc A. Allergens and Respiratory Pollutants: Woodhead Publishing; 2011. p. 245-75.
122. Rothenfusser S, Goutagny N, DiPerna G, Gong M, Monks BG, Schoenemeyer A, et al. The RNA helicase Lgp2 inhibits TLR-independent sensing of viral replication by retinoic acid-inducible gene-I. J Immunol. 2005;175(8):5260-8.
123. Robinson MJ, Sancho D, Slack EC, LeibundGut-Landmann S, Reis e Sousa C. Myeloid C-type lectins in innate immunity. Nat Immunol. 2006;7(12):1258-65.
124. Zelensky AN, Gready JE. The C-type lectin-like domain superfamily. FEBS J. 2005;272(24):6179-217.
125. Salazar F, Hall L, Negm OH, Awuah D, Tighe PJ, Shakib F, et al. The mannose receptor negatively modulates the Toll-like receptor 4-aryl hydrocarbon receptor-indoleamine 2,3-dioxygenase axis in dendritic cells affecting T helper cell polarization. J Allergy Clin Immunol. 2016;137(6):1841-51 e2.
126. Gordon S. The macrophage: Past, present and future. European Journal of Immunology. 2007;37(S1):S9-S17.
127. Gordon S, Taylor PR. Monocyte and macrophage heterogeneity. Nature reviews Immunology. 2005;5(12):953-64.

128. Wynn TA, Chawla A, Pollard JW. Macrophage biology in development, homeostasis and disease. Nature. 2013;496(7446):445-55.
129. Vogel DY, Glim JE, Stavenuiter AW, Breur M, Heijnen P, Amor S, et al. Human macrophage polarization in vitro: maturation and activation methods compared. Immunobiology. 2014;219(9):695-703.
130. Ambarus CA, Krausz S, van Eijk M, Hamann J, Radstake TR, Reedquist KA, et al. Systematic validation of specific phenotypic markers for in vitro polarized human macrophages. Journal of immunological methods. 2012;375(1-2):196-206.
131. Gordon S. Alternative activation of macrophages. Nature reviews Immunology. 2003;3(1):23-35.
132. Sica A, Mantovani A. Macrophage plasticity and polarization: in vivo veritas. J Clin Invest. 2012;122(3):787-95.
133. Biswas SK, Mantovani A. Macrophage plasticity and interaction with lymphocyte subsets: cancer as a paradigm. Nat Immunol. 2010;11(10):889-96.
134. Gordon S, Martinez FO. Alternative activation of macrophages: mechanism and functions. Immunity. 2010;32(5):593-604.
135. Lawrence T, Natoli G. Transcriptional regulation of macrophage polarization: enabling diversity with identity. Nature reviews Immunology. 2011;11(11):750-61.
136. Mantovani A, Sica A, Locati M. Macrophage Polarization Comes of Age. Immunity. 2005;23(4):344-6.
137. Murray PJ, Wynn TA. Protective and pathogenic functions of macrophage subsets. Nature reviews Immunology. 2011;11(11):723-37.
138. Wynn TA, Chawla A, Pollard JW. Macrophage biology in development, homeostasis and disease. Nature. 2013;496(7446):445-55.
139. Xue J, Schmidt SV, Sander J, Draffehn A, Krebs W, Quester I, et al. Transcriptome-based network analysis reveals a spectrum model of human macrophage activation. Immunity. 2014;40(2):274-88.
140. Filardy AA, Pires DR, Nunes MP, Takiya CM, Freire-de-Lima CG, Ribeiro-Gomes FL, et al. Proinflammatory clearance of apoptotic neutrophils induces an IL-12(low)IL-10(high) regulatory phenotype in macrophages. Journal of immunology (Baltimore, Md : 1950). 2010;185(4):2044-50.
141. Boorsma CE, Draijer C, Melgert BN. Macrophage heterogeneity in respiratory diseases. Mediators of inflammation. 2013;2013:769214.
142. Chow A, Brown BD, Merad M. Studying the mononuclear phagocyte system in the molecular age. Nature reviews Immunology. 2011;11(11):788-98.
143. Chistiakov DA, Bobryshev YV, Nikiforov NG, Elizova NV, Sobenin IA, Orekhov AN. Macrophage phenotypic plasticity in atherosclerosis: The associated features and the peculiarities of the expression of inflammatory genes. International journal of cardiology. 2015;184:436-45.
144. Adams DO. Molecular interactions in macrophage activation. Immunology today. 1989;10(2):33-5.
145. Leidi M, Gotti E, Bologna L, Miranda E, Rimoldi M, Sica A, et al. M2 macrophages phagocytose rituximab-opsonized leukemic targets more efficiently than m1 cells in vitro. Journal of immunology (Baltimore, Md : 1950). 2009;182(7):4415-22.
146. Shapouri-Moghaddam A, Mohammadian S, Vazini H, Taghadosi M, Esmaeili S-A, Mardani F, et al. Macrophage plasticity, polarization and function in health and disease: Macrophages in Health and Disease. Journal of cellular physiology. 2018;233.
147. Dale DC, Boxer L, Liles WC. The phagocytes: neutrophils and monocytes. Blood. 2008;112(4):935-45.
148. Ezekowitz RA, Gordon S. Alterations of surface properties by macrophage activation: expression of receptors for Fc and mannose-terminal glycoproteins and differentiation antigens. Contemporary topics in immunobiology. 1984;13:33-56.

149. Mosser DM, Handman E. Treatment of murine macrophages with interferon-gamma inhibits their ability to bind leishmania promastigotes. Journal of leukocyte biology. 1992;52(4):369-76.
150. O'Shea JJ, Murray PJ. Cytokine signaling modules in inflammatory responses. Immunity. 2008;28(4):477-87.
151. Mackaness GB. Cellular immunity and the parasite. Advances in experimental medicine and biology. 1977;93:65-73.
152. Kolls JK, Linden A. Interleukin-17 family members and inflammation. Immunity. 2004;21(4):467-76.
153. Bashir S, Sharma Y, Elahi A, Khan F. Macrophage polarization: the link between inflammation and related diseases. Inflammation research : official journal of the European Histamine Research Society [et al]. 2016;65(1):1-11.
154. Erwig LP, Henson PM. Immunological consequences of apoptotic cell phagocytosis. The American journal of pathology. 2007;171(1):2-8.
155. Wang N, Liang H, Zen K. Molecular mechanisms that influence the macrophage m1-m2 polarization balance. Frontiers in immunology. 2014;5:614-.
156. Loke P, Gallagher I, Nair MG, Zang X, Brombacher F, Mohrs M, et al. Alternative activation is an innate response to injury that requires CD4+ T cells to be sustained during chronic infection. Journal of immunology (Baltimore, Md : 1950). 2007;179(6):3926-36.
157. Reese TA, Liang HE, Tager AM, Luster AD, Van Rooijen N, Voehringer D, et al. Chitin induces accumulation in tissue of innate immune cells associated with allergy. Nature. 2007;447(7140):92-6.
158. Kreider T, Anthony RM, Urban JF, Jr., Gause WC. Alternatively activated macrophages in helminth infections. Current opinion in immunology. 2007;19(4):448-53.
159. Chanput W, Mes JJ, Savelkoul HF, Wichers HJ. Characterization of polarized THP-1 macrophages and polarizing ability of LPS and food compounds. Food & function. 2013;4(2):266-76.
160. Braga TT, Agudelo JS, Camara NO. Macrophages During the Fibrotic Process: M2 as Friend and Foe. Front Immunol. 2015;6:602.
161. Locati M, Mantovani A, Sica A. Chapter Six - Macrophage Activation and Polarization as an Adaptive Component of Innate Immunity. In: Murphy KM, Merad M, editors. Advances in immunology. 120: Academic Press; 2013. p. 163-84.
162. Beschin A, De Baetselier P, Van Ginderachter JA. Contribution of myeloid cell subsets to liver fibrosis in parasite infection. The Journal of pathology. 2013;229(2):186-97.
163. Chua CL, Brown G, Hamilton JA, Rogerson S, Boeuf P. Monocytes and macrophages in malaria: protection or pathology? Trends in parasitology. 2013;29(1):26-34.
164. Hinz B, Phan SH, Thannickal VJ, Prunotto M, Desmouliere A, Varga J, et al. Recent developments in myofibroblast biology: paradigms for connective tissue remodeling. The American journal of pathology. 2012;180(4):1340-55.
165. Belgiovine C, D'Incalci M, Allavena P, Frapolli R. Tumor-associated macrophages and anti-tumor therapies: complex links. Cellular and molecular life sciences : CMLS. 2016;73(13):2411-24.
166. Porta C, Riboldi E, Ippolito A, Sica A. Molecular and epigenetic basis of macrophage polarized activation. Seminars in immunology. 2015;27(4):237-48.
167. Qian BZ, Pollard JW. Macrophage diversity enhances tumor progression and metastasis. Cell. 2010;141(1):39-51.
168. Sternberg EM. Neural regulation of innate immunity: a coordinated nonspecific host response to pathogens. Nature reviews Immunology. 2006;6(4):318-28.

169. Mosser DM. The many faces of macrophage activation. Journal of leukocyte biology. 2003;73(2):209-12.
170. Gerber JS, Mosser DM. Reversing lipopolysaccharide toxicity by ligating the macrophage Fc gamma receptors. Journal of immunology (Baltimore, Md : 1950). 2001;166(11):6861-8.
171. Strassmann G, Patil-Koota V, Finkelman F, Fong M, Kambayashi T. Evidence for the involvement of interleukin 10 in the differential deactivation of murine peritoneal macrophages by prostaglandin E2. The Journal of experimental medicine. 1994;180(6):2365-70.
172. Hasko G, Pacher P, Deitch EA, Vizi ES. Shaping of monocyte and macrophage function by adenosine receptors. Pharmacology & therapeutics. 2007;113(2):264-75.
173. Bogdan C, Paik J, Vodovotz Y, Nathan C. Contrasting mechanisms for suppression of macrophage cytokine release by transforming growth factor-beta and interleukin-10. The Journal of biological chemistry. 1992;267(32):23301-8.
174. Liu YC, Zou XB, Chai YF, Yao YM. Macrophage polarization in inflammatory diseases. International journal of biological sciences. 2014;10(5):520-9.
175. Gu Q, Yang H, Shi Q. Macrophages and bone inflammation. Journal of Orthopaedic Translation. 2017;10:86-93.
176. Bruck W, Sommermeier N, Bergmann M, Zettl U, Goebel HH, Kretzschmar HA, et al. Macrophages in multiple sclerosis. Immunobiology. 1996;195(4-5):588-600.
177. Smith AM, Rahman FZ, Hayee B, Graham SJ, Marks DJ, Sewell GW, et al. Disordered macrophage cytokine secretion underlies impaired acute inflammation and bacterial clearance in Crohn's disease. The Journal of experimental medicine. 2009;206(9):1883-97.
178. Tilg H, Diehl AM. Cytokines in alcoholic and nonalcoholic steatohepatitis. The New England journal of medicine. 2000;343(20):1467-76.
179. Viola J, Soehnlein O. Atherosclerosis - A matter of unresolved inflammation. Seminars in immunology. 2015;27(3):184-93.
180. Kraakman MJ, Murphy AJ, Jandeleit-Dahm K, Kammoun HL. Macrophage Polarization in Obesity and Type 2 Diabetes: Weighing Down Our Understanding of Macrophage Function? Frontiers in Immunology. 2014;5:470.
181. Cuda CM, Pope RM, Perlman H. The inflammatory role of phagocyte apoptotic pathways in rheumatic diseases. Nature reviews Rheumatology. 2016;12(9):543-58.
182. Jiang Z, Jiang JX, Zhang GX. Macrophages: a double-edged sword in experimental autoimmune encephalomyelitis. Immunology letters. 2014;160(1):17-22.
183. Udalova IA, Mantovani A, Feldmann M. Macrophage heterogeneity in the context of rheumatoid arthritis. Nature reviews Rheumatology. 2016;12(8):472-85.
184. Klareskog L, Padyukov L, Ronnelid J, Alfredsson L. Genes, environment and immunity in the development of rheumatoid arthritis. Current opinion in immunology. 2006;18(6):650-5.
185. McVicker BL, Tuma DJ, Casey CA. Effect of ethanol on pro-apoptotic mechanisms in polarized hepatic cells. World J Gastroenterol. 2007;13(37):4960-6.
186. Nagy LE. Recent insights into the role of the innate immune system in the development of alcoholic liver disease. Experimental biology and medicine (Maywood, NJ). 2003;228(8):882-90.
187. Marks DJB, Segal AW. Innate immunity in inflammatory bowel disease: a disease hypothesis. The Journal of pathology. 2008;214(2):260-6.
188. Pugliatti M, Sotgiu S, Rosati G. The worldwide prevalence of multiple sclerosis. Clinical neurology and neurosurgery. 2002;104(3):182-91.
189. Martin R, McFarland HF, McFarlin DE. Immunological aspects of demyelinating diseases. Annual review of immunology. 1992;10:153-87.

190. van der Valk P, De Groot CJ. Staging of multiple sclerosis (MS) lesions: pathology of the time frame of MS. Neuropathology and applied neurobiology. 2000;26(1):2-10.
191. Kigerl KA, Gensel JC, Ankeny DP, Alexander JK, Donnelly DJ, Popovich PG. Identification of two distinct macrophage subsets with divergent effects causing either neurotoxicity or regeneration in the injured mouse spinal cord. J Neurosci. 2009;29(43):13435-44.
192. Abdul-Majid KB, Stefferl A, Bourquin C, Lassmann H, Linington C, Olsson T, et al. Fc receptors are critical for autoimmune inflammatory damage to the central nervous system in experimental autoimmune encephalomyelitis. Scandinavian journal of immunology. 2002;55(1):70-81.
193. Bitsch A, Kuhlmann T, Da Costa C, Bunkowski S, Polak T, Bruck W. Tumour necrosis factor alpha mRNA expression in early multiple sclerosis lesions: correlation with demyelinating activity and oligodendrocyte pathology. Glia. 2000;29(4):366-75.
194. Sarchielli P, Greco L, Floridi A, Floridi A, Gallai V. Excitatory amino acids and multiple sclerosis: evidence from cerebrospinal fluid. Archives of neurology. 2003;60(8):1082-8.
195. Smith KJ, Lassmann H. The role of nitric oxide in multiple sclerosis. The Lancet Neurology. 2002;1(4):232-41.
196. Tabas I, Bornfeldt KE. Macrophage Phenotype and Function in Different Stages of Atherosclerosis. Circulation research. 2016;118(4):653-67.
197. Moore KJ, Sheedy FJ, Fisher EA. Macrophages in atherosclerosis: a dynamic balance. Nature reviews Immunology. 2013;13(10):709-21.
198. Moore KJ, Tabas I. Macrophages in the pathogenesis of atherosclerosis. Cell. 2011;145(3):341-55.
199. Randolph GJ. Emigration of monocyte-derived cells to lymph nodes during resolution of inflammation and its failure in atherosclerosis. Curr Opin Lipidol. 2008;19(5):462-8.
200. Lewis CE, Pollard JW. Distinct role of macrophages in different tumor microenvironments. Cancer research. 2006;66(2):605-12.
201. Pollard JW. Tumour-educated macrophages promote tumour progression and metastasis. Nat Rev Cancer. 2004;4(1):71-8.
202. Ruffell B, Affara NI, Coussens LM. Differential macrophage programming in the tumor microenvironment. Trends in immunology. 2012;33(3):119-26.
203. Squadrito ML, De Palma M. Macrophage regulation of tumor angiogenesis: implications for cancer therapy. Molecular aspects of medicine. 2011;32(2):123-45.
204. Funes SC, Rios M, Escobar-Vera J, Kalergis AM. Implications of macrophage polarization in autoimmunity. Immunology. 2018;154(2):186-95.
205. Galli SJ, Borregaard N, Wynn TA. Phenotypic and functional plasticity of cells of innate immunity: macrophages, mast cells and neutrophils. Nature immunology. 2011;12(11):1035-44.
206. Biswas SK, Mantovani A. Orchestration of metabolism by macrophages. Cell metabolism. 2012;15(4):432-7.
207. Lackey DE, Olefsky JM. Regulation of metabolism by the innate immune system. Nature reviews Endocrinology. 2016;12(1):15-28.
208. Pearce EL. Metabolism in T cell activation and differentiation. Current opinion in immunology. 2010;22(3):314-20.
209. Pearce EL, Poffenberger MC, Chang CH, Jones RG. Fueling immunity: insights into metabolism and lymphocyte function. Science (New York, NY). 2013;342(6155):1242454.
210. Kelly B, O'Neill LA. Metabolic reprogramming in macrophages and dendritic cells in innate immunity. Cell research. 2015;25(7):771-84.

211. Orihuela R, McPherson CA, Harry GJ. Microglial M1/M2 polarization and metabolic states. British journal of pharmacology. 2016;173(4):649-65.
212. Galván-Peña S, O'Neill LAJ. Metabolic Reprograming in Macrophage Polarization. Frontiers in Immunology. 2014;5:420.
213. Cheng CI, Chen PH, Lin YC, Kao YH. High glucose activates Raw264.7 macrophages through RhoA kinase-mediated signaling pathway. Cellular signalling. 2015;27(2):283-92.
214. Suzuki H, Hisamatsu T, Chiba S, Mori K, Kitazume MT, Shimamura K, et al. Glycolytic pathway affects differentiation of human monocytes to regulatory macrophages. Immunology letters. 2016;176:18-27.
215. Covarrubias AJ, Aksoylar HI, Horng T. Control of macrophage metabolism and activation by mTOR and Akt signaling. Seminars in immunology. 2015;27(4):286-96.
216. Biswas SK, Chittezhath M, Shalova IN, Lim JY. Macrophage polarization and plasticity in health and disease. Immunologic research. 2012;53(1-3):11-24.
217. Mantovani A, Sica A, Sozzani S, Allavena P, Vecchi A, Locati M. The chemokine system in diverse forms of macrophage activation and polarization. Trends in immunology. 2004;25(12):677-86.
218. Lopez-Castejon G, Baroja-Mazo A, Pelegrin P. Novel macrophage polarization model: from gene expression to identification of new anti-inflammatory molecules. Cell Mol Life Sci. 2011;68(18):3095-107.
219. Kosmides AK, Kamisoglu K, Calvano SE, Corbett SA, Androulakis IP. Metabolomic Fingerprinting: Challenges and Opportunities. Critical reviews in biomedical engineering. 2013;41(3):205-21.
220. Geissmann F, Gordon S, Hume DA, Mowat AM, Randolph GJ. Unravelling mononuclear phagocyte heterogeneity. Nature reviews Immunology. 2010;10(6):453-60.
221. Alqarni AM, Ferro VA, Parkinson JA, Dufton MJ, Watson DG. Effect of Melittin on Metabolomic Profile and Cytokine Production in PMA-Differentiated THP-1 Cells. Vaccines. 2018;6(4).
222. McClenathan BM, Stewart DA, Spooner CE, Pathmasiri WW, Burgess JP, McRitchie SL, et al. Metabolites as biomarkers of adverse reactions following vaccination: A pilot study using nuclear magnetic resonance metabolomics. Vaccine. 2017;35(9):1238-45.
223. Engler RJ, Nelson MR, Collins LC, Jr., Spooner C, Hemann BA, Gibbs BT, et al. A prospective study of the incidence of myocarditis/pericarditis and new onset cardiac symptoms following smallpox and influenza vaccination. PLoS One. 2015;10(3):e0118283.
224. Rattigan KM, Pountain AW, Regnault C, Achcar F, Vincent IM, Goodyear CS, et al. Metabolomic profiling of macrophages determines the discrete metabolomic signature and metabolomic interactome triggered by polarising immune stimuli. PloS one. 2018;13(3):e0194126-e.
225. Mills EL, Ryan DG, Prag HA, Dikovskaya D, Menon D, Zaslona Z, et al. Itaconate is an anti-inflammatory metabolite that activates Nrf2 via alkylation of KEAP1. Nature. 2018;556(7699):113-7.
226. Tannahill GM, Curtis AM, Adamik J, Palsson-McDermott EM, McGettrick AF, Goel G, et al. Succinate is an inflammatory signal that induces IL-1beta through HIF-1alpha. Nature. 2013;496(7444):238-42.
227. Jha AK, Huang SC, Sergushichev A, Lampropoulou V, Ivanova Y, Loginicheva E, et al. Network integration of parallel metabolic and transcriptional data reveals metabolic modules that regulate macrophage polarization. Immunity. 2015;42(3):419-30.
228. Grice EA, Segre JA. The human microbiome: our second genome. Annual review of genomics and human genetics. 2012;13:151-70.

229. Dethlefsen L, McFall-Ngai M, Relman DA. An ecological and evolutionary perspective on human-microbe mutualism and disease. Nature. 2007;449(7164):811-8.
230. Neuhaus FC, Baddiley J. A Continuum of Anionic Charge: Structures and Functions of D-Alanyl-Teichoic Acids in Gram-Positive Bacteria. Microbiology and Molecular Biology Reviews. 2003;67(4):686-723.
231. Schleifer KH, Kandler O. Peptidoglycan types of bacterial cell walls and their taxonomic implications. Bacteriological reviews. 1972;36(4):407-77.
232. Paul WE. Fundamental Immunology: Wolters Kluwer/Lippincott Williams & Wilkins; 2008.
233. Kamio Y, Nikaido H. Outer membrane of Salmonella typhimurium: accessibility of phospholipid head groups to phospholipase c and cyanogen bromide activated dextran in the external medium. Biochemistry. 1976;15(12):2561-70.
234. Silhavy TJ, Kahne D, Walker S. The bacterial cell envelope. Cold Spring Harb Perspect Biol. 2010;2(5):a000414-a.
235. Slavin YN, Asnis J, Häfeli UO, Bach H. Metal nanoparticles: understanding the mechanisms behind antibacterial activity. Journal of Nanobiotechnology. 2017;15(1):65.
236. Hamer M, Kivimaki M, Stamatakis E, David Batty G. Psychological distress and infectious disease mortality in the general population. Brain, Behavior, and Immunity. 2019;76:280-3.
237. Holmberg SD, Solomon SL, Blake PA. Health and economic impacts of antimicrobial resistance. Reviews of infectious diseases. 1987;9(6):1065-78.
238. Wilson JW. Bacterial pathogens. Cancer Treat Res. 2014;161:91-128.
239. Tong SYC, Davis JS, Eichenberger E, Holland TL, Fowler VG, Jr. Staphylococcus aureus infections: epidemiology, pathophysiology, clinical manifestations, and management. Clinical microbiology reviews. 2015;28(3):603-61.
240. Gellatly SL, Hancock REW. Pseudomonas aeruginosa : new insights into pathogenesis and host defenses. Pathogens and Disease. 2013;67(3):159-73.
241. Cohen TS, Boland ML, Boland BB, Takahashi V, Tovchigrechko A, Lee Y, et al. S. aureus Evades Macrophage Killing through NLRP3-Dependent Effects on Mitochondrial Trafficking. Cell reports. 2018;22(9):2431-41.
242. Gorwitz RJ, Kruszon-Moran D, McAllister SK, McQuillan G, McDougal LK, Fosheim GE, et al. Changes in the prevalence of nasal colonization with Staphylococcus aureus in the United States, 2001-2004. The Journal of infectious diseases. 2008;197(9):1226-34.
243. Oliveira D, Borges A, Simões M. Staphylococcus aureus Toxins and Their Molecular Activity in Infectious Diseases. Toxins. 2018;10(6):252.
244. Howden BP, Davies JK, Johnson PDR, Stinear TP, Grayson ML. Reduced vancomycin susceptibility in Staphylococcus aureus, including vancomycin-intermediate and heterogeneous vancomycin-intermediate strains: resistance mechanisms, laboratory detection, and clinical implications. Clinical microbiology reviews. 2010;23(1):99-139.
245. Archer NK, Mazaitis MJ, Costerton JW, Leid JG, Powers ME, Shirtliff ME. Staphylococcus aureus biofilms: properties, regulation, and roles in human disease. Virulence. 2011;2(5):445-59.
246. Bien J, Sokolova O, Bozko P. Characterization of Virulence Factors of Staphylococcus aureus: Novel Function of Known Virulence Factors That Are Implicated in Activation of Airway Epithelial Proinflammatory Response. Journal of Pathogens. 2011;2011:13.
247. Grumann D, Nubel U, Broker BM. Staphylococcus aureus toxins--their functions and genetics. Infection, genetics and evolution : journal of molecular epidemiology and evolutionary genetics in infectious diseases. 2014;21:583-92.

248. Jarraud S, Cozon G, Vandenesch F, Bes M, Etienne J, Lina G. Involvement of enterotoxins G and I in staphylococcal toxic shock syndrome and staphylococcal scarlet fever. Journal of clinical microbiology. 1999;37(8):2446-9.
249. Jarraud S, Mougel C, Thioulouse J, Lina G, Meugnier H, Forey F, et al. Relationships between Staphylococcus aureus genetic background, virulence factors, agr groups (alleles), and human disease. Infection and immunity. 2002;70(2):631-41.
250. Ahearn DG, Borazjani RN, Simmons RB, Gabriel MM. Primary adhesion of Pseudomonas aeruginosa to inanimate surfaces including biomaterials. Methods in enzymology. 1999;310:551-7.
251. Crouch Brewer S, Wunderink RG, Jones CB, Leeper KV, Jr. Ventilator-associated pneumonia due to Pseudomonas aeruginosa. Chest. 1996;109(4):1019-29.
252. Bodey GP, Bolivar R, Fainstein V, Jadeja L. Infections caused by Pseudomonas aeruginosa. Reviews of infectious diseases. 1983;5(2):279-313.
253. Boucher HW, Talbot GH, Bradley JS, Edwards JE, Gilbert D, Rice LB, et al. Bad bugs, no drugs: no ESKAPE! An update from the Infectious Diseases Society of America. Clinical infectious diseases : an official publication of the Infectious Diseases Society of America. 2009;48(1):1-12.
254. Bodey GP. Pseudomonas aeruginosa infections in cancer patients: have they gone away? Current opinion in infectious diseases. 2001;14(4):403-7.
255. Ohmagari N, Hanna H, Graviss L, Hackett B, Perego C, Gonzalez V, et al. Risk factors for infections with multidrug-resistant Pseudomonas aeruginosa in patients with cancer. Cancer. 2005;104(1):205-12.
256. de Bentzmann S, Plesiat P. The Pseudomonas aeruginosa opportunistic pathogen and human infections. Environmental microbiology. 2011;13(7):1655-65.
257. Liu PV. Extracellular toxins of Pseudomonas aeruginosa. The Journal of infectious diseases. 1974;130 Suppl(0):S94-9.
258. Mancini N, Carletti S, Ghidoli N, Cichero P, Burioni R, Clementi M. The era of molecular and other non-culture-based methods in diagnosis of sepsis. Clinical microbiology reviews. 2010;23(1):235-51.
259. Irwin AD, Marriage F, Mankhambo LA, Study IPDG, Jeffers G, Kolamunnage-Dona R, et al. Novel biomarker combination improves the diagnosis of serious bacterial infections in Malawian children. BMC medical genomics. 2012;5:13-.
260. Zhu L, Zhao Q, Yang T, Ding W, Zhao Y. Cellular metabolism and macrophage functional polarization. International reviews of immunology. 2015;34(1):82-100.
261. Fujino T, Nakamuta M, Yada R, Aoyagi Y, Yasutake K, Kohjima M, et al. Expression profile of lipid metabolism-associated genes in hepatitis C virus-infected human liver. Hepatology research : the official journal of the Japan Society of Hepatology. 2010;40(9):923-9.
262. Sanchez EL, Lagunoff M. Viral activation of cellular metabolism. Virology. 2015;479-480:609-18.
263. DeVito SR, Ortiz-Riaño E, Martínez-Sobrido L, Munger J. Cytomegalovirus-mediated activation of pyrimidine biosynthesis drives UDP-sugar synthesis to support viral protein glycosylation. Proceedings of the National Academy of Sciences of the United States of America. 2014;111(50):18019-24.
264. Noto A, Dessi A, Puddu M, Mussap M, Fanos V. Metabolomics technology and their application to the study of the viral infection. The journal of maternal-fetal & neonatal medicine : the official journal of the European Association of Perinatal Medicine, the Federation of Asia and Oceania Perinatal Societies, the International Society of Perinatal Obstet. 2014;27 Suppl 2:53-7.
265. Brunton J, Steele S, Ziehr B, Moorman N, Kawula T. Feeding uninvited guests: mTOR and AMPK set the table for intracellular pathogens. PLoS Pathog. 2013;9(10):e1003552-e.

266. Takeuchi O, Hoshino K, Kawai T, Sanjo H, Takada H, Ogawa T, et al. Differential roles of TLR2 and TLR4 in recognition of gram-negative and gram-positive bacterial cell wall components. Immunity. 1999;11(4):443-51.
267. Hoshino K, Takeuchi O, Kawai T, Sanjo H, Ogawa T, Takeda Y, et al. Cutting edge: Toll-like receptor 4 (TLR4)-deficient mice are hyporesponsive to lipopolysaccharide: evidence for TLR4 as the Lps gene product. Journal of immunology (Baltimore, Md : 1950). 1999;162(7):3749-52.
268. Hollywood K, Brison DR, Goodacre R. Metabolomics: Current technologies and future trends. PROTEOMICS. 2006;6(17):4716-23.
269. Maertzdorf J, Weiner J, 3rd, Kaufmann SH. Enabling biomarkers for tuberculosis control. The international journal of tuberculosis and lung disease : the official journal of the International Union against Tuberculosis and Lung Disease. 2012;16(9):1140-8.
270. Klass MR. A method for the isolation of longevity mutants in the nematode Caenorhabditis elegans and initial results. Mechanisms of ageing and development. 1983;22(3-4):279-86.
271. Dorshkind K, Montecino-Rodriguez E, Signer RA. The ageing immune system: is it ever too old to become young again? Nature reviews Immunology. 2009;9(1):57-62.
272. Aw D, Silva AB, Palmer DB. Immunosenescence: emerging challenges for an ageing population. Immunology. 2007;120(4):435-46.
273. López-Otín C, Blasco MA, Partridge L, Serrano M, Kroemer G. The Hallmarks of Aging. Cell. 2013;153(6):1194-217.
274. Bender BS. Infectious disease risk in the elderly. Immunology and allergy clinics of North America. 2003;23(1):57-64, vi.
275. Linehan E, Fitzgerald DC. Ageing and the immune system: focus on macrophages. Eur J Microbiol Immunol (Bp). 2015;5(1):14-24.
276. Goronzy JJ, Weyand CM. Understanding immunosenescence to improve responses to vaccines. Nat Immunol. 2013;14(5):428-36.
277. Meyer KC. The role of immunity in susceptibility to respiratory infection in the aging lung. Respiration physiology. 2001;128(1):23-31.
278. Ginaldi L, Loreto MF, Corsi MP, Modesti M, De Martinis M. Immunosenescence and infectious diseases. Microbes and infection. 2001;3(10):851-7.
279. Fulop T, Kotb R, Fortin CF, Pawelec G, de Angelis F, Larbi A. Potential role of immunosenescence in cancer development. Annals of the New York Academy of Sciences. 2010;1197:158-65.
280. Sadighi Akha AA. Aging and the immune system: An overview. Journal of immunological methods. 2018;463:21-6.
281. Iwasaki A, Medzhitov R. Regulation of adaptive immunity by the innate immune system. Science (New York, NY). 2010;327(5963):291-5.
282. Plowden J, Renshaw-Hoelscher M, Engleman C, Katz J, Sambhara S. Innate immunity in aging: impact on macrophage function. Aging cell. 2004;3(4):161-7.
283. Renshaw M, Rockwell J, Engleman C, Gewirtz A, Katz J, Sambhara S. Cutting edge: impaired Toll-like receptor expression and function in aging. Journal of immunology (Baltimore, Md : 1950). 2002;169(9):4697-701.
284. Boehmer ED, Goral J, Faunce DE, Kovacs EJ. Age-dependent decrease in Toll-like receptor 4-mediated proinflammatory cytokine production and mitogen-activated protein kinase expression. Journal of leukocyte biology. 2004;75(2):342-9.
285. Chelvarajan RL, Collins SM, Van Willigen JM, Bondada S. The unresponsiveness of aged mice to polysaccharide antigens is a result of a defect in macrophage function. Journal of leukocyte biology. 2005;77(4):503-12.
286. Mahbub S, Deburghgraeve CR, Kovacs EJ. Advanced age impairs macrophage polarization. Journal of interferon & cytokine research : the official journal of the International Society for Interferon and Cytokine Research. 2012;32(1):18-26.

287. Kelly J, Ali Khan A, Yin J, Ferguson TA, Apte RS. Senescence regulates macrophage activation and angiogenic fate at sites of tissue injury in mice. The Journal of clinical investigation. 2007;117(11):3421-6.
288. Bradley SF, Kauffman CA. Aging and the response to Salmonella infection. Experimental gerontology. 1990;25(1):75-80.
289. Lynch AM, Murphy KJ, Deighan BF, O'Reilly J-A, Gun'ko YK, Cowley TR, et al. The impact of glial activation in the aging brain. Aging Dis. 2010;1(3):262-78.
290. Swift ME, Kleinman HK, DiPietro LA. Impaired wound repair and delayed angiogenesis in aged mice. Laboratory investigation; a journal of technical methods and pathology. 1999;79(12):1479-87.
291. Piper MD, Bartke A. Diet and aging. Cell metabolism. 2008;8(2):99-104.
292. Kerber RA, O'Brien E, Cawthon RM. Gene expression profiles associated with aging and mortality in humans. Aging cell. 2009;8(3):239-50.
293. Seaman C, Wyss S, Piomelli S. The decline in energetic metabolism with aging of the erythrocyte and its relationship to cell death. American Journal of Hematology. 1980;8(1):31-42.
294. Wang Y, Lawler D, Larson B, Ramadan Z, Kochhar S, Holmes E, et al. Metabonomic investigations of aging and caloric restriction in a life-long dog study. Journal of proteome research. 2007;6(5):1846-54.
295. Williams RE, Lenz EM, Lowden JS, Rantalainen M, Wilson ID. The metabonomics of aging and development in the rat: an investigation into the effect of age on the profile of endogenous metabolites in the urine of male rats using 1H NMR and HPLC-TOF MS. Molecular bioSystems. 2005;1(2):166-75.
296. Nevedomskaya E, Meissner A, Goraler S, de Waard M, Ridwan Y, Zondag G, et al. Metabolic profiling of accelerated aging ERCC1 d/- mice. Journal of proteome research. 2010;9(7):3680-7.
297. Yu Z, Zhai G, Singmann P, He Y, Xu T, Prehn C, et al. Human serum metabolic profiles are age dependent. Aging cell. 2012;11(6):960-7.
298. Lawton KA, Berger A, Mitchell M, Milgram KE, Evans AM, Guo L, et al. Analysis of the adult human plasma metabolome. Pharmacogenomics. 2008;9(4):383-97.
299. Rathmell JC. Metabolism and autophagy in the immune system: immunometabolism comes of age. Immunological reviews. 2012;249(1):5-13.
300. Seidler S, Zimmermann HW, Bartneck M, Trautwein C, Tacke F. Age-dependent alterations of monocyte subsets and monocyte-related chemokine pathways in healthy adults. BMC immunology. 2010;11:30.
301. Fei F, Lee KM, McCarry BE, Bowdish DME. Age-associated metabolic dysregulation in bone marrow-derived macrophages stimulated with lipopolysaccharide. Scientific reports. 2016;6:22637-.
302. Mandal P, Pratt BT, Barnes M, McMullen MR, Nagy LE. Molecular Mechanism for Adiponectin-dependent M2 Macrophage Polarization: LINK BETWEEN THE METABOLIC AND INNATE IMMUNE ACTIVITY OF FULL-LENGTH ADIPONECTIN. The Journal of biological chemistry. 2011;286(15):13460-9.
303. Murphy CA, Langrish CL, Chen Y, Blumenschein W, McClanahan T, Kastelein RA, et al. Divergent Pro- and Antiinflammatory Roles for IL-23 and IL-12 in Joint Autoimmune Inflammation. The Journal of experimental medicine. 2003;198(12):1951-7.
304. Sierra-Filardi E, Nieto C, Domínguez-Soto Á, Barroso R, Sánchez-Mateos P, Puig-Kroger A, et al. CCL2 Shapes Macrophage Polarization by GM-CSF and M-CSF: Identification of CCL2/CCR2-Dependent Gene Expression Profile. The Journal of Immunology. 2014;192(8):3858.
305. Rath M, Müller I, Kropf P, Closs EI, Munder M. Metabolism via Arginase or Nitric Oxide Synthase: Two Competing Arginine Pathways in Macrophages. Frontiers in Immunology. 2014;5:532.

306. Surrati A, Linforth R, Fisk ID, Sottile V, Kim DH. Non-destructive characterisation of mesenchymal stem cell differentiation using LC-MS-based metabolite footprinting. The Analyst. 2016;141(12):3776-87.
307. Jansson J, Willing B, Lucio M, Fekete A, Dicksved J, Halfvarson J, et al. Metabolomics Reveals Metabolic Biomarkers of Crohn's Disease. PLOS ONE. 2009;4(7):e6386.
308. Sun J, Schnackenberg LK, Beger RD. Studies of Acetaminophen and Metabolites in Urine and Their Correlations with Toxicity Using Metabolomics. Drug Metabolism Letters. 2009;3(3):130-6.
309. Hollenbaugh JA, Munger J, Kim B. Metabolite Profiles of Human Immunodeficiency Virus Infected CD4+ T Cells and Macrophages using LC-MS/MS Analysis. Virology. 2011;415(2):153-9.
310. Suh JH, Kim RY, Lee DS. A new metabolomic assay to examine inflammation and redox pathways following LPS challenge. Journal of Inflammation. 2012;9(1):37.
311. Freemerman AJ, Johnson AR, Sacks GN, Milner JJ, Kirk EL, Troester MA, et al. Metabolic reprogramming of macrophages: glucose transporter 1 (GLUT1)-mediated glucose metabolism drives a proinflammatory phenotype. The Journal of biological chemistry. 2014;289(11):7884-96.
312. Caras I, Tucureanu C, Lerescu L, Pitica R, Melinceanu L, Neagu S, et al. Influence of tumor cell culture supernatants on macrophage functional polarization: in vitro models of macrophage-tumor environment interaction. Tumori. 2011;97(5):647-54.
313. Rostam HM, Reynolds PM, Alexander MR, Gadegaard N, Ghaemmaghami AM. Image based Machine Learning for identification of macrophage subsets. Scientific Reports. 2017;7(1):3521.
314. Kim D-H, Achcar F, Breitling R, Burgess KE, Barrett MP. LC–MS-based absolute metabolite quantification: application to metabolic flux measurement in trypanosomes. Metabolomics. 2015;11(6):1721-32.
315. Creek DJ, Jankevics A, Burgess KE, Breitling R, Barrett MP. IDEOM: an Excel interface for analysis of LC-MS-based metabolomics data. Bioinformatics. 2012;28(7):1048-9.
316. Gordon S, Plüddemann A. Tissue macrophages: heterogeneity and functions. BMC Biology. 2017;15(1):53.
317. Rostam HM, Reynolds PM, Singh S, Alexander MR, Gadegaard N, Ghaemmaghami A. Image based machine learning for identification of M1 and M2 macrophages. The Journal of Immunology. 2016;196(1 Supplement):126.25.
318. Toniolo A, Fadini GP, Tedesco S, Cappellari R, Vegeto E, Maggi A, et al. Alternative Activation of Human Macrophages Is Rescued by Estrogen Treatment In Vitro and Impaired by Menopausal Status. The Journal of Clinical Endocrinology & Metabolism. 2015;100(1):E50-E8.
319. Huang SC-C, Everts B, Ivanova Y, O'Sullivan D, Nascimento M, Smith AM, et al. Cell-intrinsic lysosomal lipolysis is essential for alternative activation of macrophages. Nat Immunol. 2014;15(9):846-55.
320. Worley B, Powers R. Multivariate Analysis in Metabolomics. Curr Metabolomics. 2013;1(1):92-107.
321. Qi Y, Pi Z, Liu S, Song F, Lin N, Liu Z. A metabonomic study of adjuvant-induced arthritis in rats using ultra-performance liquid chromatography coupled with quadrupole time-of-flight mass spectrometry. Molecular bioSystems. 2014;10(10):2617-25.
322. Shang J, Liu J, He M, Shang E, Zhang L, Shan M, et al. UHPLC/Q-TOF MS-based plasma metabolic profiling analysis of the bleeding mechanism in a rat model of yeast and ethanol-induced blood heat and hemorrhage syndrome. Journal of Pharmaceutical and Biomedical Analysis. 2014;92:26-34.

323. Alazzo A, Al-Natour MA, Spriggs K, Stolnik S, Ghaemmaghami A, Kim DH, et al. Investigating the intracellular effects of hyperbranched polycation-DNA complexes on lung cancer cells using LC-MS-based metabolite profiling. Molecular omics. 2019;15(1):77-87.
324. Eriksson L, Kettaneh-Wold N, Trygg J, Wikström C, Wold S. Multi- and Megavariate Data Analysis : Part I: Basic Principles and Applications: Umetrics Inc; 2006 2006. 425 p.
325. Strickland KP, Subrahmanyam D, Pritchard ET, Thompson W, Rossiter RJ. Biosynthesis of lecithin in brain. Participation of cytidine diphosphate choline and phosphatidic acid. Biochemical Journal. 1963;87(1):128-36.
326. Zhang C, Wang Y, Wang F, Wang Z, Lu Y, Xu Y, et al. Quantitative profiling of glycerophospholipids during mouse and human macrophage differentiation using targeted mass spectrometry. Scientific Reports. 2017;7(1):412.
327. Mukundan L, Odegaard JI, Morel CR, Heredia JE, Mwangi JW, Ricardo-Gonzalez RR, et al. PPAR-delta senses and orchestrates clearance of apoptotic cells to promote tolerance. Nature medicine. 2009;15(11):1266-72.
328. Masoodi M, Kuda O, Rossmeisl M, Flachs P, Kopecky J. Lipid signaling in adipose tissue: Connecting inflammation & metabolism. Biochimica et biophysica acta. 2015;1851(4):503-18.
329. Kihara A, Mitsutake S, Mizutani Y, Igarashi Y. Metabolism and biological functions of two phosphorylated sphingolipids, sphingosine 1-phosphate and ceramide 1-phosphate. Prog Lipid Res. 2007;46(2):126-44.
330. El Alwani M, Wu BX, Obeid LM, Hannun YA. Bioactive sphingolipids in the modulation of the inflammatory response. Pharmacology & therapeutics. 2006;112(1):171-83.
331. Zheng W, Kollmeyer J, Symolon H, Momin A, Munter E, Wang E, et al. Ceramides and other bioactive sphingolipid backbones in health and disease: lipidomic analysis, metabolism and roles in membrane structure, dynamics, signaling and autophagy. Biochimica et biophysica acta. 2006;1758(12):1864-84.
332. Siow D, Wattenberg B. The histone deacetylase-6 inhibitor tubacin directly inhibits de novo sphingolipid biosynthesis as an off-target effect. Biochemical and biophysical research communications. 2014;449(3):268-71.
333. Sims K, Haynes CA, Kelly S, Allegood JC, Wang E, Momin A, et al. Kdo2-lipid A, a TLR4-specific agonist, induces de novo sphingolipid biosynthesis in RAW264.7 macrophages, which is essential for induction of autophagy. The Journal of biological chemistry. 2010;285(49):38568-79.
334. Cuschieri J, Bulger E, Billgrin J, Garcia I, Maier RV. Acid sphingomyelinase is required for lipid Raft TLR4 complex formation. Surgical infections. 2007;8(1):91-106.
335. Cuschieri J, Billgren J, Maier RV. Phosphatidylcholine-specific phospholipase C (PC-PLC) is required for LPS-mediated macrophage activation through CD14. Journal of leukocyte biology. 2006;80(2):407-14.
336. Sims K, Haynes CA, Kelly S, Allegood JC, Wang E, Momin A, et al. Kdo(2)-Lipid A, a TLR4-specific Agonist, Induces de Novo Sphingolipid Biosynthesis in RAW264.7 Macrophages, Which Is Essential for Induction of Autophagy. The Journal of biological chemistry. 2010;285(49):38568-79.
337. Bhat K I, Kumar A. Pyrimidines as potent cytotoxic and anti-inflammatory agents2017. 237 p.
338. Sharma V, Chitranshi N, Agarwal AK. Significance and Biological Importance of Pyrimidine in the Microbial World. International Journal of Medicinal Chemistry. 2014;2014:202784.

339. Nargund LV, Badiger VV, Yarnal SM. Synthesis and antimicrobial and anti-inflammatory activities of substituted 2-mercapto-3-(N-aryl)pyrimido[5,4-c]cinnolin-4-(3H)-ones. Journal of pharmaceutical sciences. 1992;81(4):365-6.
340. Sawant R, Kawade D. Synthesis and biological evaluation of some novel 2-phenyl benzimidazole-1-acetamide derivatives as potential anthelmintic agents. Acta pharmaceutica (Zagreb, Croatia). 2011;61(3):353-61.
341. Bonnert RV, Cage,P.A.,Hunt,S.F.,Walters,I.J.S. and Austin,R.P., inventor; Astrazeneca Uk Limited, assignee. Pyrimidine compounds and their use as modulators of chemokine receptor activity patent WO2001058906A1. 2003 2003.
342. Jankowski V, Tolle M, Vanholder R, Schonfelder G, van der Giet M, Henning L, et al. Uridine adenosine tetraphosphate: a novel endothelium- derived vasoconstrictive factor. Nature medicine. 2005;11(2):223-7.
343. Bedard K, Krause KH. The NOX family of ROS-generating NADPH oxidases: physiology and pathophysiology. Physiological reviews. 2007;87(1):245-313.
344. Rattigan KM, Pountain AW, Regnault C, Achcar F, Vincent IM, Goodyear CS, et al. Metabolomic profiling of macrophages determines the discrete metabolomic signature and metabolomic interactome triggered by polarising immune stimuli. PLOS ONE. 2018;13(3):e0194126.
345. West AP, Brodsky IE, Rahner C, Woo DK, Erdjument-Bromage H, Tempst P, et al. TLR signalling augments macrophage bactericidal activity through mitochondrial ROS. Nature. 2011;472(7344):476-80.
346. Krajewski SS, Isoz I, Johansson J. Antibacterial and antivirulence effect of 6-N-hydroxylaminopurine in Listeria monocytogenes. Nucleic acids research. 2017;45(4):1914-24.
347. Moffett JR, Namboodiri MA. Tryptophan and the immune response. Immunology and cell biology. 2003;81(4):247-65.
348. Kushnir-Sukhov NM, Gilfillan AM, Coleman JW, Brown JM, Bruening S, Toth M, et al. 5-hydroxytryptamine induces mast cell adhesion and migration. Journal of immunology (Baltimore, Md : 1950). 2006;177(9):6422-32.
349. Nakamura K, Sato T, Ohashi A, Tsurui H, Hasegawa H. Role of a serotonin precursor in development of gut microvilli. The American journal of pathology. 2008;172(2):333-44.
350. Tarique AA, Logan J, Thomas E, Holt PG, Sly PD, Fantino E. Phenotypic, functional, and plasticity features of classical and alternatively activated human macrophages. American journal of respiratory cell and molecular biology. 2015;53(5):676-88.
351. Bansal V, Ochoa JB. Arginine availability, arginase, and the immune response. Current opinion in clinical nutrition and metabolic care. 2003;6(2):223-8.
352. Morris SM, Jr. Arginine: beyond protein. The American journal of clinical nutrition. 2006;83(2):508s-12s.
353. Wu G, Morris SM, Jr. Arginine metabolism: nitric oxide and beyond. The Biochemical journal. 1998;336 (Pt 1):1-17.
354. Corraliza IM, Soler G, Eichmann K, Modolell M. Arginase induction by suppressors of nitric oxide synthesis (IL-4, IL-10 and PGE2) in murine bone-marrow-derived macrophages. Biochemical and biophysical research communications. 1995;206(2):667-73.
355. Sugimoto M, Sakagami H, Yokote Y, Onuma H, Kaneko M, Mori M, et al. Non-targeted metabolite profiling in activated macrophage secretion. Metabolomics. 2012;8(4):624-33.
356. Martinez FO, Helming L, Milde R, Varin A, Melgert BN, Draijer C, et al. Genetic programs expressed in resting and IL-4 alternatively activated mouse and human macrophages: similarities and differences. Blood. 2013;121(9):e57-e69.

357. Weigert A, von Knethen A, Fuhrmann D, Dehne N, Brune B. Redox-signals and macrophage biology. Molecular aspects of medicine. 2018;63:70-87.
358. Akagawa KS. Functional heterogeneity of colony-stimulating factor-induced human monocyte-derived macrophages. International journal of hematology. 2002;76(1):27-34.
359. Artyomov MN, Sergushichev A, Schilling JD. Integrating immunometabolism and macrophage diversity. Seminars in immunology. 2016;28(5):417-24.
360. Lachmandas E, Boutens L, Ratter JM, Hijmans A, Hooiveld GJ, Joosten LAB, et al. Microbial stimulation of different Toll-like receptor signalling pathways induces diverse metabolic programmes in human monocytes. Nature Microbiology. 2016;2(3):16246.
361. Galli SJ, Borregaard N, Wynn TA. Phenotypic and functional plasticity of cells of innate immunity: macrophages, mast cells and neutrophils. Nat Immunol. 2011;12(11):1035-44.
362. Verreck FA, de Boer T, Langenberg DM, Hoeve MA, Kramer M, Vaisberg E, et al. Human IL-23-producing type 1 macrophages promote but IL-10-producing type 2 macrophages subvert immunity to (myco)bacteria. Proceedings of the National Academy of Sciences of the United States of America. 2004;101(13):4560-5.
363. Murray PJ, Allen JE, Biswas SK, Fisher EA, Gilroy DW, Goerdt S, et al. Macrophage activation and polarization: nomenclature and experimental guidelines. Immunity. 2014;41(1):14-20.
364. Stout RD, Suttles J. Functional plasticity of macrophages: reversible adaptation to changing microenvironments. Journal of leukocyte biology. 2004;76(3):509-13.
365. Gu Q, Yang H, Shi Q. Macrophages and bone inflammation. Journal of Orthopaedic Translation. 2017;10(Supplement C):86-93.
366. Fleming BD, Mosser DM. Regulatory macrophages: setting the threshold for therapy. European journal of immunology. 2011;41(9):2498-502.
367. Hutchinson JA, Riquelme P, Geissler EK, Fandrich F. Human regulatory macrophages. Methods in molecular biology (Clifton, NJ). 2011;677:181-92.
368. Trinchieri G. Interleukin-12 and the regulation of innate resistance and adaptive immunity. Nature reviews Immunology. 2003;3(2):133-46.
369. Gruenheid S, Gros P. Genetic susceptibility to intracellular infections: Nramp1, macrophage function and divalent cations transport. Current opinion in microbiology. 2000;3(1):43-8.
370. Carlin JM, Borden EC, Byrne GI. Interferon-induced indoleamine 2,3-dioxygenase activity inhibits Chlamydia psittaci replication in human macrophages. Journal of interferon research. 1989;9(3):329-37.
371. MacMicking J, Xie QW, Nathan C. Nitric oxide and macrophage function. Annual review of immunology. 1997;15:323-50.
372. Edwards JP, Zhang X, Frauwirth KA, Mosser DM. Biochemical and functional characterization of three activated macrophage populations. Journal of leukocyte biology. 2006;80(6):1298-307.
373. Cordeiro-da-Silva A, Tavares J, Araujo N, Cerqueira F, Tomas A, Kong Thoo Lin P, et al. Immunological alterations induced by polyamine derivatives on murine splenocytes and human mononuclear cells. International immunopharmacology. 2004;4(4):547-56.
374. Stout RD, Jiang C, Matta B, Tietzel I, Watkins SK, Suttles J. Macrophages sequentially change their functional phenotype in response to changes in microenvironmental influences. Journal of immunology (Baltimore, Md : 1950). 2005;175(1):342-9.
375. Ramsey SA, Klemm SL, Zak DE, Kennedy KA, Thorsson V, Li B, et al. Uncovering a macrophage transcriptional program by integrating evidence from motif scanning and expression dynamics. PLoS computational biology. 2008;4(3):e1000021.

376. Nau GJ, Richmond JF, Schlesinger A, Jennings EG, Lander ES, Young RA. Human macrophage activation programs induced by bacterial pathogens. Proceedings of the National Academy of Sciences of the United States of America. 2002;99(3):1503-8.
377. McDermott JE, Archuleta M, Thrall BD, Adkins JN, Waters KM. Controlling the Response: Predictive Modeling of a Highly Central, Pathogen-Targeted Core Response Module in Macrophage Activation. PLOS ONE. 2011;6(2):e14673.
378. Martinez FO, Gordon S, Locati M, Mantovani A. Transcriptional profiling of the human monocyte-to-macrophage differentiation and polarization: new molecules and patterns of gene expression. Journal of immunology (Baltimore, Md : 1950). 2006;177(10):7303-11.
379. Miller JC, Brown BD, Shay T, Gautier EL, Jojic V, Cohain A, et al. Deciphering the transcriptional network of the dendritic cell lineage. Nat Immunol. 2012;13(9):888-99.
380. Gautier EL, Shay T, Miller J, Greter M, Jakubzick C, Ivanov S, et al. Gene-expression profiles and transcriptional regulatory pathways that underlie the identity and diversity of mouse tissue macrophages. Nat Immunol. 2012;13(11):1118-28.
381. Mabbott NA, Kenneth Baillie J, Hume DA, Freeman TC. Meta-analysis of lineage-specific gene expression signatures in mouse leukocyte populations. Immunobiology. 2010;215(9-10):724-36.
382. Hume DA, Summers KM, Raza S, Baillie JK, Freeman TC. Functional clustering and lineage markers: insights into cellular differentiation and gene function from large-scale microarray studies of purified primary cell populations. Genomics. 2010;95(6):328-38.
383. Shay T, Jojic V, Zuk O, Rothamel K, Puyraimond-Zemmour D, Feng T, et al. Conservation and divergence in the transcriptional programs of the human and mouse immune systems. Proceedings of the National Academy of Sciences of the United States of America. 2013;110(8):2946-51.
384. Schroder K, Irvine KM, Taylor MS, Bokil NJ, Le Cao KA, Masterman KA, et al. Conservation and divergence in Toll-like receptor 4-regulated gene expression in primary human versus mouse macrophages. Proceedings of the National Academy of Sciences of the United States of America. 2012;109(16):E944-53.
385. Ganeshan K, Chawla A. Metabolic Regulation of Immune Responses. Annual review of immunology. 2014;32(1):609-34.
386. Olenchock BA, Rathmell JC, Vander Heiden MG. Biochemical Underpinnings of Immune Cell Metabolic Phenotypes. Immunity. 2017;46(5):703-13.
387. Sinclair LV, Rolf J, Emslie E, Shi Y-B, Taylor PM, Cantrell DA. Control of amino-acid transport by antigen receptors coordinates the metabolic reprogramming essential for T cell differentiation. Nature Immunology. 2013;14:500.
388. Doedens AL, Phan AT, Stradner MH, Fujimoto JK, Nguyen JV, Yang E, et al. Hypoxia-inducible factors enhance the effector responses of CD8+ T cells to persistent antigen. Nature Immunology. 2013;14:1173.
389. Cattin AL, Burden JJ, Van Emmenis L, Mackenzie FE, Hoving JJ, Garcia Calavia N, et al. Macrophage-Induced Blood Vessels Guide Schwann Cell-Mediated Regeneration of Peripheral Nerves. Cell. 2015;162(5):1127-39.
390. Man K, Kutyavin VI, Chawla A. Tissue Immunometabolism: Development, Physiology, and Pathobiology. Cell metabolism. 2017;25(1):11-26.
391. Hobson-Gutierrez SA, Carmona-Fontaine C. The metabolic axis of macrophage and immune cell polarization. Disease Models & Mechanisms. 2018;11(8):dmm034462.
392. O'Neill LAJ, Pearce EJ. Immunometabolism governs dendritic cell and macrophage function. The Journal of experimental medicine. 2016;213(1):15.
393. Corcoran SE, O'Neill LAJ. HIF1α and metabolic reprogramming in inflammation. The Journal of Clinical Investigation. 2016;126(10):3699-707.

394. Guijas C, Montenegro-Burke JR, Warth B, Spilker ME, Siuzdak G. Metabolomics activity screening for identifying metabolites that modulate phenotype. Nature biotechnology. 2018;36(4):316-20.
395. Yosef N, Shalek AK, Gaublomme JT, Jin H, Lee Y, Awasthi A, et al. Dynamic regulatory network controlling TH17 cell differentiation. Nature. 2013;496(7446):461-8.
396. Patel S, Ahmed S. Emerging Field of Metabolomics: Big Promise for Cancer Biomarker Identification and Drug Discovery2014.
397. Everts B. Metabolomics in Immunology Research. Methods in molecular biology (Clifton, NJ). 2018;1730:29-42.
398. Sperber H, Mathieu J, Wang Y, Ferreccio A, Hesson J, Xu Z, et al. The metabolome regulates the epigenetic landscape during naive-to-primed human embryonic stem cell transition. Nature cell biology. 2015;17(12):1523-35.
399. Geiger R, Rieckmann JC, Wolf T, Basso C, Feng Y, Fuhrer T, et al. L-Arginine Modulates T Cell Metabolism and Enhances Survival and Anti-tumor Activity. Cell. 2016;167(3):829-42.e13.
400. Beyer BA, Fang M, Sadrian B, Montenegro-Burke JR, Plaisted WC, Kok BPC, et al. Metabolomics-based discovery of a metabolite that enhances oligodendrocyte maturation. Nature chemical biology. 2018;14(1):22-8.
401. Pollard JW. Macrophages define the invasive microenvironment in breast cancer. Journal of leukocyte biology. 2008;84(3):623-30.
402. Hagemann T, Lawrence T, McNeish I, Charles KA, Kulbe H, Thompson RG, et al. "Re-educating" tumor-associated macrophages by targeting NF-kappaB. The Journal of experimental medicine. 2008;205(6):1261-8.
403. Baay M, Brouwer A, Pauwels P, Peeters M, Lardon F. Tumor cells and tumor-associated macrophages: secreted proteins as potential targets for therapy. Clin Dev Immunol. 2011;2011:565187-.
404. Tumitan AR, Monnazzi LG, Ghiraldi FR, Cilli EM, Machado de Medeiros BM. Pattern of macrophage activation in yersinia-resistant and yersinia-susceptible strains of mice. Microbiology and immunology. 2007;51(10):1021-8.
405. Sumner LW, Lei Z, Nikolau BJ, Saito K, Roessner U, Trengove R. Proposed quantitative and alphanumeric metabolite identification metrics. Metabolomics. 2014;10(6):0.
406. Puig-Kroger A, Serrano-Gomez D, Caparros E, Dominguez-Soto A, Relloso M, Colmenares M, et al. Regulated expression of the pathogen receptor dendritic cell-specific intercellular adhesion molecule 3 (ICAM-3)-grabbing nonintegrin in THP-1 human leukemic cells, monocytes, and macrophages. The Journal of biological chemistry. 2004;279(24):25680-8.
407. Zizzo G, Hilliard BA, Monestier M, Cohen PL. Efficient clearance of early apoptotic cells by human macrophages requires M2c polarization and MerTK induction. Journal of immunology (Baltimore, Md : 1950). 2012;189(7):3508-20.
408. Law KP, Han TL, Mao X, Zhang H. Tryptophan and purine metabolites are consistently upregulated in the urinary metabolome of patients diagnosed with gestational diabetes mellitus throughout pregnancy: A longitudinal metabolomics study of Chinese pregnant women part 2. Clinica chimica acta; international journal of clinical chemistry. 2017;468:126-39.
409. Handford M, Rodriguez-Furlan C, Orellana A. Nucleotide-sugar transporters: structure, function and roles in vivo. Brazilian journal of medical and biological research = Revista brasileira de pesquisas medicas e biologicas. 2006;39(9):1149-58.
410. Haschemi A, Kosma P, Gille L, Evans CR, Burant CF, Starkl P, et al. The sedoheptulose kinase CARKL directs macrophage polarization through control of glucose metabolism. Cell metabolism. 2012;15(6):813-26.

411. Ruiz-Garcia A, Monsalve E, Novellasdemunt L, Navarro-Sabate A, Manzano A, Rivero S, et al. Cooperation of adenosine with macrophage Toll-4 receptor agonists leads to increased glycolytic flux through the enhanced expression of PFKFB3 gene. The Journal of biological chemistry. 2011;286(22):19247-58.
412. Vinaixa M, Schymanski EL, Neumann S, Navarro M, Salek RM, Yanes O. Mass spectral databases for LC/MS- and GC/MS-based metabolomics: State of the field and future prospects. TrAC Trends in Analytical Chemistry. 2016;78:23-35.
413. Al-Janabi AAHS. Potential activity of the purine compounds caffeine and aminophylline on bacteria. Journal of global infectious diseases. 2011;3(2):133-7.
414. M Tannahill G, O'Neill L. The emerging role of metabolic regulation in the functioning of Toll-like receptors and the NOD-like receptor Nlrp32011. 1568-72 p.
415. Mills EL, O'Neill LA. Reprogramming mitochondrial metabolism in macrophages as an anti-inflammatory signal. Eur J Immunol. 2016;46(1):13-21.
416. Rodriguez-Prados JC, Traves PG, Cuenca J, Rico D, Aragones J, Martin-Sanz P, et al. Substrate fate in activated macrophages: a comparison between innate, classic, and alternative activation. Journal of immunology (Baltimore, Md : 1950). 2010;185(1):605-14.
417. O'Neill Luke AJ. A Broken Krebs Cycle in Macrophages. Immunity. 2015;42(3):393-4.
418. O'Neill LA. A critical role for citrate metabolism in LPS signalling. The Biochemical journal. 2011;438(3):e5-6.
419. Wei X, Song H, Yin L, Rizzo MG, Sidhu R, Covey DF, et al. Fatty acid synthesis configures the plasma membrane for inflammation in diabetes. Nature. 2016;539:294.
420. Ehrensvard G, Fischer A, Stjernholm R. Protein metabolism of tissue cells in vitro; the chemical nature of some obligate factors of tissue cell nutrition. Acta physiologica Scandinavica. 1949;18(2-3):218-30.
421. Curi R, Lagranha CJ, Doi SQ, Sellitti DF, Procopio J, Pithon-Curi TC, et al. Molecular mechanisms of glutamine action. Journal of cellular physiology. 2005;204(2):392-401.
422. Newsholme P, Procopio J, Lima MM, Pithon-Curi TC, Curi R. Glutamine and glutamate--their central role in cell metabolism and function. Cell biochemistry and function. 2003;21(1):1-9.
423. Seeley JJ, Ghosh S. Molecular mechanisms of innate memory and tolerance to LPS. Journal of leukocyte biology. 2017;101(1):107-19.
424. Anderson DD, Stover PJ. SHMT1 and SHMT2 are functionally redundant in nuclear de novo thymidylate biosynthesis. PloS one. 2009;4(6):e5839-e.
425. Mehrmohamadi M, Liu X, Shestov Alexander A, Locasale Jason W. Characterization of the Usage of the Serine Metabolic Network in Human Cancer. Cell reports. 2014;9(4):1507-19.
426. Garrow TA, Brenner AA, Whitehead VM, Chen XN, Duncan RG, Korenberg JR, et al. Cloning of human cDNAs encoding mitochondrial and cytosolic serine hydroxymethyltransferases and chromosomal localization. The Journal of biological chemistry. 1993;268(16):11910-6.
427. Ma EH, Bantug G, Griss T, Condotta S, Johnson RM, Samborska B, et al. Serine Is an Essential Metabolite for Effector T Cell Expansion. Cell metabolism. 2017;25(2):345-57.
428. Liu PS, Wang H, Li X, Chao T, Teav T, Christen S, et al. alpha-ketoglutarate orchestrates macrophage activation through metabolic and epigenetic reprogramming. Nat Immunol. 2017;18(9):985-94.
429. Sornasse T, Larenas PV, Davis KA, de Vries JE, Yssel H. Differentiation and stability of T helper 1 and 2 cells derived from naive human neonatal CD4+ T cells,

analyzed at the single-cell level. The Journal of experimental medicine. 1996;184(2):473-83.
430. Coffman RL, Mocci S, O'Garra A. The Stability and Reversibility of Th1 and Th2 Populations. In: Coffman RL, Romagnani S, editors. Redirection of Th1 and Th2 Responses. Berlin, Heidelberg: Springer Berlin Heidelberg; 1999. p. 1-12.
431. Malyshev I, Malyshev Y. Current Concept and Update of the Macrophage Plasticity Concept: Intracellular Mechanisms of Reprogramming and M3 Macrophage "Switch" Phenotype. BioMed research international. 2015;2015:341308.
432. Romieu-Mourez R, Solis M, Nardin A, Goubau D, Baron-Bodo V, Lin R, et al. Distinct roles for IFN regulatory factor (IRF)-3 and IRF-7 in the activation of antitumor properties of human macrophages. Cancer research. 2006;66(21):10576-85.
433. Nardin A, Abastado JP. Macrophages and cancer. Frontiers in bioscience : a journal and virtual library. 2008;13:3494-505.
434. Morens DM, Folkers GK, Fauci AS. The challenge of emerging and re-emerging infectious diseases. Nature. 2004;430(6996):242-9.
435. Scheld WM. Maintaining fluoroquinolone class efficacy: review of influencing factors. Emerging infectious diseases. 2003;9(1):1-9.
436. Gootz TD. The global problem of antibiotic resistance. Critical reviews in immunology. 2010;30(1):79-93.
437. Brightbill HD, Libraty DH, Krutzik SR, Yang R-B, Belisle JT, Bleharski JR, et al. Host Defense Mechanisms Triggered by Microbial Lipoproteins Through Toll-Like Receptors. Science (New York, NY). 1999;285(5428):732.
438. Travassos LH, Girardin SE, Philpott DJ, Blanot D, Nahori MA, Werts C, et al. Toll-like receptor 2-dependent bacterial sensing does not occur via peptidoglycan recognition. EMBO reports. 2004;5(10):1000-6.
439. Janeway CA, Jr., Medzhitov R. Innate immune recognition. Annual review of immunology. 2002;20:197-216.
440. Takeda K, Akira S. Toll receptors and pathogen resistance. Cellular microbiology. 2003;5(3):143-53.
441. Kanwar M, Brar N, Khatib R, Fakih MG. Misdiagnosis of community-acquired pneumonia and inappropriate utilization of antibiotics: side effects of the 4-h antibiotic administration rule. Chest. 2007;131(6):1865-9.
442. Christ-Crain M, Opal SM. Clinical review: the role of biomarkers in the diagnosis and management of community-acquired pneumonia. Critical care (London, England). 2010;14(1):203.
443. Wunderink RG. Surrogate markers and microbiologic end points. Clinical infectious diseases : an official publication of the Infectious Diseases Society of America. 2010;51 Suppl 1:S126-30.
444. Hoerr V, Zbytnuik L, Leger C, Tam PP, Kubes P, Vogel HJ. Gram-negative and Gram-positive bacterial infections give rise to a different metabolic response in a mouse model. Journal of proteome research. 2012;11(6):3231-45.
445. Zhang L, Zhang X, Ma Q, Ma F, Zhou H. Transcriptomics and proteomics in the study of H1N1 2009. Genomics Proteomics Bioinformatics. 2010;8(3):139-44.
446. Vincent JL, de Souza Barros D, Cianferoni S. Diagnosis, management and prevention of ventilator-associated pneumonia: an update. Drugs. 2010;70(15):1927-44.
447. Claus RA, Otto GP, Deigner HP, Bauer M. Approaching clinical reality: markers for monitoring systemic inflammation and sepsis. Current molecular medicine. 2010;10(2):227-35.
448. Muller C, Dietz I, Tziotis D, Moritz F, Rupp J, Schmitt-Kopplin P. Molecular cartography in acute Chlamydia pneumoniae infections--a non-targeted metabolomics approach. Analytical and bioanalytical chemistry. 2013;405(15):5119-31.

449. Lv H, Hung CS, Chaturvedi KS, Hooton TM, Henderson JP. Development of an integrated metabolomic profiling approach for infectious diseases research. The Analyst. 2011;136(22):4752-63.
450. Al-Mubarak R, Vander Heiden J, Broeckling CD, Balagon M, Brennan PJ, Vissa VD. Serum Metabolomics Reveals Higher Levels of Polyunsaturated Fatty Acids in Lepromatous Leprosy: Potential Markers for Susceptibility and Pathogenesis. PLOS Neglected Tropical Diseases. 2011;5(9):e1303.
451. Teng R, Junankar PR, Bubb WA, Rae C, Mercier P, Kirk K. Metabolite profiling of the intraerythrocytic malaria parasite Plasmodium falciparum by (1)H NMR spectroscopy. NMR in biomedicine. 2009;22(3):292-302.
452. Steketee PC, Vincent IM, Achcar F, Giordani F, Kim D-H, Creek DJ, et al. Benzoxaborole treatment perturbs S-adenosyl-L-methionine metabolism in Trypanosoma brucei. PLOS Neglected Tropical Diseases. 2018;12(5):e0006450.
453. Creek DJ, Mazet M, Achcar F, Anderson J, Kim D-H, Kamour R, et al. Probing the Metabolic Network in Bloodstream-Form Trypanosoma brucei Using Untargeted Metabolomics with Stable Isotope Labelled Glucose. PLoS Pathog. 2015;11(3):e1004689.
454. Patel S, Ahmed S. Emerging field of metabolomics: Big promise for cancer biomarker identification and drug discovery. Journal of Pharmaceutical and Biomedical Analysis. 2015;107:63-74.
455. Becker S, Kortz L, Helmschrodt C, Thiery J, Ceglarek U. LC–MS-based metabolomics in the clinical laboratory. Journal of Chromatography B. 2012;883-884:68-75.
456. Trygg J, Holmes E, Lundstedt T. Chemometrics in metabonomics. Journal of proteome research. 2007;6(2):469-79.
457. Vinayavekhin N, Homan EA, Saghatelian A. Exploring disease through metabolomics. ACS Chem Biol. 2010;5(1):91-103.
458. Antunes LC, Arena ET, Menendez A, Han J, Ferreira RB, Buckner MM, et al. Impact of salmonella infection on host hormone metabolism revealed by metabolomics. Infection and immunity. 2011;79(4):1759-69.
459. Romero M, Silistre H, Lovelock L, Wright VJ, Chan KG, Hong KW, et al. Genome-wide mapping of the RNA targets of the Pseudomonas aeruginosa riboregulatory protein RsmN. Nucleic acids research. 2018;46(13):6823-40.
460. Allsopp LP, Wood TE, Howard SA, Maggiorelli F, Nolan LM, Wettstadt S, et al. RsmA and AmrZ orchestrate the assembly of all three type VI secretion systems in Pseudomonas aeruginosa. Proceedings of the National Academy of Sciences of the United States of America. 2017;114(29):7707-12.
461. Irie Y, Starkey M, Edwards AN, Wozniak DJ, Romeo T, Parsek MR. Pseudomonas aeruginosa biofilm matrix polysaccharide Psl is regulated transcriptionally by RpoS and post-transcriptionally by RsmA. Molecular microbiology. 2010;78(1):158-72.
462. Brencic A, Lory S. Determination of the regulon and identification of novel mRNA targets of Pseudomonas aeruginosa RsmA. Molecular microbiology. 2009;72(3):612-32.
463. Goodman AL, Kulasekara B, Rietsch A, Boyd D, Smith RS, Lory S. A signaling network reciprocally regulates genes associated with acute infection and chronic persistence in Pseudomonas aeruginosa. Developmental cell. 2004;7(5):745-54.
464. Heurlier K, Williams F, Heeb S, Dormond C, Pessi G, Singer D, et al. Positive control of swarming, rhamnolipid synthesis, and lipase production by the posttranscriptional RsmA/RsmZ system in Pseudomonas aeruginosa PAO1. Journal of bacteriology. 2004;186(10):2936-45.
465. Wolfgang MC, Kulasekara BR, Liang X, Boyd D, Wu K, Yang Q, et al. Conservation of genome content and virulence determinants among clinical and environmental

isolates of Pseudomonas aeruginosa. Proceedings of the National Academy of Sciences of the United States of America. 2003;100(14):8484-9.
466. Ren W, Rajendran R, Zhao Y, Tan B, Wu G, Bazer FW, et al. Amino Acids As Mediators of Metabolic Cross Talk between Host and Pathogen. Frontiers in immunology. 2018;9:319-.
467. Xiong L, Teng JLL, Botelho MG, Lo RC, Lau SKP, Woo PCY. Arginine Metabolism in Bacterial Pathogenesis and Cancer Therapy. International journal of molecular sciences. 2016;17(3):363-.
468. Appleton J. Arginine: Clinical potential of a semi-essential amino acid. Alternative medicine review : a journal of clinical therapeutic. 2002;7(6):512-22.
469. Qiu F, Huang J, Sui M. Targeting arginine metabolism pathway to treat arginine-dependent cancers. Cancer letters. 2015;364(1):1-7.
470. Kuo MT, Savaraj N, Feun LG. Targeted cellular metabolism for cancer chemotherapy with recombinant arginine-degrading enzymes. Oncotarget. 2010;1(4):246-51.
471. Lu C-D. Pathways and regulation of bacterial arginine metabolism and perspectives for obtaining arginine overproducing strains2006. 261-72 p.
472. Morris SM, Jr. Arginine metabolism: boundaries of our knowledge. The Journal of nutrition. 2007;137(6 Suppl 2):1602s-9s.
473. Bogdan C, Rollinghoff M, Diefenbach A. The role of nitric oxide in innate immunity. Immunological reviews. 2000;173:17-26.
474. Iniesta V, Gomez-Nieto LC, Corraliza I. The inhibition of arginase by N(omega)-hydroxy-l-arginine controls the growth of Leishmania inside macrophages. The Journal of experimental medicine. 2001;193(6):777-84.
475. Kropf P, Fuentes JM, Fahnrich E, Arpa L, Herath S, Weber V, et al. Arginase and polyamine synthesis are key factors in the regulation of experimental leishmaniasis in vivo. FASEB journal : official publication of the Federation of American Societies for Experimental Biology. 2005;19(8):1000-2.
476. Boucher JL, Moali C, Tenu JP. Nitric oxide biosynthesis, nitric oxide synthase inhibitors and arginase competition for L-arginine utilization. Cellular and molecular life sciences : CMLS. 1999;55(8-9):1015-28.
477. Gobert AP, McGee DJ, Akhtar M, Mendz GL, Newton JC, Cheng Y, et al. Helicobacter pylori arginase inhibits nitric oxide production by eukaryotic cells: a strategy for bacterial survival. Proceedings of the National Academy of Sciences of the United States of America. 2001;98(24):13844-9.
478. Fang Y-Z, Yang S, Lupton JR, Turner ND, Wu G. Glutathione Metabolism and Its Implications for Health. The Journal of nutrition. 2004;134(3):489-92.
479. Dringen R. Metabolism and functions of glutathione in brain. Progress in neurobiology. 2000;62(6):649-71.
480. Sies H. Oxidative stress: from basic research to clinical application. The American journal of medicine. 1991;91(3c):31s-8s.
481. Fan J, Ye J, Kamphorst JJ, Shlomi T, Thompson CB, Rabinowitz JD. Quantitative flux analysis reveals folate-dependent NADPH production. Nature. 2014;510(7504):298-302.
482. Sassone-Corsi P. Physiology. When metabolism and epigenetics converge. Science (New York, NY). 2013;339(6116):148-50.
483. Locasale JW. Serine, glycine and one-carbon units: cancer metabolism in full circle. Nature reviews Cancer. 2013;13(8):572-83.
484. Griffith OW. Biologic and pharmacologic regulation of mammalian glutathione synthesis. Free Radical Biology and Medicine. 1999;27(9):922-35.

485. Persaud C, Forrester T, Jackson AA. Urinary excretion of 5-L-oxoproline (pyroglutamic acid) is increased during recovery from severe childhood malnutrition and responds to supplemental glycine. The Journal of nutrition. 1996;126(11):2823-30.
486. Yu YM, Ryan CM, Fei ZW, Lu XM, Castillo L, Schultz JT, et al. Plasma L-5-oxoproline kinetics and whole blood glutathione synthesis rates in severely burned adult humans. American journal of physiology Endocrinology and metabolism. 2002;282(2):E247-58.
487. Antonov A, Agostini M, Morello M, Minieri M, Melino G, Amelio I. Bioinformatics analysis of the serine and glycine pathway in cancer cells. Oncotarget. 2014;5(22):11004-13.
488. Maddocks OD, Berkers CR, Mason SM, Zheng L, Blyth K, Gottlieb E, et al. Serine starvation induces stress and p53-dependent metabolic remodelling in cancer cells. Nature. 2013;493(7433):542-6.
489. Kim SK, Jung WH, Koo JS. Differential expression of enzymes associated with serine/glycine metabolism in different breast cancer subtypes. PloS one. 2014;9(6):e101004-e.
490. Amelio I, Cutruzzolá F, Antonov A, Agostini M, Melino G. Serine and glycine metabolism in cancer. Trends in biochemical sciences. 2014;39(4):191-8.
491. Baruch M, Belotserkovsky I, Hertzog BB, Ravins M, Dov E, McIver KS, et al. An extracellular bacterial pathogen modulates host metabolism to regulate its own sensing and proliferation. Cell. 2014;156(1-2):97-108.
492. Moffett J, Aryan Namboodiri M. Tryptophan and the immune response2003. 247-65 p.
493. Love AC, Schwartz I, Petzke MM. Induction of indoleamine 2,3-dioxygenase by Borrelia burgdorferi in human immune cells correlates with pathogenic potential. Journal of leukocyte biology. 2015;97(2):379-90.
494. Wymann MP, Schneiter R. Lipid signalling in disease. Nature Reviews Molecular Cell Biology. 2008;9:162.
495. van Meer G, Voelker DR, Feigenson GW. Membrane lipids: where they are and how they behave. Nature Reviews Molecular Cell Biology. 2008;9:112.
496. Teng O, Ang CKE, Guan XL. Macrophage–Bacteria Interactions—A Lipid-Centric Relationship. Frontiers in Immunology. 2017;8(1836).
497. Endemann G, Stanton LW, Madden KS, Bryant CM, White RT, Protter AA. CD36 is a receptor for oxidized low density lipoprotein. The Journal of biological chemistry. 1993;268(16):11811-6.
498. Saka HA, Valdivia R. Emerging roles for lipid droplets in immunity and host-pathogen interactions. Annual review of cell and developmental biology. 2012;28:411-37.
499. Bansal K, Narayana Y, Patil SA, Balaji KN. M. bovis BCG induced expression of COX-2 involves nitric oxide-dependent and -independent signaling pathways. Journal of leukocyte biology. 2009;85(5):804-16.
500. Grassme H, Gulbins E, Brenner B, Ferlinz K, Sandhoff K, Harzer K, et al. Acidic sphingomyelinase mediates entry of N. gonorrhoeae into nonphagocytic cells. Cell. 1997;91(5):605-15.
501. Esen M, Schreiner B, Jendrossek V, Lang F, Fassbender K, Grassme H, et al. Mechanisms of Staphylococcus aureus induced apoptosis of human endothelial cells. Apoptosis : an international journal on programmed cell death. 2001;6(6):431-9.
502. Grassme H, Jendrossek V, Riehle A, von Kurthy G, Berger J, Schwarz H, et al. Host defense against Pseudomonas aeruginosa requires ceramide-rich membrane rafts. Nature medicine. 2003;9(3):322-30.
503. Cannon CL, Kowalski MP, Stopak KS, Pier GB. Pseudomonas aeruginosa-induced apoptosis is defective in respiratory epithelial cells expressing mutant cystic fibrosis

transmembrane conductance regulator. American journal of respiratory cell and molecular biology. 2003;29(2):188-97.
504. Lau SK, Lee KC, Curreem SO, Chow WN, To KK, Hung IF, et al. Metabolomic Profiling of Plasma from Patients with Tuberculosis by Use of Untargeted Mass Spectrometry Reveals Novel Biomarkers for Diagnosis. Journal of clinical microbiology. 2015;53(12):3750-9.
505. Ecker J, Liebisch G, Englmaier M, Grandl M, Robenek H, Schmitz G. Induction of fatty acid synthesis is a key requirement for phagocytic differentiation of human monocytes. Proceedings of the National Academy of Sciences of the United States of America. 2010;107(17):7817-22.
506. Grant R, Coggan S, Smythe G. The Physiological Action of Picolinic Acid in the Human Brain2009. 71-9 p.
507. Melillo G, Bosco MC, Musso T, Varesio L. Immunobiology of Picolinic Acid. In: Filippini GA, Costa CVL, Bertazzo A, editors. Recent Advances in Tryptophan Research: Tryptophan and Serotonin Pathways. Boston, MA: Springer US; 1996. p. 135-41.
508. Blasi E, Mazzolla R, Pitzurra L, Barluzzi R, Bistoni F. Protective effect of picolinic acid on mice intracerebrally infected with lethal doses of Candida albicans. Antimicrobial agents and chemotherapy. 1993;37(11):2422-6.
509. Melillo G, Musso T, Sica A, Taylor LS, Cox GW, Varesio L. A hypoxia-responsive element mediates a novel pathway of activation of the inducible nitric oxide synthase promoter. The Journal of experimental medicine. 1995;182(6):1683-93.
510. Griffith RS, Norins AL, Kagan C. A multicentered study of lysine therapy in Herpes simplex infection. Dermatologica. 1978;156(5):257-67.
511. Katz JM, Plowden J, Renshaw-Hoelscher M, Lu X, Tumpey TM, Sambhara S. Immunity to influenza: the challenges of protecting an aging population. Immunologic research. 2004;29(1-3):113-24.
512. Medzhitov R. Recognition of microorganisms and activation of the immune response. Nature. 2007;449(7164):819-26.
513. Plackett TP, Boehmer ED, Faunce DE, Kovacs EJ. Aging and innate immune cells. Journal of leukocyte biology. 2004;76(2):291-9.
514. Hirayama D, Iida T, Nakase H. The Phagocytic Function of Macrophage-Enforcing Innate Immunity and Tissue Homeostasis. International journal of molecular sciences. 2017;19(1):92.
515. Janeway CA, Jr. Approaching the asymptote? Evolution and revolution in immunology. Cold Spring Harbor symposia on quantitative biology. 1989;54 Pt 1:1-13.
516. Aspinall R. Age-related changes in the function of T cells. Microscopy Research and Technique. 2003;62(6):508-13.
517. Gomez CR, Boehmer ED, Kovacs EJ. The aging innate immune system. Current opinion in immunology. 2005;17(5):457-62.
518. Wong C, Goldstein DR. Impact of aging on antigen presentation cell function of dendritic cells. Current opinion in immunology. 2013;25(4):535-41.
519. Vu T, Farish S, Jenkins M, Kelly H. A meta-analysis of effectiveness of influenza vaccine in persons aged 65 years and over living in the community. Vaccine. 2002;20(13-14):1831-6.
520. Thomas-Crusells J, McElhaney JE, Aguado MT. Report of the ad-hoc consultation on aging and immunization for a future WHO research agenda on life-course immunization. Vaccine. 2012;30(42):6007-12.
521. Prelog M. Aging of the immune system: a risk factor for autoimmunity? Autoimmunity reviews. 2006;5(2):136-9.
522. Oishi Y, Manabe I. Macrophages in age-related chronic inflammatory diseases. Npj Aging And Mechanisms Of Disease. 2016;2:16018.

523. Bauer ME, Fuente Mde L. The role of oxidative and inflammatory stress and persistent viral infections in immunosenescence. Mechanisms of ageing and development. 2016;158:27-37.
524. De la Fuente M, Miquel J. An update of the oxidation-inflammation theory of aging: the involvement of the immune system in oxi-inflamm-aging. Current pharmaceutical design. 2009;15(26):3003-26.
525. Xaus J, Comalada M, Valledor AF, Cardó M, Herrero C, Soler C, et al. Molecular Mechanisms Involved in Macrophage Survival, Proliferation, Activation or Apoptosis. Immunobiology. 2001;204(5):543-50.
526. Gordon S. The macrophage: past, present and future. Eur J Immunol. 2007;37 Suppl 1:S9-17.
527. Sebastián C, Espia M, Serra M, Celada A, Lloberas J. MacrophAging: A cellular and molecular review. Immunobiology. 2005;210(2):121-6.
528. Leibovich SJ, Ross R. The role of the macrophage in wound repair. A study with hydrocortisone and antimacrophage serum. The American journal of pathology. 1975;78(1):71-100.
529. Kawai T, Akira S. The role of pattern-recognition receptors in innate immunity: update on Toll-like receptors. Nat Immunol. 2010;11(5):373-84.
530. Shaw AC, Joshi S, Greenwood H, Panda A, Lord JM. Aging of the innate immune system. Current opinion in immunology. 2010;22(4):507-13.
531. Lloberas J, Celada A. Effect of aging on macrophage function. Experimental gerontology. 2002;37(12):1325-31.
532. Vida C, de Toda IM, Cruces J, Garrido A, Gonzalez-Sanchez M, De la Fuente M. Role of macrophages in age-related oxidative stress and lipofuscin accumulation in mice. Redox Biol. 2017;12:423-37.
533. Chelvarajan RL, Liu Y, Popa D, Getchell ML, Getchell TV, Stromberg AJ, et al. Molecular basis of age-associated cytokine dysregulation in LPS-stimulated macrophages. Journal of leukocyte biology. 2006;79(6):1314-27.
534. Karasik D, Demissie S, Cupples LA, Kiel DP. Disentangling the genetic determinants of human aging: biological age as an alternative to the use of survival measures. The journals of gerontology Series A, Biological sciences and medical sciences. 2005;60(5):574-87.
535. Kerber RA, O'Brien E, Cawthon RM. Gene expression profiles associated with aging and mortality in humans. Aging cell. 2009;8(3):239-50.
536. Deelen J, Beekman M, Uh HW, Helmer Q, Kuningas M, Christiansen L, et al. Genome-wide association study identifies a single major locus contributing to survival into old age; the APOE locus revisited. Aging cell. 2011;10(4):686-98.
537. Toth MJ, Tchernof A. Lipid metabolism in the elderly. European journal of clinical nutrition. 2000;54 Suppl 3:S121-5.
538. Dennis JW, Nabi IR, Demetriou M. Metabolism, cell surface organization, and disease. Cell. 2009;139(7):1229-41.
539. Partridge L, Thornton J, Bates G. The new science of ageing. Philos Trans R Soc Lond B Biol Sci. 2011;366(1561):6-8.
540. Feltes BC, de Faria Poloni J, Bonatto D. The developmental aging and origins of health and disease hypotheses explained by different protein networks. Biogerontology. 2011;12(4):293-308.
541. Houtkooper RH, Argmann C, Houten SM, Cantó C, Jeninga EH, Andreux PA, et al. The metabolic footprint of aging in mice. Scientific reports. 2011;1:134-.
542. Yu Z, Zhai G, Singmann P, He Y, Xu T, Prehn C, et al. Human serum metabolic profiles are age dependent. Aging cell. 2012;11(6):960-7.
543. Lin MT, Beal MF. Mitochondrial dysfunction and oxidative stress in neurodegenerative diseases. Nature. 2006;443(7113):787-95.

544. Houtkooper RH, Williams RW, Auwerx J. Metabolic networks of longevity. Cell. 2010;142(1):9-14.
545. Menni C, Kastenmüller G, Petersen AK, Bell JT, Psatha M, Tsai P-C, et al. Metabolomic markers reveal novel pathways of ageing and early development in human populations. Int J Epidemiol. 2013;42(4):1111-9.
546. Houtkooper RH, Argmann C, Houten SM, Cantó C, Jeninga EH, Andreux PA, et al. The metabolic footprint of aging in mice. Scientific Reports. 2011;1:134.
547. Neumann B, Held M, Liebel U, Erfle H, Rogers P, Pepperkok R, et al. High-throughput RNAi screening by time-lapse imaging of live human cells. Nature methods. 2006;3(5):385-90.
548. Harrington H, Cato P, Salazar F, Wilkinson M, Knox A, Haycock JW, et al. Immunocompetent 3D model of human upper airway for disease modeling and in vitro drug evaluation. Molecular pharmaceutics. 2014;11(7):2082-91.
549. Lemonakis N, Poudyal H, Halabalaki M, Brown L, Tsarbopoulos A, Skaltsounis AL, et al. The LC-MS-based metabolomics of hydroxytyrosol administration in rats reveals amelioration of the metabolic syndrome. Journal of chromatography B, Analytical technologies in the biomedical and life sciences. 2017;1041-1042:45-59.
550. De La Fuente M. Changes in the macrophage function with aging. Comparative biochemistry and physiology A, Comparative physiology. 1985;81(4):935-8.
551. Mancuso P, McNish RW, Peters-Golden M, Brock TG. Evaluation of phagocytosis and arachidonate metabolism by alveolar macrophages and recruited neutrophils from F344xBN rats of different ages. Mechanisms of ageing and development. 2001;122(15):1899-913.
552. Aprahamian T, Takemura Y, Goukassian D, Walsh K. Ageing is associated with diminished apoptotic cell clearance in vivo. Clin Exp Immunol. 2008;152(3):448-55.
553. Hearps AC, Martin GE, Angelovich TA, Cheng WJ, Maisa A, Landay AL, et al. Aging is associated with chronic innate immune activation and dysregulation of monocyte phenotype and function. Aging cell. 2012;11(5):867-75.
554. Fietta A, Merlini C, Dos Santos C, Rovida S, Grassi C. Influence of Aging on Some Specific and Nonspecific Mechanisms of the Host Defense System in 146 Healthy Subjects. Gerontology. 1994;40(5):237-45.
555. Schlaermann P, Toelle B, Berger H, Schmidt SC, Glanemann M, Ordemann J, et al. A novel human gastric primary cell culture system for modelling Helicobacter pylori infection in vitro. Gut. 2016;65(2):202-13.
556. Giavalisco P, Kohl K, Hummel J, Seiwert B, Willmitzer L. 13C isotope-labeled metabolomes allowing for improved compound annotation and relative quantification in liquid chromatography-mass spectrometry-based metabolomic research. Analytical chemistry. 2009;81(15):6546-51.
557. Bueschl C, Kluger B, Berthiller F, Lirk G, Winkler S, Krska R, et al. MetExtract: a new software tool for the automated comprehensive extraction of metabolite-derived LC/MS signals in metabolomics research. Bioinformatics (Oxford, England). 2012;28(5):736-8.

Appendix

Table A1: A list of total identified metabolites in macrophages in response to polarization into M0, M1 and M2.

Putative metabolite	Mass	RT	FORMULA	Confidence
5-Hydroxyferulate	210.0528	6.18	C10H10O5	L2
Phenylacetylglycine	193.0741	5.94	C10H11NO3	L2
L-Kynurenine	208.0849	10.62	C10H12N2O3	L2
Inosine	268.0808	10.64	C10H12N4O5	L1
Xanthosine	284.0756	10.01	C10H12N4O6	L2
phlorisobutyrophenone	196.0737	4.61	C10H12O4	L2
IMP	348.0471	11.69	C10H13N4O8P	L1
Deoxyadenosine	251.1018	8.77	C10H13N5O3	L1
Adenosine	267.0967	9.63	C10H13N5O4	L1
(R)-2-Methylimino-1-phenylpropan-1-ol	163.0997	5.59	C10H13NO	L2
(-)-Salsolinol	179.0946	6.29	C10H13NO2	L2
2,6-Dihydroxypseudooxynicotine	210.1005	8.57	C10H14N2O3	L2
Porphobilinogen	226.0953	6.38	C10H14N2O4	L2
(1-Ribosylimidazole)-4-acetate	258.0852	10.74	C10H14N2O6	L2
AMP	347.0629	10.68	C10H14N5O7P	L2
5-Methyl-2'-deoxycytidine	241.1062	8.56	C10H15N3O4	L2
5-Methylcytidine	257.1011	9.64	C10H15N3O5	L2
XTP	261.9874	11.97	C10H15N4O15P3	L2
ADP	427.0292	11.11	C10H15N5O10P2	L2
Biotin	244.0881	6.37	C10H16N2O3S	L2
Biotin amide	243.1042	9.75	C10H17N3O2S	L2
Glutathione	307.0837	11.27	C10H17N3O6S	L1
3-Hydroxysebacic acid	218.1155	5.66	C10H18O5	L2
Propanoylcarnitine	217.1314	9.60	C10H19NO4	L2
Decanoic acid	172.1463	4.93	C10H20O2	L2
[PC acety] 1-acetyl-sn-glycero-3-phosphocholine	299.1133	10.07	C10H22NO7P	L2
2-Quinolinecarboxylic acid	173.0477	6.19	C10H7NO2	L2
Indole-3-acetaldehyde	159.0684	7.06	C10H9NO	L2
5-Hydroxyindoleacetaldehyde	175.0634	4.97	C10H9NO2	L2
5-Hydroxyindoleacetate	191.0582	10.07	C10H9NO3	L2
Indolelactate	205.0739	8.49	C11H11NO3	L2
L-Tryptophan	204.0899	11.27	C11H12N2O2	L2
5-Hydroxy-L-tryptophan	220.0847	9.21	C11H12N2O3	L2
L-Formylkynurenine	236.0797	9.81	C11H12N2O4	L2
N-Acetyl-L-phenylalanine	207.0897	4.80	C11H13NO3	L2
N-Ribosylnicotinamide	254.0902	20.67	C11H14N2O5	L2
7-Methylinosine	282.0963	9.30	C11H14N4O5	L2
5'-Methylthioadenosine	297.0895	8.59	C11H15N5O3S	L2
1-Methyladenosine	281.1123	13.42	C11H15N5O4	L2
beta-Citryl-L-glutamic acid	321.0695	13.85	C11H15NO10	L2
1-(beta-D-Ribofuranosyl)-1,4-dihydronicotinamide	256.1059	9.52	C11H16N2O5	L2
N-Acetyl-aspartyl-glutamate	304.0904	12.17	C11H16N2O8	L2
2,7-Anhydro-alpha-N-acetylneuraminic acid	291.0954	10.28	C11H17NO8	L2
gamma-L-Glutamyl-L-cysteinyl-beta-alanine	321.0994	10.21	C11H19N3O6S	L2
N-Glycoloyl-neuraminate	325.1006	11.45	C11H19NO10	L2
O-Acetylneuraminic acid	309.1060	11.37	C11H19NO9	L2
L-isoleucyl-L-proline	228.1475	8.45	C11H20N2O3	L2
Butanoylcarnitine	231.1470	9.12	C11H21NO4	L2

Hydroxybutyrylcarnitine	247.1419	10.33	C11H21NO5	L2
[FA (11:0)] undecanoic acid	186.1619	4.85	C11H22O2	L2
N1,N8-diacetylspermidine	229.1790	15.04	C11H23N3O2	L2
N-Acetylserotonin	218.1055	6.34	C12H14N2O2	L2
Thiamine aldehyde	262.0889	8.72	C12H14N4OS	L2
[FA (12:4/2:0)]	222.0892	4.96	C12H14O4	L2
Thiamin	264.1044	19.92	C12H16N4OS	L2
N2-N2-Dimethylguanosine	311.1229	9.27	C12H17N5O5	L2
N4-(Acetyl-beta-D-glucosaminyl)asparagine	335.1329	12.53	C12H21N3O8	L2
Tiglylcarnitine	243.1470	8.89	C12H21NO4	L2
3-Hydroxydodecanedioicacid	246.1467	5.21	C12H22O5	L2
2-Methylbutyroylcarnitine	245.1627	7.01	C12H23NO4	L2
Dodecanoic acid	200.1777	4.77	C12H24O2	L2
Ac-Tyr-OEt	251.1157	5.05	C13H17NO4	L2
N-(4-nitrophenyl)validamine	298.1165	8.94	C13H18N2O6	L2
(R)-S-Lactoylglutathione	379.1049	9.83	C13H21N3O8S	L2
(L-Seryl)adenylate	218.0556	11.64	C13H21N6O9P	L2
S-glutathionyl-L-cysteine	426.0879	12.19	C13H22N4O8S2	L2
[FA hydroxy(10:0)]	275.1733	9.32	C13H25NO5	L2
Hypaphorine	246.1367	9.39	C14H18N2O2	L2
N(alpha)-Benzyloxycarbonyl-L-leucine	265.1313	8.94	C14H19NO4	L2
[FA oxo(14:0)]	242.1882	4.78	C14H26O3	L2
Butyl 3-O-beta-D-glucopyranosyl-butanoate	322.1628	6.30	C14H26O8	L2
Tetradecanoic acid	228.2090	4.72	C14H28O2	L2
indole-3-acetyl-valine	274.1317	6.36	C15H18N2O3	L2
UDP-glucose	566.0546	12.06	C15H24N2O17P2	L2
[FA methyl(14:0)]	242.2247	4.71	C15H30O2	L2
Indole-3-acetyl-isoleucine	288.1475	4.78	C16H20N2O3	L2
Alpha-CEHC	278.1517	4.65	C16H22O4	L2
[FA oxo(5:2/5:0/6:0)] (1R,2R)	268.2038	4.79	C16H28O3	L2
(2E,6E)-(10R,11S)-10,11-Epoxy-3,7,11-trimethyltrideca-2,6-dienoic acid	284.1987	4.80	C16H28O4	L2
[FA oxo(16:0)]	270.2195	4.70	C16H30O3	L2
Myristoylglycine	285.2303	4.60	C16H31NO3	L2
Hexadecanal	240.2454	5.31	C16H32O	L2
Hexadecanoic acid	256.2404	4.67	C16H32O2	L2
16-hydroxypalmitate	272.2351	4.63	C16H32O3	L2
[FA amino(16:0)]	271.2512	8.54	C16H33NO2	L2
p-(3,4-Dihydro-6-methoxy-2-naphthyl)phenol	252.1150	4.77	C17H16O2	L2
Trp-Asp-Gly	376.1382	9.29	C17H20N4O6	L2
UDP-N-acetyl-D-glucosamine	607.0814	11.30	C17H27N3O17P2	L2
[FA methoxy(16:1)]	284.2351	4.70	C17H32O3	L2
[FA (17:0)]	270.2560	4.66	C17H34O2	L2
[SP (17:0)]	287.2823	5.79	C17H37NO2	L2
8-Allyl-2-phenyl-8H-1,3a,8-triaza-cyclopenta[a]indene	273.1267	4.18	C18H15N3	L2
[FA hydroxy(18:0/4:0)] tetraynoic acid	280.1100	4.76	C18H16O3	L2
[FA (18:3)]	278.2243	4.66	C18H30O2	L2
[FA oxo(5:1/5:0/8:0)]	294.2195	4.72	C18H30O3	L2
[FA (18:3)]	310.2144	4.76	C18H30O4	L2
Linoleate	280.2403	4.66	C18H32O2	L2
[FA hydroxy(18:2)]	296.2351	4.66	C18H32O3	L2
[FA (18:2)]	312.2299	4.81	C18H32O4	L2
[FA (18:1)]	282.2559	4.65	C18H34O2	L2
2-Oxooctadecanoic acid	298.2508	4.65	C18H34O3	L2
[FA (18:1)]	281.2718	6.91	C18H35NO	L2
[SP (2:0)]	297.2666	6.74	C18H35NO2	L2

4-8dimethylnonanoylcarnitine	329.2566	4.73	C18H35NO4	L2
Octadecanoic acid	284.2716	4.75	C18H36O2	L2
[FA hydroxy(18:0)]	300.2664	4.68	C18H36O3	L2
[FA hydroxy(18:0)]	316.2613	4.79	C18H36O4	L2
[FA (16:2)]	299.2823	6.69	C18H37NO2	L2
Sphinganine	301.2980	8.57	C18H39NO2	L2
[SP hydrox] 4-hydroxysphinganine	317.2928	8.60	C18H39NO3	L2
[FA oxo(19:0)]	312.2663	4.55	C19H36O3	L2
1,2-dioctanoyl-1-amino-2,3-propanediol	343.2721	6.26	C19H37NO4	L2
[GP (16:0)]	392.2326	4.73	C19H37O6P	L2
5-methyl-octadecanoic acid	298.2872	4.66	C19H38O2	L2
[FA hydroxy(19:0)]	314.2822	5.33	C19H38O3	L2
LPA(0:0/16:0)	410.2432	5.96	C19H39O7P	L2
1-O-Hexadecyl-sn-glycerol	316.2977	5.33	C19H40O3	L2
PA(O-16:0/0:0)	396.2640	6.00	C19H41O6P	L2
2,2-Dimethyl-3-(4-methoxyphenyl)-4-ethyl-2H-1-benzopyran-7-ol	310.1568	5.10	C20H22O3	L2
CMP-N-acetylneuraminate	614.1464	11.43	C20H31N4O16P	L2
Glutathione disulfide	306.0759	12.03	C20H32N6O12S2	L2
[FA hydroxy(20:2)]	324.2663	4.48	C20H36O3	L2
[FA (20:0)] eicosenoic acid	310.2874	4.64	C20H38O2	L2
2-Oxophytanate	326.2821	4.58	C20H38O3	L2
1,4-Bis(2-ethylhexyl) sulfosuccinate	422.2340	4.44	C20H38O7S	L2
[FA (20:0)] eicosanoic acid	312.3030	4.63	C20H40O2	L2
Dihydrochelirubine	363.1101	9.48	C21H17NO5	L2
Anthocyanin 3'-O-beta-D-glucoside	384.1215	11.47	C21H20O7	L2
NADH	665.1256	10.45	C21H29N7O14P2	L2
NADPH	372.5454	12.26	C21H30N7O17P3	L2
CoA	383.5576	10.41	C21H36N7O16P3S	L2
5beta-Pregnane-3alpha,17alpha,20alpha-triol	336.2663	4.44	C21H36O3	L2
[FA methoxy,trihydrox] prostadiene	354.2769	5.25	C21H38O4	L2
cis-5-Tetradecenoylcarnitine	369.2878	6.13	C21H39NO4	L2
[FA oxo(21:0)]	340.2977	5.05	C21H40O3	L2
1,2-dioctanoyl-3-methyl-1,2,3-butanetriol	372.2873	5.26	C21H40O5	L2
Tetradecanoylcarnitine	371.3035	6.06	C21H41NO4	L2
LPA(0:0/18:1)	436.2588	5.88	C21H41O7P	L2
Lysophosphatidylethanolamine	451.2700	5.81	C21H42NO7P	L2
[FA hydroxy(21:0)]	342.3134	5.29	C21H42O3	L2
[GL (18:0)]	358.3084	5.25	C21H42O4	L2
[PE (16:1)]	437.2903	5.72	C21H44NO6P	L2
[PE (16:0)]	453.2852	5.78	C21H44NO7P	L2
1-O-Octadecyl-sn-glycerol	344.3291	5.28	C21H44O3	L2
LPA(18:0e/0:0)	424.2951	4.72	C21H45O6P	L2
[PC methyl(12:2)]	439.3061	5.87	C21H46NO6P	L2
Docosahexaenoic acid	328.2405	4.60	C22H32O2	L2
[FA trihydroxy(22:0/6:0)]	376.2257	5.59	C22H32O5	L2
[FA trihydroxy(2:0/2:0)]	381.2879	4.71	C22H39NO4	L2
[SP amino,tetramethyl(4:0/18:0/3:0)]	369.3240	4.78	C22H43NO3	L2
[PS (16:0)]	497.2753	4.90	C22H44NO9P	L2
[PG (16:0)]	484.2801	4.63	C22H45O9P	L2
[PC (14:1)]	451.3060	6.00	C22H46NO6P	L2
[PC (14:0)]	467.3010	6.11	C22H46NO7P	L2
di-n-Undecylamine	325.3707	9.34	C22H47N	L2
[PC ethyl(12:2)]	453.3217	6.17	C22H48NO6P	L2
3beta-Chloro-N,N-bis(2-chloroethyl)-androst-5-en-17beta-amine	431.1918	4.60	C23H36NCl3	L2
[ST (3:0)]	362.2820	4.44	C23H38O3	L2
[GL (8:0)]	364.2976	4.45	C23H40O3	L2

9-Hexadecenoylcarnitine	397.3191	5.94	C23H43NO4	L2
3-Hydroxy-9-hexadecenoylcarnitine	413.3139	4.47	C23H43NO5	L2
[FA] O-Palmitoyl-R-carnitine	399.3347	5.88	C23H45NO4	L2
LysoPE(0:0/18:1)	479.3009	5.68	C23H46NO7P	L2
[PC (7:0/8:0)]	495.2962	5.72	C23H46NO8P	L2
[PC (15:1)]	465.3217	5.83	C23H48NO6P	L2
[PC (15:0)]	481.3165	5.65	C23H48NO7P	L2
[PC methyl(14:2)]	467.3375	5.77	C23H50NO6P	L2
[FA (24:6)]	344.1776	5.37	C24H24O2	L2
[ST hydrox] 3alpha,12alpha-Dihydroxy-5beta-chol-6-en-24-oic Acid	390.2768	5.11	C24H38O4	L2
[PS (18:1)]	523.2909	4.85	C24H46NO9P	L2
[FA (24:0)]-tetracosenoic acid	366.3498	4.61	C24H46O2	L2
[PG (18:1)]	510.2955	4.60	C24H47O9P	L2
[PC (16:1)]	493.3166	6.00	C24H48NO7P	L2
[PS (18:0)]	525.3065	4.83	C24H48NO9P	L2
Octadecyl hexanoate	368.3655	4.60	C24H48O2	L2
[PG (18:0)]	512.3117	4.60	C24H49O9P	L2
[PC (16:1)]	479.3372	5.87	C24H50NO6P	L2
[PC (16:0)]	495.3321	5.94	C24H50NO7P	L2
[PC (16:2)]	481.3530	6.00	C24H52NO6P	L2
[ST methoxy,hydroxy(3:0)]	476.2045	5.38	C25H32O9	L2
Testosterone isocaproate	386.2817	4.44	C25H38O3	L2
LysoPE(20:4/0:0)	501.2855	5.65	C25H44NO7P	L2
LysoPE(0:0/20:3)	503.3016	5.62	C25H46NO7P	L2
Elaidic carnitine	425.3502	5.82	C25H47NO4	L2
Stearoylcarnitine	427.3658	5.76	C25H49NO4	L2
[PI (16:0)]	572.2960	4.94	C25H49O12P	L2
[PC (17:0)]	507.3318	5.92	C25H50NO7P	L2
PS(19:0/0:0)	539.3226	5.67	C25H50NO9P	L2
[PC (17:1)]	493.3531	5.76	C25H52NO6P	L2
LysoPC(17:0)	509.3477	5.88	C25H52NO7P	L2
Glycodeoxycholate	449.3142	5.21	C26H43NO5	L2
[ST hydrox] N-(3alpha,7alpha-dihydroxy-5beta-cholan-24-oyl)-taurine	499.2968	4.92	C26H45NO6S	L2
1-Oleoylglycerophosphocholine	521.3478	5.86	C26H52NO7P	L2
[PC (18:1)]	507.3686	5.82	C26H54NO6P	L2
[PC (18:0)]	523.3637	5.82	C26H54NO7P	L2
LysoPC(O-18:0)	509.3845	5.85	C26H56NO6P	L2
[ST hydroxy(3:0)]	428.2926	4.84	C27H40O4	L2
[ST (3:0/3:0/3:0)]	470.3006	6.13	C27H41F3O3	L2
LysoPE(0:0/22:6)	525.2852	5.60	C27H44NO7P	L2
LysoPE(0:0/22:5)	527.3012	5.57	C27H46NO7P	L2
Cholesterolsulfate	466.3115	4.49	C27H46O4S	L2
[PI (18:1)]	598.3117	4.88	C27H51O12P	L2
LysoPE(0:0/22:2)	533.3484	5.13	C27H52NO7P	L2
Ercalcitriol	428.3291	4.78	C28H44O3	L2
PG(22:6/0:0)	556.2798	4.57	C28H45O9P	L2
PS(22:4/0:0)	573.3063	4.57	C28H48NO9P	L2
LysoPC(20:4)	543.3319	5.84	C28H50NO7P	L2
LysoPC(20:2)	547.3636	5.10	C28H54NO7P	L2
LysoPC(20:1)	549.3791	5.75	C28H56NO7P	L2
PC(P-20:0/0:0)	535.3997	5.66	C28H58NO6P	L2
Iminoglycine	73.0164	11.17	C2H3NO2	L2
Glycine	75.0320	13.02	C2H5NO2	L2
Phosphonoacetaldehyde	123.9926	11.62	C2H5O4P	L2
2-Hydroxyethanesulfonate	125.9987	9.52	C2H6O4S	L2
Hypotaurine	109.0198	12.65	C2H7NO2S	L2

Taurine	125.0146	12.57	C2H7NO3S	L1
Ethanolamine phosphate	141.0191	12.22	C2H8NO4P	L1
24-isopropenyl-22E-dehydrocholesterol	424.3701	5.12	C30H48O	L2
[PC (22:6)]	567.3321	5.79	C30H50NO7P	L2
LysoPC(22:5)	569.3481	5.77	C30H52NO7P	L2
C14 Ceramide	509.4806	5.12	C32H63NO3	L2
Cer(d16:1/17:0)	523.4962	5.08	C33H65NO3	L2
Cer(d18:0/15:0)	525.5121	5.11	C33H67NO3	L2
3-O-(Galb)-(25R)-12-oxo-5alpha-spirostan-3beta-ol	608.3933	5.16	C34H56O9	L2
Cer(d18:2/16:0)	535.4962	5.06	C34H65NO3	L2
Cer (d18:1/16:0)	537.5120	5.10	C34H67NO3	L2
PA(32:1)	646.4573	4.47	C35H67O8P	L2
PS(12:0/17:0)	693.4578	5.02	C35H68NO10P	L2
PE(30:0)	663.4837	4.47	C35H70NO8P	L2
Cer(d18:0/17:0)	553.5431	5.08	C35H71NO3	L2
[SP (18:0)]	563.5277	5.10	C36H69NO3	L2
PS(O-16:0/14:1)	691.4787	5.00	C36H70NO9P	L2
Ceramide (d18:1/18:0)	565.5435	5.10	C36H71NO3	L2
[PC (14:0/14:0)]	677.4992	5.31	C36H72NO8P	L2
PC(O-16:0/12:0)	663.5202	5.32	C36H74NO7P	L2
PA(34:1)	674.4885	4.46	C37H71O8P	L2
PE(14:0/P-18:1)	673.5046	5.04	C37H72NO7P	L2
PE(32:1)	689.4995	5.05	C37H72NO8P	L2
PE(32:0)	691.5148	5.30	C37H74NO8P	L2
SM(d18:1/14:0)	674.5359	5.53	C37H75N2O6P	L2
PA(13:0/22:6)	678.4274	4.45	C38H63O8P	L2
PS(32:1)	733.4890	4.54	C38H72NO10P	L2
[PC (14:0/16:1)]	703.5147	5.28	C38H74NO8P	L2
PG(32:0)	722.5102	4.42	C38H75O10P	L2
PC (14:2/16:0)	689.5357	5.28	C38H76NO7P	L2
PC(30:0)	705.5306	5.27	C38H76NO8P	L2
[SP (18:0/14:0)]	688.5517	5.50	C38H77N2O6P	L2
PC(O-14:0/16:0)	691.5514	5.27	C38H78NO7P	L2
[GL methyl(15:0/8:0)]	602.5273	4.55	C39H70O4	L2
PE(16:1/P-18:1)	699.5190	5.03	C39H74NO7P	L2
PE(34:2)	715.5147	5.03	C39H74NO8P	L2
PE(16:0/P-18:1)	701.5358	5.03	C39H76NO7P	L2
PE(34:1)	717.5308	5.15	C39H76NO8P	L2
SM(d16:1/18:1)	700.5513	5.48	C39H77N2O6P	L2
PE-NMe2(16:0/16:0)	719.5479	5.27	C39H78NO8P	L2
SM(d16:1/18:0)	702.5672	5.48	C39H79N2O6P	L2
[PE (18:2/16:0)]	705.5669	5.26	C39H80NO7P	L2
N-Methylethanolamine phosphate	155.0347	11.59	C3H10NO4P	L2
Hydantoin	100.0273	9.66	C3H4N2O2	L2
3-Oxopropanoate	88.0161	8.59	C3H4O3	L2
N-Formiminoglycine	102.0429	11.29	C3H6N2O2	L2
3-Hydroxypropanoate	90.0317	8.58	C3H6O3	L2
3-sulfopropanoate	153.9935	12.27	C3H6O5S	L2
Guanidinoacetate	117.0538	13.32	C3H7N3O2	L1
L-Alanine	89.0477	12.48	C3H7NO2	L2
L-Cysteine	121.0197	8.52	C3H7NO2S	L2
D-Serine	105.0426	9.20	C3H7NO3	L2
Propanoyl phosphate	154.0031	9.96	C3H7O5P	L2
D-Glyceraldehyde 3-phosphate	169.9981	12.10	C3H7O6P	L2
Glycerol	92.0473	10.46	C3H8O3	L2
(R)-1-Aminopropan-2-ol	75.0684	10.30	C3H9NO	L2

Propane-1,2-diol 1-phosphate	156.0188	9.88	C3H9O5P	L2
sn-Glycerol 3-phosphate	172.0136	10.62	C3H9O6P	L2
PG(34:3)	744.4941	4.42	C40H73O10P	L2
PS(34:2)	759.5048	4.54	C40H74NO10P	L2
PG(34:2)	746.5097	4.42	C40H75O10P	L2
PS(14:1/20:0)	761.5204	4.53	C40H76NO10P	L2
PC(32:2)	729.5306	5.28	C40H76NO8P	L2
Cer(d18:1/22:1)	619.5899	5.03	C40H77NO3	L2
Glucosylceramide (d18:1/16:0)	699.5656	5.22	C40H77NO8	L2
PG(34:1)	748.5254	4.42	C40H77O10P	L2
PS(34:0)	763.5362	4.46	C40H78NO10P	L2
PC(32:1)	731.5461	5.26	C40H78NO8P	L2
Ceramide (d18:1/22:0)	621.6068	5.10	C40H79NO3	L2
PA(38:7)	718.4585	5.15	C41H67O8P	L2
[FA methyl(18:0/18:0/3:0/2:0)]	641.5380	5.01	C41H71NO4	L2
PE(18:4/18:1)	721.5059	5.00	C41H72NO7P	L2
PE(18:3/P-18:1)	723.5201	4.99	C41H74NO7P	L2
PE(36:4)	739.5152	5.00	C41H74NO8P	L2
PE(36:3)	741.5308	5.00	C41H76NO8P	L2
PI(32:1)	808.5098	4.59	C41H77O13P	L2
PE(18:1/P-18:1)	727.5523	5.01	C41H78NO7P	L2
PE(36:2)	743.5468	5.06	C41H78NO8P	L2
Cer(d18:2/23:0)	633.6057	5.10	C41H79NO3	L2
[PE (18:1/18:1)]	729.5679	5.23	C41H80NO7P	L2
[PE dimethyl(18:1/16:0)]	745.5622	5.25	C41H80NO8P	L2
SM(d18:0/18:1)	730.5986	5.43	C41H83N2O6P	L2
PS(36:4)	783.5049	4.51	C42H74NO10P	L2
PC(18:4/16:0)	737.5365	5.01	C42H76NO7P	L2
PC(34:4)	753.5306	5.24	C42H76NO8P	L2
PS(36:2)	787.5362	4.57	C42H78NO10P	L2
PC(34:3)	755.5465	5.25	C42H78NO8P	L2
PG(36:2)	774.5411	4.41	C42H79O10P	L2
PS(20:0/16:1)	789.5518	4.54	C42H80NO10P	L2
PC(34:2)	757.5617	5.24	C42H80NO8P	L2
[SP (24:0)]	647.6217	5.08	C42H81NO3	L2
PG(36:1)	776.5568	4.62	C42H81O10P	L2
PS(36:0)	791.5673	4.44	C42H82NO10P	L2
1-Hexadecanoyl-2-(octadecenoyl)-sn-glycero-3-phosphonocholine	743.5825	5.23	C42H82NO7P	L2
PC(34:1)	759.5773	5.23	C42H82NO8P	L2
Ceramide (d18:1/24:0)	649.6385	5.10	C42H83NO3	L2
PC(16:0/P-18:0)	745.5983	5.24	C42H84NO7P	L2
PE(38:6)	763.5148	4.99	C43H74NO8P	L2
PE(20:4/P-18:1)	749.5362	4.98	C43H76NO7P	L2
PE(38:5)	765.5309	4.99	C43H76NO8P	L2
[PE (18:1/20:4)]	751.5519	4.98	C43H78NO7P	L2
PE(38:4)	767.5469	4.98	C43H78NO8P	L2
PI(34:2)	834.5257	4.59	C43H79O13P	L2
PE(20:2/P-18:1)	753.5684	5.03	C43H80NO7P	L2
PI(18:1/16:0)	836.5413	4.58	C43H81O13P	L2
[GP (18:0/18:0)]	803.5676	4.53	C43H82NO10P	L2
PE(38:2)	771.5773	5.24	C43H82NO8P	L2
[PS (18:0/19:0)]	805.5832	5.24	C43H84NO10P	L2
PE(38:1)	773.5937	5.22	C43H84NO8P	L2
[PG (6:0/8:0)]	776.4996	5.14	C44H73O9P	L2
PS(38:6)	807.5048	4.52	C44H74NO10P	L2
PG(38:6)	794.5096	4.41	C44H75O10P	L2

PG(38:5)	796.5255	4.39	C44H77O10P	L2
PS(18:0/20:4)	811.5364	4.56	C44H78NO10P	L2
PC(36:5)	779.5462	5.22	C44H78NO8P	L2
PG(20:4/18:0)	798.5411	4.41	C44H79O10P	L2
PS(18:0/20:3)	813.5521	4.57	C44H80NO10P	L2
PI(13:0/22:1)	850.5567	4.59	C44H83O13P	L2
PS(38:1)	817.5832	4.46	C44H84NO10P	L2
PC(36:2)	785.5929	5.22	C44H84NO8P	L2
[PC (18:1/18:0)]	771.6142	5.23	C44H86NO7P	L2
PC(36:1)	787.6086	5.22	C44H86NO8P	L2
PC(18:0/P-18:0)	773.6297	5.23	C44H88NO7P	L2
PG(17:1/22:6)	806.5100	5.15	C45H75O10P	L2
PE (18:1/22:6)	775.5513	4.96	C45H78NO7P	L2
PE(40:6)	791.5462	4.97	C45H78NO8P	L2
PI(36:4)	858.5261	4.58	C45H79O13P	L2
PE(22:4/18:1)	777.5681	4.97	C45H80NO7P	L2
PI(36:2)	862.5574	4.58	C45H83O13P	L2
PI(36:1)	864.5728	4.59	C45H85O13P	L2
[PI (18:0/18:0)]	879.5841	4.54	C45H86NO13P	L2
PE(40:2)	799.6097	5.21	C45H86NO8P	L2
SM(d18:1/22:1)	784.6446	5.36	C45H89N2O6P	L2
[PG (8:0/8:0)]	802.5147	4.43	C46H75O9P	L2
PG(40:7)	820.5255	4.40	C46H77O10P	L2
PS(22:4/18:2)	835.5363	4.50	C46H78NO10P	L2
PS(18:0/22:5)	837.5518	4.46	C46H80NO10P	L2
PS(20:2/20:2)	839.5667	4.46	C46H82NO10P	L2
PC(20:4/18:1)	791.5823	5.19	C46H82NO7P	L2
PC(18:3/20:2)	807.5778	5.20	C46H82NO8P	L2
[PC (18:1/20:4)]	793.5983	5.19	C46H84NO7P	L2
PC(38:4)	809.5935	5.19	C46H84NO8P	L2
PC(38:3)	811.6087	5.19	C46H86NO8P	L2
PC(38:2)	813.6248	5.20	C46H88NO8P	L2
PI(38:6)	882.5262	4.57	C47H79O13P	L2
PS(19:0/22:6)	849.5520	4.49	C47H80NO10P	L2
PI(38:5)	884.5418	4.56	C47H81O13P	L2
PI(38:4)	886.5574	4.56	C47H83O13P	L2
PS(19:0/22:4)	853.5830	5.19	C47H84NO10P	L2
PI(38:3)	888.5724	4.58	C47H85O13P	L2
PS(19:1/22:2)	855.5981	5.18	C47H86NO10P	L2
SM(d18:2/24:1)	810.6614	5.39	C47H91N2O6P	L2
SM(d18:1/24:1)	812.6769	5.37	C47H93N2O6P	L2
PC(40:6)	833.5931	5.17	C48H84NO8P	L2
PC(22:4/P-18:1)	819.6137	5.17	C48H86NO7P	L2
PC(22:4/P-18:0)	821.6294	5.18	C48H88NO7P	L2
PI(22:3/18:3)	910.5575	4.57	C49H83O13P	L2
PI(40:5)	912.5730	4.57	C49H85O13P	L2
Phosphocreatine	211.0359	11.46	C4H10N3O5P	L2
1-butanesulfonate	138.0350	9.70	C4H10O3S	L2
Diethanolamine	105.0790	16.71	C4H11NO2	L2
Phosphodimethylethanolamine	169.0504	11.02	C4H12NO4P	L2
4-Hydroxy-2-butynal	84.0211	6.37	C4H4O2	L2
Allantoin	158.0439	12.74	C4H6N4O3	L1
2-Oxobutanoate	102.0317	12.31	C4H6O3	L2
Succinate	118.0266	11.51	C4H6O4	L1
(S)-Malate	134.0215	11.97	C4H6O5	L2
Creatinine	113.0589	10.08	C4H7N3O	L2

2-Pyrrolidinone	85.0528	8.64	C4H7NO	L2
2-Aminobutan-4-olide	101.0477	11.57	C4H7NO2	L2
L-2-Amino-3-oxobutanoic acid	117.0426	8.86	C4H7NO3	L2
L-Aspartate	133.0375	11.70	C4H7NO4	L1
L-Asparagine	132.0535	12.49	C4H8N2O3	L2
Butanal	72.0576	5.64	C4H8O	L2
(R)-3-Hydroxyisobutyrate	104.0474	6.36	C4H8O3	L2
D-Erythrose	120.0423	8.62	C4H8O4	L2
[FA trihydroxy(4:0)]	136.0372	10.29	C4H8O5	L2
3-Buten-1-amine	71.0736	11.37	C4H9N	L2
Creatine	131.0694	12.51	C4H9N3O2	L1
4-Aminobutanoate	103.0633	12.69	C4H9NO2	L2
L-Threonine	119.0582	12.09	C4H9NO3	L2
Homocysteinesulfinic acid	167.0252	8.54	C4H9NO4S	L2
S-Acetylthioethanolamine	119.0405	8.57	C4H9NOS	L2
PG(22:6/22:6)	866.5097	4.39	C50H75O10P	L2
PS(22:4/22:6)	883.5361	4.43	C50H78NO10P	L2
Butylene	70.0783	5.10	C5H10	L2
L-proline amide	114.0793	10.71	C5H10N2O	L2
L-Glutamine	146.0690	12.40	C5H10N2O3	L1
Pentanoate	102.0681	6.32	C5H10O2	L2
5-Hydroxypentanoate	118.0630	6.33	C5H10O3	L2
D-Xylulose	150.0527	10.08	C5H10O5	L2
L-Arabinonate	166.0478	10.46	C5H10O6	L2
4-Guanidinobutanoate	145.0850	12.81	C5H11N3O2	L2
L-Valine	117.0789	10.51	C5H11NO2	L1
L-Methionine	149.0510	10.82	C5H11NO2S	L1
N-hydroxyvaline	133.0738	8.62	C5H11NO3	L2
L-Methionine S-oxide	165.0460	11.34	C5H11NO3S	L2
DL-Methionine sulfone	181.0409	8.47	C5H11NO4S	L2
Tauropine	197.0358	8.60	C5H11NO5S	L2
2-Deoxy-D-ribose 5-phosphate	214.0242	11.28	C5H11O7P	L2
D-Ribose 5-phosphate	230.0191	11.78	C5H11O8P	L2
L-Ornithine	132.0898	17.66	C5H12N2O2	L2
Choline	103.0997	18.78	C5H13NO	L2
2-C-Methyl-D-erythritol 4-phosphate	216.0401	11.91	C5H13O7P	L2
Choline phosphate	183.0661	11.55	C5H14NO4P	L1
sn-glycero-3-Phosphoethanolamine	215.0560	12.47	C5H14NO6P	L2
Orotate	156.0170	9.11	C5H4N2O4	L1
Hypoxanthine	136.0384	10.48	C5H4N4O	L1
Xanthine	152.0334	10.49	C5H4N4O2	L1
Urate	168.0282	10.82	C5H4N4O3	L1
Adenine	135.0545	9.69	C5H5N5	L1
Guanine	151.0494	9.93	C5H5N5O	L2
Imidazole-4-acetate	126.0429	10.15	C5H6N2O2	L2
2-Hydroxy-2,4-pentadienoate	114.0317	12.64	C5H6O3	L2
Itaconate	130.0266	7.74	C5H6O4	L2
2-Oxoglutarate	146.0215	11.81	C5H6O5	L2
5-Methylcytosine	125.0589	10.30	C5H7N3O	L2
(S)-1-Pyrroline-5-carboxylate	113.0477	6.39	C5H7NO2	L2
5-Oxoproline	129.0426	12.30	C5H7NO3	L2
2-Oxoglutaramate	145.0375	9.11	C5H7NO4	L2
gamma-Amino-gamma-cyanobutanoate	128.0585	9.46	C5H8N2O2	L2
N-Carbamoyl-L-aspartate	176.0432	12.40	C5H8N2O5	L2
L-2-amino-4-oxo-5-chloropentanoate	165.0191	11.73	C5H8NO3Cl	L2
3-Methyl-2-oxobutanoic acid	116.0473	9.75	C5H8O3	L2

2-Acetolactate	132.0422	12.66	C5H8O4	L2
(R)-2-Hydroxyglutarate	148.0372	11.39	C5H8O5	L2
2-Dehydro-D-xylonate	164.0321	11.87	C5H8O6	L2
N-Methyl-2-pyrrolidinone	99.0684	6.50	C5H9NO	L2
L-Proline	115.0633	11.50	C5H9NO2	L1
Thiomorpholine 3-carboxylate	147.0353	7.76	C5H9NO2S	L2
cis-4-Hydroxy-L-proline	131.0583	6.39	C5H9NO3	L2
L-4-Hydroxyglutamate semialdehyde	147.0531	9.09	C5H9NO4	L2
Phosphinomethyl malate	212.0086	10.92	C5H9O7P	L2
(S)-3-Methyl-2-oxopentanoic acid	130.0630	5.39	C6H10O3	L2
1,2-Dihydroxy-5-(methylthio)pent-1-en-3-one	162.0350	8.61	C6H10O3S	L2
(R)-3-Hydroxy-3-methyl-2-oxopentanoate	146.0579	5.39	C6H10O4	L2
2-Dehydro-3-deoxy-L-rhamnonate	162.0528	10.83	C6H10O5	L2
5-Guanidino-2-oxopentanoate	173.0801	12.57	C6H11N3O3	L2
L-Pipecolate	129.0790	8.53	C6H11NO2	L2
allylcysteine	161.0510	5.93	C6H11NO2S	L2
6-Amino-2-oxohexanoate	145.0739	11.64	C6H11NO3	L2
N-Formyl-L-methionine	177.0459	6.31	C6H11NO3S	L2
Acetyl-L-homoserine	161.0688	10.32	C6H11NO4	L2
gamma-thiomethyl glutamate	193.0409	8.48	C6H11NO4S	L2
D-Alanyl-D-alanine	160.0847	8.59	C6H12N2O3	L2
[FA methyl,hydroxy(5:0)]	148.0736	6.36	C6H12O4	L2
L-Rhamnose	164.0685	8.53	C6H12O5	L2
D-Glucose	180.0634	13.68	C6H12O6	L2
D-Gluconic acid	196.0582	11.08	C6H12O7	L1
delta-Guanidinovaleric acid	159.1007	10.77	C6H13N3O2	L2
L-Citrulline	175.0957	12.87	C6H13N3O3	L1
L-Leucine	131.0946	10.45	C6H13NO2	L1
Fucosamine	163.0845	12.18	C6H13NO4	L2
D-Glucosamine	179.0793	11.92	C6H13NO5	L2
L-Lysine	146.1054	18.69	C6H14N2O2	L2
L-Arginine	174.1117	19.93	C6H14N4O2	L1
D-Glucosamine 6-phosphate	259.0457	11.78	C6H14NO8P	L2
Triethanolamine	149.1052	9.91	C6H15NO3	L2
Glycerophosphoglycerol	246.0504	10.55	C6H15O8P	L2
Picolinamide	122.0480	8.65	C6H6N2O	L2
Urocanate	138.0429	9.57	C6H6N2O2	L2
Phenol sulfate	173.9986	5.87	C6H6O4S	L2
cis-Aconitate	174.0163	12.84	C6H6O6	L2
7-Methyladenine	149.0702	13.42	C6H7N5	L2
3-Methylguanine	165.0650	10.20	C6H7N5O	L2
2-Pyridyl hydroxymethane sulfonic acid	189.0096	6.35	C6H7NO4S	L2
Methylimidazoleacetic acid	140.0585	8.74	C6H8N2O2	L2
4-Imidazolone-5-propanoate	156.0534	9.76	C6H8N2O3	L2
(4E)-2-Oxohexenoic acid	128.0473	6.38	C6H8O3	L2
2-Methyleneglutarate	144.0422	11.99	C6H8O4	L2
Citrate	192.0270	13.20	C6H8O7	L2
L-Histidinal	139.0745	8.93	C6H9N3O	L2
L-Histidine	155.0694	12.68	C6H9N3O2	L2
Vinylacetylglycine	143.0582	8.60	C6H9NO3	L2
beta-Alanopine	159.0531	6.37	C6H9NO4	L2
N-Acetyl-L-aspartate	175.0480	11.16	C6H9NO5	L2
2-Isopropylmaleate	158.0579	9.62	C7H10O4	L2
[FA hydroxy,oxo(7:0/2:0)]	190.0477	9.31	C7H10O6	L2
N(alpha)-Methylhistidine	169.0851	11.39	C7H11N3O2	L2
N-Acetyl-L-glutamate 5-semialdehyde	173.0688	6.39	C7H11NO4	L2

N-Acetyl-L-glutamate	189.0636	10.85	C7H11NO5	L1
S-(3-oxo-3-carboxy-n-propyl)cysteine	221.0358	9.74	C7H11NO5S	L2
[FA (7:0/2:0)] Heptanedioic acid	160.0736	8.91	C7H12O4	L2
N-Acetylmethionine	191.0615	6.07	C7H13NO3S	L2
2-amino-3,7-dideoxy-D-threo-hept-6-ulosonate	191.0794	8.61	C7H13NO5	L2
alpha-(2,6-anhydro-3-deoxy-D-arabino-heptulopyranosid)onate 7-phosphate	272.0298	17.66	C7H13O9P	L2
N5-Ethyl-L-glutamine	174.1005	11.52	C7H14N2O3	L2
meso-2,6-Diaminoheptanedioate	190.0953	18.67	C7H14N2O4	L2
[FA methyl(6:0)]	130.0993	5.64	C7H14O2	L2
[FA hydroxy(7:0)]	146.0943	5.30	C7H14O3	L2
3-Dehydroxycarnitine	145.1102	6.15	C7H15NO2	L2
L-Carnitine	161.1051	11.42	C7H15NO3	L1
D-Sedoheptulose 7-phosphate	290.0403	12.14	C7H15O10P	L2
1-Deoxy-D-altro-heptulose 7-phosphate	274.0454	11.68	C7H15O9P	L2
N6-Methyl-L-lysine	160.1211	18.13	C7H16N2O2	L2
N-gamma-Monomethyl-L-arginine	188.1274	18.59	C7H16N4O2	L2
Pyridine-2,3-dicarboxylate	167.0218	11.75	C7H5NO4	L2
Benzimidazole	118.0530	8.62	C7H6N2	L2
Benzoate	122.0368	6.30	C7H6O2	L1
4-Hydroxybenzoate	138.0316	5.64	C7H6O3	L2
3-Hydroxyanthranilate	153.0425	10.39	C7H7NO3	L2
1-Methylnicotinamide	136.0636	21.89	C7H8N2O	L2
N-Acetyl-L-histidine	197.0801	6.37	C8H11N3O3	L2
L-Noradrenaline	169.0739	8.84	C8H11NO3	L2
3-(3,4-Dihydroxypyridin-1-yl)-L-alanine	200.0797	9.17	C8H12N2O4	L2
N(alpha),N(alpha)-Dimethyl-L-histidine	183.1007	12.80	C8H13N3O2	L2
N2-Acetyl-L-aminoadipate	203.0794	9.95	C8H13NO5	L2
Succinyl-L-homoserine	219.0742	10.84	C8H13NO6	L2
gamma-L-Glutamyl-L-cysteine	250.0621	11.35	C8H14N2O5S	L2
6-Acetyl-D-glucose	222.0739	12.26	C8H14O7	L2
N-(3-hydroxybutanoyl)-L-homoserine	205.0951	8.77	C8H15NO5	L2
N-Acetyl-D-glucosamine	221.0898	11.06	C8H15NO6	L2
3-methyl-1-heptene	112.1252	5.11	C8H16	L2
N6-Acetyl-N6-hydroxy-L-lysine	204.1109	10.56	C8H16N2O4	L2
N-acetyl-(L)-arginine	216.1224	12.34	C8H16N4O3	L2
N-Acetyl-D-glucosamine 6-phosphate	301.0563	11.31	C8H16NO9P	L2
[FA (8:0)]	144.1150	5.14	C8H16O2	L2
N-acetyl -D- glucosaminitol	223.1056	11.45	C8H17NO6	L2
Ne,Ne dimethyllysine	174.1368	16.86	C8H18N2O2	L2
NG,NG-Dimethyl-L-arginine	202.1431	17.26	C8H18N4O2	L2
sn-glycero-3-Phosphocholine	257.1029	11.84	C8H20NO6P	L1
Indole	117.0578	5.94	C8H7N	L2
Indoxyl	133.0527	8.86	C8H7NO	L2
Formylanthranilate	165.0426	5.71	C8H7NO3	L2
Phenylacetic acid	136.0524	6.25	C8H8O2	L2
2-Phenylacetamide	135.0684	4.87	C8H9NO	L2
Phenylpropanoate	150.0680	5.59	C9H10O2	L2
3-(3-Hydroxy-phenyl)-propanoic acid	166.0628	5.77	C9H10O3	L2
3-(4-Hydroxyphenyl)lactate	182.0580	8.59	C9H10O4	L2
L-Phenylalanine	165.0790	9.98	C9H11NO2	L2
L-Tyrosine	181.0740	11.82	C9H11NO3	L1
Pseudouridine	244.0695	11.30	C9H12N2O6	L2
Deoxycytidine	227.0906	9.58	C9H13N3O4	L2
Cytidine	243.0854	11.26	C9H13N3O5	L2
Dihydrobiopterin	239.1019	10.46	C9H13N5O3	L2

Epinephrine sulfate	263.0463	10.41	C9H13NO6S	L2
UDP	404.0022	12.08	C9H14N2O12P2	L2
5-6-Dihydrouridine	246.0851	10.19	C9H14N2O6	L2
Carnosine	226.1066	12.67	C9H14N4O3	L2
4-(1-methyl-2-pyrrolidinyl)-3-oxobutanoate	185.1052	5.85	C9H15NO3	L2
N2-Succinyl-L-ornithine	232.1060	6.36	C9H16N2O5	L2
2-(alpha-D-Mannosyl)-D-glycerate	268.0794	11.68	C9H16O9	L2
8-Amino-7-oxononanoate	187.1209	6.31	C9H17NO3	L2
Acetylcarnitine	203.1159	10.22	C9H17NO4	L1
Pantothenate	219.1107	6.37	C9H17NO5	L1
N2-(D-1-Carboxyethyl)-L-lysine	218.1264	9.84	C9H18N2O4	L2
N2-(D-1-Carboxyethyl)-L-arginine	246.1329	12.09	C9H18N4O4	L2
beta-Alanyl-L-arginine	245.1488	12.89	C9H19N5O3	L2
Pantothenol	205.1314	6.62	C9H19NO4	L2
sn-glycero-3-Phospho-1-inositol	334.0665	12.13	C9H19O11P	L2
N6,N6,N6-Trimethyl-L-lysine	188.1525	17.07	C9H20N2O2	L2
3-Hydroxy-N6,N6,N6-trimethyl-L-lysine	204.1475	15.52	C9H20N2O3	L2
Indanone	132.0575	5.45	C9H8O	L2
Phenylpyruvate	164.0474	5.41	C9H8O3	L1
3-(4-Hydroxyphenyl)pyruvate	180.0423	8.52	C9H8O4	L2
Hippurate	179.0582	6.21	C9H9NO3	L1
Monomethyl sulfate	111.9830	7.96	CH4O4S	L2
Hydroxymethylphosphonate	111.9926	11.18	CH5O4P	L2
Sulfate	97.9674	13.26	H2O4S	L2
Orthophosphate	97.9770	12.28	H3O4P	L2

Table A2: A list of total identified metabolites in macrophages in response to polarization into M0, M1, M2 and Mreg.

Putative metabolite	Mass	RT	FORMULA	confidence
Phenylacetylglycine	193.0740	4.91	C10H11NO3	L2
L-Kynurenine	208.0849	8.82	C10H12N2O3	L1
Inosine	268.0808	8.95	C10H12N4O5	L1
3',5'-Cyclic AMP	329.0525	7.67	C10H12N5O6P	L1
IMP	348.0472	10.64	C10H13N4O8P	L1
Deoxyadenosine	251.1019	7.13	C10H13N5O3	L1
Adenosine	267.0968	7.78	C10H13N5O4	L1
L-Tyrosine methyl ester	195.0895	4.94	C10H13NO3	L2
AMP	347.0632	9.59	C10H14N5O7P	L1
dTMP	322.0566	9.11	C10H15N2O8P	L2
XTP	261.9875	12.06	C10H15N4O15P3	L2
ADP	427.0296	10.54	C10H15N5O10P2	L1
Biotin	244.0882	5.31	C10H16N2O3S	L2
ATP	506.9956	11.60	C10H16N5O13P3	L2
[FA (10:1/2:0)]	200.1049	4.76	C10H16O4	L2
N-(L-Arginino)succinate	290.1227	11.15	C10H18N4O6	L2
10-Oxodecanoate	186.1257	4.22	C10H18O3	L2
3-Hydroxysebacicacid	218.1154	4.74	C10H18O5	L2
Propanoylcarnitine	217.1314	7.75	C10H19NO4	L2
Decanoic acid	172.1463	3.98	C10H20O2	L2
10-Hydroxydecanoic acid	188.1413	4.04	C10H20O3	L2
[PC acety] 1-acetyl-sn-glycero-3-phosphocholine	299.1135	8.19	C10H22NO7P	L2
Kynurenate	189.0427	4.92	C10H7NO3	L2
Indole-3-acetaldehyde	159.0684	5.42	C10H9NO	L2
5-Hydroxyindoleacetaldehyde	175.0633	4.14	C10H9NO2	L2
Indolelactate	205.0739	7.10	C11H11NO3	L2
L-Tryptophan	204.0900	9.48	C11H12N2O2	L1
5-Hydroxy-L-tryptophan	220.0848	7.98	C11H12N2O3	L2
L-Formylkynurenine	236.0797	8.02	C11H12N2O4	L2
CMP-2-aminoethylphosphonate	430.0655	10.37	C11H20N4O10P2	L2
CDP-ethanolamine	446.0605	11.01	C11H20N4O11P2	L2
Butanoylcarnitine	231.1471	7.23	C11H21NO4	L1
N-Acetylserotonin	218.1055	4.95	C12H14N2O2	L2
[FA (12:5)]	190.0994	4.15	C12H14O2	L2
[FA (12:4/2:0)]	222.0891	4.13	C12H14O4	L2
Thiamin	264.1045	21.02	C12H16N4OS	L2
N-((R)-Pantothenoyl)-L-cysteine	322.1200	8.01	C12H22N2O6S	L2
3-Hydroxydodecanedioicacid	246.1467	4.32	C12H22O5	L2
Dodecanoic acid	200.1776	3.90	C12H24O2	L2
(R)-S-Lactoylglutathione	379.1050	9.01	C13H21N3O8S	L2
[FA hydroxy(10:0)] -L-serine	275.1733	7.35	C13H25NO5	L2
S-Adenosyl-L-homocysteine	384.1217	9.69	C14H20N6O5S	L2
CMP-N-trimethyl-2-aminoethylphosphonate	472.1127	9.67	C14H26N4O10P2	L2
CDP-choline	488.1072	10.21	C14H26N4O11P2	L2
Tetradecenoic acid	226.1935	3.87	C14H26O2	L2
[FA oxo(14:0)]	242.1884	3.88	C14H26O3	L2
[FA (14:0/2:0)]	258.1832	4.60	C14H26O4	L2
Butyl 3-O-beta-D-glucopyranosyl-butanoate	322.1628	4.79	C14H26O8	L2
Tetradecanoic acid	228.2090	3.86	C14H28O2	L2
Ceramide (d18:1/14:0)]	229.2406	4.61	C14H31NO	L2
UDP-glucuronate	580.0344	12.71	C15H22N2O18P2	L2

S-Adenosyl-L-methionine	398.1374	11.47	C15H22N6O5S	L2
Phosphoribosyl-AMP	559.0714	10.27	C15H23N5O14P2	L2
UDP-glucose	566.0548	11.13	C15H24N2O17P2	L1
[FA methyl(14:0)]	242.2247	3.83	C15H30O2	L2
dTDP-glucose	282.0382	10.99	C16H26N2O16P2	L2
Hexadecenoic acid	254.2247	3.82	C16H30O2	L2
[FA oxo(16:0)]	270.2195	3.85	C16H30O3	L2
Hexadecanoic acid	256.2404	3.89	C16H32O2	L2
UDP-N-acetyl-D-glucosamine	607.0815	10.38	C17H27N3O17P2	L2
[FA hydroxy(18:2)]	296.2352	3.86	C18H32O3	L2
[FA (18:2)]	312.2297	3.84	C18H32O4	L2
[FA (18:2)]	266.2610	3.94	C18H34O	L2
[FA (18:1)]	282.2560	3.81	C18H34O2	L2
2-Oxooctadecanoic acid	298.2508	3.81	C18H34O3	L2
[FA trihydroxy(18:1)]	330.2407	3.94	C18H34O5	L2
Octadecanoic acid	284.2717	4.03	C18H36O2	L2
[FA hydroxy(18:0)]	300.2664	3.85	C18H36O3	L2
[FA hydroxy(4:0/18:0)]	348.2513	4.22	C18H36O6	L2
[FA (16:2)]	299.2824	5.54	C18H37NO2	L2
[SP] Sphing-4-enine-1-phosphate	379.2489	4.69	C18H38NO5P	L2
Sphinganine	301.2981	7.04	C18H39NO2	L2
Folate	441.1398	11.36	C19H19N7O6	L1
[GP (16:0)]	410.2434	4.43	C19H39O7P	L2
[FA (20:5)]	302.2247	3.80	C20H30O2	L2
Glutathione disulfide	306.0760	11.19	C20H32N6O12S2	L1
[FA (20:4)]	304.2405	3.80	C20H32O2	L2
Icosatrienoic acid	306.2556	3.79	C20H34O2	L2
[FA (20:0)]	310.2876	3.76	C20H38O2	L2
[FA (20:0/2:0)]	342.2770	3.75	C20H38O4	L2
[FA (20:0)]	312.3030	3.89	C20H40O2	L2
NAD+	663.1091	9.59	C21H27N7O14P2	L1
[FA methoxy,trihydrox] -prostadiene	354.2771	3.98	C21H38O4	L2
[GL (18:0)]	358.3084	3.94	C21H42O4	L2
[GP (18:0)]	438.2749	4.34	C21H43O7P	L2
[PE (16:1)]	437.2907	4.35	C21H44NO6P	L2
[PE (16:0)]	453.2855	4.41	C21H44NO7P	L2
[PC methyl(12:2)]	439.3064	4.42	C21H46NO6P	L2
O-methylandrocymbine	385.1886	9.77	C22H27NO5	L2
Docosahexaenoicacid	328.2404	3.77	C22H32O2	L2
[PG (16:0)]	484.2803	3.85	C22H45O9P	L2
[PC (14:1)]	451.3061	4.50	C22H46NO6P	L2
[PC (14:0)]	467.3012	4.57	C22H46NO7P	L2
PI(14:1/0:0)	271.1242	4.01	C23H43O12P	L2
LysoPE(0:0/18:2)	477.2855	4.35	C23H44NO7P	L2
[PE (18:1)]	479.3014	4.32	C23H46NO7P	L2
[PC methyl(14:2)]	467.3377	4.34	C23H50NO6P	L2
[FA (24:6)]	344.1777	4.15	C24H24O2	L2
[ST hydrox] 3alpha,12alpha-Dihydroxy-5beta-chol-6-en-24-oic Acid	390.2771	3.85	C24H38O4	L2
[PS (18:1)]	523.2910	3.95	C24H46NO9P	L2
[FA (24:0)]	366.3499	3.67	C24H46O2	L2
[PG (18:1)]	510.2957	3.77	C24H47O9P	L2
[PC (16:1)]	493.3169	4.49	C24H48NO7P	L2
[PS (18:0)]	525.3067	3.94	C24H48NO9P	L2
Tetracosanoic acid	368.3655	3.70	C24H48O2	L2
[FA hydroxy(24:0)]	384.3605	3.65	C24H48O3	L2
[PC (16:1)]	479.3376	4.44	C24H50NO6P	L2
[PC (16:0)]	495.3325	4.47	C24H50NO7P	L2
[PC (16:2)]	481.3533	4.49	C24H52NO6P	L2

LysoPE(0:0/20:5)	499.2702	4.32	C25H42NO7P	L2
[PE (20:4)]	501.2857	4.29	C25H44NO7P	L2
LysoPE(0:0/20:3)	503.3019	4.29	C25H46NO7P	L2
Glycodeoxycholate	449.3144	4.20	C26H43NO5	L2
[ST hydrox] N-(3alpha,7alpha-dihydroxy-5beta-cholan-24-oyl)-taurine	499.2971	4.06	C26H45NO6S	L2
PG(20:3/0:0)	534.2959	3.80	C26H47O9P	L2
[FA (26:0)]	396.3967	3.65	C26H52O2	L2
[PC (18:1)]	507.3688	4.40	C26H54NO6P	L2
[PC (18:0)]	523.3642	4.41	C26H54NO7P	L2
LysoPC(O-18:0)	509.3848	4.43	C26H56NO6P	L2
LysoPE(0:0/22:6)	525.2855	4.26	C27H44NO7P	L2
LysoPE(0:0/22:5)	527.3015	4.23	C27H46NO7P	L2
[PI (18:0)]	600.3278	3.97	C27H53O12P	L2
PG(22:6/0:0)	556.2800	3.75	C28H45O9P	L2
LysoPC(20:4)	543.3324	4.43	C28H50NO7P	L2
LysoPC(20:3)	545.3486	4.41	C28H52NO7P	L2
Oxalate	89.9954	12.48	C2H2O4	L2
Iminoglycine	73.0164	10.46	C2H3NO2	L2
Glycine	75.0320	11.41	C2H5NO2	L1
Phosphonoacetaldehyde	123.9926	10.07	C2H5O4P	L2
2-Hydroxyethanesulfonate	125.9987	8.92	C2H6O4S	L2
Hypotaurine	109.0197	11.08	C2H7NO2S	L2
Taurine	125.0147	11.30	C2H7NO3S	L1
[PC (22:6)]	567.3323	4.40	C30H50NO7P	L2
LysoPC(22:5)	569.3485	4.39	C30H52NO7P	L2
N-(Tetradecanoyl)-sphing-4-enine	509.4806	3.80	C32H63NO3	L2
Cer(d18:2/16:0)	535.4965	3.77	C34H65NO3	L2
Ceramide (d18:1/16:0)]	537.5122	3.72	C34H67NO3	L2
PA(32:1)	646.4575	3.61	C35H67O8P	L2
PC(28:0)	677.4993	3.88	C36H72NO8P	L2
PA(34:2)	672.4733	3.63	C37H69O8P	L2
PA(34:1)	674.4890	3.57	C37H71O8P	L2
PE(14:0/P-18:1	673.5047	3.92	C37H72NO7P	L2
PE(32:1)	689.4999	3.78	C37H72NO8P	L2
PE(32:0)	691.5152	3.87	C37H74NO8P	L2
SM(d18:1/14:0)	674.5361	4.06	C37H75N2O6P	L2
PS(32:1)	733.4892	3.58	C38H72NO10P	L2
PC(30:1)	703.5148	3.86	C38H74NO8P	L2
PC(14:0/P-16:0)	689.5364	3.85	C38H76NO7P	L2
PC(30:0)	705.5307	3.85	C38H76NO8P	L2
Ceramide (d18:1/18:0/14:0)]	688.5519	4.02	C38H77N2O6P	L2
[PC (14:2/16:0)]	691.5514	3.85	C38H78NO7P	L2
PE(34:2)	715.5142	3.78	C39H74NO8P	L2
PE(16:0/P-18:1)	701.5359	3.84	C39H76NO7P	L2
PE(34:1)	717.5308	3.82	C39H76NO8P	L2
SM(d16:1/18:1)	700.5514	3.98	C39H77N2O6P	L2
PE(34:0)	719.5472	3.84	C39H78NO8P	L2
Ceramide (d18:1/16:0)]	702.5673	3.94	C39H79N2O6P	L2
N-Methylethanolamine phosphate	155.0346	10.23	C3H10NO4P	L2
3-Oxopropanoate	88.0161	12.46	C3H4O3	L2
Phosphoenolpyruvate	167.9824	12.14	C3H5O6P	L1
Propanoate	74.0367	7.12	C3H6O2	L2
Lactate	90.0317	7.72	C3H6O3	L1
3-Mercaptolactate	122.0038	10.65	C3H6O3S	L2
D-Glycerate	106.0266	9.08	C3H6O4	L1
Guanidinoacetate	117.0538	11.63	C3H7N3O2	L1
L-Alanine	89.0477	10.78	C3H7NO2	L1
L-Serine	105.0426	11.37	C3H7NO3	L1

Propanoyl phosphate	154.0031	8.96	C3H7O5P	L2
D-Glyceraldehyde 3-phosphate	169.9979	11.29	C3H7O6P	L2
3-Phospho-D-glycerate	185.9929	11.77	C3H7O7P	L1
Trimethylamine N-oxide	75.0684	8.49	C3H9NO	L2
sn-Glycerol 3-phosphate	172.0137	10.04	C3H9O6P	L1
PS(34:2)	759.5049	3.58	C40H74NO10P	L2
PG(34:2)	746.5101	3.55	C40H75O10P	L2
PS(34:1)	761.5205	3.58	C40H76NO10P	L2
PC(32:2)	729.5307	3.85	C40H76NO8P	L2
Cer(d18:1/22:1)	619.5902	3.76	C40H77NO3	L2
PS(34:0)	763.5366	3.53	C40H78NO10P	L2
PC(32:1)	731.5463	3.83	C40H78NO8P	L2
PC(32:0)	733.5626	3.82	C40H80NO8P	L2
[PC (14:2/18:0)]	719.5836	3.84	C40H82NO7P	L2
PE(18:4/P-18:1)	721.5049	3.73	C41H72NO7P	L2
PE(18:3/P-18:1)	723.5202	3.71	C41H74NO7P	L2
PE(36:4)	739.5154	3.74	C41H74NO8P	L2
PI(32:1)	808.5092	3.59	C41H77O13P	L2
PE(36:2)	743.5467	3.79	C41H78NO8P	L2
PE(36:1)	745.5622	3.81	C41H80NO8P	L2
PS(36:4)	783.5051	3.57	C42H74NO10P	L2
PC(34:4)	753.5312	3.84	C42H76NO8P	L2
PS(36:2)	787.5363	3.58	C42H78NO10P	L2
PG(36:2)	774.5413	3.53	C42H79O10P	L2
PS(36:1)	789.5523	3.57	C42H80NO10P	L2
PC(34:2)	757.5620	3.81	C42H80NO8P	L2
Ceramide (d18:1/24:0)]	647.6221	3.68	C42H81NO3	L2
PS(36:0)	791.5678	3.52	C42H82NO10P	L2
1-Hexadecanoyl-2-(octadecenoyl)-sn-glycero-3-phosphonocholine	743.5827	3.81	C42H82NO7P	L2
PC(34:1)	759.5775	3.80	C42H82NO8P	L2
PC(16:0/P-18:0)	745.5984	3.80	C42H84NO7P	L2
[PE (16:1/22:6)]	747.5199	3.68	C43H74NO7P	L2
PE(38:6)	763.5139	3.77	C43H74NO8P	L2
PE(20:4/P-18:1)	749.5360	3.71	C43H76NO7P	L2
PE(38:5)	765.5324	3.69	C43H76NO8P	L2
[PE (18:1/20:4)]	751.5519	3.71	C43H78NO7P	L2
PE(38:4)	767.5474	3.72	C43H78NO8P	L2
[GP (18:0/18:0)]	803.5678	3.55	C43H82NO10P	L2
PE(38:2)	771.5776	3.80	C43H82NO8P	L2
PE(38:1)	773.5938	3.79	C43H84NO8P	L2
PS(38:6)	807.5049	3.57	C44H74NO10P	L2
PS(38:5)	809.5205	3.55	C44H76NO10P	L2
PG(38:4)	798.5417	3.53	C44H79O10P	L2
PC(36:4)	781.5620	3.79	C44H80NO8P	L2
PS(38:2)	815.5674	3.54	C44H82NO10P	L2
PC(36:2)	785.5932	3.79	C44H84NO8P	L2
PC (18:1/18:0)	771.6145	3.80	C44H86NO7P	L2
PC(36:1)	787.6081	3.78	C44H86NO8P	L2
PC(18:0/P-18:0)	773.6297	3.79	C44H88NO7P	L2
PE(22:6)	773.5371	3.69	C45H76NO7P	L2
PI(36:5)	856.5103	3.59	C45H77O13P	L2
PE(40:6)	791.5453	3.72	C45H78NO8P	L2
PI(36:4)	858.5260	3.58	C45H79O13P	L2
PI(36:3)	860.5418	3.59	C45H81O13P	L2
PI(36:2)	862.5574	3.57	C45H83O13P	L2
PE(40:3)	797.5943	3.80	C45H84NO8P	L2
PI(36:1)	864.5718	3.57	C45H85O13P	L2
[PI (18:0/18:0)]	879.5845	3.57	C45H86NO13P	L2
PE(40:2)	799.6098	3.77	C45H86NO8P	L2

[PG (8:0/8:0)]	802.5149	3.53	C46H75O9P	L2
PG(40:7)	820.5257	3.53	C46H77O10P	L2
PS(40:6)	835.5363	3.57	C46H78NO10P	L2
PS(40:5)	837.5522	3.54	C46H80NO10P	L2
PS(40:4)	839.5666	3.54	C46H82NO10P	L2
PC(38:5)	807.5779	3.79	C46H82NO8P	L2
PC (18:1/20:4)	793.5983	3.78	C46H84NO7P	L2
PC(38:4)	809.5937	3.77	C46H84NO8P	L2
PC(20:2/P-18:1)	795.6134	3.76	C46H86NO7P	L2
PC(38:3)	811.6090	3.77	C46H86NO8P	L2
PC(38:2)	813.6252	3.76	C46H88NO8P	L2
PI(38:6)	882.5266	3.58	C47H79O13P	L2
PI(38:5)	884.5416	3.58	C47H81O13P	L2
PI(38:4)	886.5569	3.57	C47H83O13P	L2
PI(38:3)	888.5711	3.57	C47H85O13P	L2
SM(d18:2/24:1)	810.6622	3.85	C47H91N2O6P	L2
SM(d18:1/24:1)	812.6770	3.84	C47H93N2O6P	L2
PG(22:6)	840.4940	3.54	C48H73O10P	L2
PG(42:10)	842.5101	3.53	C48H75O10P	L2
PG(42:9)	844.5253	3.53	C48H77O10P	L2
PG(42:8)	846.5397	3.53	C48H79O10P	L2
PS(42:7)	861.5519	3.53	C48H80NO10P	L2
PC(40:6)	833.5924	3.75	C48H84NO8P	L2
PC(22:4)	819.6149	3.76	C48H86NO7P	L2
PC(40:5)	835.6093	3.75	C48H86NO8P	L2
Phosphocreatine	211.0359	10.46	C4H10N3O5P	L2
Diethanolamine	105.0790	15.58	C4H11NO2	L2
Phosphodimethylethanolamine	169.0504	9.61	C4H12NO4P	L2
3-Butynoate	84.0211	8.38	C4H4O2	L2
[FA (4:0)] butenoic acid	86.0368	10.61	C4H6O2	L2
2-Oxobutanoate	102.0317	4.90	C4H6O3	L2
Succinate	118.0267	10.83	C4H6O4	L1
L-Malate	134.0216	11.36	C4H6O5	L2
L-Aspartate 4-semialdehyde	117.0426	10.04	C4H7NO3	L2
L-Aspartate	133.0374	10.44	C4H7NO4	L1
L-Asparagine	132.0535	11.06	C4H8N2O3	L1
Butanoic acid	88.0524	4.92	C4H8O2	L2
(R)-3-Hydroxybutanoate	104.0474	7.08	C4H8O3	L2
L-Erythrulose	120.0423	8.40	C4H8O4	L2
[FA trihydroxy(4:0)]	136.0372	9.23	C4H8O5	L2
Creatine	131.0694	10.77	C4H9N3O2	L1
4-Aminobutanoate	103.0633	11.03	C4H9NO2	L1
L-Threonine	119.0583	10.59	C4H9NO3	L2
D-Erythrose 4-phosphate	200.0085	9.28	C4H9O7P	L2
PG(22:6)	866.5101	3.53	C50H75O10P	L2
PS(44:10)	883.5360	3.53	C50H78NO10P	L2
PC(42:7)	859.6094	3.76	C50H86NO8P	L2
D-Glutamine	146.0691	8.38	C5H10N2O3	L2
5-Hydroxypentanoate	118.0631	7.14	C5H10O3	L2
D-Ribose	150.0527	8.92	C5H10O5	L2
4-Guanidinobutanoate	145.0851	11.03	C5H11N3O2	L2
L-Valine	117.0790	8.82	C5H11NO2	L2
L-Methionine	149.0510	9.06	C5H11NO2S	L1
L-Methionine S-oxide	165.0460	9.79	C5H11NO3S	L2
2-Deoxy-D-ribose 5-phosphate	214.0242	10.09	C5H11O7P	L2
D-Ribose 5-phosphate	230.0188	10.87	C5H11O8P	L1
L-Ornithine	132.0898	16.17	C5H12N2O2	L2
2-C-Methyl-D-erythritol 4-phosphate	216.0400	11.06	C5H13O7P	L2
sn-glycero-3-Phosphoethanolamine	215.0559	10.87	C5H14NO6P	L2

Orotate	156.0171	8.41	C5H4N2O4	L1
Hypoxanthine	136.0385	8.76	C5H4N4O	L1
Xanthine	152.0334	9.21	C5H4N4O2	L1
Urate	168.0283	9.85	C5H4N4O3	L1
Guanine	151.0493	10.22	C5H5N5O	L2
Thymine	126.0430	7.08	C5H6N2O2	L1
(S)-Dihydroorotate	158.0327	8.80	C5H6N2O4	L2
Itaconate	130.0267	7.78	C5H6O4	L2
2-Oxoglutarate	146.0215	11.27	C5H6O5	L2
5-Methylcytosine	125.0589	8.62	C5H7N3O	L2
(S)-1-Pyrroline-5-carboxylate	113.0477	7.27	C5H7NO2	L2
L-1-Pyrroline-3-hydroxy-5-carboxylate	129.0426	7.90	C5H7NO3	L2
2-Oxoglutaramate	145.0375	8.34	C5H7NO4	L2
5,6-Dihydrothymine	128.0586	10.76	C5H8N2O2	L2
N-Carbamoyl-L-aspartate	176.0433	11.67	C5H8N2O5	L2
3-Methyl-2-oxobutanoic acid	116.0474	7.06	C5H8O3	L2
(R)-2-Hydroxyglutarate	148.0372	10.84	C5H8O5	L1
L-Proline	115.0633	9.75	C5H9NO2	L1
L-Glutamate 5-semialdehyde	131.0582	7.12	C5H9NO3	L2
L-Glutamate	147.0531	10.36	C5H9NO4	L1
4-Methylene-L-glutamine	158.0691	8.62	C6H10N2O3	L2
N-Formimino-L-glutamate	174.0641	8.55	C6H10N2O4	L2
N-Carbamyl-L-glutamate	190.0590	10.69	C6H10N2O5	L2
(S)-3-Methyl-2-oxopentanoic acid	130.0630	7.04	C6H10O3	L2
(R)-3-Hydroxy-3-methyl-2-oxopentanoate	146.0579	4.78	C6H10O4	L2
2-Dehydro-3-deoxy-L-rhamnonate	162.0528	10.20	C6H10O5	L2
D-Glucono-1,5-lactone	178.0477	10.88	C6H10O6	L2
D-Glucuronate	194.0427	11.32	C6H10O7	L2
5-Guanidino-2-oxopentanoate	173.0800	10.84	C6H11N3O3	L2
N4-Acetylaminobutanal	129.0790	4.94	C6H11NO2	L2
4-Acetamidobutanoate	145.0739	5.39	C6H11NO3	L2
N-Formyl-L-methionine	177.0460	4.92	C6H11NO3S	L2
O-Acetyl-L-homoserine	161.0688	7.38	C6H11NO4	L2
L-Lysine 1,6-lactam	128.0949	11.37	C6H12N2O	L2
D-Alanyl-D-alanine	160.0848	7.09	C6H12N2O3	L2
Hexanoic acid	116.0838	4.66	C6H12O2	L2
myo-Inositol	180.0634	12.13	C6H12O6	L1
D-Gluconic acid	196.0583	10.02	C6H12O7	L1
L-Citrulline	175.0957	11.20	C6H13N3O3	L1
L-Leucine	131.0946	8.86	C6H13NO2	L1
D-Glucosamine	179.0793	8.87	C6H13NO5	L2
L-Fucose 1-phosphate	244.0348	9.56	C6H13O8P	L2
D-Glucose 6-phosphate	260.0297	11.11	C6H13O9P	L1
L-Lysine	146.1055	16.98	C6H14N2O2	L1
L-Arginine	174.1117	18.40	C6H14N4O2	L1
D-Glucosamine 6-phosphate	259.0458	10.63	C6H14NO8P	L2
D-Sorbitol	182.0791	10.47	C6H14O6	L2
Urocanate	138.0429	8.69	C6H6N2O2	L2
Thiourocanic acid	170.0149	7.08	C6H6N2O2S	L2
cis-Aconitate	174.0164	12.35	C6H6O6	L2
7-Methyladenine	149.0702	12.07	C6H7N5	L2
Monodehydroascorbate	175.0242	8.58	C6H7O6	L2
Methylimidazoleacetic acid	140.0585	7.52	C6H8N2O2	L2
4-Imidazolone-5-propanoate	156.0535	7.09	C6H8N2O3	L2
Hydantoin-5-propionate	172.0483	10.69	C6H8N2O4	L2
(4E)-2-Oxohexenoic acid	128.0473	4.91	C6H8O3	L2
D-Glucuronolactone	176.0321	11.03	C6H8O6	L2
Citrate	192.0270	12.47	C6H8O7	L2
L-Histidine	155.0695	11.10	C6H9N3O2	L2

N-Acetyl-L-aspartate	175.0481	10.40	C6H9NO5	L2
2-Isopropylmaleate	158.0579	7.70	C7H10O4	L2
2-Hydroxybutane-1,2,4-tricarboxylate	206.0426	12.03	C7H10O7	L2
N(pi)-Methyl-L-histidine	169.0851	9.89	C7H11N3O2	L2
N-Acetyl-L-glutamate	189.0637	10.08	C7H11NO5	L1
2-Isopropylmalate	176.0685	9.56	C7H12O5	L2
5-Acetamidopentanoate	159.0895	4.93	C7H13NO3	L2
L-Cystathionine	222.0674	11.53	C7H14N2O4S	L1
[FA methyl(6:0)]	130.0994	4.35	C7H14O2	L2
Sedoheptulose	210.0739	10.69	C7H14O7	L2
4-Trimethylammoniobutanoate	145.1102	9.59	C7H15NO2	L1
N6-Methyl-L-lysine	160.1212	16.37	C7H16N2O2	L1
Pyridine-2,3-dicarboxylate	167.0218	11.02	C7H5NO4	L2
3-Hydroxyanthranilate	153.0426	9.81	C7H7NO3	L2
2-(Acetamidomethylene)succinate	187.0481	7.09	C7H9NO5	L2
Pyridoxine	169.0739	7.21	C8H11NO3	L2
Pyridoxamine	168.0898	7.05	C8H12N2O2	L2
[FA dioxo(8:0)]	172.0735	8.34	C8H12O4	L2
6-Acetamido-2-oxohexanoate	187.0845	4.91	C8H13NO4	L2
O-Succinyl-L-homoserine	219.0742	10.02	C8H13NO6	L2
gamma-L-Glutamyl-L-cysteine	250.0624	7.12	C8H14N2O5S	L2
[FA (8:1)]	142.0994	4.87	C8H14O2	L2
N-Acetyl-D-glucosamine	221.0897	9.26	C8H15NO6	L2
3-methyl-1-heptene	112.1252	3.86	C8H16	L2
N-Acetyl-D-glucosamine 6-phosphate	301.0563	10.28	C8H16NO9P	L2
[FA (8:0)]	144.1150	4.17	C8H16O2	L2
[FA hydroxy(8:0)]	176.1048	4.48	C8H16O4	L2
sn-glycero-3-Phosphocholine	257.1029	10.03	C8H20NO6P	L1
Formylanthranilate	165.0427	4.92	C8H7NO3	L2
Nicotinurate	180.0534	10.00	C8H8N2O3	L2
Phenylacetic acid	136.0525	4.91	C8H8O2	L2
3,4-Dihydroxyphenylacetate	168.0422	9.04	C8H8O4	L1
2-Phenylacetamide	135.0684	8.82	C8H9NO	L2
4-Pyridoxate	183.0532	7.81	C8H9NO4	L2
Phenylpropanoate	150.0680	4.73	C9H10O2	L2
3-(3-Hydroxy-phenyl)-propanoic acid	166.0630	4.90	C9H10O3	L2
3-(4-Hydroxyphenyl) lactate	182.0579	7.65	C9H10O4	L2
2',3'-Cyclic UMP	306.0253	8.43	C9H11N2O8P	L2
L-Phenylalanine	165.0790	8.21	C9H11NO2	L2
L-Tyrosine	181.0740	10.17	C9H11NO3	L1
Uridine	244.0695	8.52	C9H12N2O6	L1
2',3'-Cyclic CMP	305.0413	9.45	C9H12N3O7P	L2
dUMP	308.0411	9.66	C9H13N2O8P	L1
UMP	324.0359	10.43	C9H13N2O9P	L1
Deoxycytidine	227.0906	8.39	C9H13N3O4	L2
Cytidine	243.0855	9.55	C9H13N3O5	L1
UDP	404.0023	11.17	C9H14N2O12P2	L2
CMP	323.0519	10.32	C9H14N3O8P	L1
CDP	403.0182	11.60	C9H15N3O11P2	L1
8-Amino-7-oxononanoate	187.1207	4.91	C9H17NO3	L2
O-Acetylcarnitine	203.1158	8.36	C9H17NO4	L1
N2-(D-1-Carboxyethyl)-L-lysine	218.1264	7.92	C9H18N2O4	L2
N2-(D-1-Carboxyethyl)-L-arginine	246.1330	10.27	C9H18N4O4	L2
N6,N6,N6-Trimethyl-L-lysine	188.1525	15.31	C9H20N2O2	L2
3-Hydroxy-N6,N6,N6-trimethyl-L-lysine	204.1474	15.30	C9H20N2O3	L2
Phenylpyruvate	164.0475	4.84	C9H8O3	L1
3-(4-Hydroxyphenyl)pyruvate	180.0422	7.21	C9H8O4	L2
Hydroxymethylphosphonate	111.9926	10.18	CH5O4P	L2
Orthophosphate	97.9770	11.28	H3O4P	L2

Table A3: A list of total identified metabolites in macrophages in response to polarization into M0, M1, M2, Mreg, M0-LPS and Mreg-LPS.

Putative metabolite	Mass	RT	FORMULA	confidence
PI(40:6)	910.5561	3.32	C49H83O13P	L2
PI(38:4)	886.5567	3.31	C47H83O13P	L2
PI(38:5)	884.5413	3.31	C47H81O13P	L2
PS(44:10)	883.5356	3.22	C50H78NO10P	L2
PI(38:6)	882.5266	3.31	C47H79O13P	L2
[PI (18:0/18:0)]	879.5849	3.30	C45H86NO13P	L2
PI(15:0/22:4)	872.5413	3.31	C46H81O13P	L2
PG(22:6)	866.5109	3.24	C50H75O10P	L2
PI(36:1)	864.5730	6.99	C45H85O13P	L2
PI(36:2)	862.5574	3.31	C45H83O13P	L2
PC(42:6)	861.6236	3.51	C50H88NO8P	L2
PI(36:3)	860.5413	3.32	C45H81O13P	L2
PC(42:7)	859.6090	3.50	C50H86NO8P	L2
PI(36:4)	858.5265	3.31	C45H79O13P	L2
PI(36:5)	856.5110	3.32	C45H77O13P	L2
PS(19:0/22:4)	853.5839	3.55	C47H84NO10P	L2
PS(19:0/22:6)	849.5507	3.25	C47H80NO10P	L2
PG(42:9)	844.5247	3.24	C48H77O10P	L2
PG(42:10)	842.5099	3.24	C48H75O10P	L2
PG(22:6)	840.4954	3.25	C48H73O10P	L2
PS(40:5)	837.5521	3.23	C46H80NO10P	L2
PI(34:1)	836.5410	3.31	C43H81O13P	L2
PC(40:5)	835.6082	3.49	C48H86NO8P	L2
PS(40:6)	835.5361	3.30	C46H78NO10P	L2
PC(40:6)	833.5928	3.49	C48H84NO8P	L2
PC(40:7)	831.5780	3.49	C48H82NO8P	L2
PC(40:8)	829.5623	3.48	C48H80NO8P	L2
PE(42:5)	821.5923	3.52	C47H84NO8P	L2
PG(40:7)	820.5261	3.25	C46H77O10P	L2
PC(22:4/P-18:1)	819.6140	3.47	C48H86NO7P	L2
PE(42:6)	819.5790	3.51	C47H82NO8P	L2
PS(38:1)	817.5821	3.23	C44H84NO10P	L2
PS(38:2)	815.5678	3.23	C44H82NO10P	L2
PC(38:2)	813.6244	4.03	C46H88NO8P	L2
PS(38:3)	813.5521	3.29	C44H80NO10P	L2
SM(d18:2/24:0)	812.6771	6.69	C47H93N2O6P	L2
PS(38:4)	811.5366	3.30	C44H78NO10P	L2
PC(38:4)	809.5926	3.51	C46H84NO8P	L2
PS(38:5)	809.5214	3.24	C44H76NO10P	L2
PI(32:1)	808.5101	3.32	C41H77O13P	L2
PS(38:6)	807.5064	3.29	C44H74NO10P	L2
PC(38:6)	805.5621	3.50	C46H80NO8P	L2
[GP (18:0/18:0)]	803.5686	3.22	C43H82NO10P	L2
PC(38:7)	803.5469	3.50	C46H78NO8P	L2
PG(38:3)	800.5552	3.26	C44H81O10P	L2
PE(40:2)	799.6095	3.96	C45H86NO8P	L2
PG(38:4)	798.5417	3.25	C44H79O10P	L2
PS(36:0)	791.5683	3.23	C42H82NO10P	L2
PE(40:6)	791.5477	3.52	C45H78NO8P	L2

PS(36:1)	789.5526	3.22	C42H80NO10P	L2
PC(36:1)	787.6079	4.01	C44H86NO8P	L2
PS(36:2)	787.5369	3.31	C42H78NO10P	L2
PC(36:2)	785.5932	3.54	C44H84NO8P	L2
PS(36:3)	785.5212	3.32	C42H76NO10P	L2
PC(36:3)	783.5773	3.52	C44H82NO8P	L2
PS(36:4)	783.5057	3.30	C42H74NO10P	L2
PC(36:4)	781.5620	3.52	C44H80NO8P	L2
PC(36:5)	779.5467	3.51	C44H78NO8P	L2
PS(13:0/22:0)	777.5518	3.24	C41H80NO10P	L2
PG(36:2)	774.5417	3.27	C42H79O10P	L2
PE(38:1)	773.5924	4.02	C43H84NO8P	L2
[PC (18:1/18:0)]	771.6131	4.09	C44H86NO7P	L2
PE(38:2)	771.5774	3.54	C43H82NO8P	L2
PE(38:4)	767.5459	3.72	C43H78NO8P	L2
PE(38:5)	765.5312	4.62	C43H76NO8P	L2
PE(38:5)	765.5308	3.57	C43H76NO8P	L2
PS(34:0)	763.5373	3.24	C40H78NO10P	L2
PE(38:6)	763.5156	3.46	C43H74NO8P	L2
PS(34:1)	761.5213	3.31	C40H76NO10P	L2
[PC (16:0/18:1)]	759.5777	7.57	C42H82NO8P	L2
PC(34:1)	759.5774	3.65	C42H82NO8P	L2
PC(34:2)	757.5620	3.54	C42H80NO8P	L2
PC(34:3)	755.5465	3.54	C42H78NO8P	L2
[PE (18:1/20:4)]	751.5507	3.47	C43H78NO7P	L2
PE(20:4/P-18:1)	749.5349	3.42	C43H76NO7P	L2
PG(34:1)	748.5258	3.28	C40H77O10P	L2
[PE (16:1/22:6)]	747.5199	3.42	C43H74NO7P	L2
PG(34:2)	746.5101	3.26	C40H75O10P	L2
PC(16:0/P-18:0)	745.5981	4.08	C42H84NO7P	L2
PC(18:0/P-16:0)	745.5979	5.93	C42H84NO7P	L2
PE(36:1)	745.5617	3.57	C41H80NO8P	L2
PS(O-16:0/18:2)	745.5269	3.30	C40H76NO9P	L2
1-Hexadecanoyl-2-(octadecenoyl)-sn-glycero-3-phosphonocholine	743.5827	3.59	C42H82NO7P	L2
PE(36:2)	743.5466	3.57	C41H78NO8P	L2
NADP+	743.0756	10.82	C21H28N7O17P3	L1
PE(36:3)	741.5311	3.60	C41H76NO8P	L2
PE(36:5)	737.4997	3.55	C41H72NO8P	L2
PS(32:0)	735.5058	3.25	C38H74NO10P	L2
[PC (16:0/16:0)]	733.5618	5.86	C40H80NO8P	L2
PC(32:0)	733.5609	3.64	C40H80NO8P	L2
PS(32:1)	733.4895	3.31	C38H72NO10P	L2
PC(32:1)	731.5464	3.56	C40H78NO8P	L2
PC(32:2)	729.5311	3.55	C40H76NO8P	L2
SM(d18:1/18:1)	728.5834	3.73	C41H81N2O6P	L2
PC(32:3)	727.5152	3.59	C40H74NO8P	L2
PE(18:3/P-18:1)	723.5198	3.56	C41H74NO7P	L2
PE(18:4/P-18:1)	721.5040	3.48	C41H72NO7P	L2
PG(32:1)	720.4955	3.27	C38H73O10P	L2
PE(34:0)	719.5454	3.60	C39H78NO8P	L2
PE(34:1)	717.5309	3.58	C39H76NO8P	L2
PE(34:2)	715.5153	3.67	C39H74NO8P	L2
PC(30:0)	705.5308	3.59	C38H76NO8P	L2
PC(30:1)	703.5157	3.59	C38H74NO8P	L2
SM(d16:1/18:0)	702.5673	6.61	C39H79N2O6P	L2
[SP (16:0)]	702.5672	3.72	C39H79N2O6P	L2
PE(16:0/P-18:1)	701.5359	3.77	C39H76NO7P	L2
SM(d16:1/18:1)	700.5513	3.70	C39H77N2O6P	L2
PE(16:1/P-18:1)	699.5202	3.92	C39H74NO7P	L2

[PC (14:2/16:0)]	691.5511	3.61	C38H78NO7P	L2
PE(32:0)	691.5153	3.61	C37H74NO8P	L2
PC(14:0/P-16:0)	689.5349	3.59	C38H76NO7P	L2
PE(32:1)	689.4985	3.68	C37H72NO8P	L2
[SP (18:0/14:0)]	688.5514	3.74	C38H77N2O6P	L2
PC(28:0)	677.4992	3.60	C36H72NO8P	L2
SM(d18:1/14:0)	674.5356	3.74	C37H75N2O6P	L2
PA(34:1)	674.4885	3.30	C37H71O8P	L2
SM(d18:2/14:0)	672.5213	3.65	C37H73N2O6P	L2
PA(34:2)	672.4732	3.29	C37H69O8P	L2
PC(O-16:0/12:0)	663.5198	3.63	C36H74NO7P	L2
PE(30:0)	663.4840	3.48	C35H70NO8P	L2
PE(O-16:0/14:0)	649.5044	3.62	C35H72NO7P	L2
PA(32:0)	648.4724	3.29	C35H69O8P	L2
[SP (24:0)]	647.6215	3.35	C42H81NO3	L2
PA(32:1)	646.4575	3.30	C35H67O8P	L2
[SP (22:0)]	621.6054	4.03	C40H79NO3	L2
[PI (20:4)]	620.2961	7.08	C29H49O12P	L2
Cer(d18:1/22:1)	619.5902	3.36	C40H77NO3	L2
CMP-N-acetylneuraminate	614.1468	10.20	C20H31N4O16P	L2
UDP-N-acetyl-D-glucosamine	607.0812	10.23	C17H27N3O17P2	L2
[PI (18:0)]	600.3270	3.67	C27H53O12P	L2
GDP-L-fucose	589.0821	11.60	C16H25N5O15P2	L2
PS(22:4/0:0)	573.3066	3.42	C28H48NO9P	L2
[PI (16:0)]	572.2959	7.18	C25H49O12P	L2
LysoPC(22:5)	569.3485	7.23	C30H52NO7P	L2
[PC (22:6)]	567.3322	7.24	C30H50NO7P	L2
UDP-glucose	566.0547	11.02	C15H24N2O17P2	L1
Phosphoribosyl-AMP	559.0714	10.19	C15H23N5O14P2	L2
PG(22:6/0:0)	556.2799	3.46	C28H45O9P	L2
LysoPC(20:1)	549.3793	7.22	C28H56NO7P	L2
LysoPC(20:3)	545.3486	4.07	C28H52NO7P	L2
LysoPC(20:4)	543.3324	7.25	C28H50NO7P	L2
[SP (16:0)]	537.5121	4.29	C34H67NO3	L2
UDP-D-xylose	536.0440	10.99	C14H22N2O16P2	L2
Cer(d18:2/16:0)	535.4964	3.39	C34H65NO3	L2
PG(20:3/0:0)	534.2955	3.46	C26H47O9P	L2
LysoPE(0:0/22:5)	527.3020	7.24	C27H46NO7P	L2
[PS (18:0)]	525.3066	7.13	C24H48NO9P	L2
LysoPE(0:0/22:6))	525.2854	4.00	C27H44NO7P	L2
[PC (18:0)]	523.3645	7.25	C26H54NO7P	L2
[PS (18:1)]	523.2907	3.66	C24H46NO9P	L2
LysoPC(18:1)	521.3481	4.10	C26H52NO7P	L2
[PC (18:2)]	519.3323	4.12	C26H50NO7P	L2
[PG (18:1)]	510.2954	3.46	C24H47O9P	L2
LysoPC(O-18:0)	509.3848	7.26	C26H56NO6P	L2
[PC methyl(16:0)]	509.3481	4.12	C25H52NO7P	L2
[PC (18:1)]	507.3690	4.06	C26H54NO6P	L2
LysoPE(0:0/20:1)	507.3325	4.15	C25H50NO7P	L2
ATP	506.9958	11.10	C10H16N5O13P3	L1
LysoPE(0:0/20:3))	503.3016	4.01	C25H46NO7P	L2
[PE (20:4)]	501.2858	4.03	C25H44NO7P	L2
[ST hydrox] N-(3alpha,7alpha-dihydroxy-5beta-cholan-24-oyl)-taurine	499.2966	3.75	C26H45NO6S	L2
LysoPE(20:5/0:0)	499.2696	7.16	C25H42NO7P	L2
[PS (16:0)]	497.2755	7.17	C22H44NO9P	L2
[PC (16:0)]	495.3324	7.27	C24H50NO7P	L2
[PC (16:1)]	493.3167	4.20	C24H48NO7P	L2
[PG (16:0)]	484.2803	3.49	C22H45O9P	L2

[PC (16:2)]	481.3532	7.27	C24H52NO6P	L2
[PE (18:0)]	481.3169	4.17	C23H48NO7P	L2
[PC (16:1)]	479.3374	7.26	C24H50NO6P	L2
[PE (18:1)]	479.3012	7.13	C23H46NO7P	L2
LysoPE(0:0/18:2)	477.2856	7.16	C23H44NO7P	L2
CMP-N-trimethyl-2-aminoethylphosphonate	472.1123	9.61	C14H26N4O10P2	L2
[PC (14:0)]	467.3012	7.27	C22H46NO7P	L2
[PE (18:1)]	465.3219	7.25	C23H48NO6P	L2
[PE (16:0)]	453.2855	7.22	C21H44NO7P	L2
LysoPE(0:0/16:1)	451.2698	4.16	C21H42NO7P	L2
Glycodeoxycholate	449.3142	3.92	C26H43NO5	L2
CDP-ethanolamine	446.0603	10.88	C11H20N4O11P2	L2
GDP	443.0241	11.60	C10H15N5O11P2	L1
[PE (16:2)]	439.3069	4.21	C21H46NO6P	L2
[PE (16:1)]	437.2906	7.11	C21H44NO6P	L2
LPA(0:0/18:1)	436.2592	3.55	C21H41O7P	L2
CMP-2-aminoethylphosphonate	430.0655	10.30	C11H20N4O10P2	L2
ADP	427.0294	10.38	C10H15N5O10P2	L1
Chitobiose	424.1699	8.12	C16H28N2O11	L2
Thiamin diphosphate	424.0369	9.70	C12H18N4O7P2S	L2
N-oleoyl glutamine	410.3144	5.14	C23H42N2O4	L2
Acetyl-CoA	404.5631	8.63	C23H38N7O17P3S	L2
PG(O-18:0/21:0)	403.3198	5.45	C45H91O9P	L2
CDP	403.0183	11.31	C9H15N3O11P2	L1
5S-HETE di-endoperoxide	402.2254	3.58	C20H34O8	L2
[FA] O-Palmitoyl-R-carnitine	399.3348	4.17	C23H45NO4	L2
[FA (26:0)]	396.3969	3.38	C26H52O2	L2
PA(O-16:0/0:0)	396.2642	5.11	C19H41O6P	L2
[ST hydrox] 3alpha,12alpha-Dihydroxy-5beta-chol-6-en-24-oic Acid	390.2769	4.41	C24H38O4	L2
N-Acetylneuraminate 9-phosphate	389.0723	11.26	C11H20NO12P	L2
S-Adenosyl-L-homocysteine	384.1218	9.66	C14H20N6O5S	L2
[FA hydroxy(24:0)]	382.3449	3.35	C24H46O3	L2
(R)-S-Lactoylglutathione	379.1052	8.87	C13H21N3O8S	L2
Riboflavin	376.1383	7.42	C17H20N4O6	L2
NADPH	372.5456	11.13	C21H30N7O17P3	L2
N-stearoyl serine	371.3036	7.27	C21H41NO4	L2
Tetracosanoic acid	368.3657	3.38	C24H48O2	L2
[FA (24:0)]	366.3500	3.38	C24H46O2	L2
GMP	363.0579	11.23	C10H14N5O8P	L1
[FA (12:0)]	360.3030	3.42	C24H40O2	L2
[GL (18:0)]	358.3085	3.77	C21H42O4	L2
[FA (12:0)]	358.2876	3.44	C24H38O2	L2
N-palmitoyl threonine	357.2878	4.34	C20H39NO4	L2
deacetylcolchicine	357.1569	10.77	C20H23NO5	L2
Deacetoxycephalosporin C	357.0998	8.30	C14H19N3O6S	L2
[FA (24:6)]	356.2718	3.43	C24H36O2	L2
IMP	348.0473	10.52	C10H13N4O8P	L1
AMP	347.0631	9.49	C10H14N5O7P	L1
[FA (24:6)]	344.1776	5.20	C24H24O2	L2
Thiamin monophosphate	344.0707	9.36	C12H17N4O4PS	L2
Sucrose	342.1163	11.20	C12H22O11	L1
[FA (18:0)]	341.2931	4.01	C20H39NO3	L2
Docosanoic acid	340.3343	3.43	C22H44O2	L2
D-Fructose 1,6-bisphosphate	339.9964	11.74	C6H14O12P2	L2
[FA (22:0)]	338.3186	3.44	C22H42O2	L2
S-Formylglutathione	335.0789	9.46	C11H17N3O7S	L2
13,16,19-Docosatrienoic acid	334.2875	3.44	C22H38O2	L2
NADH	332.5625	9.35	C21H29N7O14P2	L2
[FA (22:4)]	332.2717	3.47	C22H36O2	L2

NAD+	331.5545	9.52	C21H27N7O14P2	L2
[GL (16:0)]	330.2772	3.76	C19H38O4	L2
3',5'-Cyclic AMP	329.0527	7.42	C10H12N5O6P	L1
Docosahexaenoicacid	328.2404	3.46	C22H32O2	L2
[FA (18:0)]	325.2981	4.52	C20H39NO2	L2
UMP	324.0360	10.34	C9H13N2O9P	L1
[FA (18:2)]	323.2824	4.47	C20H37NO2	L2
CMP	323.0518	10.20	C9H14N3O8P	L1
dTMP	322.0567	9.05	C10H15N2O8P	L2
[FA (18:0)]	316.2614	3.66	C18H36O4	L2
[SP hydrox] 6-hydroxysphing-4E-enine	315.2774	3.51	C18H37NO3	L2
[FA (16:0)]	313.2616	4.00	C18H35NO3	L2
[FA (20:0)]	312.3030	3.45	C20H40O2	L2
Spongipregnoloside A	312.1760	3.42	C33H52O11	L2
[FA (20:0)]	310.2873	3.48	C20H38O2	L2
Icosadienoic acid	308.2714	3.47	C20H36O2	L2
dUMP	308.0410	9.56	C9H13N2O8P	L1
Icosatrienoic acid	306.2560	3.49	C20H34O2	L2
Glutathione disulfide	306.0760	11.02	C20H32N6O12S2	L1
[FA (20:4)]	304.2402	3.50	C20H32O2	L2
[FA (20:5)]	302.2246	3.56	C20H30O2	L2
Sphinganine	301.2980	7.29	C18H39NO2	L2
N-Acetyl-D-glucosamine 6-phosphate	301.0561	10.14	C8H16NO9P	L2
[FA hydroxy(18:0)]	300.2664	3.51	C18H36O3	L2
[FA (16:2)]	299.2825	5.36	C18H37NO2	L2
Nonadecanoicacid	298.2871	3.47	C19H38O2	L2
2-Oxooctadecanoic acid	298.2507	3.51	C18H34O3	L2
[FA methyl(18:0)]	296.2713	3.48	C19H36O2	L2
[FA hydroxy(18:2)]	296.2351	3.55	C18H32O3	L2
N-(L-Arginino)succinate	290.1227	11.06	C10H18N4O6	L2
D-Sedoheptulose 7-phosphate	290.0404	10.96	C7H15O10P	L2
L-Octanoylcarnitine	287.2097	4.49	C15H29NO4	L2
[FA hydroxy,oxo(16:0)]	286.2143	3.72	C16H30O4	L2
Octadecanoic acid	284.2714	3.48	C18H36O2	L1
Octadecanamide	283.2876	4.90	C18H37NO	L2
[FA (18:1)]	281.2719	4.92	C18H35NO	L2
[SP (4:0)]	277.2406	4.11	C18H31NO	L2
6-Phospho-D-gluconate	276.0247	11.66	C6H13O10P	L1
[FA amino(16:0)]	271.2511	7.25	C16H33NO2	L2
[FA oxo(16:0)]	270.2195	3.55	C16H30O3	L2
omega-Cyclohexylundecanoic acid	268.2402	3.51	C17H32O2	L2
Inosine	268.0808	8.87	C10H12N4O5	L1
Adenosine	267.0967	7.76	C10H13N5O4	L1
Thiamin	264.1046	16.47	C12H16N4OS	L2
Sorbitol 6-phosphate	262.0452	10.48	C6H15O9P	L2
D-Glucose 6-phosphate	260.0295	10.88	C6H13O9P	L1
[FA (6:0)] O-hexanoyl-R-carnitine	259.1784	4.51	C13H25NO4	L2
D-Glucosamine 6-phosphate	259.0457	10.74	C6H14NO8P	L2
[FA (14:0/2:0)]	258.1831	3.67	C14H26O4	L2
sn-glycero-3-Phosphocholine	257.1029	9.93	C8H20NO6P	L1
Hexadecanoic acid	256.2402	3.51	C16H32O2	L2
Hexadecenoic acid	254.2246	3.51	C16H30O2	L2
3-beta-D-Galactosyl-sn-glycerol	254.1000	9.83	C9H18O8	L2
[Fv Hydroxy,methox] 4'-Hydroxy-2'-methoxychalcone	254.0941	3.90	C16H14O3	L2
N-Ribosylnicotinamide	254.0903	18.61	C11H14N2O5	L2
Palmitoleamide	253.2405	4.96	C16H31NO	L2
Deoxyinosine	252.0860	8.03	C10H12N4O4	L2
Deoxyadenosine	251.1016	7.37	C10H13N5O3	L1
gamma-L-Glutamyl-L-cysteine	250.0625	9.92	C8H14N2O5S	L2

Pyridoxal phosphate	247.0245	9.90	C8H10NO6P	L2
3-Hydroxydodecanedioicacid	246.1467	4.01	C12H22O5	L2
N2-(D-1-Carboxyethyl)-L-arginine	246.1329	10.17	C9H18N4O4	L2
[PR methyl(4:0)]	246.0058	9.21	C5H12O7P2	L2
beta-Alanyl-L-arginine	245.1489	10.77	C9H19N5O3	L2
2S-Hydroxytetradecanoic acid	244.2036	3.58	C14H28O3	L2
Biotin	244.0882	4.55	C10H16N2O3S	L2
Uridine	244.0694	8.42	C9H12N2O6	L1
CDP-choline	244.0538	10.15	C14H26N4O11P2	L2
Cytidine	243.0857	9.44	C9H13N3O5	L1
[FA methyl(14:0)]	242.2246	3.53	C15H30O2	L2
[FA oxo(14:0)]	242.1881	3.61	C14H26O3	L2
Lumichrome	242.0804	7.30	C12H10N4O2	L2
[SP (14:0/2:0)]	241.2041	4.07	C14H27NO2	L2
N-(3-Oxooctanoyl)homoserine lactone	241.1314	4.51	C12H19NO4	L2
Dihydrobiopterin	239.1017	8.65	C9H13N5O3	L2
[Fv Methox] 4'-Methoxychalcone	238.0993	5.14	C16H14O2	L2
L-Formylkynurenine	236.0797	7.93	C11H12N2O4	L2
N2-Succinyl-L-ornithine	232.1058	9.59	C9H16N2O5	L2
D-Ribitol 5-phosphate	232.0347	10.64	C5H13O8P	L2
O-Butanoylcarnitine	231.1471	7.32	C11H21NO4	L1
Dodecanedioic acid	230.1518	4.16	C12H22O4	L2
D-Ribose 5-phosphate	230.0191	10.45	C5H11O8P	L1
[SP (14:0)]	229.2406	7.23	C14H31NO	L2
Tetradecanoic acid	228.2090	3.55	C14H28O2	L2
Deoxycytidine	227.0905	8.58	C9H13N3O4	L2
Tetradecenoic acid	226.1934	3.56	C14H26O2	L2
Carnosine	226.1065	10.87	C9H14N4O3	L2
[FA (12:4/2:0)]	222.0892	3.85	C12H14O4	L2
L-Cystathionine	222.0675	11.33	C7H14N2O4S	L1
N-Acetyl-D-glucosamine	221.0900	9.11	C8H15NO6	L2
5-Hydroxy-L-tryptophan	220.0847	7.79	C11H12N2O3	L2
Pantothenate	219.1107	7.32	C9H17NO5	L1
O-Succinyl-L-homoserine	219.0742	9.86	C8H13NO6	L2
8-Methoxykynurenate	219.0530	6.83	C11H9NO4	L2
N2-(D-1-Carboxyethyl)-L-lysine	218.1266	7.85	C9H18N2O4	L2
3-Hydroxysebacicacid	218.1154	4.47	C10H18O5	L2
N-Acetylserotonin	218.1055	5.34	C12H14N2O2	L2
gamma-L-Glutamylputrescine	217.1426	14.88	C9H19N3O3	L2
O-Propanoylcarnitine	217.1314	5.39	C10H19NO4	L2
N-Acetyl-L-citrulline	217.1063	8.45	C8H15N3O4	L2
12-Hydroxydodecanoic acid	216.1725	3.62	C12H24O3	L2
gamma-Glutamyl-gamma-aminobutyraldehyde	216.1111	8.11	C9H16N2O4	L2
2-C-Methyl-D-erythritol 4-phosphate	216.0401	10.92	C5H13O7P	L2
sn-glycero-3-Phosphoethanolamine	215.0559	10.77	C5H14NO6P	L2
2-Deoxy-D-ribose 5-phosphate	214.0243	10.09	C5H11O7P	L2
N-Heptanoylhomoserine lactone	213.1364	4.46	C11H19NO3	L2
[FA oxo(12:1)]	212.1413	3.86	C12H20O3	L2
Phosphocreatine	211.0358	10.31	C4H10N3O5P	L2
Sedoheptulose	210.0740	10.51	C7H14O7	L2
L-Kynurenine	208.0848	8.75	C10H12N2O3	L1
2-Hydroxybutane-1,2,4-tricarboxylate	206.0428	9.59	C7H10O7	L2
Indolelactate	205.0738	7.32	C11H11NO3	L2
3-Hydroxy-N6,N6,N6-trimethyl-L-lysine	204.1473	14.67	C9H20N2O3	L2
N6-Acetyl-N6-hydroxy-L-lysine	204.1110	15.83	C8H16N2O4	L2
L-Tryptophan	204.0899	9.37	C11H12N2O2	L1
O-Acetylcarnitine	203.1158	8.34	C9H17NO4	L1
[FA (10:0/2:0)]	202.1206	4.51	C10H18O4	L2
Dodecanoic acid	200.1776	3.61	C12H24O2	L2

Dihydroclavaminic acid	200.0797	7.99	C8H12N2O4	L2
Erythrulose 1-phosphate	200.0086	9.18	C4H9O7P	L2
S-Adenosyl-L-methionine	199.0687	11.11	C15H22N6O5S	L2
3,4-Dihydroxy-L-phenylalanine	197.0688	9.61	C9H11NO4	L2
D-Gluconic acid	196.0583	10.03	C6H12O7	L1
L-Tyrosine methyl ester	195.0896	5.13	C10H13NO3	L2
2-Carboxy-2,3-dihydro-5,6-dihydroxyindole	195.0530	10.61	C9H9NO4	L2
D-Glucuronate	194.0426	11.24	C6H10O7	L2
Phenylacetylglycine	193.0740	7.28	C10H11NO3	L2
Citrate	192.0270	12.14	C6H8O7	L2
5-Hydroxyindoleacetate	191.0582	7.26	C10H9NO3	L2
2,6-Diaminoheptanedioate	190.0952	10.18	C7H14N2O4	L2
N-Carbamyl-L-glutamate	190.0590	10.91	C6H10N2O5	L2
N-Acetyl-L-glutamate	189.0637	9.84	C7H11NO5	L2
N6,N6,N6-Trimethyl-L-lysine	188.1524	14.79	C9H20N2O2	L2
10-Hydroxydecanoic acid	188.1413	3.74	C10H20O3	L2
Homoarginine	188.1273	17.96	C7H16N4O2	L2
N2-Acetyl-L-lysine	188.1161	7.30	C8H16N2O3	L2
8-Amino-7-oxononanoate	187.1208	4.50	C9H17NO3	L2
6-Acetamido-2-oxohexanoate	187.0846	8.92	C8H13NO4	L2
2-(Acetamidomethylene)succinate	187.0481	10.45	C7H9NO5	L2
10-Oxodecanoate	186.1256	3.92	C10H18O3	L2
3-Phospho-D-glycerate	185.9929	11.47	C3H7O7P	L1
L-Adrenaline	183.0895	7.17	C9H13NO3	L2
Choline phosphate	183.0660	10.11	C5H14NO4P	L1
Salicin 6-phosphate	183.0355	6.70	C13H19O10P	L2
D-Sorbitol	182.0791	10.35	C6H14O6	L2
3-(4-Hydroxyphenyl)lactate	182.0580	7.37	C9H10O4	L2
L-Tyrosine	181.0739	10.05	C9H11NO3	L2
D-Glucose	180.0634	11.93	C6H12O6	L2
3-(4-Hydroxyphenyl)pyruvate	180.0423	7.31	C9H8O4	L2
D-Glucosamine	179.0794	8.71	C6H13NO5	L2
D-Glucono-1,5-lactone	178.0477	10.62	C6H10O6	L2
N-Formyl-L-methionine	177.0459	4.51	C6H11NO3S	L2
2-Isopropylmalate	176.0684	9.77	C7H12O5	L2
N-Carbamoyl-L-aspartate	176.0433	11.45	C5H8N2O5	L2
D-Glucuronolactone	176.0321	10.92	C6H8O6	L2
L-Citrulline	175.0957	11.06	C6H13N3O3	L1
5-Hydroxyindoleacetaldehyde	175.0632	3.88	C10H9NO2	L2
N-Acetyl-L-aspartate	175.0480	10.23	C6H9NO5	L2
L-Arginine	174.1117	17.73	C6H14N4O2	L1
N-Formimino-L-glutamate	174.0640	8.18	C6H10N2O4	L2
3-oxopimelic acid	174.0528	4.55	C7H10O5	L2
5-Guanidino-2-oxopentanoate	173.0800	10.70	C6H11N3O3	L2
N-Acetyl-L-glutamate 5-semialdehyde	173.0688	7.33	C7H11NO4	L2
Decanoic acid	172.1464	3.70	C10H20O2	L2
9-Oxononanoic acid	172.1100	4.04	C9H16O3	L2
[FA dioxo(8:0)]	172.0736	7.99	C8H12O4	L2
Hydantoin-5-propionate	172.0485	8.48	C6H8N2O4	L2
sn-Glycerol 3-phosphate	172.0137	9.96	C3H9O6P	L1
2,3,4,5-Tetrahydrodipicolinate	171.0531	7.17	C7H9NO4	L2
D-Glyceraldehyde 3-phosphate	169.9980	11.01	C3H7O6P	L2
N(pi)-Methyl-L-histidine	169.0851	9.25	C7H11N3O2	L2
Pyridoxine	169.0738	7.34	C8H11NO3	L1
Phosphodimethylethanolamine	169.0503	9.55	C4H12NO4P	L2
L-Cysteate	169.0045	11.24	C3H7NO5S	L1
1,3,5-trimethoxybenzene	168.0786	4.33	C9H12O3	L2
3,4-Dihydroxyphenylacetate	168.0423	8.80	C8H8O4	L2
Urate	168.0283	9.81	C5H4N4O3	L1

Butanoylphosphate	168.0187	10.02	C4H9O5P	L2
3-Phosphonopyruvate	167.9824	9.19	C3H5O6P	L2
Taurocyamine	167.0365	11.77	C3H9N3O3S	L2
Pyridine-2,3-dicarboxylate	167.0218	10.84	C7H5NO4	L2
3-(2-Hydroxyphenyl)propanoate	166.0630	6.72	C9H10O3	L2
L-Phenylalanine	165.0790	8.12	C9H11NO2	L2
L-Methionine S-oxide	165.0459	9.69	C5H11NO3S	L2
Formylanthranilate	165.0427	6.24	C8H7NO3	L2
L-Rhamnose	164.0685	7.27	C6H12O5	L2
Phenylpyruvate	164.0474	4.48	C9H8O3	L1
S-Methyl-L-methionine	163.0667	11.69	C6H13NO2S	L2
N6-Hydroxy-L-lysine	162.1005	15.18	C6H14N2O3	L2
2-Dehydro-3-deoxy-L-rhamnonate	162.0529	10.08	C6H10O5	L2
4-Hydroxy-2-oxoglutarate	162.0165	8.92	C5H6O6	L2
O-Acetyl-L-homoserine	161.0689	7.32	C6H11NO4	L2
N6-Methyl-L-lysine	160.1212	15.81	C7H16N2O2	L1
D-Alanyl-D-alanine	160.0847	7.31	C6H12N2O3	L2
2-Oxoadipate	160.0372	11.85	C6H8O5	L2
5-Acetamidopentanoate	159.0895	9.31	C7H13NO3	L2
Indole-3-acetaldehyde	159.0684	5.53	C10H9NO	L2
4-Methylene-L-glutamate	159.0532	11.39	C6H9NO4	L2
[FA oxo(8:0)] 3-oxo-octanoic acid	158.0943	4.46	C8H14O3	L2
4-Methylene-L-glutamine	158.0692	7.95	C6H10N2O3	L2
2-Isopropylmaleate	158.0579	7.63	C7H10O4	L2
Allantoin	158.0439	11.19	C4H6N4O3	L1
(S)-Dihydroorotate	158.0328	8.53	C5H6N2O4	L2
4-Imidazolone-5-propanoate	156.0535	8.33	C6H8N2O3	L2
2,3-Dihydro-2,3-dihydroxybenzoate	156.0424	9.67	C7H8O4	L2
Orotate	156.0172	8.16	C5H4N2O4	L1
N-Methylethanolamine phosphate	155.0347	10.13	C3H10NO4P	L2
Imidazol-5-yl-pyruvate	154.0379	11.42	C6H6N2O3	L2
Propanoyl phosphate	154.0032	8.70	C3H7O5P	L2
4-(beta-Acetylaminoethyl)imidazole	153.0902	5.33	C7H11N3O	L2
3-Hydroxyanthranilate	153.0426	9.34	C7H7NO3	L2
Xylitol	152.0685	9.90	C5H12O5	L2
Xanthine	152.0334	9.00	C5H4N4O2	L1
Guanine	151.0494	10.08	C5H5N5O	L2
Phenylpropanoate	150.0681	4.45	C9H10O2	L2
D-Ribose	150.0528	8.80	C5H10O5	L2
7-Methyladenine	149.0701	11.22	C6H7N5	L2
L-Methionine	149.0511	9.01	C5H11NO2S	L2
5,6-Dihydroxyindole	149.0477	11.75	C8H7NO2	L2
(R)-2-Hydroxyglutarate	148.0372	10.69	C5H8O5	L1
L-Glutamate	147.0531	10.32	C5H9NO4	L1
L-Lysine	146.1055	16.38	C6H14N2O2	L1
L-Glutamine	146.0691	10.77	C5H10N2O3	L1
(R)-3-Hydroxy-3-methyl-2-oxopentanoate	146.0580	9.96	C6H10O4	L2
2-Oxoglutarate	146.0216	11.10	C5H6O5	L2
4-Trimethylammoniobutanoate	145.1103	9.53	C7H15NO2	L1
4-Guanidinobutanoate	145.0852	10.88	C5H11N3O2	L2
2-Oxoglutaramate	145.0376	7.99	C5H7NO4	L2
[FA (8:0)]	144.1151	3.89	C8H16O2	L2
4-Guanidinobutanamide	144.1012	17.78	C5H12N4O	L2
7-oxoheptanoate	144.0787	4.49	C7H12O3	L2
2,3-Dimethylmaleate	144.0424	10.25	C6H8O4	L2
[FA (8:1)]	142.0995	3.93	C8H14O2	L2
Ethanolamine phosphate	141.0191	10.75	C2H8NO4P	L1
Methylimidazoleacetic acid	140.0586	7.33	C6H8N2O2	L2
Urocanate	138.0429	8.29	C6H6N2O2	L2

Phenylacetic acid	136.0525	7.16	C8H8O2	L2
Hypoxanthine	136.0385	8.64	C5H4N4O	L1
[FA trihydroxy(4:0)]	136.0373	9.35	C4H8O5	L2
Adenine	135.0545	8.04	C5H5N5	L1
L-Homocysteine	135.0354	9.12	C4H9NO2S	L2
L-Malate	134.0216	11.20	C4H6O5	L1
L-Aspartate	133.0376	10.57	C4H7NO4	L1
L-Ornithine	132.0899	15.53	C5H12N2O2	L1
L-Asparagine	132.0535	10.93	C4H8N2O3	L1
2-Acetolactate	132.0424	11.34	C5H8O4	L2
Oxalureate	132.0172	8.18	C3H4N2O4	L2
L-Leucine	131.0946	8.54	C6H13NO2	L1
Creatine	131.0694	10.63	C4H9N3O2	L1
L-Glutamate 5-semialdehyde	131.0583	10.55	C5H9NO3	L2
Iminoaspartate	131.0220	7.95	C4H5NO4	L2
(S)-3-Methyl-2-oxopentanoic acid	130.0630	8.86	C6H10O3	L2
N4-Acetylaminobutanal	129.0790	7.25	C6H11NO2	L2
L-1-Pyrroline-3-hydroxy-5-carboxylate	129.0427	7.75	C5H7NO3	L2
L-Lysine 1,6-lactam	128.0950	11.16	C6H12N2O	L2
5,6-Dihydrothymine	128.0586	10.61	C5H8N2O2	L2
2,3,4,5-Tetrahydropyridine-2-carboxylate	127.0633	8.42	C6H9NO2	L2
5-Methylcytosine	125.0589	7.35	C5H7N3O	L2
Taurine	125.0147	11.25	C2H7NO3S	L1
[FA (8:2)]	124.0888	4.70	C8H12O	L2
L-Cysteine	121.0198	21.07	C3H7NO2S	L2
D-Erythrose	120.0423	7.38	C4H8O4	L2
L-Threonine	119.0583	10.54	C4H9NO3	L1
L-Valine	117.0790	8.74	C5H11NO2	L2
Indole	117.0578	8.04	C8H7N	L2
Guanidinoacetate	117.0538	11.49	C3H7N3O2	L1
L-2-Amino-3-oxobutanoic acid	117.0426	7.49	C4H7NO3	L2
3-Methyl-2-oxobutanoic acid	116.0473	8.05	C5H8O3	L2
L-Proline	115.0633	9.65	C5H9NO2	L1
2-Hydroxy-2,4-pentadienoate	114.0317	11.04	C5H6O3	L2
Creatinine	113.0590	8.21	C4H7N3O	L1
Uracil	112.0273	7.81	C4H4N2O2	L1
Hypotaurine	109.0198	10.91	C2H7NO2S	L2
L-Serine	105.0427	11.25	C3H7NO3	L1
4-Aminobutanoate	103.0633	10.90	C4H9NO2	L2
Pentanoate	102.0680	4.46	C5H10O2	L2
Acetoacetate	102.0316	7.27	C4H6O3	L2
Orthophosphate	97.9769	10.95	H3O4P	L2
Glyceraldehyde	90.0318	7.33	C3H6O3	L2
L-Alanine	89.0477	10.76	C3H7NO2	L1
Putrescine	88.1001	23.94	C4H12N2	L2
N,N'-Dimethylurea	88.0637	6.50	C3H8N2O	L2
Pyruvate	88.0161	7.29	C3H4O3	L2
[FA (4:0)]	86.0368	11.97	C4H6O2	L2
3-Butynoate	84.0210	8.35	C4H4O2	L2
Trimethylamine N-oxide	75.0685	8.43	C3H9NO	L2
Glycine	75.0321	11.26	C2H5NO2	L1

Table A4: A list of total identified metabolites in plasticity experiment.

Putative metabolite	Mass	RT	FORMULA	confidence
Phenylacetylglycine	193.0739	5.14	C10H11NO3	L1
L-Kynurenine	208.0849	8.95	C10H12N2O3	L1
Inosine	268.0808	9.15	C10H12N4O5	L1
3',5'-Cyclic AMP	329.0526	7.78	C10H12N5O6P	L1
IMP	348.0469	10.80	C10H13N4O8P	L1
Deoxyadenosine	251.1018	7.26	C10H13N5O3	L1
Adenosine	267.0968	7.96	C10H13N5O4	L1
L-Tyrosine methyl ester	195.0895	5.15	C10H13NO3	L2
(1-Ribosylimidazole)-4-acetate	258.0852	9.64	C10H14N2O6	L2
AMP	347.0631	9.72	C10H14N5O7P	L1
GMP	363.0579	11.54	C10H14N5O8P	L1
ADP	427.0295	10.73	C10H15N5O10P2	L1
Biotin	244.0882	7.22	C10H16N2O3S	L1
ATP	506.9960	11.65	C10H16N5O13P3	L2
Glutathione	307.0838	10.08	C10H17N3O6S	L1
2-Amino-9,10-epoxy-8-oxodecanoic acid	215.1160	4.76	C10H17NO4	L2
N-(L-Arginino)succinate	290.1226	11.30	C10H18N4O6	L2
10-Oxodecanoate	186.1256	4.59	C10H18O3	L2
[FA (10:0/2:0)] Decanedioic acid	202.1205	4.21	C10H18O4	L2
3-Hydroxysebacicacid	218.1154	4.69	C10H18O5	L2
Propanoylcarnitine	217.1314	7.94	C10H19NO4	L2
10-Hydroxydecanoic acid	188.1412	4.12	C10H20O3	L2
[FA amino(10:0)]	187.1572	4.89	C10H21NO2	L2
[PC acety] 1-acetyl-sn-glycero-3-phosphocholine	299.1134	7.27	C10H22NO7P	L2
Indole-3-acetaldehyde	159.0684	5.57	C10H9NO	L2
5-Hydroxyindoleacetaldehyde	175.0633	4.25	C10H9NO2	L2
5-Hydroxyindoleacetate	191.0583	7.09	C10H9NO3	L2
Indolelactate	205.0739	7.20	C11H11NO3	L2
L-Tryptophan	204.0900	9.63	C11H12N2O2	L1
5-Hydroxy-L-tryptophan	220.0847	8.05	C11H12N2O3	L2
L-Formylkynurenine	236.0797	8.11	C11H12N2O4	L2
N-Ribosylnicotinamide	254.0902	19.99	C11H14N2O5	L2
5'-Methylthioadenosine	297.0896	7.18	C11H15N5O3S	L1
N-Heptanoylhomoserine lactone	213.1363	7.14	C11H19NO3	L2
CDP-ethanolamine	446.0602	11.18	C11H20N4O11P2	L2
Butanoylcarnitine	231.1470	7.40	C11H21NO4	L1
N-Acetylserotonin	218.1055	5.08	C12H14N2O2	L2
[FA (12:5)]	190.0995	4.25	C12H14O2	L2
[FA (12:4/2:0)]	222.0893	4.24	C12H14O4	L2
Thiamin	264.1045	21.09	C12H16N4OS	L2
Thiamin monophosphate	344.0710	9.55	C12H17N4O4PS	L2
[FA (12:3)]	180.1514	4.17	C12H20O	L2
Dodecanedioic acid	230.1518	4.20	C12H22O4	L2
3-Hydroxydodecanedioicacid	246.1466	4.39	C12H22O5	L2
(R)-S-Lactoylglutathione	379.1047	9.04	C13H21N3O8S	L2
S-glutathionyl-L-cysteine	426.0880	11.21	C13H22N4O8S2	L2
S-Adenosyl-L-homocysteine	384.1217	9.82	C14H20N6O5S	L1
CDP-choline	488.1076	10.38	C14H26N4O11P2	L2
[SP (14:0/2:0)]	241.2041	4.38	C14H27NO2	L2
[SP (14:0)]	229.2406	4.77	C14H31NO	L2
S-Adenosyl-L-methionine	398.1375	11.54	C15H22N6O5S	L2
UDP-glucose	566.0545	11.30	C15H24N2O17P2	L1

[FA oxo(16:0)]	270.2195	3.88	C16H30O3	L2
Palmitoleamide	253.2405	4.36	C16H31NO	L2
Hexadecanal	240.2454	4.19	C16H32O	L2
Hexadecanoic acid	256.2404	3.92	C16H32O2	L2
[FA amino(16:0)]	271.2510	4.38	C16H33NO2	L2
UDP-N-acetyl-D-glucosamine	607.0811	10.49	C17H27N3O17P2	L2
[FA hydroxy(18:2)]	296.2352	3.91	C18H32O3	L2
[FA (18:2)]	312.2298	3.97	C18H32O4	L2
[FA (18:1)]	282.2559	3.88	C18H34O2	L2
2-Oxooctadecanoic acid	298.2508	3.88	C18H34O3	L2
[FA hydroxy(18:1)]	314.2460	3.91	C18H34O4	L2
[FA trihydroxy(18:1)]octadecenoic acid	330.2411	4.00	C18H34O5	L2
[FA hydroxy(18:0)]	346.2355	4.30	C18H34O6	L2
[FA (16:0)]	313.2616	4.31	C18H35NO3	L2
4-8dimethylnonanoylcarnitine	329.2566	4.20	C18H35NO4	L2
Octadecanoic acid	284.2716	4.07	C18H36O2	L1
[FA hydroxy(18:0)]	300.2663	3.90	C18H36O3	L2
Octadecanamide	283.2874	4.26	C18H37NO	L2
[FA (16:2)]	299.2824	5.37	C18H37NO2	L2
[SP] Sphing-4-enine-1-phosphate	379.2487	4.82	C18H38NO5P	L2
Sphinganine	301.2981	7.14	C18H39NO2	L2
Folate	441.1397	11.44	C19H19N7O6	L1
[FA methyl(18:0)]	296.2710	3.87	C19H36O2	L2
[GL (16:0)]	330.2770	4.20	C19H38O4	L2
[GP (16:0)]	410.2432	4.55	C19H39O7P	L2
PA(O-16:0/0:0)	396.2638	4.58	C19H41O6P	L2
deacetylcolchicine	357.1570	11.05	C20H23NO5	L2
[FA (20:5)]	302.2247	3.96	C20H30O2	L2
CMP-N-acetylneuraminate	614.1463	10.47	C20H31N4O16P	L2
Glutathione disulfide	612.1520	11.28	C20H32N6O12S2	L1
[FA (20:4)]	304.2402	3.87	C20H32O2	L2
Icosatrienoic acid	306.2555	3.88	C20H34O2	L2
Icosadienoic acid	308.2711	3.87	C20H36O2	L2
[FA (18:2)]	323.2825	4.20	C20H37NO2	L2
[FA (20:0)]-eicosenoic acid	310.2874	3.85	C20H38O2	L2
[FA (20:0/2:0)]	342.2769	3.82	C20H38O4	L2
[FA (18:0)]	325.2981	4.17	C20H39NO2	L2
[FA (18:0)]	341.2930	4.22	C20H39NO3	L2
N-palmitoyl threonine	357.2882	4.17	C20H39NO4	L2
[FA (20:0)] eicosanoic acid	312.3029	3.87	C20H40O2	L2
NAD+	663.1090	9.74	C21H27N7O14P2	L1
NADP+	743.0754	11.15	C21H28N7O17P3	L1
NADH	665.1253	9.55	C21H29N7O14P2	L1
NADPH	745.0909	11.57	C21H30N7O17P3	L1
CoA	767.1144	9.60	C21H36N7O16P3S	L2
[FA methoxy,trihydrox]-prostadiene	354.2769	4.12	C21H38O4	L2
[GL (18:0)]	358.3083	4.14	C21H42O4	L2
[GP (18:0)]	438.2745	4.44	C21H43O7P	L2
[PE (16:1)]	437.2907	4.45	C21H44NO6P	L2
[PE (16:0)]	453.2854	4.49	C21H44NO7P	L2
[PC methyl(12:2)]	439.3061	4.52	C21H46NO6P	L2
[Fv] 4'-O-Methylxanthohumol	368.1620	4.23	C22H24O5	L2
Docosahexaenoicacid	328.2402	3.86	C22H32O2	L2
[FA (22:4)]	332.2714	3.85	C22H36O2	L2
N-oleoyl asparagine	396.2988	4.07	C22H40N2O4	L2
[FA (20:2)]	351.3137	4.15	C22H41NO2	L2
[FA (20:0)]	353.3295	4.12	C22H43NO2	L2
[FA hydroxy(22:0)]	372.3236	4.11	C22H44O4	L2
[PG (16:0)]	484.2799	3.88	C22H45O9P	L2

[PC (14:1)]	451.3061	4.58	C22H46NO6P	L2
[PC (14:0)]	467.3012	4.67	C22H46NO7P	L2
[PC ethyl(12:2)]	453.3220	4.72	C22H48NO6P	L2
LysoPE(0:0/18:2)	477.2853	4.43	C23H44NO7P	L2
[FA] O-Palmitoyl-R-carnitine	399.3350	4.54	C23H45NO4	L2
[PE (18:1)]	479.3013	4.42	C23H46NO7P	L2
[SP] sphinganine-1-phosphocholine	467.3610	3.87	C23H52N2O5P	L2
[FA (24:6)]	344.1777	4.33	C24H24O2	L2
[ST hydrox] 3alpha,12alpha-Dihydroxy-5beta-chol-6-en-24-oic Acid	390.2771	3.93	C24H38O4	L2
[PS (18:1)]	523.2907	4.08	C24H46NO9P	L2
[FA (24:0)]	366.3496	3.77	C24H46O2	L2
[PG (18:1)]	510.2954	3.86	C24H47O9P	L2
[PC (16:1)]	493.3169	4.61	C24H48NO7P	L2
[PS (18:0)]	525.3064	4.04	C24H48NO9P	L2
Tetracosanoic acid	368.3652	3.75	C24H48O2	L2
[FA hydroxy(24:0)	384.3604	3.74	C24H48O3	L2
[PC (16:0)]	495.3325	4.59	C24H50NO7P	L2
[PC (16:2)]	481.3533	4.60	C24H52NO6P	L2
LysoPE(0:0/20:5)	499.2697	4.41	C25H42NO7P	L2
[PE (20:4)]	501.2854	4.38	C25H44NO7P	L2
LysoPE(0:0/20:3)	503.3015	4.36	C25H46NO7P	L2
Glycodeoxycholate	449.3137	4.29	C26H43NO5	L2
[ST hydrox] N-(3alpha,7alpha-dihydroxy-5beta-cholan-24-oyl)-taurine	499.2966	4.15	C26H45NO6S	L2
[FA (26:0)]	394.3812	3.73	C26H50O2	L2
[FA (26:0)]	396.3967	3.73	C26H52O2	L2
[PC (18:1)]	507.3689	4.48	C26H54NO6P	L2
[PC (18:0)]	523.3642	4.49	C26H54NO7P	L2
LysoPC(O-18:0)	509.3848	4.52	C26H56NO6P	L2
LysoPE(0:0/22:6)	525.2855	4.35	C27H44NO7P	L2
LysoPE(0:0/22:5)	527.3011	4.32	C27H46NO7P	L2
Cholesterolsulfate	466.3113	3.69	C27H46O4S	L2
[PI (18:1)]	598.3115	4.09	C27H51O12P	L2
PG(22:6/0:0)	556.2798	3.84	C28H45O9P	L2
LysoPC(20:4)	543.3324	4.51	C28H50NO7P	L2
LysoPC(20:3)	545.3484	4.49	C28H52NO7P	L2
LysoPC(20:1)	549.3795	4.44	C28H56NO7P	L2
Iminoglycine	73.0164	9.49	C2H3NO2	L2
Glycine	75.0320	11.62	C2H5NO2	L1
Phosphonoacetaldehyde	123.9926	10.21	C2H5O4P	L2
2-Hydroxyethanesulfonate	125.9987	9.01	C2H6O4S	L2
Hypotaurine	109.0198	11.27	C2H7NO2S	L2
Taurine	125.0147	11.45	C2H7NO3S	L1
2-Hydroxyethylphosphonate	126.0082	7.46	C2H7O4P	L2
Ethanolamine phosphate	141.0191	11.11	C2H8NO4P	L1
[PC (22:6)]	567.3324	4.47	C30H50NO7P	L2
LysoPC(22:5)	569.3482	4.45	C30H52NO7P	L2
Cer(d18:2/16:0)	535.4962	3.88	C34H65NO3	L2
[SP (16:0)]	537.5123	3.82	C34H67NO3	L2
PA(32:1)	646.4574	3.69	C35H67O8P	L2
PA(32:0)	648.4735	3.66	C35H69O8P	L2
PC(28:0)	677.4995	3.97	C36H72NO8P	L2
PC(O-16:0/12:0)	663.5202	3.99	C36H74NO7P	L2
PA(34:2)	672.4732	3.77	C37H69O8P	L2
PA(34:1)	674.4889	3.67	C37H71O8P	L2
PE(14:0/P-18:1)	673.5052	3.87	C37H72NO7P	L2
PE(32:1)	689.4998	3.89	C37H72NO8P	L2
PE(32:0)	691.5155	3.95	C37H74NO8P	L2
SM(d18:1/14:0)	674.5363	4.14	C37H75N2O6P	L2
PS(32:1)	733.4889	3.68	C38H72NO10P	L2

PC(30:1)	703.5150	3.95	C38H74NO8P	L2
PC(14:0/P-16:0)	689.5360	3.96	C38H76NO7P	L2
PC(30:0)	705.5309	3.94	C38H76NO8P	L2
[PC (14:2/16:0)]	691.5517	3.94	C38H78NO7P	L2
PE(34:2)	715.5144	3.88	C39H74NO8P	L2
PE(16:0/P-18:1)	701.5361	3.83	C39H76NO7P	L2
PE(34:1)	717.5310	3.91	C39H76NO8P	L2
SM(d16:1/18:1)	700.5514	4.06	C39H77N2O6P	L2
[SP (16:0)]	702.5675	4.01	C39H79N2O6P	L2
N-Methylethanolamine phosphate	155.0348	10.38	C3H10NO4P	L2
Oxalureate	132.0171	8.67	C3H4N2O4	L2
2-Aminoacrylate	87.0320	11.37	C3H5NO2	L2
Phosphoenolpyruvate	167.9824	12.27	C3H5O6P	L2
L-Lactate	90.0317	7.79	C3H6O3	L1
Guanidinoacetate	117.0538	11.88	C3H7N3O2	L1
L-Alanine	89.0477	11.08	C3H7NO2	L1
L-Serine	105.0426	11.55	C3H7NO3	L1
Propanoyl phosphate	154.0031	9.09	C3H7O5P	L2
D-Glyceraldehyde 3-phosphate	169.9980	11.37	C3H7O6P	L2
3-Phospho-D-glycerate	185.9929	11.85	C3H7O7P	L2
sn-Glycerol 3-phosphate	172.0137	10.23	C3H9O6P	L1
PS(34:2)	759.5048	3.68	C40H74NO10P	L2
PG(34:2)	746.5098	3.63	C40H75O10P	L2
PS(34:1)	761.5202	3.67	C40H76NO10P	L2
PC(32:2)	729.5309	3.94	C40H76NO8P	L2
Cer(d18:1/22:1)	619.5901	3.84	C40H77NO3	L2
PG(34:1)	748.5251	3.63	C40H77O10P	L2
PS(34:0)	763.5364	3.63	C40H78NO10P	L2
PC(32:1)	731.5463	3.93	C40H78NO8P	L2
[GP (16:0/18:0)]	414.2465	4.55	C40H78O13P2	L2
PC(32:0)	733.5625	3.92	C40H80NO8P	L2
[PC (14:2/18:0)]	719.5835	3.92	C40H82NO7P	L2
PE(18:4/P-18:1)	721.5044	3.81	C41H72NO7P	L2
PE(18:3/P-18:1)	723.5203	3.80	C41H74NO7P	L2
PE(36:4)	739.5157	3.82	C41H74NO8P	L2
PI(32:1)	808.5087	3.69	C41H77O13P	L2
PE(36:2)	743.5472	3.89	C41H78NO8P	L2
[PE (18:1/18:1)]	729.5678	3.90	C41H80NO7P	L2
PE(36:1)	745.5625	3.91	C41H80NO8P	L2
SM(d18:1/18:1)	728.5823	4.01	C41H81N2O6P	L2
PS(36:3)	785.5207	3.67	C42H76NO10P	L2
PC(34:4)	753.5314	3.93	C42H76NO8P	L2
PS(36:2)	787.5362	3.66	C42H78NO10P	L2
PG(36:2)	774.5410	3.62	C42H79O10P	L2
PS(36:1)	789.5520	3.66	C42H80NO10P	L2
PC(34:2)	757.5619	3.91	C42H80NO8P	L2
[SP (24:0)]	647.6217	3.85	C42H81NO3	L2
PG(36:1)	776.5582	3.64	C42H81O10P	L2
PS(36:0)	791.5672	3.62	C42H82NO10P	L2
PC(34:1)	759.5776	3.90	C42H82NO8P	L2
Ceramide (d18:1/16:0)	649.6386	3.88	C42H83NO3	L2
PC(16:0/P-18:0)	745.5985	3.90	C42H84NO7P	L2
PA(18:4/22:6)	370.2202	4.63	C43H65O8P	L2
[PE (16:1/22:6)]	747.5203	3.80	C43H74NO7P	L2
PE(20:4/P-18:1)	749.5360	3.79	C43H76NO7P	L2
PE(38:5)	765.5321	3.79	C43H76NO8P	L2
[PE (18:1/20:4)]	751.5519	3.79	C43H78NO7P	L2
PE(38:4)	767.5477	3.82	C43H78NO8P	L2
PI(34:2)	834.5251	3.68	C43H79O13P	L2

PI(34:1)	836.5409	3.66	C43H81O13P	L2
[GP (18:0/18:0)]	803.5675	3.78	C43H82NO10P	L2
PE(38:2)	771.5777	3.90	C43H82NO8P	L2
PE(38:1)	773.5939	3.89	C43H84NO8P	L2
PS(38:5)	809.5203	3.67	C44H76NO10P	L2
PS(38:4)	811.5359	3.64	C44H78NO10P	L2
PC(36:5)	779.5467	3.91	C44H78NO8P	L2
PS(38:3)	813.5520	3.66	C44H80NO10P	L2
PC(36:4)	781.5620	3.90	C44H80NO8P	L2
PG(38:3)	800.5576	3.61	C44H81O10P	L2
PC(36:3)	783.5778	3.89	C44H82NO8P	L2
PC(36:2)	785.5932	3.88	C44H84NO8P	L2
[PC (18:1/18:0)]	771.6144	3.89	C44H86NO7P	L2
PC(36:1)	787.6089	3.88	C44H86NO8P	L2
PC(18:0/P-18:0)	773.6299	3.89	C44H88NO7P	L2
PI(36:5)	856.5101	3.68	C45H77O13P	L2
[PE (18:1/22:6)]	775.5523	3.78	C45H78NO7P	L2
PI(36:4)	858.5261	3.68	C45H79O13P	L2
PE(22:4/P-18:1)	777.5676	3.82	C45H80NO7P	L2
PI(36:3)	860.5418	3.68	C45H81O13P	L2
PG(17:1/22:2)	407.2858	4.03	C45H83O10P	L2
PI(36:2)	862.5575	3.67	C45H83O13P	L2
PI(36:1)	864.5716	3.67	C45H85O13P	L2
[PI (18:0/18:0)]	879.5840	3.68	C45H86NO13P	L2
PS(40:6)	835.5361	3.65	C46H78NO10P	L2
PS(40:5)	837.5520	3.62	C46H80NO10P	L2
PS(40:4)	839.5678	3.65	C46H82NO10P	L2
PC(20:4/P-18:1)	791.5827	3.87	C46H82NO7P	L2
PC(38:5)	807.5787	3.87	C46H82NO8P	L2
[PC (18:1/20:4)]	793.5987	3.87	C46H84NO7P	L2
PC(38:4)	809.5936	3.86	C46H84NO8P	L2
PC(38:3)	811.6091	3.86	C46H86NO8P	L2
PC(20:1(11Z)/P-18:1(11Z))	797.6297	3.87	C46H88NO7P	L2
PC(38:2)	813.6250	3.86	C46H88NO8P	L2
PC(20:0/P-18:0)	801.6616	3.89	C46H92NO7P	L2
PI(38:6)	882.5268	3.67	C47H79O13P	L2
PI(38:5)	884.5418	3.66	C47H81O13P	L2
PI(38:4)	886.5575	3.66	C47H83O13P	L2
PI(38:3)	888.5722	3.66	C47H85O13P	L2
SM(d18:2/24:1)	810.6624	3.94	C47H91N2O6P	L2
SM(d18:1/24:1)	812.6769	3.93	C47H93N2O6P	L2
SM(d18:0/24:1)	814.6915	3.94	C47H95N2O6P	L2
PG(42:10)	842.5098	3.60	C48H75O10P	L2
PC(40:6)	833.5938	3.85	C48H84NO8P	L2
PC(22:4/P-18:1)	819.6146	3.85	C48H86NO7P	L2
PC(40:5)	835.6097	3.85	C48H86NO8P	L2
PC(22:4/P-18:0)	821.6300	3.85	C48H88NO7P	L2
PC(40:4)	837.6241	3.86	C48H88NO8P	L2
PC(22:2/P-18:1)	823.6461	3.85	C48H90NO7P	L2
Phosphocreatine	211.0359	10.57	C4H10N3O5P	L2
Diethanolamine	105.0789	15.36	C4H11NO2	L2
Phosphodimethylethanolamine	169.0504	9.74	C4H12NO4P	L2
3-Butynoate	84.0211	8.54	C4H4O2	L2
Cytosine	111.0433	9.76	C4H5N3O	L1
Iminoaspartate	131.0218	8.40	C4H5NO4	L2
Allantoin	158.0439	11.59	C4H6N4O3	L2
Acetoacetate	102.0317	5.16	C4H6O3	L2
L-Malate	134.0215	11.50	C4H6O5	L2
Creatinine	113.0589	8.50	C4H7N3O	L1

L-Aspartate	133.0375	10.80	C4H7NO4	L1
L-Asparagine	132.0535	11.21	C4H8N2O3	L1
Allantoate	176.0545	11.14	C4H8N4O4	L2
Butanoic acid	88.0524	5.15	C4H8O2	L2
(R)-3-Hydroxybutanoate	104.0474	7.15	C4H8O3	L2
D-Erythrose	120.0423	11.23	C4H8O4	L2
[FA trihydroxy(4:0)]	136.0372	9.37	C4H8O5	L2
Creatine	131.0695	11.00	C4H9N3O2	L1
L-Threonine	119.0583	10.77	C4H9NO3	L1
Erythrulose 1-phosphate	200.0086	9.40	C4H9O7P	L2
PG(22:6/22:6)	866.5102	3.59	C50H75O10P	L2
L-Glutamine	146.0691	11.03	C5H10N2O3	L1
Deoxyribose	134.0579	7.20	C5H10O4	L2
D-Xylulose	150.0527	9.07	C5H10O5	L2
4-Guanidinobutanoate	145.0851	11.26	C5H11N3O2	L2
L-Valine	117.0790	9.67	C5H11NO2	L1
L-Methionine	149.0511	9.18	C5H11NO2S	L1
L-Methionine S-oxide	165.0460	9.84	C5H11NO3S	L2
2-Deoxy-D-ribose 5-phosphate	214.0242	10.31	C5H11O7P	L2
D-Ribose 5-phosphate	230.0189	11.00	C5H11O8P	L1
L-Ornithine	132.0899	15.96	C5H12N2O2	L1
4-Guanidinobutanamide	144.1011	13.85	C5H12N4O	L2
2-C-Methyl-D-erythritol 4-phosphate	216.0401	11.24	C5H13O7P	L2
Choline phosphate	183.0661	10.20	C5H14NO4P	L1
sn-glycero-3-Phosphoethanolamine	215.0559	11.04	C5H14NO6P	L2
Orotate	156.0171	8.51	C5H4N2O4	L2
Hypoxanthine	136.0385	8.99	C5H4N4O	L1
Xanthine	152.0334	9.38	C5H4N4O2	L1
Urate	168.0283	9.97	C5H4N4O3	L1
Adenine	135.0545	8.35	C5H5N5	L1
Guanine	151.0495	10.44	C5H5N5O	L1
Imidazole-4-acetate	126.0431	9.01	C5H6N2O2	L1
(S)-Dihydroorotate	158.0327	8.89	C5H6N2O4	L2
2-Hydroxy-2,4-pentadienoate	114.0317	11.25	C5H6O3	L2
Itaconate	130.0267	8.29	C5H6O4	L2
2-Oxoglutarate	146.0215	11.38	C5H6O5	L2
4-Hydroxy-2-oxoglutarate	162.0165	9.29	C5H6O6	L2
5-Methylcytosine	125.0589	8.57	C5H7N3O	L2
L-1-Pyrroline-5-carboxylate	113.0477	11.08	C5H7NO2	L2
L-1-Pyrroline-3-hydroxy-5-carboxylate	129.0427	8.04	C5H7NO3	L2
2-Oxoglutaramate	145.0375	8.43	C5H7NO4	L2
5,6-Dihydrothymine	128.0586	10.91	C5H8N2O2	L2
N-Carbamoyl-L-aspartate	176.0433	11.76	C5H8N2O5	L2
3-Methylbut-2-enal	84.0575	4.26	C5H8O	L2
5-Oxopentanoate	116.0474	5.12	C5H8O3	L2
D-Xylonolactone	148.0372	10.97	C5H8O5	L2
L-Proline	115.0634	9.96	C5H9NO2	L1
L-Glutamate 5-semialdehyde	131.0585	10.86	C5H9NO3	L2
L-Glutamate	147.0531	10.51	C5H9NO4	L1
4-Methylene-L-glutamine	158.0691	8.19	C6H10N2O3	L2
N-Formimino-L-glutamate	174.0641	8.70	C6H10N2O4	L2
N-Carbamyl-L-glutamate	190.0590	11.27	C6H10N2O5	L2
(S)-3-Methyl-2-oxopentanoic acid	130.0631	4.87	C6H10O3	L2
1,2-Dihydroxy-5-(methylthio)pent-1-en-3-one	162.0350	7.21	C6H10O3S	L2
2-Dehydro-3-deoxy-L-rhamnonate	162.0528	10.28	C6H10O5	L2
D-Glucono-1,5-lactone	178.0477	11.03	C6H10O6	L2
D-Glucuronate	194.0426	11.50	C6H10O7	L2
5-Guanidino-2-oxopentanoate	173.0801	11.09	C6H11N3O3	L2
4-Acetamidobutanoate	145.0739	5.70	C6H11NO3	L2

N-Formyl-L-methionine	177.0460	5.17	C6H11NO3S	L2
O-Acetyl-L-homoserine	161.0688	7.42	C6H11NO4	L2
L-Lysine 1,6-lactam	128.0949	11.32	C6H12N2O	L2
D-Alanyl-D-alanine	160.0848	7.20	C6H12N2O3	L2
L-Cystine	240.0241	11.13	C6H12N2O4S2	L1
5-Methylthio-D-ribose	180.0457	8.05	C6H12O4S	L2
L-Rhamnulose	164.0685	9.21	C6H12O5	L2
myo-Inositol	180.0634	12.25	C6H12O6	L1
D-Gluconic acid	196.0583	10.17	C6H12O7	L1
L-Citrulline	175.0957	11.38	C6H13N3O3	L1
L-Leucine	131.0947	9.02	C6H13NO2	L1
D-Galactosamine	179.0794	8.94	C6H13NO5	L2
L-Fucose 1-phosphate	244.0347	9.68	C6H13O8P	L2
D-Glucose 6-phosphate	260.0298	11.60	C6H13O9P	L1
L-Lysine	146.1055	16.99	C6H14N2O2	L2
L-Arginine	174.1117	18.31	C6H14N4O2	L1
D-Glucosamine 6-phosphate	259.0457	10.78	C6H14NO8P	L1
D-Sorbitol	182.0791	10.65	C6H14O6	L2
Triethanolamine	149.1052	8.24	C6H15NO3	L2
Nicotinate	123.0321	5.52	C6H5NO2	L2
Nicotinamide	122.0480	7.19	C6H6N2O	L1
Urocanate	138.0429	7.18	C6H6N2O2	L2
Methylimidazoleacetic acid	140.0586	7.59	C6H8N2O2	L2
4-Imidazolone-5-propanoate	156.0535	8.73	C6H8N2O3	L2
(4E)-2-Oxohexenoic acid	128.0473	5.10	C6H8O3	L2
2,3-Dimethylmaleate	144.0422	11.27	C6H8O4	L2
Citrate	192.0270	12.50	C6H8O7	L1
L-Histidine	155.0695	11.22	C6H9N3O2	L1
N-Acetyl-L-aspartate	175.0481	10.52	C6H9NO5	L2
(2S,3R)-3-Hydroxybutane-1,2,3-tricarboxylate	206.0425	9.92	C7H10O7	L2
4-(beta-Acetylaminoethyl)imidazole	153.0903	9.48	C7H11N3O	L2
N(pi)-Methyl-L-histidine	169.0851	9.65	C7H11N3O2	L1
N-Acetyl-L-glutamate 5-semialdehyde	173.0688	7.39	C7H11NO4	L2
N-Acetyl-L-glutamate	189.0637	10.18	C7H11NO5	L2
(2S)-2-Isopropylmalate	176.0684	9.97	C7H12O5	L2
5-Acetamidopentanoate	159.0895	7.32	C7H13NO3	L2
L-Cystathionine	222.0673	11.65	C7H14N2O4S	L1
Sedoheptulose	210.0739	10.87	C7H14O7	L2
4-Trimethylammoniobutanoate	145.1103	9.79	C7H15NO2	L1
L-Carnitine	161.1052	9.83	C7H15NO3	L1
D-Sedoheptulose 7-phosphate	290.0403	11.29	C7H15O10P	L2
N6-Methyl-L-lysine	160.1211	16.41	C7H16N2O2	L1
Spermidine	145.1579	18.27	C7H19N3	L2
Pyridine-2,3-dicarboxylate	167.0219	11.14	C7H5NO4	L2
4-Hydroxybenzoate	138.0317	5.14	C7H6O3	L2
2-(Acetamidomethylene)succinate	187.0481	8.51	C7H9NO5	L2
3,4-Dihydroxyphenylethyleneglycol	170.0579	5.18	C8H10O4	L2
Pyridoxine	169.0739	7.37	C8H11NO3	L1
Dihydroclavaminic acid	200.0796	8.29	C8H12N2O4	L2
[FA (8:2)]	124.0888	4.17	C8H12O	L2
[FA dioxo(8:0)]	172.0735	8.42	C8H12O4	L2
N2-Acetyl-L-aminoadipate	203.0794	9.02	C8H13NO5	L2
O-Succinyl-L-homoserine	219.0743	7.96	C8H13NO6	L2
[FA (8:1)]	142.0994	4.38	C8H14O2	L2
N-Acetyl-L-citrulline	217.1062	8.62	C8H15N3O4	L2
N-Acetyl-D-glucosamine	221.0900	9.54	C8H15NO6	L1
3-methyl-1-heptene	112.1252	3.95	C8H16	L2
N6-Acetyl-N6-hydroxy-L-lysine	204.1109	10.61	C8H16N2O4	L2
N-Acetyl-D-glucosamine 6-phosphate	301.0561	10.33	C8H16NO9P	L2

sn-glycero-3-Phosphocholine	257.1030	10.23	C8H20NO6P	L1
Indole	117.0578	4.21	C8H7N	L2
Formylanthranilate	165.0426	5.12	C8H7NO3	L2
Phenylacetic acid	136.0525	5.14	C8H8O2	L2
Phenylpropanoate	150.0680	4.86	C9H10O2	L2
3-(4-Hydroxyphenyl)lactate	182.0579	7.78	C9H10O4	L2
D-Phenylalanine	165.0790	8.19	C9H11NO2	L2
L-Tyrosine	181.0740	10.34	C9H11NO3	L1
3,4-Dihydroxy-L-phenylalanine	197.0689	11.50	C9H11NO4	L2
Uridine	244.0695	8.72	C9H12N2O6	L1
UMP	324.0357	10.57	C9H13N2O9P	L1
Deoxycytidine	227.0907	8.10	C9H13N3O4	L2
Cytidine	243.0855	9.76	C9H13N3O5	L1
UDP	404.0023	11.31	C9H14N2O12P2	L2
CMP	323.0517	10.45	C9H14N3O8P	L1
CDP	403.0181	11.73	C9H15N3O11P2	L1
N2-Succinyl-L-ornithine	232.1059	9.75	C9H16N2O5	L2
9-Oxononanoic acid	172.1099	4.78	C9H16O3	L2
8-Amino-7-oxononanoate	187.1209	5.14	C9H17NO3	L2
O-Acetylcarnitine	203.1158	8.54	C9H17NO4	L1
N2-(D-1-Carboxyethyl)-L-lysine	218.1266	10.46	C9H18N2O4	L2
N2-(D-1-Carboxyethyl)-L-arginine	246.1329	10.48	C9H18N4O4	L2
gamma-L-Glutamylputrescine	217.1423	11.31	C9H19N3O3	L2
beta-Alanyl-L-arginine	245.1489	11.12	C9H19N5O3	L2
Pantothenol	205.1314	7.16	C9H19NO4	L2
N6,N6,N6-Trimethyl-L-lysine	188.1525	15.36	C9H20N2O2	L2
3-Hydroxy-N6,N6,N6-trimethyl-L-lysine	204.1474	13.85	C9H20N2O3	L2
Phenylpyruvate	164.0474	4.90	C9H8O3	L1
3-(4-Hydroxyphenyl)pyruvate	180.0423	7.36	C9H8O4	L1
Carbamoyl phosphate	140.9828	16.37	CH4NO5P	L2
Hydroxymethylphosphonate	111.9925	10.30	CH5O4P	L2
Sulfate	97.9674	12.68	H2O4S	L2
Orthophosphate	97.9771	11.42	H3O4P	L2

Table A5: A list of total identified metabolites in macrophages in response to challenging with secretome of *P. aeruginosa* and *S. aureus.*

Putative metabolite	Mass	RT	FORMULA	confidence
Phenylacetylglycine	193.0740	4.93	C10H11NO3	L1
4-Hydroxyphenylacetylglycine	209.0688	11.03	C10H11NO4	L2
L-Kynurenine	208.0849	8.73	C10H12N2O3	L1
3-Hydroxy-L-kynurenine	224.0794	8.73	C10H12N2O4	L2
Deoxyinosine	252.0859	8.37	C10H12N4O4	L2
Inosine	268.0808	8.91	C10H12N4O5	L1
IMP	348.0471	10.51	C10H13N4O8P	L1
5'-Deoxyadenosine	251.1017	9.00	C10H13N5O3	L2
Adenosine	267.0968	7.74	C10H13N5O4	L2
Thymidine	242.0904	4.95	C10H14N2O5	L2
(1-Ribosylimidazole)-4-acetate	258.0852	9.42	C10H14N2O6	L2
AMP	347.0631	9.41	C10H14N5O7P	L1
GMP	363.0581	11.27	C10H14N5O8P	L1
dTMP	322.0566	8.97	C10H15N2O8P	L2
ADP	427.0296	10.36	C10H15N5O10P2	L1
Biotin	244.0882	6.97	C10H16N2O3S	L1
ATP	506.9960	11.21	C10H16N5O13P3	L2
[FA (10:1/2:0)]	200.1049	4.70	C10H16O4	L2
Glutathione	307.0839	9.81	C10H17N3O6S	L1
10-Oxodecanoate	186.1256	4.28	C10H18O3	L2
[FA (10:0/2:0)]	202.1206	4.29	C10H18O4	L2
3-Hydroxysebacicacid	218.1155	4.70	C10H18O5	L2
Propanoylcarnitine	217.1314	7.61	C10H19NO4	L2
Decanoic acid	172.1463	3.95	C10H20O2	L2
[FA hydroxy(10:0)]	188.1413	3.65	C10H20O3	L2
Indole-3-acetaldehyde	159.0684	5.87	C10H9NO	L2
5-Hydroxyindoleacetaldehyde	175.0633	4.14	C10H9NO2	L2
5-Hydroxyindoleacetate	191.0583	7.22	C10H9NO3	L2
Indolelactate	205.0739	6.99	C11H11NO3	L2
L-Tryptophan	204.0900	9.38	C11H12N2O2	L1
5-Hydroxy-L-tryptophan	220.0847	7.83	C11H12N2O3	L2
L-Formylkynurenine	236.0797	7.90	C11H12N2O4	L2
N-Acetyl-L-phenylalanine	207.0897	4.71	C11H13NO3	L1
Nicotinate D-ribonucleoside	255.0739	9.93	C11H13NO6	L2
N-Ribosylnicotinamide	254.0902	19.53	C11H14N2O5	L2
5'-Methylthioadenosine	297.0896	6.96	C11H15N5O3S	L1
N-Heptanoylhomoserine lactone	213.1367	4.34	C11H19NO3	L2
N6-(L-1,3-Dicarboxypropyl)-L-lysine	276.1320	10.35	C11H20N2O6	L2
CMP-2-aminoethylphosphonate	430.0654	10.29	C11H20N4O10P2	L2
CDP-ethanolamine	446.0604	10.90	C11H20N4O11P2	L2
5-Hydroxyindolepyruvate	219.0532	6.82	C11H9NO4	L2
N-Acetylserotonin	218.1055	4.98	C12H14N2O2	L2
[FA oxo(12:1)]	212.1413	4.15	C12H20O3	L2
Sucrose	342.1162	10.92	C12H22O11	L1
3-Hydroxydodecanedioicacid	246.1468	4.24	C12H22O5	L2
Lactosamine	341.1324	11.21	C12H23NO10	L2
Dodecanoic acid	200.1777	3.87	C12H24O2	L2
12-Hydroxydodecanoic acid	216.1726	3.85	C12H24O3	L2
[FA amino(12:0)]	215.1886	4.49	C12H25NO2	L2
(R)-S-Lactoylglutathione	379.1051	8.82	C13H21N3O8S	L2
S-glutathionyl-L-cysteine	426.0880	10.91	C13H22N4O8S2	L2

[FA (6:0)]	259.1784	4.98	C13H25NO4	L2
N6-(1,2-Dicarboxyethyl)-AMP	463.0743	11.87	C14H18N5O11P	L2
S-Adenosyl-L-homocysteine	384.1216	9.58	C14H20N6O5S	L2
2-(alpha-Hydroxyethyl)thiamine diphosphate	468.0636	9.26	C14H22N4O8P2S	L2
CMP-N-trimethyl-2-aminoethylphosphonate	472.1126	9.56	C14H26N4O10P2	L2
CDP-choline	488.1074	10.13	C14H26N4O11P2	L2
Tetradecenoic acid	226.1934	3.81	C14H26O2	L2
[FA oxo(14:0)]	242.1885	3.85	C14H26O3	L2
2S-Hydroxytetradecanoic acid	244.2038	3.82	C14H28O3	L2
[SP (14:0)]	229.2406	4.57	C14H31NO	L2
UDP-glucuronate	580.0343	12.47	C15H22N2O18P2	L2
S-Adenosyl-L-methionine	398.1374	11.24	C15H22N6O5S	L2
Phosphoribosyl-AMP	559.0716	10.19	C15H23N5O14P2	L2
UDP-glucose	566.0548	10.99	C15H24N2O17P2	L1
[FA methyl(14:0)]	242.2247	3.82	C15H30O2	L2
GDP-L-fucose	589.0823	11.69	C16H25N5O15P2	L2
Dihydrozeatin-O-glucoside	383.1806	7.82	C16H25N5O6	L2
[FA (16:2)]	252.2089	3.88	C16H28O2	L2
7,8-dichloro-hexadecanoic acid	324.1617	4.32	C16H30Cl2O2	L2
Hexadecenoic acid	254.2247	3.78	C16H30O2	L2
[FA oxo(16:0)]	270.2195	3.81	C16H30O3	L2
Palmitoleamide	253.2406	4.20	C16H31NO	L2
Hexadecanal	240.2455	4.09	C16H32O	L2
Hexadecanoic acid	256.2404	3.97	C16H32O2	L2
[FA amino(16:0)]	271.2511	6.82	C16H33NO2	L2
UDP-N-acetyl-D-glucosamine	607.0814	10.21	C17H27N3O17P2	L2
[FA (18:3)]	278.2243	3.80	C18H30O2	L2
[FA hydroxy(18:2)]	296.2352	3.82	C18H32O3	L2
[FA (18:2)]	312.2298	3.85	C18H32O4	L2
2-Oxooctadecanoic acid	298.2508	3.74	C18H34O3	L2
[FA trihydroxy(18:1)]	330.2406	3.96	C18H34O5	L2
[SP (2:0)]	297.2668	4.17	C18H35NO2	L2
[FA (16:0)]	313.2619	4.18	C18H35NO3	L2
4-8dimethylnonanoylcarnitine	329.2568	4.13	C18H35NO4	L2
[FA (16:2)]	299.2825	5.37	C18H37NO2	L2
[SP hydrox] 6-hydroxysphing-4E-enine	315.2773	4.22	C18H37NO3	L2
[SP] Sphing-4-enine-1-phosphate	379.2489	4.63	C18H38NO5P	L2
Sphinganine	301.2980	6.91	C18H39NO2	L2
Folate	441.1398	11.15	C19H19N7O6	L1
17beta-Hydroxyandrostan-3-one	290.2247	4.21	C19H30O2	L2
[FA methoxy,hydroxy(18:2)]	326.2458	4.06	C19H34O4	L2
[FA methyl(18:0)]	296.2714	3.77	C19H36O2	L2
Nonadecanoicacid	298.2873	3.94	C19H38O2	L2
[GL (16:0)]	330.2771	4.06	C19H38O4	L2
[GP (16:0)]	410.2437	4.40	C19H39O7P	L2
deacetylcolchicine	357.1570	10.79	C20H23NO5	L2
[FA (20:5)]	302.2246	3.91	C20H30O2	L2
CMP-N-acetylneuraminate	614.1463	10.19	C20H31N4O16P	L2
Glutathione disulfide	306.0760	11.05	C20H32N6O12S2	L1
[FA (20:4)]	304.2404	3.79	C20H32O2	L2
Icosadienoic acid	308.2716	3.76	C20H36O2	L2
[FA (18:2)]	323.2826	4.11	C20H37NO2	L2
[FA (20:0)]	310.2873	3.75	C20H38O2	L2
[FA hydroxy(18:0)]	358.2720	3.66	C20H38O5	L2
[FA (18:0)]	325.2982	4.07	C20H39NO2	L2
[PC acetyl(10:2)]	439.2697	4.64	C20H42NO7P	L2
Chelirubine	361.0946	9.03	C21H15NO5	L2
Dihydrochelirubine	363.1103	8.76	C21H17NO5	L2
NAD+	663.1089	9.45	C21H27N7O14P2	L1

NADH	665.1258	9.30	C21H29N7O14P2	L1
CoA	767.1155	9.35	C21H36N7O16P3S	L2
[GL (18:0)]	358.3084	4.02	C21H42O4	L2
[GP (18:0)]	438.2752	4.36	C21H43O7P	L2
[PE (16:1)]	437.2907	4.30	C21H44NO6P	L2
[PE (16:0)]	453.2856	4.36	C21H44NO7P	L2
[PC methyl(12:2)]	439.3064	4.40	C21H46NO6P	L2
Docosahexaenoicacid	328.2403	3.75	C22H32O2	L2
[FA (22:4)]	332.2715	3.75	C22H36O2	L2
N-oleoyl threonine	383.3038	3.65	C22H41NO4	L2
[FA (22:0)]	338.3186	3.70	C22H42O2	L2
[PC (14:1)]	465.2855	4.52	C22H44NO7P	L2
Docosanoic acid	340.3341	3.93	C22H44O2	L2
[FA hydroxy(22:0)]	372.3239	4.00	C22H44O4	L2
[PG (16:0)]	484.2801	3.77	C22H45O9P	L2
[PC (14:1)]	451.3063	4.45	C22H46NO6P	L2
[PC (14:0)]	467.3013	4.50	C22H46NO7P	L2
PI(14:1/0:0)	271.1242	4.01	C23H43O12P	L2
LysoPE(0:0/18:2)	477.2857	4.31	C23H44NO7P	L2
[FA] O-Palmitoyl-R-carnitine	399.3349	4.38	C23H45NO4	L2
[PE (18:1)]	479.3011	4.28	C23H46NO7P	L2
[PC methyl(14:2)]	467.3378	4.38	C23H50NO6P	L2
[FA (24:6)] Tetracosahexaynoic acid	344.1777	4.21	C24H24O2	L2
[PS (18:1)]	523.2911	3.93	C24H46NO9P	L2
[FA (24:0)]	366.3498	3.66	C24H46O2	L2
[FA hydroxy(24:0)]	382.3450	3.64	C24H46O3	L2
[PG (18:1)]	510.2958	3.73	C24H47O9P	L2
[PC (16:1)]	493.3168	4.44	C24H48NO7P	L2
[PS (18:0)]	525.3067	3.93	C24H48NO9P	L2
Tetracosanoic acid	368.3655	3.65	C24H48O2	L2
[FA hydroxy(24:0)]	384.3605	3.64	C24H48O3	L2
[PC (16:1)]	479.3376	4.37	C24H50NO6P	L2
[PC (16:0)]	495.3325	4.39	C24H50NO7P	L2
[PC (16:2)]	481.3533	4.43	C24H52NO6P	L2
Folate	403.3087	3.65	C25H41NO3	L2
LysoPE(0:0/20:5)	499.2699	4.28	C25H42NO7P	L2
[PE (20:4)]	501.2852	4.24	C25H44NO7P	L2
LysoPE(0:0/20:3)	503.3013	4.23	C25H46NO7P	L2
[ST hydrox] N-(3alpha,7alpha-dihydroxy-5beta-cholan-24-oyl)-taurine	499.2973	4.03	C26H45NO6S	L2
[PC (18:2)]	519.3327	4.39	C26H50NO7P	L2
[FA (26:0)]	394.3814	3.63	C26H50O2	L2
[PC acetyl(16:0)]	537.3428	4.47	C26H52NO8P	L2
[PC (18:1)]	507.3689	4.35	C26H54NO6P	L2
[PC (18:0)]	523.3638	4.32	C26H54NO7P	L2
LysoPC(O-18:0)	509.3850	4.35	C26H56NO6P	L2
[ST (4:0/2:0)]	398.3183	4.22	C27H42O2	L2
LysoPE(0:0/22:5)	527.3019	4.15	C27H46NO7P	L2
LysoPE(0:0/22:4)	529.3175	4.19	C27H48NO7P	L2
[PI (18:0)]	600.3278	3.94	C27H53O12P	L2
PG(22:6/0:0)	556.2800	3.71	C28H45O9P	L2
[PC (20:5)]	541.3167	4.37	C28H48NO7P	L2
LysoPC(20:4)	543.3323	4.34	C28H50NO7P	L2
LysoPC(20:3)	545.3483	4.34	C28H52NO7P	L2
LysoPC(20:2)	547.3642	4.30	C28H54NO7P	L2
LysoPC(20:1)	549.3797	4.28	C28H56NO7P	L2
4alpha-Methylzymosterol-4-carboxylate	442.3446	4.08	C29H46O3	L2
[ST (2:0)]	458.3396	4.12	C29H46O4	L2
[PI (20:4)]	620.2963	3.94	C29H49O12P	L2
PI(20:3/0:0)	622.3116	3.94	C29H51O12P	L2

PI(20:1/0:0)	626.3425	4.17	C29H55O12P	L2
Oxalate	89.9953	12.26	C2H2O4	L1
Iminoglycine	73.0164	10.97	C2H3NO2	L2
Sulfoacetate	139.9779	12.54	C2H4O5S	L2
Glycine	75.0320	11.38	C2H5NO2	L1
Phosphonoacetaldehyde	123.9927	9.98	C2H5O4P	L2
2-Hydroxyethanesulfonate	125.9987	8.79	C2H6O4S	L2
Hypotaurine	109.0197	10.99	C2H7NO2S	L2
Taurine	125.0147	11.17	C2H7NO3S	L1
Ethanolamine phosphate	141.0191	10.78	C2H8NO4P	L1
[PC (22:6)]	567.3322	4.31	C30H50NO7P	L2
LysoPC(22:5)	569.3483	4.30	C30H52NO7P	L2
LysoPC(22:4)	571.3645	4.28	C30H54NO7P	L2
[FA hydroxy(20:0)]	650.3876	3.77	C32H58O13	L2
Cer(d18:2/14:0)	507.4652	3.84	C32H61NO3	L2
N-(Tetradecanoyl)-sphing-4-enine	509.4809	3.88	C32H63NO3	L2
Cer(d18:2/16:0)	535.4962	3.85	C34H65NO3	L2
[SP (16:0)]	537.5122	3.81	C34H67NO3	L2
[SP (18:0)]	565.5442	3.79	C36H71NO3	L2
PC(28:0)	677.4993	3.89	C36H72NO8P	L2
PC(O-16:0/12:0)	663.5198	3.88	C36H74NO7P	L2
PA(34:1)	674.4888	3.57	C37H71O8P	L2
PE(32:1)	689.4998	3.81	C37H72NO8P	L2
PE(32:0)	691.5152	3.86	C37H74NO8P	L2
SM(d18:1/14:0)	674.5362	3.99	C37H75N2O6P	L2
PS(32:1)	733.4889	3.59	C38H72NO10P	L2
PC(30:1)	703.5149	3.85	C38H74NO8P	L2
PC(14:0/P-16:0)	689.5359	3.86	C38H76NO7P	L2
PC(30:0)	705.5308	3.84	C38H76NO8P	L2
[SP (18:0/14:0)]	688.5521	3.97	C38H77N2O6P	L2
[PC (14:2/16:0)]	691.5516	3.86	C38H78NO7P	L2
PE(34:2)	715.5143	3.79	C39H74NO8P	L2
PE(16:0/P-18:1)	701.5354	3.77	C39H76NO7P	L2
PE(34:1)	717.5307	3.83	C39H76NO8P	L2
SM(d16:1/18:1)	700.5510	3.97	C39H77N2O6P	L2
[PE (16:2/18:1)]	703.5530	3.75	C39H78NO7P	L2
PE(34:0)	719.5469	3.83	C39H78NO8P	L2
[SP (16:0)]	702.5673	3.91	C39H79N2O6P	L2
N-Methylethanolamine phosphate	155.0347	10.13	C3H10NO4P	L2
Oxalureate	132.0171	8.44	C3H4N2O4	L2
Pyruvate	88.0161	6.96	C3H4O3	L1
Phosphoenolpyruvate	167.9823	11.98	C3H5O6P	L1
N-Formiminoglycine	102.0429	8.92	C3H6N2O2	L2
L-Lactate	90.0317	7.54	C3H6O3	L1
Guanidinoacetate	117.0538	11.60	C3H7N3O2	L1
Sarcosine	89.0477	7.00	C3H7NO2	L2
L-Serine	105.0426	11.28	C3H7NO3	L1
L-Cysteate	169.0044	11.19	C3H7NO5S	L1
Propanoyl phosphate	154.0031	8.84	C3H7O5P	L2
D-Glyceraldehyde 3-phosphate	169.9980	11.03	C3H7O6P	L2
3-Phospho-D-glycerate	185.9929	11.60	C3H7O7P	L1
N,N'-Dimethylurea	88.0636	6.94	C3H8N2O	L2
2,3-Bisphospho-D-glycerate	265.9593	11.96	C3H8O10P2	L2
Glycerol	92.0474	8.76	C3H8O3	L1
(R)-1-Aminopropan-2-ol	75.0684	8.41	C3H9NO	L2
sn-Glycerol 3-phosphate	172.0137	9.99	C3H9O6P	L1
PS(34:2)	759.5043	3.58	C40H74NO10P	L2
PG(34:2)	746.5097	3.53	C40H75O10P	L2
PS(34:1)	761.5205	3.57	C40H76NO10P	L2

PC(32:2)	729.5307	3.83	C40H76NO8P	L2
Cer(d18:1/22:1)	619.5904	3.70	C40H77NO3	L2
Glucosylceramide (d18:1/16:0)	699.5659	3.86	C40H77NO8	L2
PG(34:1)	748.5252	3.54	C40H77O10P	L2
PS(34:0)	763.5369	3.54	C40H78NO10P	L2
PC(32:1)	731.5462	3.81	C40H78NO8P	L2
PC(32:0)	733.5615	3.82	C40H80NO8P	L2
[PC (14:2/18:0)]	719.5829	3.83	C40H82NO7P	L2
PE(18:4(/P-18:1)	721.5038	3.71	C41H72NO7P	L2
PE(18:3)/P-18:1)	723.5200	3.70	C41H74NO7P	L2
PE(36:4)	739.5154	3.73	C41H74NO8P	L2
PE(18:2/P-18:1)	725.5365	3.73	C41H76NO7P	L2
PE(36:3)	741.5313	3.73	C41H76NO8P	L2
PE(36:2)	743.5466	3.79	C41H78NO8P	L2
PE(36:1)	745.5622	3.81	C41H80NO8P	L2
SM(d18:1/18:1)	728.5819	3.91	C41H81N2O6P	L2
PS(36:3)	785.5204	3.57	C42H76NO10P	L2
PC(34:4)	753.5309	3.83	C42H76NO8P	L2
PS(36:2)	787.5360	3.57	C42H78NO10P	L2
PC(34:3)	755.5463	3.82	C42H78NO8P	L2
PG(36:2)	774.5408	3.52	C42H79O10P	L2
PS(36:1)	789.5515	3.58	C42H80NO10P	L2
Cer(d18:1/24:0)	647.6224	3.70	C42H81NO3	L2
PG(36:1)	776.5580	3.54	C42H81O10P	L2
PC(34:1)	759.5775	3.79	C42H82NO8P	L2
PS(O-16:0/20:1)	775.5738	3.87	C42H82NO9P	L2
PC(16:0/P-18:0)	745.5984	3.80	C42H84NO7P	L2
[PE (16:1/22:6)]	747.5203	3.68	C43H74NO7P	L2
PE(20:4/P-18:1)	749.5357	3.68	C43H76NO7P	L2
PE(38:5)	765.5315	3.70	C43H76NO8P	L2
[PE (18:1/20:4)]	751.5514	3.71	C43H78NO7P	L2
PE(38:4)	767.5470	3.72	C43H78NO8P	L2
PI(34:2)	834.5251	3.58	C43H79O13P	L2
PI(34:1)	836.5409	3.57	C43H81O13P	L2
PE(38:2)	771.5775	3.79	C43H82NO8P	L2
[PS (18:0/19:0)]	805.5830	3.86	C43H84NO10P	L2
PE(38:1)	773.5937	3.78	C43H84NO8P	L2
PG(38:8)	790.4778	3.54	C44H71O10P	L2
PG(38:7)	792.4936	3.53	C44H73O10P	L2
PS(38:4)	811.5360	3.54	C44H78NO10P	L2
PG(38:4)	798.5415	3.52	C44H79O10P	L2
PS(38:3)	813.5521	3.56	C44H80NO10P	L2
PC(36:4)	781.5619	3.78	C44H80NO8P	L2
PS(38:2)	815.5675	3.61	C44H82NO10P	L2
PC(36:2)	785.5931	3.76	C44H84NO8P	L2
[PC (18:1/18:0)]	771.6141	3.78	C44H86NO7P	L2
PC(36:1)	787.6086	3.76	C44H86NO8P	L2
PC(18:0/P-18:0)	773.6296	3.79	C44H88NO7P	L2
MGDG(18:3/18:4)	772.5114	4.11	C45H72O10	L2
[PE (18:1/22:6)]	775.5520	3.69	C45H78NO7P	L2
PI(36:4)	858.5259	3.57	C45H79O13P	L2
PE(22:4/P-18:1)	777.5677	3.71	C45H80NO7P	L2
PI(36:3)	860.5421	3.57	C45H81O13P	L2
PE(22:4/P-18:0)	779.5827	3.77	C45H82NO7P	L2
PI(36:2)	862.5575	3.57	C45H83O13P	L2
PI(36:1)	864.5719	3.57	C45H85O13P	L2
[PI (18:0/18:0)]	879.5839	3.59	C45H86NO13P	L2
PE(40:2)	799.6096	3.78	C45H86NO8P	L2
[PG (8:0/8:0)]	802.5148	3.52	C46H75O9P	L2

PG(40:7)	820.5256	3.52	C46H77O10P	L2
PS(40:6)	835.5362	3.55	C46H78NO10P	L2
PS(40:5)	837.5520	3.53	C46H80NO10P	L2
PS(40:4)	839.5664	3.61	C46H82NO10P	L2
PC(38:5)	807.5778	3.77	C46H82NO8P	L2
PS(40:3)	841.5825	3.69	C46H84NO10P	L2
[PC (18:1/20:4)]	793.5983	3.76	C46H84NO7P	L2
PC(38:4)	809.5935	3.75	C46H84NO8P	L2
PC(20:2/P-18:1)	795.6138	3.76	C46H86NO7P	L2
PC(38:3)	811.6091	3.76	C46H86NO8P	L2
PC(20:1/P-18:1)	797.6296	3.78	C46H88NO7P	L2
PC(38:2)	813.6249	3.76	C46H88NO8P	L2
DG(44:6)	724.6018	4.03	C47H80O5	L2
PI(38:5)	884.5424	3.56	C47H81O13P	L2
PI(38:4)	886.5582	3.56	C47H83O13P	L2
PI(38:3)	888.5732	3.56	C47H85O13P	L2
SM(d18:2/24:1)	810.6625	3.86	C47H91N2O6P	L2
SM(d18:1/24:1)	812.6767	3.83	C47H93N2O6P	L2
PG(42:9)	844.5254	3.52	C48H77O10P	L2
PG(42:8)	846.5417	3.52	C48H79O10P	L2
PS(42:7)	861.5516	3.53	C48H80NO10P	L2
PC(40:6)	833.5933	3.75	C48H84NO8P	L2
PC(22:4/P-18:1)	819.6152	3.75	C48H86NO7P	L2
PC(40:5)	835.6090	3.75	C48H86NO8P	L2
PC(22:4/P-18:0)	821.6298	3.77	C48H88NO7P	L2
PC(40:4)	837.6245	3.76	C48H88NO8P	L2
PC(22:2/P-18:1)	823.6462	3.76	C48H90NO7P	L2
PC(40:3)	839.6396	3.76	C48H90NO8P	L2
Phosphocreatine	211.0360	10.31	C4H10N3O5P	L2
Diethanolamine	105.0790	15.13	C4H11NO2	L2
Phosphodimethylethanolamine	169.0504	9.46	C4H12NO4P	L2
Pyrimidine	80.0374	8.56	C4H4N2	L2
3-Butynoate	84.0211	10.41	C4H4O2	L2
Cytosine	111.0433	9.44	C4H5N3O	L1
5,6-Dihydrouracil	114.0430	7.87	C4H6N2O2	L2
5-Amino-4-imidazolecarboxyamide	126.0542	9.10	C4H6N4O	L2
Allantoin	158.0440	11.29	C4H6N4O3	L1
Succinate	118.0266	10.66	C4H6O4	L1
L-Malate	134.0216	11.14	C4H6O5	L1
Creatinine	113.0589	10.57	C4H7N3O	L2
L-2-Amino-3-oxobutanoic acid	117.0426	8.09	C4H7NO3	L2
L-Aspartate	133.0375	10.52	C4H7NO4	L1
L-Asparagine	132.0535	10.90	C4H8N2O3	L1
Butanal	72.0575	4.31	C4H8O	L2
Butanoic acid	88.0524	4.94	C4H8O2	L2
3-(Methylthio)propionic acid	120.0245	4.99	C4H8O2S	L2
2-Hydroxybutanoic acid	104.0474	6.94	C4H8O3	L2
D-Erythrose	120.0423	8.26	C4H8O4	L2
[FA trihydroxy(4:0)]	136.0372	9.09	C4H8O5	L2
Creatine	131.0695	10.70	C4H9N3O2	L2
N,N-Dimethylglycine	103.0634	10.11	C4H9NO2	L2
L-Threonine	119.0583	10.49	C4H9NO3	L1
Erythrulose 1-phosphate	200.0086	9.12	C4H9O7P	L2
PG(22:6/22:6)	866.5107	3.51	C50H75O10P	L2
PS(44:10)	883.5362	3.52	C50H78NO10P	L2
PC(42:7)	859.6090	3.74	C50H86NO8P	L2
L-Glutamine	146.0691	10.77	C5H10N2O3	L1
Pentanoate	102.0681	4.93	C5H10O2	L2
5-Hydroxypentanoate	118.0631	6.90	C5H10O3	L2

D-Xylulose	150.0527	8.80	C5H10O5	L2
4-Guanidinobutanoate	145.0851	10.99	C5H11N3O2	L2
5-Aminopentanoate	117.0790	10.94	C5H11NO2	L2
D-Methionine	149.0510	8.93	C5H11NO2S	L2
L-Methionine S-oxide	165.0459	9.57	C5H11NO3S	L2
2-Deoxy-D-ribose 5-phosphate	214.0242	9.99	C5H11O7P	L2
5-Aminopentanamide	116.0950	7.11	C5H12N2O	L2
L-Ornithine	132.0899	15.77	C5H12N2O2	L1
Xylitol	152.0684	9.95	C5H12O5	L2
Choline	103.0997	10.00	C5H13NO	L2
2-C-Methyl-D-erythritol 4-phosphate	216.0400	10.89	C5H13O7P	L2
sn-glycero-3-Phosphoethanolamine	215.0558	10.79	C5H14NO6P	L2
Orotate	156.0171	8.28	C5H4N2O4	L1
Hypoxanthine	136.0384	8.71	C5H4N4O	L1
Xanthine	152.0334	9.12	C5H4N4O2	L1
Urate	168.0283	9.70	C5H4N4O3	L1
Adenine	135.0545	8.19	C5H5N5	L1
Guanine	151.0494	10.17	C5H5N5O	L1
Thymine	126.0430	8.80	C5H6N2O2	L2
(S)-Dihydroorotate	158.0327	8.66	C5H6N2O4	L2
2-Hydroxy-2,4-pentadienoate	114.0318	10.91	C5H6O3	L2
2-Oxoglutarate	146.0215	11.07	C5H6O5	L1
5-Methylcytosine	125.0589	8.48	C5H7N3O	L2
L-1-Pyrroline-5-carboxylate	113.0477	10.82	C5H7NO2	L2
L-1-Pyrroline-3-hydroxy-5-carboxylate	129.0426	7.87	C5H7NO3	L2
5,6-Dihydrothymine	128.0586	8.16	C5H8N2O2	L2
N-Formimino-L-aspartate	160.0483	9.03	C5H8N2O4	L2
N-Carbamoyl-L-aspartate	176.0434	11.50	C5H8N2O5	L2
3-Methyl-2-oxobutanoic acid	116.0474	4.95	C5H8O3	L1
2-Acetolactate	132.0423	10.33	C5H8O4	L2
(R)-2-Hydroxyglutarate	148.0371	10.60	C5H8O5	L1
L-Proline	115.0633	9.68	C5H9NO2	L1
L-Glutamate 5-semialdehyde	131.0584	10.57	C5H9NO3	L2
O-Acetyl-L-serine	147.0531	8.05	C5H9NO4	L2
L-Glutamate	147.0531	10.21	C5H9NO4	L2
4-Methylene-L-glutamine	158.0690	7.92	C6H10N2O3	L2
N-Formimino-L-glutamate	174.0641	8.35	C6H10N2O4	L2
(S)-3-Methyl-2-oxopentanoic acid	130.0631	4.71	C6H10O3	L2
[FA oxo,hydroxy(6:0)]	146.0579	4.82	C6H10O4	L2
2-Dehydro-3-deoxy-L-rhamnonate	162.0528	9.91	C6H10O5	L2
D-Galactono-1,4-lactone	178.0476	6.98	C6H10O6	L2
D-Glucuronate	194.0426	10.71	C6H10O7	L2
D-Glucarate	210.0375	11.69	C6H10O8	L2
5-Guanidino-2-oxopentanoate	173.0800	10.78	C6H11N3O3	L2
4-Acetamidobutanoate	145.0739	5.33	C6H11NO3	L2
N-Formyl-L-methionine	177.0460	4.96	C6H11NO3S	L2
O-Acetyl-L-homoserine	161.0688	7.03	C6H11NO4	L2
4-Hydroxy-4-methylglutamate	177.0637	9.49	C6H11NO5	L2
D-Glucuronate 1-phosphate	274.0090	11.00	C6H11O10P	L2
D-Alanyl-D-alanine	160.0849	7.75	C6H12N2O3	L2
[FA (6:1)]	100.0888	4.42	C6H12O	L2
Hexanoic acid	116.0838	4.57	C6H12O2	L2
L-Rhamnulose	164.0685	8.69	C6H12O5	L2
myo-Inositol	180.0634	11.90	C6H12O6	L1
D-Gluconic acid	196.0582	9.84	C6H12O7	L1
L-Citrulline	175.0958	11.13	C6H13N3O3	L1
L-Leucine	131.0947	8.55	C6H13NO2	L2
D-Glucosamine	179.0794	10.37	C6H13NO5	L1
6-Phospho-D-gluconate	276.0247	11.82	C6H13O10P	L1

L-Fucose 1-phosphate	244.0348	10.35	C6H13O8P	L2
N-Acetylputrescine	130.1106	17.28	C6H14N2O	L1
L-Lysine	146.1055	16.74	C6H14N2O2	L2
L-Arginine	174.1117	18.06	C6H14N4O2	L1
D-Glucosamine 6-phosphate	259.0457	10.53	C6H14NO8P	L1
D-Sorbitol	182.0791	10.39	C6H14O6	L2
Triethanolamine	149.1052	8.04	C6H15NO3	L2
Nicotinate	123.0321	9.86	C6H5NO2	L2
6-Hydroxynicotinate	139.0269	8.35	C6H5NO3	L2
Urocanate	138.0429	8.53	C6H6N2O2	L2
Thiourocanic acid	170.0149	6.99	C6H6N2O2S	L2
7-Methyladenine	149.0702	7.18	C6H7N5	L2
2-Aminophenol	109.0528	6.05	C6H7NO	L2
Methylimidazole acetaldehyde	124.0637	7.42	C6H8N2O	L2
Methylimidazoleacetic acid	140.0586	8.06	C6H8N2O2	L2
4-Imidazolone-5-propanoate	156.0535	8.50	C6H8N2O3	L2
Hydantoin-5-propionate	172.0484	8.52	C6H8N2O4	L2
(4E)-2-Oxohexenoic acid	128.0473	4.88	C6H8O3	L2
2,3-Dimethylmaleate	144.0422	10.48	C6H8O4	L2
Ascorbate	176.0321	10.91	C6H8O6	L1
Citrate	192.0270	12.15	C6H8O7	L1
L-Histidine	155.0694	10.85	C6H9N3O2	L1
N-Acetyl-L-aspartate	175.0480	10.22	C6H9NO5	L2
L-Ascorbate 6-phosphate	255.9984	11.15	C6H9O9P	L2
2-Hydroxybutane-1,2,4-tricarboxylate	206.0426	11.79	C7H10O7	L2
N(pi)-Methyl-L-histidine	169.0851	9.46	C7H11N3O2	L1
N-Acetyl-L-glutamate 5-semialdehyde	173.0689	7.10	C7H11NO4	L2
N-Acetyl-L-glutamate	189.0638	6.96	C7H11NO5	L2
3-Isopropylbut-3-enoic acid	128.0838	4.46	C7H12O2	L2
5-Acetamidopentanoate	159.0896	4.96	C7H13NO3	L2
N-Acetylornithine	174.1005	9.69	C7H14N2O3	L2
2,6-Diaminoheptanedioate	190.0953	16.78	C7H14N2O4	L2
L-Cystathionine	222.0673	11.41	C7H14N2O4S	L1
[FA methyl(6:0)]	130.0994	4.34	C7H14O2	L2
1-O-Methyl-myo-inositol	194.0789	9.97	C7H14O6	L2
Sedoheptulose	210.0739	10.61	C7H14O7	L2
3-Dehydroxycarnitine	145.1102	14.79	C7H15NO2	L2
L-Carnitine	161.1052	9.56	C7H15NO3	L1
D-Sedoheptulose 7-phosphate	290.0403	10.97	C7H15O10P	L2
1-(3-aminopropyl)-4-aminobutanal	144.1263	17.05	C7H16N2O	L2
N6-Methyl-L-lysine	160.1212	16.19	C7H16N2O2	L1
Pyridine-2,3-dicarboxylate	167.0218	10.86	C7H5NO4	L2
Benzoate	122.0368	4.98	C7H6O2	L1
N1-Methyl-4-pyridone-5-carboxamide	152.0585	6.94	C7H8N2O2	L2
3,5-dihydroxyanisole	140.0473	4.86	C7H8O3	L2
2-(Acetamidomethylene)succinate	187.0482	8.28	C7H9NO5	L2
Pyridoxine	169.0739	7.11	C8H11NO3	L2
2-(Hydroxymethyl)-3-(acetamidomethylene)succinate	217.0586	13.16	C8H11NO6	L2
[FA (8:2)]	124.0888	4.21	C8H12O	L2
[FA dioxo(8:0)]	172.0735	8.15	C8H12O4	L2
gamma-Glutamyl-beta-aminopropiononitrile	199.0958	7.77	C8H13N3O3	L2
N-Butyryl-L-homoserine lactone	171.0895	4.93	C8H13NO3	L2
6-Acetamido-2-oxohexanoate	187.0844	4.56	C8H13NO4	L2
N2-Acetyl-L-aminoadipate	203.0793	10.23	C8H13NO5	L2
O-Succinyl-L-homoserine	219.0743	10.63	C8H13NO6	L2
[FA (8:1)] octenoic acid	142.0994	4.86	C8H14O2	L2
[FA oxo(8:0)]	158.0943	4.74	C8H14O3	L2
N-Acetyl-L-citrulline	217.1063	8.54	C8H15N3O4	L2
N-Acetyl-D-glucosamine	221.0900	9.32	C8H15NO6	L1

N6-Acetyl-L-lysine	188.1162	10.41	C8H16N2O3	L2
N6-Acetyl-N6-hydroxy-L-lysine	204.1109	7.09	C8H16N2O4	L2
N-Acetyl-D-glucosamine 6-phosphate	301.0562	10.05	C8H16NO9P	L2
[FA (8:0)] octanoic acid	144.1150	4.14	C8H16O2	L2
sn-glycero-3-Phosphocholine	257.1030	9.96	C8H20NO6P	L2
Formylanthranilate	165.0427	4.93	C8H7NO3	L2
Phenylacetic acid	136.0525	4.92	C8H8O2	L2
3,4-Dihydroxyphenylacetate	168.0422	8.91	C8H8O4	L1
Phenylpropanoate	150.0680	4.71	C9H10O2	L2
3-(3-Hydroxy-phenyl)-propanoic acid	166.0630	4.94	C9H10O3	L2
3-(4-Hydroxyphenyl)lactate	182.0579	7.58	C9H10O4	L2
2',3'-Cyclic UMP	306.0253	8.30	C9H11N2O8P	L2
L-Phenylalanine	165.0790	8.07	C9H11NO2	L2
L-Tyrosine	181.0740	10.04	C9H11NO3	L1
cis-(homo)3aconitate	216.0635	8.76	C9H12O6	L2
UMP	324.0359	10.27	C9H13N2O9P	L1
Deoxycytidine	227.0906	8.07	C9H13N3O4	L2
Cytidine	243.0855	9.53	C9H13N3O5	L1
2-Amino-4-hydroxy-6-(D-erythro-1,2,3-trihydroxypropyl)-7,8-dihydropteridine	255.0967	10.99	C9H13N5O4	L2
N-Succinyl-L-glutamate	247.0693	11.71	C9H13NO7	L2
UDP	404.0022	10.96	C9H14N2O12P2	L2
CMP	323.0517	10.24	C9H14N3O8P	L1
CDP	403.0184	11.39	C9H15N3O11P2	L1
N2-Succinyl-L-ornithine	232.1059	9.03	C9H16N2O5	L2
9-Oxononanoic acid	172.1100	4.58	C9H16O3	L2
8-Amino-7-oxononanoate	187.1209	4.92	C9H17NO3	L2
O-Acetylcarnitine	203.1158	8.31	C9H17NO4	L1
N2-(D-1-Carboxyethyl)-L-lysine	218.1265	12.23	C9H18N2O4	L2
N2-(D-1-Carboxyethyl)-L-arginine	246.1328	11.43	C9H18N4O4	L2
N6,N6,N6-Trimethyl-L-lysine	188.1525	15.12	C9H20N2O2	L2
3-Hydroxy-N6,N6,N6-trimethyl-L-lysine	204.1473	15.06	C9H20N2O3	L2
Phenylpyruvate	164.0474	4.79	C9H8O3	L1
3-(4-Hydroxyphenyl)pyruvate	180.0423	7.05	C9H8O4	L1
3-Methyldioxyindole	163.0632	7.92	C9H9NO2	L2
Hydroxymethylphosphonate	111.9926	10.02	CH5O4P	L2
Sulfate	97.9675	12.37	H2O4S	L2
Orthophosphate	97.9770	11.13	H3O4P	L2

Table A6: A list of total identified metabolites in primary macrophages of old compared to young samples.

Putative metabolite	Mass	RT	FORMULA	confidence
Phenylacetylglycine	193.0740	4.77	C10H11NO3	L2
3',5'-Cyclic AMP	329.0528	9.67	C10H12N5O6P	L2
IMP	348.0471	10.40	C10H13N4O8P	L2
Adenosine	267.0968	7.58	C10H13N5O4	L1
(1-Ribosylimidazole)-4-acetate	258.0853	7.68	C10H14N2O6	L2
AMP	347.0631	9.34	C10H14N5O7P	L1
ADP	427.0295	10.33	C10H15N5O10P2	L1
Biotin	244.0881	6.90	C10H16N2O3S	L2
Glutathione	307.0838	9.71	C10H17N3O6S	L2
Acetylpseudotropine	183.1260	6.82	C10H17NO2	L2
10-Oxodecanoate	186.1256	4.38	C10H18O3	L2
O-Propanoylcarnitine	217.1314	7.54	C10H19NO4	L2
Decanoic acid	172.1463	3.87	C10H20O2	L2
[FA amino(10:0)]decanoic acid	187.1572	4.64	C10H21NO2	L2
5-Hydroxyindoleacetaldehyde	175.0634	4.15	C10H9NO2	L2
Indolelactate	205.0739	6.91	C11H11NO3	L2
L-Tryptophan	204.0900	9.25	C11H12N2O2	L1
5-Hydroxy-L-tryptophan	220.0847	7.66	C11H12N2O3	L2
N-Ribosylnicotinamide	254.0902	19.39	C11H14N2O5	L2
N-Heptanoylhomoserine lactone	213.1365	4.66	C11H19NO3	L2
CDP-ethanolamine	446.0604	10.78	C11H20N4O11P2	L2
O-Butanoylcarnitine	231.1470	7.04	C11H21NO4	L1
N-Acetylserotonin	218.1055	4.86	C12H14N2O2	L2
[FA (12:4/2:0)]	222.0892	3.98	C12H14O4	L2
Thiamin	264.1045	19.92	C12H16N4OS	L2
Dodecanedioic acid	230.1518	4.00	C12H22O4	L2
Dodecanoic acid	200.1777	3.79	C12H24O2	L2
[FA amino(12:0)] dodecanoic acid	215.1884	4.42	C12H25NO2	L2
(R)-S-Lactoylglutathione	379.1049	8.68	C13H21N3O8S	L2
[FA (6:0)]	259.1784	4.79	C13H25NO4	L2
S-Adenosyl-L-homocysteine	384.1216	9.50	C14H20N6O5S	L2
[FA oxo(14:0)]	242.1883	3.75	C14H26O3	L2
Tetradecanoic acid	228.2090	3.73	C14H28O2	L2
[SP (14:0)]	229.2406	4.49	C14H31NO	L2
UDP-glucuronate	580.0343	12.41	C15H22N2O18P2	L2
S-Adenosyl-L-methionine	398.1375	11.27	C15H22N6O5S	L2
Xanthoxin	250.1569	4.31	C15H22O3	L2
UDP-glucose	566.0548	10.87	C15H24N2O17P2	L1
L-Octanoylcarnitine	287.2096	4.80	C15H29NO4	L2
[FA methyl(14:0)]	242.2247	3.71	C15H30O2	L2
[FA oxo(16:0)]	270.2195	3.74	C16H30O3	L2
Palmitoleamide	253.2405	4.16	C16H31NO	L2
Hexadecanoic acid	256.2404	3.72	C16H32O2	L2
UDP-N-acetyl-D-glucosamine	607.0813	10.11	C17H27N3O17P2	L2
[FA (10:0)]	315.2409	4.74	C17H33NO4	L1
[FA (18:3)]	310.2142	3.76	C18H30O4	L2
[FA hydroxy(18:2)]	296.2350	3.71	C18H32O3	L2
[FA (18:2)]	312.2300	3.75	C18H32O4	L2
[FA (18:1)]	282.2559	3.69	C18H34O2	L2

2-Oxooctadecanoic acid	298.2508	3.69	C18H34O3	L2
[FA hydroxy(18:1)]	314.2459	3.77	C18H34O4	L2
[FA trihydroxy(18:1)]	330.2408	3.91	C18H34O5	L2
[FA (18:1)]	281.2719	4.10	C18H35NO	L2
[SP (2:0)]	297.2668	4.05	C18H35NO2	L2
[FA (16:0)]	313.2616	4.09	C18H35NO3	L2
4-8dimethylnonanoylcarnitine	329.2567	4.12	C18H35NO4	L2
Octadecanoic acid	284.2716	3.84	C18H36O2	L1
[FA hydroxy(18:0)]	300.2663	3.69	C18H36O3	L2
[FA hydroxy(18:0)]	316.2614	3.80	C18H36O4	L2
Octadecanamide	283.2874	4.11	C18H37NO	L2
[FA (16:2)]	299.2825	5.34	C18H37NO2	L2
Sphinganine	301.2980	6.85	C18H39NO2	L2
[GL (16:0)]	330.2770	3.95	C19H38O4	L2
[GP (16:0)]	410.2433	4.30	C19H39O7P	L2
Crocetin	328.1669	9.33	C20H24O4	L2
[FA (20:5)]	302.2246	3.88	C20H30O2	L2
CMP-N-acetylneuraminate	614.1469	10.08	C20H31N4O16P	L2
Glutathione disulfide	306.0759	10.96	C20H32N6O12S2	L1
[FA (20:4)]	304.2402	3.75	C20H32O2	L2
[FA oxo,hydroxy(2:0)]	352.2250	4.38	C20H32O5	L2
[FA (18:2)]	323.2824	4.01	C20H37NO2	L2
[FA (20:0/2:0)]	342.2768	3.64	C20H38O4	L2
[FA (18:0)]	325.2981	3.96	C20H39NO2	L2
[FA (18:0)]	341.2930	4.02	C20H39NO3	L2
[FA (20:0)]	312.3029	3.70	C20H40O2	L2
NAD+	663.1091	9.36	C21H27N7O14P2	L1
[FA methoxy,trihydrox]prostadiene	354.2770	3.89	C21H38O4	L2
[GL (18:0)]	358.3084	3.96	C21H42O4	L2
[PE (16:1)]	437.2906	4.23	C21H44NO6P	L2
[PE (16:0)]	453.2856	4.26	C21H44NO7P	L2
[FA hydroxy(22:0/6:0)]	360.2302	3.68	C22H32O4	L2
[FA (20:2)]	351.3138	3.93	C22H41NO2	L2
[FA (20:0)] ethanolamine	353.3295	3.96	C22H43NO2	L2
Docosanoic acid	340.3340	3.71	C22H44O2	L2
[FA hydroxy(22:0)]	356.3291	3.67	C22H44O3	L2
[PC (14:0)]	467.3011	4.40	C22H46NO7P	L2
LysoPE(0:0/18:2)	477.2855	4.22	C23H44NO7P	L2
[FA] O-Palmitoyl-R-carnitine	399.3349	4.30	C23H45NO4	L2
[PE (18:1)]	479.3012	4.19	C23H46NO7P	L2
[FA (24:6)]	344.1776	4.14	C24H24O2	L2
[ST hydrox] 3alpha,12alpha-Dihydroxy-5beta-chol-6-en-24-oic Acid	390.2771	3.77	C24H38O4	L2
[PS (18:1)]	523.2909	3.85	C24H46NO9P	L2
[PC (16:1)]	493.3168	4.37	C24H48NO7P	L2
[PS (18:0)]	525.3066	3.82	C24H48NO9P	L2
Tetracosanoic acid	368.3654	3.60	C24H48O2	L2
[FA hydroxy(24:0)]	384.3604	3.63	C24H48O3	L2
[PC (16:1)]	479.3376	4.31	C24H50NO6P	L2
[PC (16:0)]	495.3325	4.35	C24H50NO7P	L2
[PC (16:2)]	481.3534	4.37	C24H52NO6P	L2
LysoPE(0:0/20:5)	499.2700	4.19	C25H42NO7P	L2
[PE (20:4)]	501.2856	4.17	C25H44NO7P	L2
[FA (26:0)]	396.3967	3.56	C26H52O2	L2
[FA hydroxy(26:0)]	412.3917	3.60	C26H52O3	L2
[PC (18:1)]	507.3688	4.23	C26H54NO6P	L2
[PC (18:0)]	523.3639	4.26	C26H54NO7P	L2
LysoPE(0:0/22:6)	525.2854	4.13	C27H44NO7P	L2
LysoPE(0:0/22:5)	527.3014	4.12	C27H46NO7P	L2
LysoPC(20:4)	543.3324	4.26	C28H50NO7P	L2

Oxalate	89.9953	12.21	C2H2O4	L1
Glycine	75.0320	11.24	C2H5NO2	L1
Phosphonoacetaldehyde	123.9926	9.85	C2H5O4P	L2
2-Hydroxyethanesulfonate	125.9987	8.58	C2H6O4S	L2
Hypotaurine	109.0198	10.86	C2H7NO2S	L2
Taurine	125.0147	11.06	C2H7NO3S	L1
Ethanolamine phosphate	141.0191	10.68	C2H8NO4P	L1
[SP (16:0)]	537.5120	3.72	C34H67NO3	L2
PC(28:0)	677.4994	3.80	C36H72NO8P	L2
PA(34:1)	674.4886	3.48	C37H71O8P	L2
PE(32:0)	691.5155	3.77	C37H74NO8P	L2
SM(d18:1/14:0)	674.5361	3.90	C37H75N2O6P	L2
PC(30:1)	703.5150	3.77	C38H74NO8P	L2
PC(14:0/P-16:0)	689.5372	3.76	C38H76NO7P	L2
PC(30:0)	705.5307	3.76	C38H76NO8P	L2
[SP (18:0/14:0)]	688.5518	3.87	C38H77N2O6P	L2
[PC (14:2/16:0)]	691.5516	3.77	C38H78NO7P	L2
PE(34:2)	715.5142	3.70	C39H74NO8P	L2
PE(16:0/P-18:1)	701.5356	3.73	C39H76NO7P	L2
PE(34:1)	717.5308	3.73	C39H76NO8P	L2
SM(d16:1/18:1)	700.5515	3.89	C39H77N2O6P	L2
PE(34:0)	719.5471	3.75	C39H78NO8P	L2
[SP (16:0)]	702.5673	3.83	C39H79N2O6P	L2
[SP (16:0)]	704.5839	3.79	C39H81N2O6P	L2
N-Methylethanolamine phosphate	155.0347	9.98	C3H10NO4P	L2
Oxalureate	132.0171	8.23	C3H4N2O4	L2
Pyruvate	88.0160	6.91	C3H4O3	L2
L-Lactate	90.0317	7.16	C3H6O3	L1
Guanidinoacetate	117.0538	11.46	C3H7N3O2	L1
L-Alanine	89.0477	10.85	C3H7NO2	L1
L-Serine	105.0426	11.18	C3H7NO3	L1
L-cysteine sulfinate	153.0095	7.94	C3H7NO4S	L2
L-Cysteate	169.0044	11.07	C3H7NO5S	L1
Propanoyl phosphate	154.0031	8.66	C3H7O5P	L2
D-Glyceraldehyde 3-phosphate	169.9979	11.03	C3H7O6P	L2
3-Phospho-D-glycerate	185.9929	11.47	C3H7O7P	L1
Glycerol	92.0474	8.07	C3H8O3	L2
Taurocyamine	167.0365	11.80	C3H9N3O3S	L2
sn-Glycerol 3-phosphate	172.0137	10.17	C3H9O6P	L1
PS(34:2)	759.5044	3.50	C40H74NO10P	L2
PS(34:1)	761.5200	3.50	C40H76NO10P	L2
PC(32:2)	729.5307	3.75	C40H76NO8P	L2
PC(32:1)	731.5464	3.73	C40H78NO8P	L2
PC(32:0)	733.5621	3.73	C40H80NO8P	L2
[PC (14:2/18:0)]	719.5831	3.73	C40H82NO7P	L2
PE(18:4/P-18:1)	721.5039	3.63	C41H72NO7P	L2
PE(18:3/P-18:1)	723.5202	3.65	C41H74NO7P	L2
PE(36:4)	739.5156	3.63	C41H74NO8P	L2
PE(36:2)	743.5465	3.70	C41H78NO8P	L2
PE(36:1)	745.5621	3.71	C41H80NO8P	L2
SM(d18:1/18:1)	728.5819	3.83	C41H81N2O6P	L2
PS(36:3)	785.5204	3.49	C42H76NO10P	L2
PC(18:4/P-16:0)	737.5374	3.90	C42H76NO7P	L2
PS(36:2)	787.5359	3.49	C42H78NO10P	L2
PC(34:3)	755.5464	3.74	C42H78NO8P	L2
PS(36:1)	789.5517	3.49	C42H80NO10P	L2
PC(34:2)	757.5620	3.72	C42H80NO8P	L2
1-Hexadecanoyl-2-(octadecenoyl)-sn-glycero-3-phosphonocholine	743.5827	3.72	C42H82NO7P	L2
PC(34:1)	759.5776	3.71	C42H82NO8P	L2

PC(16:0/P-18:0)	745.5984	3.72	C42H84NO7P	L2
[PE (16:1/22:6)]	747.5198	3.61	C43H74NO7P	L2
PE(20:4/P-18:1)	749.5359	3.61	C43H76NO7P	L2
PE(38:5)	765.5310	3.62	C43H76NO8P	L2
[PE (18:1/20:4)]	751.5519	3.63	C43H78NO7P	L2
PE(38:4)	767.5470	3.63	C43H78NO8P	L2
PI(34:2)	834.5251	3.50	C43H79O13P	L2
PE(38:2)	771.5776	3.70	C43H82NO8P	L2
PE(38:1)	773.5937	3.69	C43H84NO8P	L2
PS(38:5)	809.5204	3.48	C44H76NO10P	L2
PS(38:4)	811.5361	3.49	C44H78NO10P	L2
PC(36:5)	779.5464	3.71	C44H78NO8P	L2
PG(38:4)	798.5415	3.45	C44H79O10P	L2
PC(36:4)	781.5621	3.70	C44H80NO8P	L2
PC(36:3)	783.5779	3.69	C44H82NO8P	L2
PC(36:2)	785.5933	3.70	C44H84NO8P	L2
[PC (18:1/18:0)]	771.6145	3.68	C44H86NO7P	L2
PC(36:1)	787.6089	3.70	C44H86NO8P	L2
MGDG(18:3/18:4)	772.5114	4.02	C45H72O10	L2
PE(22:6/P-18:1)	773.5362	3.65	C45H76NO7P	L2
[PE (18:1/22:6)]	775.5512	3.61	C45H78NO7P	L2
PE(40:6)	791.5458	3.65	C45H78NO8P	L2
PI(36:4)	858.5254	3.51	C45H79O13P	L2
PE(22:4/P-18:1)	777.5674	3.63	C45H80NO7P	L2
PI(36:3)	860.5418	3.49	C45H81O13P	L2
PE(22:4/P-18:0)	779.5828	3.67	C45H82NO7P	L2
PI(36:2)	862.5575	3.50	C45H83O13P	L2
PI(36:1)	864.5724	3.48	C45H85O13P	L2
[PI (18:0/18:0)]	879.5846	3.48	C45H86NO13P	L2
PE(40:2)	799.6098	3.68	C45H86NO8P	L2
SM(d18:1/22:1)	784.6450	3.77	C45H89N2O6P	L2
[PG (8:0/8:0)]	802.5151	3.43	C46H75O9P	L2
PS(40:6)	835.5365	3.45	C46H78NO10P	L2
PI(15:1/22:4)	435.2622	4.66	C46H79O13P	L2
PS(40:5)	837.5522	3.44	C46H80NO10P	L2
PS(40:4)	839.5673	3.48	C46H82NO10P	L2
PC(38:5)	807.5779	3.68	C46H82NO8P	L2
[PC (18:1/20:4)]	793.5984	3.68	C46H84NO7P	L2
PC(38:4)	809.5936	3.67	C46H84NO8P	L2
PC(20:2/P-18:1)	795.6134	3.68	C46H86NO7P	L2
PC(38:3)	811.6087	3.68	C46H86NO8P	L2
PC(38:2)	813.6247	3.68	C46H88NO8P	L2
SM(d17:1/24:1)	798.6612	3.76	C46H91N2O6P	L2
PI(38:5)	884.5406	3.43	C47H81O13P	L2
PI(38:4)	886.5579	3.50	C47H83O13P	L2
PI(38:3)	888.5716	3.49	C47H85O13P	L2
PS(19:1/22:2)	855.5991	3.74	C47H86NO10P	L2
SM(d18:2/24:1)	810.6620	3.75	C47H91N2O6P	L2
SM(d18:1/24:1)	812.6770	3.73	C47H93N2O6P	L2
PG(42:9)	844.5253	3.44	C48H77O10P	L2
PS(42:7)	861.5524	3.42	C48H80NO10P	L2
PC(40:8)	829.5624	3.71	C48H80NO8P	L2
PC(40:7)	831.5780	3.67	C48H82NO8P	L2
PC(40:6)	833.5933	3.67	C48H84NO8P	L2
PC(22:4/P-18:1)	819.6148	3.66	C48H86NO7P	L2
PC(40:5)	835.6093	3.66	C48H86NO8P	L2
PC(22:4/P-18:0)	821.6299	3.66	C48H88NO7P	L2
PC(40:4)	837.6245	3.68	C48H88NO8P	L2
PI(40:6)	910.5577	3.49	C49H83O13P	L2

PI(40:5)	912.5723	3.48	C49H85O13P	L2
Phosphocreatine	211.0359	10.18	C4H10N3O5P	L2
Diethanolamine	105.0790	8.38	C4H11NO2	L2
Phosphodimethylethanolamine	169.0504	9.37	C4H12NO4P	L2
3-Butynoate	84.0211	8.14	C4H4O2	L2
Allantoin	158.0439	11.14	C4H6N4O3	L1
2-Oxobutanoate	102.0317	4.80	C4H6O3	L2
Succinate	118.0266	10.56	C4H6O4	L1
L-Malate	134.0215	11.06	C4H6O5	L1
Creatinine	113.0589	8.11	C4H7N3O	L1
L-Aspartate	133.0375	10.41	C4H7NO4	L1
L-Asparagine	132.0535	10.84	C4H8N2O3	L1
Allantoate	176.0545	10.72	C4H8N4O4	L2
[FA trihydroxy(4:0)]	136.0372	8.98	C4H8O5	L2
Creatine	131.0694	10.60	C4H9N3O2	L1
L-Threonine	119.0583	10.41	C4H9NO3	L1
PG(22:6/22:6)	866.5101	3.44	C50H75O10P	L2
PC(42:7)	859.6097	3.66	C50H86NO8P	L2
PC(42:6)	861.6249	3.66	C50H88NO8P	L2
PC(42:5)	863.6414	3.67	C50H90NO8P	L2
L-Glutamine	146.0690	10.65	C5H10N2O3	L1
Pentanoate	102.0681	4.70	C5H10O2	L2
5-Hydroxypentanoate	118.0630	8.20	C5H10O3	L2
D-Xylulose	150.0527	8.64	C5H10O5	L2
4-Guanidinobutanoate	145.0851	10.87	C5H11N3O2	L2
Betaine	117.0790	8.65	C5H11NO2	L1
L-Methionine	149.0511	8.84	C5H11NO2S	L1
L-Methionine S-oxide	165.0459	9.54	C5H11NO3S	L2
2-Deoxy-D-ribose 5-phosphate	214.0242	9.98	C5H11O7P	L2
D-Ribose 5-phosphate	230.0190	10.59	C5H11O8P	L1
L-Ornithine	132.0898	15.92	C5H12N2O2	L1
Xylitol	152.0684	9.83	C5H12O5	L2
Choline	103.0997	17.82	C5H13NO	L2
2-C-Methyl-D-erythritol 4-phosphate	216.0401	10.81	C5H13O7P	L2
Choline phosphate	183.0661	9.84	C5H14NO4P	L1
sn-glycero-3-Phosphoethanolamine	215.0560	10.65	C5H14NO6P	L2
Orotate	156.0171	8.08	C5H4N2O4	L1
Hypoxanthine	136.0385	8.60	C5H4N4O	L1
Xanthine	152.0334	8.95	C5H4N4O2	L1
Urate	168.0283	9.57	C5H4N4O3	L1
Adenine	135.0545	8.02	C5H5N5	L1
2,5-Dioxopentanoate	130.0267	6.85	C5H6O4	L2
2-Oxoglutarate	146.0215	10.96	C5H6O5	L2
5-Methylcytosine	125.0589	7.04	C5H7N3O	L2
L-1-Pyrroline-5-carboxylate	113.0477	7.06	C5H7NO2	L2
L-1-Pyrroline-3-hydroxy-5-carboxylate	129.0427	7.58	C5H7NO3	L2
2-Oxoglutaramate	145.0375	7.96	C5H7NO4	L2
5,6-Dihydrothymine	128.0586	8.05	C5H8N2O2	L2
N-Carbamoyl-L-aspartate	176.0434	11.38	C5H8N2O5	L2
3-Methylbut-2-enal	84.0575	4.21	C5H8O	L2
(R)-2-Hydroxyglutarate	148.0372	10.55	C5H8O5	L1
L-Proline	115.0633	9.55	C5H9NO2	L1
L-Glutamate 5-semialdehyde	131.0584	10.46	C5H9NO3	L2
L-Glutamate	147.0531	10.13	C5H9NO4	L1
N-Formimino-L-glutamate	174.0640	8.36	C6H10N2O4	L2
N-Carbamyl-L-glutamate	190.0589	10.47	C6H10N2O5	L2
(S)-3-Methyl-2-oxopentanoic acid	130.0631	4.60	C6H10O3	L2
2-Dehydro-3-deoxy-L-rhamnonate	162.0528	9.92	C6H10O5	L2
D-Glucono-1,5-lactone	178.0477	10.61	C6H10O6	L2

5-Guanidino-2-oxopentanoate	173.0800	10.65	C6H11N3O3	L2
[FA oxo,amino(6:0)]	145.0739	9.56	C6H11NO3	L2
N-Formyl-L-methionine	177.0460	4.82	C6H11NO3S	L2
O-Acetyl-L-homoserine	161.0688	8.42	C6H11NO4	L2
D-Alanyl-D-alanine	160.0848	6.94	C6H12N2O3	L2
L-Rhamnose	164.0685	8.80	C6H12O5	L2
myo-Inositol	180.0634	11.95	C6H12O6	L1
D-Gluconic acid	196.0583	9.94	C6H12O7	L1
L-Citrulline	175.0957	11.04	C6H13N3O3	L1
L-Leucine	131.0946	8.60	C6H13NO2	L1
D-Galactosamine	179.0793	8.62	C6H13NO5	L2
L-Lysine	146.1055	16.82	C6H14N2O2	L1
L-Arginine	174.1117	18.19	C6H14N4O2	L1
D-Glucosamine 6-phosphate	259.0458	10.41	C6H14NO8P	L1
D-Sorbitol	182.0792	10.30	C6H14O6	L2
Triethanolamine	149.1052	8.05	C6H15NO3	L2
Urocanate	138.0429	8.36	C6H6N2O2	L2
Phenol	94.0419	4.06	C6H6O	L2
cis-Aconitate	174.0164	12.03	C6H6O6	L2
Methylimidazoleacetic acid	140.0585	7.07	C6H8N2O2	L2
(4E)-2-Oxohexenoic acid	128.0473	4.80	C6H8O3	L2
3,5/4-Trihydroxycyclohexa-1,2-dione	160.0371	6.96	C6H8O5	L2
D-Glucuronolactone	176.0320	11.94	C6H8O6	L2
Citrate	192.0270	12.16	C6H8O7	L2
L-Histidine	155.0695	10.83	C6H9N3O2	L2
N-Acetyl-L-aspartate	175.0481	10.13	C6H9NO5	L2
N(pi)-Methyl-L-histidine	169.0851	9.35	C7H11N3O2	L1
N-Acetyl-L-glutamate	189.0637	9.82	C7H11NO5	L1
4-Trimethylammoniobutanoate	145.1102	9.42	C7H15NO2	L1
L-Carnitine	161.1052	9.43	C7H15NO3	L1
N6-Methyl-L-lysine	160.1211	16.23	C7H16N2O2	L1
Homoarginine	188.1274	18.47	C7H16N4O2	L2
Pyridine-2,3-dicarboxylate	167.0219	10.75	C7H5NO4	L2
Pyridoxine	169.0739	7.00	C8H11NO3	L1
[FA (8:2)]	124.0888	4.11	C8H12O	L2
[FA dioxo(8:0)]	172.0735	8.00	C8H12O4	L2
N2-Acetyl-L-aminoadipate	203.0794	8.62	C8H13NO5	L2
O-Succinyl-L-homoserine	219.0743	9.74	C8H13NO6	L2
gamma-L-Glutamyl-L-cysteine	250.0624	9.74	C8H14N2O5S	L2
N-Acetyl-D-glucosamine	221.0900	9.21	C8H15NO6	L2
3-methyl-1-heptene	112.1252	3.79	C8H16	L2
N2-Acetyl-L-lysine	188.1161	6.89	C8H16N2O3	L2
N6-Acetyl-N6-hydroxy-L-lysine	204.1109	6.90	C8H16N2O4	L2
N-Acetyl-D-glucosamine 6-phosphate	301.0562	9.97	C8H16NO9P	L2
sn-glycero-3-Phosphocholine	257.1029	9.85	C8H20NO6P	L1
Indole	117.0578	4.06	C8H7N	L2
Phenylpropanoate	150.0681	4.60	C9H10O2	L2
3-(4-Hydroxyphenyl)lactate	182.0579	7.29	C9H10O4	L2
L-Phenylalanine	165.0790	8.05	C9H11NO2	L2
L-Tyrosine	181.0740	9.93	C9H11NO3	L1
Pseudouridine	244.0695	9.43	C9H12N2O6	L2
UMP	324.0357	10.18	C9H13N2O9P	L1
Deoxycytidine	227.0906	8.08	C9H13N3O4	L2
gamma-Glutamyl-gamma-aminobutyraldehyde	216.1107	7.08	C9H16N2O4	L2
N2-Succinyl-L-ornithine	232.1059	9.22	C9H16N2O5	L2
9-Oxononanoic acid	172.1099	4.54	C9H16O3	L2
8-Amino-7-oxononanoate	187.1209	4.81	C9H17NO3	L2
O-Acetylcarnitine	203.1158	8.17	C9H17NO4	L1
Pantothenate	219.1106	6.88	C9H17NO5	L2

N2-(D-1-Carboxyethyl)-L-arginine	246.1328	10.09	C9H18N4O4	L2
N6,N6,N6-Trimethyl-L-lysine	188.1525	15.16	C9H20N2O2	L2
3-(4-Hydroxyphenyl)pyruvate	180.0422	6.95	C9H8O4	L2
3-(3,4-Dihydroxyphenyl)pyruvate	196.0373	4.37	C9H8O5	L2
Dopaquinone	195.0531	10.47	C9H9NO4	L2
Carbamoyl phosphate	140.9828	15.61	CH4NO5P	L2
Hydroxymethylphosphonat	111.9926	9.91	CH5O4P	L2

Table A7: A list of total identified metabolites in primary macrophages of old-LPS compared to young-LPS samlpes.

Putative metabolite	Mass	RT	FORMULA	confidence
5-Hydroxyferulate	210.0529	4.79	C10H10O5	L2
Phenylacetylglycine	193.0740	4.75	C10H11NO3	L1
4-Hydroxyphenylacetylglycine	209.0688	4.67	C10H11NO4	L2
L-Kynurenine	208.0849	8.58	C10H12N2O3	L1
2',3'-Cyclic AMP	329.0529	9.55	C10H12N5O6P	L2
Deoxyadenosine	251.1018	6.81	C10H13N5O3	L1
Adenosine	267.0967	7.53	C10H13N5O4	L1
AMP	347.0631	9.20	C10H14N5O7P	L1
ADP	427.0296	10.07	C10H15N5O10P2	L1
Biotin	244.0882	6.78	C10H16N2O3S	L1
ATP	506.9957	10.97	C10H16N5O13P3	L2
[FA (10:1/2:0)]	200.1049	4.45	C10H16O4	L2
Glutathione	307.0838	9.61	C10H17N3O6S	L1
Acetylpseudotropine	183.1259	4.68	C10H17NO2	L2
3-Hydroxysebacicacid	218.1154	4.63	C10H18O5	L2
O-Propanoylcarnitine	217.1314	7.49	C10H19NO4	L2
Decanoic acid	172.1463	3.80	C10H20O2	L2
10-Hydroxydecanoic acid	188.1412	3.83	C10H20O3	L2
Indole-3-acetaldehyde	159.0684	5.45	C10H9NO	L2
5-Hydroxyindoleacetaldehyde	175.0633	3.94	C10H9NO2	L2
Indolelactate	205.0739	6.74	C11H11NO3	L2
L-Tryptophan	204.0899	9.21	C11H12N2O2	L1
5-Hydroxy-L-tryptophan	220.0847	7.64	C11H12N2O3	L2
L-Formylkynurenine	236.0797	7.79	C11H12N2O4	L2
N-Ribosylnicotinamide	254.0902	19.54	C11H14N2O5	L2
CDP-ethanolamine	446.0606	10.66	C11H20N4O11P2	L2
O-Butanoylcarnitine	231.1470	6.91	C11H21NO4	L1
N-Acetylserotonin	218.1055	4.81	C12H14N2O2	L2
[FA (12:5)]	190.0995	4.00	C12H14O2	L2
[FA (12:4/2:0)]	222.0892	3.94	C12H14O4	L2
N-(3-Oxooctanoyl)homoserine lactone	241.1314	4.83	C12H19NO4	L2
[FA oxo(12:1)]	212.1413	3.98	C12H20O3	L2
Sucrose	342.1161	11.02	C12H22O11	L1
Dodecanedioic acid	230.1517	4.78	C12H22O4	L2
3-Hydroxydodecanedioicacid	246.1467	4.07	C12H22O5	L2
Dodecanoic acid	200.1777	3.72	C12H24O2	L2
(R)-S-Lactoylglutathione	379.1050	8.55	C13H21N3O8S	L2
S-glutathionyl-L-cysteine	426.0880	10.74	C13H22N4O8S2	L2
[FA (6:0)]	259.1783	4.81	C13H25NO4	L2
[FA hydroxy(10:0)]	275.1732	6.65	C13H25NO5	L2
S-Adenosyl-L-homocysteine	384.1217	9.44	C14H20N6O5S	L1
Tetradecenoic acid	226.1933	3.65	C14H26O2	L2
Tetradecanoic acid	228.2090	3.68	C14H28O2	L2
S-Adenosyl-L-methionine	398.1374	11.25	C15H22N6O5S	L2
UDP-glucose	566.0551	10.75	C15H24N2O17P2	L1
[FA methyl(14:0)]	242.2247	3.67	C15H30O2	L2
GDP-L-fucose	589.0823	11.41	C16H25N5O15P2	L2
(9Z)-Hexadecenoic acid	254.2247	3.67	C16H30O2	L2
[FA oxo(16:0)]	270.2194	3.67	C16H30O3	L2
Hexadecanoic acid	256.2404	3.67	C16H32O2	L2
[FA amino(16:0)]	271.2509	6.60	C16H33NO2	L2

UDP-N-acetyl-D-glucosamine	607.0817	9.96	C17H27N3O17P2	L2
[FA hydroxy(18:2)]	296.2351	3.70	C18H32O3	L2
[FA (18:2)]	312.2299	3.67	C18H32O4	L2
[FA (18:1)]	282.2559	3.62	C18H34O2	L2
2-Oxooctadecanoic acid	298.2507	3.64	C18H34O3	L2
[FA hydroxy(18:1)]	314.2459	3.73	C18H34O4	L2
[FA trihydroxy(18:1)]	330.2407	3.81	C18H34O5	L2
[FA hydroxy(18:0)]	346.2357	3.95	C18H34O6	L2
[FA hydroxy(18:0)]	300.2663	3.62	C18H36O3	L2
[FA hydroxy(4:0/18:0)]	348.2513	4.01	C18H36O6	L2
[FA (16:2)]	299.2825	5.47	C18H37NO2	L2
Sphinganine	301.2980	6.70	C18H39NO2	L2
Phenolsulfonphthalein	354.0563	4.72	C19H14O5S	L1
Folate	441.1397	10.86	C19H19N7O6	L1
[GP (16:0)]	410.2435	4.24	C19H39O7P	L2
deacetylcolchicine	357.1571	10.60	C20H23NO5	L2
[FA (20:5)]	302.2245	3.82	C20H30O2	L2
Glutathione disulfide	612.1519	10.79	C20H32N6O12S2	L1
N-palmitoyl threonine	357.2880	4.45	C20H39NO4	L2
[FA (20:0)]	312.3030	3.73	C20H40O2	L2
NAD+	663.1090	9.26	C21H27N7O14P2	L1
NADH	665.1261	9.06	C21H29N7O14P2	L1
NADPH	372.5455	11.06	C21H30N7O17P3	L1
[FA methoxy,trihydrox] prostadiene	354.2771	3.88	C21H38O4	L2
[GL (18:0)]	358.3084	3.89	C21H42O4	L2
[PE (16:1)]	437.2907	4.17	C21H44NO6P	L2
[PE (16:0)]	453.2855	4.21	C21H44NO7P	L2
Docosahexaenoicacid	328.2403	3.59	C22H32O2	L2
[FA (20:2)]	351.3138	3.92	C22H41NO2	L2
[FA (20:0)]	353.3293	3.88	C22H43NO2	L2
Docosanoic acid	340.3341	3.74	C22H44O2	L2
[PC (14:1)]	451.3062	4.28	C22H46NO6P	L2
[PC (14:0)]	467.3012	4.37	C22H46NO7P	L2
LysoPE(0:0/18:2)	477.2855	4.17	C23H44NO7P	L2
[FA] O-Palmitoyl-R-carnitine	399.3350	4.24	C23H45NO4	L2
[PE (18:1)]	479.3012	4.16	C23H46NO7P	L2
[FA (24:6)]	344.1777	4.02	C24H24O2	L2
[ST hydrox] 3alpha,12alpha-Dihydroxy-5beta-chol-6-en-24-oic Acid	390.2770	3.73	C24H38O4	L2
[PS (18:1)]	523.2912	3.77	C24H46NO9P	L2
[PG (18:1)]	510.2956	3.58	C24H47O9P	L2
[PC (16:1)]	493.3168	4.28	C24H48NO7P	L2
[PS (18:0)]	525.3068	3.74	C24H48NO9P	L2
[PC (16:1)]	479.3376	4.22	C24H50NO6P	L2
[PC (16:0)]	495.3324	4.25	C24H50NO7P	L2
[PC (16:2)]	481.3535	4.29	C24H52NO6P	L2
LysoPE(0:0/20:5)	499.2700	4.17	C25H42NO7P	L2
[PE (20:4)]	501.2858	4.14	C25H44NO7P	L2
[PC (17:0)]	507.3322	4.23	C25H50NO7P	L2
His-Lys-Phe-Val	529.3018	4.39	C26H39N7O5	L2
Glycodeoxycholate	449.3144	3.99	C26H43NO5	L2
[PC (18:1)]	507.3689	4.12	C26H54NO6P	L2
[PC (18:0)]	523.3640	4.18	C26H54NO7P	L2
LysoPE(0:0/22:6)	525.2855	4.06	C27H44NO7P	L2
LysoPE(0:0/22:5)	527.3015	4.07	C27H46NO7P	L2
[PI (18:1)]	598.3119	3.79	C27H51O12P	L2
PI(18:0/0:0)	600.3279	3.77	C27H53O12P	L2
LysoPC(20:4)	543.3323	4.22	C28H50NO7P	L2
LysoPC(20:3)	545.3483	4.17	C28H52NO7P	L2
Oxalate	89.9953	11.97	C2H2O4	L1

Glycine	75.0320	11.19	C2H5NO2	L1
Phosphonoacetaldehyde	123.9926	9.74	C2H5O4P	L2
2-Hydroxyethanesulfonate	125.9987	8.55	C2H6O4S	L2
Hypotaurine	109.0198	10.80	C2H7NO2S	L2
Taurine	125.0147	11.03	C2H7NO3S	L1
Ethanolamine phosphate	141.0191	10.51	C2H8NO4P	L1
[PC (22:6)]	567.3324	4.16	C30H50NO7P	L2
Ceramide (d18:1/16:0)	537.5122	3.64	C34H67NO3	L2
PC(28:0)	677.4993	3.72	C36H72NO8P	L2
PA(34:1)	674.4890	3.41	C37H71O8P	L2
PE(32:0)	691.5153	3.73	C37H74NO8P	L2
SM(d18:1/14:0)	674.5360	3.83	C37H75N2O6P	L2
SM(d18:0/14:0)	676.5530	3.79	C37H77N2O6P	L2
PC(30:1)	703.5152	3.71	C38H74NO8P	L2
PC(30:0)	705.5306	3.71	C38H76NO8P	L2
PE-Cer(d14:1/22:0)	688.5517	3.80	C38H77N2O6P	L2
[PC (14:2/16:0)]	691.5517	3.69	C38H78NO7P	L2
PE(34:2)	715.5146	3.66	C39H74NO8P	L2
PE(16:0/P-18:1)	701.5359	3.65	C39H76NO7P	L2
PE(34:1)	717.5308	3.69	C39H76NO8P	L2
SM(d16:1/18:1)	700.5516	3.81	C39H77N2O6P	L2
PE(34:0)	719.5465	3.69	C39H78NO8P	L2
Ceramide (d18:1/16:0)]	704.5840	3.74	C39H81N2O6P	L2
N-Methylethanolamine phosphate	155.0347	9.87	C3H10NO4P	L2
Oxalureate	132.0170	8.17	C3H4N2O4	L2
Pyruvate	88.0160	6.76	C3H4O3	L1
Hydroxypyruvate	104.0110	9.99	C3H4O4	L2
L-Lactate	90.0317	7.67	C3H6O3	L1
Guanidinoacetate	117.0538	11.39	C3H7N3O2	L1
L-Alanine	89.0477	10.61	C3H7NO2	L1
L-Serine	105.0426	11.16	C3H7NO3	L1
L-cysteine sulfinate	153.0095	7.91	C3H7NO4S	L2
L-Cysteate	169.0045	11.03	C3H7NO5S	L1
Glycerol	92.0473	8.57	C3H8O3	L1
(R)-1-Aminopropan-2-ol	75.0684	8.23	C3H9NO	L2
sn-Glycerol 3-phosphate	172.0137	9.80	C3H9O6P	L1
PS(34:2)	759.5047	3.41	C40H74NO10P	L2
PG(34:2)	746.5101	3.36	C40H75O10P	L2
PS(34:1)	761.5202	3.40	C40H76NO10P	L2
PC(32:2)	729.5305	3.70	C40H76NO8P	L2
PC(32:1)	731.5462	3.69	C40H78NO8P	L2
PC(32:0)	733.5623	3.68	C40H80NO8P	L2
[PC (14:2/18:0)]	719.5833	3.67	C40H82NO7P	L2
PE(18:4/P-18:1)	721.5037	3.57	C41H72NO7P	L2
PE(18:3/P-18:1)	723.5202	3.57	C41H74NO7P	L2
PE(36:4)	739.5157	3.61	C41H74NO8P	L2
PE(36:2)	743.5465	3.64	C41H78NO8P	L2
PE(36:1)	745.5620	3.66	C41H80NO8P	L2
SM(d18:1/18:1)	728.5823	3.75	C41H81N2O6P	L2
PE(36:0)	747.5790	3.68	C41H82NO8P	L2
SM(d18:0/18:1)	730.5992	3.73	C41H83N2O6P	L2
PS(36:3)	785.5207	3.42	C42H76NO10P	L2
PC(18:4/P-16:0)	737.5364	3.62	C42H76NO7P	L2
PC(34:4)	753.5308	3.70	C42H76NO8P	L2
PS(36:2)	787.5359	3.41	C42H78NO10P	L2
PG(36:2)	774.5410	3.39	C42H79O10P	L2
PS(36:1)	789.5516	3.41	C42H80NO10P	L2
PC(34:2)	757.5618	3.67	C42H80NO8P	L2
Ceramide (d18:1/24:0)]	647.6219	3.61	C42H81NO3	L2

1-Hexadecanoyl-2-(octadecenoyl)-sn-glycero-3-phosphonocholine	743.5825	3.66	C42H82NO7P	L2
PC(34:1)	759.5773	3.66	C42H82NO8P	L2
PC(16:0/P-18:0)	745.5982	3.66	C42H84NO7P	L2
[PE (16:1/22:6)]	747.5201	3.56	C43H74NO7P	L2
PE(38:6)	763.5155	3.58	C43H74NO8P	L2
PE(20:4/P-18:1)	749.5360	3.57	C43H76NO7P	L2
PE(38:5)	765.5309	3.58	C43H76NO8P	L2
[PE (18:1/20:4)]	751.5519	3.58	C43H78NO7P	L2
PE(38:4)	767.5468	3.58	C43H78NO8P	L2
PI(34:2)	834.5252	3.42	C43H79O13P	L2
PE(38:2)	771.5775	3.65	C43H82NO8P	L2
PE(38:1)	773.5936	3.64	C43H84NO8P	L2
PS(38:4)	811.5362	3.40	C44H78NO10P	L2
PC(36:5)	779.5461	3.67	C44H78NO8P	L2
PC(36:4)	781.5618	3.65	C44H80NO8P	L2
PC(36:2)	785.5931	3.64	C44H84NO8P	L2
[PC (18:1/18:0)]	771.6141	3.64	C44H86NO7P	L2
PC(36:1)	787.6087	3.64	C44H86NO8P	L2
MGDG(18:3/18:4)	772.5120	3.95	C45H72O10	L2
[PE (18:1/22:6)]	775.5528	3.55	C45H78NO7P	L2
PE(40:6)	791.5460	3.59	C45H78NO8P	L2
PI(36:4)	858.5255	3.40	C45H79O13P	L2
PE(40:5)	793.5630	3.62	C45H80NO8P	L2
PI(36:3)	860.5420	3.42	C45H81O13P	L2
PE(40:4)	795.5792	3.63	C45H82NO8P	L2
PI(36:2)	862.5577	3.41	C45H83O13P	L2
PE(40:3)	797.5941	3.63	C45H84NO8P	L2
PI(36:1)	864.5714	3.41	C45H85O13P	L2
[PI (18:0/18:0)]	879.5839	3.41	C45H86NO13P	L2
PE(40:2)	799.6095	3.63	C45H86NO8P	L2
PE(40:1)	801.6246	3.63	C45H88NO8P	L2
SM(d18:1/22:1)	784.6451	3.71	C45H89N2O6P	L2
SM(d18:1/22:0)	786.6621	3.71	C45H91N2O6P	L2
PS(40:7)	833.5208	3.39	C46H76NO10P	L2
PS(40:6)	835.5365	3.40	C46H78NO10P	L2
PS(40:5)	837.5522	3.39	C46H80NO10P	L2
PC(38:6)	805.5624	6.09	C46H80NO8P	L2
PS(40:4)	839.5675	3.39	C46H82NO10P	L2
[PC (18:1/20:4)]	793.5985	3.62	C46H84NO7P	L2
PC(38:4)	809.5932	3.61	C46H84NO8P	L2
PC(38:3)	811.6083	3.62	C46H86NO8P	L2
PC(38:2)	813.6246	3.63	C46H88NO8P	L2
SM(d17:1/24:1)	798.6611	3.72	C46H91N2O6P	L2
SM(d18:1/23:0)	800.6770	3.71	C46H93N2O6P	L2
PI(38:5)	884.5425	3.41	C47H81O13P	L2
PI(38:4)	886.5579	3.41	C47H83O13P	L2
PE(42:5)	821.5949	3.62	C47H84NO8P	L2
PI(38:3)	888.5717	3.41	C47H85O13P	L2
PE(42:4)	823.6095	3.62	C47H86NO8P	L2
SM(d18:2/24:1)	810.6618	3.69	C47H91N2O6P	L2
SM(d18:2/24:0)	812.6775	6.46	C47H93N2O6P	L2
PG(42:9)	844.5258	3.36	C48H77O10P	L2
PS(42:7)	861.5523	3.37	C48H80NO10P	L2
PC(40:6)	833.5933	3.60	C48H84NO8P	L2
PC(40:5)	835.6091	3.60	C48H86NO8P	L2
PC(22:4/P-18:0)	821.6291	3.61	C48H88NO7P	L2
PC(40:4)	837.6241	3.60	C48H88NO8P	L2
PC(22:2/P-18:1)	823.6461	3.63	C48H90NO7P	L2
PI(40:6)	910.5569	3.40	C49H83O13P	L2

Phosphocreatine	211.0359	10.04	C4H10N3O5P	L2
Diethanolamine	105.0790	15.72	C4H11NO2	L2
Phosphodimethylethanolamine	169.0504	9.28	C4H12NO4P	L2
Uracil	112.0273	8.24	C4H4N2O2	L2
Maleamate	115.0269	10.59	C4H5NO3	L2
Allantoin	158.0439	11.10	C4H6N4O3	L1
[FA (4:0)]	86.0368	4.68	C4H6O2	L2
Succinate	118.0266	10.37	C4H6O4	L1
L-Malate	134.0215	10.88	C4H6O5	L1
(R,R)-Tartaric acid	150.0164	11.58	C4H6O6	L2
Creatinine	113.0589	8.05	C4H7N3O	L1
L-Aspartate	133.0374	10.23	C4H7NO4	L1
L-Asparagine	132.0535	10.78	C4H8N2O3	L1
Allantoate	176.0544	10.59	C4H8N4O4	L2
Butanoic acid	88.0524	4.81	C4H8O2	L2
L-Erythrulose	120.0422	10.79	C4H8O4	L2
[FA trihydroxy(4:0)]	136.0372	8.92	C4H8O5	L2
Creatine	131.0694	10.51	C4H9N3O2	L1
N,N-Dimethylglycine	103.0633	9.13	C4H9NO2	L2
L-Threonine	119.0583	10.33	C4H9NO3	L1
PG(22:6)	866.5104	3.36	C50H75O10P	L2
PS(44:10)	883.5362	3.37	C50H78NO10P	L2
PC(42:7)	859.6093	3.59	C50H86NO8P	L2
PC(42:6)	861.6241	3.61	C50H88NO8P	L2
L-Glutamine	146.0690	10.56	C5H10N2O3	L1
Pentanoate	102.0681	4.77	C5H10O2	L2
D-Xylulose	150.0527	8.59	C5H10O5	L2
L-Arabinonate	166.0477	9.20	C5H10O6	L2
4-Guanidinobutanoate	145.0851	10.80	C5H11N3O2	L2
Betaine	117.0790	8.59	C5H11NO2	L1
L-Methionine	149.0510	8.82	C5H11NO2S	L1
L-Methionine S-oxide	165.0459	9.52	C5H11NO3S	L2
2-Deoxy-D-ribose 5-phosphate	214.0243	9.83	C5H11O7P	L2
L-Ornithine	132.0899	16.15	C5H12N2O2	L1
4-Guanidinobutanamide	144.1011	18.48	C5H12N4O	L2
Xylitol	152.0684	9.78	C5H12O5	L2
Choline	103.0997	17.85	C5H13NO	L2
2-C-Methyl-D-erythritol 4-phosphate	216.0401	10.70	C5H13O7P	L2
Choline phosphate	183.0661	9.73	C5H14NO4P	L1
sn-glycero-3-Phosphoethanolamine	215.0559	10.64	C5H14NO6P	L2
Hypoxanthine	136.0385	8.50	C5H4N4O	L1
Xanthine	152.0334	8.88	C5H4N4O2	L1
Urate	168.0283	9.45	C5H4N4O3	L1
Adenine	135.0545	8.00	C5H5N5	L1
Imidazole-4-acetate	126.0430	8.58	C5H6N2O2	L1
2-Hydroxy-2,4-pentadienoate	114.0317	10.83	C5H6O3	L2
Mesaconate	130.0267	10.35	C5H6O4	L1
2-Oxoglutarate	146.0215	10.77	C5H6O5	L1
5-Methylcytosine	125.0589	6.99	C5H7N3O	L2
(S)-1-Pyrroline-5-carboxylate	113.0477	10.52	C5H7NO2	L2
L-1-Pyrroline-3-hydroxy-5-carboxylate	129.0427	7.63	C5H7NO3	L2
2-Oxoglutaramate	145.0375	7.95	C5H7NO4	L2
N-Formyl-L-aspartate	161.0325	10.57	C5H7NO5	L2
3-Methyl-2-oxobutanoic acid	116.0474	4.82	C5H8O3	L1
(R)-2-Hydroxyglutarate	148.0372	10.38	C5H8O5	L1
L-Proline	115.0633	9.51	C5H9NO2	L1
N-Acetyl-beta-alanine	131.0582	6.78	C5H9NO3	L2
Acetylcysteine	163.0303	6.71	C5H9NO3S	L1
L-Glutamate	147.0531	9.98	C5H9NO4	L1

L-erythro-4-Hydroxyglutamate	163.0481	10.38	C5H9NO5	L2
N-Formimino-L-glutamate	174.0641	9.98	C6H10N2O4	L2
N-Carbamyl-L-glutamate	190.0589	10.32	C6H10N2O5	L2
(S)-3-Methyl-2-oxopentanoic acid	130.0631	4.58	C6H10O3	L2
2-Dehydro-3-deoxy-L-rhamnonate	162.0528	9.76	C6H10O5	L2
D-Glucono-1,5-lactone	178.0477	10.35	C6H10O6	L2
D-Glucarate	210.0376	11.37	C6H10O8	L2
5-Guanidino-2-oxopentanoate	173.0800	10.58	C6H11N3O3	L2
[FA oxo,amino(6:0)]	145.0738	9.56	C6H11NO3	L2
N-Formyl-L-methionine	177.0460	4.80	C6H11NO3S	L2
O-Acetyl-L-homoserine	161.0688	7.01	C6H11NO4	L2
4-Hydroxy-4-methylglutamate	177.0637	9.25	C6H11NO5	L2
D-Alanyl-D-alanine	160.0848	6.72	C6H12N2O3	L2
L-Cystine	240.0241	10.69	C6H12N2O4S2	L1
Hexanoic acid	116.0838	4.43	C6H12O2	L2
L-Rhamnulose	164.0685	8.76	C6H12O5	L2
D-Glucose	180.0634	11.88	C6H12O6	L1
D-Gluconic acid	196.0583	9.89	C6H12O7	L1
L-Citrulline	175.0957	10.97	C6H13N3O3	L1
L-Leucine	131.0946	8.56	C6H13NO2	L1
D-Galactosamine	179.0794	8.55	C6H13NO5	L2
D-Fructose 6-phosphate	260.0296	10.22	C6H13O9P	L1
D-Lysine	146.1055	17.02	C6H14N2O2	L2
L-Arginine	174.1117	18.51	C6H14N4O2	L1
D-Glucosamine 6-phosphate	259.0457	10.29	C6H14NO8P	L1
D-Sorbitol	182.0791	10.16	C6H14O6	L2
Triethanolamine	149.1052	8.10	C6H15NO3	L2
Nicotinamide	122.0480	6.75	C6H6N2O	L1
Urocanate	138.0429	8.29	C6H6N2O2	L2
cis-Aconitate	174.0164	11.82	C6H6O6	L2
2-Aminomuconate semialdehyde	141.0426	11.50	C6H7NO3	L2
Methylimidazoleacetic acid	140.0585	7.11	C6H8N2O2	L2
4-Imidazolone-5-propanoate	156.0534	10.34	C6H8N2O3	L2
2-Oxohexenoic acid	128.0473	4.77	C6H8O3	L2
2,3-Dimethylmaleate	144.0422	8.13	C6H8O4	L2
Citrate	192.0270	11.96	C6H8O7	L1
L-Histidine	155.0695	10.63	C6H9N3O2	L1
N-Acetyl-L-aspartate	175.0481	9.97	C6H9NO5	L2
2-Hydroxybutane-1,2,4-tricarboxylate	206.0426	11.52	C7H10O7	L2
N(pi)-Methyl-L-histidine	169.0851	9.29	C7H11N3O2	L1
N-Acetyl-L-glutamate	189.0637	9.64	C7H11NO5	L2
5-Acetamidopentanoate	159.0896	9.04	C7H13NO3	L2
L-Cystathionine	222.0674	11.28	C7H14N2O4S	L1
5-L-Glutamyl-taurine	254.0573	10.47	C7H14N2O6S	L2
[FA methyl(6:0)]	130.0994	4.14	C7H14O2	L2
4-Trimethylammoniobutanoate	145.1102	9.35	C7H15NO2	L1
L-Carnitine	161.1052	9.39	C7H15NO3	L1
N6-Methyl-L-lysine	160.1212	16.38	C7H16N2O2	L1
Homoarginine	188.1273	18.73	C7H16N4O2	L2
Pyridine-2,3-dicarboxylate	167.0218	10.61	C7H5NO4	L2
4-Hydroxybenzoate	138.0317	4.74	C7H6O3	L2
3-Hydroxyanthranilate	153.0426	9.34	C7H7NO3	L2
2-Amino-3-carboxymuconate semialdehyde	185.0324	11.58	C7H7NO5	L2
1-Methylnicotinamide	136.0636	9.02	C7H8N2O	L2
N1-Methyl-2-pyridone-5-carboxamide	152.0585	7.03	C7H8N2O2	L2
2-(Acetamidomethylene)succinate	187.0481	6.75	C7H9NO5	L2
Pyridoxine	169.0739	6.90	C8H11NO3	L1
Dihydroclavaminic acid	200.0797	7.88	C8H12N2O4	L2
[FA dioxo(8:0)]	172.0736	4.79	C8H12O4	L2

N2-Acetyl-L-aminoadipate	203.0794	8.48	C8H13NO5	L2
O-Succinyl-L-homoserine	219.0743	9.58	C8H13NO6	L2
[FA (8:1)]	142.0994	4.03	C8H14O2	L2
N-Acetyl-D-glucosamine	221.0899	9.00	C8H15NO6	L1
3-methyl-1-heptene	112.1252	3.72	C8H16	L2
N6-Acetyl-L-lysine	188.1161	10.22	C8H16N2O3	L2
N-Acetyl-D-glucosamine 6-phosphate	301.0563	9.82	C8H16NO9P	L2
[FA (8:0)]	144.1150	3.97	C8H16O2	L2
sn-glycero-3-Phosphocholine	257.1029	9.81	C8H20NO6P	L1
Formylanthranilate	165.0427	4.76	C8H7NO3	L2
Phenylacetic acid	136.0525	4.75	C8H8O2	L2
Phenylpropanoate	150.0680	4.49	C9H10O2	L2
Phenyllactate	166.0629	4.74	C9H10O3	L2
3-(4-Hydroxyphenyl)lactate	182.0579	7.35	C9H10O4	L2
L-Phenylalanine	165.0790	7.95	C9H11NO2	L2
L-Tyrosine	181.0739	9.89	C9H11NO3	L1
Uridine	244.0695	8.27	C9H12N2O6	L1
UMP	324.0358	10.04	C9H13N2O9P	L1
Deoxycytidine	227.0906	8.04	C9H13N3O4	L2
Cytidine	243.0854	9.31	C9H13N3O5	L1
2-Amino-4-hydroxy-6-(D-erythro-1,2,3-trihydroxypropyl)-7,8-dihydropteridine	255.0967	10.80	C9H13N5O4	L2
Aspartyl-L-proline	230.0902	10.16	C9H14N2O5	L2
Carnosine	226.1066	10.78	C9H14N4O3	L2
8-Amino-7-oxononanoate	187.1208	4.80	C9H17NO3	L2
O-Acetylcarnitine	203.1158	8.12	C9H17NO4	L1
Pantothenate	219.1107	6.74	C9H17NO5	L1
N2-(D-1-Carboxyethyl)-L-arginine	246.1328	10.02	C9H18N4O4	L2
Nonanoic acid	158.1306	3.87	C9H18O2	L2
Pantothenol	205.1314	6.68	C9H19NO4	L2
N6,N6,N6-Trimethyl-L-lysine	188.1525	15.29	C9H20N2O2	L2
3-Hydroxy-N6,N6,N6-trimethyl-L-lysine	204.1474	13.83	C9H20N2O3	L2
Phenylpyruvate	164.0474	4.53	C9H8O3	L1
3-(4-Hydroxyphenyl)pyruvate	180.0422	6.96	C9H8O4	L1
Hippurate	179.0583	4.79	C9H9NO3	L1
Dopaquinone	195.0533	10.26	C9H9NO4	L2
Carbamoyl phosphate	140.9828	15.65	CH4NO5P	L2
Hydroxymethylphosphonate	111.9926	9.77	CH5O4P	L2
Orthophosphate	97.9771	10.77	H3O4P	L2

Appendix A8: A list that shows the batch analysis by LC-MS and sample's order.

Suitability QC (Standard mix)

Suitability QC (Standard mix)

Suitability QC (Standard mix)

Suitability QC (Standard mix)

Suitability QC (Standard mix)

Process blank

Intrastudy QC sample (8 to 10 QC)

Experiment's samples

Intrastudy QC every 5 to 10 samples

Suitability QC (Standard mix)

Suitability QC (Standard mix)

Suitability QC (Standard mix)

Suitability QC (Standard mix)

Suitability QC (Standard mix)

Process blank